

UCLA

UCLA Electronic Theses and Dissertations

Title

Defining a Minimal Pharmacophore to Selectively Inhibit MBOAT4 (Ghrelin O-Acyl Transferase)

Permalink

<https://escholarship.org/uc/item/0971212d>

Author

Hollibaugh, Ryan

Publication Date

2016

Peer reviewed|Thesis/dissertation

UNIVERSITY OF CALIFORNIA

Los Angeles

Defining a Minimal Pharmacophore to Selectively Inhibit MBOAT4
(Ghrelin O-Acyl Transferase)

A dissertation submitted in partial satisfaction of the requirements
for the degree Doctor of Philosophy in Chemistry

by

Ryan A Hollibaugh

2016

© Copyright by
Ryan A Hollibaugh
2016

ABSTRACT OF THE DISSERTATION

Defining a Minimal Pharmacophore to Selectively Inhibit MBOAT4

(Ghrelin O-Acyl Transferase)

by

Ryan A Hollibaugh

Doctor of Philosophy in Chemistry

University of California, Los Angeles, 2015

Professor Patrick G. Harran, Chair

Ghrelin O-acyl Transferase (GOAT) is a recently discovered member of the membrane bound O-acyl transferase (MBOAT) family of enzymes. GOAT is uniquely able to catalyze the transfer of an n-octanoyl group to its substrate, the peptide hormone ghrelin. Acylated ghrelin is insulinostatic and can promote feeding behavior in higher mammals. Pharmacological inhibition of GOAT has emerged as an attractive means to modulate the ghrelin signaling pathway. GOAT is the only human enzyme known to promote octanoylation. Ghrelin is the only substrate of GOAT, and ghrelin is the only known octanoylated hormone. Further, ghrelin and GOAT are produced principally in the digestive tract. Unlike ligands of the ghrelin receptor, a GOAT inhibitor would not need to penetrate the blood brain barrier.

Herein, we detail our efforts to develop potent, in vivo active small molecule GOAT inhibitors by a peptidomimetic approach. Towards this goal we outline experimental procedures for assaying GOAT activity in vitro, and address unique challenges overcome during this work. Our medicinal chemistry has been driven by hypotheses concerning the catalytic mechanism and binding mode of GOAT and its co-substrates ghrelin and octanoyl-CoA. We unify our understanding of structure-activity relationships for a new class of GOAT inhibitors, and examine the progression of inhibitor structure which has led to these conclusions. Multiple synthetic routes appropriate for small and large scale syntheses of GOAT inhibitors are presented.

Top performing inhibitors exhibit high nanomolar potency in vitro, and suppress circulating acyl-ghrelin in-vivo for up to three hours in a mouse. We have extensively characterized the in vivo and in vitro pharmacokinetic properties of these materials. These inhibitors lay a strong foundation for further medicinal chemistry refinement, and provide a powerful new means of interrogating ghrelin biology and assessing the therapeutic potential of GOAT inhibition.

The dissertation of Ryan A Hollibaugh is approved.

Jorge R. Barrio

Kendall N. Houk

Patrick G. Harran, Committee Chair

University of California, Los Angeles

2016

This dissertation is dedicated to my parents who inspired me, to Christina who supported me, and to my friends who have helped me along the way.

TABLE OF CONTENTS

1. Introduction	1
1.1. Discovery of ghrelin and GHS-r	1
1.2. Physiological Functions of Ghrelin	3
1.3. Ghrelin O-Acyl Transferase	5
1.4. Inhibitors of GOAT	8
1.5. Need for a Small Molecule GOAT Inhibitor	11
2. GOAT Assays	14
2.1. Enzyme Inhibitors	14
2.2. Literature GOAT Activity Assays	14
2.3. Implementation of a GOAT Activity Assay	19
2.4. Expression of Mouse GOAT in Sf9 Insect Cells	20
2.5. His-Tagged Proghrelin	22
2.6. GOAT Activity Assay	26
3. Hypothesis Driven Design and Synthesis of In Vivo Inhibitors of Ghrelin O-Acyl Transferase	29
3.1. Approach	29
3.2. Design of GHS-r Ligand/Ghrelin Hybrids	31
3.3. Syntheses of GHS/Ghrelin Hybrids	33
3.4. Linker Optimization	34
3.5. Synthesis of Carbamoyl GOAT Inhibitors	36
3.6. Methyl Scan	37
3.7. Synthesis of Methylated GOAT Inhibitors	38

3.8. Conformationally Restrained Octanoate Mimics	40
3.9. Representative Syntheses of Alkynyl and Cyclobutyl Octanoate Mimics	42
3.10. Efforts to Optimize the C-Terminal Heterocycle	43
3.11. Synthesis of Simplified C-Terminal Fragments	45
3.12. C-Terminal Truncation and P2 Residue Optimization	46
3.13. Synthesis of Aminomethylpyrrolidine GOAT Inhibitors	48
3.14. Optimization of N-Terminal Residue	50
3.15. Synthesis of Thioamides	52
3.16. In Vitro Activity of Lead Inhibitors Compared to Reported GOAT Inhibitors	53
3.17. Competitive Inhibition and Divergent SAR of Aminomethylpyrrolidines	54
3.18. Conclusion	55
4. In Vivo Performance of Novel Small Molecule GOAT Inhibitors	58
4.1. Selection and Preparation of In Vivo Candidates	58
4.2. Evaluation of Inhibitor Efficacy In Vivo	70
4.3. Observation of Lethargy in Mice Treated with GOAT Inhibitors	79
4.4. Pharmacokinetics of GOAT Inhibitors	80
4.5. Membrane Permeability Assays	85
4.6. PAMPA Measurement of Inhibitor Permeability	87
4.7. Cellular Model of Inhibitor Permeability	89
4.8. Inhibitor Plasma Binding	92
4.9. Conclusions	93
5. Experimental Appendices	97

Experimental Procedures Supporting Chapter 2	98
5.1. GOAT Membrane Preparation	99
5.2. Ghrelin Production	103
5.3. GOAT Activity Assay	105
5.4. Engineering and Production of GST-TEV	107
Experimental Procedures Supporting Chapter 3	109
5.5. General Procedures for Inhibitor Synthesis or Homologation	110
5.6. GHS and GHS/Ghrelin Hybrids	110
5.7. Synthesis and Characterization of Carbamoyl GOAT inhibitors	113
5.8. Characterization of Methyl Scan Inhibitors	115
5.9. Conformationally Constrained GOAT inhibitors	119
5.10. Synthesis and Characterization of C-terminal Variants	123
5.11. Synthesis and Characterization of Aminomethylpyrrolidine GOAT Inhibitors	130
5.12. Synthesis and Characterization of Branched GOAT Inhibitors	133
5.13. Thioamide Synthesis using Thioacyl Donors	139
5.14. Literature GOAT Inhibitors	142
Experimental Procedures Supporting Chapter 4	143
5.15. Thioacylation using Nitrotriazolyl Thioacyl Donors	144
5.16. Evaluation of Lawesson's Reagent Selectivity	145
5.17. Synthesis of Lead Inhibitor 1	147
5.18. Synthesis of Lead Inhibitor 2	151
5.19. Pd-Mediated Alloc Cleavage	154
5.20. Synthesis of Lead Inhibitor 3	157

5.21. Syntheses of Negative Control 4 and Inhibitor 19	161
5.22. Synthesis and Characterization of Amidyl Inhibitors for Pharmacokinetic Analysis	164
5.23. Crystallography	166
5.24. In Vivo Evaluation of GOAT Inhibitor Efficacy	176
5.25. Efficacy Evaluation by IP Dosing	176
5.26. Inhibitor Quantitation in Mouse Excrement	177
5.27. INS-1 Cellular Assay	178
5.28. PAMPA Permeability	178
5.29. Permeability in Caco2 and MDCK Monolayers	179
5.30. Plasma Binding Measurement	179
6. Compiled In Vitro GOAT Inhibition Assay Results	181
UT Southwestern / Dr. Tongjin Zhao Results	182
UCLA / Dr. David Strugatsky Results	334

ACKNOWLEDGMENTS

I wish to thank everyone in Athens, in Atlanta, and in Los Angeles who has helped me along the way. I would not be here without you.

This project would have been impossible without the assistance of Dr. Tongjin Zhao in the lab of Drs. Michael Brown and Joseph Goldstein at UTSW. The in vitro assay implemented in chapter two was developed by him, many of the inhibitors described in chapter three were evaluated by him, and much of the in vivo experimentation described in chapter four was designed and performed by him. His assistance in transferring the biology portion of the project to UCLA was invaluable.

Dr. David Strugatsky has been invaluable. His efforts have rendered the inhibitor assay routine. He has taken over where Tongjin left off, and ably pushes the biology side of the project. Dr. Peter Tontonoz and the members of his lab have been generous with their time and advice. Dr. Elisabeth Tarling was incredibly generous with her time, energy, and equipment for the culture of sf9 cells used for GOAT expression.

I thank in particular Dr. Haixia Liu, who preceded me on this project. Many of the inhibitors described here were prepared in whole or in part by her, and her work laid the foundation for my own. I have had the honor of supervising several undergraduates on this project; of these, Ryan Quiroz and Brandon Sumida in particular were each tremendous aids. Dr. Hui Ding and Tyler Allred have at various times joined me on this project.

Pharmacology work was largely performed by Dr. Noelle Williams of UTSW and the members of her lab. I appreciate her incredible diligence and thoroughness, as well as her willingness to spend time discussing results with a non-expert.

Funding support was provided by the NIH through the CBI program (2T32GM008496), by the NIDDK (1R01DK100627), and by the NSF (CHE-1048804).

Discussions with Dr. Tristin Rose have been invaluable for both the advancement of the project and for my growth as a scientist and researcher. I aspire to match her breadth and depth of knowledge. Andrew Roberts has been all I could hope for in a friend and colleague. Brice, Ken, Jack, and all the other Harran lab members have been tremendous sources of information and advice.

Special thanks to my advisor and mentor Dr. Patrick Harran. His challenge to be a better scientist and to do better science has inspired me and sharpened my mind. To my parents Terry Hastings and Tim Hollibaugh, for teaching me at a very young age that $PV=nRT$, and for their love and support. To Christina, for always being my #1 advocate.

Thanks, everyone.

CURRICULUM VITAE

Education:

B.S. Chemistry Emory University, Atlanta, GA. 2009

Publications & Patents:

Ryan A. Hollibaugh, David Strugatsky, Tyler Allred, Peter Tontonoz, Patrick G. Harran. Defining a Minimal Pharmacophore to Selectively Inhibit MBOAT4 (Ghrelin O-Acyl Transferase). Manuscript in preparation.

Patrick G. Harran, Ryan A. Hollibaugh, Haixia Liu (2014). Small Lipopeptidomimetic Inhibitors of Ghrelin O-Acyl Transferase. **US Provisional Patent Application #62/051,701**. Filed September 17, 2014.

Sulfide oxidation coupled to arsenate reduction by a diverse microbial community in a soda lake. Applied Environmental Microbiology. 2006 Mar;72(3):2043-9.

Anaerobic oxidation of arsenite in Mono Lake water and by a facultative, arsenite-oxidizing chemoautotroph, strain MLHE-1. Applied Environmental Microbiology. 2002 Oct;68(10):4795-802.

Awards:

January – March 2010: UCLA Foundation Fellowship

July 2010 – July 2013: Chemistry and Biology Interface (CBI) Training Grant

1 Introduction

1.1 Discovery of Ghrelin and GHS-r

Ghrelin (**1**) is a 28 amino acid lipopeptide,¹ which has been shown to play a role in the regulation of growth hormone (GH) release, feeding behavior, energy homeostasis, and glucose homeostasis. The discovery of ghrelin began with the identification of its receptor, originally termed the growth hormone secretagogue receptor (GHS-r).² In the 1990s, researchers at Merck prepared small molecule analogs of a short peptide motif (**3**),³ which was known to promote release of GH via a mechanism distinct from the canonical growth hormone releasing hormone (GHRH) axis (Figure 1.1A). These molecules, typified by MK-0677 (**2**), were termed growth hormone secretagogues (GHSs). The cellular target of these compounds was initially unknown, however a ³⁵S radiolabeled analog of **2** was used to identify the receptor for these molecules (GHS-r).² As shown in in figure 1.1B, action of GHS-r ligands on GHS-r in the pituitary leads to secretion of GH,³ while binding in the hypothalamus promotes GHRH release, ultimately resulting in additional GH release. Small molecules agonists of this receptor received considerable interest for their potential utility in the treatment of patients with GH deficiencies. MK-0677, and other related GHSr agonists have been clinically evaluated for the treatment of a variety of GH related diseases.³

Although a suite of synthetic GHS-r ligands had been identified and their interactions with the receptor well characterized,³ the endogenous ligand for the receptor remained unknown until 1999, when Kojima and coworkers, who screened

tissue extracts for receptor activity, identified a lipidated 28 amino acid peptide hormone as the endogenous ligand for the receptor and named it ghrelin (1).¹ It was determined

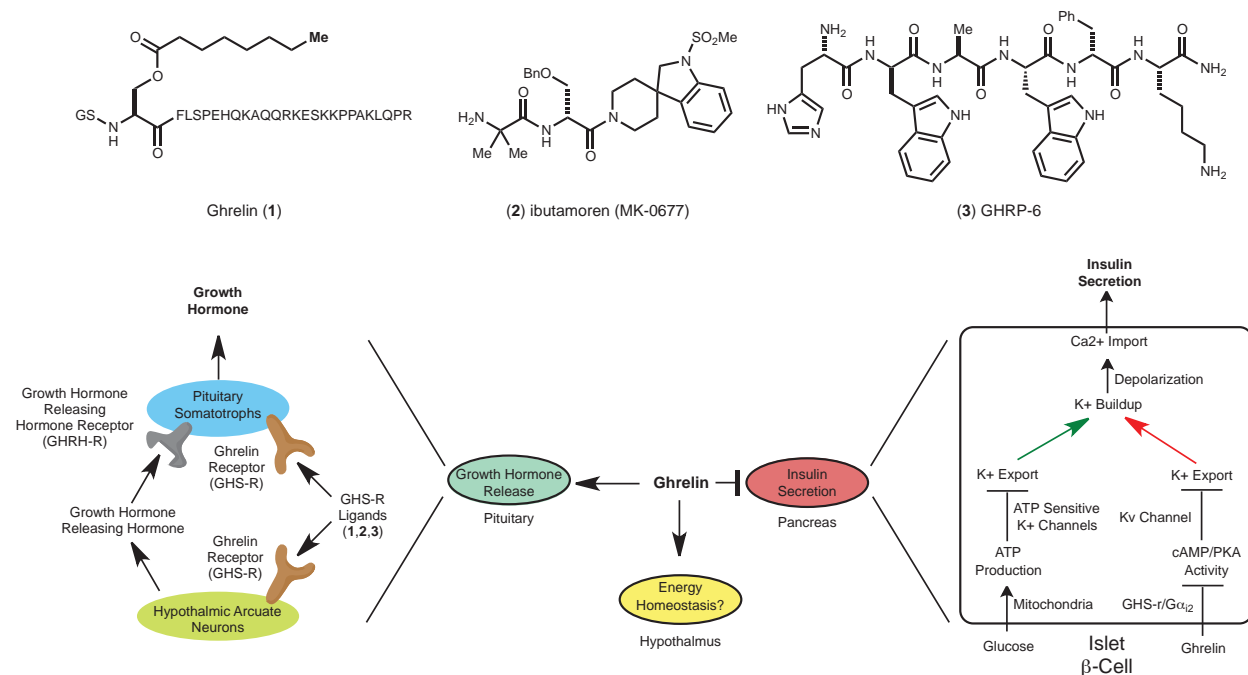


Figure 1.1: Ghrelin, Ibutamoren, and GHRP-6 are all agonists of GHS-r and the diverse signaling pathways originating from ghrelin. (A) Structure of three structurally distinct GHS-r agonists. (B) GHS-r is a G-protein coupled receptor, which has several functions, depending on tissue type. In the pituitary gland, GHS-r regulates production of growth hormone both directly and indirectly through additional production of GHRH. In pancreatic islets, GHS-r is coupled to a different G-protein, and receptor activation prevents accumulation of intracellular calcium, which in turn suppresses insulin release in response to glucose. Ghrelin also influences hunger, feeding behavior, and energy homeostasis, although these effects are highly context dependent.

that the active form of ghrelin required a medium chain (natively almost exclusively octanoyl) fatty acid appendage on serine-3 for endocrine activity. Ghrelin was the first octanoylated peptide identified, and it remains the only known hormone having this modification.⁴ At the time, the mechanism by which octanoate was appended was unknown. Select and truncated forms of the ghrelin peptide have been identified, but the

most abundant form of ghrelin is the 28 amino acid ser-3 form, which is found in the blood in both acyl and des-acyl forms.⁵

1.2 Physiological Functions of Ghrelin

Following its discovery, ghrelin was found to be linked not just to GH secretion in the hypothalamus, but also to overall metabolism and to glucose homeostasis (Figure 1.1B). It was noted that ghrelin levels rise before a meal and fall afterwards.⁶ This finding led to speculation that ghrelin functioned as a hunger signal, apparently antipodally to the satiety inducing hormone leptin.⁷ This hypothesis was supported by studies demonstrating that infusion of ghrelin peptides to mice or humans induced feeding.⁸ A more recent study, however, determined that in mice the amount of ghrelin required to induce a change in feeding behavior exceeds the levels of circulating ghrelin observed physiologically, even under fasting conditions.⁹ These data cast doubt on the physiological relevance of ghrelin as a direct mediator of the hunger response.

Whereas induction of ghrelin signaling was found to promote feeding, blockade of ghrelin signaling does not affect feeding behavior or weight gain with a standard diet.^{10,11} Unlike leptin knockout mice, ghrelin knockout (KO) mice under standard feeding conditions are reportedly healthy, and outwardly indistinguishable from wild type cohorts. Examination of these animals under a wide variety of non-standard feeding conditions has yielded mixed results. Some studies have shown that ghrelin KO mice have a modest resistance to weight gain when fed a high fat diet.¹² This effect is directly linked to the amount of food the animal consumes, suggesting that ghrelin regulates

metabolism at multiple levels, rather than simply controlling caloric intake. Yet, other studies failed to observe this effect, even under similar feeding conditions.¹³

While ghrelin's role in feeding behavior and metabolism is both complex and inconsistently observed in laboratory experiments, its function in glucose homeostasis is better understood.^{14,15} The action of ghrelin on its receptor in pancreatic islets suppresses insulin release via a well-characterized signaling pathway (Figure 1.1B). This effect has been observed in systems ranging from isolated pancreatic islets¹⁶ to whole organism models,¹⁷ and is consistently observed across multiple studies.⁵ Animals lacking ghrelin or its receptor show improved performance in a glucose tolerance test (GTT), such animals are better able to clear oral or intraperitoneally administered glucose. Ghrelin signaling has also been linked to a wide variety of other disease processes. However the most compelling data are from literature linking ghrelin signaling pathways to deleterious effects on metabolism and glucose homeostasis, and our goal is to develop pharmacological tools to control ghrelin production in vivo.

Pharmacological ablation of ghrelin signaling has garnered considerable interest in the medicinal chemistry community.¹⁸ Ghrelin receptor ligands are well developed; useful small molecule agonists, antagonists, and inverse agonists of the GHSr have been reported in the literature.^{3,19,20} All of these molecules must penetrate the blood-brain barrier to reach the receptor, and thus have potential to cause unintended neurological effects. Ghrelin is produced in the digestive tract, especially in the gastric oxyntic mucosa.^{1,21} A compound that blocked ghrelin production, rather than receptor binding, could therefore act peripherally, and might offer distinct advantages over CNS-penetrating GHSr antagonists.

1.3 Ghrelin O-Acyl Transferase

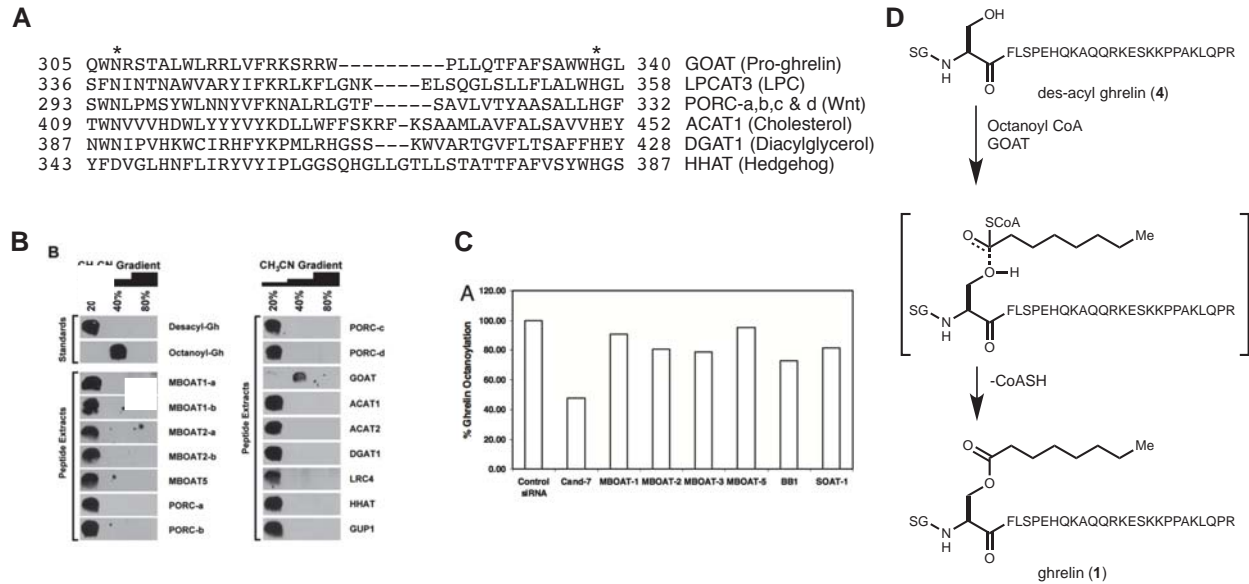


Figure 1.2: Identification of the enzyme responsible for ghrelin octanoylation. (A) Sequence alignment of select MBOATs demonstrating the high degree of conservation amongst this family of proteins. Absolutely conserved Asn and His residues are indicated. (B) Approaches to the identification of the MBOAT that transfers octanoate to ghrelin. Yang et al cloned candidate enzymes to identify an enzyme capable of performing this modification. Gutierrez et al silenced candidate enzymes to identify an enzyme or enzymes required for octanoylation of ghrelin. (C) Mechanism of GOATs action on ghrelin. No evidence of a covalent interaction between any substrate and GOAT has been reported.

Ghrelin requires post-translational octanoylation of serine-3 for its activity, but the enzyme responsible for this unique acylation was unknown until 2008. It stood to reason that if the enzyme or enzymes that mediated this lipidation could be identified, then inhibition of this pathway might provide a means to modulate ghrelin signaling without affecting receptor activity. The membrane bound O-acyl transferases (MBOATs) are a family of membrane bound enzymes that transfer long and medium chain fatty acids to a variety of peptidal and non-peptidal hydroxyl and sulfhydryl nucleophiles. The

MBOATs were originally characterized by Hofmann, who identified the family by sequence homology.²² This family of enzymes is characterized by tightly conserved histidine and asparagine residues, which are believed to participate in catalysis. Sequence alignments of several well-studied MBOATs are shown in figure 1.2A, with the conserved His and Asn residues indicated. ACAT and DGAT, in particular, have each been the subject of extensive medicinal chemistry investigation,^{23,24} and numerous compounds targeting each have advanced to clinical trials.

Searching for the acyltransferase responsible for the octanoylation of ghrelin, Yang et al. identified the MBOAT family of enzymes as likely candidates, and screened all sixteen MBOATs encoded by the mouse genome for the ability to acylate ghrelin.²⁵ Each candidate MBOAT was expressed alongside ghrelin in a rat insulinoma (INS-1) cell line. Following the addition of octanoic acid to the culture medium, media and cell lysate were analyzed for the presence of octanoyl ghrelin. Acyl and des-acyl ghrelin were separated by chromatography and the eluent fractions analyzed by immunostaining (Figure 1.2B). Only transformation with MBOAT 4 conferred the ability to produce acyl ghrelin. Concurrently with this study, Gutierrez et al. identified a cell line that required only the addition of octanoic acid to produce mature acyl ghrelin.²⁶ Reasoning that these cells must express the correct acyltransferase, siRNAs targeting a series of candidate acyltransferases were added to probe candidate genes. Only the siRNA targeting MBOAT 4 suppressed acyl-ghrelin formation (Figure 1.2C). MBOAT 4 was thus termed Ghrelin O-Acyl Transferase (GOAT). Octanoyl CoA was subsequently identified as the acyl donor in the reaction.²⁷ Since then, no other GOAT substrates have been identified, and no other enzyme has been found which can octanoylate

ghrelin. In addition, both GOAT and ghrelin are principally and co-locally expressed in the digestive tract, especially the oxyntic portion of the stomach.²²

The mutual specificity of GOAT, Ghrelin, and octanoate, and the peripheral (rather than CNS) localization of the key acylation event suggest that a small molecule inhibitor of GOAT would not need to penetrate the brain, should have no mechanism-based toxic effects, and that inhibition of related enzymes is unlikely. These facts, coupled with the potential therapeutic utility of suppressing circulating ghrelin levels, warrant the development of small molecule inhibitors of this enzyme, as several research groups have noted.^{26, 27,5}

GOAT knockout mice have been generated, and show a relatively mild phenotype. If a beneficial phenotype were observed for mice of this genetic background, it would provide strong support for the potential utility of a GOAT inhibitor. However, as was observed for ghrelin and GHS-r KO mice, GOAT knockout mice show no detectable phenotype under standard or high fat (HF) feeding conditions.¹³ However, a recent study using a new strain of GOAT knockout mice identified dietary characteristics required to observe a phenotypic effect.²⁸ GOAT knockout mice fed medium chain triglyceride (MCT) or HF diets supplemented with sucrose showed marked resistance to obesity relative to WT and KO mice fed an un-supplemented HF or MCT diet. They further identified a contribution of ghrelin signaling to impulse based feeding. Most importantly, they found that knockout mice fed a sucrose supplemented high fat or medium chain triglyceride diet were measurably more resistant to weight gain than WT mice. While phenotypic differences under conditions of calorie surplus have been difficult to identify, a strong phenotype is observed under conditions of severe calorie

restriction. Zhao et al. noted that GOAT and ghrelin knockout mice were more susceptible than WT mice to hypoglycemia induced mortality.¹³ This effect is mediated through the GH axis of ghrelin signaling, as infusion of GH to calorie restricted GOAT KO mice was sufficient to rescue them.

1.4 Inhibitors of GOAT

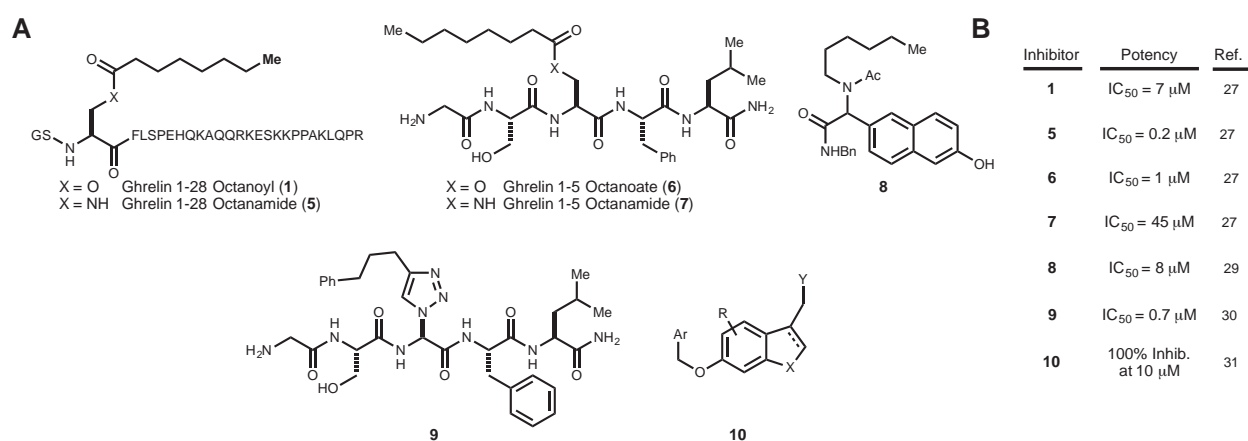


Figure 1.3: Reported inhibitors of ghrelin O-acyl transferase. (A) Several classes of inhibitor have been reported in the literature. (B) Reported in vitro potency of GOAT inhibitors.

Shortly after GOAT was identified as the enzyme responsible for ghrelin octanoylation, Yang and coworkers reported that the enzyme was inhibited by its reaction product, octanoyl ghrelin 1-28 (**1**) [IC₅₀ 7μM] and much more potently by octylamide analog **5** [IC₅₀ 200nM] (Figure 1.3).²⁸ They also showed that GOAT can catalyze the octanoylation of much shorter peptides derived from the N-terminus of ghrelin. Oligomers as short as five residues are readily acylated by the enzyme. Small acyl-ghrelin derived pentapeptides (**6** and **7**) also inhibit GOAT, albeit with roughly 40 fold reduced potency relative to full-length ghrelin sequences.

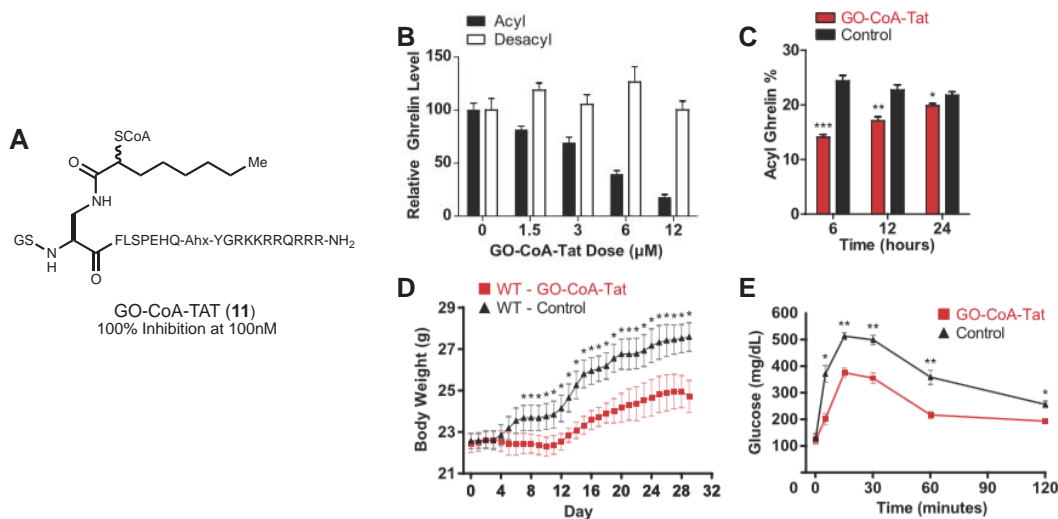


Figure 1.4: Structure and in vivo pharmacology of GO-CoA-TAT. (A) GO-CoA-TAT is a fusion peptide consisting of the first ten amino acids of acyl-ghrelin octanamide (**5**) with an intact CoA unit and TAT sequence appended. (B) GOAT activity in Hela cells transfected to express GOAT and ghrelin is inhibited in a dose dependent fashion by GO-CoA-Tat. (C) In mice GO-CoA-Tat reduces the fraction of acyl ghrelin, with maximum effect observed after 6 hours; followed by slow recovery to the resting state. (D) Chronic administration of **11** to mice fed a MCT diet reduces weight gain. (E) Treatment with **11** also improves glucose tolerance test performance relative to a control group.

In addition to the peptidyl GOAT inhibitors, four other classes of GOAT inhibitors have been disclosed (Figure 1.3). In 2011 Garner and Janda reported that benzamide **8** inhibited GOAT.²⁹ This compound was identified from a small library of compounds derived from Ugi multicomponent reactions. No further development of these small molecules has so far been reported. Houglund has identified a set of “click” reaction derived triazoles, the most potent of which is **9**, as inhibitors of GOAT.³⁰ While these compounds utilize the same pentapeptide skeleton as **6** and **7**, they demonstrate the enzyme’s ability to tolerate modification of the octanoate side chain. Takeda Pharmaceuticals has patented a class of heterocycle based GOAT inhibitors.³¹ They

report several compounds having general structure **10** that fully inhibit GOAT activity at 10 μ M in vitro. These compounds have thus far not been characterized further in the literature.

To date the most well-studied GOAT inhibitor was reported by Barnett et al. in 2010.³² The authors noted that, as shown in figure 1.2C, the enzyme must bind both octanoyl CoA and ghrelin during catalysis. A bisubstrate mimetic, termed GO-CoA-Tat (**11**), was designed to take advantage of both binding sites. GO-CoA-Tat incorporates the first ten amino acids of octanamide ghrelin 1-28 (**5**) and an intact CoA unit. A Tat, which promotes endocytosis, is appended to the C-terminus of the ghrelin peptide via an aminohexanoate linker. Peptide inhibitors such as **5** and **6** are inactive in cellular culture, likely due to poor membrane permeability and poor stability. By contrast, GO-CoA-Tat retains activity in cell-based assays, and reduces circulating acyl-ghrelin concentrations in vivo. Chronic administration of GO-CoA-Tat was reported to decrease weight gain in mice fed a high fat diet. Additionally, GO-CoA-Tat improved GTT performance when administered in advance of a glucose challenge. These results reinforce the pharmacological potential of GOAT inhibition, but it is unclear whether GO-CoA-Tat itself will be clinically useful. While **11** has been used in a few studies since its development, it is limited by high molecular weight and peptidal character. GO-CoA-Tat is presumably not orally available, so repeated IP dosing is required for long-term studies. In addition, the metabolic stability of this construct has not been demonstrated. To our knowledge, no other reported inhibitors have been tested in vivo.

1.5 Need for a Small Molecule GOAT Inhibitor

Despite the apparently conflicting results obtained with knockout animals lacking components of the ghrelin signaling pathway, interest in this hormone has persisted. Numerous authors have suggested that an inhibitor of GOAT production would serve at the very least as a useful probe of this system. The results obtained using Go-CoA-TAT suggest that such a compound may even be clinically useful. An orally available small molecule inhibitor of GOAT would be an ideal means to determine the potential of such a compound for the treatment of human disease and to answer longstanding questions in the area of ghrelin signaling as well as obesity and diabetes research.

-
- 1 Kojima M, Hosoda H, Date Y, Nakazato M, Matsuo H, Kangawa K (1999). Ghrelin is a growth-hormone-releasing acylated peptide from stomach. *Nature* 402:656-660.
 - 2 Pong SS, Chaung LY, Dean DC, Nargund RP, Patchett AA, Smith RG (1996). Identification of a new G-protein-linked receptor for growth hormone secretagogues. *Mol. Endocrinol.* 10(1):57-61.
 - 3 Smith RG (2005). Development of growth hormone secretagogues. *Endocr Rev.* 26(3):346-60.
 - 4 Romero A, Kirchner H, Heppner K, Pfluger PT, Tschöp MH, Nogueiras R (2010). GOAT: the master switch for the ghrelin system?. *European Journal of Endocrinology* 163(1):1-8.
 - 5 Müller TD, et al. (2015) Ghrelin. *Molecular Metabolism* 4(6):437-460.
 - 6 Diabetes. 2001 Aug;50(8):1714-9. A preprandial rise in plasma ghrelin levels suggests a role in meal initiation in humans. Cummings DE¹, Purnell JQ, Frayo RS, Schmidova K, Wisse BE, Weigle DS.
 - 7 *Obes Rev.* 2007 Jan;8(1):21-34. The role of leptin and ghrelin in the regulation of food intake and body weight in humans: a review. Klok MD¹, Jakobsdottir S, Drent ML.
 - 8 A.M. Wren, L.J. Seal, M.A. Cohen, A.E. Brynes, G.S. Frost, K.G. Murphy, W.S. Dhillo, M.A. Ghatei, S.R. Bloom Ghrelin enhances appetite and increases food intake in humans. *J. Clin. Endocrinol. Metab.*, 86 (2001), pp. 5992–5995.
 - 9 McFarlane MR, Brown MS, Goldstein JL, Zhao TJ (2014) Induced ablation of ghrelin cells in adult mice does not decrease food intake, body weight, or response to high-fat diet. *Cell Metab.* 20(1): 54–60.
 - 10 Y. Sun, S. Ahmed, R.G. Smith. Deletion of ghrelin impairs neither growth nor appetite. *Mol. Cell. Biol.*, 23 (2003), pp. 7973–7981.

-
- 11 K.E. Wortley, K.D. Anderson, K. Garcia, J.D. Murray, L. Malinova, R. Liu, M. Moncrieffe, K. Thabet, H.J. Cox, G.D. Yancopoulos, et al. Genetic deletion of ghrelin does not decrease food intake but influences metabolic fuel preference. *Proc. Natl. Acad. Sci. USA*, 101 (2004), pp. 8227–8232.
 - 12 Wortley KE, del Rincon JP, Murray JD, Garcia K, Iida K, Thorner MO, and Sleeman, MW (2005). Absence of ghrelin protects against early-onset obesity. *J. Clin. Invest.* 115(12):3573-3578.
 - 13 Zhao TJ, et al. (2010). Ghrelin O-acyltransferase (GOAT) is essential for growth hormone-mediated survival of calorie-restricted mice. *Proc. Natl. Acad. Sci. USA* 107(16):7467-7472.
 - 14 Kurashina T. et al. (2015). The β -cell GHSR and downstream cAMP/TRPM2 signaling account for insulinostatic and glycemic effects of ghrelin. *Sci Rep* 15(5):14041.
 - 15 Dezaki, K. (2006). Blockade of pancreatic islet-derived ghrelin enhances insulin secretion to prevent high-fat diet-induced glucose intolerance. *Diabetes* 55(12):3486-93.
 - 16 Dezaki, K., Hosoda, H., Kakei, M., Hashiguchi, S., Watanabe, M., Kangawa, K., et al., 2004. Endogenous ghrelin in pancreatic islets restricts insulin release by attenuating Ca²⁺ signaling in beta-cells: implication in the glycemic control in rodents. *Diabetes* 53:3142e3151.
 - 17 Salehi, A., Dornonville de la Cour, C., Hakanson, R., Lundquist, I., 2004. Effects of ghrelin on insulin and glucagon secretion: a study of isolated pancreatic islets and intact mice. *Regulatory Peptides* 118:143e150.
 - 18 *Nat Rev Neurosci.* 2001. Aug;2(8):551-60. Ghrelin: an orexigenic and somatotrophic signal from the stomach. Inui A1.
 - 19 Yua, M, et al. (2010). Identification of piperazine-bisamide GHSR antagonists for the treatment of obesity. *Bioorganic & Medicinal Chemistry Letters* 20(5):1758–1762.
 - 20 Takahashi B, et al. (2015) 2-Aminoalkyl nicotinamide derivatives as pure inverse agonists of the ghrelin receptor. *Bioorganic & Medicinal Chemistry Letters* 25(13):2707–2712.
 - 21 Stengel A, et al. (2010). Differential distribution of ghrelin-O-acyltransferase (GOAT) immunoreactive cells in the mouse and rat gastric oxyntic mucosa. *Biochem Biophys Res Commun.* 392(1):67-71.
 - 22 Hofmann K (2000) A superfamily of membrane-bound O-acyltransferases with implications for Wnt signaling. *Trends Biochem Sci.* 25(3):111–112.
 - 23 *Mini Rev Med Chem.* 2013. Jun 1;13(8):1195-219. ACAT inhibitors: the search for novel cholesterol lowering agents. Pal P1, Gandhi H, Giridhar R, Yadav MR.
 - 24 *Curr Opin Drug Discov Devel.* 2010 Jul;13(4):489-96. DGAT1 inhibitors as anti-obesity and anti-diabetic agents. Birch AM1, Buckett LK, Turnbull AV.
 - 25 Yang J, Brown MS, Liang G, Grishin NV, Goldstein JL (2008) Identification of the Acyltransferase that Octanoylates Ghrelin, an Appetite-Stimulating Peptide Hormone. *Cell* 132(3):387-396.
 - 26 Gutierrez JA, et al. (2008). Ghrelin octanoylation mediated by an orphan lipid transferase. *Proc. Nat. Acad. Sci. USA* 105(17):6320-6325.

-
- 27 Yang J, Zhao TJ, Goldstein JL, Brown MS (2008). Inhibition of ghrelin O-acyltransferase (GOAT) by octanoylated pentapeptides. *Proc. Natl. Acad. Sci. USA* 105(31):10750-10755.
- 28 Kouno T, Akiyama N, Ito T, Okuda T, Nanchi I, Notoya M, Oka S, Yukioka H (2016). Ghrelin O-acyltransferase knockout mice show resistance to obesity when fed high-sucrose diet.
- 29 Garner A, Janda K (2011). A small molecule antagonist of ghrelin O-acyltransferase (GOAT). *Chem. Commun.* 47(26):7512-7514.
- 30 Zhao F, Darling JE, Gibbs RA, Hougland JL. (2015). A new class of ghrelin O-acyltransferase inhibitors incorporating triazole-linked lipid mimetic groups. *Bioorg Med Chem Lett.* 25(14):2800-3.
- 31 Aromatic ring compound. WO 2013125732 A1.
- 32 Barnett BP, et al. (2010). Glucose and weight control in mice with a designed ghrelin O-acyltransferase inhibitor. *Science* 330(6011):1689-1692.

2. GOAT Assays

2.1 Enzyme Inhibitors

Successful medicinal chemistry programs critically depend upon a method or set of methods to score the efficacy of candidate compounds. Among many molecular features that could be scored, perhaps the most fundamental of these is the nature and strength of interaction between a given ligand and its target receptor.¹ The method(s) used to evaluate this interaction underpins the entire program, and should be robust as possible, such that many compounds can be routinely screened and reproducible results obtained.² This chapter will first detail literature methods to measure ghrelin O-acyl transferase (GOAT) activity, then describe in detail the assay implemented to evaluate novel GOAT inhibitors. Despite invaluable advice and assistance from our collaborators at University of Texas Southwestern Medical Center, especially Dr. Tongjin Zhao, establishing this assay proved challenging in our hands, and special attention will be paid to the pitfalls encountered and the means with which they were overcome. A detailed step-by-step protocol is included in the supporting information for this chapter.

2.2 Literature GOAT Activity Assays

Following the identification of ghrelin in 1999, methods were developed to rapidly quantify levels of both the acyl and des-acyl forms of ghrelin.³ The most standard and widely adopted of these is a sandwich ELISA, which has been commercialized by two

manufacturers. Both kits are reported to give reliable quantitation of ghrelin species, even in complex media such as animal plasma. While these assays have also been used for analysis of GOAT activity in vitro, their expense – a single 96 well plate costs >\$450 – limits throughput and renders this strategy cost prohibitive for use in a medicinal chemistry program.

Each of the groups having reported the development of a GOAT inhibitor has also independently developed at least one in vitro enzyme activity assay. While the reported assays are distinct, they necessarily share some common features. Natively, GOAT catalyzes the transfer of an n-octanoate fragment from octanoyl CoA to serine-3 of proghrelin.⁴ Thus, any enzyme assay must contain these three components, or an appropriate surrogate, and provide a means to detect product formation.⁵ Octanoyl CoA is commercially available in both unlabeled and radiolabeled form. Reported assay systems vary widely in the form of ghrelin used and the means to detect octanoylation (see the discussion of individual assay systems below for further details).

The MBOAT family, including GOAT, comprises integral membrane proteins. As such, recombinant enzymes must remain in a lipid membrane in order to retain catalytic activity.⁴ Instead membrane fractions of GOAT expressing cells are used as a source of enzyme activity. Integral membrane proteins like MBOATS generally fail to fold correctly when produced in bacterial expression vectors, and are therefore most often produced in eukaryotic cells.⁶ The most commonly used cell type for MBOAT production is *Spodoptera frugiperda* (fall armyworm) derived Sf9 cells, which may be infected with a recombinant baculovirus encoding mammalian genes such as GOAT under transcriptional control of a viral polyhedrin promoter.⁷ A major advantage of this

expression system relative to cells of mammalian origin is reduced background activity, most likely because insects lack endogenous GOAT.³ Low background rate of acyl-transfer is essential for accurate evaluation of enzyme inhibitors. Additionally, insect cell based protein expression is generally less expensive and more scalable than mammalian derived expression systems.

The first in vitro assay of GOAT activity was reported by Yang et al. in 2008.⁸ In this assay format (Figure 2.1A), transfer of ³H-octanoate from ³H-octanoyl CoA to an affinity tagged proghrelin construct is catalyzed by membranes from GOAT expressing Sf9 cells. Palmitoyl-CoA, which is not used by GOAT, is also included at high concentration in the reaction mixture. In the absence of this additive, complex kinetics are observed and the reaction is poorly reproducible. The long chain acyl-CoA is believed to act as an alternative substrate for hydrolases present in the crude Sf9 thereby slowing degradation of radiolabeled octanoyl-CoA. Affinity purification of acyl as well as des-acyl proghrelin peptides separates product acyl ghrelin from residual ³H-octanoyl CoA, and the extent of octanoylation is then quantified by liquid scintillation counting. This method was used extensively in the identification of the first inhibitors of GOAT by Yang et al., and a minor modification was used in the development of GO-CoA-Tat.⁹ In this implementation, GOAT-containing membrane fractions were isolated from HEK-293 cells, and synthetic biotin tagged ghrelin 1-28 used as substrate. Purification of the reaction mixture using streptavidin beads allows incorporation of labeled octanoate to be quantified by liquid scintillation counting. While this method is robust, and the use of radiometric detection provides a large dynamic range, the need to purify product away from ³H-octanoyl CoA reduces sample throughput.

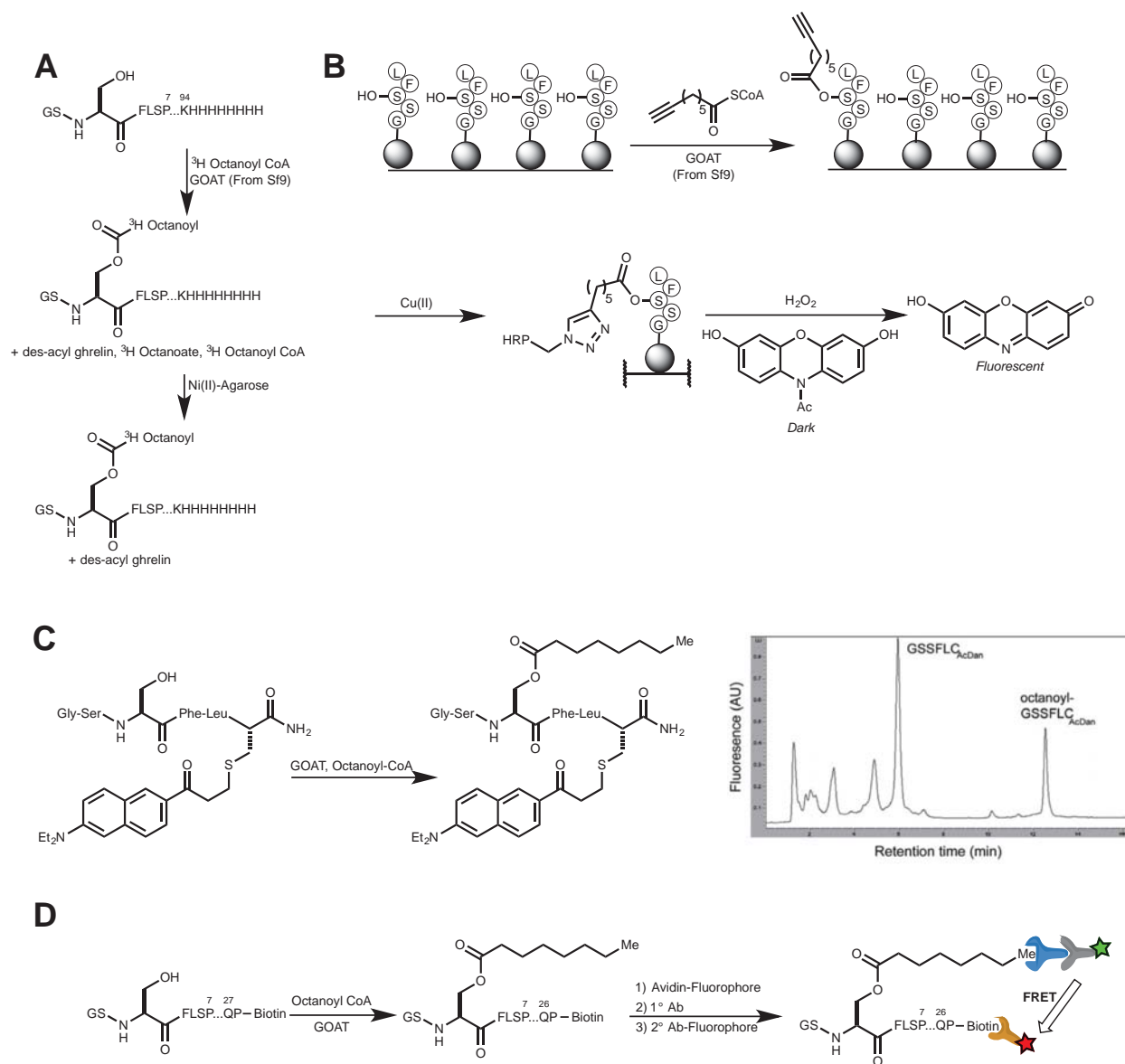


Figure 2.1: Reported GOAT Activity assays. (A) A radiochemical assay format reported by Yang et al. quantifies the extent of ³H octanoyl transfer to a tagged proghrelin construct.⁸ (B) A “cat-ELCCA” assay reported by Garner and Janda relies on the ability of GOAT to utilize 7-octynoyl-CoA as co-substrate, followed by “click” crosslinking to a HRP enzyme and fluorescence readout.¹⁰ (C) The HPLC-fluorescence based method reported utilizes a fluorescence tagged ghrelin peptide. Separation of acyl and des-acyl peptide is achieved by reverse phase HPLC. Image adapted from Zhao et al. *Bioorg Med Chem Lett*. 2015. 2800. (D) Takeda has reported the use of a FRET based assay format.

Several alternative assay formats have been reported in the literature that do not rely on radiochemical detection. The first of these was a modified ELISA format GOAT

assay (Figure 2.1B), was reported by Garner and Janda.¹⁰ In vivo, GOAT catalyzes the octanoylation of 94aa proghrelin, but will readily acylate ghrelin 1-28 or shorter ghrelin 1-5 peptides.⁸ A biotin tagged ghrelin pentapeptide was immobilized on streptavidin coated 96-well plates. Addition of Sf9 derived GOAT membranes, palmitoyl CoA, and 7-octynoyl CoA leads to transfer of octynoate to the immobilized ghrelin peptide. Following washing to remove excess reagents, the terminal alkyne is cross-linked to a horseradish peroxidase (HRP) alkyl-azide conjugate via a Cu promoted azide/alkyne cycloaddition. Incubation of the enzyme linked ghrelin peptides with hydrogen peroxide and amplex red, leads to the formation of fluorescent resorufin. The fluorescence is proportional to the amount of acyl-ghrelin produced during the reaction, and can be quantified using a standard fluorescence plate reader.

Another fluorescence-based system utilizing a different synthetic N-terminal ghrelin fragment was reported by Darling et al. in 2013.¹¹ They report the synthesis of a GSSFLC peptide, which is then covalently linked via the cysteine residue to an acrylodan fluorophore to generate a fluorescent GOAT substrate (figure 2.1C). Incubation of this conjugate with Sf9 derived GOAT membranes, octanoyl CoA, and palmitoyl CoA generates a fluorescently labeled acyl-ghrelin product. The reaction mixture is then analyzed by HPLC with in-line fluorescence detection. Peaks corresponding to the octanoyl and des-acyl forms of the peptide are readily separable, and integration of the fluorescence signal from each species allows determination of their relative abundance.

Takeda Pharmaceuticals has reported the development of a series of heterocyclic GOAT inhibitors. Their patent describes a FRET based assay format based

on the HTRF platform developed by CisBio (figure 2.1D).¹² A biotinylated ghrelin 1-27 peptide serves as enzyme substrate, and Sf9 GOAT membranes are used as the enzyme activity source. Addition of octanoyl CoA initiates the reaction. Following quenching of the reaction mixture, an acyl-ghrelin specific antibody is added. Double labeling by a FRET matched fluorophore-linked secondary antibody and a fluorophore-streptavidin completes the reaction. Quantitation of the FRET signal using a plate reader allows the extent of ghrelin acylation to be determined. The efficacy of this system depends heavily on the quality of the antibodies used, which appear to be proprietary. Anti-ghrelin antibodies such as those used in the ELISA ghrelin detection kits are commercially available, but to our knowledge this assay has not been evaluated outside of Takeda.

2.3 Implementation of a GOAT Activity Assay

In initial efforts to develop GOAT inhibitors (see chapters three and four), we collaborated closely with the Brown and Goldstein laboratory at UTSW. Dr. Tongjin Zhao in their group graciously screened many small molecule analogs using the radioassay system described above.⁸ It subsequently became necessary to establish an assay system in house, and we chose to re-establish this same. Switching to a new assay system would unnecessarily interrupt our SAR progression, and would necessitate reevaluation of old inhibitors to establish consistency across formats. Additionally, because the native substrates are most closely mimicked, this system was considered to be most representative of in vivo GOAT inhibition. As described above, the reaction system utilizes four components: GOAT containing membranes from Sf9

cells, poly-histidine tagged proghrelin, palmitoyl CoA, and ³H-octanoyl CoA. Both CoA derivatives are commercially available, but production of GOAT containing membranes and proghrelin required the development of suitable expression systems. Dr. Zhao was generous with his time and advice in aiding our efforts to establish this assay.

2.4 Expression of Mouse GOAT in Sf9 Insect Cells

Ghrelin-O-Acyl Transferase is a polytopic membrane protein that belongs to Membrane Bound O Acyl Transferases (MBOAT) superfamily of enzymes.^{13, 14} Murine GOAT is 435 amino acids in length, and current models of its membrane architecture predict 11 transmembrane helices as well as a single reentrant loop.¹⁵ Overexpression and purification of globular proteins is routinely performed, but heterologous expression of membrane associated proteins, especially those containing large numbers of transmembrane helices such as GOAT, can be more challenging.⁶ Several MBOATS, including GOAT, have been successfully generated in Sf9 cells using the Bac-to-Bac baculoviral expression system developed by Monsanto and marketed by Life technologies.^{16, 17, 18} We adopted this method for its high protein expression level, robustness, and low maintenance cost. This insect cell culture system is suitable for production of mammalian proteins on relatively large scale for various studies including drug screening and structural biology.⁷

As shown by the workflow shown in figure 2.2A, the gene of interest is cloned into a small bacterial vector, pFastBac, downstream of the viral polyhedrin promoter.¹⁹ The expression cassette, which includes the gene of interest and a gentamicin resistance gene, is flanked by Tn7 transposon sequences. The resultant plasmid is

transformed into a specialized *E. coli* strain containing a large baculovirus encoding plasmid (bacmid). The expression cassette is transferred into the bacmid via transposition, which occurs between Tn7 sites on pFastBac and attTn7 sites on the bacmid. Bacmid DNA is isolated from *E. coli* cells using standard plasmid purification methods, and then transfected into host Sf9 insect cells. The host line is then able to express the gene of interest and to generate additional virus, thereby amplifying expression of the target gene throughout the cell culture. Viral titer is increased through several rounds of infection until maximal expression of the gene of interest is achieved.

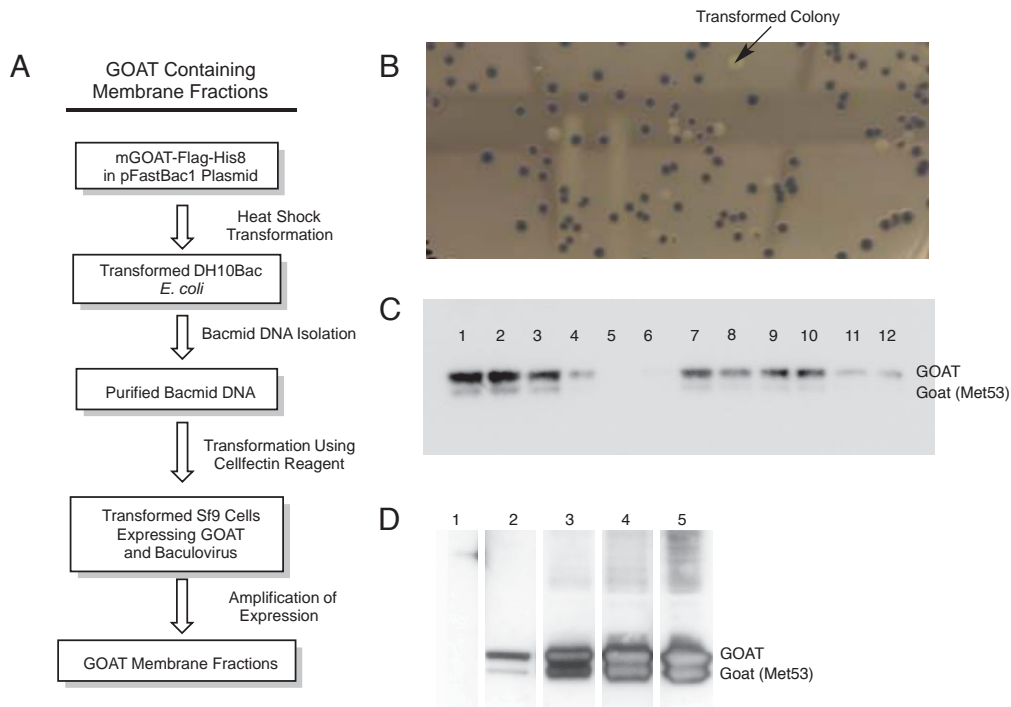


Figure 2.2: Production of GOAT containing membranes in sf9 cells. (A) Workflow outlining steps required for the generation of GOAT containing membranes from Sf9. (B) Transformed and Untransformed DH10Bac *E. coli* were identified on the basis of gentamycin resistance and blue/white selection. (C) GOAT production, as determined by western blot, in second generation (P2) Sf9 cells varied depending on which bacmid isolate was used for transfection. 15ug of total protein were run on SDS page and transferred to a PVDF membrane, then blotted with anti-Flag M2 antibody. Each lane represents Sf9 cells transfected with an individual bacmid isolate. The lower band reflects the presence of an alternate start codon at Met53 mGOAT. (D) Increasing GOAT expression in Sf9 cells through viral amplification. lane 1: uninfected Sf9 cells, lane 2: P2 whole cell lysate, lane 3: P3

whole cell lysate, lane 4: p4 whole cell lysate, lane 5: p4 cell membrane fractions. No GOAT production was detectable in P1 cells.

Murine GOAT containing bacmids were generated by transforming of a poly-His, FLAG tagged mGOAT construct into competent DH10Bac *E. coli*. Transformed colonies were identified on the basis of antibiotic resistance as well as blue/white selection (figure 2.2B). Bacmid DNA from several transformed colonies was isolated and purified using standard protocols.¹⁹ This DNA was then transformed into Sf9 insect cells using the Cellfectin II reagent. Following transfection, adherent cells were incubated for a period of 4 days at 27 °C and the media (containing 1st generation (P1) virus) was collected. Cells were also collected for subsequent GOAT expression analysis. P1 virus containing media was used to infect a second set of adherent insect cells, which were cultured for a further three days. P2 virus containing media and the P2 cells were then collected. To this point we had maintained parallel cultures infected with bacmid DNA originating from one of twelve selected colonies. Using western blot (anti-FLAG) analysis of these cells, we observed a range of mGOAT expression in Sf9 cells infected with virus of differing lineage (Figure 2.2C). We selected a single viral isolate giving the best expression of MGOAT, and further amplified expression through a P3 generation (figure 2.2D). Membranes were isolated from a 1L culture of Sf9 cells infected with P3 virus by ultracentrifugation.⁸

2.5 His-Tagged Proghrelin

The primary endogenous substrate of GOAT is proghrelin, a 94-amino acid form of the hormone.⁴ This length precludes solution or solid-phase peptide synthesis of the

hormone, though a native chemical ligation route to this material is likely possible.^{20, 21} Instead we have relied on traditional bacterial protein expression, and adapted the recombinant pro-ghrelin preparation developed Yang et al.⁸

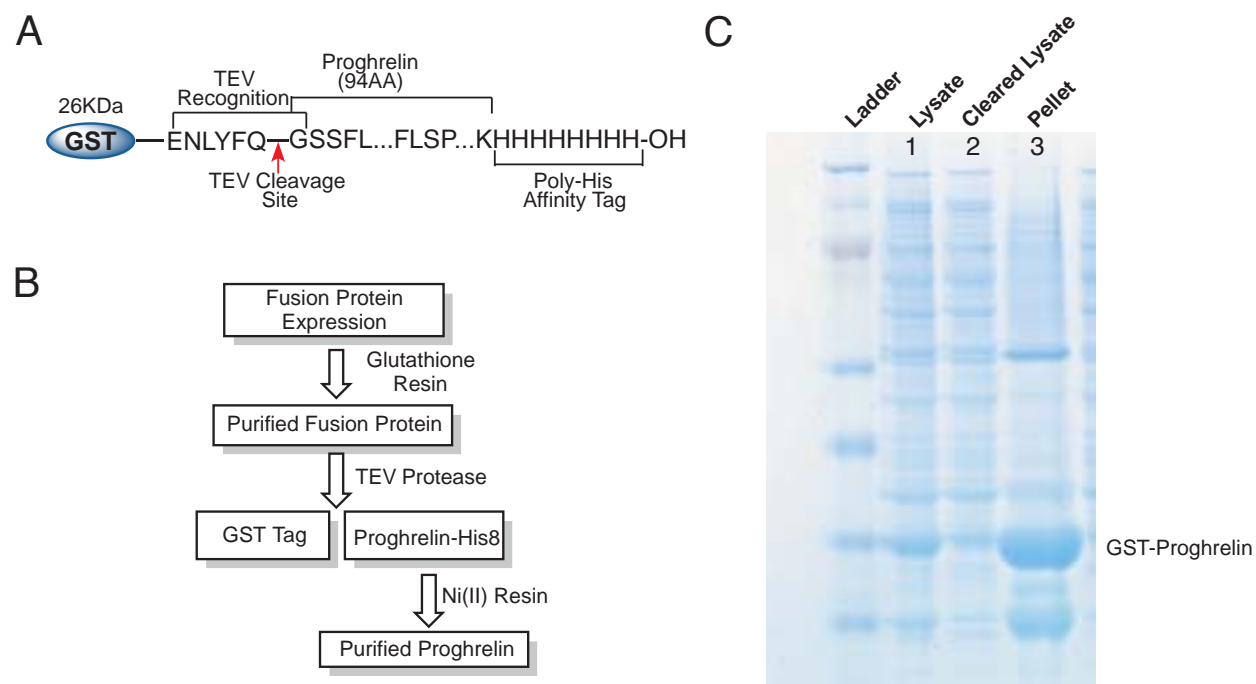


Figure 2.3: Proghrelin expression in *E. coli*. (A) Tagged GST-proghrelin fusion protein to be expressed in *E. coli*. (B) Workflow outlining steps required for the production of purified proghrelin for use in *in vitro* enzyme activity assay. (C) The GST-proghrelin fusion protein is poorly soluble and precipitates upon expression in bacterial host, as demonstrated by SDS PAGE. Following IPTG induction of expression, cells were harvested by centrifugation, suspended in Tris buffer and lysed by sonication. Soluble and insoluble fractions were separated by centrifugation at 10,000g. The insoluble portion was resuspended in 8M urea. Total protein (lane 1), Soluble fraction (lane 2), and insoluble fraction (lane 3) were run on SDS-PAGE and stained with Coomassie blue to visualize protein. A band corresponding to molecule weight of GST-proghrelin fusion protein is labeled as such.

Figure 2.3A depicts the proghrelin fusion protein used for proghrelin production. GOAT requires a N-terminal glycine residue for substrate recognition.⁸ Even conservative substitution of alanine at this position blocks enzyme activity. Translation in prokaryotes most commonly originates at a fMet start codon. Consequently, to

produce proghrelin in *E. coli*, an N-terminal fusion protein must be appended to the transcript and then removed post-translationally to reveal the native N-terminal Gly1 residue. The tobacco etch virus (TEV) protease is suitable for this purpose, as it recognizes a ENLYFQG sequence and cleaves between the Gln and Gly residues.¹⁴ The use of a TEV cleavage site enables the preparation of a proghrelin construct having the requisite N-terminal glycine using the double purification scheme depicted in Figure 2.3B. A C-terminal polyhistidine tag allows cleaved proghrelin to be separated from the liberated GST fragment and from residual protease. Glutathione S- Transferase (GST) was chosen as the N-terminal fusion partner to aid in expression and purification of the fusion protein.²² GST binds to immobilized glutathione, and acts as a primary affinity tag, with the His tag being used to repurify the protein following cleavage of the GST and also in the course of the GOAT activity assay.

Initial expression attempts were performed at 37°C in standard LB broth using BL21 *E. coli*. SDS-PAGE and Coomassie staining of soluble and insoluble fractions prepared from induced bacterial culture revealed that the GST-proghrelin fusion protein was insoluble and accumulated as inclusion bodies (Figure 2.3B). It has been shown in many instances that performing protein expression at a lower temperature can increase the fraction of soluble protein.²² While the amounts of protein in each fraction were difficult to directly quantify, in the case of GST-proghrelin, decreasing the temperature from 37 °C to 18 °C during induction increased the yield of purified protein approximately 10-fold.

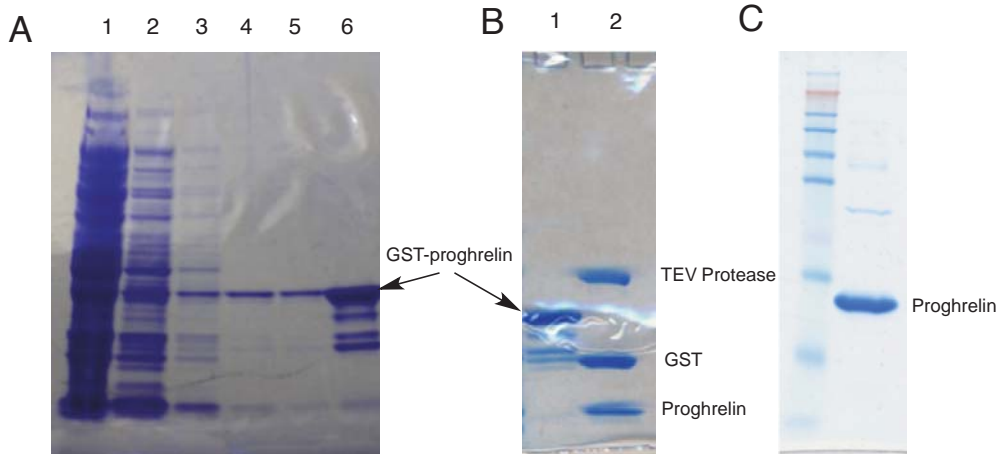


Figure 2.3: Proghrelin purification in *E. coli*. (A) GST affinity purification of proghrelin fusion protein. The soluble portion of cell lysate from proghrelin producing cells (lane 1) was incubated with glutathione agarose, then washed to remove excess protein (lanes 2-5). Fusion protein was liberated by incubation of the beads with reduced glutathione in buffer (lane 6) (B) Following release from the GST beads (lane 1), proghrelin was incubated with in house produced GST-TEV protease to provide cleaved GST and free proghrelin (lane 2) alongside the enzyme. (C) Ni(II) affinity chromatography of the cleaved proteins yielded proghrelin with >90% purity. Left lane is a molecular weight marker confirming the expected ~12 kDa mass of proghrelin-His8. Each described fraction was run on SDS-PAGE and stained with Coomassie blue to visualize protein.

Following induction, cells were lysed by sonication in a buffered solution containing a cocktail of protease inhibitors, and the insoluble fraction was removed by centrifugation. The supernatant was incubated with glutathione linked agarose beads for several hours to capture the GST protein. The beads were washed several times, and GST fusion was liberated by addition of free glutathione (Figure 2.4A). Commercially available TEV proteases are His-tagged, so in order to facilitate downstream purification of proghrelin, we generated a GST fused TEV protease (not shown). Incubation of the GST-fusion protein with TEV protease cleaves GST from proghrelin (Figure 2.4B), and proghrelin-His8 can then be purified by Ni(II) chromatography. The purified protein was then concentrated and stored in buffer prior to usage in the GOAT activity assay. The final material generated by this method was >90% pure as judged by SDS PAGE (figure

2.4C). We have routinely purified milligram quantities of proghrelin from six liters of bacterial culture, which is sufficient for several hundred in vitro enzymatic assays.

2.6 GOAT Activity Assay

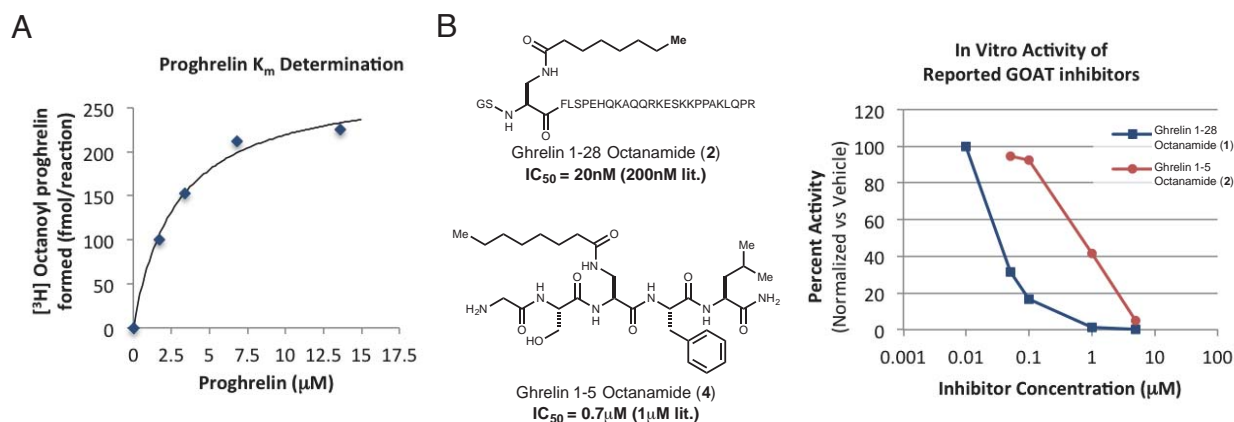


Figure 2.3: GOAT enzyme activity assay. (A) K_m determination for proghrelin. To a solution containing the indicated concentration of proghrelin, 100 μM palmitoyl CoA, and 50 μg of GOAT containing membranes on ice was added ^3H octanoyl-CoA (6.5dpm/fmol, 1 μM final concentration) to a total volume of 50 μL . The vessel was then transferred to a prepared 37 $^\circ\text{C}$ heating block and maintained at this temperature for 10m. The reactions were then quenched by addition of 10 μl of 1N HCl following by addition of 0.75 ml of 50 mM NaPi buffer containing 0.1% Triton X-100, 150 mM NaCl, 10 mM imidazole and 200 μl of 50% Ni-NTA slurry (pH 7.3). The pro-ghrelin-His8 was bound to Ni(II) resin by incubation for 1 hour in a cold room. The resin was washed 3 times with 50 mM NaPi buffer containing 150 mM NaCl and 10 mM imidazole (pH 7.3). Bound pro-ghrelin was eluted with 250 mM imidazole in the same buffer. Reactions were performed in duplicate. (B) Structures of reported peptidal GOAT inhibitors alongside their measured and reported in vitro efficacy. Assays were performed as described above using the indicated concentration of inhibitor, 5 μg proghrelin, 100 μM palmitoyl CoA, 50 μg of GOAT containing membranes, and 1 μM ^3H octanoyl-CoA (6.5dpm/fmol).

With the key reaction components in hand, we were able to establish an in vitro assay for GOAT inhibition. We again closely followed the procedure outlined by Brown and Goldstein. To a solution containing proghrelin, palmitoyl CoA, and GOAT containing membranes on ice was added ^3H octanoyl-CoA. The solutions were incubated 37 $^\circ\text{C}$ for 10 minutes, then quenched by addition of HCl. Proghrelin was recovered by incubation

of the reaction mixture with Ni-NTA beads at 4°C. The resin was washed and bound proghrelin was eluted with 250 mM imidazole in phosphate buffer. The eluate was subjected to liquid scintillation counting to quantify the extent of octanoyl transfer.

Under the described conditions, we have routinely observed formation of up to 300 fmol of acyl ghrelin, similar to the results obtained by Yang et al.⁸ To further confirm that our system conformed to expectations, we measured a K_m value for proghrelin (Figure 2.4A) as well as octanoyl CoA. Our measured constants (3 μ M for proghrelin and 0.6 μ M for octanoyl CoA) compared favorably to previously reported values (6 μ M and 0.6 μ M).⁸ Satisfied that our system behaved similarly to the reported protocol, we measured inhibition curves for prototype peptidal GOAT inhibitors **1** and **2**.⁸ IC_{50} values for these two compounds again matched those reported in the literature (Figure 2.4B). With reliable methods for the production of critical assay components established and the assay itself giving results consistent with literature values, we were prepared to push towards the development of a novel class of small molecule GOAT inhibitor.

-
- 1 Copeland, RA. Evaluation of enzyme inhibitors in drug discovery: A guide for Medicinal Chemists and Pharmacologists. (John Wiley and Sons, Hoboken, New Jersey).
 - 2 Janzen, WP, ed. *High throughput screening methods and protocols*. (Humana Press, Totowa, New Jersey).
 - 3 Taylor MS, Hwang Y, Hsiao PY, Boeke JD, Cole PA. (2012) Ghrelin O-acyltransferase assays and inhibition. *Methods Enzymol.* 514:205-28.
 - 4 Müller TD, et al. (2015) Ghrelin. *Molecular Metabolism* 4(6):437-460.
 - 5 Eisenthal R, Danson MJ, *Enzyme Assays: a practical approach* (Oxford Press, New York, New York).
 - 6 Production of Membrane Proteins: Strategies for Expression and Isolation.
 - 7 Schneider EH, Seifert R (2010) Sf9 cells: a versatile model system to investigate the pharmacological properties of G protein-coupled receptors. *Pharmacol Ther.* 128(3):387-418.

-
- 8 Yang J, Zhao TJ, Goldstein JL, Brown MS (2008) Inhibition of ghrelin O-acyltransferase (GOAT) by octanoylated pentapeptides. *Proc. Natl. Acad. Sci. USA* 105(31):10750-10755.
 - 9 Barnett BP, et al. (2010) Glucose and weight control in mice with a designed ghrelin O-acyltransferase inhibitor. *Science* 330(6011):1689-1692.
 - 10 Garner AL, Janda KD (2010) Cat-ELCCA: a robust method to monitor the fatty acid acyltransferase activity of ghrelin O-acyltransferase (GOAT). *Angew. Chem. Int. Engl. Ed.* 49(50):9630-4.
 - 11 Darling JE, Prybolsky EP, Sieburg M, Hougland JL (2013) A fluorescent peptide substrate facilitates investigation of ghrelin recognition and acylation by ghrelin O-acyltransferase. *Anal Biochem.* 437(1):68-76.
 - 12 Takakura N et al. (2013) Aromatic ring compound. *US Patent* 9238639 B2.
 - 13 Gutierrez JA, et al. (2008) Ghrelin octanoylation mediated by an orphan lipid transferase. *Proc. Nat. Acad. Sci. USA* 105(17):6320-6325.
 - 14 Yang J, Brown MS, Liang G, Grishin NV, Goldstein JL (2008) Identification of the Acyltransferase that Octanoylates Ghrelin, an Appetite-Stimulating Peptide Hormone. *Cell* 132(3):387-396.
 - 15 Taylor MS, et al. (2013). Architectural Organization of the Metabolic Regulatory Enzyme Ghrelin-O-Acyltransferase. *J. Biol. Chem.* 288(45):32211.
 - 16 Cao J, et al. (2011) Targeting Acyl-CoA:diacylglycerol acyltransferase 1 (DGAT1) with small molecule inhibitors for the treatment of metabolic diseases. *286(48):41838-51.*
 - 17 Cheng D, Chang CC, Qu X, Chang TY. (1995) Activation of acyl-coenzyme A:cholesterol acyltransferase by cholesterol or by oxysterol in a cell-free system. *J Biol Chem.* 270(2):685-95.
 - 18 Masumoto N, Lanyon-Hogg T, Rodgers UR, Konitsiotis AD, Magee AI, Tate EW (2015) Membrane bound O-acyltransferases and their inhibitors. *Biochem Soc Trans.* 43(2):246-52.
 - 19 Life Technologies. (2015) Bac-to-Bac® Baculovirus Expression System.
 - 20 Dawson PE, Kent SB (2000) Synthesis of native proteins by chemical ligation. *Annu Rev Biochem.* 69:923-60.
 - 21 Thapa P, Zhang RY, Menon V, Bingham JP. (2014) Native chemical ligation: a boon to peptide chemistry. *Molecules.* 19(9):14461-83.
 - 22 Walls D, Loughran ST, ed. *Protein Chromatography: Methods and Protocols* (Springer, New York, USA) pp 259.

3 Hypothesis Driven Design and Synthesis of In Vivo inhibitors of Ghrelin O-Acyl Transferase

3.1 Approach

Our strategy for developing a small molecule GOAT inhibitor was to transform the known pentapeptide recognition sequence into a peptidomimetic – a small molecule which retained the binding properties of the parent peptide, but which had improved membrane permeability and metabolic stability.^{1,2} We would need to identify and enhance the critical recognition elements while trimming away superfluous polar functionality. This is a classic strategy in medicinal chemistry, which has been applied to the development of several marketed drugs. Aliskiren, which is a marketed renin inhibitor, barely resembles the angiotensinogen sequence from which it is derived.³ Small molecule growth hormone secretagogues (GHSs) (ie ligands of the growth hormone secretagogue receptor (GHS-r)) such as Ibutamoren (**1**) are derived from peptidal GHS hexarelin.⁴ Both Aliskiren and Ibutamoren were derived from the parent peptides by a rational development process. The daughter small molecules had significantly improved potency and, more importantly, dramatically improved pharmacokinetic characteristics. For the development of GOAT inhibitors we sought to emulate strategy of these classic cases.

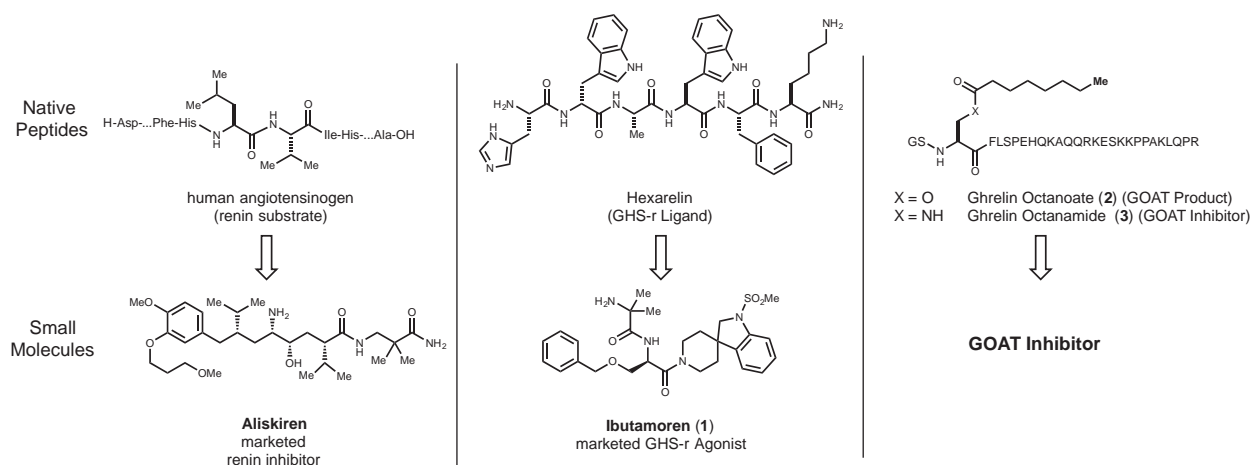


Figure 3.1: Peptidomimetic small molecule drugs. Aliskiren and Ibutamoren (1) are small molecule marketed drugs derived from peptide sequences. We sought to convert ghrelin 2, the substrate of GOAT, or its amide congener 3 to a small molecule inhibitor of the enzyme.

As a primary screen for GOAT inhibition we would make use of the radiochemical assay described in chapter 2. Results from this assay would drive hypothesis generation and inhibitor design. While we were most concerned with inhibitor potency, we were also conscious of the necessity to improve inhibitor pharmacokinetic properties – as exemplified by the development of Aliskiren and Ibutamoren. Because GOAT is located in the endoplasmic reticulum,⁵ we would need a compound with good membrane permeability. We took advantage of the well-documented correlation of membrane permeability with readily measured or computed characteristics of the molecules themselves, such as LogD, polar surface area, number of hydrogen bond donors, and molecular weight.^{6, 7} For the early phases of inhibitor development, we attempted to design compounds that would best match the profile of a typical small molecule drug while maintaining or improving activity against GOAT.

3.2 Design of GHS-r Ligand/Ghrelin Hybrids

As discussed in chapter 1, Yang et al. had demonstrated that GOAT was inhibited by octanoyl ghrelin **2** and its amidated derivative **3**.⁸ They also showed that ghrelin 1-5 pentapeptide **4** (Figure 3.2A), but not a tetrameric ghrelin 1-4 congener, was capable of inhibiting GOAT, albeit with reduced potency relative to full-length derivative **3**. Additionally, GOAT acylation of ghrelin mutants having alanine at residues 1, 3, 4 or 5 was impeded relative to the wild type sequence (Figure 3.2B).

Ghrelin is the endogenous ligand of GHS-r ligand.⁹ The minimal portion of ghrelin required for full activation of GHS-r has been identified (Figure 3.2C).¹⁰ Octanoylated peptides ghrelin 1-5, ghrelin 1-4, and full-length ghrelin all had similar EC₅₀, but an octanoyl ghrelin 1-3 peptide was unable to bind the receptor. Both GOAT and GHS-r principally recognize the N-terminal five amino acids of ghrelin, and a recent study suggested that ghrelin and ibutamoren (**1**) occupy overlapping binding sites on GHSr.¹¹ Taken together; these results suggested that small molecules able to bind GHS-r might also bind GOAT. We prepared a sample of **1** and found that it did not inhibit GOAT. However, hybrid compound **5**, wherein the C-terminal dipeptide of **4** is replaced with the C-terminal spiroindoline from **1**, was an inhibitor of GOAT, albeit with reduced potency relative to the parent pentapeptide. Although this substitution decreased inhibitor potency, it also decreased polar surface area and the number of hydrogen bond donors. Since this fragment had been highly optimized for a different system, we thought it likely that recovery of the lost potency would be possible by optimizing this fragment for GOAT inhibition.

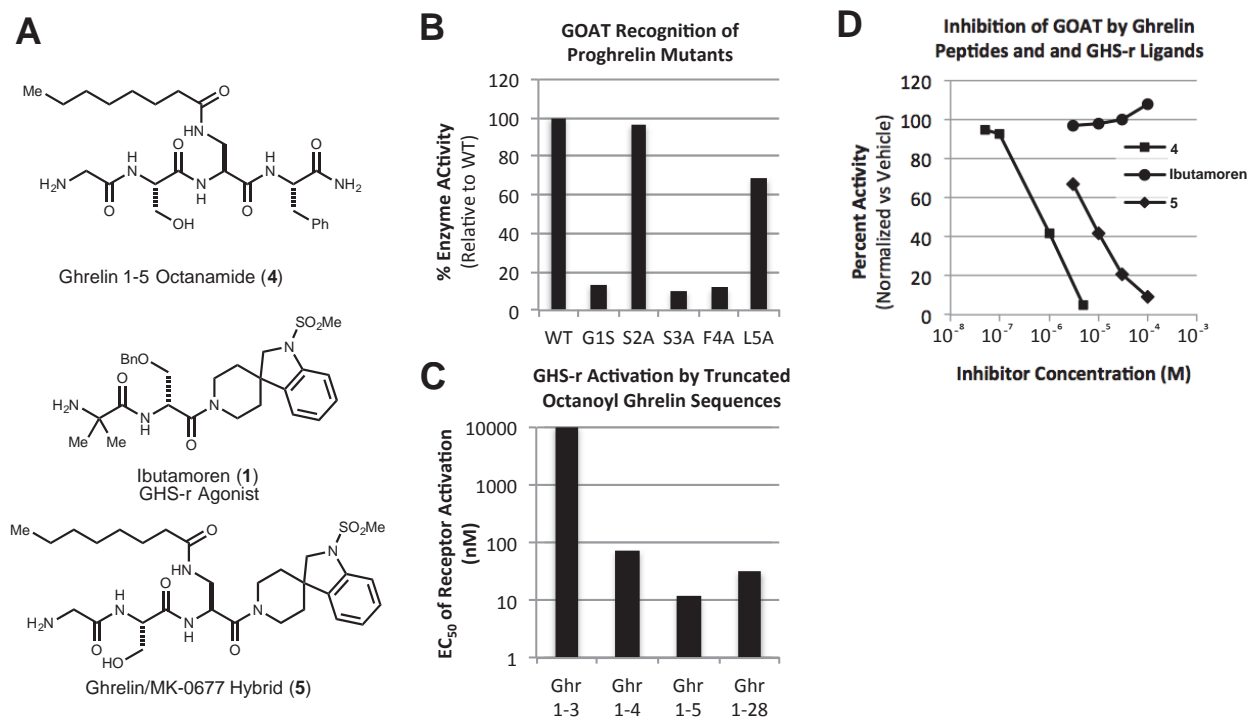
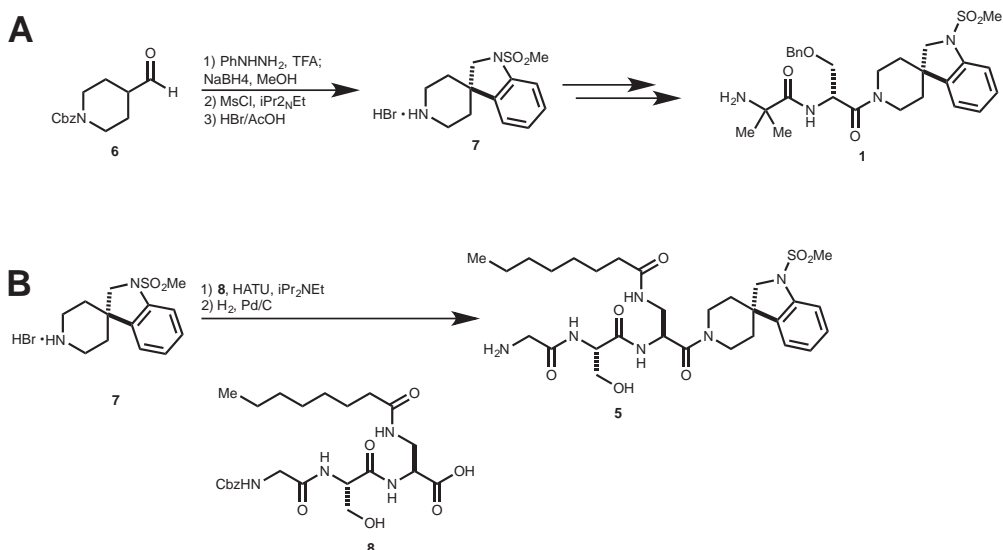


Fig 3.2: Development of a ghrelin/Ghs-r agonist hybrid GOAT inhibitor. (A) Both GOAT and the ghrelin receptor [growth hormone secretagogue receptor (GHS-r)] minimally bind the N-terminal 5 amino acids of ghrelin. GHS-r agonists such as **1** mimic the N-terminus of ghrelin. A GOAT inhibitor incorporating the portion of ibutamoren corresponding to the c-terminal dipeptide is expected to have improved pharmacology. (B) GOAT catalyzed octanoylation of proghrelin mutants. Enzyme activity was measured using the radiometric assay described in chapter 2, and the data are expressed as a percentage of the transfer observed for WT proghrelin. Adapted from Yang et al. Proc. Natl. Acad. Sci. USA 105. 10750. (C) Recognition of truncated ghrelin sequences by the GHS-r. Data reflect activation of GHS-r by the indicated peptides at 10mM as a percentage of the receptor relative to the signal achieved using full length ghrelin (**2**). Adapted from Bednarek et al. J Med. Chem. 43. 4370. (D) Inhibition titrations of ghrelin pentapeptide **4**, ibutamoren (**1**) and a hybrid of the two (**5**). Assays were conducted as described in chapter 2.

3.3 Syntheses of GHS/Ghrelin Hybrids



Scheme 3.1: Synthesis of GHS/Ghrelin Hybrid GOAT inhibitors. (A) Preparation of ibutamoren from isonipenaldehyde via spironindoline **7**. (B) Elaboration of **7** to ibutamoren/ghrelin hybrid **5**.

Syntheses of these molecules began with synthesis of the N-terminal heterocycle **7**, was prepared in three steps starting with commercially available isonipenaldehyde acid (**6**) via a Fisher-type indolization followed by sodium borohydride reduction of the resultant imine (Scheme 3.1A).¹² The aniline was derivatized as the methanesulfonamide, and the piperidyl protection was removed by treatment with hydrogen bromide in acetic acid. The amine was then elaborated to **1** according to published methods.

Amide **5** was prepared by reverse coupling of **7** with ghrelin N-terminal tripeptide **8**. Deprotection of this material by hydrogenolysis afforded the targeted hybrid inhibitor. Ghrelin pentapeptide **4** was readily prepared by solid phase peptide synthesis (SPPS) using a Fmoc/Alloc protection strategy.

3.4 Linker Optimization

We next turned our attention to the central octanoylated residue. As previously discussed, substitution of serine 3 for a diaminopropionic acid (DAP) residue (ie **2** vs **3**) resulted in a 35-fold improvement in inhibitor potency.⁸ To determine if this was due to the increased stability of the amide under the reaction conditions or to increased affinity for the enzyme, carbamates **9** and **10**, which differ only in heteroatom position, were prepared (Figure 3.3A). DAP derived *O*-hexyl carbamate **9** had potency similar to that of parent amide **4** [$IC_{50} = 10\mu\text{M}$], while serine derived *N*-hexyl carbamate **10** was nearly inactive at the tested concentrations (Figure 2.3B). Both **9** and **10** are expected to be stable under in vitro GOAT activity assay conditions,¹³ so the observed difference in potency is most likely due to improved binding. An *N*-methylated derivative of **9** (see figure 3.4 below) was also inactive, further supporting this hypothesis. To account for this observation, we envisioned a mechanism of catalysis related to that of a classic serine protease (Figure 3.3C).¹⁴

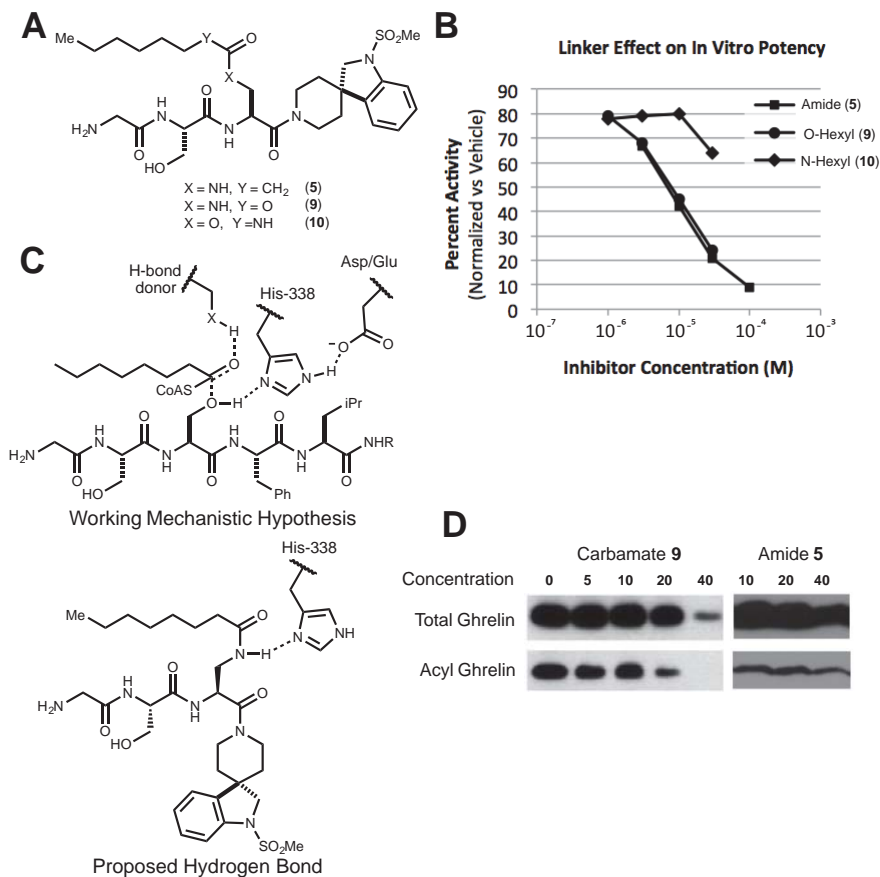
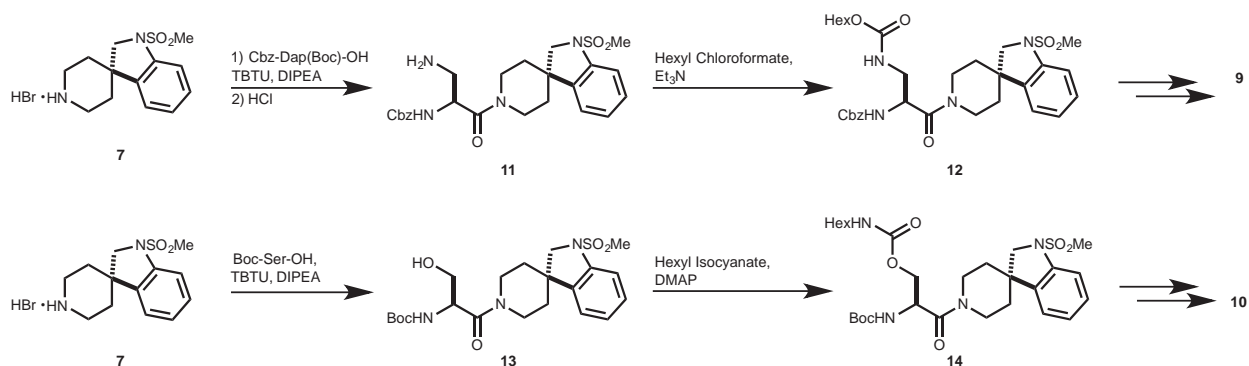


Fig 3.3: Effects of octanoate linker structure and backbone methylation on inhibitor potency. (A) Structures of amide and carbamate linked GOAT inhibitors. (B) Inhibition titrations of **5**, **9**, and **10**. Inhibitors were assayed normally. (C) Conserved His-338 residue is required for GOAT catalysis. Working mechanistic hypothesis of GOAT catalysis. (D) Effect of GOAT inhibitors **11** and **5** in a cellular assay. Carbamate **9** partially blocks acyl ghrelin production at 20mM in INS-1 cells stably expressing GOAT and ghrelin, while amide **5** has no observable effect at the tested concentrations. INS-1 cells stably transfected to express ghrelin and GOAT were incubated with octanoic acid and inhibitor at the indicated concentrations. Ghrelin species were detected by western blot using antibodies specific for acyl or total ghrelin.

His-338, acting as a base in conjunction with some carboxylate residue, could facilitate attack of ghrelin's Ser3 residue on octanoyl CoA. A hydrogen bond donating residue would act to stabilize the developing oxyanion. The product ester would lack a suitable hydrogen bond donor to interact with the histidine and be ejected from the active site, allowing enzyme turnover. Amide **5** and carbamate **11**, but not carbamate

12, would be able to form a hydrogen bond with His-338, thus accounting for the increased potency of **2** relative to **1** and **6** relative to **7**. Unlike our previous compounds, carbamate **11** was also active in a cellular assay format (Figure 4D). At a concentration of 20 μ M carbamate **11** decreased the production of acyl ghrelin in a line of INS-1 cells stably transfected to produce GOAT and ghrelin,¹⁵ while total ghrelin levels remained unchanged. Amide **5** did not affect ghrelin production at any tested concentration.

3.5 Synthesis of Carbamoyl GOAT Inhibitors



Scheme 3.2: Synthesis of GHS/Ghrelin Hybrid GOAT inhibitors 11 and 12.

Carbamoyl GOAT inhibitors **9** and **10** were prepared as shown in scheme 3.2. Spiroindoline **7** was coupled to a protected DAP derivative and the β -amino protection removed by hydrogenolysis, providing primary amine **11**. Treatment of **11** with hexyl chloroformate provided the desired *O*-hexyl carbamate **12**, which was readily elaborated to **9**. Amidation of **7** with Boc-serine afforded primary alcohol **13**. Formation of desired carbamate **14** was achieved by treatment of this material with hexyl isocyanate and

DMAP. The C-terminal dipeptide was then appended to **14** to provide *n*-hexyl carbamate **10**.

3.6 Methyl Scan

Systematic substitution of methyl units along a pharmacophore is a well-established strategy for identifying sites of interaction between a ligand and its receptor,¹⁶ especially in cases where crystallographic or other structural data are unavailable. We prepared analogs of **9** having a single methyl substitution at the positions indicated in figure 3.4A (**15a-k**). We sought to identify positions where substitution might be tolerated or beneficial, which we could then investigate more thoroughly. In particular, if amide *N*-methylation were tolerated, the resultant compound would have less polar surface area and fewer hydrogen bond donors.¹⁷ Figure 3.4B shows the IC₅₀ of the daughter, methylated compounds relative to the reference IC₅₀ of parent inhibitor **9**.

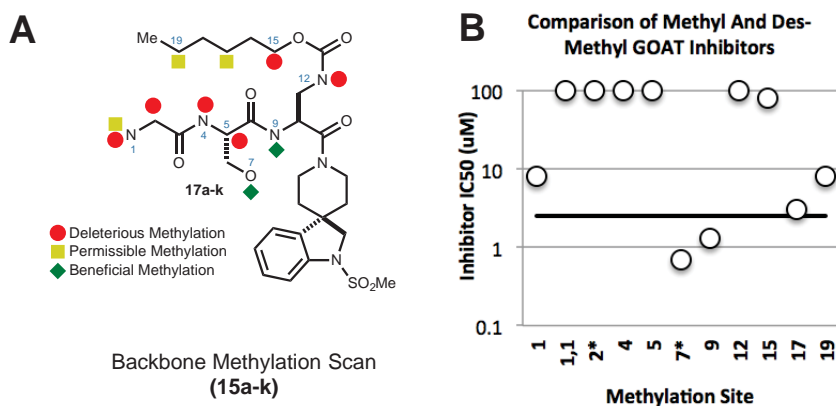
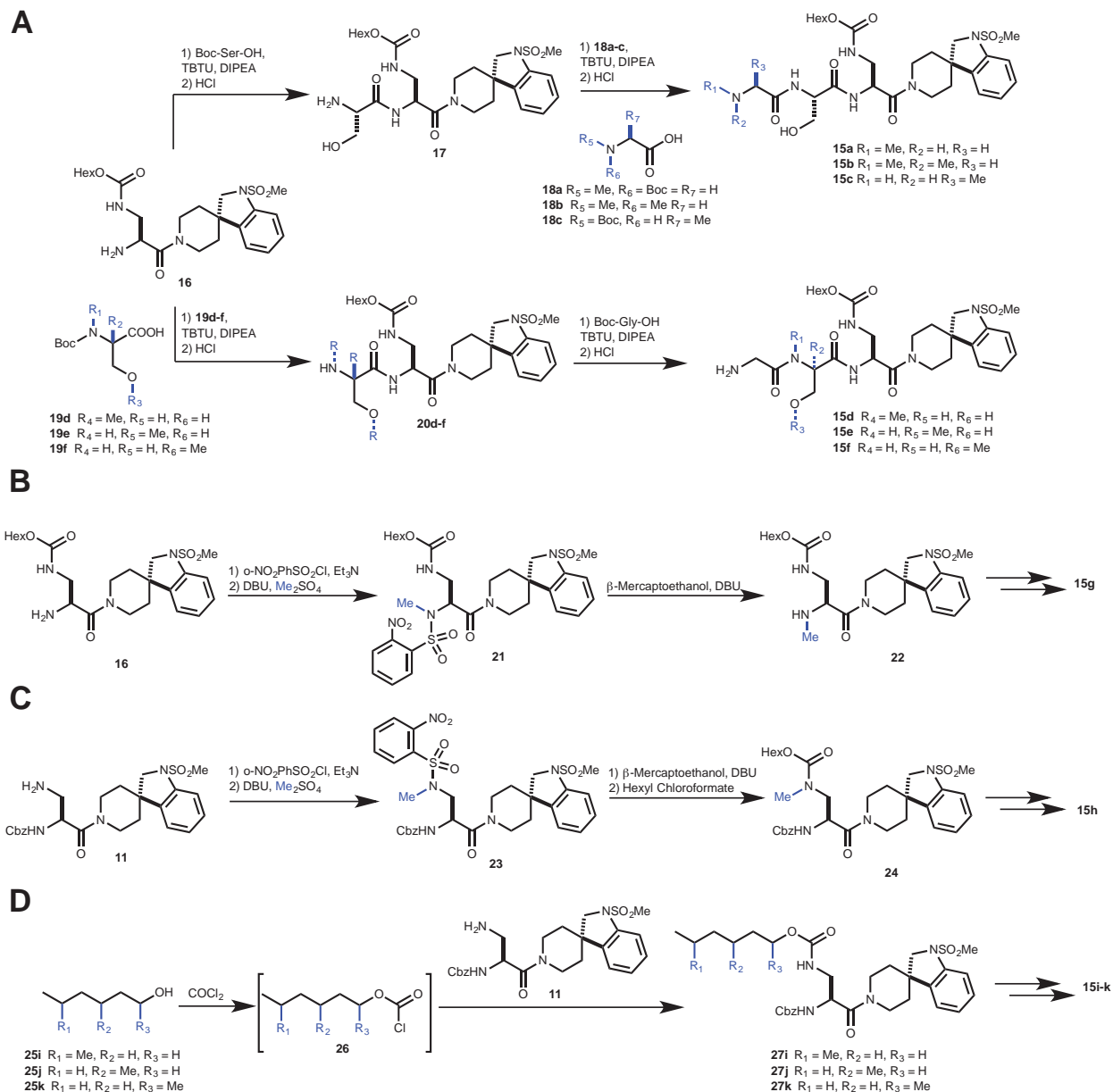


Fig 3.4: Sites of methylation and effect on GOAT inhibitor potency. (A) Sites selected for methylation with coloration indicating whether the methylation had a positive or negative effect on potency. (B) Plot of IC₅₀ of methylated derivatives relative to the reference potency of parent des-methyl inhibitor **9**.

We found that monomethylation, but not dimethylation, of the N-terminal glycine residue was tolerated, as has been reported by others.¹⁸ We were surprised to find that even conservative Gly to Ala substitution led to a completely inactive inhibitor. Backbone methylation of the second residue at either N or C- α was also not tolerated. Consistent with the observations of Darling et al., O-methylation of the serine residue was deleterious. Methylation of the DAP α -amine proved beneficial, while as discussed above, methylation of the DAP β -amide obviated enzyme inhibition. This latter observation further supports the previously described hydrogen bond interaction of this amide bond. Finally, methylation along the O-hexyl tail was unhelpful.

3.7 Synthesis of Methylated GOAT Inhibitors

Methylated inhibitors **15a-k** were prepared according to the methods shown in scheme 3.3. Each inhibitor, other than dimethylglycine derivative **15b** has only a single site of methylation. Coupling of Boc-serine to **16** followed by deprotection afforded amino alcohol **17**, which was amidated using Boc-sarcosine (**18a**) or Boc-alanine (**18c**). Deprotection afforded the target compounds **15a** and **15c** (Scheme 3.3A). Coupling of **16** to dimethylglycine directly provided **15b**. Inhibitors having methylation on the P2 residue (**17d-f**) were synthesized by coupling of intermediate **16** with commercially available serine analogs having the correct methylation state (**19d-f**), followed by deprotection to afford amines of type **20**. Glycine was then appended to provide **15d-f**. DAP α - and β -N-methylated inhibitors were prepared from the corresponding primary amines **16** and **11** using Fukuyama's nitrobenesulfonyl alkylation chemistry via intermediates **21** and **23**.¹⁹ Following removal of the auxiliary, the secondary amines



Scheme 3.3: Synthesis of methyl scan targets. (A) Compounds 17a-f were prepared from DAP derivative 14 using solution phase peptide synthesis methods and appropriately methylated serine and glycine derivatives. (B and C) Methylation of the DAP α and β amines was achieved using Fukuyama's 2-nitrobenzenesulfonyl (Nosyl) alkylation chemistry, these methylated derivatives were readily elaborated to intact inhibitors 17g and 17h. (D) Inhibitors having methylation in the tail region were prepared from commercially available monomethylated hexanol derivatives.

could then be elaborated to target inhibitors **15g** and **15h**. Inhibitors having methylation along the *n*-hexyl tail region (**17i-k**) were derived from the corresponding methyl hexanol derivatives (**25i-k**). Treatment of such alcohols with phosgene afforded chloroformates of type **26**. Addition of primary amine **11** to **26** afforded methylated analogs **27i-k**, which could then be elaborated to the target inhibitors.

3.8 Conformationally Restrained Octanoate Mimics

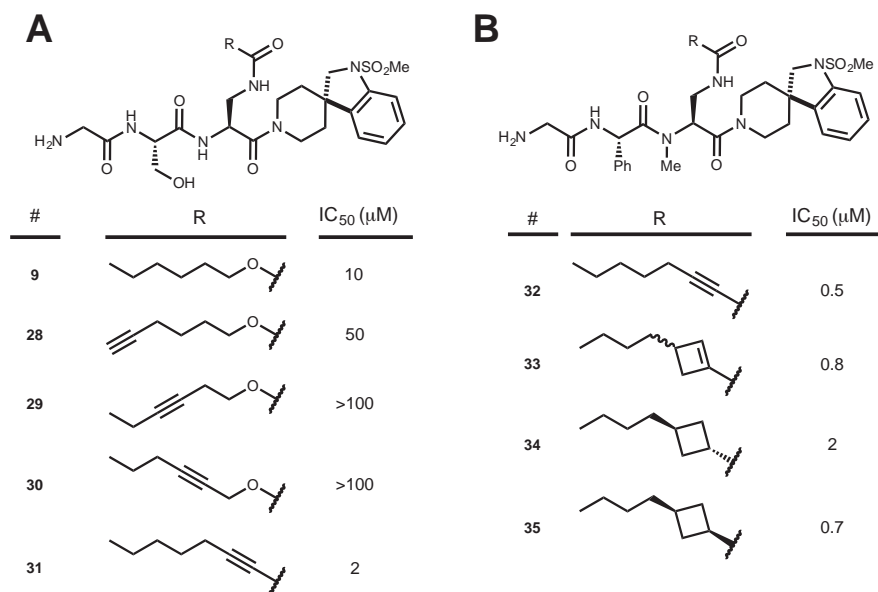


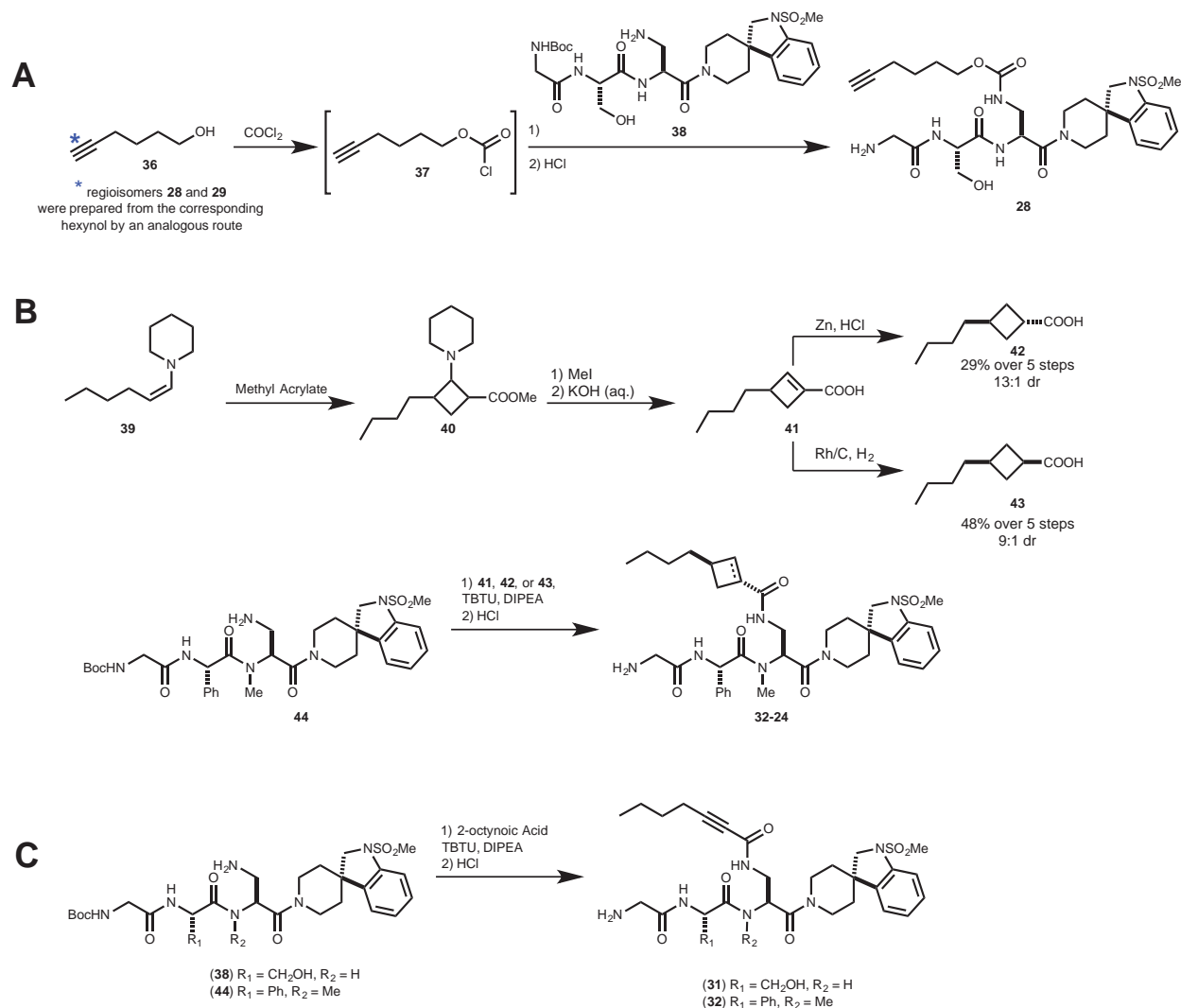
Fig. 3.5: Conformationally restrained octanoate mimics. (A) Structure and potency of GOAT inhibitors **28-31** having an alkyne at various position along the side chain. Saturated carbamate **9** is included in the data set as a reference. (B) 3-Butyl-cyclobutane and cyclobutene carboxylic acid containing analogs of 2-octynoic acid derivatives retain enzyme inhibitory activity. Inhibitors **32-35** are N-methylated and contain a phenylglycine residue at P2 in place of the serine found in **9** and **28-31**.

While the hexyl carbamate side chain of inhibitors such as **9** is anticipated to be flexible, upon binding of the inhibitor to GOAT, the octanoate most likely adopts a defined low energy conformation or suite of conformations.²⁰ The use of a side chain

analog having its conformation restricted to a preferred binding mode would reduce the entropic penalty of binding, and increase inhibitor potency. We prepared a set of inhibitors (**28-31**) containing an alkyne at a variety of positions along the octanoate chain. Of these, hexynol derivatives **28-30** had decreased activity relative to the parent, but conjugated octynyl amide **30** (Figure 3.5A) was more potent than carbamate **9**.

While this result was promising, despite being more potent in vitro, **30** was inactive in a cell based assay (not shown). We noticed during the synthesis of **30** that it was electrophilic, readily forming an adduct with HCl, for example. Cytosol is a reducing medium²¹; in such an environment **30** could react with nucleophiles such as glutathione, which are present at high concentrations. We sought, therefore, to devise an analog of **30** that would adopt a similar conformation, but lack the reactivity. We envisioned that a *cis*- or *trans*-3-butylcyclobutane-carboxylic acid could approximate the geometry of the octynoic acid fragment (Figure 3.5B). Inhibitors **33-35**, which incorporated *cis*- or *trans*-cyclobutanecarboxylic acid as well as a cyclobutene (figure 5A) fragment, each had similar potency as the alkynyl congener (**32**) in a phenylglycine containing series of inhibitors (see below for further discussion of the P2 residue).

3.9 Representative Syntheses of Alkynyl and Cyclobutyl Octanoate Mimics



Scheme 3.4: Synthesis of conformationally restrained octanoate mimics. (A) Alkynyl inhibitors **28-30** were each prepared from hexynols of type **36**. The shown synthesis of **28** is representative of the route used to prepare each of these compounds. (B) Cyclobutenecarboxylic acid **41** was derived from enamine **39** and methyl acrylate. **41** was selectively reduced to either *cis*- (**43**) or *trans*- cyclobutanecarboxylic acid (**42**). Each carboxylic acid was then elaborated to GOAT inhibitors **33-35**. (C) Coupling of 2-octynoic acid to an appropriate peptidic fragment provided targeted GOAT inhibitors **31** and **32**.

Alkynyl GOAT inhibitors **28-30** were prepared using a variation of the strategy used to prepare methylated analogs **17i-k** (Scheme 3.4A). Regioisomeric hexynols of type **36** were treated with phosgene to generate the corresponding chloroformates **37**.

Addition of amine **38** to each chloroformate afforded the desired amides, which were then deprotected using HCl to provide desired GOAT inhibitors **28**, **29** and **30**. *Cis*- and *trans*-butylcyclobutanecarboxylic acids **42** and **43** were prepared using a modification of the methods reported by Brannock and Dehmlow (Scheme 3.4B).^{22, 23} Enamine **39** was condensed by Michael/Mannich cascade with methyl acrylate to provide aminocyclobutane **40** as a mixture of diastereomers. The tertiary amine could be quaternized with methyl iodide, and treatment of the resulting salt with aqueous potassium hydroxide afforded the desired 3-butylcyclobutene carboxylic acid **41**. A stereoselective zinc/HCl reduction was used to prepare the *trans*-cyclobutane **42** with 13:1 dr, while a rhodium catalyzed hydrogenation afforded the *cis*- diastereomer **43** with 9:1 dr. Cyclobutanes **42** and **43**, as well as cyclobutene **41** were then coupled to phenylglycine derivative **44** and treated with HCl to provide the targeted GOAT inhibitors. Coupling of either **38** or **44** with 2-octynoic acid followed by acid promoted Boc cleavage afforded the desired octynamides **31** and **32** (Scheme 3.4C).

3.10 Efforts to Optimize the C-terminal Heterocycle

We had continued throughout this process using the ibutamoren derived spiroindoline (figure 3.2A) as a C-terminal surrogate under the assumption that we would be able to revisit this fragment and optimize it for our system. Despite extensive effort only marginal progress was made in this direction. Attempts to improve binding by altering the substitution and composition of the spiroindolyl portion of the C-terminal heterocycle led, in some cases, to new compounds with activity comparable to the parent, but none were superior.

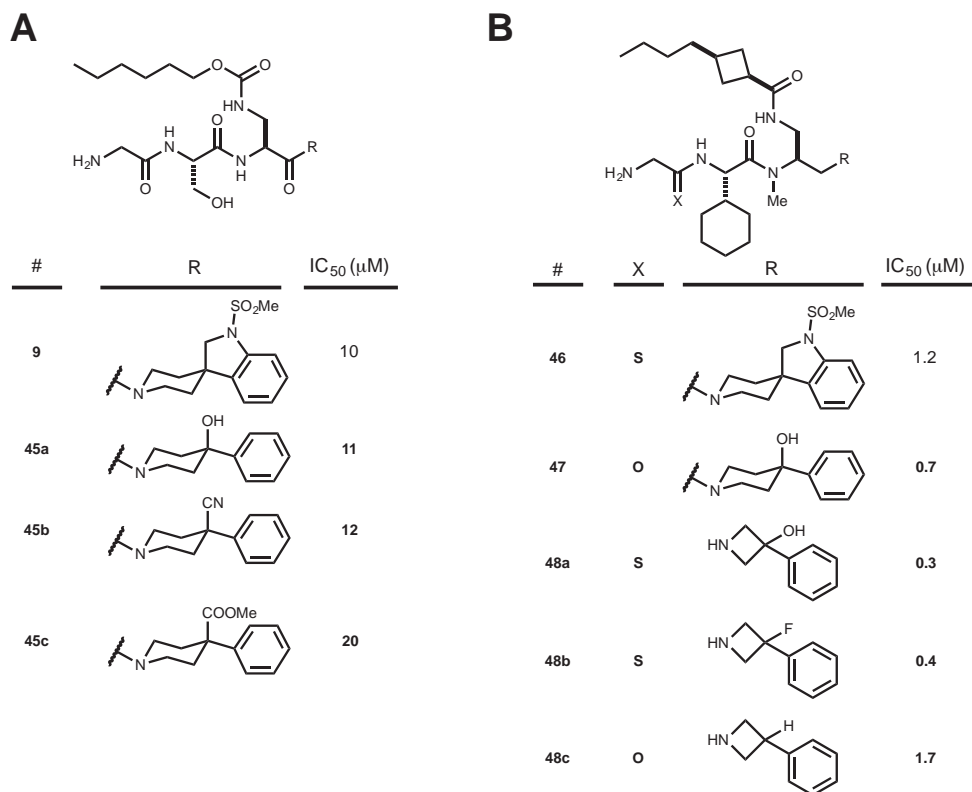
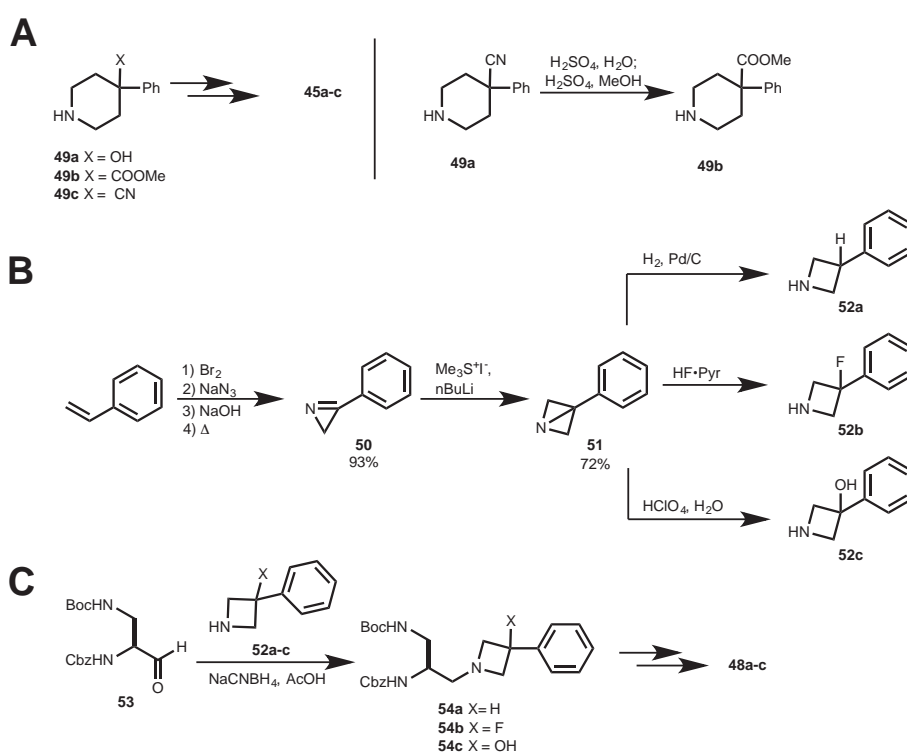


Fig. 3.5: Optimization of C-terminal heterocycle. (A) Inhibitors containing disubstituted piperidines inhibit GOAT with potency similar to **9**, and have reduced molecular weight. (B) Further reduction in molecular weight without loss of potency is achieved by the use of 3-phenyl azetidines.

However, efforts to prepare simplified, lower molecular weight analogs did meet with success. The spiroindoline was expected to adopt the conformation shown for **11** (Figure 3.5A). As a means to simplify the structure, we wondered whether the five membered ring was necessary or if simpler 4,4 disubstituted piperidines could serve as substitutes. A set of three piperidines having a range of functionality opposite the phenyl ring was elaborated to GOAT inhibitors **45a-c**. (Figure 3.6A). All of the compounds prepared inhibited the enzyme with potency near 10 μM. A further reduction in molecular weight was achieved when we found that in a related series of inhibitors, 3-phenyl azetidines (**48a-c**, Figure 3.6B) were also effective C-terminal fragments. As was

observed for the piperidine series of inhibitors, both polar and nonpolar functional groups opposite the aryl ring were tolerated by the enzyme. Thioamidation (ie. **46**, **48a**, **48b**) has little effect on inhibitor potency. For a more detailed discussion of the importance of thionation in GOAT inhibitors, see section 3.14 below.

3.11 Synthesis of Simplified C-Terminal Fragments



Scheme 3.5: Syntheses of simplified C-termini. (A) Compounds **45a-f** were prepared from the corresponding piperidines. Methyl ester **45b** was prepared from the commercially available nitrile **45a** by a hydrolysis/esterification sequence. (B) 3-phenyl azetidines derivatives **52a-52c** were prepared by addition across the central sigma bond of [1.1.0] bicyclic compound **51**. (C) Reductive amination of azirines **52a-c** afforded with commercially available DAP aldehyde **53** afforded tertiary amines **54a-c**, which were readily elaborated to target compounds **48a-c**.

Piperidyl inhibitors **45a-c** were prepared from 4,4 disubstituted piperidines **49a-c**. Methyl ester **49b** was prepared by hydrolysis and esterification of commercially

available nitrile **49a**. Homologation of these amines by a route analogous to that used for the preparation of **9** provided the target inhibitors.

To prepare 3,3-disubstituted azetidines, styrene was converted by the dibromination, azide displacement, elimination, and pyrolysis sequence shown in scheme 3.5B to 2-phenyl-azirine (**50**).²⁴ Strained [1.1.0] bicyclic intermediate **51** was prepared from **50** by methylene transfer using trimethylsulfonium ylide.²⁵ We found **51** to be a versatile intermediate that could be readily transformed to a wide variety of azetidines. Reduced azetidine **52a** was prepared by catalytic hydrogenation of **51**, though this procedure was reported to be unsuccessful in the literature.²⁵ Fluorinated derivative **52b** was prepared in low yield by treatment of **51** with HF-pyridine,²⁶ while hydroxylated analog **52c** was synthesized by perchloric acid promoted hydration.²⁵ These secondary amines were then appended to DAP aldehyde **53** by reductive amination using sodium cyanoborohydride to provide tertiary amines **54a-c**, which were then elaborated to the shown inhibitors.

3.12 C-Terminal Truncation and P2 Residue Optimization

Due to the lack of selectivity we had observed for functionality within the C-terminal fragment, we speculated that its contribution to binding was modest. We wondered if an inhibitor lacking this fragment might retain activity. As demonstrated by the compounds in figure 3.5B, reduction of the amide linking the DAP residue and the heterocyclic fragment was tolerated and, as previously discussed, methylation of the DAP α -amide was beneficial (Figure 3.4). A cyclic structure such as **55**, wherein the reduced C-terminus was connected to the *N*-alkyl substituent would mimic the DAP

stereochemistry and retain conformational control while dramatically reducing molecular weight and polar surface area (Figure 3.6A). We were pleased to find that **55** retained activity, having potency comparable to **48a** (Figure 3.6B). Relative to **48a**, aminomethylpyrrolidine derived inhibitors such as **55** had the additional advantages of reduced molecular weight, polar surface area, and hydrogen bonding capacity.

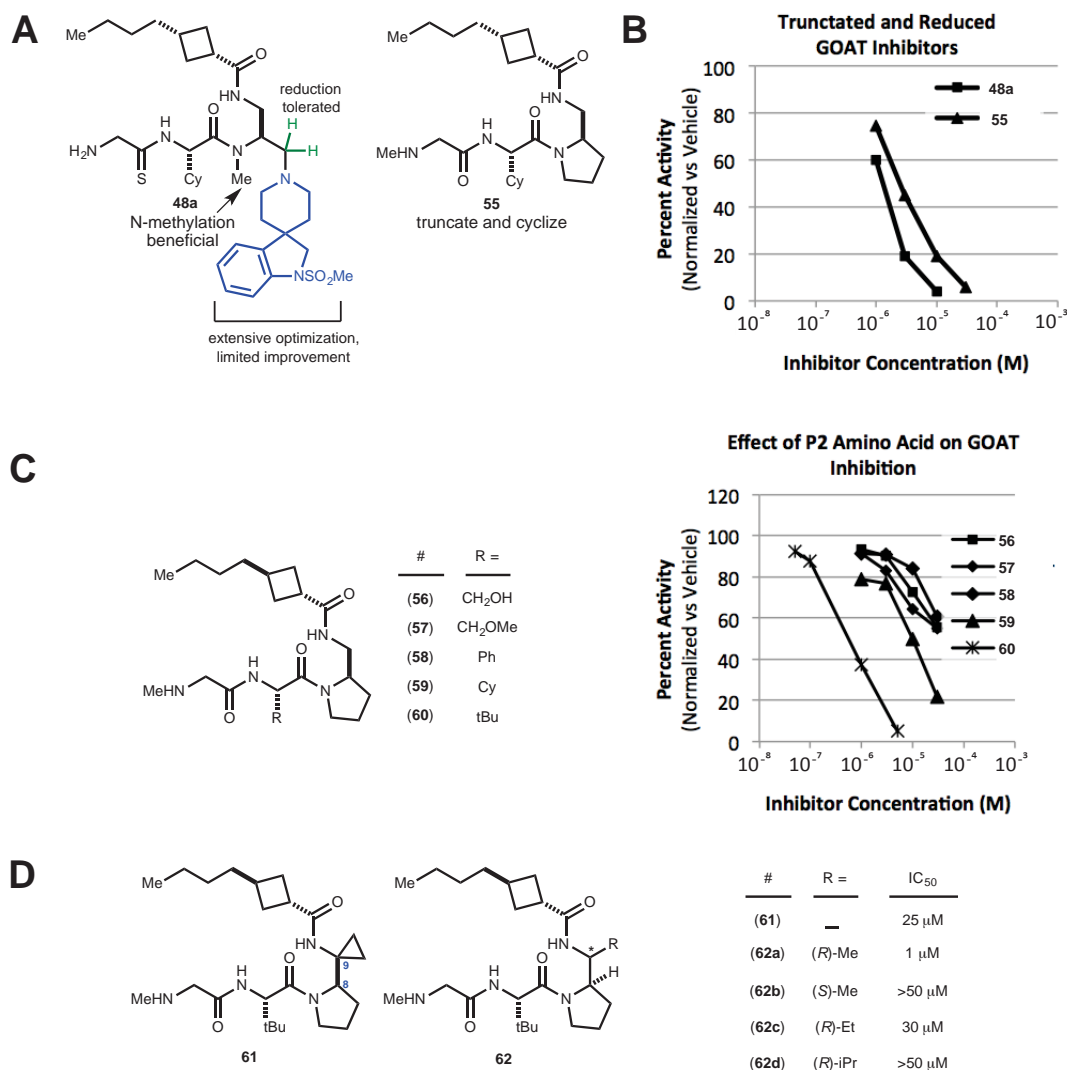
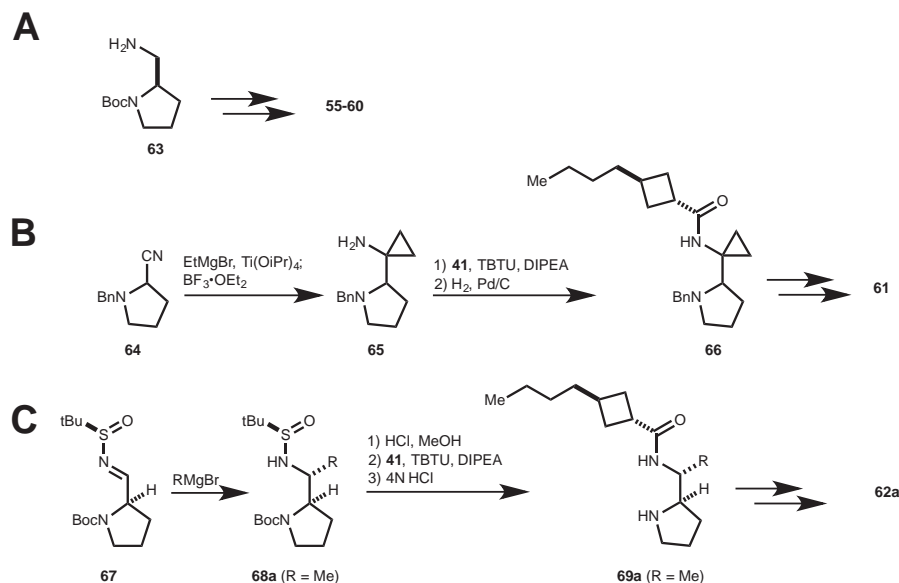


Fig. 3.6: Truncation and optimization of the C-terminal heterocycle. (A) Tolerance for *N*-methylation and DAP amide reduction coupled with broad SAR in the C-terminal fragment suggested that a truncated and cyclized inhibitor such as **55** might retain activity. (B) Comparison of the enzyme inhibitory activity of inhibitors **48a** and **55**. (C) Comparison of in vitro potency of a series of P2 residue variants. (D) Certain β -branched aminoalkylpyrrolidine inhibitors retain activity against GOAT.

We had noticed that in certain series of compounds, such as those in figure 3.5B, bulky and hydrophobic residues were preferred at the P2 position. Within the new aminomethylpyrrolidine scaffold, we found that this effect was even more pronounced (Figure 3.6C). A serine derivative (**57**) was essentially inactive, while *tert*-leucine containing analog **61** was the most potent compound we had so far prepared. The new scaffold also provided the opportunity to prepare branched analogs of the aminomethyl appendage, a position we had not examined in the DAP-derived inhibitors. Initially we prepared a pair of diastereomeric cyclopropanated derivatives. One of these isomers had weak activity against GOAT, and was assumed to have the shown *R* stereochemistry at the C8 position (**61**). We then prepared a pair of diastereomeric 2-(1-aminoethyl)-pyrrolidine derivatives (**62a** and **62b**). We were pleased to find that **62a**, having *R*-stereochemistry at carbon 9, had potency equivalent to **61**, while *S* isomer **62b** was inactive. Larger alkyl substituents were not tolerated (**62c** and **62d**).

3.13 Synthesis of Aminomethylpyrrolidine GOAT Inhibitors

(*R*)-1-Boc-2-aminomethylpyrrolidine (**63**) is commercially available in either enantiomeric form. Diamine **65** is then readily elaborated using standard solution phase peptide synthesis methods to the targeted GOAT inhibitors **56-61** (Scheme 3.6A).



Scheme 3.6: Synthesis of β -branched GOAT inhibitors. (A) Solution phase peptide synthesis methods may then be used to prepare GOAT inhibitors from monoprotected diamine **63**. (B) Aminocyclopropanes are prepared by Kulinkovich cyclopropanation of 2-cyanopyrrolidine. Elaboration to inhibitors proceeded normally. (C) Other aminoalkylpyrrolidines are prepared by addition of grignard reagents to D-prolinaldehyde derived Ellman sulfimine **67**. Following selective cleavage of the auxiliary and amidation with trans-cyclobutane **41**, conversion to full-length GOAT inhibitors proceeded normally.

Towards the synthesis of cyclopropanated inhibitor **61**, known nitrile **64**²⁷ was treated with ethylmagnesium bromide, titanium isopropoxide, and boron trifluoride under Szymoniak-Kulinkovich conditions, thus providing cyclopropylamine **65**.²⁸ Appendage of the side chain carboxylic acid was followed by benzyl deprotection to provide secondary amine **66**. Sequential peptide extension with L-Boc-*tert*-Leucine and Boc-sarcosine provided two separable diastereomeric GOAT inhibitors. The bioactive diastereomer was assumed to have the *R* stereochemistry shown.

Branched aminoalkylpyrrolidines **62a-d** were prepared by addition of the appropriate Grignard reagent to sulfimine **67**.²⁹ Shown in scheme 3.6C is an exemplary route to **62b**. Organometallic additions proceeded in fair to good yields and with >10:1

dr in each case. A single crystal of the major isomer derived from isopropyl addition was obtained, allowing assignment of the absolute and relative stereochemistry. Ethyl and methyl additions were assumed to give the same stereochemical outcome. In each case the *tert*-butyl sulfinamide was removed with methanolic HCl,³⁰ and *trans*-cyclobutane **41** appended using standard amidation conditions to provide **69a-d** following Boc cleavage. The latter could then be elaborated as before to inhibitors **62a-d**.

3.14 Optimization of N-Terminal Residue

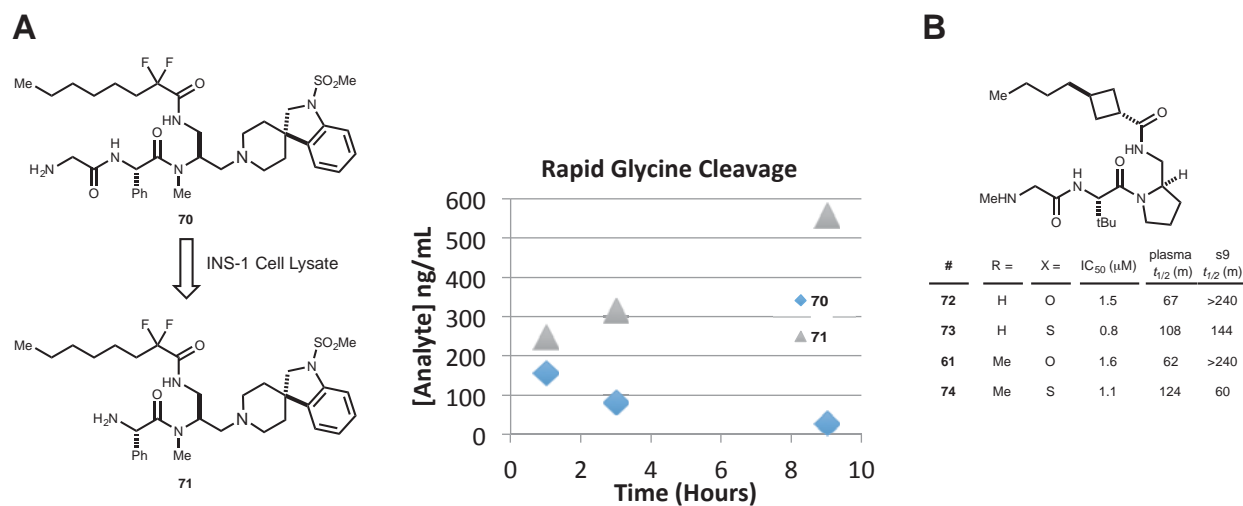
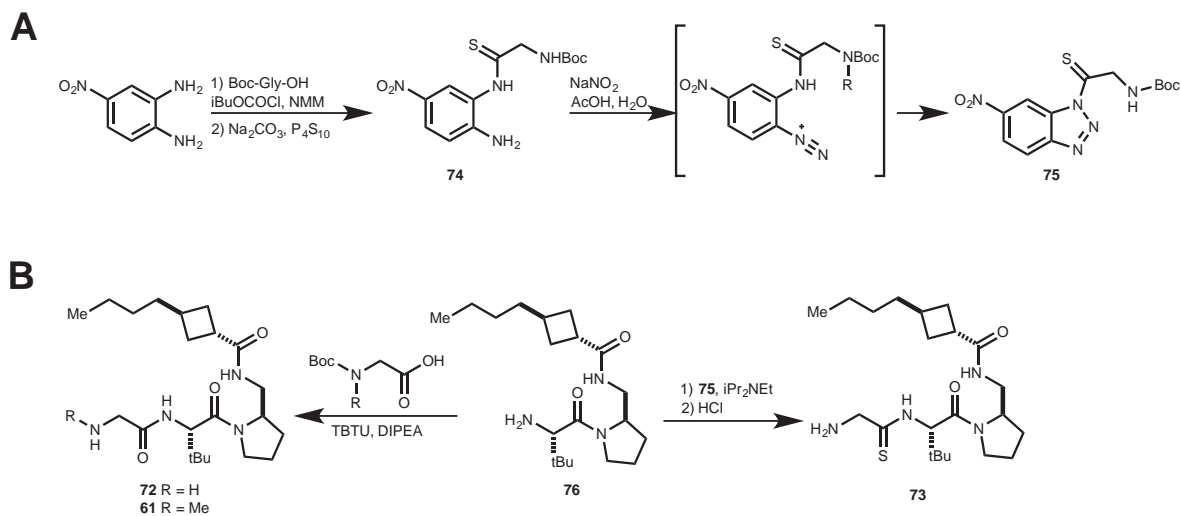


Fig. 3.7: Optimization of the N-terminal residue for proteolytic stability. (A) Incubation of previous generation inhibitor **70** in INS-1 cell extract resulted in rapid cleavage of the N-terminal glycine residue and formation of the truncated product **71** (B) We analyzed the stability of a set of thioamidated and *N*-methylated inhibitors using *in vitro* measures of inhibitor stability.

Data from a previous series of inhibitors (Figure 3.7A) suggested that proteolytic cleavage of the N-terminal glycine residue was a major degradation pathway. We observed rapid production of truncated compound **73** when a GOAT inhibitor (**72**) was incubated with INS-1 cell lysate. *N*-methylation is a common method to protect peptides

against proteolysis,¹⁷ and we had already demonstrated tolerance for monomethylation of the glycine residue (Figure 3.4). Thioamidation is another modification that has been shown to improve proteolytic stability of amide bonds.^{31, 32} We prepared a set of inhibitors (**61**, **72-74**) wherein the N-terminal residue had been methylated, thionated, or both to examine the effects of these modifications on inhibitor potency and on metabolism (figure 3.7B). We found that thionation effectively increased the proteolytic stability (as modeled by stability in murine plasma)³³ of the inhibitor with minimal effect on potency. Incubation of the compounds with liver S9 fractions demonstrated that the introduction of a thioamide increased the rate of hepatic metabolism (as modeled by liver S9 fraction incubation),³⁴ however the measured half-life of the thioamide inhibitors (**75** and **76**) under these conditions was sufficient to recommend them for in vivo examination. For a more detailed discussion of the pharmacokinetics of GOAT inhibitors, see chapter 4.

3.15 Synthesis of Thioamides



Scheme 3.7: Synthesis of thioamide inhibitors. (A) Thioacylating reagent **75** was prepared from 4-nitrobenzene-1,2-diamine by the shown three-step acylation/thionation/diazotization sequence. (B) Primary amine **76** could be converted to amides **61** and **72** by peptide coupling with glycine or sarcosine followed by deprotection. Thioamide **73** was prepared by thioamidation using **75** followed by deprotection.

Several authors have reported the use of thioacyl donor reagents as a general approach to the synthesis of thioamide containing peptides.³⁵ We made use of the nitrotriazolyl reagents reported by Shalaby et al.³⁶ These reagents were prepared in three steps from 4-nitrobenzene-1,2-diamine. Mixed carbonic anhydride coupling of the diamine with glycine selectively acylated the *m*-nitro aniline to provide the desired anilide, which was then treated with sodium carbonate and P_4S_{10} to afford thioanilides **74**. Diazotization of **74** with sodium nitrite and acetic acid afforded the aryldiazonium, which spontaneously cyclized to the desired triazoles **75**. Thioamide **73** was prepared from **76** by treatment with **75** followed by Boc cleavage using HCl. Peptide coupling of **76** with glycine or sarcosine followed by deprotection provided amides **61** and **72**.

3.16 In Vitro Activity of Lead Inhibitors Compared to Reported GOAT Inhibitors

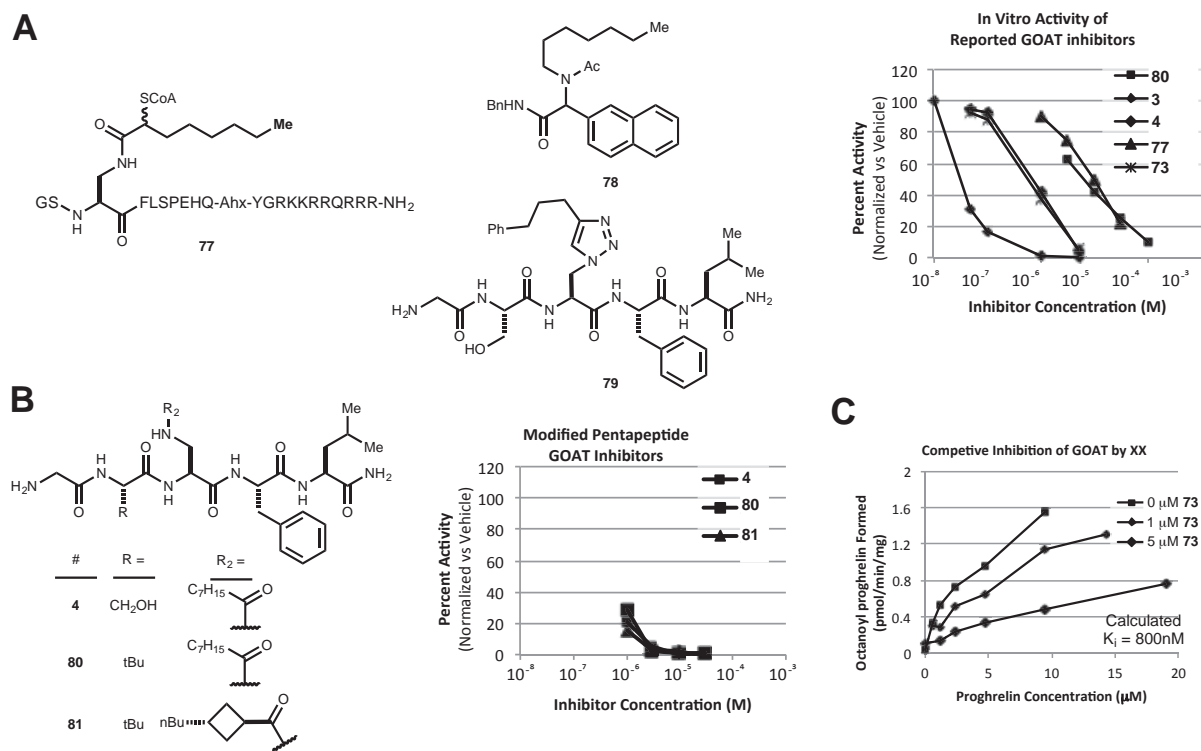


Figure 3.8: Comparison of GOAT inhibitors, divergent SAR, and mode of inhibition determination. (A) Reported GOAT inhibitors were independently synthesized and directly compared in our radioassay format. (B) Efforts to prepare a highly potent peptidal GOAT inhibitor by application of key SAR points to the peptidal series of inhibitors failed to improve peptide binding. (C) We assayed a lead inhibitor (**73**) in the presence of varying ghrelin concentrations and found that our inhibitor did not affect V_{max}, and our data best fit a competitive (with ghrelin) binding mode.

As described in chapter 1, several distinct classes of GOAT inhibitor have been reported.^{8, 37, 38, 39} We were able to prepare each of these according to literature methods and directly compare them in our assay system. Ghrelin 1-28 octanamide **3** is by far the most potent inhibitor so far developed. Lead inhibitor **73** was the most potent non-peptidyl inhibitor, matching ghrelin pentapeptide **4**. We found that GO-CoA-Tat (**77**)

and triazole linked inhibitor **79** had similar potency, while benzamide **78** was inactive in our assay format.

3.17 Competitive Inhibition and Divergent SAR of Aminomethylpyrrolidines

Our inhibitors were developed by the hypothesis driven and rational process described above from the known binding sequence of ghrelin 1-5, and were expected to bind the same active site pocket as ghrelin itself. Nonetheless, they are structurally dissimilar to the parent peptides, and our assay results did not rule out uncompetitive or non-competitive binding.⁴⁰ We were able to confirm a competitive binding mode by assaying our inhibitors at varying concentrations of ghrelin. We found that V_{max} was unaffected by our inhibitors and that increased initial rates were observed for higher ghrelin concentrations. Computationally, our data best fit a competitive binding model, confirming that the binding mode of our inhibitors had not been altered by the development process.

Based on these results, we wondered if it were possible to develop a highly potent short peptide GOAT inhibitor by incorporating key motifs from the aminomethylpyrrolidine series into the pentapeptide scaffold. We prepared peptides **81** and **82** containing a *tert*-leucine residue or a *tert*-leucine and the *trans*-cyclobutane side chain using solid phase peptide synthesis. We found that **4**, **81**, and **82** had very similar in vitro potency, despite the importance of the *tert*-leucine and cyclobutane to potency in the aminomethylpyrrolidine series of inhibitors (i.e. Figure 3.6D). This suggests that the latter compounds likely adopt a binding conformation distinct from that of the parent peptides.

3.18 Conclusion

We have successfully developed a novel class of small molecule GOAT inhibitor. Our inhibitors match the best reported small molecule GOAT inhibitors and are significantly more drug-like. We have developed a thorough understanding of SAR within the present aminomethylpyrrolidine series of inhibitors. Preliminary evaluation of inhibitor pharmacokinetics suggested that they were likely to have acceptable in vivo performance. Our next task was, then, to identify a suitable route for the large-scale preparation of a series of lead inhibitors and to evaluate their ability to inhibit GOAT in vivo.

-
- 1 Vagner J, Qu H, Hruby VJ, (2008) Peptidomimetics, a synthetic tool of drug discovery. *Curr Opin Chem Biol.* 12(3):292–296.
 - 2 Hruby VJ, Cai M (2013) Design of peptide and peptidomimetic ligands with novel pharmacological activity profiles. *Annu Rev Pharmacol Toxicol.* 53:557-80.
 - 3 Jensen C, Herold, P. Brunner, HR (2008) Aliskiren: the first renin inhibitor for clinical treatment. *Nature Reviews Drug Discovery* 7(5):399.
 - 4 Smith RG (2005) Development of growth hormone secretagogues. *Endocr Rev.* 26(3):346-60.
 - 5 Müller TD, et al. (2015) Ghrelin. *Molecular Metabolism* 4(6):437-460.
 - 6 Lipinski CA, Lombardo F, Dominy BW, Feeney PJ (2001) Experimental and computational approaches to estimate solubility and permeability in drug discovery and development settings. *Adv. Drug Deliv. Rev.* 46(1-3):3-26.
 - 7 Veber DF, Johnson SR, Cheng HY, Smith BR, Ward KW, Kopple KD (2002). Molecular properties that influence the oral bioavailability of drug candidates. *J. Med. Chem.* 45(12):2615-23.
 - 8 Yang J, Zhao TJ, Goldstein JL, Brown MS (2008) Inhibition of ghrelin O-acyltransferase (GOAT) by octanoylated pentapeptides. *Proc. Natl. Acad. Sci. USA* 105(31):10750-10755.
 - 9 Pong SS, Chung LY, Dean DC, Nargund RP, Patchett AA, Smith RG (1996) Identification of a new G-protein-linked receptor for growth hormone secretagogues. *Mol. Endocrinol.* 10(1):57-61.
 - 10 Bednarek MA, et al. (2000) Structure–Function Studies on the New Growth Hormone-Releasing Peptide, Ghrelin: Minimal Sequence of Ghrelin Necessary for Activation of Growth Hormone Secretagogue Receptor 1a. *J. Med. Chem.* 43(23):4370–4376.

-
- 11 Holst B, et al. (2009) Overlapping Binding Site for the Endogenous Agonist, Small-Molecule Agonists, and Allosteric Modulators on the Ghrelin Receptor. *Molecular Pharmacology* 75(1):44-59.
 - 12 Maligres PE, et al. (1997). Synthesis of the orally active spiroindoline-based growth hormone secretagogue, MK-677. *Tetrahedron* 53(32):10983-10992.
 - 13 Ghosh AK, Brindisi M (2015) Organic carbamates in drug design and medicinal chemistry. *J Med Chem.* 58(7):2895-940.
 - 14 Hedstrom L (2002) Serine protease mechanism and specificity. *Chem Rev.* 102(12):4501-24.
 - 15 Yang J, Brown MS, Liang G, Grishin NV, Goldstein JL (2008) Identification of the Acyltransferase that Octanoylates Ghrelin, an Appetite-Stimulating Peptide Hormone. *Cell* 132(3):387-396.
 - 16 Rajeswaran WG, Hocart, SJ, Murphy WA, Taylor JE, Coy DH (2001) Highly Potent and Subtype Selective Ligands Derived by N-Methyl Scan of a Somatostatin Antagonist. *Journal of Medicinal Chemistry* 44(8):1305-1311.
 - 17 Chatterjee J, Gilon C, Hoffman A, Kessler H (2008) N-Methylation of Peptides: A New Perspective in Medicinal Chemistry. *Acc. Chem. Res.* 41(10):1331-1342.
 - 18 Darling JE, et al. (2015) Structure-activity analysis of human ghrelin O-acyltransferase reveals chemical determinants of ghrelin selectivity and acyl group recognition. *Biochemistry.* 54(4):1100-10.
 - 19 Kan T, Fukuyama T (2004) Ns strategies: a highly versatile synthetic method for amines. *Chem Commun.* 21;(4):353-9.
 - 20 Koshland DE (1995) The Key-Lock Theory and the Induced Fit Theory. *Angew. Chem. Int. Ed.* 33(23-24):2375-2378.
 - 21 López-Mirabal HR, Winther JR. (2008) Redox characteristics of the eukaryotic cytosol. *Biochim Biophys Acta.* 1783(4):629-40.
 - 22 Brannock KC, Bell A, Burpitt RD, Kelly CA (1964). Enamine Chemistry. IV. Cycloaddition Reactions of Enamines Derived from Aldehydes and Acyclic Ketones. *J. Org. Chem.* 29(4):801-812.
 - 23 Dehmlow EV, Schmidt S (1990). Synthesis of Stereoisomeric 3-Substituted Cyclobutanecarboxylic Acid Derivatives. *Liebigs Annalen der Chemie.* 1990(5):411-414.
 - 24 Hortmann AG, Robertson DA, Gillard BK (1972) Convenient procedure for the preparation of 2-arylazirines. *J. Org. Chem.* 37(2):322-324.
 - 25 Hortmann AG, Robertson DA (1972) 1-Azabicyclobutanes. Synthesis and reactions. *J. Am. Chem. Soc.* 94(8):2758-2765.
 - 26 Alvernhe G, Laurent A, Touhami K, Bartnik R, Mloston G (1985). Synthèse de fluoro-3 azacyclanes : action de l'acide fluorhydrique sur les aza-1 bicyclo [n.1.0] alcanes. *Journal of Fluorine Chemistry.* 29(4):363-384.
 - 27 Couty F, David O, Larmanjat B, Marrot J (2007) Strained azetidinium ylides: new reagents for cyclopropanation. *J. Org Chem.* 72(3):1058-61.

-
- 28 Bertus P1, Szymoniak J. (2002) Ti(II)-mediated conversion of alpha-heterosubstituted (O, N, S) nitriles to functionalized cyclopropylamines. Effect of chelation on the cyclopropanation step. *J Org Chem.* 67(11):3965-8.
- 29 Song XN; Yao ZJ (2010) Short asymmetric synthesis of (S,S)-PDP using l-prolinol derivative as economic starting material. *Tetrahedron.* 66(14):2589-2593.
- 30 Yeung, KS. Bristol Meyers Squibb. Assignees. Benzofuran derivatives for the treatment of hepatitis c. US Patent US20150141395.
- 31 Zhang W, et al. (2010) A novel analog of antimicrobial peptide Polybia-MPI, with thioamide bond substitution, exhibits increased therapeutic efficacy against cancer and diminished toxicity in mice. *Peptides.* 31(10):1832-8.
- 32 Zacharie B, Lagraoui M, Dimarco M, Penney CL, Gagnon L (1999) Thioamides: synthesis, stability, and immunological activities of thioanalogues of Imreg. Preparation of new thioacylating agents using fluorobenzimidazolone derivatives. *J Med Chem.* 42(11):2046-52.
- 33 Kerns EH, Di L. *Drug-Like Properties: Concepts, Structure Design and Methods from ADME to Toxicity Optimization* (Elsevier, New York, New York).
- 34 Kang, YJ ed. *Optimization in Drug Discovery: Methods in Pharmacology and Toxicology* (Humana Press, Totowa, New Jersey).
- 35 Zacharie B, Lagraoui M, Dimarco M, Penney CL, Gagnon L (1999) Thioamides: synthesis, stability, and immunological activities of thioanalogues of Imreg. Preparation of new thioacylating agents using fluorobenzimidazolone derivatives. *J Med Chem.* 42(11):2046-52.
- 36 Shalaby MA, Grote CW, Rapoport HJ (1996) Thiopeptide Synthesis. alpha-Amino Thionoacid Derivatives of Nitrobenzotriazole as Thioacylating Agents. *J. Org Chem.* 61(25):9045-9048.
- 37 Barnett BP, et al. (2010) Glucose and weight control in mice with a designed ghrelin O-acyltransferase inhibitor. *Science* 330(6011):1689-1692.
- 38 Garner A, Janda K (2011) A small molecule antagonist of ghrelin O-acyltransferase (GOAT). *Chem. Commun.* 47(26):7512-7514.
- 39 Zhao F, Darling JE, Gibbs RA, Hougland JL. (2015) A new class of ghrelin O-acyltransferase inhibitors incorporating triazole-linked lipid mimetic groups. *Bioorg Med Chem Lett.* 25(14):2800-3.
- 40 Copeland, RA. *Evaluation of enzyme inhibitors in drug discovery: A guide for Medicinal Chemists and Pharmacologists.* (John Wiley and Sons, Hoboken, New Jersey).

4 In Vivo Performance of Novel Small Molecule GOAT Inhibitors

4.1 Selection and Preparation of In Vivo Candidates

Based on the structure-activity relationships and preliminary pharmacokinetic studies outlined in Chapter 3, we selected three candidate inhibitors and two negative control compounds for scale up and in vivo testing (Figure 4.1A). (*R*)-aminomethylpyrrolidines **1** and **2**, differing in methylation state of the N-terminal amine, and (*R, R*) aminoethylpyrrolidine derivative **3** were identified as potential lead compounds. As a negative control, we targeted truncated compound **4**, which lacks the N-terminal glycine residue.

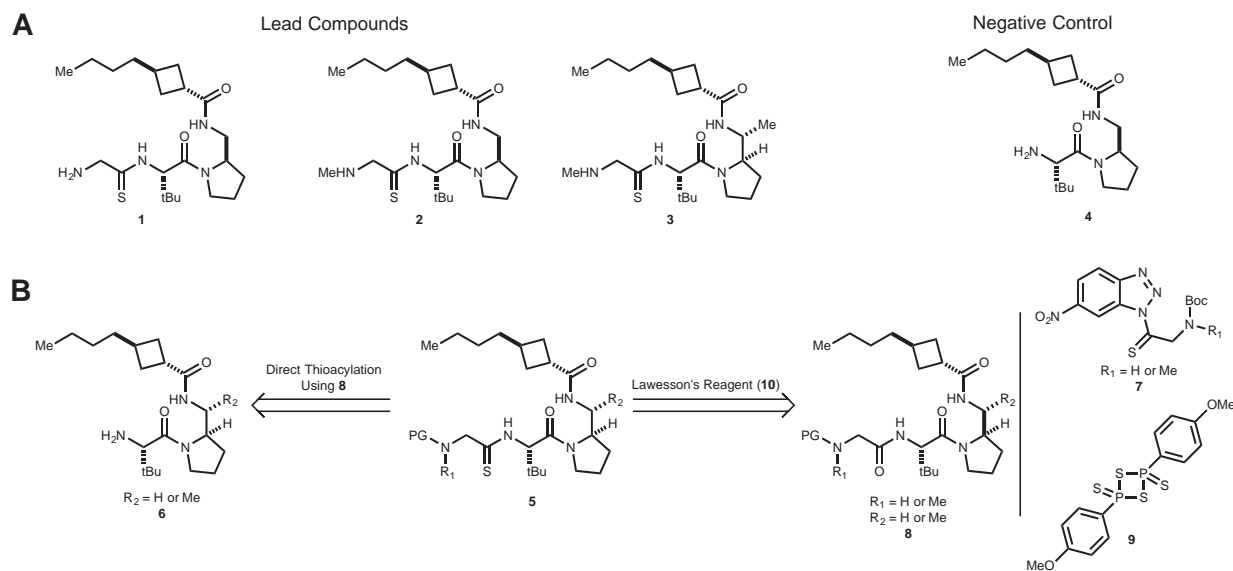


Figure 4.1: Synthetic approaches to lead structures 1-3. (A) Four inhibitors were selected and prepared for use in vivo, including three lead compounds and one negative control. (B) Potential strategies for introduction of the key thioamide present in **1-3**.

In the course of medicinal chemistry investigation, negative control **4** had been prepared on moderate scale by standard solution phase peptide synthesis methods

without incident, and further scale-up was not expected to be problematic. For thioamides **1-3**, selective and efficient introduction of the thioamide was anticipated to be the most significant challenge. Each of these compounds could be derived from a protected precursor of type **5**. We considered two possible routes for the preparation of **5**, which are shown in figure 4.1B. In both cases final removal of the glycylyl protecting group would then afford the desired product. The routes differed chiefly by the method used to introduce the thioamide. The most direct approach would be to use a thioacyl donor such as **7**¹ to append a protected thioglycine to a primary amine such as **6**, thus generating **5**. Alternatively, late stage treatment of protected amides such as **8** with Lawesson's reagent (**9**)², would also afford **7**. The latter strategy would require at least one additional synthetic step, and therefore thioacylation using **7** was explored first.

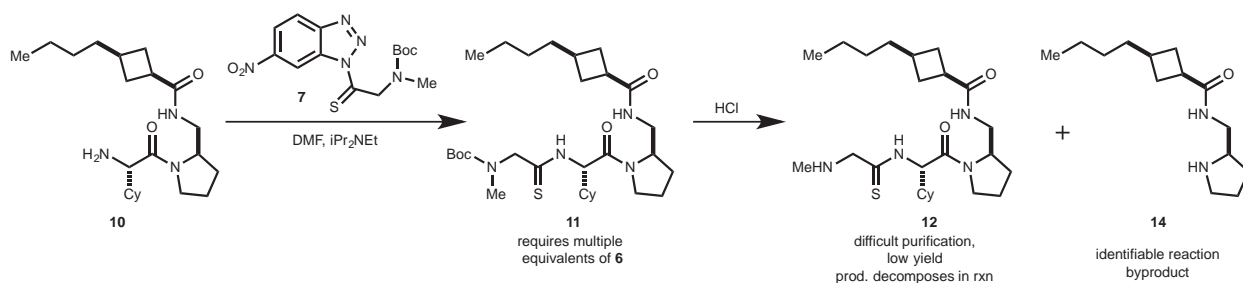


Figure 4.2: Direct thioacylation strategy for the preparation of GOAT inhibitors. The utility of the shown route was limited by poor efficiency of the initial thioacylation and by instability of the product thioamides to acidic conditions required for deprotection of the *N*-terminal Boc group.

Thioacylating reagents such as **7** had been used successfully to prepare thioamide analogs on small scale for *in vitro* testing (see Chap 3), but on scale these reactions suffered from key limitations exemplified by the reaction sequence shown in figure 4.2. First, thioacylations using **7** were low yielding and required multiple

equivalents of the acyl donor to reach full conversion. For example, the acylation of **10** required 3 equivalents of **7** to observe full consumption of the starting amine and formation of **11**. Moreover, removal of intensely colored nitroaryl byproducts proved challenging, as they tended to co-elute with desired product during chromatography. Most critically, we and others^{3,4,5} have found that thioamides such as **12** are unstable to the strong acid conditions used to remove the Boc-protecting group from precursor **11** in the final step. In some cases, we were able to observe and isolate byproducts such as **13** and **14** resulting from cyclative cleavage of the tertiary amide bond by the thioamide. To avoid the latter problem, we attempted to prepare a derivative of **7** with alternative protection on the glycyI or sarcosyl fragment. However these attempts were not successful, and late stage thionation of intact amide precursors was sought as an alternative.

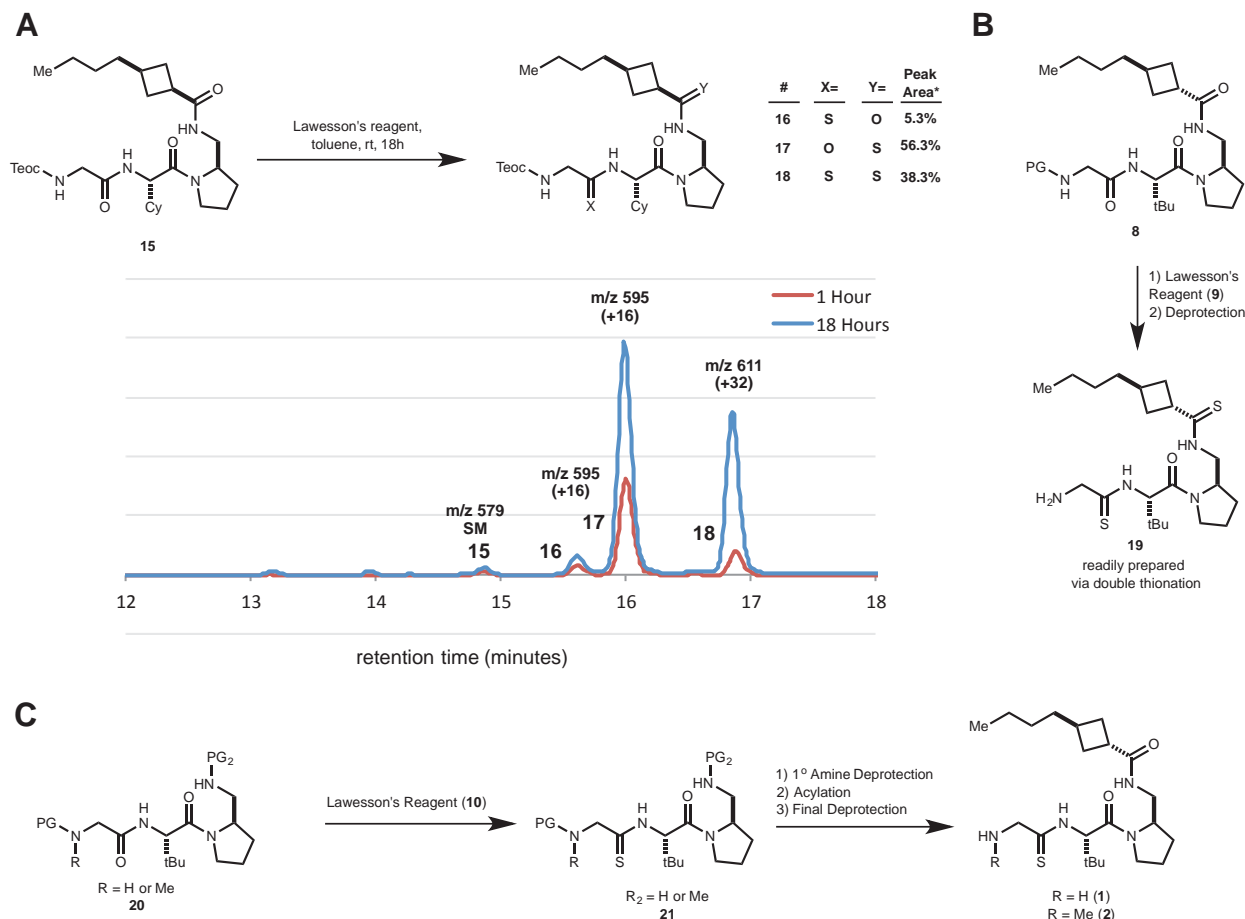


Figure 4.3: Regioselectivity of Lawesson's reagent in thionation reactions of aminomethylpyrrolidine containing GOAT inhibitors. (A) Model inhibitor 15 was treated with 0.5 equivalents of Lawesson's reagent in toluene. The reaction was monitored by HPLC-UV. Shown traces represent the UV absorbance at 280 nm. *18 absorbs UV only poorly, and so appears as a very small peak in this experiment, and is not considered in the tabulated product distribution at 18h. These values are not corrected for differences in extinction coefficient between products. (B) Preparation of target *bis*-thioamide inhibitor 19 from monoprotected *tris*-amide 8. (C) Reformulation of the synthetic approach to have carbamoyl protection of the side chain during application of Lawesson's reagent would ensure selective thionation of a single amide bond.

Direct monothionation of *tris*-amides such as **8** as shown in would only be a useful approach for the synthesis of **7** if the reaction could be selective for the glycol amide as shown in figure 4.1B. Synthesis of thioamides using Lawesson's Reagent (**9**, Figure 4.1) is well studied. When multiple amides are present the regioselectivity of the reaction depends largely on the relative steric environment of each amide bond.^{1,6} We

were uncertain which amide in substrates such as **5** would be most reactive towards Lawesson's reagent, and set out to test this experimentally. The hindered amide between the P2 *tert*-leucine residue and the (R)-2-aminomethyl pyrrolidine residue was unlikely to participate, but both of the remaining amides could be reactive.

To evaluate the regioselectivity of Lawesson's reagent in the context of our substrates, cyclohexylglycine derivative **15** was treated with 0.5 equivalents of **9** in toluene at room temperature, and the reaction was monitored by HPLC-UV (Figure 4.3A). Within one hour a mixture of starting material, a major monothioamide (**17**), and a small amount of *bis*-thioamide (**18**) was formed. A trace amount of a second monothioamide (**16**) was also observed. Additional reaction time consumed the remaining starting material, and increased the fraction of *bis*-thioamide, but did not significantly alter the selectivity of the reaction. The major monothioamide and the *bis*-thioamide products were purified by preparative HPLC and the sites of thionation determined using two-dimensional NMR analysis (COSY, HMBC). Monothioamide **17** was found to be thionated at the side chain amide, rather than at the desired glycylic amide bond. *Bis*-thioamide **18** had been thionated at both expected sites. We concluded that the thionation using **9** was moderately selective for the undesired side chain amide. A variety of mechanistically related thionation reagents have been described, but do not generally reverse the observed regioselectivity. Consequently, preparation of the desired monothioamide from a tris-amidyl starting material did not appear possible.

As discussed in chapter three, *bis*-thioamide **18** was found to have *in vitro* activity against GOAT comparable to amide **17** and monothioamide **16**. This trend was expected to hold for a P2 *tert*-leucine containing analog, and synthesis of a *bis*-

thioamide by late stage thionation using Lawesson's reagent would be possible (figure 4.3B). Moreover, such a compound might have pharmacokinetic advantages over the monothioamide congeners. We elected to prepare bis-thioamide inhibitor **19** as a fifth inhibitor for in vivo study.

To achieve selective monothionation towards lead structures 1-3, a substrate with a single reactive amide would be required. Lawesson's reagent reacts with carbamates only under forcing conditions,^{1,6} so for our initial syntheses of **1** and **2**, we elected to prepare a precursor of type **20**, harboring a single reactive amide and a carbamoylated primary amine. Treatment of **20** with Lawesson's reagent would provide monothioamide **21**. Removal of the side chain carbamate followed by acylation with *trans*-3-butyl-cyclobutanecarboxylic acid, and final deprotection of the material would afford inhibitors **1** and **2** (figure 4.3C).

The final detail to be considered was the choice of protection strategy. The two free amines present in **20** would need to be orthogonally protected, and acid-labile groups (i.e. Boc) would need to be avoided because of the instability of thioamides to acidic conditions. Standard orthogonal protecting groups such as carboxylbenzyl (Cbz) or Allyloxycarbonyl (Alloc) were initially ruled out because the palladium catalyst traditionally used to cleave these groups may be susceptible to poisoning by the thioamide. Ultimately, for our initial syntheses of **1** and **2**, we used 2-(trimethylsilyl) ethoxycarbonyloxy (Teoc) protection on the *N*-terminal residue.⁷ Teoc can be readily cleaved using nucleophilic fluoride sources, thus avoiding the acid-promoted decomposition pathway. For the aminomethylpyrrolidine primary amine, we used the

Fmoc protecting group, which is typically removed by treatment with secondary amines such as piperidine.

We designed the synthetic route to **1** and **2** shown in Figure 4.4, starting with commercially available Boc-protected (R)-aminomethylpyrrolidine (**22**). Fmoc protection of the primary amine followed by HCl mediated removal of the Boc group, afforded secondary amine **23** as its hydrochloride. Due to the potential lability of the Fmoc group in the presence of a free secondary amine, the free base of **23** was not isolated, but instead liberated *in situ*. The C-terminal dipeptide was then constructed by coupling of hydrochloride salt **23** to Boc-*tert*-leucine. Removal of the Boc-group, then coupling with Teoc-protected sarcosine or glycine provided dicarbamoyl products **24** and **25**.

In other experiments, we observed that related thioamide were thermally unstable. Thionation using **9** is most often performed in refluxing toluene or benzene due to the poor solubility of the reagent in these solvents at ambient temperatures. Nonetheless, in some cases thionation has been shown to proceed at room temperature, despite apparent insolubility of the thioanating reagent. Reaction of our tripeptides with one equivalent of **9** in toluene at room temperature for eighteen hours afforded the desired monothioamides **26** and **27** in good yields (figure 4.4). Treatment of these products with DBU and octanethiol removed the Fmoc group and gave primary amines **28** and **29**. Acylation with *trans*-3-butylcyclobutanecarboxylic acid (**31**) was performed using standard amidation conditions to afford the desired products **31** and **32**.

Cleavage of the Teoc protecting group proved more challenging than anticipated. Standard cleavage conditions using tetrabutylammonium fluoride (TBAF) generated the

desired product, but additional impurities were evident by NMR. We sought an alternative source of fluoride anion, and tris(dimethylamino)sulfonium difluorotrimethylsilicate (TASF) performed well.⁸ Use of this reagent cleanly generated the desired product, but TASF is expensive, and challenging to prepare.

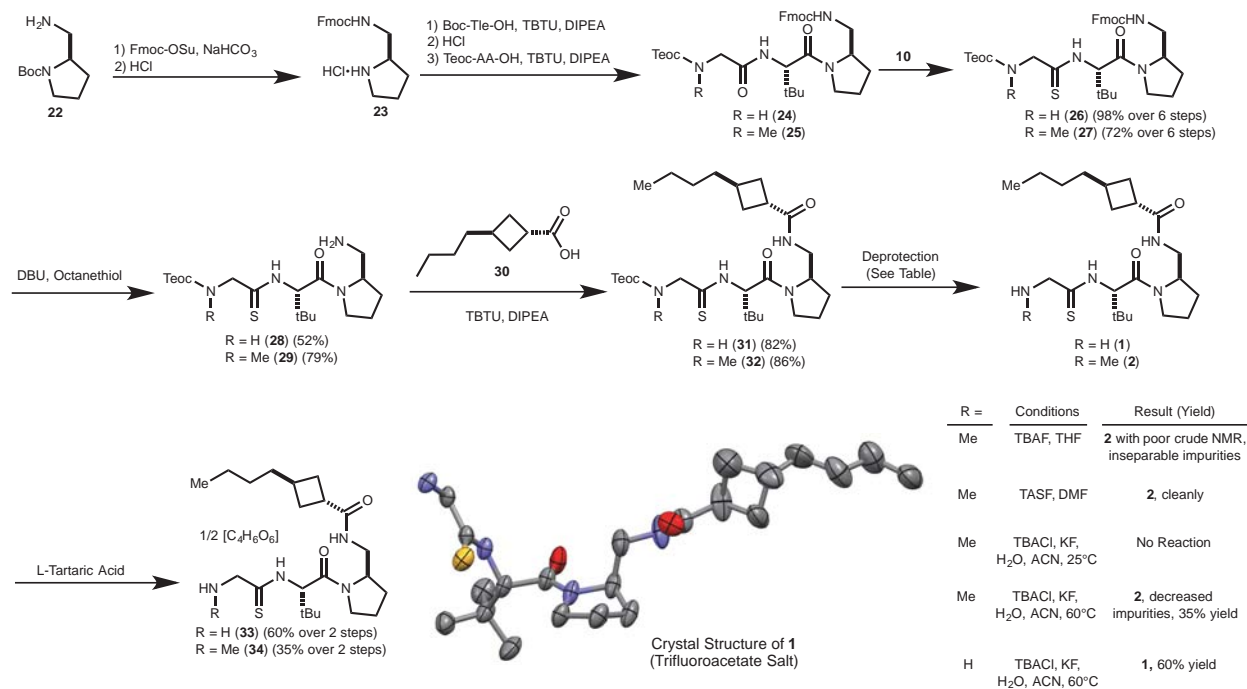


Figure 4.4: Synthetic routes to the targeted GOAT inhibitors 1 and 2.

Carpino has identified the combination of tetrabutylammonium chloride and potassium fluoride hydrate as an alternative method to generate nucleophilic fluoride.⁹ At room temperature these reagents had no effect on our substrate, but at 60°C the Teoc fragment was removed from 31 and 32 to generate 1 and 2 respectively, with greater purity observed by NMR. Because the material was to be used for in vivo testing, we needed to formulate the product as a pharmaceutically acceptable salt form.¹⁰ The 2:1 salts with L-tartaric acid (i.e. hemitartrates) 33 and 34 were isolated as

white solid materials, which were non-hygroscopic, free-flowing, stable to benchtop storage, and soluble (to >10mg/mL) in aqueous solutions containing 1% Tween-80 as a detergent. We were obtained a single crystal structure of the trifluoroacetate salt of **1** (Figure 4.4), confirming structural assignment and absolute configuration.

During the synthesis of **1** and **2**, we had assumed that a palladium-promoted deprotection of the *N*-terminal glycine or sarcosine would be difficult due to poisoning of the catalyst by the nucleophilic thioamide residue. Given the high cost of commercial Teoc precursor 2-trimethylsilylethanol, an Alloc or Cbz protection strategy, if viable, was appealing. Alloc is used extensively as an orthogonal protection strategy in peptide synthesis.¹¹ Generic conditions for its removal involve the use of a Pd(0) catalyst, or Pd(II) precatalyst, and one of several nucleophilic trapping agents to sequester the generated allyl electrophile. We prepared Alloc protected substrates **35** and **36** to evaluate potential cleavage conditions (figure 4.5A), and found that standard cleavage conditions using Pd(PPh₃)₄ and diethylamine as the nucleophile readily cleaved the alloc group and provided the free amine with very little degradation of the material. However, purification of material generated in this fashion proved challenging, as the triphenylphosphine oxide byproduct of catalyst degradation coeluted with desired product under all tested chromatography conditions. In an effort to solve this problem, we screened a set of alternative conditions using immobilized Pd catalyst, however no product was detected in these reactions. Genet has reported an alternative catalyst system, wherein Pd(0) is generated from palladium acetate and diethylamine in the presence of a sulfated phosphine ligand (TPPTS (**39**)).¹² Application of these conditions to our system resulted in full conversion to product, and the increased ligand polarity

rendered chromatographic purification of the final compound straightforward. This improved protection strategy was used in the syntheses of branched inhibitor **3** and bis-thioamide **20**.

Aminoethylpyrrolidine **41** was synthesized as described in chapter 3, by addition of methylmagnesium bromide to Ellman type sulfimine **40**.¹³ On large scale (figure 4.5B) this reaction provided branched product **41** in high yield and with better than 20:1 dr. Selective acid-promoted cleavage of the Ellman auxiliary in the presence of a potentially labile Boc group was achieved using HCl in methanol at 0°C. Fmoc protection of the primary amine and cleavage of the Boc group using HCl at room temperature afforded monoprotected aminoethylpyrrolidine **42**. Peptide extension as previously described was used to generate tripeptide **43**. Monothionation with Lawesson's reagent proceeded in high yield to provide thioamide **44**. The Fmoc protection was removed and side chain carboxylic acid **31** appended to provide protected inhibitor **45**. The Alloc group was removed using the Pd(OAc)₂/TPPTS conditions and the product amine formulated as the hemitartrate salt (**46**).

then acylated with Boc-*tert*-leucine. Acid promoted cleavage of the protecting group was followed by treatment with aqueous sodium carbonate to generate negative control **4**. To prepare **19** an alloc-sarcosyl fragment was appended to free base **4** under standard peptide coupling conditions. Treatment of this *tris*-amidyl material with excess **9** afforded the expected *bis*-thioamide, which was deprotected under the Genet¹² conditions to provide targeted *bis*-thioamide **19**. Inhibitors **4** and **19** were formulated as the hemitartrate salts (**48** and **49**). For all pharmacological studies described below, compound numbers (ie. **1-4**, **19**) refer to the corresponding hemitartrate (ie. **33**, **34**, **46**, **48**, and **49**).

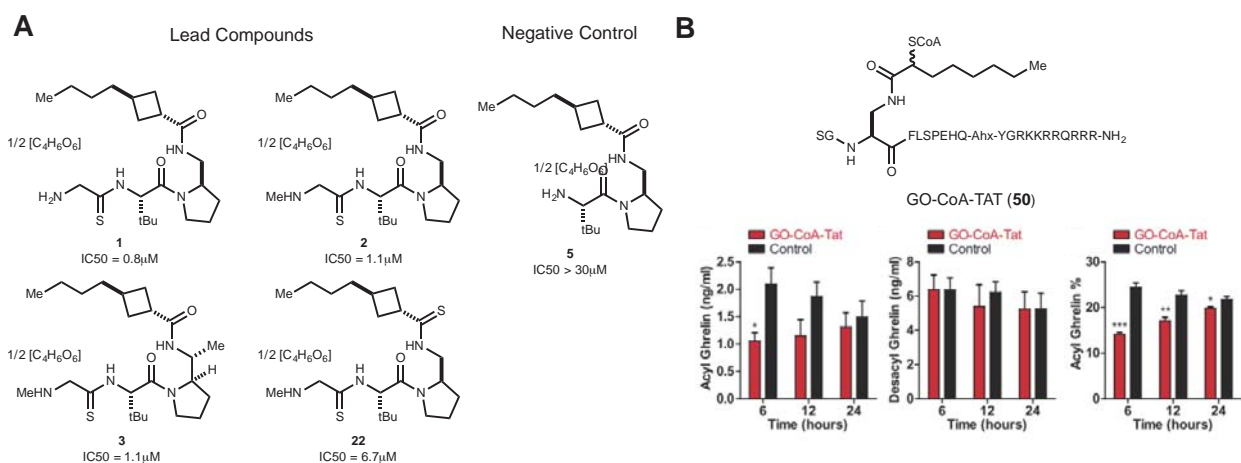


Figure 4.6: GOAT inhibitors evaluated in vivo. (A) Set of GOAT inhibitors to be evaluated in vivo with measured in vitro IC₅₀ values. (B) GO-CoA-TAT is the only other reported inhibitor of GOAT having activity in vivo. Figure reprinted from Barnett et al. *Science* 330(6011):1689-1692.

Once each of the candidate inhibitors had been prepared on scale and formulated as the hemitartrate salt, we re-assayed the in vitro activity of each sample to confirm potency (Figure 4.6A). These results were as we had anticipated; lead compounds **1**, **2**, **3** and **19** were active in vitro, having IC₅₀s of 1.1 μM, 0.8 μM, 1.1 μM,

and 6.7 μ M respectively (Figure 4.5). Designed negative control **4** had no effect on in vitro ghrelin acylation at any tested concentration.

4.2 Evaluation of Inhibitor Efficacy In Vivo

With a set of candidate inhibitors in hand we aimed to determine what effect, they would have on acyl-ghrelin levels in vivo. There was little precedent on which to base our experimental design. As discussed in chapter 1, GO-CoA-TAT (**50**) is the only reported GOAT inhibitor that has been evaluated in vivo (figure 4.6B).¹⁴ Our protocols are similar to those reported by Barnett et al. Male C57BL/6 mice of at least 8 weeks of age were maintained on standard diet. In order to maximize the levels of circulating acyl-ghrelin prior to inhibitor administration, animals were fasted overnight before experiments were performed.

We began our in vivo analysis with lead inhibitor **2**. Each of the described inhibitors was freely soluble to >10mg/mL in PBS containing 1% Tween-80. We began with an intraperitoneal dosage of 80mg/kg. Blood samples were periodically collected from anesthetized mice from 15 minutes to 24 hours after injection, and the levels of acyl and des-acyl ghrelin were quantified using commercially available ELISA assays.

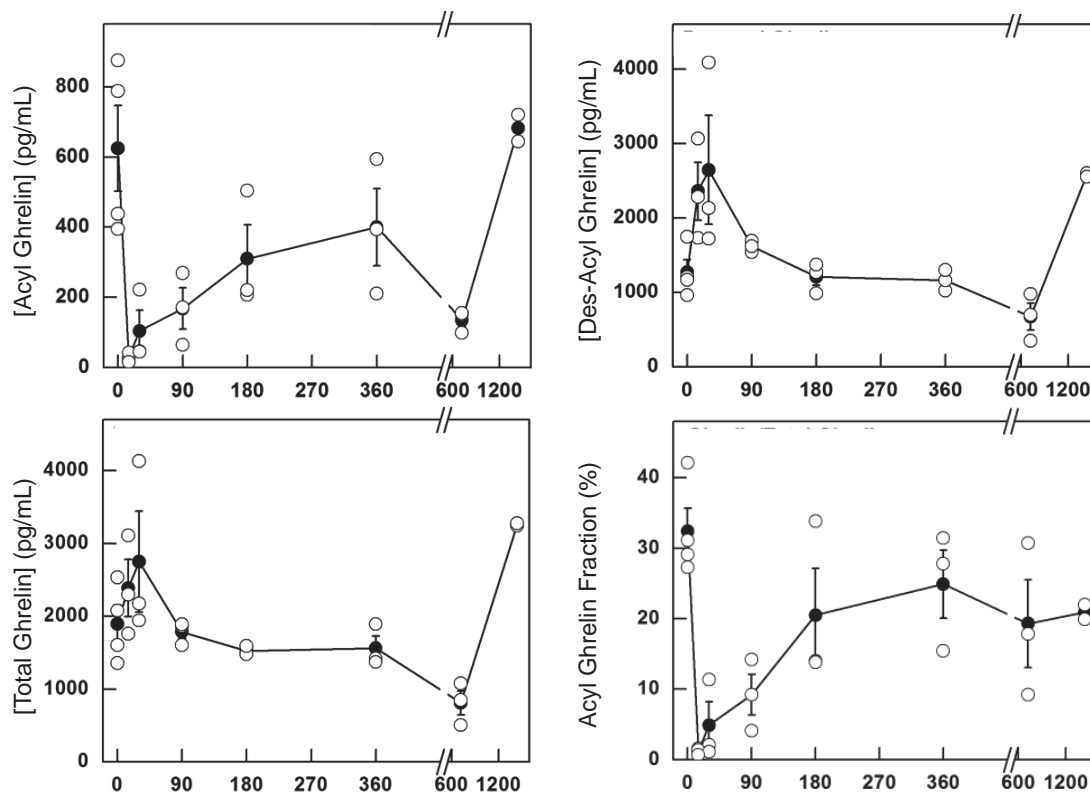


Figure 4.7: In vitro effects of administration of 2 on levels of circulating ghrelin species. Open circles represent the values obtained for individual mice, while filled circles represent the average of the group. N=3 per group. Error bars reflect standard error.

Within 15 minutes of administration, inhibitor **2** reduced the circulating concentration of acyl ghrelin below the limit of detection (Figure 4.7). Acyl ghrelin recovered to resting levels within approximately three hours. Des-acyl ghrelin levels increased markedly immediately following inhibitor injection, but quickly returned to resting levels. This latter observation could be partially explained by GOAT inhibition – without the ability to produce acyl ghrelin, all of the peptide remains in des-acyl form. However, the sum of the concentration of both des-acyl and acyl ghrelin species – ie. total ghrelin level – also spiked, suggesting an alternative perturbation potentially from a simple stress response to being handled and treated with drug.

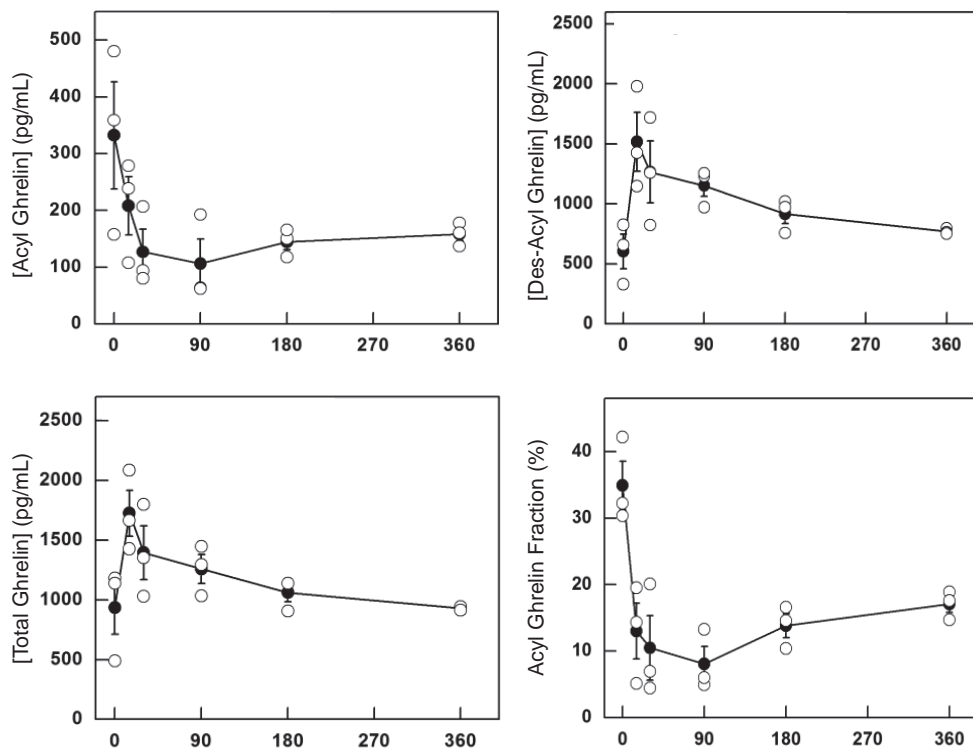


Figure 4.8: In vivo effects of administration of 1 on levels of circulating ghrelin species. Open circles represent the values obtained for individual mice, while filled circles represent the average of the group. N=3 per group. Error bars reflect standard error.

Given inter-individual variability, ghrelin levels are more reliably expressed as a fraction of acyl-ghrelin.^{14, 15} The acyl to des-acyl ghrelin ratio appears to be more physiologically relevant than the absolute concentrations of either species. When the above data are evaluated in this format, we see a similar trend: the acyl ghrelin fraction drops precipitously within 15 minutes and recovers after approximately three hours to resting levels, consistent with the absolute measurements.

We evaluated the performance of 1 in a similar manner (Figure 4.8). Intraperitoneal administration of the inhibitor at 80mg/kg led to a rapid decline in acyl ghrelin levels, as well as the fraction of acyl ghrelin. For this experiment, the response seemed to be somewhat better sustained than when 2 was used, although the initial

drop in acyl-ghrelin concentration was less pronounced. The absolute concentration of des-acyl ghrelin again spiked and then recovered to the resting state within three hours.

We repeated this same experiment a third time using branched inhibitor **3**. As had been observed for **1** and **2**, intraperitoneal treatment with 80mg/kg of **3** led to a rapid decrease in the circulating concentration of acyl-ghrelin followed by recovery to resting concentrations over about three hours.

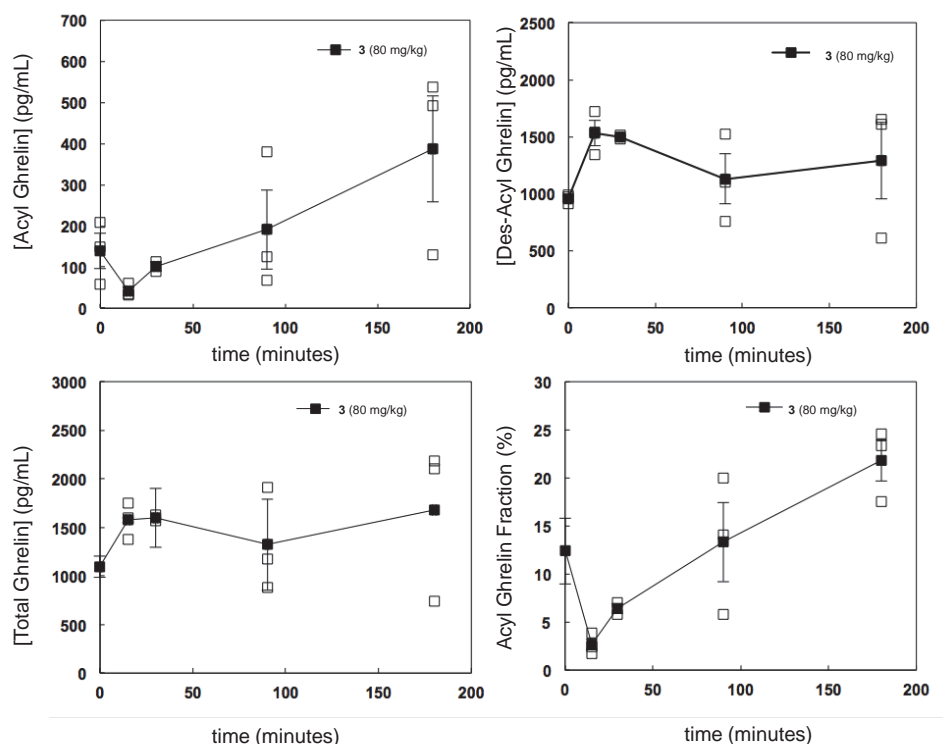


Figure 4.9: In vitro effects of administration of **3 on levels of circulating ghrelin species.** Open marks represent the values obtained for individual mice, while filled marks represent the average of the group. N=3 per group. Error bars reflect standard error.

Having evaluated the single concentration efficacy of each lead inhibitor, we sought to determine a dose-response relationship for an inhibitor. Prior experiments had been conducted using 80mg/kg of intraperitoneal GOAT inhibitor. To identify the minimal efficacious dose of a GOAT inhibitor, we administered doses of **1** from 20mg/kg

to 80mg/kg and monitored the effect on ghrelin species concentrations (Figure 4.10). To evaluate whether the spike in des-acyl ghrelin concentration observed in prior experiments was a specific response to our inhibitors or a more general response, a parallel group of mice injected only with vehicle were included as a control. Truncated compound **4** was also included as an additional negative control.

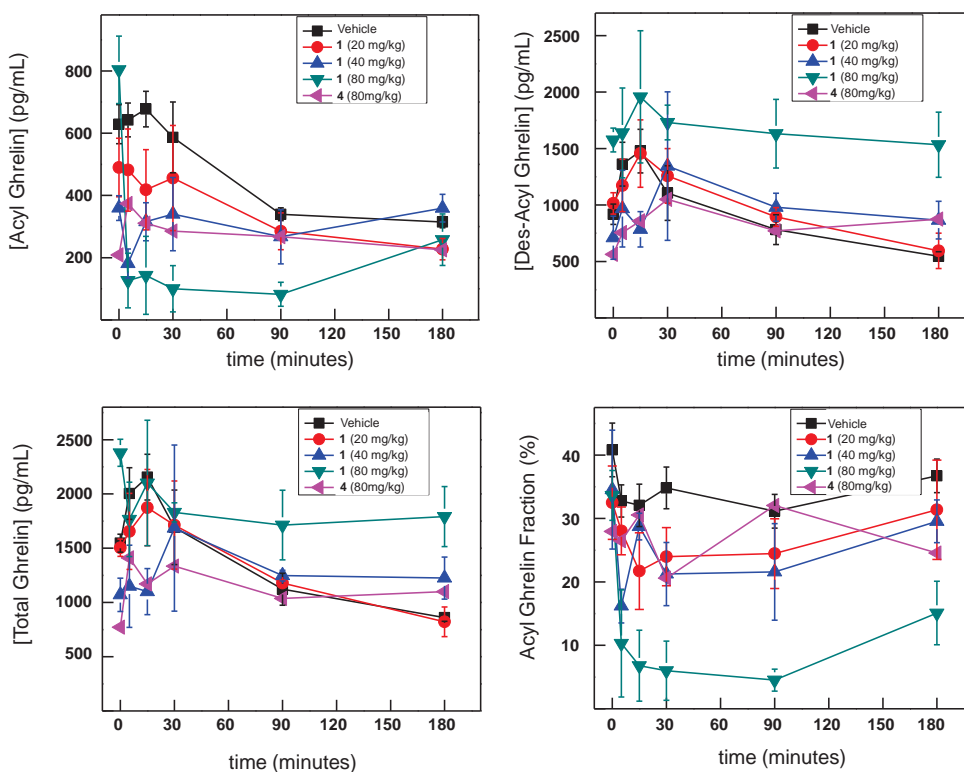


Figure 4.10: Dose titration of inhibitor 1 and negative control 4. N=3 per group. Individual mice are omitted for clarity. Error bars reflect standard error.

As was observed previously, administration of 80mg/kg of **1** led to a rapid and dramatic reduction in the fraction of acyl ghrelin, with the effect sustained for approximately three hours. At 40mg/kg, the effect was blunted, and a dose of 20mg/kg appeared to have had little effect on acyl-ghrelin concentrations. These data suggested

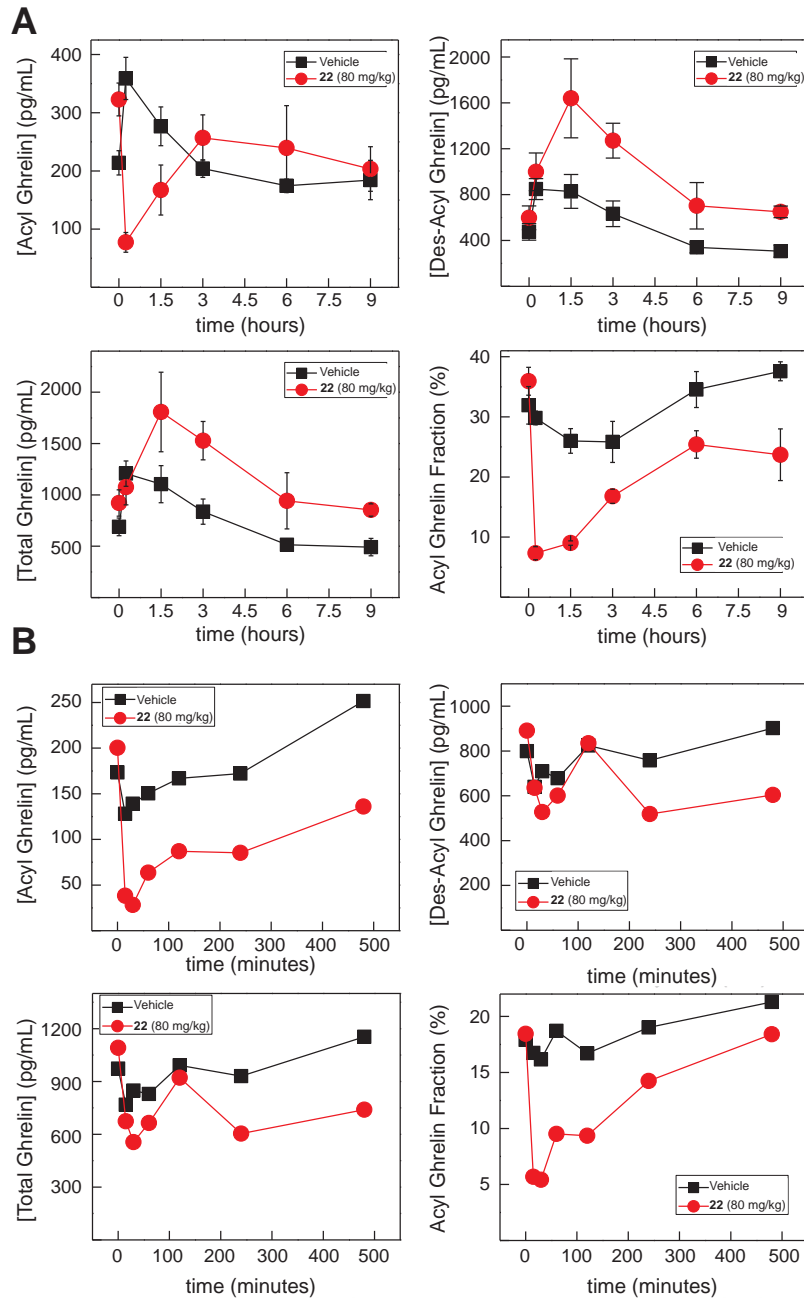


Figure 4.11: In vitro effects of 19 on levels of circulating ghrelin species in mice and rats. (A) A dose of 80mg/kg **22** was administered intraperitoneally to C57BL/6 mice. Blood samples were collected at the indicated time points, and the levels of ghrelin species quantified as described above. Individual mice are omitted for clarity. N=3 per group. Error bars reflect standard error. (B) An identical experiment was performed using rats. Animals were not sacrificed at the indicated time points, rather blood was collected via a sub-orbital bleed and ghrelin species quantified. Three rats were used for the vehicle control group, and due to difficulty recovering blood from one animal; only two were used for the treatment group.

that inhibitors **1-3** could require a dose of 80mg/kg for efficacy. As expected, **4** had no effect on acyl-ghrelin levels or fraction of acyl ghrelin. We observed a rapid increase in des-acyl ghrelin levels for all treatment groups, including both vehicle and inactive compound **4**, suggesting that this marginal effect may be a stress response.

Bisthioamide **19**, which showed reduced potency in vitro compared to the other lead inhibitors, nonetheless produced a similar response as **1-3** when administered (figure 4.11A). As with the other tested compounds, the fraction of acyl ghrelin promptly fell and recovered roughly to the resting level within about three hours.

While we were encouraged that our inhibitors appeared to have the desired effect of reducing acyl ghrelin fraction in mice, the efficacy window was deemed too short to be useful for evaluating the effects of **1-3** on phenotypes such as weight gain and glucose response. Despite their extensive use in drug development, mice are often considered to be only loose models of human biology. Ghrelin signaling, which appears to be involved at multiple levels in the overall metabolism of the animal, is likely to be quite different qualitatively in rodents than in humans. In addition, rates of drug metabolism can vary widely between mammal species. We wondered, therefore, if our compounds might have improved efficacy in an alternative model organism. The amino acid sequences of mouse and rat GOAT are 88% identical and their mature ghrelin sequences are 100% identical, suggesting that an inhibitor of mouse GOAT was likely to be an inhibitor of rat GOAT as well. We administered **19** to rats at 80mg/kg, in the hope that the effect might be more persistent. We were pleased to find that **19** was also effective in rats. However, the lifetime of the effect was not significantly extended relative to a murine model.

To briefly summarize the initial results: An immediate reduction in absolute acyl ghrelin levels as well as fraction of acyl ghrelin, in many cases to near or below the limit of detection, was observed for animals treated intraperitoneally with 80mg/kg of with inhibitors **1-3** or **19**. Designed negative control **4** had no observable effect on acyl-ghrelin concentrations. A brief increase in des-acyl and total ghrelin levels was observed following treatment with a GOAT inhibitor, negative control, or vehicle. That this effect is unrelated to the effect of the treatment on acyl-ghrelin levels suggests that this increase is most likely a response to the stress of being handled and dosed.

When inhibitors **1-3** were administered intraperitoneally, the maximum sustained effect on acyl-ghrelin levels was roughly three hours. To design an experiment that would meaningfully evaluate phenotypic effects of GOAT inhibition, however, we would need a means to reduce circulating ghrelin levels for at least 12 hours. This led us to three distinct lines of inquiry: first, could we find an alternative dosing mode that would suppress acyl-ghrelin concentrations for a longer period of time? Second, what were the circulating plasma concentrations of inhibitor and did they track with the loss of effect on acyl-ghrelin? Third, by what mechanism are GOAT inhibitors cleared from circulation?

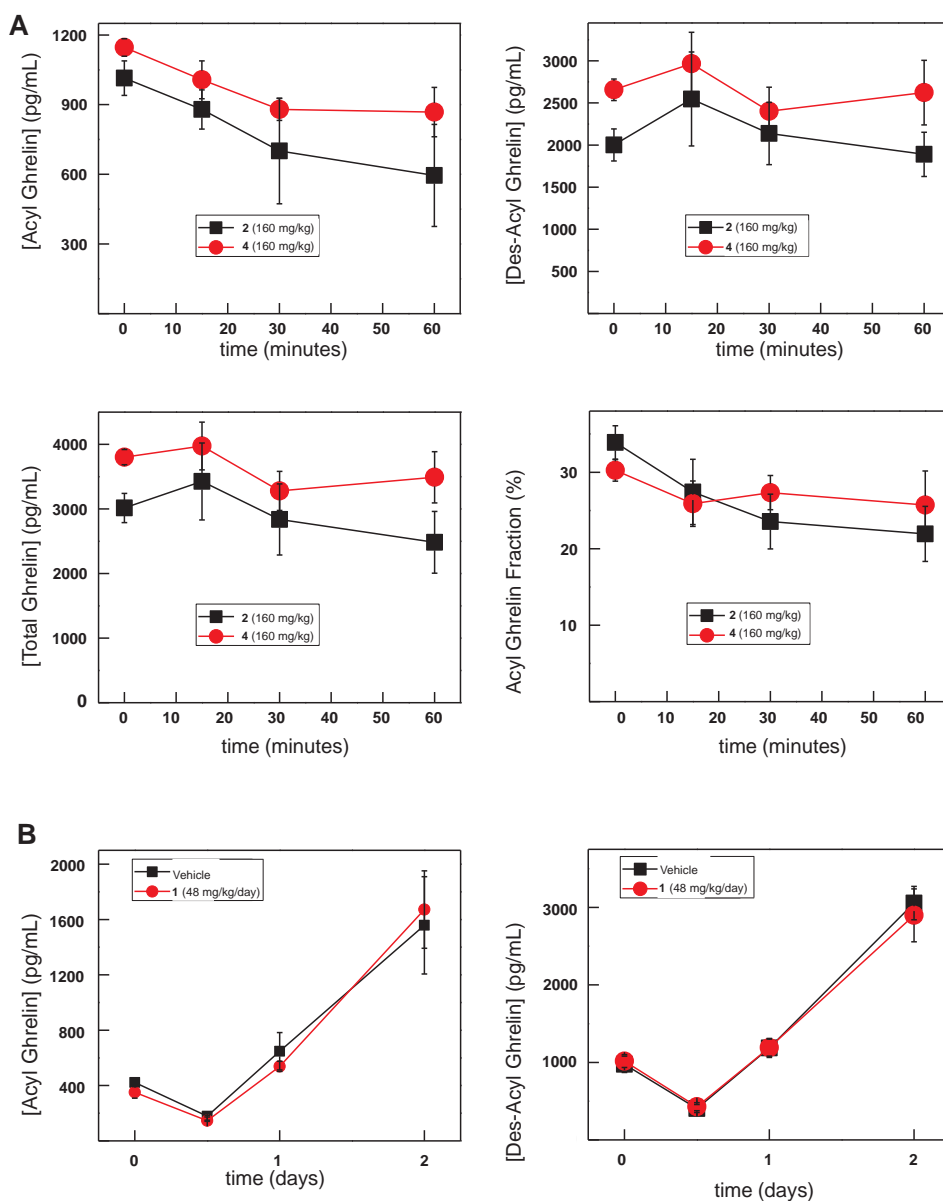


Figure 4.12: Evaluation of inhibitor efficacy with alternative dosing modes. (A) A dose of 160 mg/kg of **2** dissolved at 20 mg/mL in PBS containing 1% tween-80 was administered by oral gavage. Blood samples were collected at the indicated time points, and the levels of ghrelin species quantified as described above. Individual mice are omitted for clarity. N=4 per group. Error bars reflect standard error. (B) Mice were implanted with ALZET 1003 osmotic minipump containing a solution of 50mg/mL **2** in D5W. A one time intraperitoneal injection of 40mg/kg **2** was then administered. Blood was collected 30m after the one time injection, and then once per day subsequently. Ghrelin species were quantified normally.

To address the first point, we administered the compound in two alternative fashions intended to provide a more sustained effect. Inhibitor **2** was administered by oral gavage at 160mg/kg. Given the rapid response we had seen during IP dosing, we monitored the mice for one hour in this experiment. Compound **4** was included in this experiment at the same dose as a negative control. Unfortunately, even at these very doses of **2**, no effect was observed on acyl ghrelin levels or fraction. We speculated that our inhibitors were poorly absorbed across the gastrointestinal tract. One method to circumvent poor GI absorption but also generate a sustained serum concentration of inhibitor would be to directly infuse inhibitor using osmotic mini-pumps. Using the maximum possible dose obtainable using this technology of $48 \text{ mg}\cdot\text{kg}^{-1}\cdot\text{day}^{-1}$ of **1** we were unable to discern any difference between mice dosed only with vehicle and those treated with inhibitor **1** (figure 4.11B).

4.3 Observation of Lethargy in Mice Treated with GOAT Inhibitors.

We noted that, relative to untreated mice, mice treated intraperitoneally with 80mg/kg of GOAT inhibitors **1-3**, **19**, or negative control **4** became lethargic approximately ten minutes after the dose was administered. This effect persisted for roughly an hour, after which the mice recovered and became as active as their untreated counterparts. This effect was also observed in GOAT knockout mice treated with **2**. That this effect was observed in mice treated with negative control **4** as well as in GOAT KO mice, demonstrates that this is most likely the result of some off-mechanism toxicity. We have not yet identified the cause of this effect.

4.4 Pharmacokinetics of GOAT Inhibitors

To better understand the results of our in vivo experiments, we sought to evaluate the pharmacokinetic behavior of our inhibitors following administration. To do this, inhibitor concentration in the plasma of mice treated with 80mg/kg of IP **2** and **3** was evaluated. To evaluate the GI permeability of our compounds, we collected plasma from mice dosed with 80mg/kg of PO **2**. Inhibitor quantification was performed using standard LC/MS/MS analyses. The results of these experiments are shown in figure 4.12A and 4.12B. Following intraperitoneal administration of **2**, we observed high initial concentrations of inhibitor of nearly 10,000 ng/mL, which decayed with a $t_{1/2}$ of 32 minutes (figure 4.12A). Inhibitor is absorbed when the compound is administered orally,

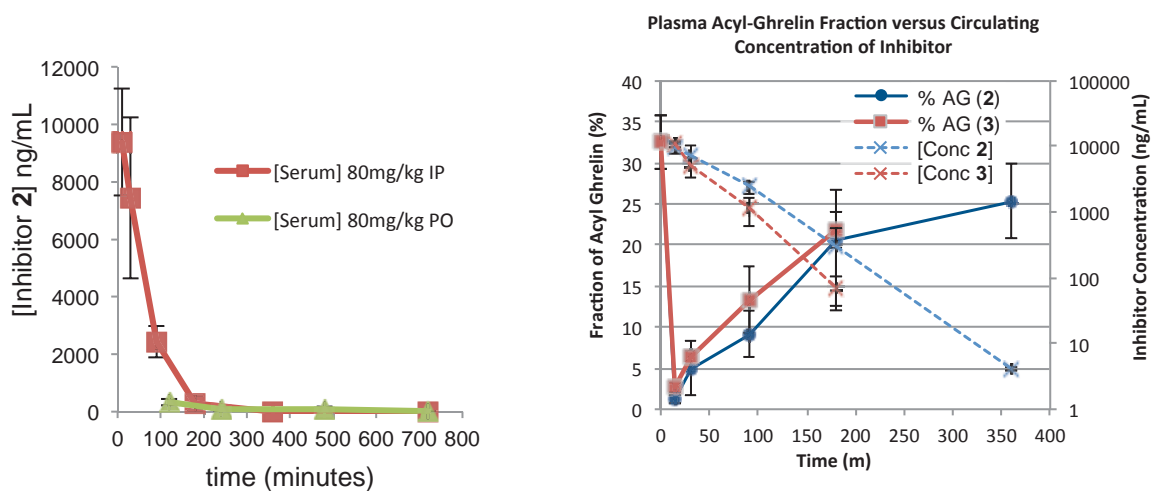


Figure 4.13: Serum concentration of GOAT inhibitors following dosing. (A) The concentration of GOAT inhibitor in mouse plasma or stomach tissue following IP or PO dosing was quantified using standard HPLC/MS/MS. (B) Comparison of plasma acyl-ghrelin fraction and inhibitor concentration.

though to a substantially lesser extent than following IP injection. This confirmed our hypothesis that **2**, and likely the other related inhibitors, are poorly absorbed through the intestine. Calculated AUC for both IP and PO dosing indicated that the relative %F (IP vs PO) was roughly 10%.

We observed a direct correlation between the acyl-ghrelin ratio in mice treated with **2** or **3** and the measured concentration of inhibitor (Figure 4.13B). These data, in conjunction with the similar in vivo performance of inhibitors **1-3** and **22**, suggested that each inhibitor was cleared quickly, possibly by the same mechanisms, given their very similar structures. It was, therefore, critical to evaluate the routes of clearance of GOAT inhibitors.

Following entry to the blood stream, the fate of a small molecule in vivo is canonically governed by the rates with which it is distributed, metabolized, and excreted.¹⁶ We aimed to determine which of these routes was responsible for the rapid clearance of our inhibitors from circulation. We first examined potential metabolic degradation of the inhibitor. Prior to evaluating GOAT inhibitors **1-3** in vivo, we had examined the stability of inhibitors **1** and **2** to in vitro models of metabolism (Figure 4.14A).¹⁷¹⁸ These data suggested that both these compounds were acceptably stable in liver S9 fraction, which is a standard model of phase I hepatic metabolism, and to murine serum, which is considered representative of proteolytic metabolism. However, in vitro PK may not be predictive of in vivo results. These results were revisited, and likely degradation pathways considered.

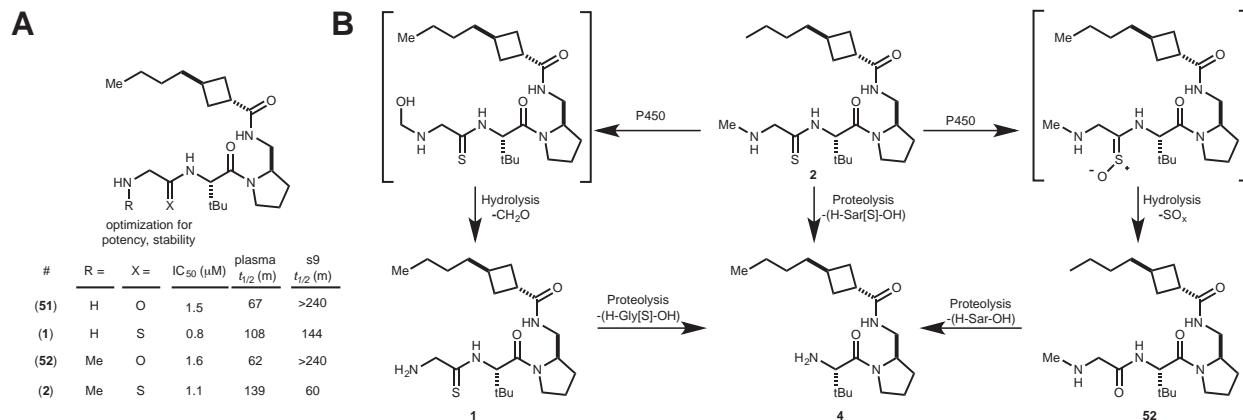


Figure 4.14: Metabolic stability of GOAT inhibitors. (A) Summary of in vitro pharmacokinetic evaluations of inhibitors **1** and **2** as well as the amide analogs **51** and **52**. (B) Potential pathways for the conversion of **2** into **4**.

For peptidyl molecules such as **2** the most likely metabolic pathways would be proteolytic (ie. hydrolysis of an amide bond) or oxidative. Several possible routes of metabolism were considered (Figure 4.14B). First, *O*- and *N*-methylated drugs are often de-alkylated oxidatively via a hydroxymethyl intermediate and loss of formaldehyde.¹⁹ In this case, the product of such an oxidation would be primary amine lead compound **1**. An alternative pathway might be oxidative desulfurization of the thioamide. Thioamides are known to be susceptible to oxidative degradation, and then the mechanism of this process has been studied.²⁰ The thioamide moiety may be oxidized at sulfur to an *S*-oxide or -dioxide type intermediate, rendering the thiocarbonyl electrophilic. These oxidized species may then react with nucleophiles such as glutathione or be hydrolyzed to the amide. The latter occurs rapidly in the case of a marketed thioamide-containing drug, Quazepam.^{21, 22} A comparison of the S9 stability of thioamides **1** and **2** relative to amides **51** and **52** (figure 4.13A) suggests that oxidation of the thioamide probably does

occur for these compounds. In the case of **2**, oxidative hydrolysis per this mechanism would likely result in the formation of amide inhibitor **52**.

A third likely metabolic pathway could be cleavage of the glycine or sarcosine residue. Proteolysis of **1**, **2**, or **52** would each generate negative control **4**. Both thionation and *N*-methylation are expected to reduce the rate of this cleavage,^{23, 24, 25} and our in vitro data suggested that the thioamide modification reduced the rate of proteolytic degradation relative to amide congener **52**.

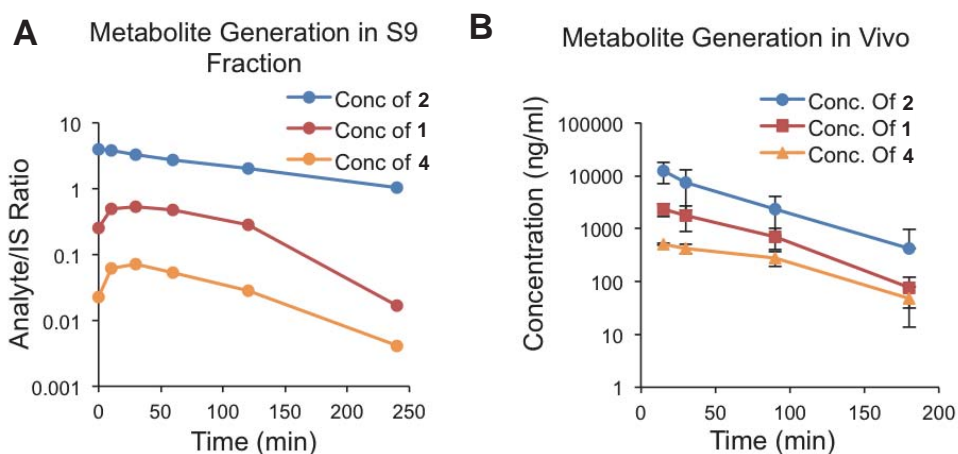


Figure 4.15: Quantification of select degradation products. (A) The indicated metabolites generated during liver S9 digestion in vitro were quantified by LC/MS/MS. (B) These same metabolites were identified in murine plasma following administration of compound **2**.

To gain information about the relative rates of these potentially competing metabolic pathways, we determined the concentration of inhibitor **2**, demethylated metabolite **1** and inactive **4** in liver S9 fraction digests of **2**, murine plasma digests of **2**, and in serum from mice that had been dosed with **2** (80mg/kg IP). If cleavage of the thioamide bond by any of the three routes shown in figure 4.13B were a major route of metabolism, we would expect to observe accumulation of **4**. When incubated with

murine plasma, neither 1 nor 4 was generated to any appreciable extent (data not shown). By contrast, when inhibitor 2 was incubated with liver S9 fractions, we observed production of both 1 and 4 (Figure 4.15A). The peak concentration of 1 in this experiment was estimated to be ~300nM (relative to 2mM initial concentration of 1) and the peak concentration of 4 was ~40nM. In vivo, significant generation of both 1 and 4 was observed (Figure 4.15B). The concentration of 1 was roughly 20% the measured concentration of 2 at each time point, and 4 was detected at still lower concentrations. Neither 1 nor 4 accumulated significantly with time. While the metabolic degradation pathways outlined in figure 4.14B clearly contribute to the clearance of 2 from circulation, the data do not support the hypothesis that the observed rapid clearance of 2 from circulation results from degradation of the N-terminus.

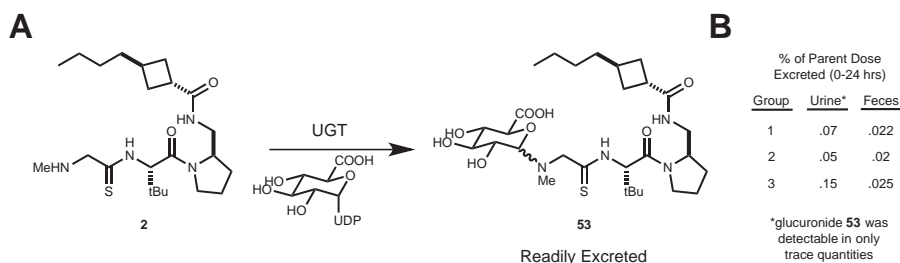


Figure 4.16: Glucuronidation and excretion of 2. (A) Glucuronic acid conjugate **53** may be formed by action of UGTs on **2**. (B) Quantitation of unmodified **2** in feces and urine from animals treated with **2**.

Glucuronic acid may be appended by UDP-glucuronosyl transferases (UGTs) to primary and secondary amines such as those found in **1** and **2**, generating a conjugate such as **53** (figure 4.15A).¹⁶ This conjugation renders the drug hydrophilic and promotes elimination in the feces or urine. We considered this pathway, as well as the possibility that the parent compound itself was readily excreted. In order to determine whether this

pathway was operative, mice were treated with inhibitor **2** (80mg/kg, IP) and the feces and urine were collected over 24 hours. These samples were then analyzed by LC/MS/MS to quantify the levels of **2** present as well as identify a potential glucuronic acid conjugate (figure 4.15B). Very little intact was **2** found in the feces or in urine. Trace amounts of glucuronic acid conjugate **53** were detectable by MS/MS, but only in very low abundance. These data suggest that excretion of intact inhibitor or its glucuronide do not contribute significantly to the clearance of GOAT inhibitor **2** from solution.

4.5 Membrane Permeability Assays

While performing preliminary pharmacokinetic analyses of our lead inhibitors, we also evaluated their efficacy in a cellular assay. Our collaborators Brown and Goldstein had developed a line of rat INS-1 cells that stably expressed ghrelin and GOAT.²⁶ Cells of this lineage were incubated with inhibitor **2** and the levels of acyl ghrelin and total ghrelin were evaluated by western blotting. In the presence of **2**, acyl-ghrelin production was inhibited with an apparent IC_{50} of $2.5\mu M$ (Figure 4.17). Negative control **4** had no apparent effect on acyl ghrelin production. As a counter-screen for cytotoxicity or off-target effects, we also evaluated the production of total ghrelin in these same samples. Neither **2** nor **5** affected total ghrelin production in this assay.

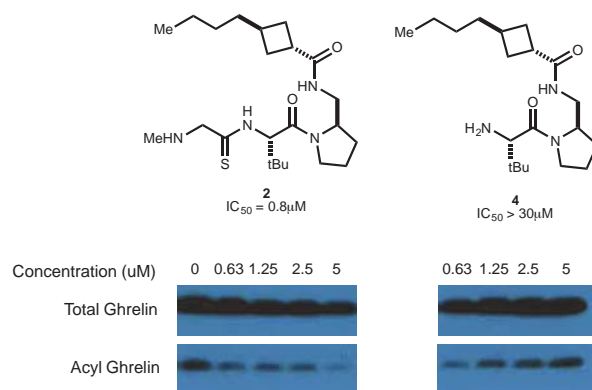


Figure 4.17: Activity of lead inhibitor 2 and negative control 4 in a cellular (INS-1) assay format.

While these compounds were effective in cell culture, we noted the roughly five-fold decrease in potency for the cell-based assay relative to the in vitro IC_{50} . While this could be caused by degradation of the compound in the assay mixture, our in vitro analyses of metabolic stability suggested that this was unlikely. GOAT is known to be embedded in the endoplasmic reticulum of expressing cells, so to reach the active site of GOAT an inhibitor would need to penetrate the outer cellular membrane. An alternative explanation for the divergence between cellular and in vitro efficacies was that the compound suffered low membrane permeability.

The passage of a hydrophobic small molecule from one aqueous phase to another via a lipid membrane is complex and much studied process (Figure 4.18A).²⁷ The major barrier to permeability is the requirement for the small molecule, which is solvated by an ordered shell of many water molecules, to desolvate prior to entering the lipid phase. To enter the second aqueous phase, the molecule must then break numerous hydrophobic interactions, substituting them for water molecules. Depending on the nature of the small molecule, either of these processes can be rate limiting. For a

given small molecule, membrane permeability depends strongly on the overall lipophilicity (ie. LogD). Numerous studies have demonstrated a strong correlation between LogD and favorable membrane permeability.²⁸ We experimentally determined a LogD value for **2** of 1.8 at pH 7.2, indicating that our compound was within the advocated range and should be membrane permeable.²⁹ We sought to confirm this prediction experimentally.

4.6 PAMPA Measurement of Inhibitor Permeability

Numerous methods have been developed to evaluate the membrane permeability of small molecules in vitro. Two of the most important methods, particularly in medicinal chemistry applications are Parallel Artificial Membrane Permeability Assay (PAMPA) and Caco-2 colorectal epithelial monolayers. 30, 31, 17 PAMPA relies on the construction of a cellular membrane surrogate, usually consisting of a phospholipid dissolved in a long chain hydrocarbon and immobilized on solid support. The artificial membrane is then sandwiched between two buffer solutions and a test compound introduced on one side of the setup. The rate of passive diffusion across the membrane can then be quantified by HPLC-MS/MS or UV spectroscopy. Permeability in a PAMPA format is well correlated with LogD and with permeability across biological membranes including cellular membranes and the GI tract. Poor permeability in a PAMPA format would suggest that inhibitor **2** was poorly cell permeable in the INS-1 cell based assay described previously.

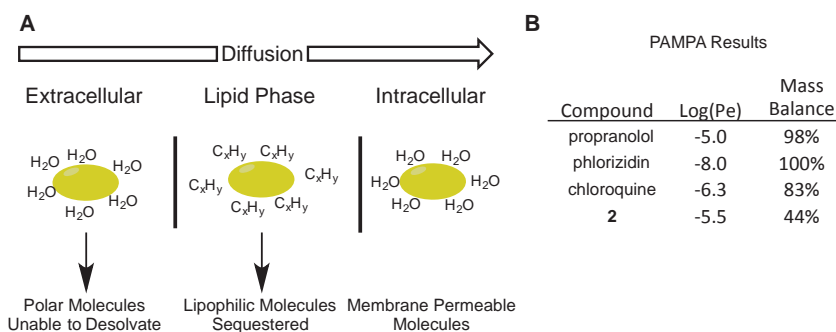


Figure 4.18: Membrane permeability considerations for small molecules. (A) Schematic of necessary events for transport of a small molecule across a lipid membrane. (B) Results of PAMPA analysis of control molecules and **2**. Results for control compounds closely match those reported in the literature.

To evaluate the PAMPA permeability of **2** we established the assay according to a published protocol.³⁰ Briefly, a 1% solution of lecithin in dodecane was added to the filter portion of a 96 well filter plate. The lipid layer was then sandwiched between a donor buffer containing test compound and a blank acceptor phase. Following an incubation period, UV absorbance of the donor and acceptor wells were recorded. PAMPA permeability coefficients and mass balance were computed according to standard formulae using external calibration of the drug UV absorbance. Propranolol, chloroquine, and phlorizidin were included as controls having high, moderate, and low permeability, respectively.

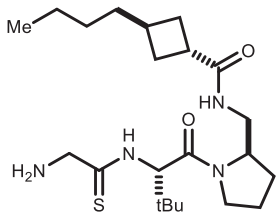
Results for all three control compounds (figure 4.18B) closely matched the literature values, suggesting that the assay was working properly.³² The PAMPA permeability coefficient (Log Pe) of compound **2** was ~-5.5, suggesting that the inhibitor was at least moderately permeable. However, only 44% of the mass could be accounted for in the donor solution and acceptor solutions. This result is common in PAMPA analyses and several common causes for the apparent apparent loss of mass

are possible. Precipitation of the inhibitor in the donor well is a frequent cause of mass loss. Alternatively, test compounds can adhere non-specifically to the plastic surfaces used for both the assay or analysis, causing an apparent loss of material. Highly lipophilic compounds may be sequestered within the lipid phase. Though we did not attempt to characterize the mechanism(s) leading to low mass recovery, these PAMPA results anticipate that inhibitor **2** will be at least moderately cell permeable.

4.7 Cellular Model of Inhibitor Permeability

A frequent problem in the development of small molecule therapeutics is the ability of an organism to actively export xenobiotics from both cells and circulation.¹⁶ This function is generally performed by one of several families of transport proteins. While PAMPA flux is well correlated with cellular and GI permeability, by nature it can only evaluate the passive permeability of a small molecule. To evaluate the potential active transport susceptibility of GOAT inhibitors such as **2**, we utilized more sophisticated cell based systems. Monolayers of Caco-2 epithelial and Madin-Darby Canine Kidney (MDCK) cells are standard models of small molecule GI absorption.³² These cell lines natively express a variety of transport proteins. Generally the most important among these are the multidrug resistance protein (MDR1) and breast cancer resistance protein (BCRP), although there are many closely related transporters that perform similar functions.¹⁶

Compound	Efflux Ratio (B to A / A to B) by Cell Line and Compound			
	Caco2	MDCK	MDCK (MDR1)	MDCK (BCRP)
2	1.0	4.5	30	1.2
Propranolol	0.7	0.5	0.4	0.5
Nadolol	2.0	4	2	3
Quinidine	1.5	6.7	70	n/d
Cimetidine	4.0	2.3	n/d	10



2

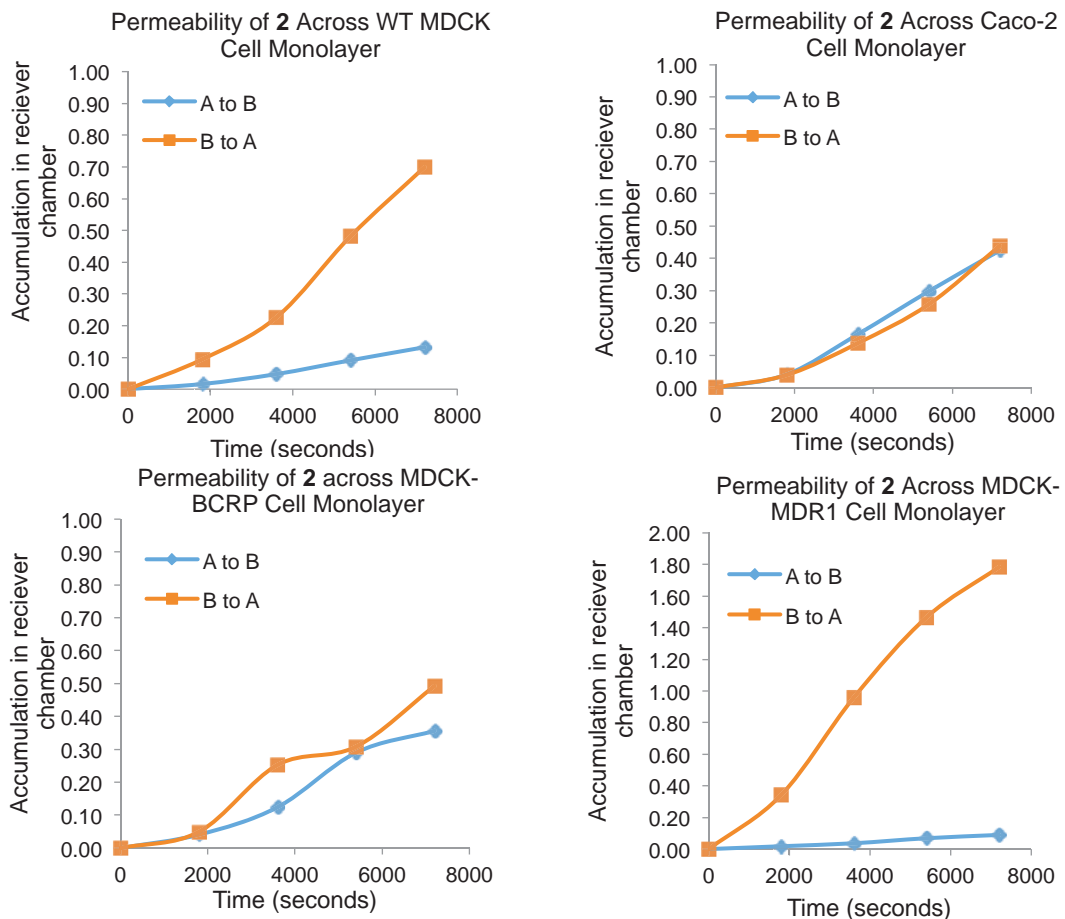


Figure 4.19: Membrane permeability in cellular assay formats. (A) Summary of results from cellular permeability experiments. Efflux ratio is a unitless value reflecting the relative rate of small molecule transport from the basolateral reservoir to the apical media. (B) Graphical representation of select data used to derive efflux ratios. Plots show accumulation of inhibitor in receiving well through time.

Caco-2 cells are derived from intestinal epithelia, and are often used to predict intestinal absorption/efflux. When grown on solid support, the resulting monolayers mimic the structure of the small intestine. Because our compounds are administered

intraperitoneally, GI absorption was not a principle concern. However, the transport proteins expressed in Caco-2 are also present in the kidney and liver. If our inhibitor was a substrate for these transport proteins, this could also which cause it to be rapidly transferred from the blood to feces or urine.³³ This could potentially account, at least in part, for the rapid clearance of our compound observed in vivo. MDCK cells are derived from kidney epithelium, and are potentially a good model for renal excretion of our inhibitors.

To examine the active transport properties of our compounds we determined the permeability of these compounds across standard Caco-2 monolayers, as well as a panel of WT, MDR1 overexpressing, or BCRP overexpressing MDCK cells.¹⁷ These assays make use of cellular monolayers grown to confluence across a polycarbonate membrane. It is important to note that both Caco-2 and MDCK cells form monolayers, with alternate faces of the monolayer mimicking the apical and basolateral portions of a membrane. Once confluence is confirmed, generally by measurement of the electrical resistance across the membrane, an analyte is introduced to either the apical or basolateral media reservoir. Compound transport can be determined by MS/MS based quantification of analyte concentration in the receptor portion of the setup. Transport directionality can be assessed by comparing the rates of transport in either direction across the membrane. We performed these analyses using inhibitor **1**, and found that it had intermediate permeability in all of the tested cell lines. This result mirrored the performance of **2** in PAMPA. In Caco-2 cells, there was no apparent directionality to the permeability of **1**, suggesting a lack of active transport. However, in wild type MDCK cells, we observed significantly faster export (B → A) than import (A → B) of the

inhibitor. This was magnified in MDCK cells overexpressing MDR1, but not in cells overexpressing BCRP, suggesting that **1** is a substrate for MDR1, but not for BCRP. These results are similar to those obtained for control compound quinidine, a known substrate of MDR1, but not cimetidine, which is a known substrate of BCRP. We conclude that **1** is a substrate for MDR1, though the physiological significance of this finding, and its relevance to the short in vivo half-life we observe, is not yet known.

4.8 Inhibitor Plasma Binding

When in circulation through the bloodstream, small molecule drugs may exist as free fully solvated molecules, or they may be bound non-covalently to plasma proteins, such as albumin. Protein-bound drug is sequestered and unavailable to diffuse across cellular membranes or to act at its target, and is also unavailable for hepatic metabolism or renal excretion. Balancing these considerations is critical, as a compound that is poorly bound is likely to be rapidly cleared, whereas a compound that is too tightly bound it is not available to act on its target. Plasma protein binding is driven primarily by non-specific hydrophobic interactions, which is closely correlated to LogD for a given small molecule. We measured the plasma protein binding for a set of closely related but increasingly hydrophilic GOAT inhibitors (figure 4.16)

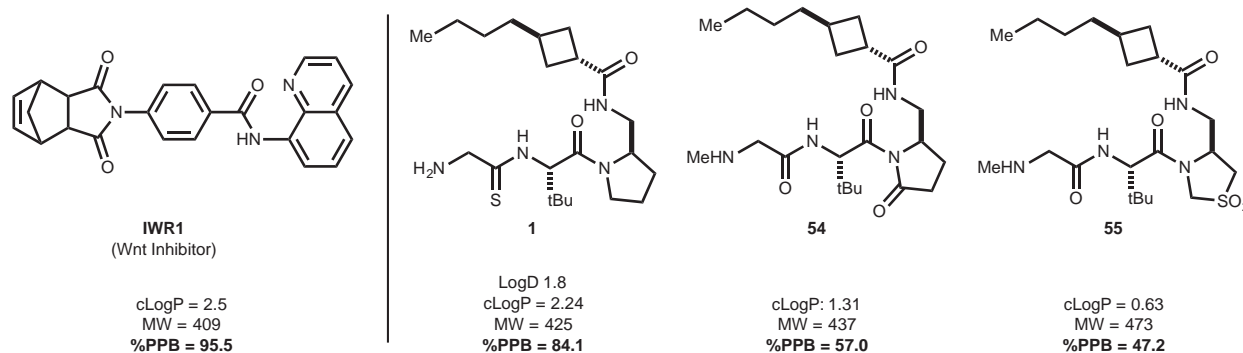


Figure 4.20 Percentage of GOAT inhibitors bound to protein in murine plasma. IWR1, an MBOAT inhibitor with good in vivo activity and has a significantly higher bound fraction, is included for reference.

As expected, the fraction of small molecule bound to plasma was well correlated with logP. Most critically, we found that **2** was 84% plasma bound. While it is difficult to directly compare isolated PK parameters between targets, we considered this value to be below optimal. IWR1, which is a small molecule inhibitor of the MBOAT Wnt, serves as a useful comparison and is >95% plasma bound. The fairly direct correlation between plasma protein binding and small molecule clearance suggests that future GOAT inhibitors may benefit from increased lipophilicity if possible.

4.9 Conclusions

We have developed the first class of small-molecule GOAT inhibitors with in vivo activity. We consistently observe rapid clearance of acyl-ghrelin from mice treated with GOAT inhibitor. Present generation inhibitors are limited by their short half-life in serum. Efforts to identify the cause of rapid inhibitor clearance have met with limited success, but efforts are presently underway to identify new chemical entities with improved

pharmacokinetic performance. We are also exploring new inhibitor formulations that have the potential to dramatically extend the window of efficacy.

-
- 1 Shalaby MA, Grote CW, Rapoport HJ (1996) Thiopeptide Synthesis. alpha-Amino Thionoacid Derivatives of Nitrobenzotriazole as Thioacylating Agents. *J. Org Chem.* 61(25):9045-9048.
 - 2 Jesberger M, Davis TP, Barner L (2003) Applications of Lawesson's Reagent in Organic and Organometallic Syntheses. *Synthesis* 2003(13):1929-1958.
 - 3 Frank R, Schutkowski, M (1996) Extremely mild reagent for Boc deprotection applicable to the synthesis of peptides with thioamide linkages. *Chem. Commun* 1996(22):2509-2510.
 - 4 Brown DW, Campbell MM, Chambers MS, Walker CV (1987) Mono- and dithiopeptide synthesis. *Tetrahedron Lett.*, 28(19):2171-2174.
 - 5 Clausen K, Thorsen M, Lawesson SO, Spatola AF (1984) Studies on amino acids and peptides. Part 6. Methods for introducing thioamide bonds into the peptide backbone: synthesis of the four monothio analogues of leucine encephalin. *J. Chem. Soc., Perkin Trans. 1.* 0:785-798.
 - 6 Moody CJ. *Comprehensive Organic Functional Group Transformations*, Volume 5. (Elsevier Scicne Inc. Tarrytown, New Jersey).
 - 7 Carpino LA, Tsao JH, Ringsdorf H, Fell E, Hettrich G (1978) The β -(trimethylsilyl)ethoxycarbonyl amino-protecting group. *J. Chem. Soc., Chem. Commun*, 1978(8):358-359.
 - 8 Middleton WJ (1985) *Org. Synth* 64:221.
 - 9 Carpino LA, Sau AC (1979) Convenient source of 'naked' fluoride: tetra-n-butylammonium chloride and potassium fluoride dehydrate. *J. Chem. Soc., Chem. Commun.*, 1979(11):514-515.
 - 10 Stahl PH, Wermuth CG ed. *Handbook of Pharmaceutical Salts: Properties, Selection and Use*, (Wiley-VCH, New York, New York).
 - 11 Wuts PGM, Greene TW *Greene's Protective Groups in Organic Synthesis*, Fourth Edition. (John Wiley & Sons, Inc. Hoboken, New Jersey).
 - 12 Lemaire-Audoire S, Savignac M, Blart E, Pourcelot G, Genêt JP, Bernard JM (1994) Selective deprotective method using palladium-water soluble catalysts. *Tetrahedron Lett.* 35(47)8783-8786.
 - 13 Song XN; Yao ZJ (2010) Short asymmetric synthesis of (S,S)-PDP using l-prolinol derivative as economic starting material. *Tetrahedron.* 66(14):2589-2593.
 - 14 Barnett BP, et al. (2010) Glucose and weight control in mice with a designed ghrelin O-acyltransferase inhibitor. *Science* 330(6011):1689-1692.
 - 15 Taylor MS, Hwang Y, Hsiao PY, Boeke JD, Cole PA. (2012) Ghrelin O-acyltransferase assays and inhibition. *Methods Enzymol.* 514:205-28.
 - 16 Lash, LH, ed. *Drug Metabolism and Transport: Molecular Methods and Mechanisms*. (Humana Press, Totowa, New Jersey).

-
- 17 Kang, YJ ed. Optimization in Drug Discovery: Methods in Pharmacology and Toxicology (Humana Press, Totowa, New Jersey).
 - 18 Kerns EH, Di L. Drug-Like Properties: Concepts, Structure Design and Methods from ADME to Toxicity Optimization (Elsevier, New York, New York).
 - 19 Guengerich FP (2001) Common and uncommon cytochrome P450 reactions related to metabolism and chemical toxicity. *Chem Res Toxicol* 14(6):611–650.
 - 20 Hanzlink RP, Cashman JR, Traiger GJ. (1980) Relative Hepatotoxicity of Substituted Thiobenzamides and Thiobenzamide-S-oxides in the Rat. *Toxicol. Appl. Pharmacol.* 55(2):260-272.
 - 21 Miura M, Ohkubo T. (2004) In vitro metabolism of quazepam in human liver and intestine and assessment of drug interactions. *Xenobiotica.* 34(11/12):1001–1011.
 - 22 Zampaglione N, Hilbert JM, Ning J, Chung M, Gural R, Symchowicz S. (1985) Disposition and metabolic fate of ¹⁴C-quazepam in man. *Drug Metab Dispos.* 13(1):25-29.
 - 23 Chatterjee J, Gilon C, Hoffman A, Kessler H (2008) N-Methylation of Peptides: A New Perspective in Medicinal Chemistry. *Acc. Chem. Res.* 41(10):1331-1342.
 - 24 Zhang W, et al. (2010) A novel analog of antimicrobial peptide Polybia-MPI, with thioamide bond substitution, exhibits increased therapeutic efficacy against cancer and diminished toxicity in mice. *Peptides.* 31(10):1832-8.
 - 25 Zacharie B, Lagraoui M, Dimarco M, Penney CL, Gagnon L (1999) Thioamides: synthesis, stability, and immunological activities of thioanalogues of Imreg. Preparation of new thioacylating agents using fluorobenzimidazolone derivatives. *J Med Chem.* 42(11):2046-52.
 - 26 Yang J, Brown MS, Liang G, Grishin NV, Goldstein JL (2008) Identification of the Acyltransferase that Octanoylates Ghrelin, an Appetite-Stimulating Peptide Hormone. *Cell* 132(3):387-396.
 - 27 Stein WD, Lieb WR. Transport and Diffusion Across Cell Membranes (Academic Press, Inc. New York, New York).
 - 28 Pade V, Stavchansky S (1998) Link Between Drug Absorption Solubility and Permeability Measurements in Caco-2 Cells. *J. Pharmacological Sciences.* 87(12):1604-1607.
 - 29 Lipinski CA, Lombardo F, Dominy BW, Feeney PJ (2001) Experimental and computational approaches to estimate solubility and permeability in drug discovery and development settings. *Adv. Drug Deliv. Rev.* 46(1-3):3-26.
 - 30 Kansy M, Senner F, Gubernator K (1998) Physicochemical High Throughput Screening: Parallel Artificial Membrane Permeation Assay in the Description of Passive Absorption Processes. *Journal of Medicinal Chemistry.* 41(7):1007-1010.
 - 31 Artursson P, Karlsson J (1991) Correlation between oral drug absorption in humans and apparent drug permeability coefficients in human intestinal epithelial (Caco-2) cells. *Biochemical and Biophysical Research Communications.* 175(3):880-885.
 - 32 Kerns EH, Di L, Petusky S, Farris M, Ley R, Jupp PJ (2004) Combined application of parallel artificial membrane permeability assay and Caco-2 permeability assays in drug discovery. *Pharm Sci.* 93(6):1440-53.

33 Karyekar CS, Eddington ND, Garimella TS, Gubbins PO, Dowling TC (2003) Evaluation of P-glycoprotein-mediated renal drug interactions in an MDR1-MDCK model. *Pharmacotherapy*. 23(4):436-42.

Experimental Appendices

Experimental Procedures Supporting Chapter 2

The protocols related below are derived from those originally developed and provided to us by Dr. Tongjin Zhao, in the lab of Dr. Michael Brown and Dr. Joseph Goldstein at UTSW Med Ctr. The GOAT containing pFASTBAC plasmid and the pGEX ghrelin plasmid were also gifts from the Brown/Goldstein group.

GOAT Membrane Preparation

A. Transformation

Summary: Small bacterial plasmid, pFASTBAC1 with cloned mouse GOAT cDNA is transformed using a standard method into DH10Bac (special for baculovirus construction) where it recombines via site-specific transposition into large bacmid (130 kbp) DNA already present in the cells. Gentamicin resistant phenotype along with Blue/white selection on Bluo-gal is used to select positive transformants. Target cells should be Gent/Kan/Tet resistant and appear white on Bluo-gal/IPTG media.

- 1) Prepare 500mL of LB with agar
 - 500mL 1X LB Media
 - 7.5g Agar
- 2) Autoclave
- 3) Once cool enough to handle, prepare 2x50mL in 50mL Falcon tubes
- 4) To each tube add
 - 750uL of 20mg/mL BluoGal in DMSO
 - 100uL of 40mg/mL IPTG
 - 25uL of 100mg/mL Kanamycin
 - 10uL of 50mg/mL Tetracyclin
 - 17.5uL of 20mg/mL Gentamycin
- 5) Pour into standard Petri dish plates (should afford 6-8 plates) and allow agar to solidify for a few hours.
- 6) Thaw on ice one vial of DH10Bac E. Coli competent cells (Invitrogen) from -80C.
- 7) Chill one 5mL culture tube on ice
- 8) Thaw one vial of SOC Media at rt
- 9) Transfer thawed cells to 5mL culture tube, then add 1uL of FASTBAC1-mouseGOAT plasmid
- 10) Incubate on ice for 30 min
- 11) Heat shock at 42C for 45s (duration matters)
- 12) Place on ice and incubate for 2 min
- 13) Add 900uL SOC media and shake at 37C for 4h.
- 14) Place culture at room temperature, and prepare 10-fold serial dilutions with LB media (no antibiotics) as follows
 - 1x 100uL of 1:10
 - 2x 100uL of 1:100 (because this is the most useful one, usually)
 - 1x 100uL of 1:1000

Remaining cells can be discarded.

15) Pipette dilutions onto plates prepared above and distribute with autoclaved glass beads

16) Cover agar plates with aluminum foil and incubate at 37C for 2 days.

This strain grows slower than some others, and blue/white selection can be subtle. Growing in dark seems to help. If color is not clear after 2 days, try growing at 4C for a few days. Color will eventually appear.

17) After color appears, select at least nine white colonies and one blue. Restreak onto quadrants of plates prepared above to reconfirm color selection.

B. Isolation of Bacmid DNA

Summary: a small (4mL) culture of DH10Bac/mouseGOAT is grown in LB media supplemented with antibiotics (Gen/Kan/Tet – see above) and the Bacmid DNA is isolated using standard molecular biology techniques.

Buffer I

50mL 1M Glucose
25mL 1M Tris HCl PH 8.0
20mL 0.5M EDTA pH 8.0
Dilute to 1000mL filter sterilize

Buffer II

20mL 10M NaOH
20mL 20% W/V SDS
Dilute to 1000mL, filter sterilize

Buffer III

60mL 5M KOAc
11.5mL AcOH
28.5mL H₂O
Filter sterilize

1) From either original plate or restreaked plate, grow overnight cultures in 4mL Kan/Gent/Tet media

For 50mL

50mL 1x LB
25uL of 100mg/mL Kanamycin
10uL of 50mg/mL Tetracyclin
17.5uL of 20mg/mL Gentamycin

2) Take 2mL of overnight culture and pellet cells at 14,000g x 1m.

- 3) Remove supernatant
- 4) Resuspend pellet in 250uL of buffer I by pipette.
- 5) Add 500uL of buffer II, mix by inversion, incubate at rt for 5m. (Cell lysis)
Add 375uL of buffer III, white precipitate forms. Incubate at rt for 10m then centrifuge at 14000g x 10m.
- 6) Transfer 1mL of supernatant (carefully avoid solids sticking to pipette) to 1mL of cold isopropanol. Incubate on ice for 10m then centrifuge at 14,000 g x 15m.
- 7) Remove supernatant, then add 0.5mL of 70% EtOH to wash. Wash by inversion (do not dislodge pellet) then centrifuge 14000g x 5m and remove supernatant. Blot dry, then air dry, then vacuum dry to remove any EtOH. When dry, resuspend in 50uL H₂O (NO VORTEX! DO NOT FREEZE!)

Solution should be entirely clear at this point. Remove any remaining insoluble material by centrifugation and reserve DNA containing supernatant. Quantity and quality of the resultant DNA can be estimated by measuring A₂₆₀ in a nanodrop instrument.

- 8) DNA should be stored at 4C and used quickly for Sf9 transfection.

C. Transfection

Summary: Bacmid DNA generated above is transfected into Sf9 insect cells using a transfection reagent. The bacmid DNA bears all necessary genes for viral amplification in insect cells. The transfection of bacmid DNA leads to expression of all viral protein components along with GOAT gene inserted into the virus genome.

- 1) For each Bacmid isolate to be transfected, prepare two wells of a six well plate containing 0.9×10^6 Sf9 cells in 2mL of media. Allow cells to attach for 1h.
- 2) While they attach prepare solutions of Cellfectin II reagent and DNA in sf900 media. Prepare 1ug/uL (A₂₆₀) solutions of DNA in sf900 media.
For each well, prepare 8uL of cellfectin in 100uL of media
For each well, prepare 1ug of DNA in 100 uL of sf900 media
- 3) Mix these two solutions (DNA binds to transfection reagent). Incubate at rt for 45m. In addition, prepare control solutions containing DNA (1ug/200uL) only and cellfectin only. (8uL/200uL)

For example, using 8 bacmid isolates:

16 wells total, plus cells only, DNA only, and reagent only controls = 19 wells.

$2 \times 8 \times 8 + 8 = 136$ uL of cellfectin needed in 1700 uL media.

Prepared 140uL of cellfectin in 1.75mL media.

And 2uL of DNA in 200uL of media per isolate

Mixed to get 8×400 uL solutions of DNA/Reagent.

Also prepared 8uL cellfectin/200uL media control and 1uL DNA/200uL media control.

- 4) After cells have settled for 1h, remove the media from the cells and replace with 0.8mL of fresh media. Then add dropwise 200uL of the DNA/Celfectin complex per well. Swirl gently to mix, then incubate at 27C for 5h. Wrap in parafilm to prevent dehydration.
- 5) Remove the media containing transfection reagent and add 2mL fresh media. Rewrap in parafilm.
- 6) After ~96h, recover the supernatant by pipette. This contains P1 virus. All viral stocks should be stored at 4C in the dark to protect the viral particles.

D. Amplification

P2 Generation

- 1) In a 6 well plate allow 2×10^6 cells/well to attach in 2mL of media (~20m). To these cells add 500uL. of p1 viral stock.
- 2) After 72h, harvest p2 viral stock. To each well add 400uL of lysis buffer

For 100mL of lysis buffer
100mL H₂O
981 mg Tris HCl
10mL of 20% SDS
pH to 6.8

- 3) Scrape each plate with cell scraper to detach cells. Pipette lysate into 1.5mL tube and store at -80 before analysis by Western Blot.

P3 Generation

- 1) Set up 50mL of Sf9 cells (in suspension) at 0.9×10^6 cells/mL.
- 2) Add 2.25mL of P2 virus (because of the way p2 expression was done, this uses most of the virus generated). Values used are based on a theoretical viral titer in P2 of 1×10^7 and MOI of 0.5.
- 3) After 72h, harvest supernatant by centrifugation of the culture at ~4000g x 10m (ensure that media is clear and cells are pelleted).
- 4) An aliquot of cells can be lysed and analyzed by Western.

E. Final Expression and Membrane Prep

- 1) Set up culture of 250mL Sf9 cells at 1×10^6 cells/mL. To this add 25mL of P3 virus (from large scale P3). Theoretically, this is an MOI of 10.
- 2) After 72h, harvest supernatant by centrifugation of the culture at $\sim 4000g \times 10m$ (ensure that media is clear and cells are pelleted).
- 3) Prepare Lysis Buffer (DO NOT USE DETERGENTS)

Lysis Buffer is

50mM Tris,
150mM NaCl
1mM EDTA
1mM DTT
10ug/ml pepstatin
10ug/ml leupeptin
5ug/ml aprotinin
100ug/ml bis(4-nitrophenyl) phosphate(BNPP)
1x diethyl *para*-nitrophenyl phosphate (from 1000x stock).

- 4) Cells from 1L of culture were resuspended in 50 mL of buffer and lysed by Douncer on ice for 50 strokes. The lysate was centrifuged at 3000g for 5m to pellet cellular debris.
- 5) This gives a cloudy/yellow supernatant, which is transferred to ultracentrifuge tubes.
- 6) Spin at 100,000g for 1h. This clarifies the solution and provides pelleted membranes. The supernatant can be discarded.
- 7) The membrane pellet is resuspended in 10 ml of storage buffer: 50mM NaPi pH 7.5, 150 mM NaCl and 5% w/v glycerol by douncer (10 strokes).
- 8) Flash freeze membrane suspension with liquid nitrogen and store at $-80C$ until use. The membrane suspension can be freeze/thawed several times without any detectable loss of GOAT enzyme activity activity of GOAT enzyme.

Ghrelin Production

A. Transformation

Construct used is GST-TevCleavageSite-Proghrelin-His8.

- 1) Remove 3 prepared Ampicillin plates from cold room
- 2) Thaw on ice BL21 DE3 (pLys) competent cells

- 3) Chill one 5mL culture tube on ice
- 4) Thaw one vial of SOC Media at rt
- 5) Transfer thawed cells to 5mL culture tube, then add 1uL of GST-TevCleavageSite-Proghrelin-His8
- 6) Incubate on ice for 30m
- 7) Heat shock at 42C for 45s
- 8) Incubate on ice for 2m
- 9) 300uL SOC media added and shake at 37C for 1h
- 10) Plate cell suspension on LB agar plate with ampicillin
- 11) Incubate culture at 37C overnight

B. Expression and isolation of Ghrelin

Summary: Protocol for expression and purification of ghrelin from the previously generated E. coli.

- 1) Inoculate 3 ml LB + Amp + Cam with a few colonies directly from agar plate. Grow culture at 37C for 6 hours and use 1 ml to inoculate 100 ml LB + Amp + Cm. Grow 200 ml culture overnight at 37C.
- 2) In the morning, inoculate 1Lx6 of LB +Amp with 10 ml overnight culture. Incubate at 37C with vigorous shaking for ~4h. When OD600 reached 0.6-0.8 place cultures on ice for 30 min. Add 0.25 mM IPTG and grow cultures at 18C overnight. Harvest cells and resuspend pellet in lysis buffer (see 3) for immediate use or store pellets in -20C for later use.
- 3) Prepare 100mL of Lysis buffer (20mM Tris, 150mM NaCl, 1mM EDTA, 1mM DTT, 1mg/mL lysozyme, pH = 7.5).
- 4) Sonicate cells. Spin at 18000x for 30 min to pellet cellular debris, then recover the supernatant.
- 5) Prepare 4-5mL of glutathione Agarose resin (Fisher) by pipetting 10mL of slurry into a 25mL chromatography column. Equilibrate resin with 5 column volumes of lysis buffer.
- 6) All chromatography step are performed in a cold room. Pour the supernatant from

step 4 into the column. Allow fusion protein to bind via gravity flow.

- 7) Wash with 50mL of lysis buffer.
- 8) Elute fusion protein with 25 ml lysis buffer with 15 mM reduced glutathione.
- 9) To eluate (contains GST-Ghrelin-His8) add 1 ml of GST-TEV protease (see protocol below) (3 mg/ml). Incubate at 16C overnight.
- 10) Equilibrate 2.5 ml bed volume Ni-NTA (Qiagen) resin with buffer containing 20 mM Tris pH 7.5, 150 mM NaCl.
- 11) Bind proghrelin-His8 on Ni-NTA via gravity
- 12) Wash with 75 ml of 20 mM Tris pH 7.5, 150 mM NaCl, 40 mM Imidazole.
- 13) Elute with 20 mM Tris pH 7.5, 150 mM NaCl, 250 mM Imidazole.
- 14) Dialyze against 10 mM Tris pH 8.5/50 mM NaCl/10% w/v glycerol/0.01 % CHAPS
- 15) Concentrate on Amicon filter device (Fisher) with 3,000 Da cutoff
- 16) Analyze purity of ghrelin by SDS-PAGE w/ Coomassie staining.

GOAT Activity Assay

A. Prepare buffers for the reaction

Reaction Buffer
50mM HEPES pH 7.0

Quench buffer
50mM NaPi/150mM NaCl/10mM imidazole (pH = 7.5) with 0.1% Triton x-100

Wash Buffer
50mM NaPi/150mM NaCl (pH = 7.5) with 40mM imidazole)

Elution Buffer
50mM NaPi/150mM NaCl (pH = 7.5) with 250mM imidazole

- 1) Readjust the pH after addition of imidazole (it will have changed).
- 2) Prepare 20x solutions of candidate GOAT inhibitor in 6% DMSO from the 10mM stock. (ie. to test an inhibitor at 20nM prepare a 400nM stock solution).

- 3) Prepare a 10 mM solution of palmitoyl CoA in H₂O.
- 4) Thaw stock of ghrelin (see relevant section for prep).
- 5) Thaw GOAT containing membrane suspension.

B. Run And Quench Assays

- 1) To the prepared reaction tubes add the following, in order. At this point the reaction is time sensitive. Concentration of all components given as final:

HEPES – to final volume 47.5 ul
Membrane suspension – 50 ug/rxn (measured as total protein using BCA method)
Bis(4-nitrophenyl) phosphate(BNPP) – 100 uM
Palmitoyl CoA - 100uM
Proghrelin - 5ug/reaction (measured at A280/1.06 – ext coefficient)
2.5 uL 20X inhibitor solution

Final volume = 47.5uL

- 2) Ensure that the contents of the tube is mixed and at the bottom of the tube.
- 3) Remove the 20 uM ³H octanoyl CoA (5.5dpm/fmol) from the refrigerator and add 2.5uL of this solution directly to the reaction mixture
- 4) Upon completion of the additions, close all the tubes and transfer them to preheated block at 37C.
- 5) 10m after the 3H octanoyl CoA was added transfer the reactions back to ice.
- 6) Add 10 ul 1N HCl to each tube and mix.
- 7) Add 0.75 mL of quench buffer including 100 uM Bis(4-nitrophenyl) phosphate(BNPP) and 1 mM PMSF to each reaction.

C. Recover proghrelin and quantify acyl-transfer

- 1) To each tube add 200 uL of Ni-NTA pre-equilibrated with 10mM Imidazole/150mM NaCl/50mM NaPi, pH 7.5.
- 2) Incubate tubes for 1 hour with rotation in cold room to bind proghrelin-His8.
- 3) Pour content of each tube into separate disposable chromatography column.
- 4) Allow the solution to drain completely,

- 5) Add a final 1mL x 3 of wash buffer (40mM Imidazole/150mM NaCl/50mM NaPi, pH 7.5. Then allow it to drain completely.
- 6) Add 1mL of 250mM Imidazole elution buffer and collect into scintillation tubes. Allow this solution to drain completely.
- 7) Add 5mL of scintillation fluid shake until the solution is clear and count.

D. Data Processing:

Data can be plotted as either a straight count vs concentration or as a percent activity.
 $\%A = (\text{measured count} - \text{count with } 2\mu\text{M Ghrelin } 1\text{-}28 \text{ octanamide}) / \text{No inhibitor count} * 100$

Engineering and Production of GST-TEV

The gene for GST protein was sub-cloned with a Gibson assembly approach from pGEX-proghrelin into pMHT vector (ref: Paul G. Blommel, Brian G. Fox. A combined approach to improving large-scale production of tobacco etch virus protease. Protein Expression and Purification 55 (2007) 53–68). The pMHT plasmid was a kind gift from Dr. Arbing (UCLA). Primers were designed to replace the MBP gene from pMHT vector with a GST gene.

The resulted plasmid with GST-TEV(234D) was transformed into the BL21Gold E. coli strain and GST-TEV protein was produced as a following:

- 1) Inoculate 3ml LB+Kan with a few colonies
- 2) Grow at 37C with shaking for 6 hours
- 3) Inoculate 50 ml LB + Kan with 1 ml of culture from step 2
- 4) Grow at 37C with shaking overnight
- 5) Inoculate 4 x 1L LB with 10 ml of overnight culture
- 6) Grow at 37C with shaking for 4 hours or till OD600 ~ 0.8
- 7) Induce protein expression with 1 mM IPTG
- 8) Continue to grow for 4 hours at 37C
- 9) Harvest cells by centrifugation

- 10) Resuspend cell pellets from 4 L culture in 200 ml of lysis buffer
- 11) 25 mM Tris-HCl pH 8.0
- 12) 150 mM NaCl
- 13) 1 mM EDTA
- 14) 5% v/v glycerol
- 15) 1 mM DTT
- 16) 0.5 mg/ml lysozyme

- 17) Sonicate
- 18) Spin at 18,000 rpm for 30 min
- 19) Load supernatant on column with 3 mL bed volume of glutathione resin by gravity
- 20) Wash with 50 ml of lysis buffer (excluding DTT and lysozyme)
- 21) Elute with 25 ml of buffer from step 14 with 15 mM reduced glutathione
- 22) Dialyze against buffer containing 25 mM Tris-HCl pH 8.0, 50 mM NaCl and 50% w/v glycerol
- 23) After dialysis add 1 mM DTT and store -20°C
- 24) Measure protein concentration using nanodrop at A280 (use ext. coeff ~ 1.39 for GST-TEV fusion protein)

Experimental Procedures Supporting Chapter 3

General Procedures for Inhibitor Synthesis or Homologation

Amide Bond Formation

Unless otherwise noted, amide bond forming reactions were performed in acetonitrile or DMF at a concentration of 0.2-0.3M, using 2-3 equivalents of $i\text{Pr}_2\text{NEt}$ as base and 1.1-1.3 equivalents of either O-(Benzotriazol-1-yl)-N,N,N',N'-tetramethyluronium tetrafluoroborate (TBTU) or 1-[Bis(dimethylamino)methylene]-1H-1,2,3-triazolo[4,5-b]pyridinium 3-oxid hexafluorophosphate (HATU) as coupling reagents. Reactions were initiated by addition of coupling reagent to the other reaction components, and stirred at room temperature until the reaction was complete, as monitored by TLC or HPLC. Once complete, the reaction was quenched by addition of the reaction solution to 1N HCl (for products lacking basic functionality) or NH_4Cl (for products having a basic nitrogen). The aqueous phase was extracted three times with ethyl acetate, and the combined organic phases were washed with saturated sodium bicarbonate and brine. The organics were then dried over sodium or magnesium sulfate, then filtered, and the solvent removed in vacuo.

Boc-Deprotection

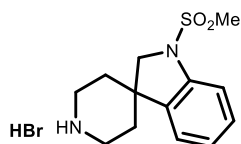
Unless otherwise noted, removal of a tert-butyloxycarbonyl (Boc) group was performed by dissolving the protected material in a solution of 4N HCl in dioxane. After the reaction was complete, the solution was concentrated to provide the hydrochloride salt of the product.

Cbz-Deprotection

Unless otherwise noted, removal of carboxybenzyl (Cbz) group was performed by dissolving the protected material in methanol. 10-20% (w/w) of palladium on carbon (Pd/C) or Palladium hydroxide on carbon ($\text{Pd}(\text{OH})_2$) was then added. The solution was then placed under a hydrogen atmosphere by evacuation of the head space followed by refilling with hydrogen three times. After the reaction was complete, the mixture was filtered over celite to remove catalyst, and then concentrated.

GHS/Ghrelin Hybrid Inhibitors

1-(methylsulfonyl)spiro[indoline-3,4'-piperidine] hydrobromide (**7**)

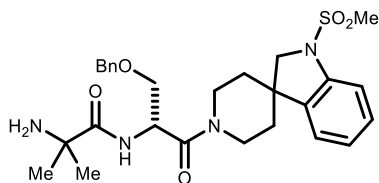


7 was prepared according to literature protocols. Recorded spectroscopic information closely matched reported data.

Ref: Maligres PE, et al. (1997). Synthesis of the orally active spiroindoline-based growth hormone secretagogue, MK-677. *Tetrahedron* 53(32):10983-10992.

^1H NMR (500 MHz, $\text{DMSO}-d_6$) δ : 8.6 (bs, 1H), 8.36 (bs, 1H), 7.27-7.21 (m, 2H), 7.16 (d, $J = 7.5$, 1H), 7.07 (td, $J = 1.9, 7$, 1H), 3.91 (s, 2H), 3.3-3.26 (m, 2H), 3.11-3.02 (m, 2H), 3.02 (s, 3H), 1.95 (td, $J = 4.0, 14.1$, 2H), 1.8 ($J = 14$, 2H)

(R)-2-amino-N-(3-(benzyloxy)-1-(1-(methylsulfonyl)spiro[indoline-3,4'-piperidin]-1'-yl)-1-oxopropan-2-yl)-2-methylpropanamide (**1**)



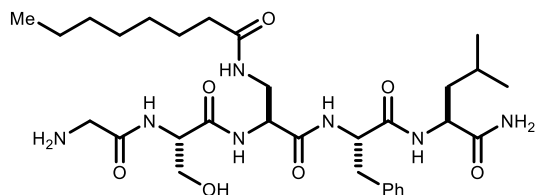
Ibutamoren (**1**) was prepared from **7** according to literature protocols (See ref above). Recorded spectroscopic information matched that reported in the literature.

1:1 rotamers present

^1H NMR (500 MHz, $\text{DMSO-}d_6$) 8.66-8.55 (m, 1H), 8.24 (bs, 3H), 7.36-6.93 (m, 9H), 5.02 (sextet, $J = 7.0$, 1H), 4.51 (s, 1H), 4.48 (quartet, $J = 11.4$, 1H), 4.36 (t, $J = 11.4$, 1H), 3.95-3.82 (m, 3H), 3.70 (ddd, $J = 6.7$, 9.7, 19.0, 1H), 3.63-3.52 (m, 1H), 3.19 (quartet, $J = 14$), 3.02 (app d, $J = 7.0$, 3H), 2.83-2.71 (m, 1H), 1.76-1.52 (m, 4H), 1.51-1.44 (m, 6H)

HPLC/MS: $M+1/Z$ Calcd = 529.2 Obsd. 529.3

N-((S)-3-(((S)-1-amino-1-oxo-3-phenylpropan-2-yl)amino)-2-((S)-2-(2-aminoacetamido)-3-hydroxypropanamido)-3-oxopropyl)octanamide (**4**)

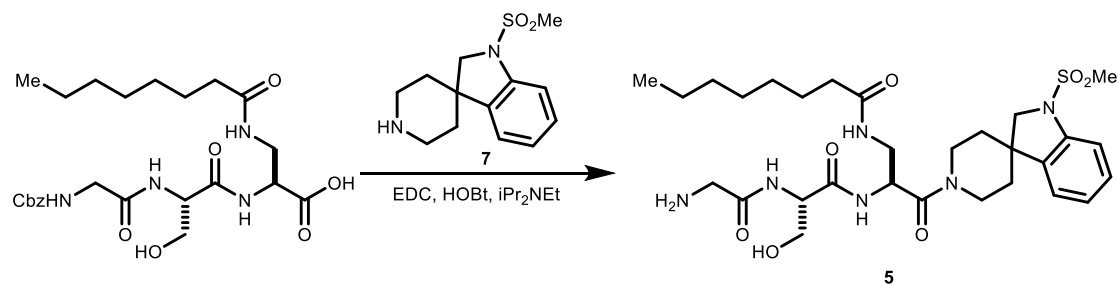


4 was prepared according to standard solid phase peptide synthesis methods using a Fmoc/Alloc protection scheme.

^1H NMR (500 MHz, $\text{DMSO-}d_6$) δ : 8.48 (d, $J = 8.0$, 1H), 8.21 (d, $J = 7.6$, 1H), 8.04 (d, $J = 7.8$, 1H), 7.93 (bs, 3H), 7.86 (d, $J = 8.3$, 1H), 7.25-7.13 (m, 5H), 7.0 (d, $J = 16.8$, 1H), 5.17 (bs, 1H), 5.06 (bs, 1H), 4.48 (ddd, $J = 6.1, 6.1, 7.8$), 4.43 (ddd, $J = 4.5, 8.0, 9.0$, 1H), 4.25 (quartet, $J = 6.7$, 1H), 4.17 (quartet, $J = 7.2$, 1H), 3.62-3.44 (m, 8H), 3.04 (dd, $J = 4.1, 13.8$, 1H), 2.77 (dd, $J = 9.25, 14.1$, 1H), 1.53 (septet, $J = 6.9$, 1H), 1.43 (t, $J = 7.5$, 2H), 0.86 (d, $J = 6.1$, 3H), 0.80 (d, $J = 6.3$, 3H).

HPLC/MS: $M+1/Z$ Calcd = 634.4 Obsd. 634.4

N-((S)-2-((S)-2-(2-aminoacetamido)-3-hydroxypropanamido)-3-(1-(methylsulfonyl)spiro[indoline-3,4'-piperidin]-1'-yl)-3-oxopropyl)octanamide (**5**)



5 was prepared from **7** (28.6mg, 0.094mmol) by reverse EDC mediated coupling to a N-terminal tripeptide, followed by Cbz-removal according to the general procedure.

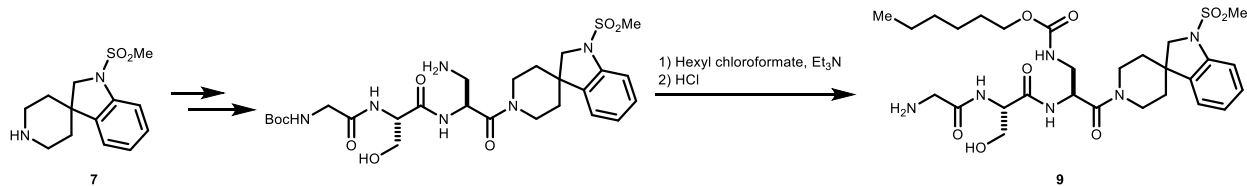
1H NMR (500 MHz MeOH- D_4) δ : 8.36-7.29 (m, 3H), 7.36-7.17 (m, 3H), 7.05-6.98 (m, 1H), 5.02-4.85 (m, 2H), 4.4-4.26 (m, 2H), 4.07-3.94 (m, 1H), 3.9 (s, 2H), 3.66-3.5 (m, 3H), 3.18 (t, $J = 11$, 1H), 2.79-2.68 (m, 1H), 2.06-1.93 (m, 2H), 1.73-1.56 (m, 3H), 1.48-1.37 (m, 2H), 1.26-1.12 (m, 8H), 0.85-0.77 (m, 3H).

^{13}C NMR (125 MHz MeOH- D_4) δ : 173.7 170.0 168.2 167.9 141.5 139.1 129.1 124.2 123.9 113.1 62.5 59.1 48.7 43.1 42.7 46.5 63.4 63.0 35.8 34.7 31.6 29.8 29.1 28.9 25.4 22.6 14.4

HPLC/MS: M+1/Z Calcd = 623.3 Obsd. 623.3.

Synthesis and Characterization of Carbamoyl GOAT Inhibitors

hexyl ((S)-2-((S)-2-(2-aminoacetamido)-3-hydroxypropanamido)-3-(1-(methylsulfonyl)spiro[indoline-3,4'-piperidin]-1'-yl)-3-oxopropyl)carbamate (**9**)



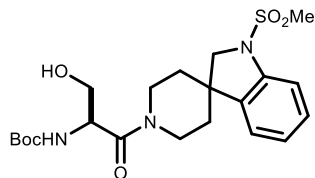
O-hexyl carbamate **9** was prepared by treatment of the corresponding DAP derivative (40mg, 0.067mmol) with hexyl chloroformate (23uL, 0.134uL) and triethylamine (23uL, 0.167mmol) in dichloromethane. Workup according to the general peptide procedure was followed by Boc deprotection according to the general procedure.

Rotamers (1:1) present.

¹H NMR (500 MHz MeOH-D₄) δ: 7.40 (dd, *J* = 2.42, 8.1, 1H), 7.37-7.23 (m, 2H), 7.12-7.06 (m, 1H), 5.11 (t, *J* = 6.3, 1H), 4.57-4.49 (m, 2H), 4.25-3.95 (m, 5H), 3.94-3.79 (m, 4H), 3.76 (t, *J* = 5.5, 1H), 3.69 (q, *J* = 5.5, 1H), 3.6 (t, *J* = 5.13, 1H), 3.53-3.45 (m, 1H), 3.44-3.37 (m, 1H), 3.01 (s, 3H), 2.97-2.85 (m, 1H), 2.19-1.74 (m, 4H), 1.74-1.58 (m, 2H), 1.46-1.26 (m, 6H), 0.96-0.87 (m, 3H).

HPLC/MS: M+1/Z Calcd = 625.3 Obsd. 625.3.

tert-Butyl (S)-(3-hydroxy-1-(1-(methylsulfonyl)spiro[indoline-3,4'-piperidin]-1'-yl)-1-oxopropan-2-yl)carbamate (**13**)

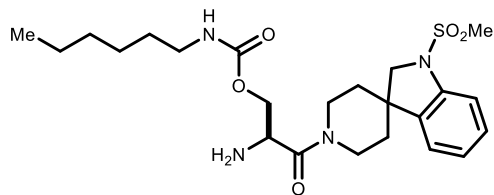


Amidation of **7** (142mg) with Boc-Serine according to the general protocol for amidation afforded **13** (187mg), which was used without further purification.

¹H NMR (500 MHz, CDCl₃) δ: 7.40 (d, *J* = 8.0, 1H), 7.25 (dd, *J* = 1.44, 7.7, 1H), 7.13 (t, *J* = 7.7, 1H), 7.08 (qd, *J* = 0.9, 7.5, 1H), 5.77 (m, 1H), 4.73-4.55 (m, 2H), 4.20-4.05 (m, 1H), 3.91-3.83 (m, 3H), 3.78-3.70 (m, 1H), 3.22 (q, *J* = 12.0, 1H), 2.92 (s, 3H), 2.83-2.74 (m, 1H), 1.94-1.72 (m, 6H), 1.44 (s, 9H)

HPLC/MS: M+1/Z Calcd = 454.2 Obsd. 354.1 (-Boc) and 476.1 (+Na)

(S)-2-amino-3-(1-(methylsulfonyl)spiro[indoline-3,4'-piperidin]-1'-yl)-3-oxopropyl hexylcarbamate (**14**)

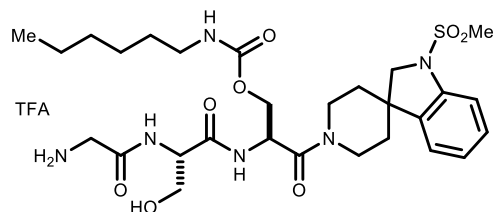


Triethylamine (107 μ L, 0.77mmol), hexyl isocyanate (83 μ L, 0.576mmol) and dimethylaminopyridine (10mg, 0.076mmol) were added to a solution of **13** (174mg) in chloroform (3mL). The mixture was then heated at 60C for 24 hours, during which time starting material was consumed and product appeared (as monitored by HPLC). The product was isolated by addition of the reaction solution to 1N HCl. The aqueous phase was extracted three times with ethyl acetate, and the combined organic phases were washed with saturated sodium bicarbonate and brine. The organics were then dried over sodium or magnesium sulfate, then filtered, and the solvent removed in vacuo. The product was deprotected according to the general procedure for Boc removal, then isolated as the free base by extraction from aqueous sodium carbonate with ethyl acetate to provide the desired product (148mg), which appeared to be contaminated with excess hexyl isocyanate, by NMR analysis. The material was used without further purification.

^1H NMR (500 MHz, CDCl_3) δ : 7.3 (d, J = 7.8, 1H), 7.15 (td, J = 1.3, 7.8, 1H), 7.12-7.01 (m, 1H), 6.97 (td, J = 0.9, 7.5, 1H), 5.22 (t, J = 5.6, 1H), 4.91-4.82 (m, 1H), 4.60-4.50 (m, 1H), 4.22-4.13 (m, 1H), 4.11-3.96 (m, 2H), 3.92-3.75 (m, 3H), 3.21-3.00 (m, 5H), 2.84 (s, 3H), 2.7 (t, J = 13.3, 1H), 1.89-1.62 (m, 2H), 1.45-1.32 (m, 2H), 1.26-1.11 (m, 4H), 0.82-.75 (m, 3H).

HPLC/MS: M+1/Z Calcd = 454.2 Obsd. 354.1 (-Boc) and 476.1 (+Na)

(S)-2-((S)-2-(2-Aminoacetamido)-3-hydroxypropanamido)-3-(1-(methylsulfonyl)spiro[indoline-3,4'-piperidin]-1'-yl)-3-oxopropyl hexylcarbamate (**10**)



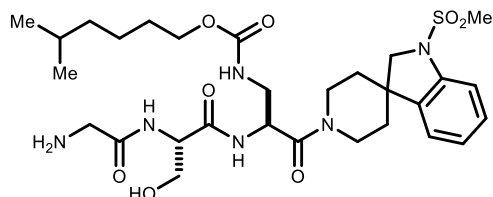
10 was prepared from **14** (148mg) by sequential homologation/deprotection with serine and glycine according to the general procedures. Yield: 29.4mg following purification by preparative HPLC.

^1H NMR (500 MHz, $\text{DMSO}-d_6$) δ : 8.58-8.34 (m, 2H), 7.96 (bs, 3H), 7.31-7.12 (m, 3H), 7.03 (ddd, J = 1.2, 7.4, 7.4, 1H), 5.00 (q, J = 8.0, 1H), 4.95 (q, J = 6.9, 1H), 4.42 (dd, J = 4.6, 7.1, 1H), 4.39-4.31 (m, 1H), 4.17-4.11 (m, 1H), 4.05 (dd, J = 5.9, 11.0, 1H), 3.98-3.85 (m, 3H), 3.57 (ddd, J = 4.7, 6.1, 11.2, 1H), 3.2 (q, J = 13.5, 1H), 3.02 (s, 3H), 2.96-2.87 (m, 2H), 2.81-2.72 (m, 1H), 1.87-1.77 (m, 1H), 1.73-1.57 (m, 3H), 1.38-1.30 (m, 2H), 1.27-1.13 (m, 4H), 0.85-0.78 (m, 3H).

HPLC/MS: M+1/Z Calcd = 625.3 Obsd. 625.3

Characterization of Methyl Scan Inhibitors

5-Methylhexyl ((S)-2-((S)-2-(2-aminoacetamido)-3-hydroxypropanamido)-3-(1-(methylsulfonyl)spiro[indoline-3,4'-piperidin]-1'-yl)-3-oxopropyl)carbamate (**15i**)

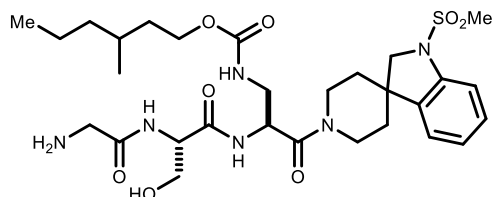


1:1 diastereomers at methyl

^1H NMR (500 MHz, MeOH- D_4) δ : 7.42-7.23 (m, 3H), 7.09 (dt, $J = 4.0, 7.2$, 1H), 5.14-5.07 (m, 1H), 4.58-4.46 (m, 2H), 4.28-4.20 (m, 1H), 4.19-3.94 (m, 5H), 3.93-3.76 (m, 4H), 3.53-3.36 (m, 3H), 3.00 (s, 3H), 2.96-2.88 (m, 1H) 1.90-1.75 (m, 2H), 1.66-1.49 (m, 3H), 1.45-1.17 (m, 4H), 0.99-0.88 (m, 6H).

HPLC/MS: M+1/Z Calcd = 639.3 Obsd. 639.4

3-Methylhexyl ((S)-2-((S)-2-(2-aminoacetamido)-3-hydroxypropanamido)-3-(1-(methylsulfonyl)spiro[indoline-3,4'-piperidin]-1'-yl)-3-oxopropyl)carbamate (**15j**)

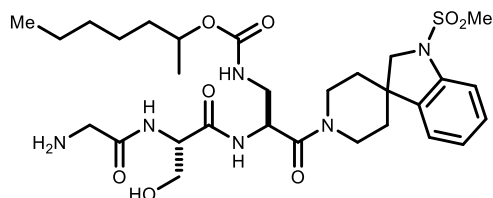


1:1 diastereomers at methyl

^1H NMR (500 MHz, MeOH- D_4) δ : 7.43-7.22 (m, 3H), 7.10 (dt, $J = 3.0, 7.5$, 1H), 4.76 (sextet, $J = 6.5$, 1H), 4.59-4.47 (m, 2H), 4.26-4.12 (m, 1H), 4.01 (AB, 2H), 3.91-3.77 (m, 4H), 3.59-3.35 (m, 3H), 3.01 (s, 3H), 2.96-2.87 (m, 1H) 2.25-1.76 (m, 4H), 1.65-1.46 (m, 2H), 1.43-1.16 (m, 9H), 0.97-0.84 (m, 3H).

HPLC/MS: M+1/Z Calcd = 639.3 Obsd. 639.3

Heptan-2-yl ((S)-2-((S)-2-(2-aminoacetamido)-3-hydroxypropanamido)-3-(1-(methylsulfonyl)spiro[indoline-3,4'-piperidin]-1'-yl)-3-oxopropyl)carbamate (**15k**)

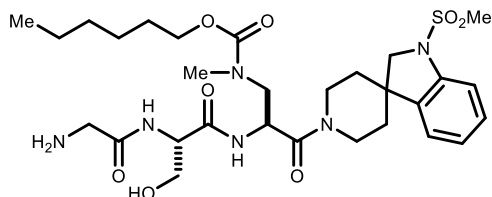


1:1 diastereomers at methyl

^1H NMR (500 MHz, MeOH- D_4) δ : 7.43-7.24 (m, 3H), 7.12-7.07 (m, 1H), 5.16-5.06 (m, 1H), 4.58-4.46 (m, 2H), 4.28-4.000 (m, 3H), 4.12 (AB, 2H), 3.93-3.76 (m, 4H), 3.53-3.36 (m, 2H), 3.00 (s, 3H), 2.96-2.88 (m, 1H) 2.2-1.76 (m, 4H), 1.73-1.53 (m, 2H), 1.48-1.10 (m, 4H), 0.99-0.87 (m, 6H).

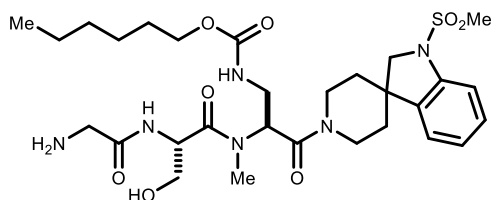
HPLC/MS: M+1/Z Calcd = 639.3 Obsd. 639.3

Hexyl ((S)-2-((S)-2-(2-aminoacetamido)-3-hydroxypropanamido)-3-(1-(methylsulfonyl)spiro[indoline-3,4'-piperidin]-1'-yl)-3-oxopropyl)(methyl)carbamate (**15h**)



^1H NMR (500 MHz, MeOH- D_4) δ : 7.35 (dd, J = 4.4, 7.3, 1H), 7.26-7.18 (m, 2H), 7.07-7.01 (m, 1H), 5.34-5.21 (m, 1H), 4.54-4.44 (m, 2H), 4.25-4.00 (m, 3H), 3.98 (m, 2H), 3.88-3.72 (m, 3H), 3.72-3.29 (2.99-2.82 (7H), 2.05-1.69 (m, 4H), 1.69-1.56 (m, 2H), 1.43-1.27 (6H), 0.98-0.8 (m, 3H).

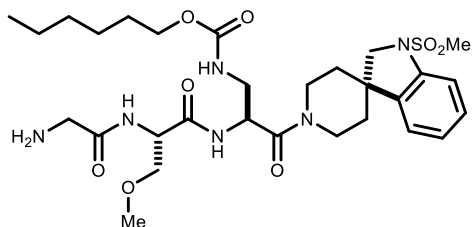
Hexyl ((S)-2-((S)-2-(2-aminoacetamido)-3-hydroxy-N-methylpropanamido)-3-(1-(methylsulfonyl)spiro[indoline-3,4'-piperidin]-1'-yl)-3-oxopropyl)carbamate (**15g**)



HPLC/MS: M+1/Z Calcd = 639.3 Obsd. 639.3

^1H NMR (500 MHz, MeOH- D_4) δ : 7.43-7.34 (m, 1H), 7.31-7.20 (m, 2H), 7.14-7.04 (m, 1H), 5.72-5.56 (m, 1H), 5.12-4.93 (m, 1H), 4.62-4.47 (m, 1H), 4.10-3.9 (m, 5H), 3.88-3.65 (m, 3H), 3.65-3.38 (m, 3H), 3.29-3.04 (m, 5H), 3.03 (m, 4H), 2.01-1.53 (m, 6H), 1.47-1.26 (m, 6H), 0.99-0.89 (m, 3H)

Hexyl ((S)-2-((S)-2-(2-aminoacetamido)-3-methoxypropanamido)-3-(1-(methylsulfonyl)spiro[indoline-3,4'-piperidin]-1'-yl)-3-oxopropyl)carbamate (**15f**)

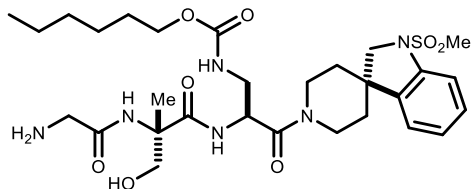


Rotamers Present

^1H NMR (500 MHz, MeOH- D_4) δ : 8.638 (app dd, J = 7.5, 14.7, 1H), 8.45-8.27 (m, 1H), 7.29-6.97 (m, 5H), 4.91 (pentet, J = 7.2, 1H), 4.59 (app pentet, J = 6.7, 1H), 4.36 (t, J = 13.63, 1H), 3.97-3.84 (m, 5H), 3.59 (quartet, 5.5, 2H), 3.53-3.42 (m, 2H), 3.53-3.42 (m, 2H), .23 (s, 3H), 3.19 (s, 2H), 3.26 (s, 3H), 2.75

(quartet, $J = 12.1$, 1H), 1.71-1.60 (m, 3H), 1.54-1.43 (m, 2H), 1.29-1.15 (m, 8H), 0.87-0.77 (m, 3H), 2.97-2.87 (m, 1H), 2.21-1.74 (m, 4H), 1.75-1.57 (m, 2H),

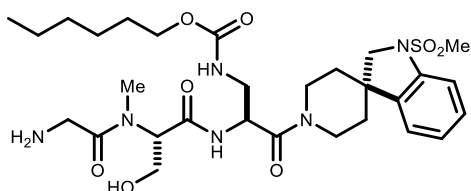
Hexyl ((S)-2-((S)-2-(2-aminoacetamido)-3-hydroxy-2-methylpropanamido)-3-(1-(methylsulfonyl)spiro[indoline-3,4'-piperidin]-1'-yl)-3-oxopropyl)carbamate (**15e**)



^1H NMR (500 MHz, MeOH- D_4) δ : 7.4 (d, $J = 8.2$, 1H), 7.38-7.29 (m, 1H), 7.29-7.23 (m, 1H), 7.13 (app sextet, $J = 3.7$, 1H), 5.16-5.10 (m, 1H), 4.54 (d, $J = 12.7$, 1H), 4.23-3.97 (m, 5H) 3.96-3.75 (m, 4H), 3.56 (m, 3H), 3.01 (s, 3H), 1.57 (app d, $J = 9.8$, 3H), 1.44-1.30 (m, 6H), 0.97-0.89 (m, 3H)

^{13}C NMR (125 MHz, CDCl_3) δ : 168.9, 167.9 166.4 157.1 141.5 138.9 128.9, 125.4 123.9, 113.3 724.4 66.9 64.5 58.9 23.9 48.8 43.2 36.5 35.8 34.8 31.4 30.9 29.1 15.5 22.5 22.4 14.4

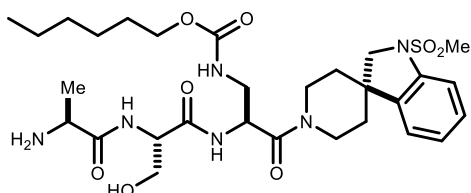
hexyl ((S)-2-((S)-2-(2-amino-N-methylacetamido)-3-hydroxypropanamido)-3-(1-(methylsulfonyl)spiro[indoline-3,4'-piperidin]-1'-yl)-3-oxopropyl)carbamate (**15d**)



^1H NMR (500 MHz, MeOH- D_4) δ : 7.38-7.16 (m, 3H), 7.04 (t, $J = 7.5$, 1H), 5.04 (bs, 1H), 4.49 (d, $J = 14.0$), 4.22-3.57 (m, 10H), 3.32 (s, 3H), 3.08-3.01 (m, 1H), 2.95 (s, 3H), 2.92-2.81 (m, 1H), 2.11-1.70 (m, 4H), 1.67-1.51 (m, 2H), 1.41-1.22 (m, 6H), 0.92-0.82 (m, 3H).

HPLC/MS

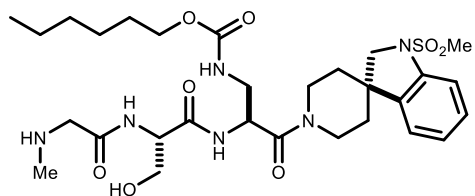
Hexyl ((S)-2-((S)-2-((S)-2-aminopropanamido)-3-hydroxypropanamido)-3-(1-(methylsulfonyl)spiro[indoline-3,4'-piperidin]-1'-yl)-3-oxopropyl)carbamate (**15c**)



^1H NMR (500 MHz, MeOH- D_4) δ : 8.69 (d, $J = 6.1$, 1H), 8.34-7.95 (m, 5H), 7.32-6.94 (m, 4H), 4.90 (q, $J = 6.8$, 1H), 4.43-4.26 (m, 2H), 4.03-3.84 (m, 5H), 3.70-3.55 (m, 2H), 3.50-3.34 (m, 2H), 3.31-3.10 (m, 2H), 3.02 (s, 3H), 2.80-2.69 (m, 1H), 2.01-1.77 (m, 1H), 1.75-1.57 (m, 2H). 1.55-1.43 (m, 2H), 1.41-1.31 (m, 3H), 1.30-1.15 (m, 6h), 0.86-0.76 (m, 3H).

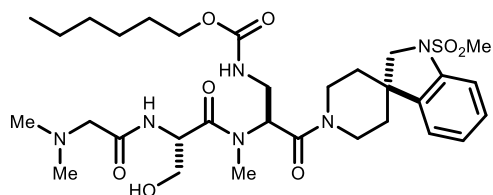
^{13}C NMR (125 MHz, CDCl_3) δ : 170.1 169.5 168.1 157.1 141.6 139.0 128.7 124.0 123.8 113.1 72.6 71.1 64.5 62.1 58.8 56.1 48.9 48.5 43.2 42.7 35.9 34.6 31.3 29.2 25.6 22.4 14.5

Hexyl ((S)-2-((S)-3-hydroxy-2-(2-(methylamino)acetamido)propanamido)-3-(1-(methylsulfonyl)spiro[indoline-3,4'-piperidin]-1'-yl)-3-oxopropyl)carbamate (**15a**)



^1H NMR (500 MHz, MeOH- D_4) δ : 8.74 (bs, 1H), 8.64 (dd, 8.11, 10.32), 8.30-8.14 (m, 1H), 7.31-7.14 (m, 3H), 5.05-4.87 (m, 1H), 4.43-4.30 (m, 1H), 4.00-3.85 (m, 3H), 3.79-3.67 (m, 2H), 3.60-3.54 (m, 2H), 3.03 (s, 3H), 2.53 (t, $J = 5.1$, 2H), 1.74-1.59 (m, 2H), 1.53-1.43 (m, 2H), 1.29-1.14 (m, 6H), 0.866-0.77 (m, 3H).

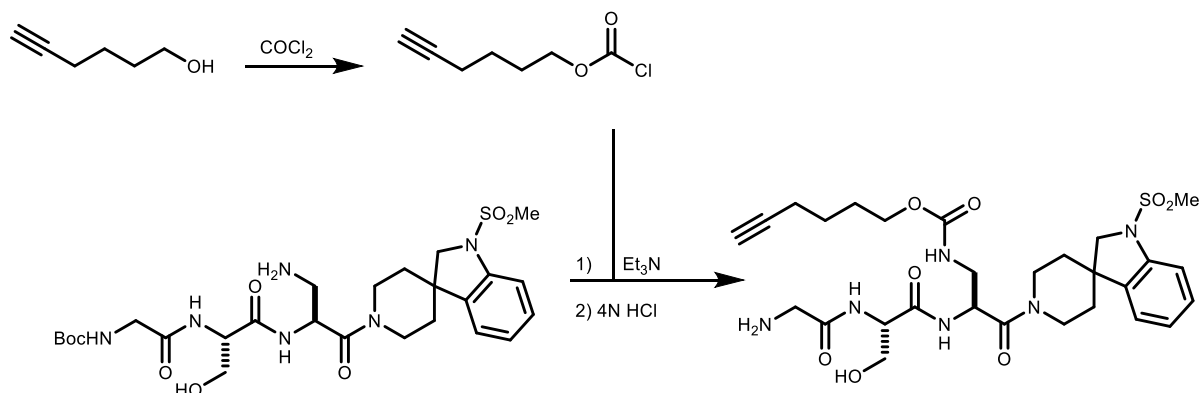
Hexyl ((S)-2-((S)-2-(2-(dimethylamino)acetamido)-3-hydroxy-N-methylpropanamido)-3-(1-(methylsulfonyl)spiro[indoline-3,4'-piperidin]-1'-yl)-3-oxopropyl)carbamate (**15b**)



^1H NMR (500 MHz, MeOH- D_4) δ : 7.4 (dd $J = 2.8, 8.0$, 1H), 7.29-7.22 (m, 2H), 7.09 (q, $J = 7$, 1H), 5.66-5.48 (m, 1H), 5.07-4.95 (m, 1H), 4.61-4.52 (m, 1H), 4.15-3.94 (m, 6H), 3.88-3.71 (m, 2H), 3.63-3.42 (m, 2H), 3.3-3.10 (m, 4H), 3.00-2.96 (m, 9H), 2.95-2.88 (m, 1H), 1.99-1.57 (m, 6H), 1.48-1.29 (m, 6H), 0.98-0.89 (m, 3H).

Conformationally Restrained Inhibitors

hex-5-yn-1-yl ((S)-2-((S)-2-(2-aminoacetamido)-3-hydroxypropanamido)-3-(1-(methylsulfonyl)spiro[indoline-3,4'-piperidin]-1'-yl)-3-oxopropyl)carbamate (**28**)



Hex-5-yn-1-ol was added to a solution of phosgene in toluene at 0C. After 1h, the solution was concentrated to provide the desired chloroformate in quantitative yield.

^1H NMR (500 MHz, CDCl_3) δ : 4.40 (t, $J = 6.5$, 2H), 2.31 (td, $J = 2.83$, 6.9, 2H), 2.02 (t, $J = 2.5$, 1H), 1.92 (p, $J = 6.9$, 2H), 1.69 (p, $J = 7.5$, 2H)

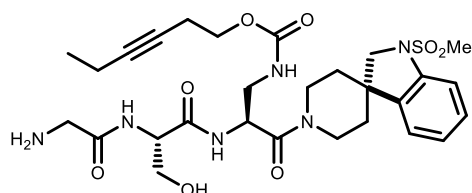
^{13}C NMR (125 MHz, CDCl_3) δ : 83.2 71.5 69 27.2 24.3 17.8

To a room temperature solution of the DAP derivative (30mg, 0.05mmol) and $i\text{Pr}_2\text{NEt}$ (22 μL , 0.125mmol) in dichloromethane was added hex-5-yn-1-yl carbonochloridate (16mg, 0.1mmol). After fifteen minutes the reaction was stopped and quenched according to the general amidation procedure. The material was purified by preparative TLC to afford 23mg of product. This material was deprotected according to the general Boc-removal procedure to afford **28** as the hydrochloride salt in quantitative yield.

^1H NMR (500 MHz, MeOH-D_4) δ : 7.43-7.24 (m, 3H), 7.10 (app q, $J = 8.0$, 1H), 5.15-5.08 (m, 1H), 4.58-4.48 (m, 2H), 4.28-4.05 (m, 3H), 4.05-3.95 (m, 2H), 3.94-3.7 (m, 7H), 3.61 (t, $J = 5.0$, 1H), 3.53-3.46 (m, 1H), 3.45-3.37 (m, 1H), 3.01 (s, 3H), 2.97-2.88 (m, 1H), 2.28-2.2 (m, 3H), 2.18-1.71 (m, 5H), 1.66-1.54 (m, 2H).

HPLC/MS: $M+1/Z$ Calcd = 621.3 Obsd. 621.3

hex-3-yn-1-yl ((S)-2-((S)-2-(2-aminoacetamido)-3-hydroxypropanamido)-3-(1-(methylsulfonyl)spiro[indoline-3,4'-piperidin]-1'-yl)-3-oxopropyl)carbamate (**29**)



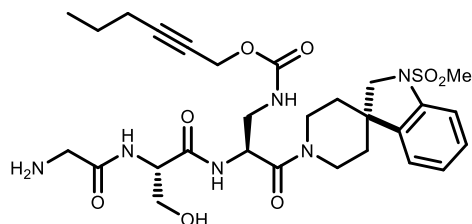
29 was prepared by a route analogous to that used for the preparation of **28**.

^1H NMR (500 MHz, MeOH-D_4) δ : 7.42-7.22 (m, 3H), 7.10 (app q, $J = 8.0$, 1H), 5.11 (bs, 1H), 4.53 (bs, 1H), 4.26-4.05 (m, 3H), 4.03-3.98 (m, 2H), 3.94-3.7 (m, 8H), 3.6 (t, $J = 5.0$, 1H), 3.48 (d, 1H), 3.45-3.37

(m, 1H), 3.01 (s, 3H), 2.92 (t, $J = 12.1$, 1H), 2.61-2.4 (m, 2H), 2.15 (p, $J = 7.3$, 2H), 2.08-1.90 (m, 1H), 1.90-1.75 (m, 2H), 1.5-1.26 (m, 2H), 1.1 (app q, $J = 7.3$, 3H), 0.99-0.91 (m, 3H).

HPLC/MS: M+1/Z Calcd = 621.3 Obsd. 621.3

hex-2-yn-1-yl ((S)-2-((S)-2-(2-aminoacetamido)-3-hydroxypropanamido)-3-(1-(methylsulfonyl)spiro[indoline-3,4'-piperidin]-1'-yl)-3-oxopropyl)carbamate (**30**)

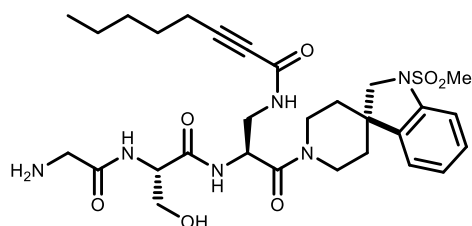


30 was prepared by a route analogous to that used for the preparation of **28**.

^1H NMR (500 MHz, MeOH- D_4) δ : 7.43-7.23 (m, 3H), 7.09 (app q, $J = 7.4$, 1H), 5.11 (bs, 1H), 4.78-4.6 (m, 2H), 4.53 (bs, 2H), 4.28-4.10 (m, 1H), 4.00 (d, $J = 4.3$, 2H), 3.92-3.72 (m, 5H), 3.68 (s, 2H), 3.722-3.66 (m, 1H), 3.61 (t, $J = 5.0$, 1H), 3.57-3.47 (m, 1H), 3.45-3.37 (m, 1H), 3.00 (s, 3H), 2.92 (app q, $J = 12.0$, 1H), 2.21 (t, $J = 6.5$, 1H), 2.14 (t, $J = 6.0$, 1H), 2.09-1.75 (m, 3H), 1.57-1.28 (m, 4H), 1.03-0.90 (m, 3H).

HPLC/MS: M+1/Z Calcd = 621.3 Obsd. 621.3

N-((S)-2-((S)-2-(2-aminoacetamido)-3-hydroxypropanamido)-3-(1-(methylsulfonyl)spiro[indoline-3,4'-piperidin]-1'-yl)-3-oxopropyl)oct-2-ynamide (**31**)

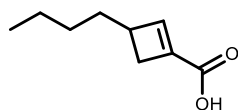


31 was prepared by amidation of the same primary amine with 2-octynoic acid according to the general procedure, followed by deprotection according to the corresponding general procedure.

^1H NMR (500 MHz, MeOH- D_4) δ : 7.41-7.21 (m, 3H), 7.08 (bs, 1H), 5.12 (bs, 1H), 4.51 (bs, 2H), 4.20-4.07 (m, 1H), 4.03-3.92 (m, 2H), 3.91-3.62 (m, 7H), 3.63-3.47 (m, 2H), 3.43-3.35 (m, 1H), 2.98 (s, 3H), 2.94-2.83 (m, 1H), 2.49-2.3 (m, 2H), 2.14-1.98 (m, 1H), 1.97-1.72 (m, 3H), 1.58 (bs, 2H), 1.47-1.25 (m, 6H), 0.96-0.87 (m, 3H).

HPLC/MS: M+1/Z Calcd = 621.3 Obsd. 619.3

3-butylcyclobut-1-enecarboxylic acid (**41**)



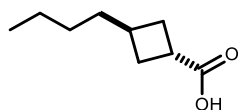
Piperidine (20mL, 202.4mmol) was dissolved in ether (75mL) containing 4A molecular sieves (50g). The solution was cooled in an ice bath, and hexanal (25mL, 202.4 mmol) was added with stirring over 5

minutes. Stirring was stopped and the solution was allowed to warm to room temperature and maintained at this temperature overnight. The solution was filtered over celite (dried in an oven overnight), the filter cake washed with additional ether, and the solvent removed *in vacuo*. The resulting colorless oil was dissolved in acetonitrile (75mL) and methyl acrylate (18.22 mL, 202.4 mmol) was added. A reflux condenser was placed on the flask, and the biphasic solution was heated at reflux for three hours. During this time the solution turned orange and became monophasic. The reaction mixture was then cooled and concentrated *in vacuo*. The resulting thick orange oil was dissolved in ether (150mL) and methyl iodide (50.4 mL, 808 mmol) was added. The solution was mixed and then allowed to stand. After 4 days, the supernatant was poured off and the precipitate was rinsed with ether and then dried *in vacuo*. A solution of KOH (1.13 mol) and water (250mL) was added, and the solution stirred at room temperature until it became homogenous. The solution was then heated to reflux for 2 hours, then cooled to room temperature. 300mL of water were added and the reaction mixture was poured into a separatory funnel, washed three times with ether, and then acidified with 12N HCl to pH<2. The aqueous phase was extracted three times with ether. These organic phases were combined, washed with 1N HCl and brine, then dried over MgSO₄ and concentrated to afford a yellow oil (18.94g, 60% yield). No further purification was required.

¹H NMR (400 MHz, CDCl₃) δ: 7.01 (s, 1H), 2.84 (dd, *J* = 13.4, 4.31, 1H) 2.69-2.62 (m, 1H) 2.26 (dd, *J* = 13.4, 1.59, 1H) 1.50-1.39 (m, 2H), 1.31-1.24 (m, 4H), 0.9 (t, *J* = 7.2, 3H).

¹³C NMR (125 MHz, CDCl₃) δ; 167.6, 153.7, 136.5, 40.1, 34.5, 32.6, 29.9, 22.5, 13.9.

Trans-3-butylcyclobutanecarboxylic acid (**42**)

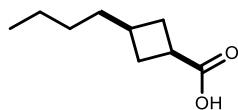


To a solution of 37% HCl (100mL), water (67mL), and THF (166mL) in a 1L round-bottom flask at room temperature was added **11** (4g, 25.9 mmol). The flask was placed in a room temperature water bath and zinc powder (13.47g, 207.2 mmol) was added in 10 portions at a rate such that the previous portion was almost completely dissolved prior to the next addition (total time was roughly 90 minutes). The reaction was filtered over celite then THF was removed *in vacuo*. The resulting aqueous phase was extracted three times with ether, the combined organic phases were washed with 1N HCl and brine, then dried over Na₂SO₄ and concentrated. Purification by column chromatography (10% EtOAc in hexanes) afforded **9** as a colorless oil (4.73g, 59% yield).

¹H NMR (400 MHz, CDCl₃) δ: 3.13-3.06 (m, 1h), 2.42-2.34 (m, 3H), 1.93-1.86 (m, 1H), 1.42 (dt, *J* = 7.7, 7.2, 2H), 1.27 (sextet, *J* = 7.4, 2H) 1.17 (m, 2H), 0.86 (t, *J* = 7.3, 3H).

¹³C NMR (125 MHz, CDCl₃) δ: 182.0, 36.3, 34.2, 31.3, 28.9, 22.4, 13.9.

(*cis*)-3-butylcyclobutane-1-carboxylic acid (**43**)

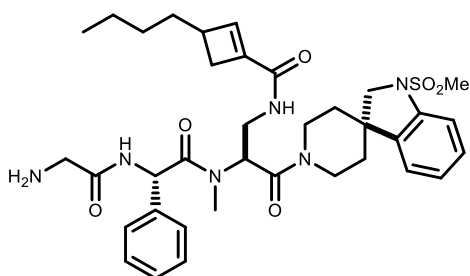


To a solution of **41** (2g) in 95:5 EtOH/AcOH (40mL) in a Parr bomb was added Rh/C (360mg). The mixture was placed under 500psi of hydrogen with stirring overnight. Evaporation of the solvents afforded the desired product, which was used without further purification. Quantitative yield.

^1H NMR (400 MHz, CDCl_3) δ : 2.96 (pent, $J = 9.0$, 1H), 2.30 (ddd, $J = 2.74, 8.22, 16.93$, 2H), 2.18 (pentet, $J = 8.0$, 1H), 1.87 (ddd, $J = 2.4, 9.73, 19$, 2H), 1.36 (q, $J = 7.3$, 2H), 1.26 (sextet, $J = 7.3$, 2H), 1.19-1.12 (m, 2H), 0.86 (t, $J = 7.6$, 3H).

^{13}C NMR (125 MHz, CDCl_3) δ : 181.9, 36.3, 34.2, 31.6, 36.4, 29.9, 22.5, 13.9.

N-((*S*)-2-((*S*)-2-(2-aminoacetamido)-*N*-methyl-2-phenylacetamido)-3-(1-(methylsulfonyl)spiro[indoline-3,4'-piperidin]-1'-yl)-3-oxopropyl)-3-butylcyclobut-1-ene-1-carboxamide (**33**)

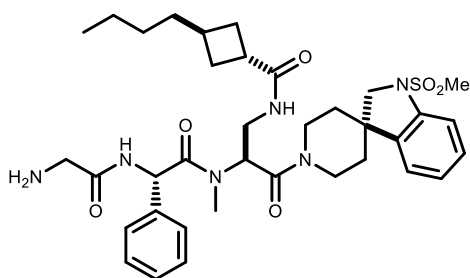


1:1 diastereomers at cyclobutane, plus likely rotamers.

^1H NMR (500 MHz, MeOH-D_4) δ : 7.47-7.02 (m, 9H), 6.69-6.64 (m, 1H), 5.87-5.51 (m, 2H), 4.55-4.45 (m, 1H), 4.01-3.94 (m, 2H), 3.92-3.81 (m, 2H), 3.75-3.53 (m, 7H), 3.00-2.86 (m, 8H), 2.77-2.64 (m, 2H), 2.14 (t, $J = 12$, 1H), 1.94-1.70 (m, 4H), 1.57-1.43 (m, 2H), 1.41-1.28 (m, 4H), 0.95-0.86 (m, 3H)

HPLC/MS: $M+1/Z$ Calcd = 693.3 Obsd. 692.9

(*trans*)-*N*-((*S*)-2-((*S*)-2-(2-aminoacetamido)-*N*-methyl-2-phenylacetamido)-3-(1-(methylsulfonyl)spiro[indoline-3,4'-piperidin]-1'-yl)-3-oxopropyl)-3-butylcyclobutane-1-carboxamide (**34**)

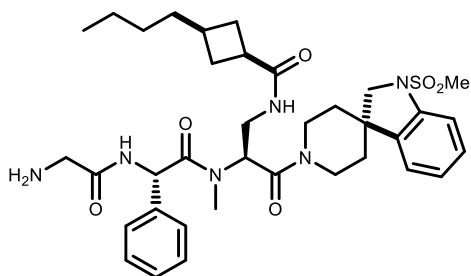


Rotamers evident ~2:1

^1H NMR (500 MHz, MeOH-D_4) δ : 7.44-6.98 (m, 9H), 5.86 and 5.79 (s, 1H), 5.77 and 5.68 (dd, $J = 5.2, 8.9$, 1H), 4.92-4.84 (m, 1H), 4.51 t, $J = 16.1$, 1H), 4.06-3.83 (m, 3H), 3.80-3.52 (m, 3H), 3.50-3.35 (m, 2H), 3.18 (t, $J = 13.9$, 1H), 3.00-2.8 (m, 9H), 2.35-2.15 (m, 3H), 1.95-1.7 (m, 6H), 1.45 (q, $J = 7.5$, 2H), 1.31 (sextet, $J = 7.3$, 2H), 1.24-1.16 (m, 2H), 0.90 (t, $J = 7.3$, 3H).

HPLC/MS: $M+1/Z$ Calcd = 695.3 Obsd. 694.9

(*cis*)-*N*-((*S*)-2-((*S*)-2-(2-aminoacetamido)-*N*-methyl-2-phenylacetamido)-3-(1-(methylsulfonyl)spiro[indoline-3,4'-piperidin]-1'-yl)-3-oxopropyl)-3-butylcyclobutane-1-carboxamide (**35**)

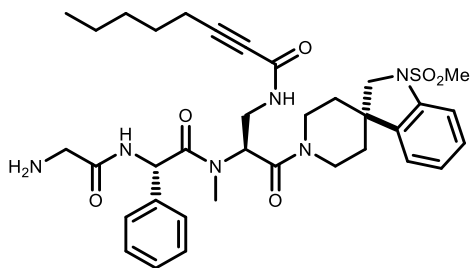


HPLC/MS: M+1/Z Calcd = 695.3 Obsd. 694.9

Rotational isomers evident in NMR.

¹H NMR (500 MHz, AcOH-D₄) δ: 7.50-7.40 (m, 3H), 7.36 (d, *J* = 8.04, 1H), 7.28-7.15 (m, 3H), 7.06 (p, *J* = 7.5, 1H), 6.95 (t, *J* = 7.5, 0.5H), 6.72 (d, *J* = 7.7, 0.5H), 5.97 (d, *J* = 10.5, 1H), 5.63 and 5.50 (t, *J* = 7.0, 1H), 4.45 and 4.34 (d, *J* = 14.0, 1H), 3.99-3.94 (m, 2H), 3.93-3.89 (m, 1H), 3.81 (AB, 1H), 3.70-3.58 (m, 3H), 3.48 (bd, *J* = 13.9, 1H), 3.12 (s, 2H), 2.97 and 2.95 (s, 3H), 2.92 (s, 3H), 2.73 (bt, *J* = 13.2, 1H), 2.23-2.04 (m), 1.86-1.7 (m, 3H), 1.35 (q, *J* = 6.7, 2H), 1.27 (Sextet, *J* = 7.5, 2H), 1.20 (m, 2H), 0.87 (t, *J* = 7.3, 3H).

N-((*S*)-2-((*S*)-2-(2-Aminoacetamido)-*N*-methyl-2-phenylacetamido)-3-(1-(methylsulfonyl)spiro[indoline-3,4'-piperidin]-1'-yl)-3-oxopropyl)oct-2-ynamide (**32**)



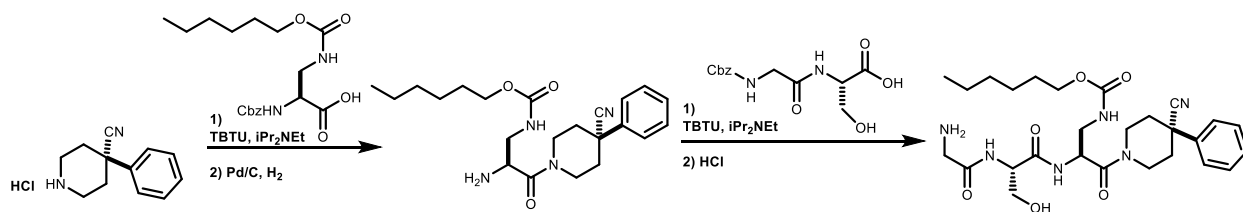
3:2 mixture of diastereomers.

¹H NMR (500 MHz, MeOH-D₄) δ: 7.6-6.8 (m, 9H), 5.91-8.82 (m, 1H), 5.66-5.47 (m, 1H), 4.63-4.33 (m, 1H), 4.05-3.50 (m, 6H), 3.12 (s, 2H), 3.01 (s, 3H), 2.98-2.94 (m, 3H), 2.82-2.70 (m, 1H), 2.55-2.34 (m, 2H), 2.00-1.24 (m, 10H), 1.00-0.92 (m, 3H).

HPLC/MS: M+1/Z Calcd = 679.3 Obsd. 679.9

Synthesis and Characterization of C-terminal Variants

Hexyl ((*S*)-2-((*S*)-2-(2-aminoacetamido)-3-hydroxypropanamido)-3-(4-cyano-4-phenylpiperidin-1-yl)-3-oxopropyl)carbamate (**45a**)

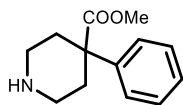


4-cyano 4-phenyl piperidine hydrochloride (250mg) was first coupled to Z-Dap(Hex)-OH according to the general procedure. The Cbz group was removed according to the general procedure and the N-terminal dipeptide appended by reverse coupling of Boc-Gly-Ser-OH according to general procedure. Following purification by column chromatography (5% MeOH/CHCl₃) 438mg was isolated. 200mg of this material was deprotected according to the general procedure to provide 153.6mg of **45a**.

¹H NMR (500 MHz, DMSO-D₆) δ: 8.60 (d, *J* = 8.1, 1H), 8.28 and 8.18 (d, *J* = 7.5, 1H), 8.12 (bt, 3H), 7.55-7.46 (m, 2H), 7.41 (t, *J* = 7.6, 2H), 7.36-7.29 (m, 1H), 7.15 and 7.04 (t, *J* = 6.8, 1H), 4.86 (q, *J* = 7.2, 1H), 4.53 (t, *J* = 13.1, 1H), 4.4-4.32 (m, 1H), 4.15 (d, *J* = 13.4, 1H), 3.96-3.75 (m, 2H), 3.68-3.48 (m, 3H), 3.33-3.20 (m, 2H), 2.82 (q, *J* = 13.4, 1H), 2.17-1.99 (m, 3H), 1.90 and 1.79 (td, *J* = 3.6, 13.0, 1H), 1.54-1.43 (m, 1H), 1.42-1.33 (m, 1H), 1.29-1.1 (m, 6H), 0.86-0.75 (m, 3H).

HPLC/MS: M+1/Z Calcd = 545.3 Obsd. 545.0

Methyl 4-phenylpiperidine-4-carboxylate (**49b**)

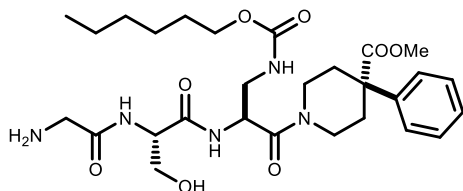


4-phenylpiperidine-4-carbonitrile hydrochloride (1g, 4.5mmol) was placed in a round bottom flask and dissolved in H₂O (1mL) and H₂SO₄ (2mL). A condenser was added and the solution was heated at 120C for four hours. The solution was then concentrated in vacuo to remove water. Following evaporation, water and an additional 1mL of H₂SO₄ were added, and the solution was heated at reflux under argon for a further four hours. The sulfuric acid was carefully neutralized with 1N NaOH (Na₂SO₄ precipitates) and the product extracted with ethyl acetate. The combined organic phases were dried over MgSO₄ and then filtered and concentrated. 554mg of desired product were obtained and used without further purification.

¹H NMR (500 MHz, CDCl₃) δ: 7.4-7.31 (m, 4H), 7.27-7.22 (m, 1H), 3.66 (s, 3H), 3.10 (dt, *J* = 3.3 13.0, 2H), 2.81 (td, *J* = 1.9, 12.6, 2H), 2.55 (d, *J* = 13.0, 2H), 2.29 (bs, 1H), 1.89 (td, *J* = 3.5, 1.89, 12.5, 2H).

HPLC/MS: M+1/Z Calcd = 220.1 Obsd. 220.0

Methyl 1-((S)-2-((S)-2-(2-aminoacetamido)-3-hydroxypropanamido)-3-((hexyloxy)carbonyl)amino)propanoyl)-4-phenylpiperidine-4-carboxylate (**45b**)



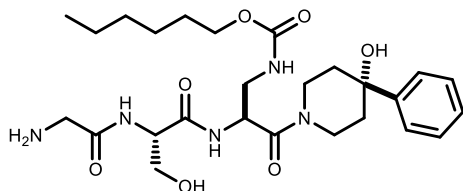
45b was prepared from **49b** (250mg) by a route analogous to that used to prepare **45a**, affording 80mg of **45b**.

^1H NMR (500 MHz MeOH- D_4) δ : 7.47-7.34 (m, 4H), 7.32-7.27 (m, 1H), 5.16-5.04 (m, 1H), 4.50 (q, $J = 5.5$, 1H), 4.33 (d, $J = 13.4$, 1H), 4.14-3.75 (m, 7H), 3.71 (app d, $J = 5.1$, 3H), 3.49-3.36 (m, 2H), 3.02 (t, $J = 11.1$, 1H), 2.68-2.54 (m, 2H), 2.11-1.84 (m, 2H), 1.74-1.57 (m, 1H), 1.56-1.46 (m, 1H), 1.44-1.23 (m, 6H), 0.97-0.89 (m, 3H).

^{13}C NMR (125 MHz, MeOH- D_4) δ : 174.0, 173.6, 170.6, 167.9, 167.8, 157.3, 141.4, 128.7, 127.4, 125.6, 64.1, 62.7, 54.7, 52.3, 50.3, 49.45, 44.5, 43.5, 42.6, 41.1, 34.0, 33.2, 31.2, 28.7, 25.3, 22.4, 13.9.

HPLC/MS: M+1/Z Calcd = 578.3 Obsd. 577.9

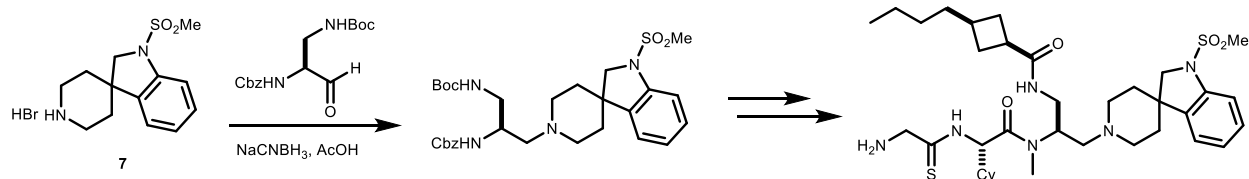
Hexyl ((S)-2-((S)-2-(2-aminoacetamido)-3-hydroxypropanamido)-3-(4-hydroxy-4-phenylpiperidin-1-yl)-3-oxopropyl)carbamate (**45c**)



45c was prepared from **49c**, affording 48mg of **45b**.

^1H NMR (500 MHz MeOH- D_4) δ : 8.55 (t, $J = 7.2$, 1H), 8.23 and 8.11 (d, $J = 7.9$, 1H), 7.99 (bs, 3H), 7.46 and 7.42 (d, $J = 7.9$, 2H), 7.28 (td, $J = 3.2, 7.2$, 2H), 7.17 (t, $J = 7.5$, 1H), 7.13 and 7.00 (t, $J = 5.8$, 1H), 5.11 (s, 1H), 4.99 (p, $J = 5.3$, 1H), 4.92-4.85 (m, 1H), 4.37 (bs, 1H), 4.27 (t, $J = 11.8$, 1H), 3.93-3.78 (m, 3H), 3.6-3.51 (m, 4H), 3.39 (q, $J = 13.4$, 1H), 3.26-3.19 (m, 1H), 2.94 (q, $J = 12.0$, 1H), 1.97 and 1.89 (t, $J = 11.1$, 1H), 1.77 and 1.67 (t, $J = 13.9$, 1H), 1.57 (t, 10.5, 2H), 1.48 and 1.42 (t, $J = 6.5$, 2H), 1.29-1.12 (m, 6H), 0.82 and 0.78 (t, $J = 6.0$, 3H).

(*cis*)-N-((*S*)-2-((*S*)-2-(2-aminoacetamido)-2-cyclohexylacetamido)-3-(1-(methylsulfonyl)spiro[indoline-3,4'-piperidin]-1'-yl)propyl)-3-butylcyclobutane-1-carboxamide (**46**)

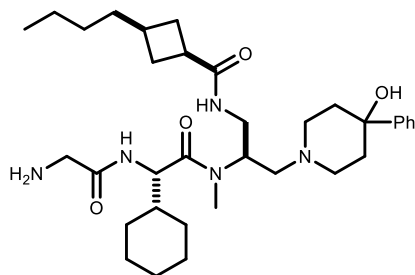


7 (2.046g, 5.92mmol) and DAP-aldehyde (1.6g, 4.93mmol) were dissolved in MeOH (54mL) and DMF (9.6mL) and stirred at 0C for 5m, then acetic acid (725uL, 17.85mmol) was added. After stirring for another 5m, sodium cyanoborohydride (557mg, 8.9mmol) was added. The reaction was stirred at room temperature overnight, then poured into NaHCO₃ and extracted with ethyl acetate three times. The combined organic phases were washed with brine, dried over sodium sulfate, and concentrated. The residue was purified by column chromatography (3:1 EtOAc/Hexane to 100% EtOAc). Yield 1.95g of an off white foam. This material was processed according to the general procedures to afford **46**.

¹H NMR (500 MHz MeOH-D₄) δ: 7.33 (d, *J* = 8.0, 1H), 7.19 (t, *J* = 8.1, 1H), 7.14 (t, *J* = 7.4, 1H), 7.02 (t, *J* = 7.3, 1H), 5.16 (d, *J* = 8.1, 1H), 4.93 (bs, 1H), 3.91-3.76 (m, 3H), 3.11 (s, 2H), 3.03 (d, *J* = 11, 1H), 2.91 (s, 3H), 2.88-2.76 (m, 2H), 2.65 (t, *J* = 11.8, 1H), 2.35-2.07 (m, 3H), 2.07-1.61 (m, 9H), 1.39-1.10 (m, 10H), 0.87 (t, *J* = 7.4, 3H).

HPLC/MS: M+1/Z Calcd = 703.4 Obsd. 703.0

(1*r*,3*R*)-N-((*S*)-2-((*S*)-2-(2-aminoacetamido)-2-cyclohexylacetamido)-3-(4-hydroxy-4-phenylpiperidin-1-yl)propyl)-3-butylcyclobutane-1-carboxamide (**47**)

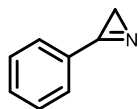


47 was prepared by a route analogous to that used to prepare **46**.

¹H NMR (500 MHz MeOH-D₄) δ: 7.43 (d, *J* = 7.8, 2H), 7.27 (t, *J* = 7.8, 2H), 7.17 (t, *J* = 7.4, 1H), 4.94 (bs, 1H), 4.67 (d, *J* = 7.4, 1H), 3.66-3.51 (m, 1H), 3.34 (dd, *J* = 4.5, 13.9, 1H), 3.15 (dd, *J* = 9.6, 14.1, 1H), 3.01 (s, 3H), 2.85-2.75 (m, 2H), 2.69-2.52 (m, 3H), 2.36 (t, *J* = 12.55, 1H), 2.30 (dd, *J* = 4.4, 13.5), 2.19-2.08 (m, 3H), 2.02 (td, *J* = 4.4, 13.2, 1H), 1.93 (td, *J* = 4.0, 13.1, 1H), 1.88-1.60 (m, 8H), 1.39-1.02 (m, 12H), 0.86 (t, *J* = 7.7, 3H)

HPLC/MS: M+1/Z Calcd = 598.4 Obsd. 598.2

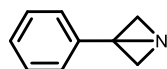
3-phenyl-2H-azirine (**50**)



To a stirred solution of styrene (20g, 192mmol) in dichloromethane in an ice bath was added dropwise a solution of bromine (30.7g, 192mol) in dichloromethane (50mL). When addition was complete and the solution became colorless it was concentrated to afford a light pink solid. (56.51g). 26.4g (0.1 mol) of this solid material was dissolved in DMSO (260m). A solution of sodium azide (9.8g, 0.15mmol) in water (25mL) was added dropwise, and the solution was stirred at room temperature overnight. A solution of 4.0g of NaOH in 4mL of water was then added dropwise, and the solution stirred overnight. The reaction mixture was diluted with NaHCO₃ and then extracted twice with DCM. The combined organic phases were washed twice with water, then dried over MgSO₄, filtered, and concentrated to a colorless oil (12.4g, 85%). 5.0g of this oil were dissolved in toluene and heated at 100C for 1h, until the evolution of gas had ceased. This solution was then concentrated to afford desired **50** in quantitative yield.

¹H NMR (500 MHz, CDCl₃) δ: 7.6-7.55 (m, 2H), 7.4-7.34 (m, 3H), 5.44 (d, *J* = 2.4, 1H) and 4.97 (d, *J* = 2.4, 1H).

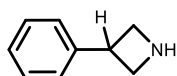
3-phenyl-1-azabicyclo[1.1.0]butane (**51**)



Trimethylsulfonium iodide (11.5g, 56.3mmol) was dissolved in THF (200mL) and cooled to -40C. nBuLi (27mL, 56.3mmol) was added dropwise. The solution was stirred at -40C for 10m, then at -20C for 10m. **50** (6.0g, 51.2mmol) was dissolved in THF (15mL), and added dropwise to the solution of ylide over 20m. The mixture was stirred for 30m, then quenched by addition to water. The product was extracted 4x with dichloromethane. The combined organic phases were dried over MgSO₄, then filtered and concentrated. The product was distilled to afford 2.8g of colorless crystals.

¹H NMR (500 MHz, CDCl₃) δ: 7.44-7.29 (m, 5H), 2.80 (t, *J* = 1.2, 2H), 1.55 (t, *J* = 1.2)

3-phenylazetidene (**52a**)

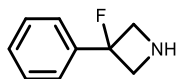


To a solution of 200mg of **21** in 60mL of THF was added 80mg of Pd/C. The solution was transferred to a Parr bomb apparatus and 500psi of H₂ pressure was applied overnight with stirring. The solution was then filtered and concentrated to afford the desired product (165mg) as the only observable material by crude NMR. No further purification.

¹H NMR (500 MHz, CDCl₃) δ: 7.37-7.16 (m, 5H), 3.99 (p, *J* = 7.9, 1H), 3.89 (t, *J* = 7.3, 2H), 3.80 (t, *J* = 7.9, 2H)

¹³C NMR (125 MHz, CDCl₃) δ: 143.0, 128.5 126.8 12.5 54.7 39.6

3-fluoro-3-phenylazetididine (**52b**)

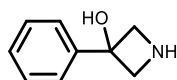


A solution of **51** (1.6g, 12.5mmol) in dichloromethane (12.5mL) was added dropwise to a -78C solution of HF-pyridine (12.5mL) and dichloromethane (12.5ml) in a plastic tube. The solution was stirred at room temperature for 2h, then poured onto ice and NH₄OH was added until the pH reached 13. The product was extracted with diethyl ether, the combined organic phase was washed with water and brine, then dried over MgSO₄ and filtered and concentrated. The product was purified by column chromatography to afford 359mg of product.

¹H NMR (500 MHz, CDCl₃) δ: 7.54 (d, *J* = 7.9, 2H), 7.39 (t, 7.4, 2H), 7.32 (tt, *J* = 7.5, 1.2, 1H), 4.15 (ddd, *J* = 1.6, 8.5, 23.5, 2H), 3.89 (ddd, *J* = 1.6, 9.0, 18.6, 2H), 2.08 (s, 1H)

¹³C NMR (125 MHz, CDCl₃) δ: 140.18 (d, *J* = 23.1), 128.4, 128.09 (d, *J* = 1.56), 123.97 (d, *J* = 8.6), 95.83 (d, *J* = 207), 59.8 (d, *J* = 24.2).

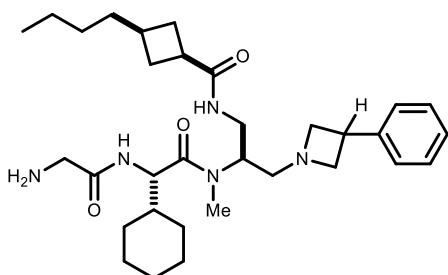
3-phenylazetididin-3-ol (**52c**)



A solution of **51** (230mg, 0.15mmol) in dioxane (20mL) was added to water (220mL) and the solution was stirred overnight, and then concentrated to afford the desired product.

¹H NMR (500 MHz, MeOH-D₄) δ: 7.63-7.55 7.44-7.36 7.34-7.28 3.96 (t, *J* = 9.5, 2H), 3.89 (t, *J* = 9.8, 2H), 3.32-3.30 (m, 1H).

(1*r*,3*R*)-*N*-((*S*)-2-((*S*)-2-(2-aminoacetamido)-2-cyclohexyl-*N*-methylacetamido)-3-(3-phenylazetididin-1-yl)propyl)-3-butylcyclobutane-1-carboxamide (**48a**)

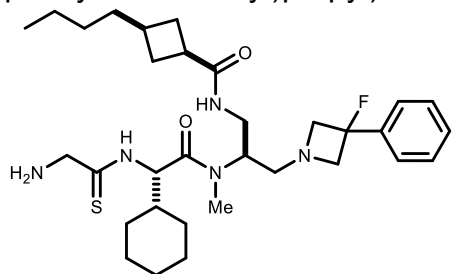


48a was prepared from **52a** by a route analogous to that used to prepare **46**.

¹H NMR (500 MHz, CD₃OD) δ: 4.65 (d, *J* = 6.85, 1H), 4.65 (m, 1H), 4.33 (t, *J* = 7.6, 1H), 4.27 (t, *J* = 7.6, 1H), 4.18-3.90 (m, 3H), 3.82-3.63 (m, 2H), 3.53-3.46 (m, 1H), 3.45-3.37 (m, 2H), 3.33-3.27 (m, 1H), 3.17 (d, *J* = 4.7, 13.5, 1H), 3.11 (s, 3H), 2.98 -2.86 (m, 1H), 2.36-2.13 (m, 3H), 1.94-1.66 (m, 7H), 1.45-1.06 (m, 11H), 0.92 (t, *J* = 7.3, 3H).

HPLC/MS: M+1/Z Calcd = 554.4 Obsd. 554.1

(1*r*,3*R*)-*N*-((*S*)-2-((*S*)-2-(2-aminoethanethioamido)-2-cyclohexylacetamido)-3-(3-fluoro-3-phenylazetidin-1-yl)propyl)-3-butylcyclobutane-1-carboxamide (**48b**)

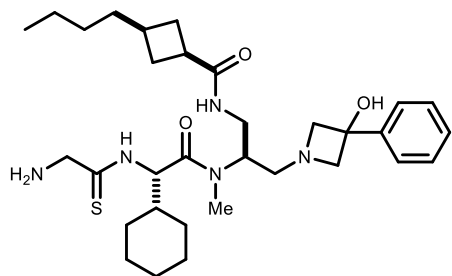


48b was prepared from **52b** by a route analogous to that used to prepare **46**.

¹H NMR (500 MHz, CD₃OD) δ: 7.49 (d, *J* = 7.8, 2H), 7.37 (t, *J* = 7.6, 2H), 7.31 (t, *J* = 7.5, 1H), 5.14 (d, *J* = 7.2, 1H), 4.6 (bs, 1H), 3.86-3.61 (m, 4H), 3.57 (dd, *J* = 8.7, 22.6, 1H), 3.36 (dd, *J* = 5.5, 14.4, 1H), 3.22 (dd, *J* = 9.0, 13.1, 1H), 3.11 (s, 3H), 2.88-2.76 (m, 2H), 2.56 (dd, *J* = 5.2, 12.5, 1H), 2.26-2.08 (m, 3H), 1.89-1.82 (m, 2H), 1.76-1.67 (m, 3H), 1.65-1.57 (m, 2H), 1.34 (q, *J* = 7.3, 2H), 1.27 (sextet, *J* = 7.3, 2H), 1.19-1.11 (m, 6H), 0.87 (t, *J* = 7.3, 3H).

HPLC/MS: M+1/Z Calcd = 588.3 Obsd. 588.3

(1*r*,3*R*)-*N*-((*S*)-2-((*S*)-2-(2-aminoethanethioamido)-2-cyclohexylacetamido)-3-(3-hydroxy-3-phenylazetidin-1-yl)propyl)-3-butylcyclobutane-1-carboxamide (**48c**)



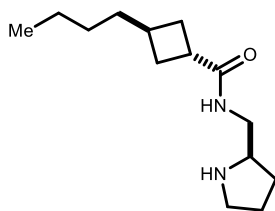
48c was prepared from **52c** by a route analogous to that used to prepare **46**.

¹H NMR (500 MHz, CD₃OD) δ: 7.62 (d, *J* = 7.8, 2H), 7.40 (t, *J* = 7.5, 2H), 7.31 (t, *J* = 7.25, 1H), 5.19 (d, *J* = 7.8, 1H), 4.6 (bs, 1H), 3.99-3.76 (m, 4H), 3.51 (d, *J* = 7.7, 2H), 7.42 (dd, *J* = 6.0, 14.1, 1H), 3.17 (s, 3H), 2.99 (dd, *J* = 9.9, 11.3, 1H), 2.92-2.80 (m, 1H), 2.76 (dd, *J* = 5.0, 12.9, 1H), 2.29-2.11 (m, 3H), 1.96-1.87 (m, 1H), 1.87-1.60 (m, 7H), 1.40 (q, *J* = 7.2, 2H), 1.36-1.27 (m, 2H), 1.27-1.13 (m, 6H), 0.92 (t, *J* = 7.3, 3H).

HPLC/MS: M+1/Z Calcd = 586.4 Obsd. 586.4

Synthesis and Characterization of Aminomethylpyrrolidine GOAT Inhibitors

(1*s*,3*R*)-3-butyl-N-(((*R*)-pyrrolidin-2-yl)methyl)cyclobutane-1-carboxamide (**47**)



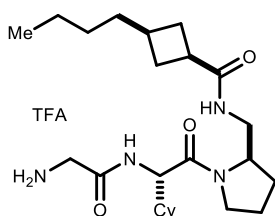
To a solution of 1-Boc-2-(aminomethyl)pyrrolidine (627mg, 3.13 mmol) in acetonitrile (10mL) was added **9** (537mg, 3.45 mmol), DIPEA (819 μ L, 4.7mmol), and TBTU (1.1g, 3.45mmol). The mixture was stirred at room temperature for 2h, then poured into 1N NCl. The aqueous layer was extracted three times with EtOAc, and the combined organic layers were washed with water, saturated NaHCO₃, water, and brine then dried over Na₂SO₄ and concentrated. The residue obtained was dissolved in 4N HCl in dioxane (10mL), stirred at room temperature for 30 minutes, then poured into 1M aqueous Na₂CO₃. The aqueous phase was extracted three times with ether and the combined organic phases were dried over Na₂SO₄ and concentrated. Purification by column chromatography (0-10% MeOH in CHCl₃) afforded **47** as a white crystalline solid. (314mg, 33% yield).

¹H NMR (500MHz, CDCl₃): δ 5.97 (bs, 1H), 3.4 (ddd, $J = 13.5, 5.8, 4.6$, 1H), 3.25 (ddd, $J = 11.5, 7.5, 4.6$, 1H), 3.04 (ddd, $J = 13.4, 7.9, 5.2$, 1H), 2.97-2.84 (m, 3H), 2.36-2.25 (m, 1H), 2.05 (bs, 1H), 2.89-1.62 (m, 5H) 1.42 (app quartet, $J = 7.4$, 1H), 1.39-1.31 (m, 1H), 1.31-1.14 (m, 4H), 0.86 (t, $J = 7.3$, 3H).

¹³C NMR (125 MHz, CDCl₃) δ : 175.9, 57.8, 46.53, 43.62, 36.7, 36.1, 31.9, 30.51, 30.49, 29.4, 29.1, 25.9, 22.6, 14.1.

HPLC/MS: M+1/Z Calcd = 239.2 Obsd. = 239.2

(1*r*,3*S*)-N-(((*R*)-1-(((*S*)-2-(2-aminoacetamido)-2-cyclohexylacetyl)pyrrolidin-2-yl)methyl)-3-butylcyclobutane-1-carboxamide (**55**)



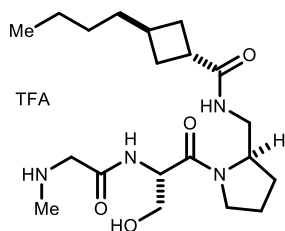
55 was readily prepared by homologation of **47** according to the general procedures.

Rotational isomers present. Major peaks characterized when not overlapping

¹H NMR (500 MHz, CD₃OD) δ : 4.38 (d, $J = 7.9$, 1H), 4.08 (bs, 1H), 3.78 (bs, 1H), 3.74-3.52 (m, 3H), 3.44-3.33 (m, 1H), 2.87 (t, $J = 7.5$, 1H), 2.29-2.10 (m, 3H), 2.05-1.54 (m, 12H), 1.411-0.96 (m, 11H), 0.86 (t, $J = 7.4$, 3H)

HPLC/MS: M+1/Z Calcd = 425.3 Obsd. = 435.3

(1s,3R)-3-butyl-N-(((R)-1-(glycyl-L-seryl)pyrrolidin-2-yl)methyl)cyclobutane-1-carboxamide (**56**)

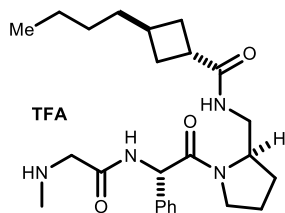


56 was prepared by homologation of **47** according to the general procedures. Yield 5.6mg of the trifluoroacetate salt.

^1H NMR (125 MHz, DMSO- D_6) δ : 8.75 and 8.69 (d, $J = 7.2$, 1H), 8.66 (bs, 1H), 7.88 and 7.64 (t, $J = 5.9$, 1H), 5.07 and 5.02 (t, $J = 5.2$, 1H), 4.70 and 4.61 (q, $J = 7.7$, 1H), 4.33 and 3.94 (bs, 1H), 3.72-3.65 (m, 2H), 3.59-3.41 (m, 4H), 3.26-1.17 (m, 1H), 3.05 and 2.97 (ddd, $J = 6.9, 8.9, 13.1$, 1H), 2.95-2.87 (m, 1H), 2.58-2.54 (m, 1H), 2.53 and 2.51 s, 3H), 2.19 and 2.10 (m, 3H), 1.91-1.61 (m, 6H), 1.42-1.32 (m, 2H), 1.23 (sextet, $J = 7.6$, 2H), 1.17-1.09 (m, 2H), 0.83 (t, $J = 7.3$, 3H).

HPLC/MS: M+1/Z Calcd = 396.3 Obsd. = 435.3

(1s,3R)-N-(((R)-1-((S)-2-(2-aminoacetamido)-2-phenylacetyl)pyrrolidin-2-yl)methyl)-3-butylcyclobutane-1-carboxamide (**58**)

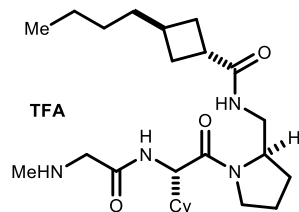


58 was prepared by homologation of **47** according to the general procedures. Yield 30.2mg of the trifluoroacetate salt.

^{13}C NMR (125 MHz, DMSO- D_6) δ : 9.16 and 9.12 (d, $J = 7.9$, 1H), 8.75 (bs, 2H), 7.92 and 7.68 (t, $J = 5.9$, 1H), 7.64 (d, $J = 8.0$, 1H), 7.38-7.28 (m, 5H), 5.89 and 5.61 (d, $J = 7.5$, 1H), 4.37 and 3.95 (ddd, $J = 3.7, 6.9$, and 10.7, 1H), 3.77-3.70 (m, 2H), 3.63 (td, $J = 2.7, 9.3$, 1H), 3.33 (td, $J = 4.7, 12.33$, 1H), 3.10 (ddd, $J = 6.3, 8.3, 14.8$, 1H), 3.03-2.85 (m, 2H), 2.67 (ddd, $J = 6.1, 10.9, 17.1$, 1H), 2.51 (s, 3H), 2.19-2.12 (m, 3H), 1.87-1.76 (m, 2H), 1.75-1.54 (m, 4H), 1.41-1.34 (m, 2H), 1.27-1.19 (m, 2H), 1.17-1.10 (m, 2H), 0.84 and 0.83 (t, $J = 7.2$, 3H).

^{13}C NMR (125 MHz, CDCl_3) δ : 175.4, 167.8, 164.9, 137.0, 129.2, 129.1, 128.6, 58.1, 55.9, 49.3, 46.8, 40.4, 63.2, 35.9, 33.0, 31.7, 30.4, 29.4, 27.3, 23.6, 22.6, 14.6.

(1s,3R)-N-(((R)-1-((S)-2-(2-aminoacetamido)-2-cyclohexylacetyl)pyrrolidin-2-yl)methyl)-3-butylcyclobutane-1-carboxamide (**59**)



59 was prepared by homologation of **47** according to the general procedures. Yield 53.6mg of the trifluoroacetate salt.

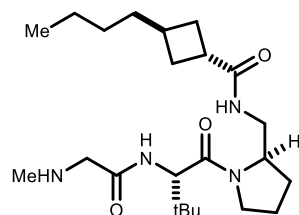
Rotamers present

^{13}C NMR (125 MHz, DMSO- D_6) δ : 8.8 and 8.77 (bs, 2H), 8.67 and 8.2 (t, $J = 8.0$, 1H), 7.92 and 7.66 (t, $J = 5.6$, 1H), 4.41 and 4.33 (t, $J = 8.7$, 1H), 4.37 and 3.93 (app sextet, $J = 4.9$, 1H), 3.79-3.66 (m, 2H), 3.62 (ddd, $J = 3.3$, 8.22, 11.4, 1H), 3.45 (q, $J = 9.0$, 1H), 3.32-3.16 (m, 2H), 3.02 (ddd, $J = 6.9$, 8.8, 15.8, 1H), 2.96-2.81 (2H), 2.52 (s, 3H), 2.20-1.99 (m, 3H), 1.90-1.78 (m, 2H), 1.75-1.45 (m, 10H), 1.40-1.33 (m, 2H), 1.27-1.18 (m, 2H), 1.18-1.07 (m, 5H), 1.06-0.87 (m, 2H), 0.84 and 0.83 (t, $J = 7.2$, 3H).

^{13}C NMR (125 MHz, CDCl_3) δ : 175.3, 169.6, 165.4, 57.2, 55.9, 49.3, 47.1, 42.0, 36.0, 35.8, 33.1, 31.7, 30.4, 30.3, 29.4, 29.4, 28.7, 27.4, 26.2, 26.0, 25.9, 23.6, 22.6, 14.4.

HPLC/MS: M+1/Z Calcd = 449.3 Obsd. = 449.0

(1s,3R)-3-butyl-N-(((R)-1-((S)-3,3-dimethyl-2-(2-(methylamino)acetamido)butanoyl)pyrrolidin-2-yl)methyl)cyclobutane-1-carboxamide (**60**)



59 was prepared by homologation of **47** according to the general procedures. Yield 250.4mg of the hemitartrate salt.

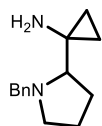
^1H NMR (500 MHz, DMSO- D_6) 5:1 rotamers, major peaks characterized. 8.18 (d, $J = 9.1$, 1H), 7.62 (t, $J = 5.6$, 1H), 4.48 (d, $J = 9.5$, 1H), 3.58-3.49 (m, 2H), 3.38 (s, 2H), 3.2 (dt, $J = 5.0$, 12.8, 1H), 3.05 (ddd, $J = 6.9$, 8.5, 12.8, 1H), 2.93-2.85 (m, 1H), 2.36 (s, 3H), 2.19-2.12 (m, 3H), 1.91-1.76 (m, 2H), 1.73-1.62 (m, 4H), 1.37 (q, $J = 7.1$, 2H), 1.22 (app pent, $J = 7.22$, 2H), 1.16-1.09 (m, 2H), 0.92 (s, 9H), 0.83 (t, $J = 7.2$, 3H).

^{13}C NMR (125 MHz, DMSO- D_6) δ : 175.3, 174.7, 169.4, 168.7, 71.6, 57.2, 56.9, 52.2, 47.8, 36.0, 35.9, 35.2 34.9, 31.7, 30.4, 30.3, 29.4, 27.5, 27.1 26.8, 23.6, 22.6, 14.5.

HPLC/MS: M+1/Z Calcd = 423.3 Obsd. = 423.3.

Synthesis and Characterization of Branched GOAT Inhibitors

1-(1-benzylpyrrolidin-2-yl)cyclopropan-1-amine (**65**)



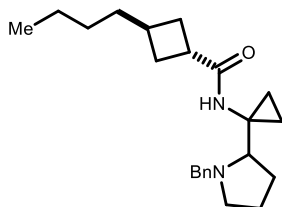
To a solution of 1-benzylpyrrolidine-2-carbonitrile (1g, 5.35mmol) in THF at room temperature was added titanium isopropoxide (1.8mL, 5.88mmol) followed by dropwise addition of ethylmagnesium bromide (4.86mL, 10.7mmol, 2.2M in Et₂O). This mixture was stirred at room temperature for 30m, then boron trifluoride etherate (1.36mL, 10.7mmol) was added all at once. This solution was stirred for 10 minutes, then 1N NaOH was added. The basic solution was extracted with ethyl acetate and the organic phases washed with brine. The organics were then dried with Na₂SO₄ and concentrated. Product was purified by column chromatography to afford 905mg of material which was ~70% pure by ¹H NMR. An analytical sample was prepared by PTLC, while the bulk of the material was used without further purification.

¹H NMR (400 MHz, CDCl₃) δ 7.38-7.28 (m, 4H), 7.25-7.21 (m, 1H), 4.3 (d, *J* = 13.04 Hz, 1H), 3.13 (d, *J* = 13.04 Hz, 1H), 2.97 (dd, *J* = 2.68, 7.00 Hz, 1H), 2.2-2.0 (m, 3H), 1.88-1.79 (m, 3H), 1.75-1.6 (m, 2H), 0.8-0.72 (ddd, *J* = 3.83, 6.1, 9.7 Hz, 1H), 0.59-0.51 (ddd, *J* = 4.5, 5.96, 10.44 Hz, 1H), 0.52-0.45 (ddd, *J* = 4.12, 5.96, 10 Hz, 1H), 0.32-0.25 (ddd, *J* = 4.48, 6.6, 10.52 Hz, 1H)

¹³C NMR (100 MHz, CDCl₃) δ 139.94, 128.63, 128.26, 126.83, 71.61, 58.82, 33.59, 27.57, 22.53, 16.46, 8.8

HPLC/MS: M+1/Z Calcd = 449.3 Obsd. = 217.2

(*trans*)-N-(1-(1-benzylpyrrolidin-2-yl)cyclopropyl)-3-butylcyclobutane-1-carboxamide (**66**)



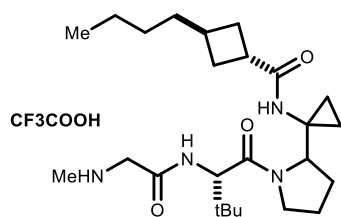
66 was prepared from **65** (910mg) by a standard peptide coupling procedure, affording 291mg of **66**.

¹H NMR (400 MHz, CDCl₃) δ 7.42-7.27 (m, 5H), 4.28 (d, *J* = 13.16 Hz, 1H), 3.6 (d, *J* = 13.16 Hz, 1H), 3.19-3.08 (m, 1H), 2.98-2.88 (m, 1H), 2.71-2.58 (m, 1H), 2.48 (q, *J* = 8.1 Hz, 1H), 2.36-2.21 (m, 3H), 1.96 (q, *J* = 7.5 Hz, 2H), 1.88-1.62 (m, 4H), 1.41 (q, *J* = 7.4 Hz, 2H), 1.3-1.09 (m, 4H), 0.93-0.68 (m, 3H), 0.86 (t, *J* = 7.3 Hz, 3H), 0.59-0.51 (m, 1H)

¹³C NMR (100 MHz, CDCl₃) δ 176.78, 129.56, 128.63, 128.62, 128.0, 71.15, 59.64, 54.42, 37.1, 36.3, 33.6, 31.8, 30.4, 30.3, 29.5, 27.9, 23.2, 22.7, 14.1, 10.2

HPLC/MS: M+1/Z Calcd = 355.3 Obsd. = 355.3

(1*s*,3*R*)-3-butyl-N-(1-((*R*)-1-((*S*)-3,3-dimethyl-2-(2-(methylamino)acetamido)butanoyl)pyrrolidin-2-yl)cyclopropyl)cyclobutane-1-carboxamide (**61a**)



A solution of **66** (290mg), and Pd/C (60mg) in MeOH (10mL), 1N HCl (1mL), was placed under pressure of hydrogen (1 atm) for 24 hours. After 24 hours the solution was filtered and concentrated. Boc-Tle-OH and Boc-Sar-OH were appended to the resulting secondary amine to provide a 1:1 mixture of diastereomeric Boc-protected secondary amines. These were separated by preparative HPLC. Each was independently dissolved in 1:1 dichloromethane/TFA for 30m, then concentrated to provide **61a** and **61b** as the trifluoroacetate salts. *R* stereochemistry at the alpha carbon of the pyrrolidine was assigned to **61a**, but not **61b** was able to inhibitor GOAT.

Yield **61a**: 32.8mg

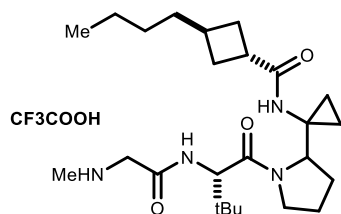
~2:1 mixture of rotational isomers evident. The larger peak is reported where they did not overlap.

¹H NMR (400 MHz, MeOD) δ: 4.55 (s, 1H), 4.34 (dd, *J* = 1.73, 8.5, 1H), 3.89-3.78 (m, 2H), 3.57-3.43 (m, 1H), 2.96-2.87 (m, 1H), 2.68 (s, 3H), 2.29-1.95 (m, 6H), 1.91-1.65 (m, 4H), 1.47-1.38 (m, 2H), 1.33-1.12 (m, 4H), 1.03 (s, 9H), 0.93-0.83 (m, 4H), 0.803-0.687 (m, 1H), 0.65-0.55 (m, 1H)

¹³C NMR (125 MHz, MeOD₃) δ: 177.54, 177.40, 171.4, 170.2, 165.0, 164.4, 61.43, 60.94, 58.27, 58.11, 49.39, 49.14, 48.67, 46.84, 36.33, 36.06, 36.00, 35.85, 35.79, 35.13, 34.30, 34.14, 32.19, 32.14, 31.62, 31.59, 29.9, 29.7, 29.66, 29.58, 29.13, 27.47, 26.30, 25.67, 25.58, 23.84, 22.31, 24.43, 13.02, 12.55, 11.57, 11.21, 10.06

HPLC/MS: M+1/Z Calcd = 449.3 Obsd. = 449.3

(1*s*,3*R*)-3-butyl-N-(1-((*R*)-1-((*S*)-3,3-dimethyl-2-(2-(methylamino)acetamido)butanoyl)pyrrolidin-2-yl)cyclopropyl)cyclobutane-1-carboxamide (**61b**)



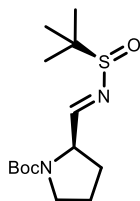
See procedure for **61a**. yield **61b**: 38.9mg.

¹H NMR (400 MHz, MeOH-D₄) δ: 4.57 (s, 1H), 3.95-3.87 (m, 3H), 3.75-3.66 (m, 1H), 3.64-3.57 (m, 1H), 2.98-2.89 (m, 1H), 2.73 (s, 3H), 2.28-1.98 (m, 5H), 1.98-1.69 (m, 4H), 1.43 (quart, *J* = 7.5, 2H), 1.32-1.22 (m, 2H), 1.22-1.12 (m, 3H), 1.00 (s, 9H), 0.87 (t, *J* = 7.8, 3H), 0.79-0.70 (m, 1H), 0.670.59 (m, 2H).

¹³C NMR (125 MHz, MeOH-D₄) δ: 177.46, 169.9, 165.2, 62.3, 58.0, 49.4, 48.0, 47.9, 47.7, 36.2, 35.8, 34.3, 34.3, 32.3, 31.5, 29.6, 29.6, 29.2, 28.3, 25.5, 23.4, 22.3, 14.6, 13.0, 10.5

HPLC/MS: M+1/Z Calcd = 449.3 Obsd. = 449.4

tert-butyl (R)-2-((E)-(((R)-*tert*-butylsulfinyl)imino)methyl)pyrrolidine-1-carboxylate (**67**)



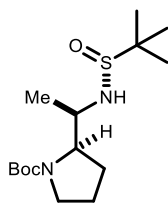
To a dried vial was added boc-Proinaldehyde (314mg, 1.57mmol), (R)-2-Methyl-2-propanesulfonamide (189mg, 1.57mmol) and THF (3mL). This solution was cooled to 0C and a solution of titanium ethoxide (1.43g, 6.3mmol) was added slowly by syringe. After stirring at room temperature overnight the solution was poured into iced brine. The resultant slurry was filtered over celite, and the solution extracted three times with ethyl acetate. The combined organic phases were dried with sodium sulfate and concentrated to afford 375 mg of **67** as a colorless oil. The material was used without further purification.

Mixture of rotational isomers

¹H NMR (500 MHz CDCl₃) δ: 7.91 (d, *J* = 3) and 7.83 (d, *J* = 4.6) 1H], 4.58-4.51 (m, 1H), 3.82 (bs, 1H), 3.45-3.32 (m, 3H), 2.17-2.03 (m, 1H), 2.02-1.70 (m, 5H), 1.42-1.34 (m, 11H), 1.15-1.12 (m, 9H)

¹³C NMR (125 MHz, CDCl₃) δ: . 169.2 and 168.75, 154.3 and 154.2, 79.95 and 79.60, 60.40 and 60.23 57.76 and 56. 76, 46.57 and 46. 25, 30.25 and 29.31, 28.36, 24.2 and 23.14 22.61 and 21.02, 22.34 and 22.14

tert-butyl (R)-2-((R)-1-(((R)-*tert*-butylsulfinyl)amino)ethyl)pyrrolidine-1-carboxylate (**68a**).



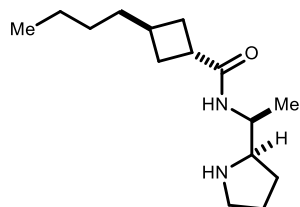
To a solution of MeMgBr (10.76 mL, 2.04M in Et₂O, 1.9 eq) in THF (19mL, 0.75M to Grignard) at -40°C, imine (3.5g, 11.57 mmol) in DCM (21mL, 0.55M) was added slowly. The reaction was stirred at -40°C for 4 hours. The reaction was then warmed to 0°C, quenched with saturated aqueous ammonium chloride, and extracted with EtOAc. The organic layer was washed with brine, dried over MgSO₄, filtered and concentrated to a clear oil. The residue was purified by flash column chromatography (1:1 → 1:2 → 1:3 → 1:4 Hex/EtOAc, SiO₂) to give **41** as a clear oil (2.96g, 80%) R_f = 0.3-0.5 streak (1:1 Hex/EtOAc).

¹H NMR (500 MHz CDCl₃) δ: 5.17 (bs, 1H) 3.82 (bs, 1H), 3.66-3.25 (m, 4H), 1.92-1.76 (m, 4H), 1.45 (s, 9H), 1.19 (s, 9H), 1.11 (d *J* = 6.2, 3H)

¹³C NMR (125 MHz, CDCl₃) δ: 157.1, 80.0, 62.0, 55.0, 46.6, 28.5, 23.7, 22.9, 20.1, 53.4, 28.4

HPLC/MS: M+1/Z Calcd = 319.2 Obsd. 319.2

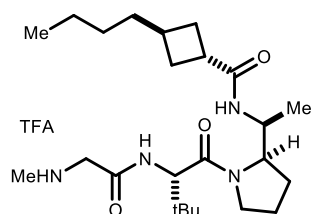
(*trans*)-3-butyl-N-((S)-1-((R)-pyrrolidin-2-yl)ethyl)cyclobutane-1-carboxamide (**69a**)



To a solution of 68a (225mg, 0.7mmol) in MeOH at 0C was added HCl (4N in dioxane, 0.6 mL, 2.4mmol). The solution was allowed to stand for 30m (reaction progress was monitored by HPLC) until cleavage of the sulfonamide was observed, after which the reaction was quenched by addition of 800uL iPr₂NEt and the solution was concentrated. The residue was dissolved in acetonitrile (10mL) and **42** (163uL, 1.05mmol), TBTU (337mg, 1.05mmol) and iPr₂NEt (200uL, 1.05mmol) were added. The solution was allowed to stir for one hour, then poured into 1N HCl, and extracted with EtOAc. The organic phases were washed with NaHCO₃ and brine, then dried over Na₂SO₄, filtered and concentrated. The resultant residue was dissolved in 4N HCl/Dioxane (4mL), stirred for 30m, and then concentrated. The residue was dissolved in 1N aqueous Na₂CO₃ and extracted with diethyl ether. The organic phases were dried over Na₂SO₄, filtered and concentrated. Finally, the oily residue was purified by column chromatography to afford **69a** (40mg)

¹H NMR (500 MHz, CDCl₃) δ: 6.76 (d, *J* = 8.6, 1H), 4.91 (bs, 1H), 4.03 (sextet, *J* = 6.8, 1H), 3.27 (ddd, *J* = 5.3, 7.9, 13.5, 1H), 3.05-2.93 (m, 3H), 2.32-2.17 (m, 3H), 1.95-1.87 (m, 1H), 1.85-1.73 (m, 3H), 1.49 (ddd, *J* = 8.23, 12.65, 16.47, 1H), 1.38 (q, *J* = 7.4, 2H), 1.22 (p, *J* = 7.5, 2H), 1.16 (d, *J* = 6.7, 3H), 1.16-1.09 (m, 2H), 0.83 (t, *J* = 7.5, 3H),

(*trans*)-3-butyl-N-((*S*)-1-((*R*)-1-((*S*)-3,3-dimethyl-2-(2-(methylamino)acetamido)butanoyl)pyrrolidin-2-yl)ethyl)cyclobutane-1-carboxamide
(62a)

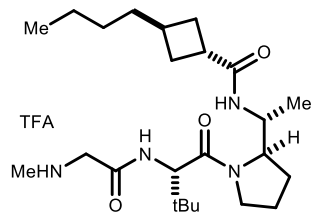


69a (43.3mg) was processed according to the standard peptide coupling procedures to afford **62a** (41.3mg) as the trifluoroacetate salt following HPLC purification.

¹H NMR (500 MHz, CD₃OD) δ 4.69 (s, 1H), 4.3-4.22 (m, 1H), 4.21-4.14 (m, 1H), 3.89 (d, *J* = 15.86 Hz, 1H), 3.83-3.75 (m, 1H), 3.73 (d, *J* = 15.86 Hz, 1H), 3.68-3.61 (m, 1H), 3.0-3.92 (m, 1H), 2.7 (s, 3H), 2.34-2.19 (m, 3H), 2.05-1.7 (m, 6H), 1.51-1.41 (m, 2H), 1.36-1.26 (m, 2H), 1.25-1.17 (m, 2H), 1.06-1.0 (m, 12H), 0.89 (t, *J* = 7.3 Hz)

¹³C NMR (125 MHz, CD₃OD) δ 176.38, 170.6, 164.77, 66.28, 60.24, 57.61, 49.16, 46.92, 36.04, 35.85, 34.67, 32.21, 31.62, 29.99, 29.77, 29.20, 26.15, 25.82, 25.5, 24.22, 23.47, 22.35, 15.23, 13.06

(*trans*)-3-butyl-N-((*R*)-1-((*R*)-1-((*S*)-3,3-dimethyl-2-(2-(methylamino)acetamido)butanoyl)pyrrolidin-2-yl)ethyl)cyclobutane-1-carboxamide
(62b)



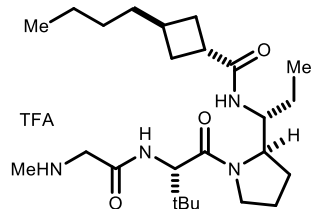
To methylmagnesium bromide (2.62mL, 5.24mmol) in THF (6mL) was slowly added sulfimine **67** (797mg) in 6mL of THF at -40°C . The reaction was stirred at -40°C for 3 hours. The reaction was then warmed to room temperature overnight. The reaction was quenched with saturated aqueous ammonium chloride, and extracted with Et_2O . The organic layer was washed with brine, dried over MgSO_4 , filtered and concentrated to a clear oil. The minor diastereomer of the product (lower rf) was purified by column chromatography (50 to 90% EtOAc in Hexanes). Yield 77mg. This material was processed as for **62a** to provide **62b**.

^1H NMR (500 MHz, CD_3OD) δ : 4.7 (s, 1H), 4.27 (pentet, $J = 7.0$, 1H), 4.18 (ddd, $J = 5.82, 7.211, 2.112$, 1H), 3.89 (app d, $J = 14.6$, 1H), 7.79 (ddd, $J = 3.5, 8.3, 15.6$, 1H), 3.72 (app d, $J = 14.6$, 1H), 3.693.63 (m, 1H), 3.011-2.93 (m, 1H), 2.71 (2, 3H), 2.35-2.21 (m, 3H), 2.05-1.75 (m, 6H), 1.47 (q, $J = 7.6$, 2H), 1.31 (pentet, $J = 7.5$, 2H), 1.26-1.20 (m, 2H), 1.05-1.02 (m, 12H), 0.9 (t, $J = 7.2$, 3H),

^{13}C NMR (125 MHz, CD_3OD) δ : 176.4, 170.6, 164.7, 60.3, 57.6, 49.1, 36.0, 35.9, 34.7, 32.2, 31.6, 30.0, 29.8, 29.2, 26.2, 25.8, 25.5, 24.2, 23.5, 22.4, 15.3, 13.1

HPLC/MS Calcd. = Obsd. =

(1*s*,3*R*)-3-butyl-N-((*R*)-1-((*R*)-1-((*S*)-3,3-dimethyl-2-(2-(methylamino)acetamido)butanoyl)pyrrolidin-2-yl)propyl)cyclobutane-1-carboxamide (**62c**)



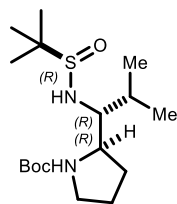
62c was prepared by a route analogous to that used to prepare **62a** and **62b**.

^1H NMR (500 MHz, $\text{DMSO}-d_6$) δ 8.86 (bs, 1H), 8.80 (bs, 1H), 8.53 (d, $J = 9.6$ Hz, 1H), 7.36 (d, $J = 9.55$, 1H), 4.56 (d, $J = 9.6$ Hz, 1H), 4.09-4.0 (m, 1H), 3.98-3.92 (m, 1H), 3.86-3.8 (m, 1H), 3.78-3.7 (m, 1H), 3.63-3.55 (m, 1H), 3.38-3.3 (m, 1H), 2.98-2.89 (m, 1H), 2.57 (m, 3H), 2.16-2.08 (m, 3H), 1.89-1.63 (m, 6H), 1.43-1.29 (m, 3H), 1.28-1.18 (m, 3H), 1.18-1.09 (m, 3H), 0.92 (s, 9H), 0.84 (t, $J = 7.27$ Hz, 3H), 0.72 (t, $J = 7.3$ Hz, 3H)

^{13}C NMR (125 MHz, $\text{DMSO}-d_6$) δ 175.24, 168.82, 165.53, 60.5, 56.87, 51.15, 49.64, 47.54, 36.10, 35.87, .0, 33.26, 31.53, 30.15, 29.46, 26.75, 25.44, 24.88, 24.32, 22.62, 14.46, 11.39

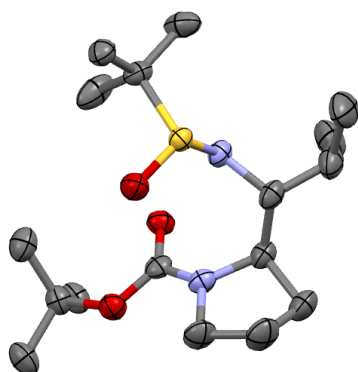
HPLC/MS Calcd. = Obsd. =

tert-butyl (*R*)-2-((*R*)-1-(((*R*)-*tert*-butylsulfinyl)amino)-2-methylpropyl)pyrrolidine-1-carboxylate (**68d**)

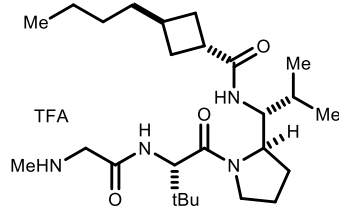


68d (271.4mg, 47% yield) was obtained in the same fashion as **68a**. The isolated material was crystalline, and a single crystal was submitted for X-Ray analysis. The structure shown below was obtained, allowing assignment of *R, R, R* stereochemistry.

XRay Structure



(*trans*)-3-butyl-N-((*R*)-1-((*R*)-1-((*S*)-3,3-dimethyl-2-(2-(methylamino)acetamido)butanoyl)pyrrolidin-2-yl)-2-methylpropyl)cyclobutane-1-carboxamide (**62d**)



62d was prepared from **68d** in a fashion analogous to that used to prepare **68a-c**.

^1H NMR (500 MHz, $\text{DMSO-}D_6$) δ 8.85 (bs, 2H), 8.58 (d, $J = 9.35$ Hz, 1H), 6.48 (d, $J = 9.46$ Hz, 1H), 4.62 (d, $J = 9.4$ Hz, 1H), 4.15-4.06 (m, 1H), 3.92-3.82 (m, 1H), 3.76-3.68 (m, 1H), 3.67-3.59 (m, 1H), 3.52-3.42 (m, 1H), 3.38-3.3 (m, 1H), 2.89-2.8 (m, 1H), 2.52 (m, 3H), 2.2-2.1 (m, 2H), 2.1-2.02 (m, 1H), 1.92-1.67 (m, 6H), 1.65-1.55 (m, 1H), 1.38 (q, $J = 7.38$ Hz, 2H), 1.29-1.18 (m, 2H), 1.18-1.09 (m, 1H), 0.91 (s, 9H), 0.86-0.78 (m, 9H)

^{13}C NMR (125 MHz, $\text{DMSO-}D_6$) δ 174.87, 170.39, 165.13, 58.18, 56.7, 56.63, 49.45, 47.81, 36.04, 35.97, 35.77, 33.17, 31.85, 31.17, 30.24, 29.92, 29.45, 28.87, 26.73, 23.72, 22.6, 21.28, 17.47, 14.47

Thioamide Synthesis using Thioacyl Donors

tert-Butyl (2-((2-amino-5-nitrophenyl)amino)-2-thioxoethyl)carbamate (**74**)



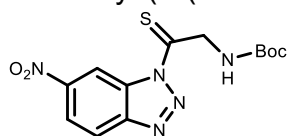
Boc-Glycine (1.575g, 9mmol) was dissolved in THF (100mL) and cooled to -40C. N-methyl morpholine (2.2mL, 20mmol) was added. Isobutyl chloroformate (1.3mL, 10mmol) was added dropwise and the reaction stirred at -40C for 20m, then *m*-nitrophenylenediamine (1.53g, 10mmol) was added and the reaction was allowed to warm to room temperature overnight. The reaction was diluted with EtOAc and aqueous NaHCO₃. The aqueous phase was extracted two more times with ethyl acetate. The combined organic phases were washed with brine, dried over MgSO₄, filtered and concentrated. Yield: 3.03g of anilide.

P₄S₁₀ (5.96, 13.4mmol) and Na₂CO₃ (1.42g, 13.4mmol) were suspended in THF (536mL) and stirred for 1h, then cooled to 0C. Anilide (8.32g, 26.8l) was added. The reaction was stirred at room temperature for three hours. The solution was concentrated onto silica gel, then purified by column chromatography (1:1 EtOAc/Hexanes to 100% EtOAc) to afford 5.372g of a yellow solid

¹H NMR (500 MHz, CDCl₃) 7.92 (dd, *J* = 2.3, 9.1, 1H), 7.85 (dd, *J* = 2.3, 5.5, 1H), 7.31 (s, 2H), 6.75 (d, *J* = 9.1, 1H), 6.49 (bs, 1H), 4.06 (s, 2H), 1.37 (s, 9H)

¹³C NMR (125 MHz, CDCl₃) δ: 202.9, 156.4, 150.9, 135.6, 128.2, 125.4, 125.2, 114.1, 79.1, 51.7, 28.6

Tert-butyl (2-(6-nitro-1H-benzo[d][1,2,3]triazol-1-yl)-2-thioxoethyl)carbamate (**75**)



75

74 (5.37g, 16.48mmol) was dissolved in AcOH (117mL) then cooled to 0C. Water (6.6mL) was added then sodium nitrite (1.66g, 24.7mmol) was added in portions over five minutes. After stirring for 30m, the reaction was diluted with 800mL of water, and precipitated products was isolated by filtration as a yellow powder.

¹H NMR (500 MHz, CDCl₃) δ: 9.67 (d *J* = 1.9, 1H), 8.46 (dd *J* 2.3, 8.8 1H), 8.32 (d *J* = 9.2, 1H), 5.44 (bs, 1H), 5.15 (d *J* = 6.0, 2H), 9.67 (d *J* = 1.9, 1H), 1.52 (s, 9H).

(*trans*)-N-(((*R*)-1-(((*S*)-2-(2-aminoethanethioamido)-2-cyclohexylacetyl)pyrrolidin-2-yl)methyl)-3-butylcyclobutane-1-carboxamide (**73**)

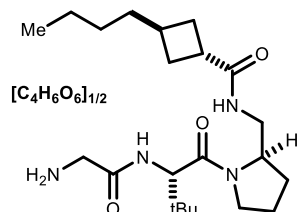


To the primary amine (50mg, 0.12mmol) in THF (1mL) was added $i\text{Pr}_2\text{NEt}$ (21 μL). Equivalents of **75** (40mg, 0.12mmol) in 1mL of THF were then added successively as the reaction was monitored by HPLC. After 3eq had been added, the reaction was still incomplete. The reaction was concentrated and product purified by pTLC. To the resultant product was added a 4N solution of HCl in dioxane. After 30m then solution was concentrated and the product (**73**) purified by HPLC. Significant quantities of degraded byproducts having mass corresponding to the shown fragment were observed, but not isolated. **12** was isolated in low yield.

^1H NMR (500 MHz, MeOH-D_4) δ : 4.12-4.07 (m, 1H), 4.03 (ddd, $J = 2.9, 8.11, 10.11$, 1H), 3.89 (AB, 15.92, 4.78, 2H), 3.61 (q, $J = 8.3$, 1H), 2.91-2.78 (m, 1H), 2.27-2.09 (m, 3H), 2.06-1.61 (m, 12H), 1.39-1.06 (m, 12H), 0.87, (t, $J = 7.2$, 3H).

HPLC/MS: $M+1/Z$ Calcd = 451.3 Obsd = 451.3

(*trans*)-N-(((*R*)-1-((*S*)-2-(2-aminoacetamido)-3,3-dimethylbutanoyl)pyrrolidin-2-yl)methyl)-3-butylcyclobutane-1-carboxamide (**51**)



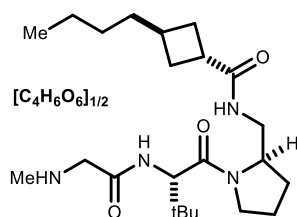
A solution of **47** (2.1mmol), Boc-Tle-OH (2.1mmol), TBTU (2.1mmol), and $i\text{Pr}_2\text{NEt}$ (4.2mmol) in acetonitrile was stirred at room temperature for four hours, then poured into 1N HCl. The aqueous layer was extracted three times with EtOAc, and the combined organic layers were washed with water, saturated NaHCO_3 , water, and brine then dried over Na_2SO_4 and concentrated. The resultant oil (1.03g) was dissolved in 4N HCl and stirred at room temperature for 30m, then concentrated. 1.05mmol of the resultant salt was dissolved in acetonitrile (5mL). To this solution was added Boc-Gly-OH (1.05mmol), TBTU (1.05mmol), and $i\text{Pr}_2\text{NEt}$ (2.1mmol). This solution was stirred at room temperature for three hours, then then poured into 1N HCl. The aqueous layer was extracted three times with EtOAc, and the combined organic layers were washed with water, saturated NaHCO_3 , water, and brine then dried over Na_2SO_4 and concentrated. The resultant oil was dissolved in 4N HCl/Dioxane, and stirred at room temperature for 30m, then concentrated. The free base was liberated by extraction with aqueous 1N Na_2CO_3 and ether, purified by column chromatography (0-5% MeOH in CHCl_3), then formulated as the hemitartrate (127.5mg yield).

^1H NMR (500 MHz, DMSO-d_6) 5:1 rotamers. Only major peak characterized. δ : 8.26 (d, $J = 9.4$, 1H), 7.64 (t, $J = 5.9$, 1H), 4.51 (d, $J = 9.3$, 1H), 3.96 (app octet, $J = 4.6$, 1H), 3.77 (s, 1H), 3.61-3.51 (m, 2H), 3.39 (s, 2H), 3.24 (dt, $J = 4.6, 12.6$, 1H), 3.07 (ddd, $J = 6.7, 8.6, 12.8$, 1H), 2.95-2.88 (m, 1H), 2.21-2.12 (m, 3H), 1.92-1.78 (m, 2H), 1.75-1.64 (m, 4H), 1.39 (q, $J = 6.9$, 2H), 1.28-1.22 (m, 2H), 1.19-1.11 (m, 2H), 0.94 (s, 9H), 0.85 (t, $J = 7.3$, 3H).

^{13}C NMR (125 MHz, DMSO-d_6) δ : 175.4, 174.8, 169.8, 169.6 71.6, 57.2, 56.8, 47.7, 42.6, 36.0, 35.8, 35.3, 31.8, 30.4, 31.3, 29.4, 27.5, 27.1, 26.7, 23.6, 22.6, 14.5

HPLC/MS: $M+1/Z$ Calcd = 409.3 3 Obsd. = 409.3

(trans)-3-butyl-N-(((R)-1-((S)-3,3-dimethyl-2-(2-(methylamino)acetamido)butanoyl)pyrrolidin-2-yl)methyl)cyclobutane-1-carboxamide (52)



A solution of **19** (2.1mmol), Boc-Tle-OH (2.1mmol), TBTU (2.1mmol), and iPr_2NEt (4.2mmol) in acetonitrile was stirred at room temperature for four hours, then poured into 1N HCl. The aqueous layer was extracted three times with EtOAc, and the combined organic layers were washed with water, saturated $NaHCO_3$, water, and brine then dried over Na_2SO_4 and concentrated. The resultant oil (1.03g) was dissolved in 4N HCl and stirred at room temperature for 30m, then concentrated. 1.05mmol of the resultant salt was dissolved in acetonitrile (5mL). To this solution was added Boc-Sar-OH (1.05mmol), TBTU (1.05mmol), and iPr_2NEt (2.1mmol). This solution was stirred at room temperature for three hours, then then poured into 1N HCl. The aqueous layer was extracted three times with EtOAc, and the combined organic layers were washed with water, saturated $NaHCO_3$, water, and brine then dried over Na_2SO_4 and concentrated. The resultant oil was dissolved in 4N HCl/Dioxane, and stirred at room temperature for 30m, then concentrated. The free base was liberated by extraction with aqueous 1N Na_2CO_3 and ether, purified by column chromatography (0-5% MeOH in $CHCl_3$), then formulated as the hemitartrate (250.4mg yield).

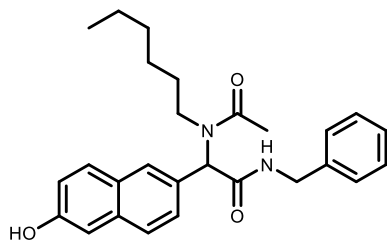
1H NMR (500 MHz, $DMSO-d_6$) 5:1 rotamers, major peaks characterized. δ : 8.18 (d, $J = 9.1$, 1H), 7.62 (t, $J = 5.6$, 1H), 4.48 (d, $J = 9.5$, 1H), 3.58-3.49 (m, 2H), 3.38 (s, 2H), 3.2 (dt, $J = 5.0$, 12.8, 1H), 3.05 (ddd, $J = 6.9$, 8.5, 12.8, 1H), 2.93-2.85 (m, 1H), 2.36 (s, 3H), 2.19-2.12 (m, 3H), 1.91-1.76 (m, 2H), 1.73-1.62 (m, 4H), 1.37 (q, $J = 7.1$, 2H), 1.22 (app pent, $J = 7.22$, 2H), 1.16-1.09 (m, 2H), 0.92 (s, 9H), 0.83 (t, $J = 7.2$, 3H).

^{13}C NMR (125 MHz, $DMSO-d_6$) δ : 175.3, 174.7, 169.4, 168.7, 71.6, 57.2, 56.9, 52.2, 47.8, 36.0, 35.9, 35.2, 34.9, 31.7, 30.4, 30.3, 29.4, 27.5, 27.1, 26.8, 23.6, 22.6, 14.5.

HPLC/MS: $M+1/Z$ Calcd = 423.3 Obsd. = 423.3

Literature GOAT inhibitors

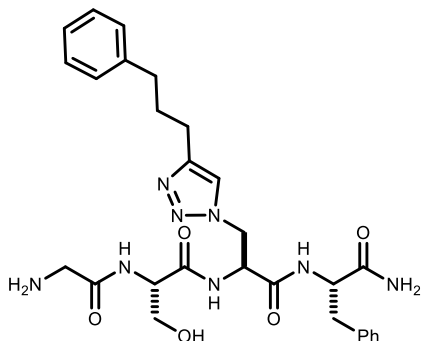
N-benzyl-2-(N-hexylacetamido)-2-(6-hydroxynaphthalen-2-yl)acetamide (**78**)



6-hydroxy-2-naphthaldehyde (200mg, 1.16mmol), hexylamine (309uL, 2.32mmol), acetic acid (94uL, 2.32mmol), and benzyl isonitrile (283uL, 2.32mmol) were refluxed in methanol for 24h. The solution was concentrated the product purified by column chromatography. Yield 482.3 mg, yellow solid.

^1H NMR (500 MHz, CDCl_3) δ : 1H 8.47 (bs, 1H), 7.51 (d, $J = 9.5$, 1H), 4.47 (d, $J = 8.5$, 1H), 7.3-7.16 (m, 6H), 7.09-7.04 (m, 2H), 7.7 (t, $J = 5.7$, 1H), 6.03 (s, 1H), 4.48 (AB, 2H), 3.36-3.28 (m, 2H), 2.17 (s, 3H), 1.43-1.34 (m, 1H), 1.33-1.21 (m, 3H), 1.06-0.83 (m, 6H), 0.67 (t, $J = 6.9$, 3H)

(S)-N-((S)-1-amino-1-oxo-3-phenylpropan-2-yl)-2-((S)-2-(2-aminoacetamido)-3-hydroxypropanamido)-3-(4-(3-phenylpropyl)-1H-1,2,3-triazol-1-yl)propanamide (**79**)



79 was prepared on solid phase according to the literature protocol, and purified by preparative HPLC.

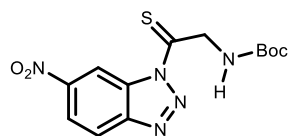
^1H NMR (500 MHz, DMSO-d_6) δ : 8.47 (d, $J = 7.75$, 1H), 8.29 (d, $J = 7.9$, 1H), 8.27 (d, $J = 8$, 1H), 8.07 (d, $J = 8.4$, 1H), 7.93 (bt, $J = 5.6$, 1H), 7.69 (s, 1H), 7.28-7.102 (m, 10H), 6.96 (bs, 1H), 4.71-4.59 (m, 2H), 4.48 (ddd, $J = 4.64$, 8.14, 9.07, 1H), 4.40 (dd, $J = 7.55$, 14.0, 1H), 4.35 (ddd, $J = 5.9$, 7.45, 11.9, 1H), 4.20 (ddd, $J = 5.6$, 8.7, 14.2, 1H), 3.57-3.46 (m, 4H), 3.04 (dd, $J = 14.3$ 4.7, 1H), 2.77 (dd, $J = 9.25$, 14.0, 1H), 2.6-2.52 (m, 4H), 1.84 (pentet, $J = 7.5$, 2H), 1.59-1.51 (m, 1H), 1.50-1.41 (m, 3H), 0.86 (d, $J = 6.6$, 3H), 0.80 (d, $J = 6.6$, 3H).

Experimental Procedures Supporting Chapter 4

Thioacylation Using Nitrotriazolyl Thioacyl Donors

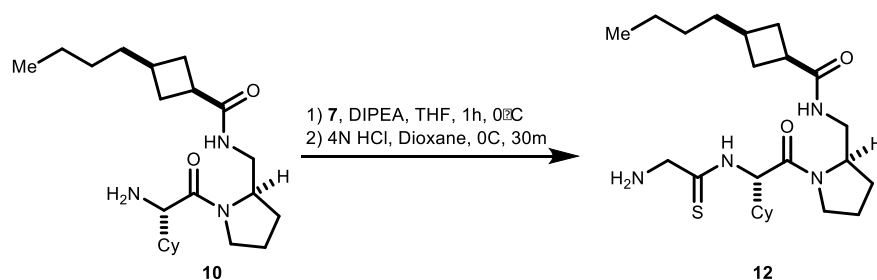
For preparation of nitrotriazole **7** see supporting information for chapter **3**.

tert-Butyl (2-(6-nitro-1H-benzo[d][1,2,3]triazol-1-yl)-2-thioxoethyl)carbamate (**7**)



^1H NMR (500 MHz, CDCl_3) (**7**) δ : 9.67 (d, $J = 1.9$, 1H), 8.46 (dd, $J = 2.3, 8.8$, 1H), 8.32 (d, $J = 9.2$, 1H), 5.44 (bs, 1H), 5.15 (d, $J = 6.0$, 2H), 9.67 (d, $J = 1.9$, 1H), 1.52 (s, 9H).

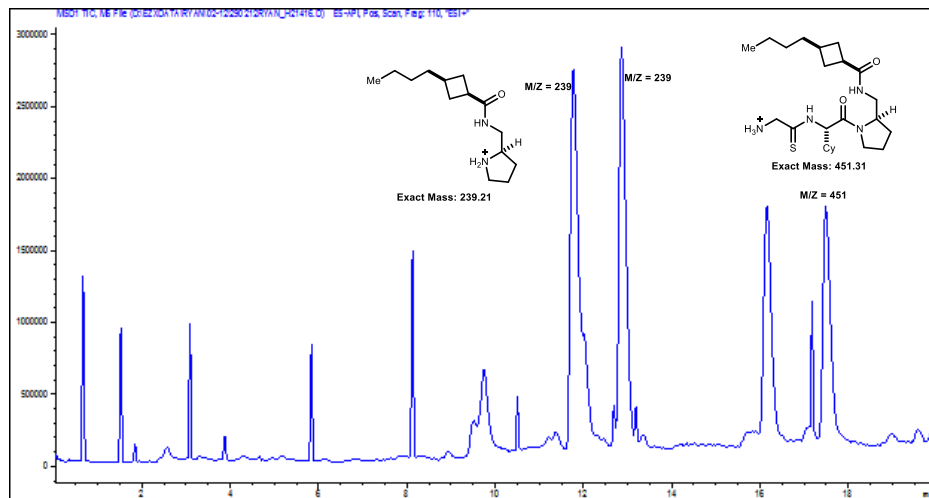
(*cis*)-N-(((*R*)-1-((*S*)-2-(2-Aminoethanethioamido)-2-cyclohexylacetyl)pyrrolidin-2-yl)methyl)-3-butylcyclobutane-1-carboxamide (**12**)



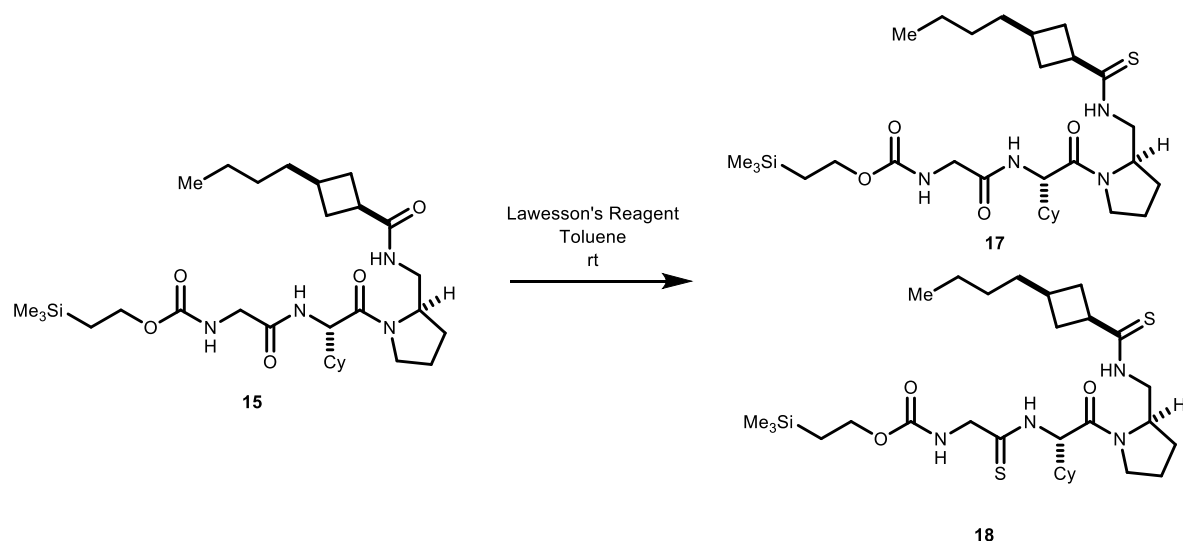
To primary amine **10** (50mg, 0.12mmol) in THF (1mL) was added $i\text{Pr}_2\text{NEt}$ (21 μL). Equivalents of **7** (40mg, 0.12mmol) in 1mL of THF were then added successively as the reaction was monitored by HPLC. After 3eq had been added, the reaction was still incomplete, but was not progressing. The reaction was concentrated and product purified by pTLC. To the resultant product was added a 4N solution of HCl in dioxane. After 30m then solution was concentrated and the product (**12**) purified by HPLC. Significant quantities of degraded byproducts having mass corresponding to the shown fragment were observed, but not isolated. **12** was isolated in low yield.

^1H NMR (500 MHz MeOD) δ : 4.12-4.07 (m, 1H), 4.03 (ddd, $J = 2.9, 8.11, 10.11$, 1H), 3.89 (AB, $J = 4.78, 15.92$, 2H), 3.61 (q, $J = 8.3$, 1H), 2.91-2.78 (m, 1H), 2.27-2.09 (m, 3H), 2.06-1.61 (m, 12H), 1.39-1.06 (m, 12H), 0.87 (t, $J = 7.2$, 3H).

HPLC/MS: $M+1/Z$ Calcd = 451.3 Obsd = 451.3.



Evaluation of Lawesson's Reagent Selectivity



(1*r*,3*S*)-3-Butyl-N-(((*R*)-1-((*S*)-2-cyclohexyl-2-(2-(3-(trimethylsilyl)propanamido)acetamido)acetyl)pyrrolidin-2-yl)methyl)cyclobutane-1-carboxamide (**15**)

15 was prepared by standard solution phase peptide chemistry.

¹H NMR (500 MHz, CDCl₃) δ: 8.3 (d, *J* = 8.9, 1H), 7.29 (bq, *J* = 3.9, 1H), 5.68 (bt, *J* = 4.3, 1H), 4.55 (t, *J* = 9.1, 1H), 3.94 (s, 1H), 4.11-3.9 (m, 3H), 3.87 (dd, *J* = 4.5, 17.1, 1H), 3.71 (t, *J* = 8.8, 1H), 3.51-3.39 (m, 2H), 3.05-2.98 (m, 1H), 2.76 (App P, *J* = 8.5, 1H), 2.16-1.94 (m, 3H), 1.93-1.47 (m, 11H), 1.25 (q, *J* = 7.2, 2H), 1.19-0.86 (m, 11H), 0.75 (t, *J* = 7.3, 3H), -0.045 (s, 9H).

¹³C NMR (125 MHz, CDCl₃) δ: 175.63, 170.79, 168.41, 156.68, 77.34, 63.24, 57.99, 55.38, 53.39, 47.47, 43.51, 40.95, 39.01, 38.47, 36.18, 35.91, 31.58, 31.38, 31.31, 29.57, 29.03, 28.70, 27.39, 25.98, 25.93, 25.81, 23.19, 22.47, 17.59, 13.99, -1.61.

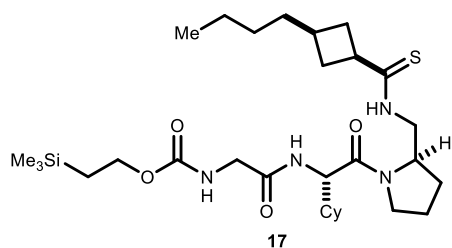
HPLC/MS: M+1/Z Calcd = 579.4 Obsd = 579.4.

2-(Trimethylsilyl)ethyl (2-(((*S*)-2-((*R*)-2-(((1*r*,3*S*)-3-butylcyclobutane-1-carbothioamido)methyl)pyrrolidin-1-yl)-1-cyclohexyl-2-oxoethyl)amino)-2-oxoethyl)carbamate (**17**)

and

2-(Trimethylsilyl)ethyl (2-(((*S*)-2-((*R*)-2-(((1*r*,3*S*)-3-butylcyclobutane-1-carbothioamido)methyl)pyrrolidin-1-yl)-1-cyclohexyl-2-oxoethyl)amino)-2-thioethyl)carbamate (**18**)

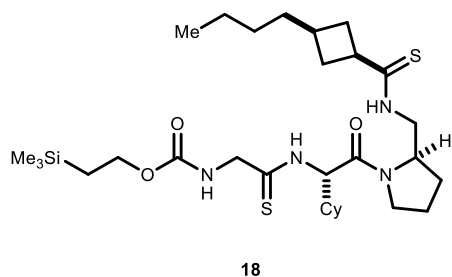
To a solution of **15** (53mg, 0.91 mmol) in toluene at room temperature was added Lawesson's Reagent (18.52mg, 0.0458mmol). The reaction was monitored periodically by HPLC (see chapter text). After 18h the reaction was concentrated and purified by HPLC. Yield **17** = 20mg. Yield **18** = 10mg. Structures of thioamides **17** and **18** were assigned by one and two dimensional NMR analyses (COSY, HMBC).



^1H NMR (500 MHz, CDCl_3) δ : 9.31 (bs, 1H), 6.9 (bs, 1H), 5.26 (t, $J = 5.4$, 1H), 4.57 (t, $J = 8.4$, 1H), 4.41-4.35 (m, 1H), 4.17 (t, $J = 8.5$, 2H), 3.94-3.86 (m, 3H) 3.81-3.75 (m, 1H), 3.59 (ddd, $J = 7.3$, 9.5, 15.4, 1H) 3.15 (app p, $J = 9.0$, 1H) 2.4-2.3 (m, 2H), 2.15-1.86 (m, 6H), 1.8-1.57 (m, 5H) 1.36 (ddd, $J = 1.9$, 7.3, 14.5) 1.3-0.95 (m, 10H), 0.86 (t, $J = 7.1$, 3H) -0.036 (s, 9H).

^{13}C NMR (125 MHz, CDCl_3) 208.67, 172.5, 169.2, 156.9, 63.9, 56.6, 55.7, 47.9, 44.4, 40.8, 36.3, 35.1, 34.7, 30.7, 29.8, 29.3, 28.6, 25.99, 25.95, 25.81, 24.0, 22.7, 17.7, 14.1, -1.5.

HPLC/MS: $M+1/Z$ Calcd = 595.4 Obsd = 595.4.



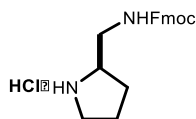
^1H NMR (500 MHz, CDCl_3) δ : 9.15 (bs, 1H), 8.59 (bs, 1H), 5.37 (bs, 1H), 5.11 (t, $J = 7.4$, 1H) 4.43-4.37 (m, 1H), 4.24-4.15 (m, 4H), 3.99 (ddd, $J = 3.5$, 7.4, 14.1, 1H), 3.89 (dt, $J = 3.8$, 14.5, 1H), 3.66-3.55 (m, 2H), 3.12 (app p, $J = 9.0$, 1H) 2.4-2.3 (m, 2H), 2.15-1.62 (m, 9H), 1.67 (t, $J = 14.5$, 2H) 1.35 (q, $J = 7.4$, 2H), 1.3-1.04 (m, 9H) 1.00 (t, $J = 7.5$, 2H) 0.86 (t, $J = 7.2$, 3H), 0.042 (s, 9H).

^{13}C NMR (125 MHz, CDCl_3) δ : 208.7, 200.2, 171.0, 157.6, 64.4, 61.8, 57.1, 52.25, 50.89, 47.98, 44.38, 40.95, 63.30, 35.01, 34.55, 30.60, 29.53, 29.28, 29.06, 25.95, 25.93, 23.97, 22.65, 17.15, 14.18, -1.5.

HPLC/MS: $M+1/Z$ Calcd = 611.4 Obsd = 611.4.

Synthesis of Lead Inhibitor 1

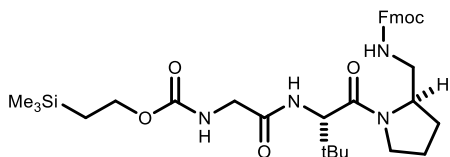
(9H-Fluoren-9-yl)methyl (R)-(pyrrolidin-2-ylmethyl)carbamate hydrochloride (**23**)



To a solution of 1- Boc(R)-2-(aminomethyl)pyrrolidine (**22**) (3.82g, 19.0 mmol) in THF (45mL) and water (45mL) was added NaHCO₃ (2.4g, 28.5 mmol) and Fmoc-OSu (7.08g, 21.0 mmol). The solution was stirred at rt for 1h then poured into 1N HCl. The aqueous layer was extracted three times with EtOAc, and the combined organic layers were washed with water, saturated NaHCO₃, water, and brine then dried over Na₂SO₄ and concentrated to afford **14** as pale yellow oil (9.18g). The *bis*-carbamate was dissolved in 50mL of 4N HCl in Dioxane and stirred for 20 minutes at rt, then concentrated to afford 7.7g of a yellow solid. The product was used without further purification.

¹H NMR (500 MHz CDCl₃) δ: 9.87 (bs, 1H), 9.16 (bs, 1H), 7.71 (d, *J* = 7.2, 2H), 7.61 (d, *J* = 7.6, 2H), 7.34 (t, *J* = 7.7, 2H), 7.27 (t, *J* = 7.3, 2H), 6.94 (bs, 1H), 4.36 (dd, *J* = 7.7, 10.2, 1H), 4.26 (dd, *J* = 7.6, 10.35, 1H), 4.17 (t, *J* = 7.1, 1H), 3.85 (bs, 1H), 3.65-3.58 (m, 1H), 3.58-3.49 (m, 1H), 3.39-3.02 (m, 3H), 2.13-1.70 (m, 3H).

(9H-Fluoren-9-yl)methyl (((R)-1-((S)-11-(tert-butyl)-2,2-dimethyl-6,9-dioxo-5-oxa-7,10-diaza-2-siladodecan-12-oyl)pyrrolidin-2-yl)methyl)carbamate (**24**)

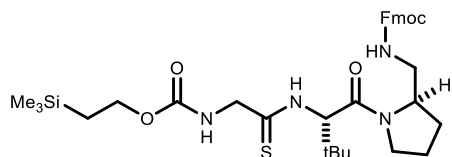


The crude hydrochloride salt **23** (7.7g) was dissolved in DMF (100 mL) along with iPr₂NEt (8.25mL, 47.3 mmol). Boc-Tle-OH (4.97g, 21.5 mmol) and TBTU (6.9g, 21.5mmol) were then added. The reaction mixture was then stirred at room temperature for 2h. DMF was removed *in vacuo*. The reaction mixture was then diluted with 1M aqueous HCl and EtOAc. The aqueous layer was then washed with EtOAc twice. The combined organics were then washed with saturated aqueous NaHCO₃ then brine. The organics were then dried over MgSO₄ and filtered. The filtrate was then concentrated to a dark orange oil (12.98g). 3.77g of the product was dissolved in 4 M HCl in Dioxane (60mL) and stirred at rt for 25m, then concentrated to afford a brown solid (12.59g). 3.77g of this material was dissolved in 30mL of acetonitrile alongside iPr₂NEt (3mL, 16mmol). Teoc-Gly-OH (1.75g, 8mmol) and TBTU (2.56g, 8 mmol) were then added. The reaction was then stirred at room temperature for two hours and then diluted with EtOAc and 1M aqueous HCl. The aqueous layer was then washed with EtOAc twice and the combined organic phases were washed with saturated aqueous NaHCO₃ and brine. The organics were dried over MgSO₄ and filtered. The filtrate was concentrated to a yellow oil and used without further purification.

¹H NMR (500 MHz CDCl₃) δ: ROTAMERS 7.75 (d, *J* = 7.5, 2H), 7.66-7.56 (m, 2H), 7.39 (t, *J* = 7.5, 2H), 7.31 (t, *J* = 7.5, 2H), 6.61 (bs, 1H), 5.86 (bs, 1H), 5.21 (bs, 1H), 4.6 (d, *J* = 9.1, 1H), 4.34 (ddd, *J* = 7.7, 10.57, 17.7), 4.25-4.1 (m, 5H), 3.9 (dd, *J* = 5.4, 16.7), 3.83-3.73 (m, 2H), 3.67-3.60 (m, 1H), 3.6-3.51 (m, 1H), 2.02-1.82 (m, 3H), 1.02 (s, 9H), 0.99-0.96 (m, 2H), 0.01 (s, 9H).

HPLC/MS: M+1/Z Calcd = 637.3 Obsd = 637.3.

(9H-Fluoren-9-yl)methyl (((R)-1-((S)-11-(tert-butyl)-2,2-dimethyl-6-oxo-9-thioxo-5-oxa-7,10-diaza-2-siladodecan-12-oyl)pyrrolidin-2-yl)methyl)carbamate (**26**)



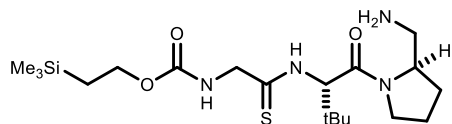
To a solution of **24** (5.7 mmol) in toluene at room temperature was added Lawesson's Reagent (**10**) (1.73g, 4.275mmol). The reaction was monitored periodically by HPLC. After 48h the reaction was diluted with EtOAc and 1M aqueous HCl. The aqueous layer was then washed with EtOAc twice and the combined organic phases were washed with saturated aqueous NaHCO₃ and brine. The organics were dried over MgSO₄ and filtered, then concentrated to a residue and purified by column chromatography (0 to 5% MeOH in CHCl₃) to afford 4.2g of **26** as a slightly green foam (76% over six steps).

¹H NMR (500 MHz CDCl₃) δ: (d, *J* = 7.6, 2H), 7.65-7.55 (m, 2H), 7.38 (t, *J* = 7.5, 2H), 7.31 (tt, *J* = 7.55, 1.62, 2H), 5.63 (bs, 1H), 5.52 (bs, 1H), 5.16 (bd, *J* = 5.7, 1H), 4.6-4.42 (m, 1H), 4.4-4.3 (m, 2H), 4.23-4.14 (m, 4H), 4.05-3.98 (m, 1H), 3.68-3.61 (m, 1H), 3.58-3.49 (m, 1H), 3.36-3.29 (m, 1H), 2.02-1.81 (m, 3H), 1.08 (s, 9H), 0.97 (dd, *J* = 1.59, 8.06, 11.0), 0.16 (s, 9H).

¹³C 200.36, 169.1, 157.3, 156.9, 144.1, 141.38, 127.7, 126.98, 125.25, 119.86, 66.76, 64.24, 58.33, 55.41, 52.56, 48.31, 47.31, 42.87, 35.50, 28.73, 26.74, 25.35, 24.22, 21.1, 17.7, -1.6.

HPLC/MS: M+1/Z Calcd = 653.3 Obsd = 653.3.

2-(Trimethylsilyl)ethyl (2-(((S)-1-((R)-2-(aminomethyl)pyrrolidin-1-yl)-3,3-dimethyl-1-oxobutan-2-yl)amino)-2-thioxoethyl)carbamate (**28**)



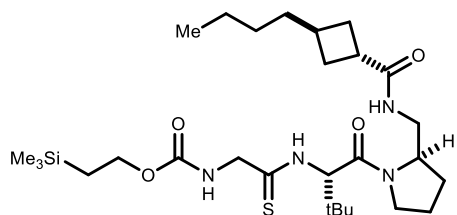
26 (4.2g, 6.45mmol) was dissolved in THF. Octanethiol (11.6mL, 64.5 mmol) was added followed by DBU (1.05mL, 7.1mmol). The resultant red solution was stirred at room temperature for 20m, then concentrated and purified by column chromatography (0-15% MeOH in CHCl₃). Yield 1.43g **28** (52%).

¹H NMR (500 MHz CDCl₃) δ: 5.98 (bs, 1H), 5.23 (s, 1H), 4.31 (dd, *J* = 5.6, 17.9, 1H), 4.15 (dd, *J* = 7.7, 9.7, 2H), 4.12-4.01 (m, 2H), 3.97-3.90 (m, 1H), 4.59 (ddd, *J* = 7.4, 10.3, 15.2, 1H), 2.83 (dd, *J* = 4.9, 13.0, 1H), 2.68 (dd, *J* = 6.7, 13.0, 1H), 2.00-1.82 (m, 3H), 1.02 (s, 9H) 0.96 (ddd, *J* = 1.5, 7.8, 11, 2H).

¹³C NMR (125 MHz, CDCl₃) δ: 199.9, 168.8, 157.3, 64.1, 63.0, 60.0, 52.3, 48.2, 43.7, 36.2, 28.3, 26.7, 21.7, 17.7, -1.5.

HPLC/MS: M+1/Z Calcd = 431.2 Obsd = 431.2.

2-(trimethylsilyl)ethyl 2-(((S)-1-((R)-2-(((1S,3R)-3-butylcyclobutane-1-carboxamido)methyl)pyrrolidin-1-yl)-3,3-dimethyl-1-oxobutan-2-yl)amino)-2-thioxoethylcarbamate (**31**)

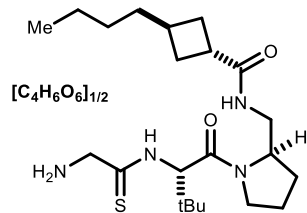


To a solution of **28** (3.3g, 7.7mmol) in acetonitrile (60mL) was added *trans*-3-butylcyclobutanecarboxylic acid **30** (1.32g, 8.5mmol), TBTU (2.718g, 8.5mmol) and *i*Pr₂NEt (2mL, 11.55mmol). The solution was stirred at room temperature for 90 minutes then concentrated and diluted with EtOAc and 1M aqueous HCl. The aqueous layer was then washed with EtOAc twice and the combined organic phases were washed with saturated aqueous NaHCO₃ and brine. The organics were dried over MgSO₄ and filtered and concentrated. Product was purified by column chromatography (0-5% MeOH in CHCl₃). Yield (2.3g as a white foam.

¹H NMR (500 MHz CDCl₃) δ: 8.58 (bs, 1H), 6.50 (t, *J* = 5.7, 1H), 5.46 (t, *J* = 5.6, 1H), 5.11 (d, *J* = 8, 1H), 4.3 (dd, *J* = 5.3, 16.7, 1H), 4.22-4.12 (m, 4H), 3.97-3.91 (m, 1H), 3.68-3.62 (m, 1H), 3.58 (dt, *J* = 4.8, 13.8, 1H), 3.38 (dt, *J* = 6, 13.7, 1H), 2.96-2.89 (m, 1H), 2.36-2.23 (m, 3H), 2.04-1.93 (m, 2H), 1.92-1.76 (m, 4H), 1.42 (q, *J* = 7.5, 2H), 1.27 (septet, *J* = 7.1, 2H), 1.21-1.14 (m, 2H), 1.06 (s, 9H), 1.02-0.97 (m, 2H), 0.87 (t, *J* = 7.1, 3H), 0.33 (s, 9H).

HPLC/MS: M+1/Z Calcd = 569.3 Obsd = 569.3.

(*trans*)-N-(((R)-1-((S)-2-(2-aminoacetamido)-3,3-dimethylbutanoyl)pyrrolidin-2-yl)methyl)-3-butylcyclobutane-1-carboxamide hemitartrate (**1**)



Solid *n*Bu₄NCl (5.07g, 18.2mmol) and anhydrous KF (1.412g, 24.32mmol) were placed in a flask. A solution of **31** (3.45g, 6.08mmol) in acetonitrile (90mL) was added, followed by water (218uL, 12.16mmol). The solution was stirred at 60C for 20 hours then concentrated to remove acetonitrile. The residue was then diluted with water and ethyl acetate. The aqueous phase was extracted three additional times with ethyl acetate and the combined organic phases were washed with water and brine, then dried over sodium sulfate, filtered, and concentrated (2.76g crude yield). The resultant product was purified by HPLC to provide the trifluoroacetate salt, which was freed by extraction with aqueous sodium carbonate and ether. The free base was dissolved in methanol and an aqueous solution of 0.5 equivalents of sodium tartrate added. This solution was concentrated, then the residue was dissolved in diethyl ether and concentrated to provide 0.82g of the desired hemitartrate salt as an off-white powder.

¹H NMR (500 MHz, DMSO) δ: 7.58 (t, *J* = 5.6, 1H), 5.20 (s, 2H), 4.05 (s, 3H), 3.95 (app sextet, *J* = 4.5, 1H), 3.83 (ddd, *J* = 3.0, 8.3, 10.7, 1H), 3.76 (s, 2H), 3.56 (ddd, *J* = 8.0, 8.1, 9.2, 1H), 3.19 (ddd, *J* = 4.6, 4.6, 12.8, 1H), 3.03 (ddd, *J* = 7.0, 8.9, 13.0, 1H), 2.92-2.85 (m, 1H), 2.31 (s, 3H), 2.21-2.10 (m, 3H), 1.92-

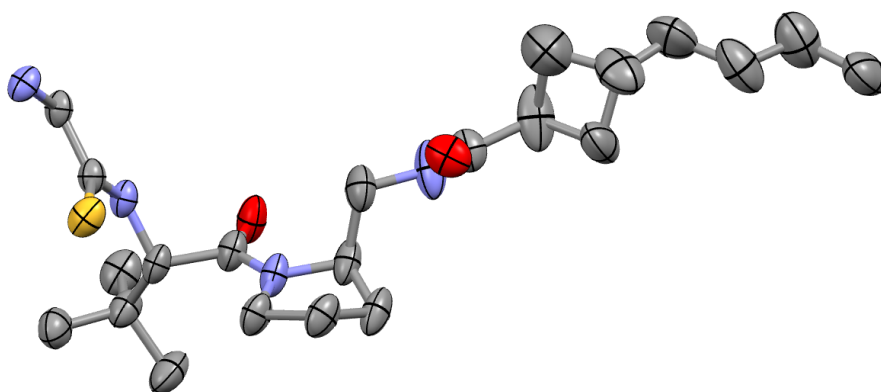
1.79 (m, 2H), 1.75-1.63 (m, 4H), 1.36 (q, $J = 7.0$, 2H), 1.23 (app sextet, $J = 7.3$, 2H), 1.17-1.09 (m, 2H), 0.99 (s, 9H), 0.84 (t, $J = 7.2$, 3H).

^{13}C NMR (125 MHz, DMSO) δ : 199.2, 175.3, 174.1, 167.8, 72.0, 63.1, 57.1, 49.1, 48.0, 36.1, 36.01, 35.9, 31.8, 30.42, 30.24, 29.42, 27.527.3, 26.9, 23.5, 22.6, 14.5.

HPLC/MS: $M+1/Z$ Calcd = 425.3 Obsd = 425.3.

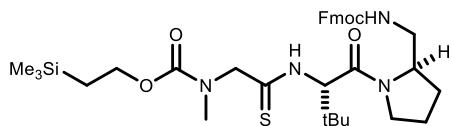
X-Ray Crystal Structure.

A single crystal of **1** (trifluoroacetate salt) was obtained upon concentration of a methanolic solution of **1**. The crystal was submitted for X-ray analysis and the shown structure obtained. We thank Dr. Saeed Khan for his assistance. Data are presented in tabular form below.



Synthesis of Lead Inhibitor 2

2-(trimethylsilyl)ethyl (2-(((S)-1-((R)-2-((((9H-fluoren-9-yl)methoxy)carbonyl)amino)methyl)pyrrolidin-1-yl)-3,3-dimethyl-1-oxobutan-2-yl)amino)-2-thioxoethyl(methyl)carbamate (**27**)



The crude hydrochloride salt **23** was dissolved in DMF (100 mL) along with $i\text{Pr}_2\text{NEt}$ (8.25mL, 47.3 mmol). Boc-Tle-OH (4.97g, 21.5 mmol) and TBTU (6.9g, 21.5mmol) were then added. The reaction mixture was then stirred at room temperature for 2h. DMF was removed *in vacuo*. The reaction mixture was then diluted with 1M aqueous HCl and EtOAc. The aqueous layer was then washed with EtOAc twice. The combined organics were then washed with saturated aqueous NaHCO_3 then brine. The organics were then dried over MgSO_4 and filtered. The filtrate was then concentrated to a dark orange oil (12.98g). The product was dissolved in 4 M HCl in Dioxane (60mL) and stirred at rt for 25m, then concentrated to afford a brown solid (12.59g). 8.81g of this material was dissolved in 30mL of acetonitrile alongside $i\text{Pr}_2\text{NEt}$ (7.16mL, 41.07mmol). Teoc-Sar-OH (1.75g, 13.05mmol) and TBTU (3.05g, 18.67 mmol) were then added. The reaction was then stirred at room temperature for two hours and then diluted with EtOAc and 1M aqueous HCl. The aqueous layer was then washed with EtOAc twice and the combined organic phases were washed with saturated aqueous NaHCO_3 and brine. The organics were dried over MgSO_4 and filtered. The filtrate was concentrated to a yellow oil and used without further purification. Yield 9.51g of **25**.

HPLC/MS: M+1/Z Calcd = 623.3 Obsd = 623.3.

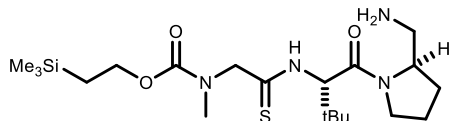
To a solution of **25** (13.3 mmol) in toluene at room temperature was added Lawesson's Reagent (**10**) (4.03g, 9.975mmol). The reaction was monitored periodically by HPLC. After 18h the reaction appeared to have stalled at ~80% conversion. An additional 2g of **10** was added and the reaction stirred for an additional 24h. The reaction was diluted with EtOAc and 1M aqueous HCl. The aqueous layer was then washed with EtOAc twice and the combined organic phases were washed with saturated aqueous NaHCO_3 and brine. The organics were dried over MgSO_4 and filtered. The filtrate was concentrated to a residue and purified by column chromatography (0 to 5% MeOH in CHCl_3) to afford 6.4g of **27** as a slightly green foam (76% over six steps).

^1H NMR (500 MHz, DMSO) δ : 7.74 (d, J = 7.8, 2H), 7.64-7.54 (m, 2H), 7.37 (t, J = 7.47, 2H), 7.30 (1.2, 2.4, 7.5, 2H), 5.76 (bs, 1H), 5.07 (bs, 1H), 4.47-4.37 (m, 1H), 4.32 (d, J = 7.5, 2H), 4.23-4.12 (m, 3H), 4.03-3.97 (m, 1H), 3.67-3.61 (m, 1H), 3.58-3.50 (m, 1H), 3.43-3.27 (m, 2H), 2.97 (s, 3H), 2.02-1.91 (m, 1H), 1.90-1.81 (m, 1H), 1.07 (s, 9H), 1.04-0.97 (m, 2H), 0.02 (s, 9H).

^{13}C NMR (125 MHz, DMSO) δ : 168.7, 168.4, 157.0, 152.7, 144.1, 141.3, 127.6, 127.1, 125.3, 119.9, 66.9, 66.6, 64.8, 58.3, 53.5, 48.3, 47.3, 43.3, 35.5, 38.8, 16.7, 25.3, 24.0, 17.9, -1.5.

HPLC/MS: M+1/Z Calcd = 667.3 Obsd = 323.1 (Fragmentation of Tle-pyrrolidine amide).

2-(trimethylsilyl)ethyl 2-(((S)-1-((R)-2-(aminomethyl)pyrrolidin-1-yl)-3,3-dimethyl-1-oxobutan-2-yl)amino)-2-thioxoethyl(methyl)carbamate (**29**)



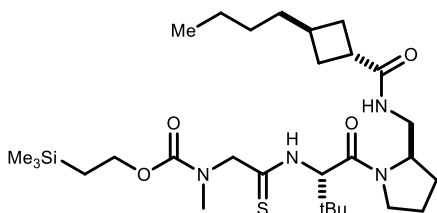
27 (6.4g, 6.45mmol) was dissolved in THF. Octanethiol (17.3mL, 96.2 mmol) was added followed by DBU (1.58mL, 10.6mmol). The resultant red solution was stirred at room temperature for 20m, then concentrated and purified by column chromatography (0-15% MeOH in CHCl₃). Yield 3.4g **29** (79%).

¹H NMR (500 MHz CDCl₃) δ: 5.07 (bs, 1H), 4.38 (bs, 1H), 4.22-4.18 (m, 3H), 4.00-3.92 (m, 1H), 3.63 (dt, J = 7.03, 10.3, 1H), 2.96 (s, 3H), 2.95-2.89 (m, 1H), 2.09-2.02 (m, 1h), 2.00-1.91 (m, 1H), 1.91-1.78 (m, 2H), 1.38-1.18 (m, 2H), 1.05-0.93 (m, 11H), 0.02 (2, 9H).

¹³C NMR (125 MHz, DMSO) δ: 200.6, 169.9, 158.2, 64.8, 63.6, 61.1, 58.7, 53.3, 48.6, 44.3, 35.8, 29.3, 26.7, 23.9, 17.9, -1.5.

HPLC/MS: M+1/Z Calcd = 445.3 Obsd = 445.3.

2-(trimethylsilyl)ethyl 2-(((S)-1-((R)-2-(((1r,3S)-3-butylcyclobutane-1-carboxamido)methyl)pyrrolidin-1-yl)-3,3-dimethyl-1-oxobutan-2-yl)amino)-2-thioxoethyl(methyl)carbamate (**32**)



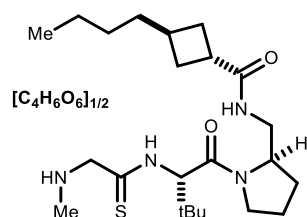
To a solution of **29** (3.4g, 7.65mmol) in acetonitrile (50mL) was added trans-3-butylcyclobutanecarboxylic acid **30** (1.31g, 8.5mmol), TBTU (2.70g, 8.41mmol) and iPr₂NEt (1.73mL, 9.45mmol). The solution was stirred at room temperature for 90 minutes then diluted with EtOAc and 1M aqueous HCl. The aqueous layer was then washed with EtOAc twice and the combined organic phases were washed with saturated aqueous NaHCO₃ and brine. The organics were dried over MgSO₄ and filtered and concentrated. Product was purified by column chromatography (0-5% MeOH in CHCl₃). Yield 3.87g of **32** as a white foam.

¹H NMR (500 MHz CDCl₃) δ: 8.80 (bs, 1H), 6.68 (bs, 1H), 5.03 (bs, 1H) 4.30 (bs, 2H, 4.25-4.12 (m, 3H), 3.97-3.91 (m, 1H), 3.68-3.60 (m, 1H), 3.55 (dt, J = 4.7, 13.8, 1H), 3.35 (bs, 1H), 2.97 (s, 3H), 2.95-2.87 (m, 1H), 2.39-2.24 (m, 3H), 2.02-1.92 (m, 2H), 1.90-1.74 (m, 5H), 1.41 (q, J = 7.6, 2H), 1.27 (septet, J = 7.3, 2H), 1.21-1.14 (m, 2H), 1.04 (s, 9H), 1.04-0.97 (m, 2H), 0.86 (t, J = 7.4, 3H), 0.033 (s, 9H).

¹³C NMR (125 MHz CDCl₃) δ: 199.1, 176.1, 169.6, 157.9, 64.8, 63.6, 61.24, 58.08, 53.46, 48.27, 42.59, 38.50, 36.64, 36.13, 35.51, 31.91, 31.51, 31.37, 29.45, 29.18, 26.69, 24.07, 22.68, 17.91, 14.16, -1.46.

HPLC/MS: M+1/Z Calcd = 583.36 Obsd = 605.3 (M+Na).

(*trans*)-3-butyl-N-(((*R*)-1-((*S*)-3,3-dimethyl-2-(2-(methylamino)ethanethioamido)butanoyl)pyrrolidin-2-yl)methyl)cyclobutane carboxamide hemitartrate (**2**)



Solid nBu₄NCl (5.54g, 19.95mmol) and anhydrous KF (1.54g, 26.6mmol) were placed in a flask. A solution of **31** (3.87g, 6.65 mmol) in acetonitrile (100mL) was added, followed by water (239uL, 13.3mmol). The solution was stirred at 60C for 20 hours then concentrated to remove acetonitrile. The residue was then diluted with water and ethyl acetate. The aqueous phase was extracted three additional times with ethyl acetate and the combined organic phases were washed with water and brine, then dried over sodium sulfate, filtered, and concentrated (2.72g crude yield). The resultant product was purified by HPLC to provide the trifluoroacetate salt, which was freed by extraction with aqueous sodium carbonate and ether. The freebase was dissolved in methanol and an aqueous solution of 0.5 equivalents of sodium tartrate added. This solution was concentrated, then the residue was dissolved in diethyl ether and concentrated to provide 1.13g of the desired hemitartrate salt as an off-white powder.

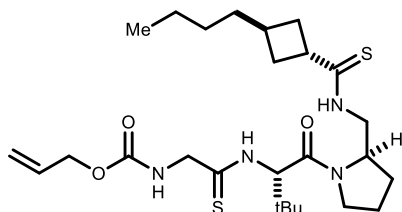
¹H NMR (500 MHz, DMSO) δ: 7.56 (t, *J* = 5.7, 1H), 5.18 (s, 2H), 4.04 (s, 1H), 3.96 (app sextet, *J* = 4.5, 1H), 3.83 (ddd, *J* = 3.3, 8.4, 10.2, 1H), 3.64 (s, 2H), 3.56 (ddd, *J* = 8.0, 8.0, 9.4, 1H), 3.19 (ddd, *J* = 4.7, 4.7, 12.8, 1H), 3.03 (ddd, *J* = 6.9, 8.7, 13.0, 1H), 2.91-2.84 (m, 1H), 2.31 (s, 3H), 2.21-2.09 (m, 3H), 1.93-1.79 (m, 2H), 1.75-1.61 (m, 4H), 1.36 (dt, *J* = 7.0, 8.0, 2H), 1.23 (app sextet, *J* = 7.3, 2H), 1.16-1.09 (m, 2H), 0.98 (s, 9H), 0.84 (t, *J* = 7.2, 3H).

¹³C NMR (125 MHz, DMSO) δ: 199.6, 175.3, 174.2, 168.0, 72.1, 62.4, 60.7, 57.4, 47.9, 36.10, 36.01, 35.9, 35.4, 31.8, 30.39, 30.25, 29.4, 27.5, 27.2, 26.9, 25.5, 22.6, 14.5.

HPLC/MS: M+1/Z Calcd = 439.3 Obsd = 439.3

Pd Mediated Alloc Cleavage

Allyl (2-(((S)-1-((R)-2-(((1s,3R)-3-butylcyclobutane-1-carbothioamido)methyl)pyrrolidin-1-yl)-3,3-dimethyl-1-oxobutan-2-yl)amino)-2-thioxoethyl)(methyl)carbamate (**35**)

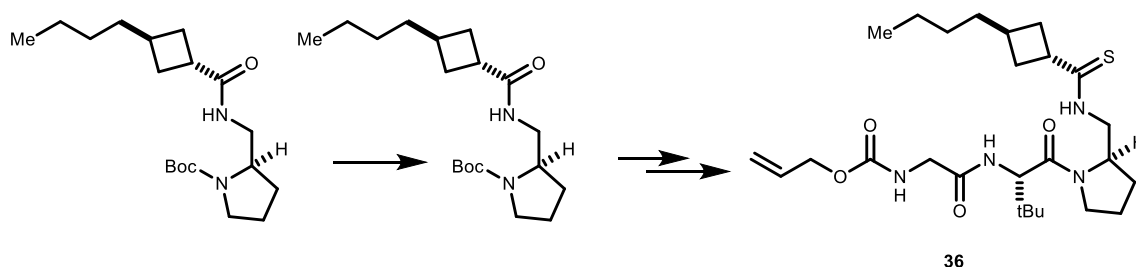


The corresponding tris-amidyl substrate (1.077g, 2.18mmol) was dissolved in toluene. Lawesson's reagent (880mg, 2.18mmol) was added and the reaction was stirred at room temperature for 24 hours. The reaction was concentrated and purified by column chromatography (0-1% MeOH in CHCl₃) to afford 1.024g of the desired product.

¹H NMR (500 MHz CDCl₃) δ: 9.28 (bs, 1H), 8.54 (bs, 1H), 5.90 (ddd, *J* = 5.4, 10.8, 17.1, 1H), 5.42 (bs, 1H), 5.32 (dd, *J* = 1.4, 17.2, 1H), 5.24 (dd, *J* = 1.2, 10.5, 1H), 5.21-5.16 (m, 1H), 4.61 (d, *J* = 5.75, 2H), 4.49-4.36 (m, 1H), 4.31-4.15 (m, 2H), 4.04-3.96 (m, 1H), 3.92-3.77 (m, 3H), 3.70 (ddd, *J* = 7.4, 9.8, 15.2, 1H), 3.57 (ddd, *J* = 3.8, 9.5, 14.8, 1H), 3.38 (p, *J* = 8.1, 1H), 2.52-2.36 (m, 2H), 2.24-2.14 (m, 1H), 2.10-1.84 (m, 6H), 1.48 (q, *J* = 7.2, 2H), 1.33-1.16 (m, 4H), 1.06 (s, 9H), 0.88 (t, *J* = 7.2, 3H).

¹³C NMR (125 MHz, CDCl₃) δ: 209.1, 199.8, 170.6, 157.1, 132.1, 118.4, 66.5, 63.1, 57.1, 52.7, 51.5, 48.3, 45.1, 36.0, 33.11, 33.04, 30.38, 29.68, 29.6, 26.7, 24.0, 22.8, 14.1.

Allyl (2-(((S)-1-((R)-2-(((1s,3R)-3-butylcyclobutane-1-carbothioamido)methyl)pyrrolidin-1-yl)-3,3-dimethyl-1-oxobutan-2-yl)amino)-2-oxoethyl)(methyl)carbamate (**36**)

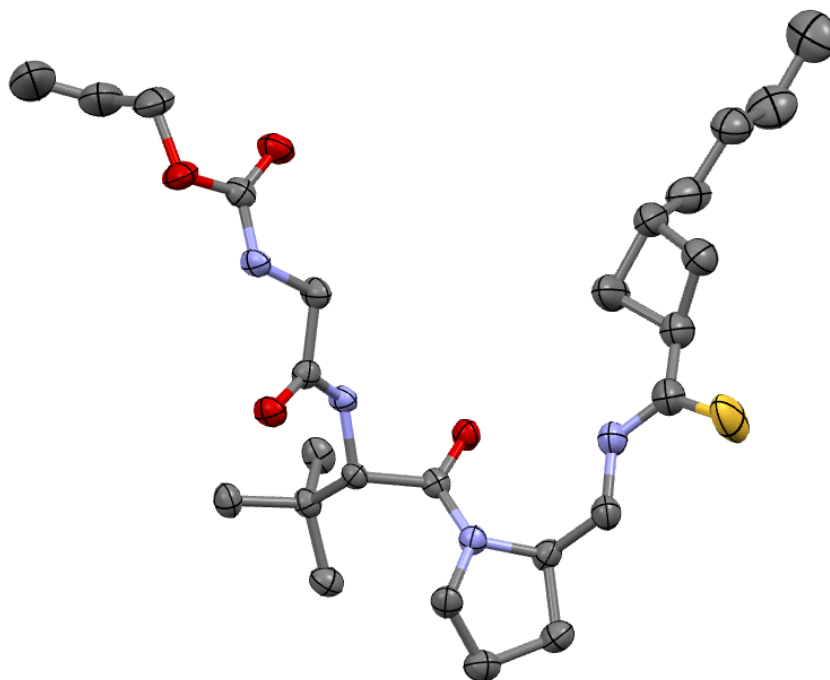


Monothioamide **36** was prepared by the shown sequence. Action of Lawesson's reagent on a monothioamide was followed by peptide extension using standard solution phase Boc peptide chemistry to provide **36**.

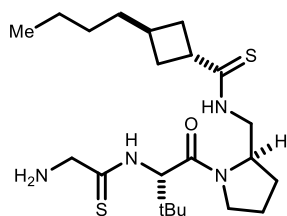
¹H NMR (500 MHz CDCl₃) δ: 9.38 (bs, 1H), 6.70 (d, *J* = 7.2, 1H), 5.90 (dddd *J* = 1.8, 5.5, 11.1, 16.0, 1H), 5.47 (t, *J* = 5.5, 1H), 5.29 (dd, *J* = 1.0, 17.2, 1H), 5.208 (dd, *J* = 1.1, 10.5, 1H), 4.67-4.55 (m, 4H) 4.38 (t, *J* = 7.2, 1H), 4.0-3.82 (m, 4H), 3.78-3.64 (m, 2H), 3.58 (t, *J* = 11.0, 1H) 3.39 (pent, *J* = 8.2, 1H), 2.51-2.36 (m, 2H), 2.24-2.14 (m, 1H), 2.07-1.82 (m, 6H), 1.47 (q, *J* = 7.7, 2H), 1.31-1.16 (m, 4H), 0.99 (s, 9H), 0.87 (t, *J* = 7.4, 3H).

X-Ray Crystal Structure: A suspension of ~40mg of **1** in hexane was prepared in a scintillation vial. A minimal volume of dichloromethane was added until **1** just dissolved. The vessel was sealed with a septa cap, which was punctured with a needle. The solvent was allowed to slowly evaporate overnight. By

morning crystals of **1** appeared as clustered colorless needles. The crystal was submitted for X-ray analysis and the shown structure obtained. We thank Dr. Saeed Khan for his assistance. Data presented in tabular form below.



(1*s*,3*R*)-*N*-(((*R*)-1-((*S*)-2-(2-Aminoethanethioamido)-3,3-dimethylbutanoyl)pyrrolidin-2-yl)methyl)-3-butylcyclobutanecarbothioamide (**37**)



To a solution of **35** (985mg, 1.88 mmol) in a degassed solution of acetonitrile (3mL), water (2mL) and diethylamine (4mL) was added triphenylphosphine-3,3',3''-trisulfonic acid trisodium salt (128.22mg, 0.224mmol) and Pd(OAc)₂ (25.1mg, 0.112mmol). The mixture was stirred at room temperature for 45m, then poured into saturated aqueous NaHCO₃. The aqueous phase was extracted three times with EtOAc and the combined organic phases were washed with brine then dried over Na₂SO₄. Purification by column chromatography (100% CHCl₃ to 1% MeOH in CHCl₃) afforded **37** (503.8mg, 61%) as a white foam.

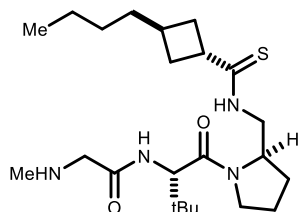
¹H NMR (400 MHz, CDCl₃) δ: 10.08 (bs, 1H), 9.26 (bs, 1H), 5.14 (s, 1H), 4.45-4.39 (m, 1H), 4.02 (ddd, *J* = 3.8, 7.55, 10.8, 1H), 3.82-3.64 (m, 4H), 3.58 (ddd, *J* = 4.0, 9.3, 13.9, 1H), 3.32 (app pentet, *J* = 8.3, 1H),

2.45-2.25 (m, 2H), 2.16-2.06 (m, 1H), 2.03-1.78 (m, 6H), 1.52 (bs, 2H), 1.4 (app quartet, $J = 7.5$, 2H), 1.22 (app pentet, $J = 7.2$, 2H), 1.17-1.1 (m, 2H), 1.04 (s, 9H), 0.81 (t, $J = 7.23$, 3H).

^{13}C NMR (125 MHz, CDCl_3) δ : 208.8, 201.9, 170.5, 62.1, 56.8, 52.5, 51.5, 48.4, 45.0, 35.8, 35.6, 32.98, 32.96, 30.3, 29.6, 29.3, 26.8, 24.0, 22.6, 14.2.

HPLC/MS: $M+1/Z$ Calcd = 441.3 Obsd = 441.3.

N-((S)-1-((R)-2-(((1s,3R)-3-Butylcyclobutane-1-carbothioamido)methyl)pyrrolidin-1-yl)-3,3-dimethyl-1-oxobutan-2-yl)-2-(methylamino)acetamide (**38**)



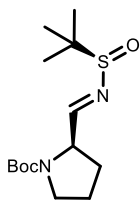
To a solution of **36** (664mg, 1.88 mmol) in a degassed solution of acetonitrile (5mL), water (0.8mL) and diethylamine (5mL) was added triphenylphosphine-3,3',3''-trisulfonic acid trisodium salt (30mg, 0.224mmol) and $\text{Pd}(\text{OAc})_2$ (6mg, 0.112mmol). The mixture was stirred at room temperature for 45m, then poured into saturated aqueous NaHCO_3 . The aqueous phase was extracted three times with EtOAc and the combined organic phases were washed with brine then dried over Na_2SO_4 . Purification by column chromatography (100% CHCl_3 to 1% MeOH in CHCl_3) afforded **38** as a white foam.

^1H NMR (500 MHz CDCl_3) δ : 9.57 (bs, 1H), 7.83 (d, $J = 9.3$, 1H), 4.58 (d, $J = 9.4$, 1H), 4.41 (ddd, $J = 2.4$, 5.0, 9.9, 1H), 3.77-3.70 (m, 2H), 3.65 (ddd, $J = 2.0$, 9.1, 18.1, 1H), 3.53 (ddd, $J = 3.6$, 10.4, 14.5, 1H), 3.4-3.24 (m, 3H), 2.46-2.39 (m, 1H), 2.36-2.29 (m, 1H), 2.17-2.08 (m, 1H), 2.03-1.75 (m, 6H), 1.46 (bs, 1H), 1.42 (q, $J = 7.5$, 2H), 1.28-1.10 (m, 4H), 0.98 (s, 9H), 0.83 (t, $J = 7.3$, 3H).

^{13}C NMR (125 MHz, CDCl_3) δ : 208.7, 172.5, 172.4, 56.6, 56.2, 52.14, 48.28, 45.0, 44.7, 34.6, 34.2, 33.0, 32.9, 30.3, 29.6, 29.3, 26.5, 23.9, 22.7, 14.1.

Synthesis of Lead Inhibitor 3

tert-butyl (R)-2-((E)-(((R)-tert-butylsulfinyl)imino)methyl)pyrrolidine-1-carboxylate (**40**)

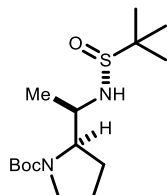


To a dried vial was added Boc-Proinaldehyde (314mg, 1.57mmol), (R)-2-Methyl-2-propanesulfonamide (189mg, 1.57mmol) and THF (3mL). This solution was cooled to 0C and a solution of titanium ethoxide (1.43g, 6.3mmol) was added slowly by syringe. After stirring at room temperature overnight the solution was poured into iced brine. The resultant slurry was filtered over celite, and the solution extracted three times with ethyl acetate. The combined organic phases were dried with sodium sulfate and concentrated to afford 375 mg of **40** as a colorless oil. The material was used without further purification.

¹H NMR (500 MHz CDCl₃) δ: 7.91 (d, *J* = 3) and 7.83 (d, *J* = 4.6) 1H], 4.58-4.51 (m, 1H), 3.82 (bs, 1H), 3.45-3.32 (m, 3H), 2.17-2.03 (m, 1H), 2.02-1.70 (m, 5H), 1.42-1.34 (m, 11H), 1.15-1.12 (m, 9H).

¹³C NMR (125 MHz, CDCl₃) δ: Mixture of rotational isomers. 169.2 and 168.8, 154.3 and 154.2, 80 and 79.6, 60.4 and 60.2 57.8 and 56. 76, 46.6 and 46. 2, 30.2 and 29.3, 28.4, 24.2 and 23.14, 22.6 and 21.0, 22.3 and 22.1.

tert-butyl (R)-2-((R)-1-(((R)-tert-butylsulfinyl)amino)ethyl)pyrrolidine-1-carboxylate (**41**)



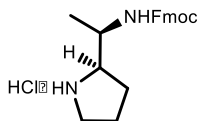
To a solution of MeMgBr (10.76 mL, 2.04M in Et₂O, 1.9 eq) in THF (19mL, 0.75M to Grignard) at -40°C, imine (3.5g, 11.57 mmol) in DCM (21mL, 0.55M) was added slowly. The reaction was stirred at -40°C for 4 hours. The reaction was then warmed to 0°C, quenched with saturated aqueous ammonium chloride, and extracted with EtOAc. The organic layer was washed with brine, dried over MgSO₄, filtered and concentrated to a clear oil. The residue was purified by flash column chromatography (1:1 → 1:2 → 1:3 → 1:4 Hex/EtOAc, SiO₂) to give **41** as a clear oil (2.96g, 80%) R_f = 0.3-0.5 streak (1:1 Hex/EtOAc).

¹H NMR (500 MHz CDCl₃) δ: 5.17 (bs, 1H) 3.82 (bs, 1H), 3.66-3.25 (m, 4H), 1.92-1.76 (m, 4H), 1.45 (s, 9H), 1.19 (s, 9H), 1.11 (d, *J* = 6.2, 3H).

¹³C NMR (125 MHz, CDCl₃) δ: 157.1, 80.0, 62.0, 55.0, 46.6, 28.5, 23.7, 22.9, 20.1, 53.4, 28.4.

HPLC/MS: M+1/Z Calcd = 319.2 Obsd. 319.2.

tert-butyl (R)-2-(((R)-1-((((9H-fluoren-9-yl)methoxy)carbonyl)amino)ethyl)pyrrolidine-1-carboxylate (**42**).

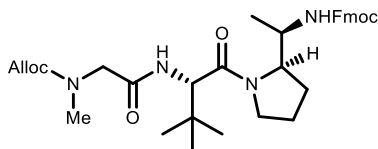


To a solution of sulfinamide (2.79g, 8.75 mmol) in methanol (60mL, 0.15M) at 0°C, HCl (4M in Dioxane, 7.65 mL, 30.6 mmol, 3.5 eq) was added dropwise. The reaction was stirred for 30 minutes until TLC indicated that starting material had been consumed. The reaction mixture was then diluted with THF (25 mL) and water (25mL, 0.08M) followed by the addition of NaHCO₃ (3.68g, 43.8mmol, 5 eq). The reaction mixture was stirred for 10 minutes then Fmoc-OSu (3.28g, 9.7 mmol, 1.1 eq) was added in one portion. The reaction was then stirred overnight (~16 hrs). The yellow solution was then diluted with brine and extracted with EtOAc. The aqueous layer was washed with EtOAc twice. The combined organic layers were then dried over MgSO₄ and filtered. The filtrate was concentrated to an orange oil. The crude was purified by column chromatography (10:1 → 4:1 Hex/EtOAc, SiO₂) to afford a yellow oil (2.99g, 78%) R_f = 0.34 (4:1 Hex/EtOAc). To carbamate **42** (2.84g, 6.5 mmol), HCl in dioxane (4M, 17mL, 68 mmol, ~10.5 eq) was added. The mixture was stirred at room temperature until TLC indicated that starting material was consumed (~1.5hrs). The reaction mixture was then concentrated to a brown solid.

¹H NMR (500 MHz CDCl₃) δ: 10.26 (bs, 1H), 8.83 (bs, 1H), 7.93-7.64 (m, 4H), 7.39-7.27 (m, 4H), 6.92 (bd, J = 7.0, 1H), 4.38-4.25 (m, 2H), 4.20 (t, J = 6.4, 1H), 4.11-4.03 (m, 1H), 3.8-3.71 (m, 1H), 3.46-3.36 (m, 1H), 3.36-3.23 (m, 1H), 2.2-1.89 (m, 3H), 1.87-1.69 (m, 3H), 1.47-1.45 (d, J = 6, 3H).

HPLC/MS: M+1/Z Calcd = 337.2 Obsd. = 337.2.

Allyl (2-(((S)-1-(((R)-2-(((R)-1-((((9H-fluoren-9-yl)methoxy)carbonyl)amino)ethyl)pyrrolidin-1-yl)-3,3-dimethyl-1-oxobutan-2-yl)amino)-2-oxoethyl)(methyl)carbamate (**43**)



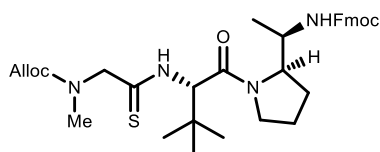
The crude hydrochloride salt was then dissolved in MeCN (32 mL, 0.2M). Boc-Tle-OH (1.51g, 6.5 mmol, 1 eq) and TBTU (2.29g, 7.1mmol, 1.1 eq) were then dissolved in the reaction mixture followed by addition of *i*Pr₂Net (5.67 mL, 32.5mmol, 5 eq). The reaction mixture was then stirred at room temperature overnight (~16 hrs). The reaction mixture was then diluted with 1M aqueous HCl and EtOAc. The aqueous layer was then washed with EtOAc twice. The combined organics were then washed with saturated aqueous NaHCO₃ then brine. The organics were then dried over MgSO₄ and filtered. The filtrate was then concentrated to a dark orange oil. The crude was purified by column chromatography (0→0.5→ 1→2% MeOH in CHCl₃) to afford a yellow-orange foam (2.81g, 78% over two steps) The carbamate (2.81g, 5.11 mmol) was dissolved in 4 M HCl in dioxane (13 mL, 52mmol, 10 eq). The reaction was stirred at room temperature until TLC indicated consumption of starting material (~1 hr). The reaction was then concentrated to a yellow foam (crude weight: 2.33g, 94%). The material was used directly in the next step. The hydrochloride salt (1.16g, 2.39 mmol) was dissolved in MeCN (12mL, 0.2M). Alloc-Sar-OH (0.41g, 2.4 mmol, 1 eq) and TBTU (0.85g, 2.65 mmol, 1.1 eq) were then dissolved in the reaction followed by the addition of *i*Pr₂NEt (2.1mL, 12.05 mmol, 5 eq). The reaction was then stirred overnight (~16hrs) at room temperature. The reaction was then diluted with Et₂O and 1M aqueous HCl. The aqueous layer was then washed with Et₂O twice and the combined organics were washed with saturated aqueous NaHCO₃ and brine. The organics were dried over MgSO₄ and filtered. The filtrate was

concentrated to an orange oil and was purified by column chromatography (0→0.5→1→2% MeOH in CHCl₃, SiO₂) to afford a yellow foam (0.717g, 50%). R_f = 0.37 (2% MeOH in CHCl₃).

¹H NMR (500MHz, CDCl₃): δ: 7.75 (d, J = 7.3, 2H), 7.63-7.57 (m, 2H), 7.42-7.36 (m, 2H), 7.34-7.28 (m, 2H), 6.31 (s, 1H), 5.96-5.76 (m, 1H), 5.31-5.09 (m, 2H), 4.72 (d, J = 9.5, 1H), 4.63-4.43 (m, 3H), 4.24-4.12 (m, 2H), 4.05-3.81 (m, 2H), 3.76-3.61 (m, 3H), 3.51-3.38 (m, 1H), 3.1-2.89 (m, 2H), 2.8 (s, 3H), 2.14-1.73 (m, 4H), 1.68-1.59 (m, 1H), 1.21 (d, J = 5.8, 3H), 1.01-0.93 (m, 9H).

HPLC/MS: M+1/Z3 Obsd = 605.3 Calcd = 605.3.

Allyl (2-(((S)-1-((R)-2-((R)-1-(((9H-fluoren-9-yl)methoxy)carbonyl)amino)ethyl)pyrrolidin-1-yl)-3,3-dimethyl-1-oxobutan-2-yl)amino)-2-thioxoethyl)(methyl)carbamate (**44**)

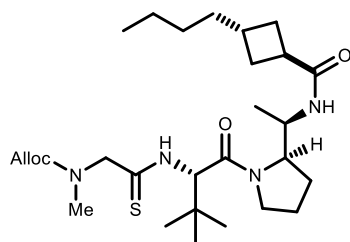


To a solution of amide (0.6994g, 1.15 mmol) in toluene (6 mL, 0.2M), Lawesson's reagent (0.4716g, 1.16 mmol, 1 eq) was added in one portion. The reaction was stirred for 24 hrs. HPLC analysis indicated that some starting material remained in the reaction, so more Lawesson's reagent (0.2345g, 0.58 mmol, 0.5 eq) was added. The reaction was stirred another 16 hours. The reaction mixture was then filtered and the solids were washed with CHCl₃. The filtrate was concentrated and purified by column chromatography (0→0.5→1→2% MeOH in CHCl₃, SiO₂) to give a gray foam (0.669g, 94%).

¹H NMR (500MHz, CDCl₃): δ: 7.74 (d, J = 7.4, 2H), 7.59 (d, J = 7.08, 1H), 7.38 (dd, J = 7.28, 2H), 7.34-7.28 (m, 2H), 5.97-5.8 (m, 1H), 5.37-5.13 (m, 3H), 4.66-4.43 (m, 4H), 4.19 (t, J = 7.0, 2H), 4.07-3.9 (m, 2H), 3.88-3.8 (m, 1H), 3.77-3.64 (m, 2H), 3.13-2.8 (m, 4H), 2.19-1.67 (m, 5H), 1.29-1.16 (m, 3H), 1.06-0.94 (m, 9H).

HPLC/MS: M+1/Z Calcd = 621.3 Obsd = 643.3 (M+Na).

Allyl (2-(((S)-1-((R)-2-((R)-1-((1s,3R)-3-butylcyclobutane-1-carboxamido)ethyl)pyrrolidin-1-yl)-3,3-dimethyl-1-oxobutan-2-yl)amino)-2-thioxoethyl)(methyl)carbamate (**45**)



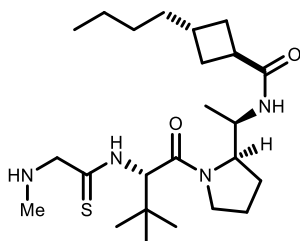
To a solution of carbamate (0.5383g, 0.86 mmol) and octanethiol (1.5 mL, 8.64 mmol, 10 eq) in THF (9 mL, 0.1M), DBU (0.15 mL, 1.00 mmol, 1.1 eq) was added. The reaction was stirred at room temperature until TLC indicated that starting material SM consumed (~15 minutes). The reaction was then concentrated and purified by column chromatography (0→2→5→15% MeOH in CHCl₃, SiO₂) to afford a yellow oil (0.2929g, 85%). To a solution of amine (0.2629g, 0.65 mmol), *trans*-acid (0.1088g, 0.69 mmol, ~1 eq), HOBT (0.1101g, 0.72 mmol, 1.1 eq), and EDC-HCl (0.1449g, 0.75 mmol, ~1.1 eq) in MeCN (4mL, 0.2M), *i*Pr₂NEt (0.57mL, 3.25 mmol, 5 eq) was added. The reaction was stirred overnight (~16 hrs). The reaction was then diluted with Et₂O and 1M aqueous HCl. The aqueous layer was then washed with Et₂O

twice and the combined organic layers were washed with saturated NaHCO_3 and brine. The organics were dried over MgSO_4 and filtered. The filtrate was concentrated to a yellow oil and purified by column chromatography (0→1→2% MeOH in CHCl_3 , SiO_2) to afford a light brown oil (0.2303g, 66%).

^1H NMR (500MHz, CDCl_3): δ : 8.73 (bs, 1H), 7.01 (bs, 1H), 5.94 (ddd, J = 5.1, 11.2, 16.6, 1H), 5.32 (d, J = 17.8, 1H), 5.24 (d, J = 10.7, 1H), 4.67-5.45 (m, 2H), 4.52-4.32 (m, 1H), 4.18-4.01 (m, 2H), 3.93-3.72 (m, 2H), 3.71-3.59 (m, 1H), 3.03 (s, 3H), 2.78 (bs, 1H), 2.29-2.13 (m, 3H), 2.12-1.99 (m, 2H), 1.98-1.61 (m, 6H), 1.44-1.06 (m, 9H), 1.02 (s, 9H), 0.86 (t, J = 7.3, 3H).

HPLC/MS: $M+1/Z$ Calcd = 537.3 Obsd = 537.3.

(*trans*)-3-butyl-N-((*R*)-1-((*R*)-1-((*S*)-3,3-dimethyl-2-(2-(methylamino)ethanethioamido)butanoyl)pyrrolidin-2-yl)ethyl)cyclobutane-1-carboxamide (**3**)



To a degassed solution of carbamate (0.21g, 0.39 mmol) in Et_2NH (1.8 mL, 0.1M), H_2O (0.6 mL, 0.1M), and MeCN (1.8 mL, 0.1M), ligand (0.022g, 0.039 mmol, 10 mol %) was added. The reaction mixture was stirred for 10 minutes until the mixture was homogenous. Then $\text{Pd}(\text{OAc})_2$ (0.0046g, 0.02 mmol, 5 mol %) was added. The reaction was stirred for 2 hours at room temperature until TLC indicated consumption of starting material. The reaction was diluted with EtOAc and washed with saturated aqueous NaHCO_3 followed by brine. The organics were dried over MgSO_4 and filtered. The filtrate was concentrated to an orange oil. The crude was purified by column chromatography (0→0.5→1→2% MeOH in CHCl_3 , SiO_2) to give a pale orange oil (0.1331g, 75%).

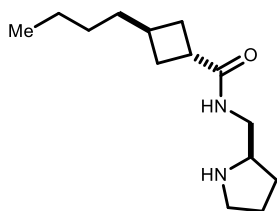
^1H NMR (500 MHz CDCl_3) δ : 5.27 (s, 1H), 4.17 (ddd, J = 3.3, 7.1, 8.36, 1H), 4.07 (ddd, J = 6.7, 8.12, 13.0, 1H), 3.96 (ddd, J = 4.3, 8.6, 10.8, 1H), 3.82 (ddd, J = 7.75, 10.7, 15.2, 1H), 3.55 (s, 2H), 2.86 (ddd, J = 5.8, 9.3, 11.7, 1H), 2.36 (s, 3H), 2.26-2.16 (m, 2H), 2.08-1.92 (m, 1H), 1.88 (ddd, J = 2.66, 5.39, 6.55, 1H), 1.79-1.70 (m, 2H), 1.44 (q, J = 7.2, 2H), (ddd J = 1.1, 7.6, 15.2, 2H), 1.24-1.18 (m, 2H), 1.08 (s, 9H), 1.06 (d, J = 6.5, 3H), 0.89 (t, J = 7.2, 3H).

^{13}C NMR (125 MHz, CDCl_3) δ : 200.0, 175.4, 170.9, 62.4, 61.3, 50.1, 47.9, 36.8, 16.4, 36.2, 36.1, 34.6, 30.4, 31.2, 29.5, 28.6, 26.8, 23.6, 22.7, 19.5, 14.1.

HPLC/MS: $M+1/Z$ Calcd = 453.3 Obsd = 453.3.

Synthesis of Negative Control 4 and Lead Inhibitor 19

(*trans*)-3-butyl-N-(((R)-pyrrolidin-2-yl)methyl)cyclobutane-1-carboxamide (**47**)



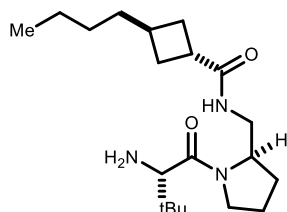
To a solution of 1-Boc-2-(aminomethyl)pyrrolidine (627mg, 3.13 mmol) in acetonitrile (10mL) was added **9** (537mg, 3.45 mmol), DIPEA (819 μ L, 4.7mmol), and TBTU (1.1g, 3.45mmol). The mixture was stirred at room temperature for 2h, then poured into 1N HCl. The aqueous layer was extracted three times with EtOAc, and the combined organic layers were washed with water, saturated NaHCO₃, water, and brine then dried over Na₂SO₄ and concentrated. The residue obtained was dissolved in 4N HCl in dioxane (10mL), stirred at room temperature for 30 minutes, then poured into 1M aqueous Na₂CO₃. The aqueous phase was extracted three times with ether and the combined organic phases were dried over Na₂SO₄ and concentrated. Purification by column chromatography (0-10% MeOH in CHCl₃) afforded **47** as a white crystalline solid. (314mg, 33% yield).

¹H NMR (500MHz, CDCl₃) δ : 5.97 (bs, 1H), 3.4 (ddd, J = 4.6, 5.8, 13.5, 1H), 3.25 (ddd, J = 4.6, 7.5, 11.5, 1H), 3.04 (ddd, J = 5.2, 7.9, 13.4, 1H), 2.97-2.84 (m, 3H), 2.36-2.25 (m, 1H), 2.05 (bs, 1H), 2.89-1.62 (m, 5H) 1.42 (app quartet, J = 7.4, 1H), 1.39-1.31 (m, 1H), 1.31-1.14 (m, 4H), 0.86 (t, J = 7.3, 3H).

¹³C NMR (125 MHz, CDCl₃) δ : 175.9, 57.8, 46.53, 43.62, 36.7, 36.1, 31.9, 30.51, 30.49, 29.4, 29.1, 25.9, 22.6, 14.1.

HPLC/MS: M+1/Z Calcd = 239.2 Obsd. = 239.2

(*trans*)-N-(((R)-1-((S)-2-amino-3,3-dimethylbutanoyl)pyrrolidin-2-yl)methyl)-3-butylcyclobutanecarboxamide (**4**)



To a solution of **12** (1.47g, 5.36 mmol) in acetonitrile (20mL) was added S-Boc-*tert*-Leucine (1.23g, 5.36 mmol), DIPEA (2.4mL, 13.4mmol), HOBt (820mg, 5.36mmol), and EDC (1.027g, 5.36mmol). The mixture was stirred at room temperature for 6h, then poured into 1N HCl. The aqueous layer was extracted three times with EtOAc, and the combined organic layers were washed with water, saturated NaHCO₃, water, and brine then dried over Na₂SO₄ and concentrated. The residue obtained was dissolved in 4N HCl in dioxane (25mL), stirred at room temperature for 30 minutes, then poured into 1M aqueous Na₂CO₃. The aqueous phase was extracted three times with ether and the combined organic phases were dried over Na₂SO₄ and concentrated. Purification by column chromatography (0-10% MeOH in CHCl₃) afforded **13** as a pale yellow oil. (932mg, 49% yield).

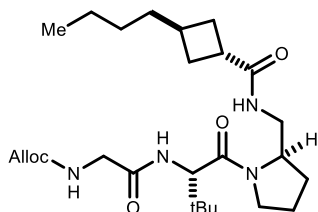
¹H NMR (400 MHz, CDCl₃) δ : 7.29 (bt, J = 3.8, 1H), 4.36-4.26 (m, 1H), 3.66-3.53 (m, 2H), 3.45 (ddd, J = 3.9, 5.2, 13.7, 1H), 3.29 (s, 1H), 3.24 (ddd, J = 4.1, 9.3, 13.7, 1H), 3.01-2.87 (m, 1H), 2.38-2.21 (m, 3H),

2.10-1.86 (m, 3H) 1.86-1.73 (m, 3H), 1.63 (bs, 2H), 1.42 (app quartet, $J = 7.2$, 2H), 1.35-1.1 (m, 5H), 0.98 (s, 9H), 0.86 (t, $J = 7.1$, 3H).

^{13}C NMR (125 MHz, CDCl_3) δ : 176.3, 175.4, 60.4, 56.8, 47.5, 45.1, 36.7, 36.0, 35.2, 31.9, 30.44, 30.41, 29.4, 29.1, 26.3, 24.0, 22.7, 14.1.

HPLC/MS: $M+1/Z$ Calcd = 352.3 Obsd. = 352.3

Allyl(2(((S)-1-((R)-2-(((*trans*)-3-butylcyclobutanecarboxamido)methyl)pyrrolidin-1-yl)-3,3-dimethyl-1-oxobutan-2-yl)amino)-2-oxoethyl)carbamate (**14**)



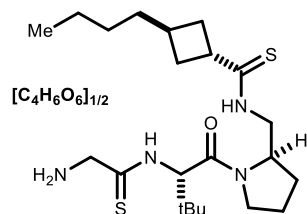
To a solution of **13** (932mg, 2.65 mmol) in acetonitrile (10mL) was added Alloc-Glycine (422.9mg, 2.66 mmol), DIPEA (713uL, 3.98 mmol), HOBt (407mg, 2.66mmol), and EDC (510, 2.66mmol). The mixture was stirred at room temperature for 18h, then poured into 1N HCl. The aqueous layer was extracted three times with EtOAc, and the combined organic layers were washed with water, saturated NaHCO_3 , water, and brine then dried over Na_2SO_4 and concentrated to afford **14** as pale yellow oil (1.08g, 82% yield). The product was used without further purification. To a solution of **14** (1.08g, 2.18 mmol) in toluene (10mL) was added Lawesson's reagent (880.7mg, 2.18mmol). The mixture was stirred at room temperature for 18h, and then concentrated to an oil. Purification by column chromatography (100% CHCl_3 to 1% MeOH in CHCl_3) afforded **15** (1.024g, 89%) as a pale yellow oil. To a solution of **15** (985mg, 1.88 mmol) in a degassed solution of acetonitrile (3mL), water (2mL) and diethylamine (4mL) was added triphenylphosphine-3,3',3''-trisulfonic acid trisodium salt (128.22mg, 0.224mmol) and $\text{Pd}(\text{OAc})_2$ (25.1mg, 0.112mmol). The mixture was stirred at room temperature for 45m, then poured into saturated aqueous NaHCO_3 . The aqueous phase was extracted three times with EtOAc and the combined organic phases were washed with brine then dried over Na_2SO_4 . Purification by column chromatography (100% CHCl_3 to 1% MeOH in CHCl_3) afforded **16** (503.8mg, 61%) as a white foam.

^1H NMR (400 MHz, CDCl_3) δ : 10.08 (bs, 1H), 9.26 (bs, 1H), 5.14 (s, 1H), 4.45-4.39 (m, 1H), 4.02 (ddd, $J = 3.8, 7.55, 10.8$, 1H), 3.82-3.64 (m, 4H), 3.58 (ddd, $J = 4.0, 9.3, 13.9$, 1H), 3.32 (app pentet, $J = 8.3$, 1H), 2.45-2.25 (m, 2H), 2.16-2.06 (m, 1H), 2.03-1.78 (m, 6H), 1.52 (bs, 2H), 1.4 (app quartet, $J = 7.5$, 2H), 1.22 (app pentet, $J = 7.2$, 2H), 1.17-1.1 (m, 2H), 1.04 (s, 9H), 0.81 (t, $J = 7.23$, 3H).

^{13}C NMR (125 MHz, CDCl_3) δ : 208.8, 201.9, 170.5, 62.1, 56.8, 52.5, 51.5, 48.4, 45.0, 35.8, 35.6, 32.98, 32.96, 30.3, 29.6, 29.3, 26.8, 24.0, 22.6, 14.2.

HPLC/MS: $M+1/Z$ Calcd = 441.3 Obsd. = 441.3

(*trans*)-N-(((*R*)-1-((*S*)-2-(2-aminoethanethioamido)-3,3-dimethylbutanoyl)pyrrolidin-2-yl)m ethyl)-3-butylcyclobutanecarbothioamide hemitartrate (**19**)



To a vial containing **19** (250mg, 0.56mmol) and solid tartaric acid (42 mg, 0.284 mmol) was added 1:1 MeOH/water with stirring until the solution became homogenous. The solution was then concentrated *in vacuo*, then dissolved in ether and concentrated again. The solid thus obtained was used without further purification for biological testing.

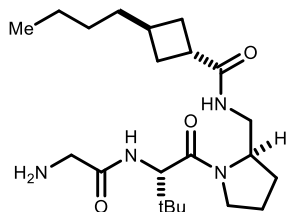
¹H NMR (500 MHz, DMSO) δ: 9.65 (bt, *J*=5.2, 1H), 7.03 (bs, 3H), 5.20 (s, 2H), 4.22 (ddd, *J* = 1.34, 7.6, 14.6, 1H), 3.94 (s, 1H), 3.89 (ddd, *J* = 2.4, 8.5, 10.9, 1H), 3.68 (d, *J* = 2.2, 2H), 3.65-3.52 (m, 3H), 3.45-3.30 (m, 1H), 2.39-2.30 (m, 2H), 2.2-2.07 (m, 2H), 1.98-1.68 (m, 6H), 1.42 (quartet, *J* = 7.4, 2H), 1.24 (pentet, *J* = 7.2, 2H), 1.19-1.12 (m, 2H), 1.00 (s, 9H), 0.84 (t, *J* = 7.3, 3H).

¹³C NMR (125 MHz, DMSO) δ: 208.7, 200.7, 174.6, 168.7, 71.8, 62.7, 56.5, 50.7, 48.0, 46.8, 43.7, 36.2, 35.7, 33.13, 33.09, 30.5, 29.6, 21.9, 26.9, 23.7, 22.6, 14.5.

HPLC/MS: M+1/Z Calcd = 441.3 Obsd. = 441.3

Characterization of Amidyl Inhibitors for Pharmacokinetic Analysis

(*trans*)-N-(((R)-1-((S)-2-(2-aminoacetamido)-3,3-dimethylbutanoyl)pyrrolidin-2-yl)methyl)-3-butylcyclobutane-1-carboxamide (**51**)



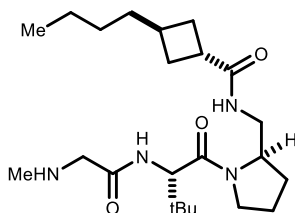
A solution of **19** (2.1mmol), Boc-Tle-OH (2.1mmol), TBTU (2.1mmol), and *i*Pr₂NEt (4.2mmol) in acetonitrile was stirred at room temperature for four hours, then poured into 1N HCl. The aqueous layer was extracted three times with EtOAc, and the combined organic layers were washed with water, saturated NaHCO₃, water, and brine then dried over Na₂SO₄ and concentrated. The resultant oil (1.03g) was dissolved in 4N HCl and stirred at room temperature for 30m, then concentrated. 1.05mmol of the resultant salt was dissolved in acetonitrile (5mL). To this solution was added Boc-Gly-OH (1.05mmol), TBTU (1.05mmol), and *i*Pr₂NEt (2.1mmol). This solution was stirred at room temperature for three hours, then poured into 1N HCl. The aqueous layer was extracted three times with EtOAc, and the combined organic layers were washed with water, saturated NaHCO₃, water, and brine then dried over Na₂SO₄ and concentrated. The resultant oil was dissolved in 4N HCl/Dioxane, and stirred at room temperature for 30m, then concentrated. The free base was liberated by extraction with aqueous 1N Na₂CO₃ and ether, purified by column chromatography (0-5% MeOH in CHCl₃), then formulated as the hemitartrate (127.5mg yield).

¹H NMR (500 MHz, CDCl₃) 5:1 rotamers. Only major peak characterized. δ: 8.26 (d, *J* = 9.4, 1H), 7.64 (t, *J* = 5.9, 1H), 4.51 (d, *J* = 9.3, 1H), 3.96 (app octet, *J* = 4.6, 1H), 3.77 (s, 1H), 3.61-3.51 (m, 2H), 3.39 (s, 2H), 3.24 (dt, *J* = 4.6, 12.6, 1H), 3.07 (ddd, *J* = 6.7, 8.6, 12.8, 1H), 2.95-2.88 (m, 1H), 2.21-2.12 (m, 3H), 1.92-1.78 (m, 2H), 1.75-1.64 (m, 4H), 1.39 (q, *J* = 6.9, 2H), 1.28-1.22 (m, 2H), 1.19-1.11 (m, 2H), 0.94 (s, 9H), 0.85 (t, *J* = 7.3, 3H).

¹³C NMR (125 MHz, CDCl₃) δ: 175.4, 174.8, 169.8, 169.6, 71.6, 57.2, 56.8, 47.7, 42.6, 36.0, 35.8, 35.3, 31.8, 30.4, 31.3, 29.4, 27.5, 27.1, 26.7, 23.6, 22.6, 14.5

HPLC/MS: M+1/Z Calcd = 409.3 3 Obsd. = 409.3

(*trans*)-3-butyl-N-(((R)-1-((S)-3,3-dimethyl-2-(2-(methylamino)acetamido)butanoyl)pyrrolidin-2-yl)methyl)cyclobutane-1-carboxamide (**52**)



A solution of **19** (2.1mmol), Boc-Tle-OH (2.1mmol), TBTU (2.1mmol), and *i*Pr₂NEt (4.2mmol) in acetonitrile was stirred at room temperature for four hours, then poured into 1N HCl. The aqueous layer

was extracted three times with EtOAc, and the combined organic layers were washed with water, saturated NaHCO₃, water, and brine then dried over Na₂SO₄ and concentrated. The resultant oil (1.03g) was dissolved in 4N HCl and stirred at room temperature for 30m, then concentrated. 1.05mmol of the resultant salt was dissolved in acetonitrile (5mL). To this solution was added Boc-Sar-OH (1.05mmol), TBTU (1.05mmol), and iPr₂NEt (2.1mmol). This solution was stirred at room temperature for three hours, then then poured into 1N HCl. The aqueous layer was extracted three times with EtOAc, and the combined organic layers were washed with water, saturated NaHCO₃, water, and brine then dried over Na₂SO₄ and concentrated. The resultant oil was dissolved in 4N HCl/Dioxane, and stirred at room temperature for 30m, then concentrated. The free base was liberated by extraction with aqueous 1N Na₂CO₃ and ether, purified by column chromatography (0-5% MeOH in CHCl₃), then formulated as the hemitartrate (250.4mg yield).

¹H NMR (500 MHz, CDCl₃) 5:1 rotamers, major peaks characterized. δ: 8.18 (d, *J* = 9.1, 1H), 7.62 (t, *J* = 5.6, 1H), 4.48 (d, *J* = 9.5, 1H), 3.58-3.49 (m, 2H), 3.38 (s, 2H), 3.2 (dt, *J* = 5.0, 12.8, 1H), 3.05 (ddd, *J* = 6.9, 8.5, 12.8, 1H), 2.93-2.85 (m, 1H), 2.36 (s, 3H), 2.19-2.12 (m, 3H), 1.91-1.76 (m, 2H), 1.73-1.62 (m, 4H), 1.37 (q, *J* = 7.1, 2H), 1.22 (app pent, *J* = 7.22, 2H), 1.16-1.09 (m, 2H), 0.92 (s, 9H), 0.83 (t, *J* = 7.2, 3H).

¹³C NMR (125 MHz, CCl₃) δ: 175.3, 174.7, 169.4, 168.7, 71.6, 57.2, 56.9, 52.2, 47.8, 36.0, 35.9, 35.2, 34.9, 31.7, 30.4, 30.3, 29.4, 27.5, 27.1, 26.8, 23.6, 22.6, 14.5.

HPLC/MS: M+1/Z Calcd =423.3 Obsd. = 423.3

Crystallography

(*trans*)-N-(((*R*)-1-((*S*)-2-(2-aminoacetamido)-3,3-dimethylbutanoyl)pyrrolidin-2-yl)methyl)-3-butylcyclobutane-1-carboxamide trifluoroacetate

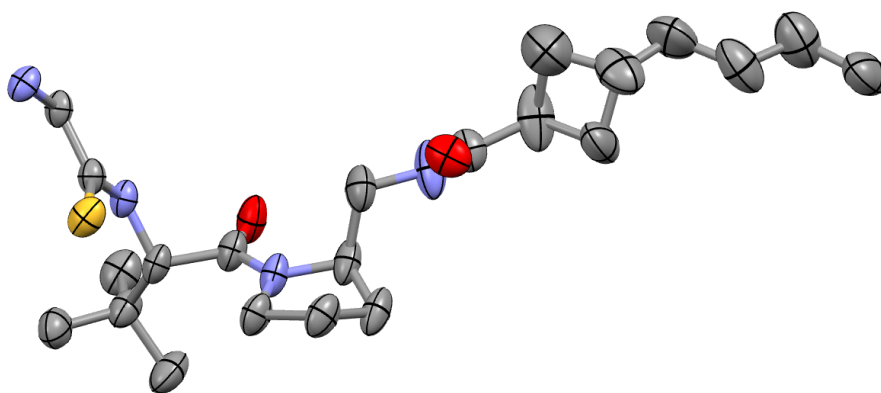
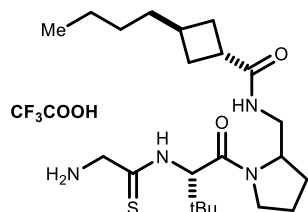


Table 1. Crystal data and structure refinement for **1**

Identification code	har1502b	
Empirical formula	C ₂₄ H ₄₀ F ₃ N ₄ O ₄ S	
Formula weight	537.66	
Temperature	100(2) K	
Wavelength	1.54178 Å	
Crystal system	Orthorhombic	
Space group	P2 ₁ 2 ₁ 2 ₁	
Unit cell dimensions	a = 13.8434(4) Å	α = 90°.
	b = 24.9214(7) Å	β = 90°.
	c = 25.0377(7) Å	γ = 90°.
Volume	8637.9(4) Å ³	
Z	12	
Density (calculated)	1.240 Mg/m ³	
Absorption coefficient	1.466 mm ⁻¹	
F(000)	3444	

Crystal size	0.200 x 0.100 x 0.050 mm ³
Theta range for data collection	2.501 to 69.206°.
Index ranges	-16<=h<=16, -29<=k<=30, -29<=l<=29
Reflections collected	50842
Independent reflections	15594 [R(int) = 0.0599]
Completeness to theta = 67.679°	99.2 %
Absorption correction	Semi-empirical from equivalents
Max. and min. transmission	0.79 and 0.60
Refinement method	Full-matrix least-squares on F ²
Data / restraints / parameters	15594 / 1339 / 1122
Goodness-of-fit on F ²	1.071
Final R indices [I>2sigma(I)]	R1 = 0.0601, wR2 = 0.1601
R indices (all data)	R1 = 0.0765, wR2 = 0.1698
Absolute structure parameter	0.052(8)
Extinction coefficient	n/a
Largest diff. peak and hole	0.536 and -0.322 e.Å ⁻³

Table 2. Atomic coordinates ($\times 10^4$) and equivalent isotropic displacement parameters ($\text{\AA}^2 \times 10^3$) for alloc. $U(\text{eq})$ is defined as one third of the trace of the orthogonalized U^{ij} tensor.

	x	y	z	$U(\text{eq})$
S(1)	3196(1)	2869(1)	3181(1)	55(1)
O(1)	1338(3)	1216(2)	2651(2)	63(1)
O(2)	5154(3)	429(2)	1968(2)	67(1)
N(1)	2671(3)	3582(2)	2279(2)	44(1)
N(2)	1639(3)	2343(2)	2832(2)	42(1)
N(3)	2718(3)	1145(2)	3126(2)	52(1)
N(4)	3572(4)	271(2)	2000(3)	78(2)
C(1)	1990(4)	3131(2)	2334(2)	41(1)
C(2)	2256(4)	2757(2)	2789(2)	40(1)
C(3)	1689(4)	1940(2)	3253(2)	46(1)
C(4)	761(4)	1935(2)	3603(3)	55(1)
C(5)	742(5)	2451(3)	3923(3)	65(2)
C(6)	-167(4)	1892(3)	3267(3)	67(2)
C(7)	826(6)	1451(3)	3985(3)	75(2)
C(8)	1903(4)	1401(2)	2983(3)	50(1)
C(9)	3422(4)	1324(2)	3524(3)	56(1)
C(10)	4263(4)	931(2)	3432(3)	61(2)
C(11)	3762(4)	421(2)	3230(3)	64(2)
C(12)	2976(4)	631(2)	2865(3)	56(1)
C(13)	3339(5)	751(2)	2298(3)	64(2)
C(14)	4456(4)	164(3)	1827(3)	57(2)
C(15)	4583(4)	-290(3)	1420(4)	93(3)
C(16)	5207(15)	-119(6)	922(6)	131(5)
C(17)	5666(9)	-672(5)	938(5)	96(4)
C(18)	5331(10)	-730(5)	1507(4)	87(4)
C(19)	5350(13)	-1073(5)	526(5)	113(5)
C(20)	5860(9)	-1596(5)	613(6)	101(4)
C(21)	5556(13)	-2056(6)	251(7)	111(5)
C(22)	6042(14)	-2587(7)	380(9)	102(6)
C(16A)	5502(14)	-298(12)	1081(11)	69(6)
C(17A)	5702(17)	-864(10)	1295(12)	74(7)

C(18A)	5037(18)	-734(9)	1759(10)	83(6)
C(19A)	5300(20)	-1280(13)	904(13)	84(8)
C(20A)	5100(30)	-1520(19)	357(14)	133(10)
C(21A)	6060(30)	-1814(13)	329(19)	118(10)
C(22A)	5810(40)	-2408(16)	330(20)	89(10)
S(2)	1752(1)	5606(1)	1580(1)	51(1)
O(3)	1562(3)	4020(2)	1506(2)	55(1)
O(4)	-1591(3)	4693(1)	2724(2)	53(1)
N(5)	3188(3)	5646(2)	2487(2)	44(1)
N(6)	2915(3)	4804(2)	1302(2)	40(1)
N(7)	507(3)	4472(2)	1005(2)	57(1)
N(8)	-933(4)	4071(2)	2179(3)	68(2)
C(23)	3488(3)	5294(2)	2043(2)	44(1)
C(24)	2717(3)	5212(2)	1624(2)	42(1)
C(25)	2269(4)	4626(2)	880(2)	45(1)
C(26)	2811(4)	4260(3)	471(2)	54(1)
C(27)	3176(5)	3734(3)	720(3)	66(2)
C(28)	3660(6)	4570(3)	244(3)	77(2)
C(29)	2099(6)	4122(4)	16(3)	77(2)
C(30)	1415(4)	4349(2)	1147(2)	47(1)
C(31)	196(5)	4863(3)	597(3)	75(2)
C(32)	-905(6)	4888(4)	680(5)	102(3)
C(33)	-1152(5)	4331(3)	898(4)	92(3)
C(34)	-300(4)	4211(3)	1280(3)	67(2)
C(35)	-423(5)	4445(3)	1833(3)	73(2)
C(36)	-1432(4)	4217(2)	2610(3)	48(1)
C(37)	-1775(4)	3760(2)	2960(2)	61(2)
C(38)	-957(8)	3568(4)	3331(4)	74(3)
C(39)	-1421(7)	3882(3)	3792(3)	63(2)
C(40)	-2332(6)	3946(5)	3460(4)	88(4)
C(41)	-1485(11)	3635(4)	4351(4)	99(4)
C(42)	-1882(12)	4015(6)	4778(4)	121(5)
C(43)	-1169(12)	4439(5)	4963(5)	108(4)
C(44)	-1570(11)	4862(6)	5320(5)	152(5)
C(38A)	-1348(16)	3668(16)	3519(7)	74(7)
C(39A)	-2240(20)	3935(12)	3766(6)	70(7)

C(40A)	-2752(11)	3870(8)	3229(9)	69(6)
C(41A)	-2550(30)	3745(12)	4331(10)	89(7)
C(42A)	-2590(30)	4240(13)	4692(12)	103(8)
C(43A)	-1740(40)	4324(9)	5058(10)	139(11)
S(3)	8249(1)	5538(1)	3988(1)	57(1)
O(5)	7403(3)	7471(2)	3668(2)	49(1)
O(6)	4080(3)	6615(2)	2466(2)	57(1)
N(9)	9610(3)	5547(2)	3033(2)	45(1)
N(10)	8651(3)	6581(2)	3867(2)	40(1)
N(11)	6239(3)	6900(2)	3940(2)	44(1)
N(12)	4840(3)	7362(2)	2746(2)	46(1)
C(45)	9733(4)	5998(2)	3410(3)	48(1)
C(46)	8838(4)	6074(2)	3757(2)	42(1)
C(47)	7916(4)	6754(2)	4248(2)	42(1)
C(48)	8355(5)	7076(2)	4713(2)	51(1)
C(49)	8990(6)	6699(3)	5036(3)	70(2)
C(50)	8963(5)	7554(2)	4529(3)	55(1)
C(51)	7537(5)	7273(3)	5068(3)	67(2)
C(52)	7152(4)	7069(2)	3929(2)	43(1)
C(53)	5838(4)	6443(3)	4239(3)	57(2)
C(54)	4804(4)	6410(3)	4036(3)	63(2)
C(55)	4549(4)	6988(3)	3894(3)	59(2)
C(56)	5480(4)	7203(2)	3648(2)	46(1)
C(57)	5551(4)	7078(2)	3054(2)	45(1)
C(58)	4159(4)	7109(2)	2465(2)	44(1)
C(59)	3542(4)	7462(2)	2113(2)	50(1)
C(60)	3901(4)	7437(3)	1526(3)	59(2)
C(61)	3124(4)	7014(3)	1422(2)	57(1)
C(62)	2598(4)	7180(3)	1931(2)	57(2)
C(63)	2573(5)	7035(3)	893(3)	68(2)
C(64)	3221(6)	7012(4)	398(3)	93(2)
C(65)	3991(10)	6588(5)	346(8)	85(5)
C(66)	3414(14)	6074(7)	282(7)	94(6)
C(65A)	3504(19)	6403(7)	379(9)	110(8)
C(66A)	3970(20)	6227(10)	-141(9)	143(12)
F(1)	6436(3)	3348(2)	1704(3)	108(2)

F(2)	6355(3)	4077(2)	1273(2)	83(1)
F(3)	6555(3)	4097(2)	2099(2)	100(2)
O(7)	4637(3)	3451(2)	2022(2)	53(1)
O(8)	4610(3)	4291(1)	1691(2)	57(1)
C(67)	5001(3)	3860(2)	1820(2)	41(1)
C(68)	6089(4)	3833(2)	1724(3)	50(1)
F(4)	1989(3)	7404(2)	3205(2)	94(2)
F(5)	1062(3)	7071(2)	3800(2)	69(1)
F(6)	1308(4)	7912(2)	3775(2)	95(2)
O(9)	-348(3)	7238(1)	3102(2)	45(1)
O(10)	390(3)	7970(2)	2797(2)	60(1)
C(69)	311(4)	7573(2)	3086(2)	46(1)
C(70)	1168(4)	7483(2)	3464(3)	55(1)
F(7)	1962(6)	4668(3)	4044(3)	153(3)
F(8)	1459(4)	3989(2)	3587(3)	149(3)
F(9)	538(4)	4662(2)	3713(3)	129(2)
O(11)	2480(3)	4524(2)	2877(2)	68(1)
O(12)	1534(3)	5238(2)	3015(2)	52(1)
C(71)	1420(5)	4510(3)	3608(4)	98(3)
C(72)	1835(4)	4778(2)	3107(3)	52(1)

Allyl (2-(((S)-1-((R)-2-(((*trans*)-3-butylcyclobutane-1-carbothioamido)methyl)pyrrolidin-1-yl)-3,3-dimethyl-1-oxobutan-2-yl)amino)-2-oxoethyl)(methyl)carbamate (**36**)

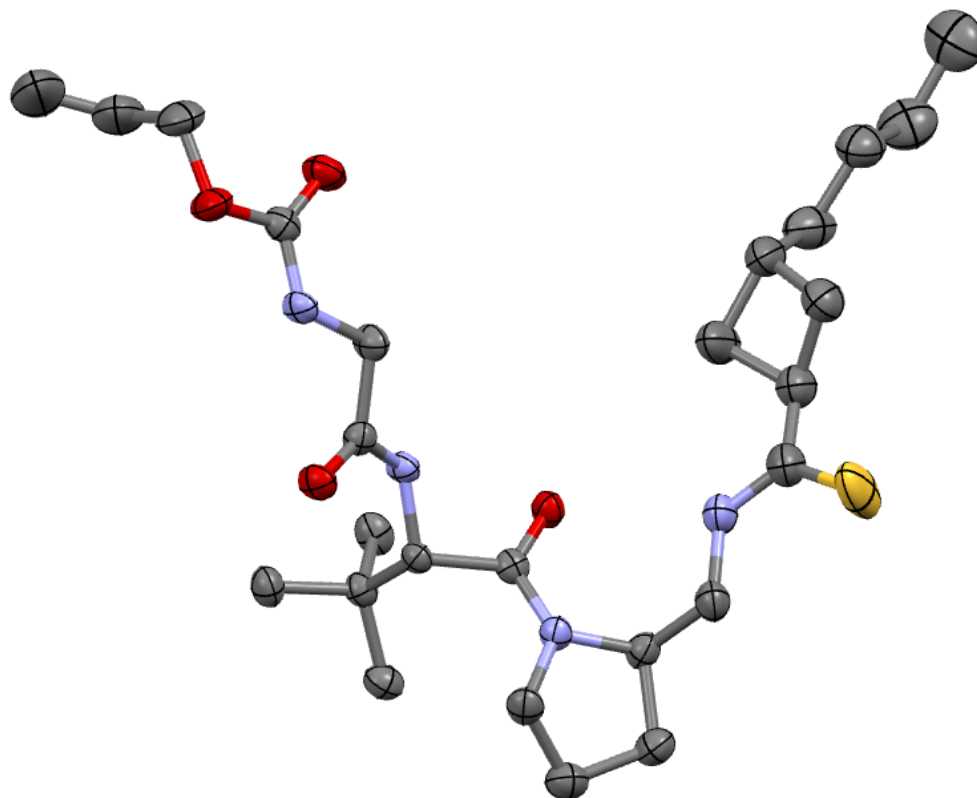
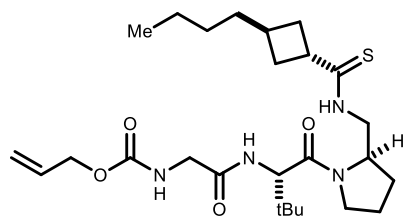


Table 1. Crystal data and structure refinement for **36**.

Identification code	har1303s	
Empirical formula	C ₂₆ H ₄₄ N ₄ O ₄ S	
Formula weight	508.71	
Temperature	100(2) K	
Wavelength	0.71073 Å	
Crystal system	Monoclinic	
Space group	P2 ₁	
Unit cell dimensions	a = 9.782(4) Å	a = 90°.
	b = 9.800(4) Å	b = 91.305(5)°.
	c = 14.421(6) Å	g = 90°.
Volume	1382.1(10) Å ³	
Z	2	
Density (calculated)	1.222 Mg/m ³	
Absorption coefficient	0.154 mm ⁻¹	
F(000)	552	
Crystal size	0.50 x 0.05 x 0.03 mm ³	
Theta range for data collection	4.05 to 28.61°.	
Index ranges	-13<=h<=13, -13<=k<=13, -18<=l<=19	
Reflections collected	17845	
Independent reflections	6976 [R(int) = 0.0404]	
Completeness to theta = 28.61°	99.1 %	
Absorption correction	Semi-empirical from equivalents	
Max. and min. transmission	0.9954 and 0.8812	
Refinement method	Full-matrix least-squares on F ²	
Data / restraints / parameters	6976 / 1 / 320	
Goodness-of-fit on F ²	1.045	
Final R indices [>2sigma(I)]	R1 = 0.0431, wR2 = 0.0929	
R indices (all data)	R1 = 0.0591, wR2 = 0.1001	
Absolute structure parameter	?	
Largest diff. peak and hole	0.318 and -0.288 e.Å ⁻³	

Table 2. Atomic coordinates ($\times 10^4$) and equivalent isotropic displacement parameters ($\text{\AA}^2 \times 10^3$) for bisthio. $U(\text{eq})$ is defined as one third of the trace of the orthogonalized U^{ij} tensor.

	x	y	z	U(eq)
S(1)	10782(1)	1989(1)	4974(1)	49(1)
O(1)	8270(1)	3130(1)	1715(1)	19(1)
O(2)	10179(1)	6849(1)	99(1)	21(1)
O(3)	13343(1)	3740(1)	-1400(1)	26(1)
O(4)	13662(2)	5845(1)	-2010(1)	28(1)
N(1)	9181(2)	2330(2)	3506(1)	25(1)
N(2)	7632(2)	4883(2)	2596(1)	17(1)
N(3)	9260(2)	4776(2)	433(1)	16(1)
N(4)	12268(2)	5603(1)	-836(1)	18(1)
C(1)	12718(3)	-6040(3)	2742(2)	50(1)
C(2)	11650(3)	-4939(3)	2689(2)	44(1)
C(3)	12191(2)	-3489(2)	2632(2)	36(1)
C(4)	11071(2)	-2434(3)	2518(2)	38(1)
C(5)	11526(2)	-962(2)	2511(2)	36(1)
C(6)	11882(2)	-341(2)	3464(2)	31(1)
C(7)	10419(2)	218(2)	3497(2)	32(1)
C(8)	10317(3)	56(3)	2439(2)	42(1)
C(9)	10103(2)	1567(2)	3948(2)	30(1)
C(10)	8505(2)	3471(2)	3941(1)	24(1)
C(11)	7284(2)	3978(2)	3376(1)	20(1)
C(12)	6376(2)	4877(2)	3985(1)	24(1)
C(13)	6025(2)	6129(2)	3404(1)	26(1)
C(14)	7284(2)	6302(2)	2819(1)	21(1)
C(15)	7996(2)	4362(2)	1788(1)	16(1)
C(16)	8060(2)	5249(2)	921(1)	15(1)
C(17)	6732(2)	5156(2)	304(1)	17(1)
C(18)	6864(2)	6199(2)	-485(1)	22(1)
C(19)	5480(2)	5529(2)	865(1)	22(1)
C(20)	6538(2)	3723(2)	-99(1)	22(1)
C(21)	10243(2)	5594(2)	119(1)	17(1)
C(22)	11506(2)	4824(2)	-174(1)	21(1)

C(23)	13101(2)	4959(2)	-1412(1)	19(1)
C(24)	14461(2)	5248(2)	-2737(2)	35(1)
C(25)	13580(3)	4960(3)	-3558(2)	46(1)
C(26)	13732(4)	5516(3)	-4379(2)	72(1)

In Vivo Evaluation of GOAT Inhibitors

Inhibitors **1,2,4**, and **19** were originally evaluated by Dr. Tongjin Zhao at UTSW. We have since reproduced much of this work at UCLA.

Efficacy Evaluation by IP Dosing

A cohort of 27-33 age matched C57BL/6 mice was acclimatized for one week prior to each experiment. All animals were housed in a temperature-controlled room under a 12 h light/12 h dark cycle and under pathogen-free conditions. All mice were fed a standard diet.

Prior to experimentation, mice were fasted overnight. For IP dosing, 10mg/mL solution of test inhibitor was prepared in 1% tween 80 in PBS. For PO dosing, compounds were suspended in cellulose prior to oral gavage. Following compound administration, blood samples were collected at the indicated time points.

For measurement of inhibitor concentration, blood was collected by cardiac puncture from anesthetized mice using EDTA coated needles and transferred to blood tubes containing EDTA as an anticoagulant. Plasma was recovered after centrifugation at 8000 rpm for 5m and snap frozen in liquid nitrogen, then stored at -80C. Inhibitor quantitation was performed by the group of Dr. Noelle Williams (Univ. Tex. Southwestern Med. Ctr). To 100uL of collected plasma was added 100uL of acetonitrile containing 0.2% formic acid and 200ng/mL benzylbenzamide or tolbutamide as an internal standard. These samples were centrifuged at 13000 rpm and the supernatant analyzed by LC/MS/MS.

These samples were analyzed for the species indicated in the chapter text. Where possible external calibration curves were prepared using authentic drug or metabolite standards to allow precise quantitation of the analyte.

For quantitation of ghrelin species, a portion of the whole blood was transferred to tubes containing 5uL of a 100mM *p*-hydroxymercuribenzoic acid in PBS at pH 7.4. Plasma was isolated by centrifugation at 3500rpm for 10 min. Freshly prepared plasma was acidified with 1/10 volume of 1N HCl then centrifuged again at 3500 rpm for 5 min. The supernatant was then analyzed for acyl- and des-acyl ghrelin species using commercially available ELISA kits (Cayman).

All animal experiments were approved by the Institutional Animal Care and Research Advisory Committee of the University of California Los Angeles.

Inhibitor Quantitation in Mouse Excrement

A cohort of 9 age matched C57BL/6 mice were housed in metabolic cages (3 mice/cage) for one day prior to experimentation. Feces and urine were collected during this period to serve as blank samples. They were maintained on a standard diet before and during the experiment. No fasting was conducted. A 10mg/mL solution of Inhibitor **2** was prepared in 1% tween 80 in PBS. Inhibitor was administered intraperitoneally at 80mg/kg to each mouse, and they were returned to cages. Feces and urine were collected separately from each cage. 0-4 hour, 4-7 hour, and 7-24 hour time period samples from each cage were collected and analyzed separately. Following collection, samples were frozen at -80 C. Inhibitor concentration was determined by the group of Dr. Noelle Williams (Univ. Tex. Southwestern Med. Ctr). Feces homogenates were prepared by homogenizing in a 5-fold volume of PBS (total volume of homogenate in ml = 6x weight in g.). For a 1:5 dilution, mixed 40 microliter of blank feces with 10 microliter of sample and for a 1:10 dilution, mixed 45 microliter of blank feces with 5 microliter of sample . To each sample, add 100 microliters of acetonitrile containing 0.15% formic acid and 75 ng/ml IS (50 ng/ml final conc.).The samples were vortexed 15 seconds, incubated at room temp for 10 min and spun twice at 13,200 rpm for 5 min 4°C in a standard microcentrifuge. The supernatant was then analyzed by LC-MS/MS. Analyte counts were compared to a standard curve for parent inhibitor. Presence of

glucuronidated metabolites was evaluated by searching for expected mass transitions corresponding to the glucuronidated product.

INS-1 Cellular Assay

A line of INS-1 cells stably expressing GOAT and ghrelin was established by Dr. Tongjin Zhao at UTSW. To evaluate the effects of a candidate GOAT inhibitor on ghrelin production in these cells, cells were plated at 1.5×10^6 cells in a 10cm dish. After 96 hours the cells were treated with 50uM octanoic acid and the indicated concentration of inhibitor. After 24 hours the cells were lysed and the protein run on SDS-PAGE. The relative abundance of ghrelin species was evaluated by western blot using antibodies specific for acyl or total ghrelin concentration. In some cases GOAT or SCAP levels were analyzed as a control for loading or cytotoxicity.

PAMPA Permeability

10mM solutions of **2**, propranolol, and phlorizidin in DMSO. A solution of 5mM chloroquine in 1:1 DMSO/Water was prepared. These stock solutions were used to prepare test solutions of the listed compounds at 100uM concentration in 5% DMSO. A suspension of 1% lecithin in dodecane was prepared and 5uL of this solution was added to the center of each used well of a Millipore Multiscreen filter plate. 150uL of test solution was added to each well of the filter plate and the filter plate (donor plate). A Teflon receiver plate was filled with 300uL per well of blank 5% DMSO/PBS solution. The donor plate was placed into the acceptor plate such that the bottom surface of the filter was in full contact with the receiving solution. The donor plate was covered and the apparatus placed in a closed bag with a wet paper towel to minimize evaporation. After sixteen hours the plates were separated and the donor and acceptor solutions transferred to Greiner UV-star 96 well plates. A solution containing the theoretical equilibrium concentration (ie. For 100uM donor, theoretical equilibrium concentration is 33uM) of inhibitor in 5% DMSO/PBS was prepared separately. The UV absorbance spectrum for each well was recorded using a Tecan M1000 plate reader. Each

compound was analyzed in triplicate, and the results of each determination averaged. The equilibrium solution was used to determine a UVmax for each analyzed compound. Comparison of the absorption in donor and acceptor solutions at the UVmax for each compound according to the formula

$$\text{LogPe} = \text{Log} (C^* - 1 * n * (1 - A_A / A_E))$$

$$\text{Where } C = (V_D * V_A) / (V_D * V_A) * \text{Area} * \text{time}$$

Mass recovery was computed according to the formula

$$\text{Mass Recovery} = (A_D * V_D + A_A * V_A) / (A_{EQ} * (V_D + V_A))$$

Permeability in Caco-2 and MDCK Monolayers

Analyses of permeability in Caco2 and MDCK Cell types were performed by Changguang Wang in the group of Dr. Noelle Williams at UTSW. Caco2, WT MDCK, MDCK MDR1, and MDCK BCRP cells were cultured on solid support until they reached confluence. The monolayers were rinsed three times with 0.5% FBS in Hank's buffered salt solution, then 5uM test compound in 0.5% FBS/HBSS (1, cimetidine, nadolol, quinidine, or propranolol) was added to the apical or basolateral portion of the culture media (depending the desired transport direction). Samples (300uL from apical portion, or 1mL from basolateral portion) were collected from the receiving portion of the setup at the indicated time points and the sample volume replaced with blank media. 100uL of the sample was diluted with 200ul of MeOH containing 15ng/mL benzylbenzamide as internal standard, 2mM ammonium formate, and 0.15% formic acid. Following centrifugation to clear protein, analyte was quantified by LC/MS/MS.

Plasma Binding Measurement

Inhibitor stocks were prepared at 2mM in DMSO. 2uL of stock was added to 400uL of commercially available mouse plasma, then vortexed to afford a 10uM test solution. Two 50ul aliquots were removed and placed into Eppendorf tubes. To one was added 50ul of water and 200uL of MeOH/internal standard solution (time zero control). The

second aliquot was incubated for twenty minutes at 37C, and then processed in the same fashion (plasma stability control). The remaining solution was placed in a centrifuge device. The upper and lower chambers were separately weighed, then the device was incubated at 37C for 20 min, and centrifuged at 1000g for 5 minutes. 50uL samples from the upper and lower chamber were collected and processed as before. Inhibitor concentration was quantified by LC/MS/MS and the data processed as described in the reference below.

Reference: Wang, C. and N.S. Williams (2013) A mass balance approach for calculation of recovery and binding enables the use of ultrafiltration as a rapid method for measurement of plasma protein binding for even highly lipophilic compounds. *Journal of Pharmaceutical and Biomedical Analysis* 75: 112-117. PMID: PMC3545278

Compiled In Vitro GOAT Inhibition Assay Results

Dr. Tongjin Zhao Results

Compound	Structure Page	In Vitro Data Page	Cellular Data Page	In Vivo Data Page
AEN 1-101	1	7	1	
AEN 1-111	1	7		
AEN 1-121	1	1,3		
AEN 1-129	1	1,3		
AEN 1-163	1	9		
AEN 1-179	1	10		
AEN 1-225-2	1	12		
AEN 1-235		12		
AEN 1-257-2	1	14		
AEN 1-295-d	1			
AEN 1-295-e	1	18		
AEN 2-32	1	24		
AEN 2-41	2	24		
AEN 2-48	2	25		
AEN 2-63	2	27		
AEN 2-66	2	27		
AEN 2-80	2	31,32		
AEN 2-88	2	33		
AEN 2-89	2	33		
AEN 2-92	2	22		
BK1114		1,3,4,5,6,8,9,10,11	1,2	
BRB 1-148		8		
CRN 1-107	3	24		
CRN 1-130	3			
CRN 1-148	3	62		
CRN 1-155	3	40		
CRN 1-89-a	3	21		
CRN 1-89-b	3	21		
CRN 1-93	3	22		
CWF 1-61	3	4		
HD 5-240	35			
HD 5-259-2A	35			
HD 5-259-2B	35			

LHX 1-100	28	13	2	
LHX 1-109	8	13		
LHX 1-11	8	1,3		
LHX 1-113	8	14		
LHX 1-114	8	14,15,17,18,22,23,24,25,26, 27,28,29,30,31,32,33,34,3 5,36,37,38,53	2,3,4,5,6,7,8,9	
LHX 1-115	8	14	2	
LHX 1-119	8	,26,27,28,29,30,31,32,33,3	3,4,5,	
LHX 1-137	8	15		
LHX 1-138	8	15	4,5	
LHX 1-144	9	17	5	
LHX 1-153	9	17		
LHX 1-160	9	17		
LHX 1-161	9	17		
LHX 1-162	9	17		
LHX 1-166		18		
LHX 1-168	9			
LHX 1-177	9	18		
LHX 1-178	9	18		
LHX 1-186	10			
LHX 1-187	10			
LHX 1-188	10			
LHX 1-19	28	4		
LHX 1-192	10	21		
LHX 1-195	10	21		
LHX 1-198	10	21	6	
LHX 1-204	11	22		
LHX 1-207	11	22	6	
LHX 1-217	11	23		
LHX 1-218	11	23		
LHX 1-221	11	23		
LHX 1-229	11	23		
LHX 1-230	11	23		

LHX 1-231	11	23		
LHX 1-236	12	23		
LHX 1-243	12	25		
LHX 1-245	12	25		
LHX 1-246	12	25		
LHX 1-249	12	26		
LHX 1-252	12	26		
LHX 1-254	12	26		
LHX 1-257	12	26		
LHX 1-262	13	27		
LHX 1-273	13	28		
LHX 1-278	13	28		
LHX 1-286	13	19		
LHX 1-287	13	19		
LHX 1-292	13	30		
LHX 1-293	13	30		
LHX 1-296	13	30		
LHX 1-45	6	6		
LHX 1-46	6	6		
LHX 1-47	6	6		
LHX 1-52	6	10		
LHX 1-64	6	10		
LHX 1-65	6	10,11,12,13,14	2	
LHX 1-69	6	10		
LHX 1-81	6			
LHX 1-87	7	12		
LHX 1-96	7	12		
LHX 1-97B	7	14		
LHX 2-100	10	36		
LHX 2-10A		31,32		
LHX 2-10B		31,32		
LHX 2-124	10	,47,48,49,50,51,52,54,55,5		
LHX 2-135	15	39		

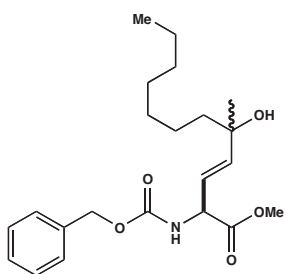
LHX 2-138	15	39		
LHX 2-152	15	62		
LHX 2-181	15	40		
LHX 2-189	15	41		
LHX 2-18A	4	33		
LHX 2-2	4	31,32		
LHX 2-203	4	42	8	
LHX 2-211		43		
LHX 2-226	4	45	8	
LHX 2-230	4	44		
LHX 2-233	4	44		
LHX 2-237	5	44		
LHX 2-251	5	45		
LHX 2-270	5	46		
LHX 2-279	5	47		
LHX 2-280	5	47		
LHX 2-281	5	47		
LHX 2-294	5	48		
LHX 2-295	5	48		
LHX 2-36	28	34		
LHX 2-37	28	34		
(mixed Dists)	28	34		
LHX 2-39	28	34		
LHX 2-4	4	31,32		
LHX 2-42	28	34		
diastereomer A	29	34		
diastereomer B	29	34		
LHX 2-47	28	35		
LHX 2-51	29	35		
LHX 2-60	15			

LHX 2-79	15			
LHX 2-8	4	31,32		
LHX 2-90		37		
LHX 2-96	15	36		
LHX 3-105	29	55	17	
LHX 3-114	29	55	17	
LHX 3-117	29	56	18,19	
LHX 3-118	29	56	18,19	
LHX 3-14	29	63		
LHX 3-140		57		
LHX 3-15	30	63		
LHX 3-151	30	58	20,21	
LHX 3-176	30	60		
LHX 3-177A	30	60		
LHX 3-177B	30	60		
LHX 3-185	31	61		
LHX 3-196A	31	61		
LHX 3-30	31	64		
LHX 3-31B	31	64		
LHX 3-40A	31			
LHX 3-40B	31			
LHX 3-42	32			
LHX 3-71	32	50		
LHX 3-72	32	50	12	
LHX 3-73	32	50	10,11,12,13,15,16	
LHX 3-74	32	50		
LHX 3-79	32	51		
LHX 3-88	32	52	8,14,15,16,17,18,19,20,22	
LHX 3-89	32	52	11	
LHX 3-90A	23	52		
LHX 3-90B	23	52	11	
LHX 3-96A	23	54		
LHX 3-96B	23	54	14	
LHX 3-97A	23	54		
LHX 3-97B	23	54	14,15,16	

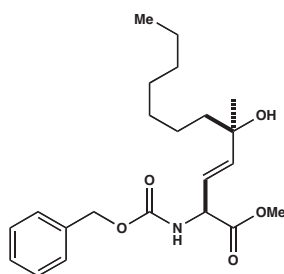
NE 1-116	27	70		
NE 1-125	27	70	29	
PHB 1-238	14			
PHB 1-241	14	8	1	
PHB 1-242A	14	8	1	
PHB 1-243	14	8		
PHB 1-248	14	8		
PHB 1-249	14	8	1	
PHB 1-260B	14	7		
PHB 1-273A	14	7		
PHB 1-273B		7		
RAH 1-127	24	45		
RAH 1-150	24	46		
RAH 1-165	24	48		
RAH 1-178	24	48		
RAH 1-179	24	49		
RAH 1-208-1	24	64		
RAH 1-208-2	24	64		
RAH 1-46	18	37		
RAH 1-50	18	36		
RAH 1-64	18			
RAH 1-69	24	38		
RAH 1-89	18	40		
RAH 2-100	20	59		
RAH 2-101	20	59		
RAH 2-102	20	60		
RAH 2-104	19	60		
RAH 2-106A	19	60		
RAH 2-106B	19	60		
RAH 2-109	20	61		
RAH 2-115	21	61	23,25,26	
RAH 2-117	21	66		
RAH 2-128	22	66,68,69,76,77	24,25,26,27,28,29,30	
RAH 2-129	22	66	23,24,26	
RAH 2-130	21	66	23,25,26	

RAH 2-131	21	66	23	
RAH 2-19	19	57		
RAH 2-20	19	57	21	
RAH 2-201	22	67	24,27	
RAH 2-202	21	67	24,27	
RAH 2-204	21	67		
RAH 2-22	19	57	21	
RAH 2-270	22	77		
RAH 2-272	22	77	28	
RAH 2-274	25	68,70,73,74	28	
RAH 2-276	25	68		
RAH 2-277	25	68		
RAH 2-288	25	69		
RAH 2-40	25	58	19	
RAH 2-57	18	65	22	
RAH 2-58	18	65		
RAH 2-58B	18	65	22	
RAH 2-58T	18	65	22	
RAH 2-59	25	65	22	
RAH 2-60	25	65	22	
RAH 2-61	25	65	22	
RAH 2-77	20	59		
RAH 2-81	20	59		
RAH 3-134	35			
RAH 3-163	33	75		
RAH 3-164	33	75		
RAH 3-167	33	75		
RAH 3-203	35			
RAH 3-209	35			
RAH 3-220	35			
RAH 3-224	35			
RAH 3-228	35			
RAH 3-28	33	70		
RAH 3-30	33	70		
RAH 3-59	33	71,73		

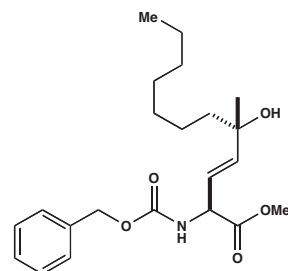
RAH 3-60	33	71,73		
RAH 3-63	33	71,72,73		
RAH 3-64	33	73		
RAH 3-65	33	74		
RAH 3-79	33	74		
RAH 3-88	33	76		
RVQ 1-33	26	77	28,30	
RVQ 1-47	26	77		
RVQ 1-72 1	26	69		
RVQ 1-72 2	26	70	28,29	
RVQ 1-75	26	70,71	29	
RVQ 1-95 d1	26	74		
RVQ 1-95 d2	26	74		
RVQ 1-96 d1	27	74		
RVQ 1-96 d2	27	74		
RVQ 1-99	26	74		
RW 1-131	16	39		
RW 1-175	16	40	7	
RW 1-176	16	40	7	
RW 1-182	16	41		
RW 1-184	16	41		
RW 1-191	16	42		
RW 1-197	16	42		
RW 1-206		43		
RW 1-220	16	46		
RW 1-258-1	17	49	10	
RW 1-258-2	17	49		
RW 1-260	17	49		
TR 1-296A	34	53		
TR 1-296B	34	53		
TR 1-296C	34	53		
TR 1-296D	34	53		
TR 1-296E	34	53		
TR 2-108	34	58	19,20	
TR 2-98A	34	58	19,20,22	



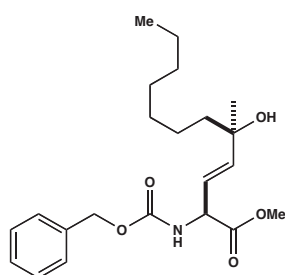
AEN1-101



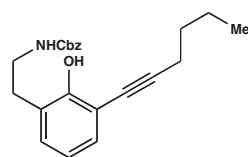
AEN1-111



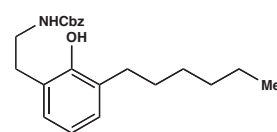
AEN1-121



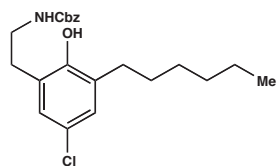
AEN1-129



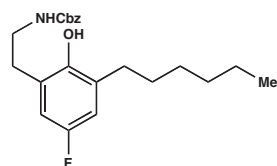
AEN1-163



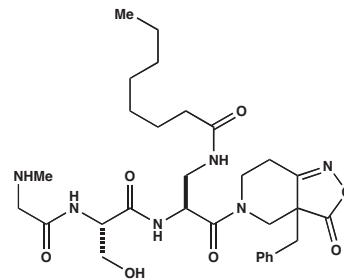
AEN1-179



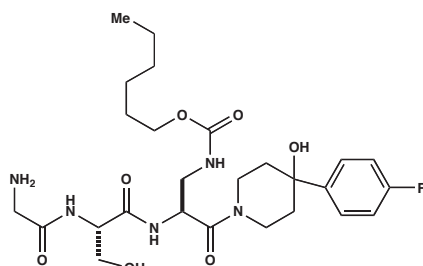
AEN1-225-2



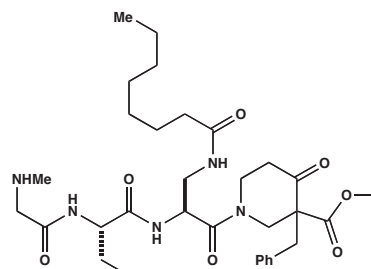
AEN1-257-2



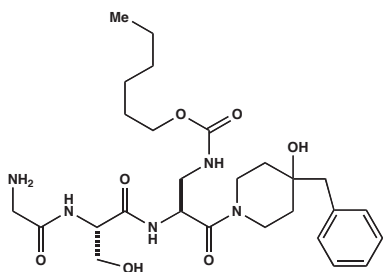
AEN1-295-d



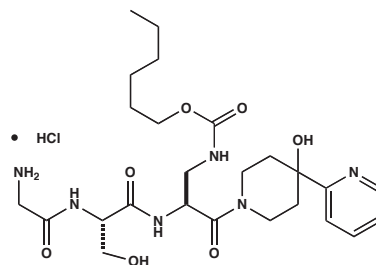
AEN2-32



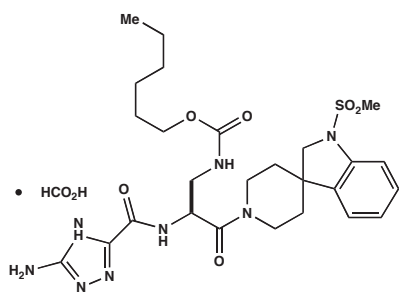
AEN1-295-e



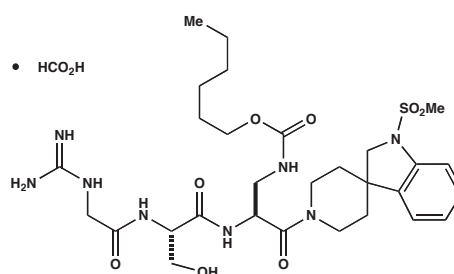
AEN2-41



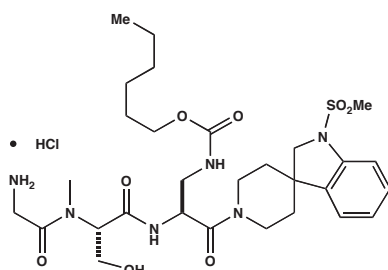
AEN2-48



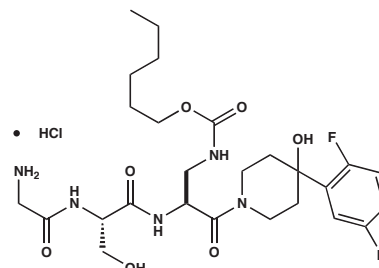
AEN2-66



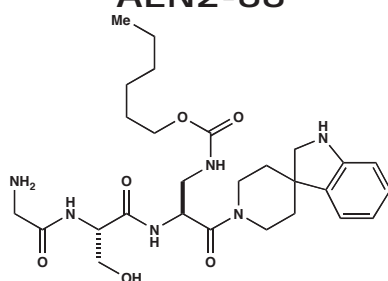
AEN2-63



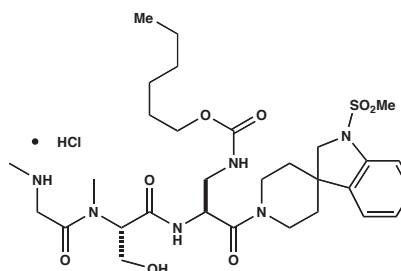
AEN2-88



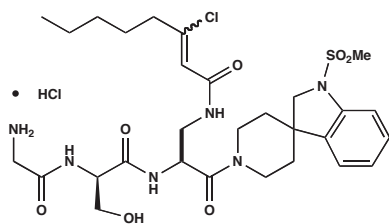
AEN2-80



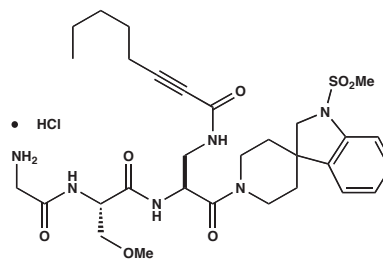
AEN2-92



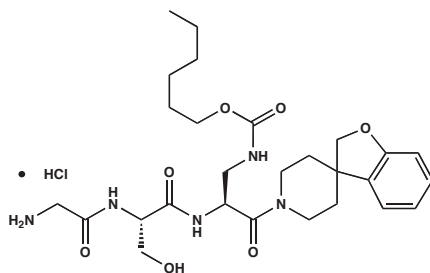
AEN2-89



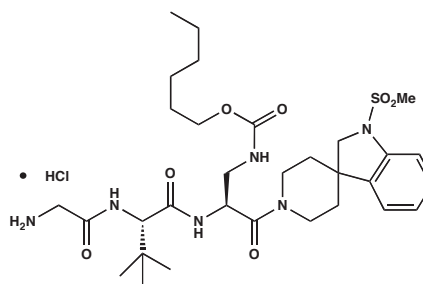
CRN1-093



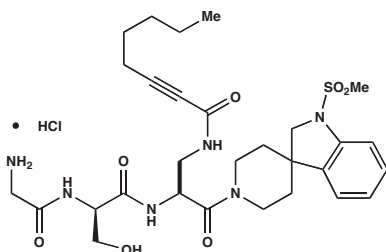
CRN-1-107



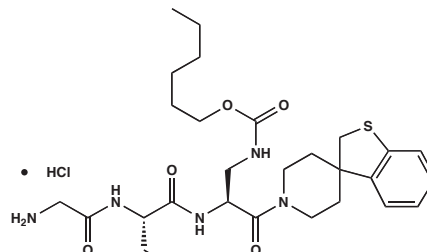
CRN1-148



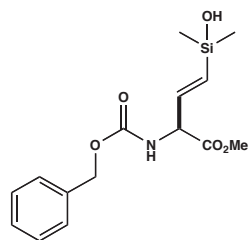
CRN1-130



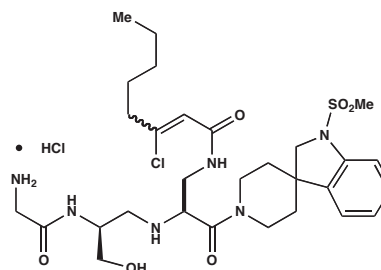
CRN1-89-a



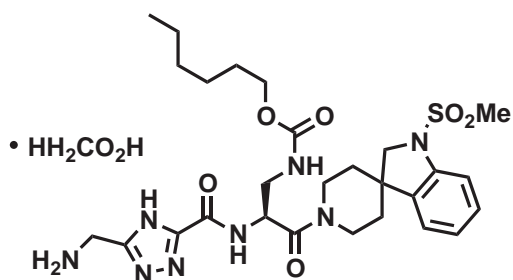
CRN1-155



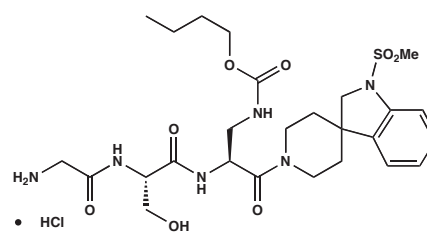
CWF-1-61



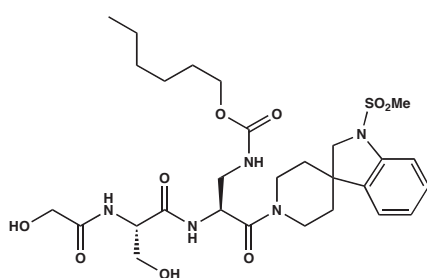
CRN1-89-b



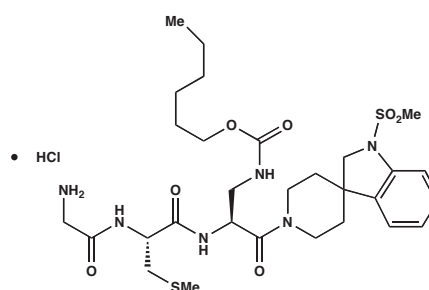
LHX_2_02



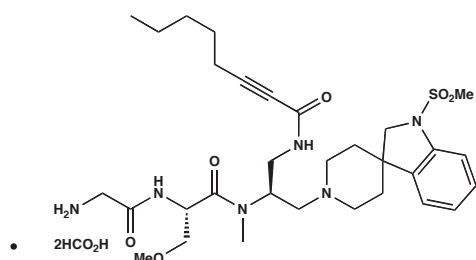
LHX_2_04



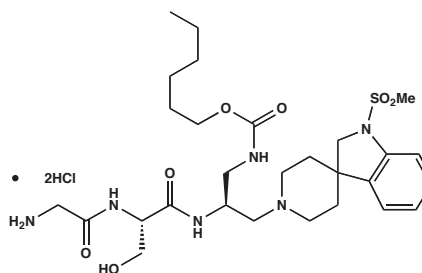
LHX_2_08



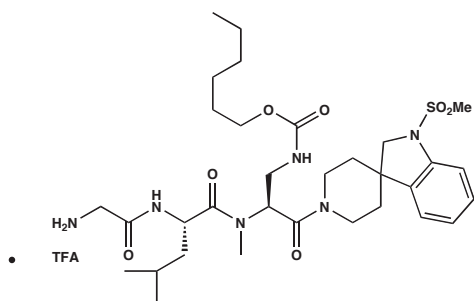
LHX_2_18A



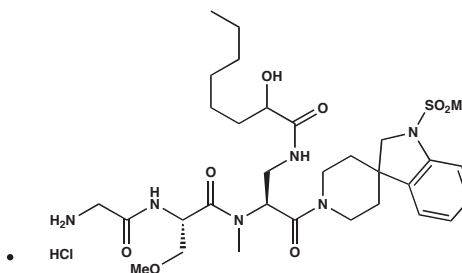
LHX_2_226



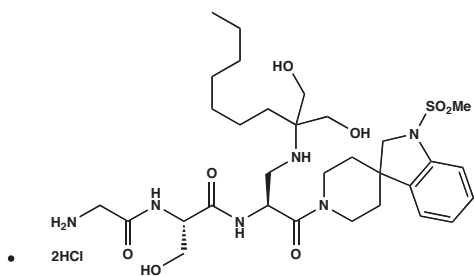
LHX_2_203



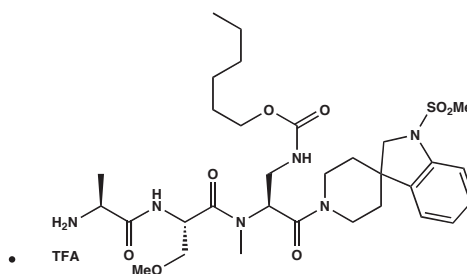
LHX_2_233



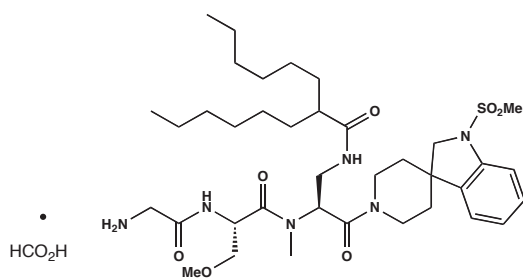
LHX_2_230



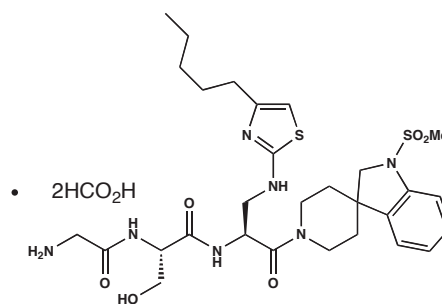
LHX_2_251



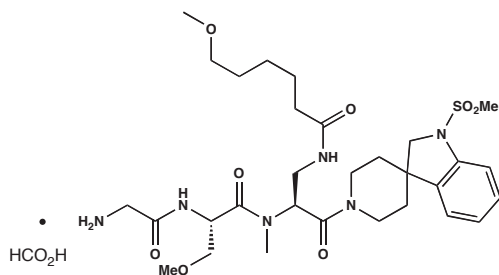
LHX_2_237



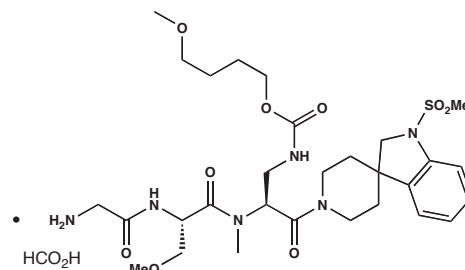
LHX_2_279



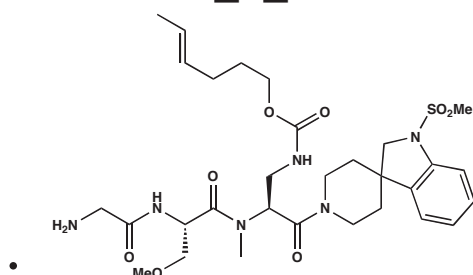
LHX_2_270



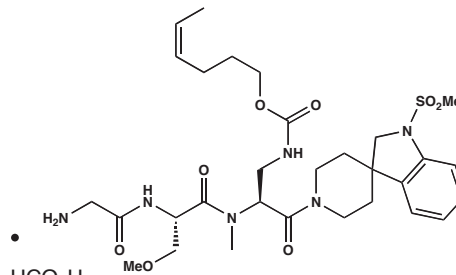
LHX_2_281



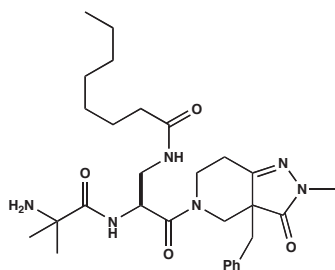
LHX_2_280



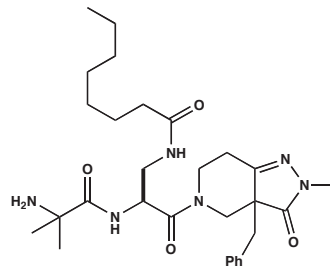
LHX_2_295



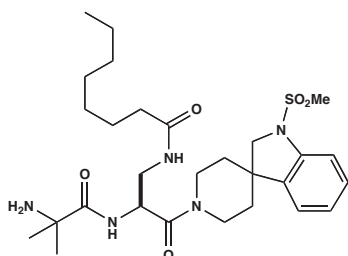
LHX_2_294



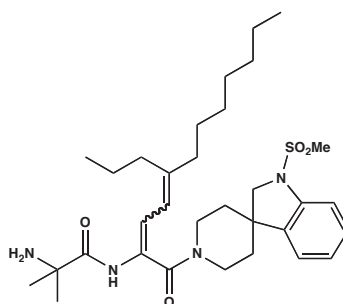
LHX-45



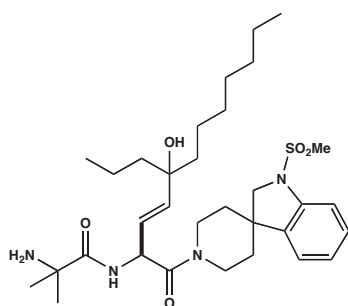
LHX-46



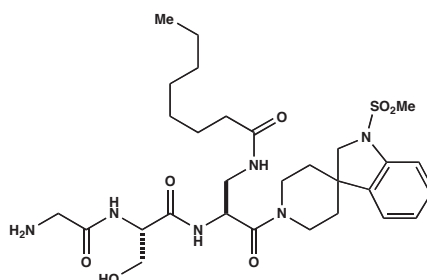
LHX-47



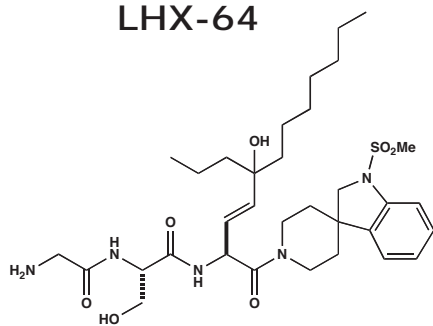
LHX-52



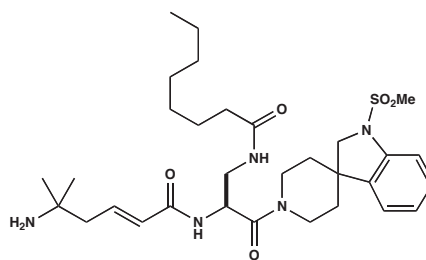
LHX-64



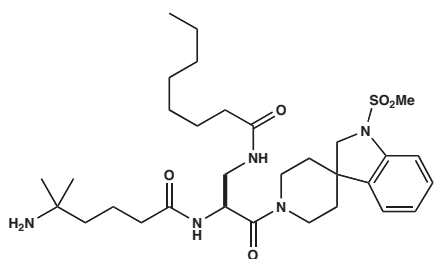
LHX-65



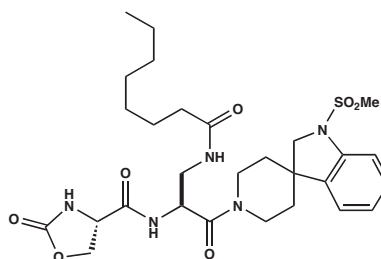
LHX-69



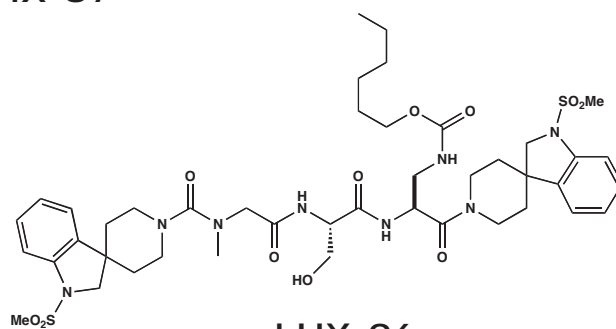
LHX-81



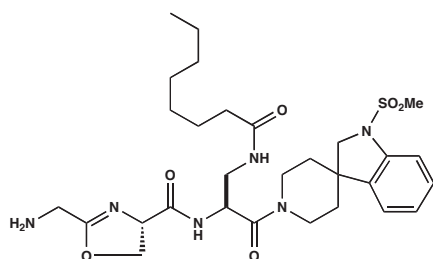
LHX-87



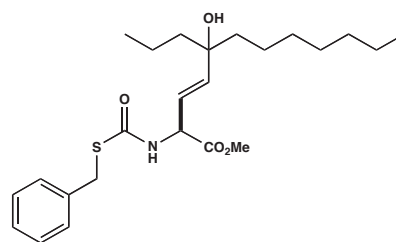
LHX-97B



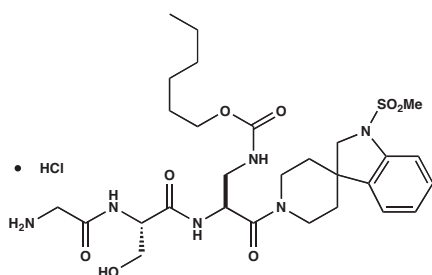
LHX-96



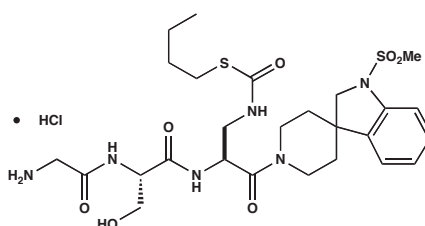
LHX-109



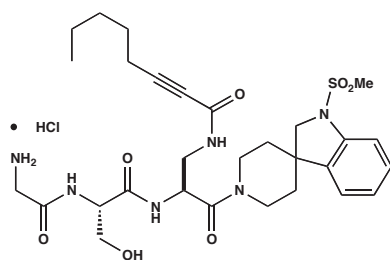
LHX-11



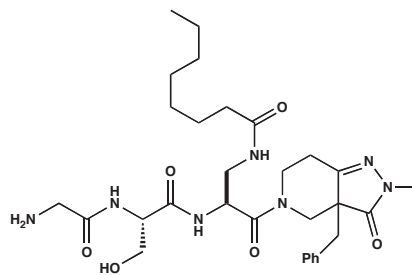
LHX-114



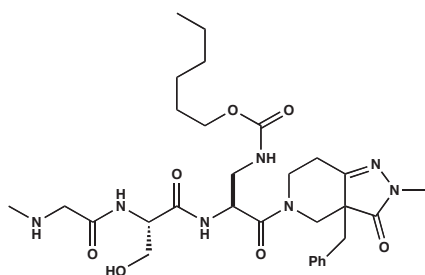
LHX-113



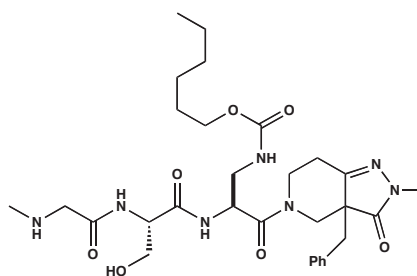
LHX-119



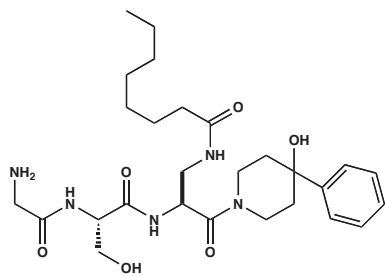
LHX-115



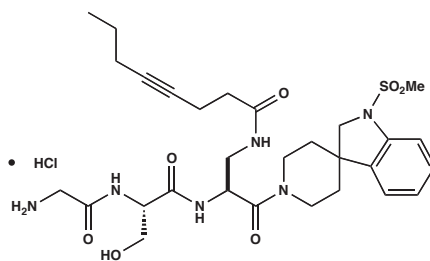
LHX-137



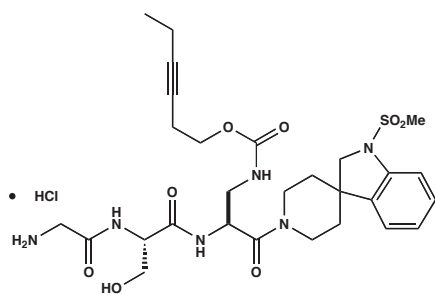
LHX-138



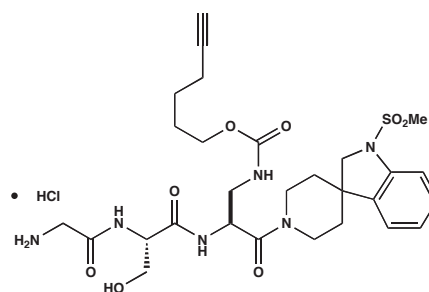
LHX-144



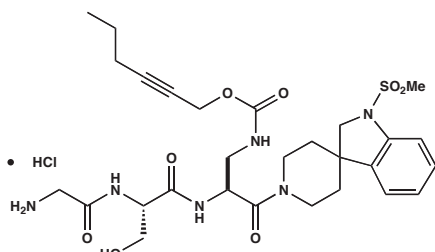
LHX-153



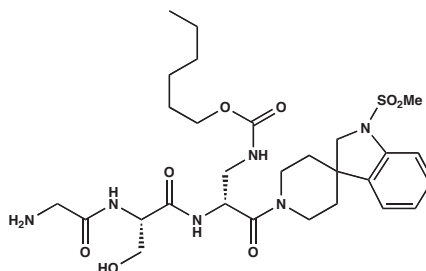
LHX-160



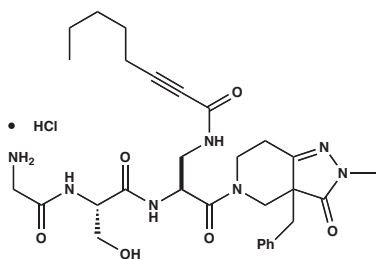
LHX-161



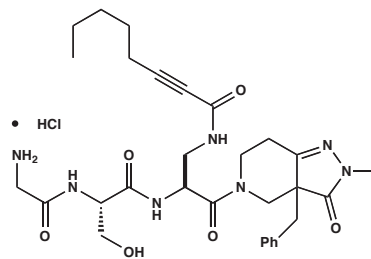
LHX-162



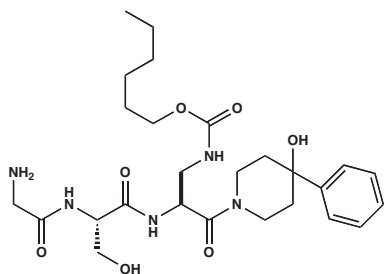
LHX-168



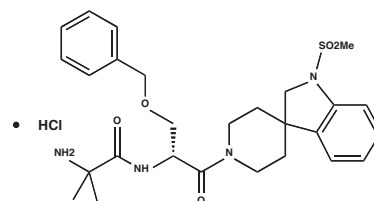
LHX-177



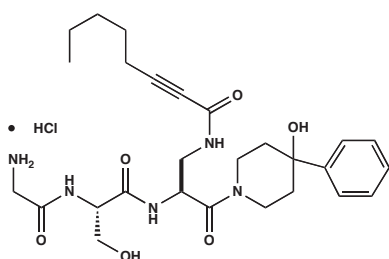
LHX-178



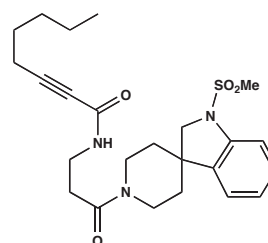
LHX-186



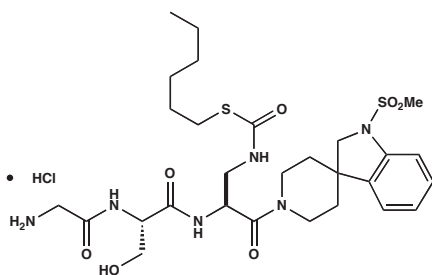
LHX-187



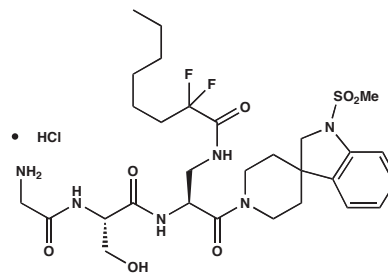
LHX-188



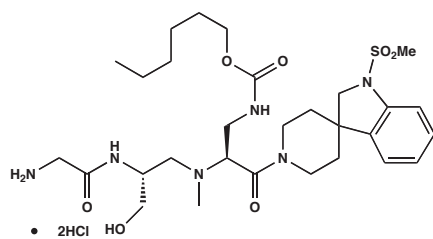
LHX-192



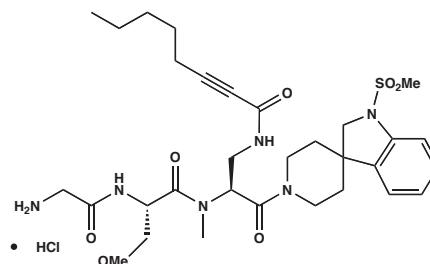
LHX-195



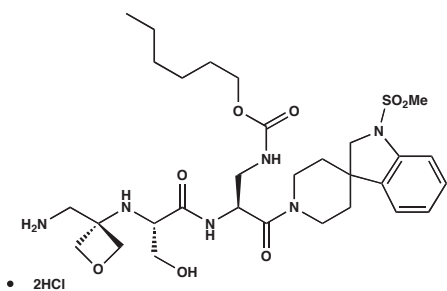
LHX-198



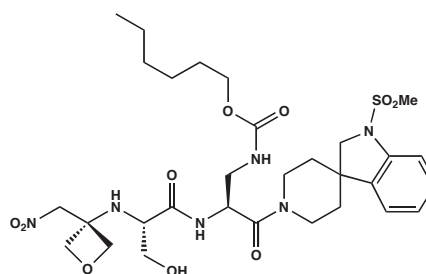
LHX-2-100



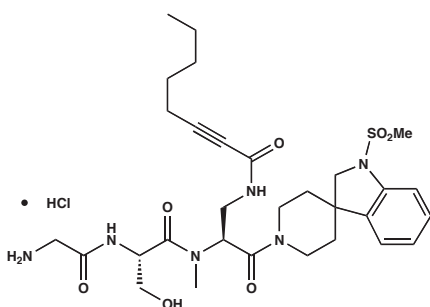
LHX-2-124



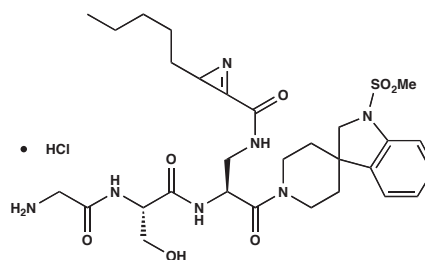
LHX-2-135



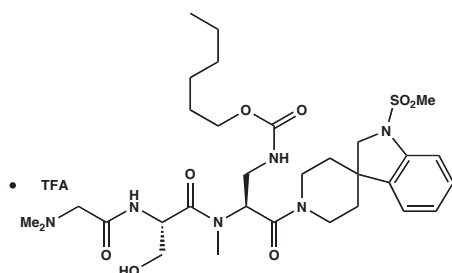
LHX-2-138



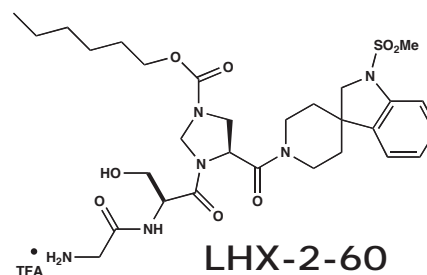
LHX-2-152



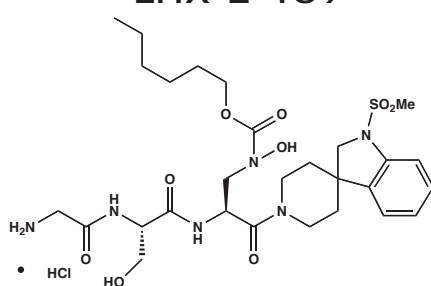
LHX-2-181



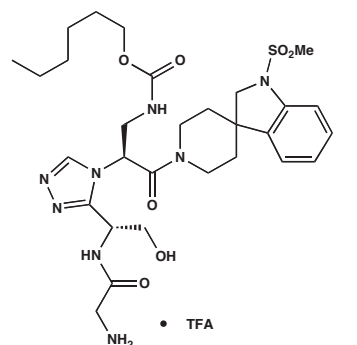
LHX-2-189



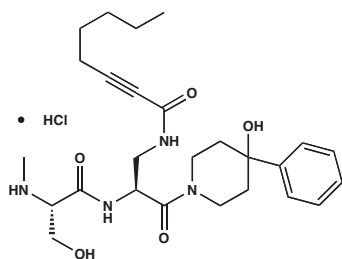
LHX-2-60



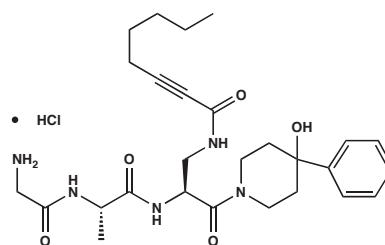
LHX-2-79



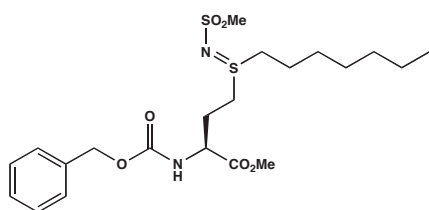
LHX-2-96



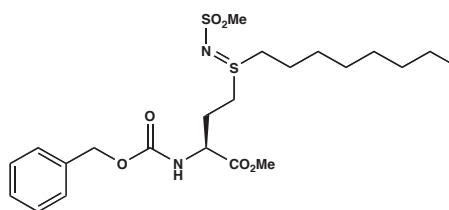
LHX-204



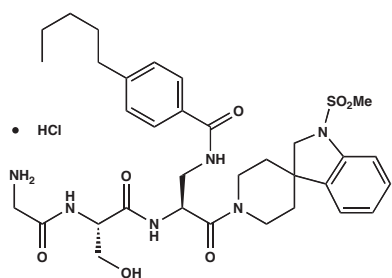
LHX-207



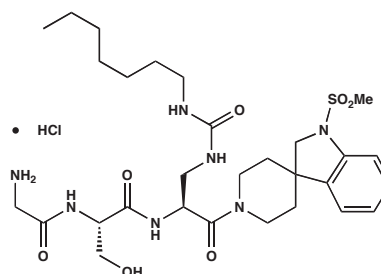
LHX-218



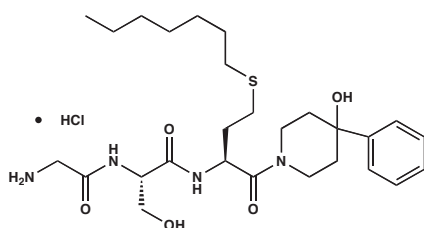
LHX-217



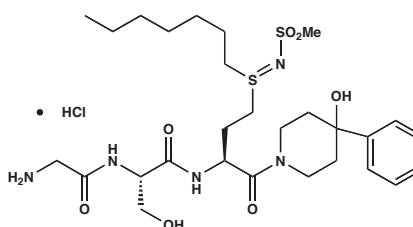
LHX-221



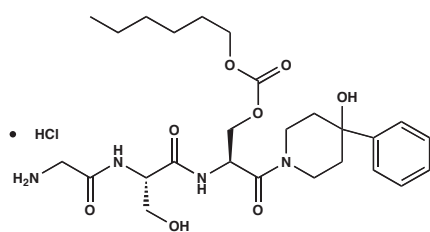
LHX-229



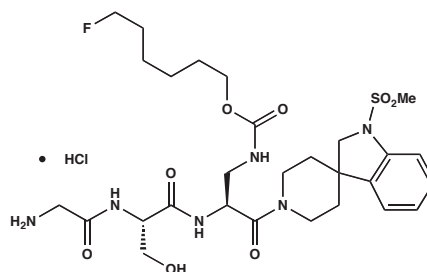
LHX-230



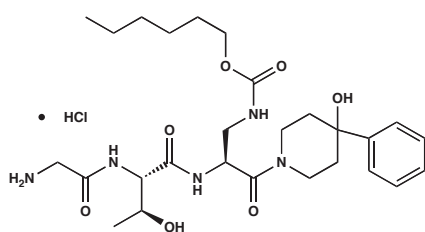
LHX-231



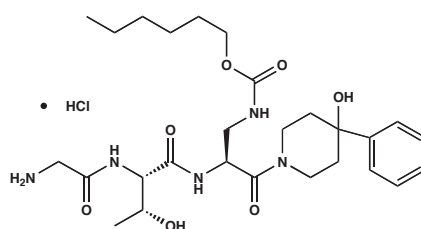
LHX-236



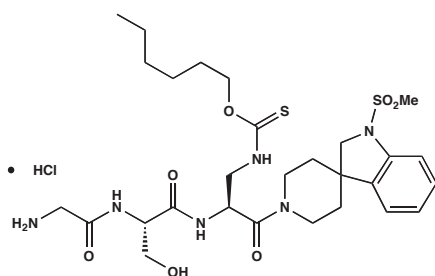
LHX-243



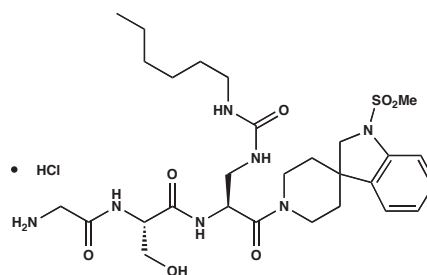
LHX-246



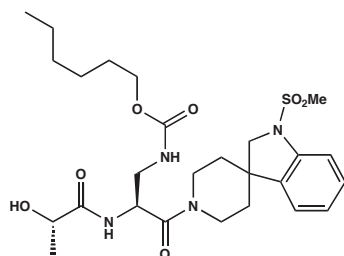
LHX-245



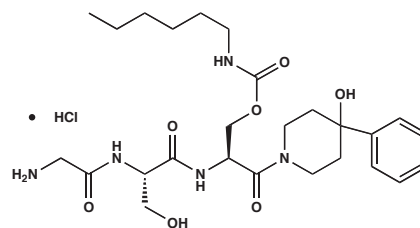
LHX-249



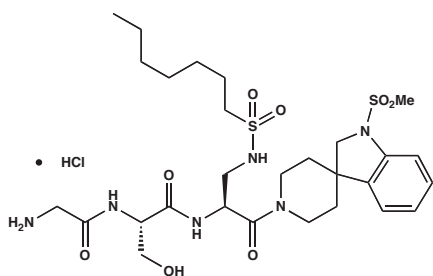
LHX-252



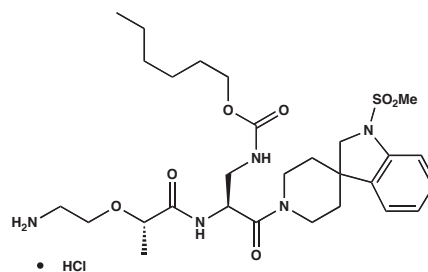
LHX-254



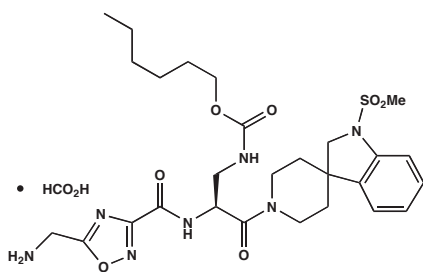
LHX-257



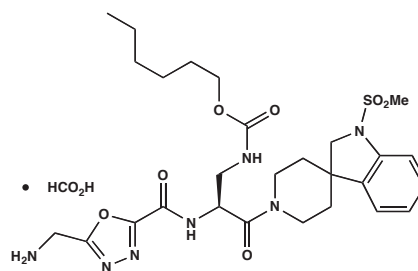
LHX-262



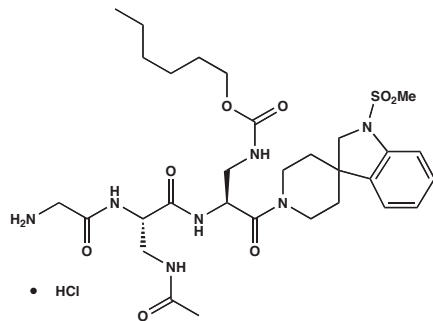
LHX-273



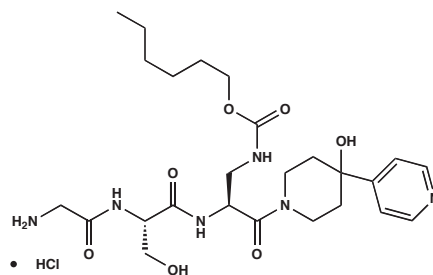
LHX-278



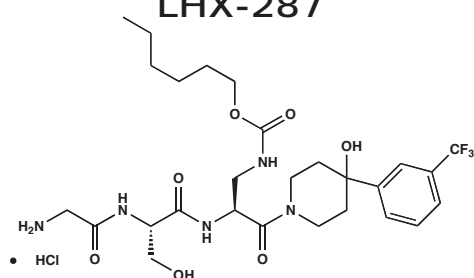
LHX-286



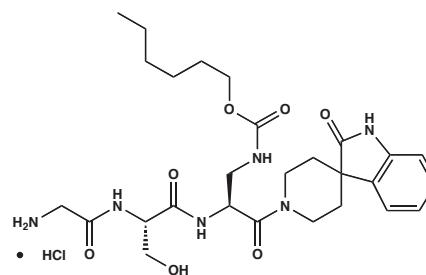
LHX-287



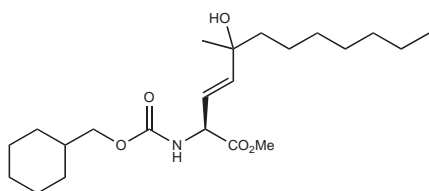
LHX-292



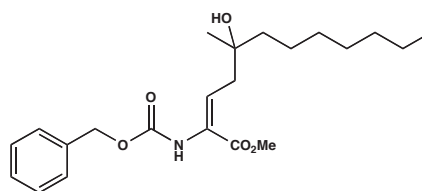
LHX-293



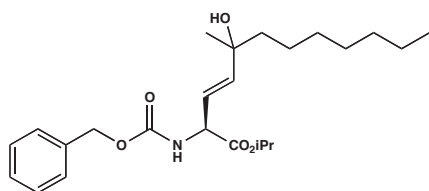
LHX-296



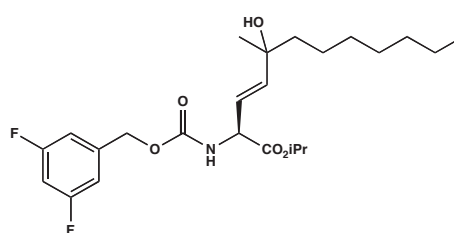
PHB238



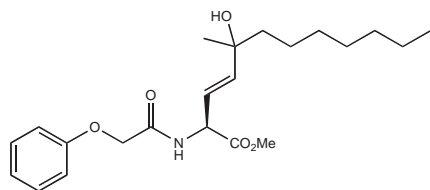
PHB241



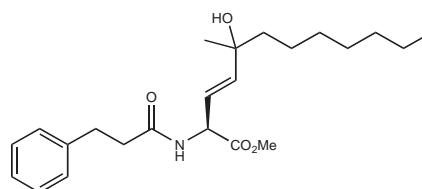
PHB242A



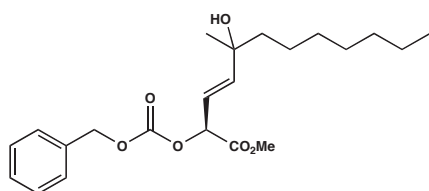
PHB243



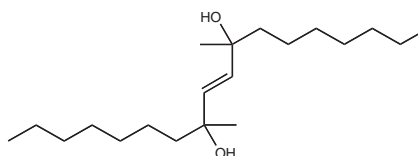
PHB248



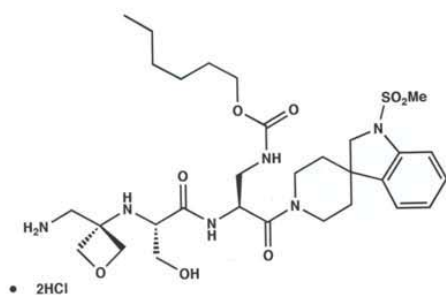
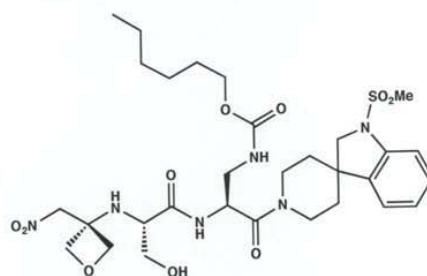
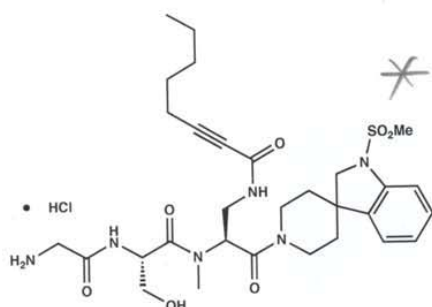
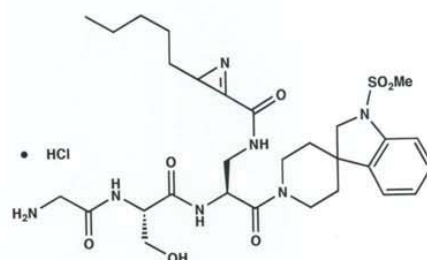
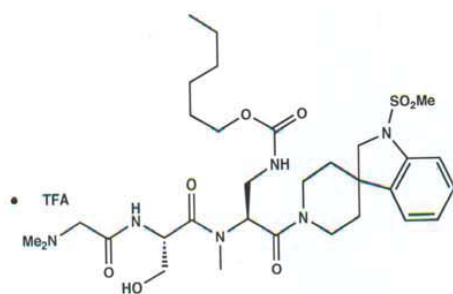
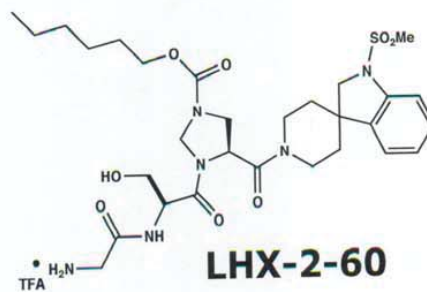
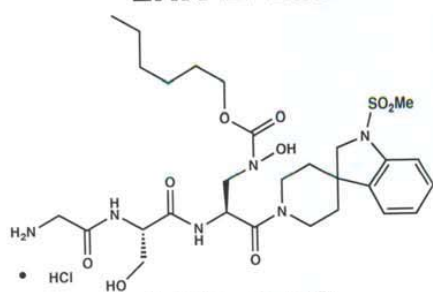
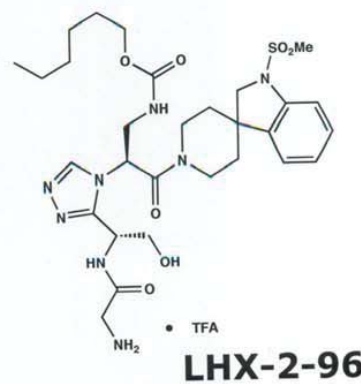
PHB249

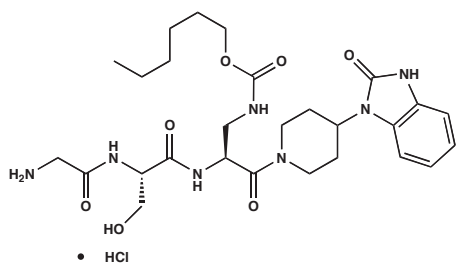


PHB273A

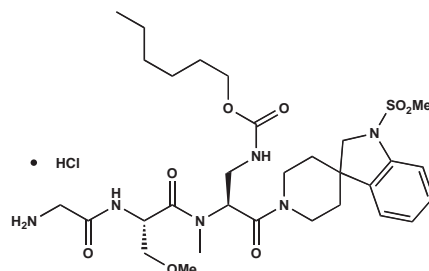


PHB260B

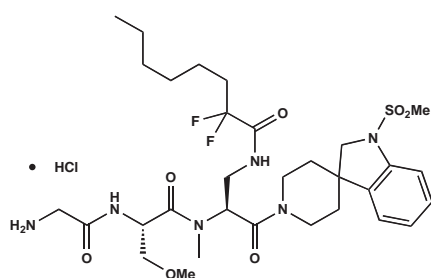
**LHX-2-135****LHX-2-138****LHX-2-152****LHX-2-181****LHX-2-189****LHX-2-60****LHX-2-79****LHX-2-96**



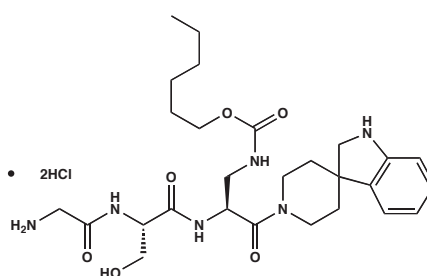
RW131



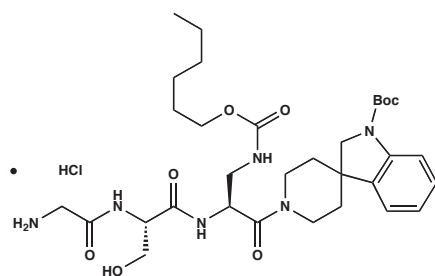
RW175



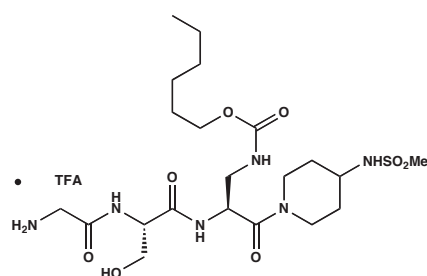
RW176



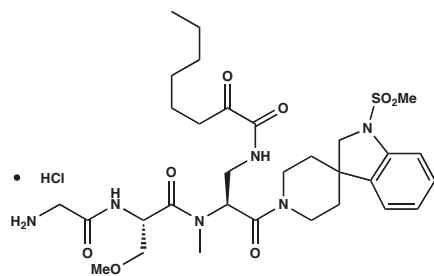
RW182



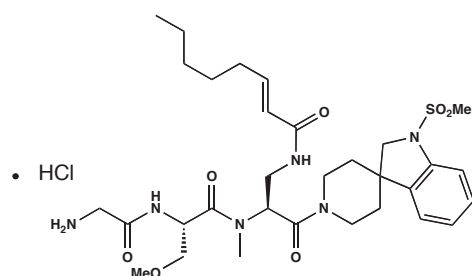
RW184



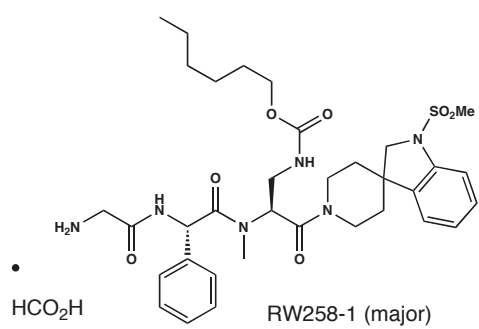
RW191



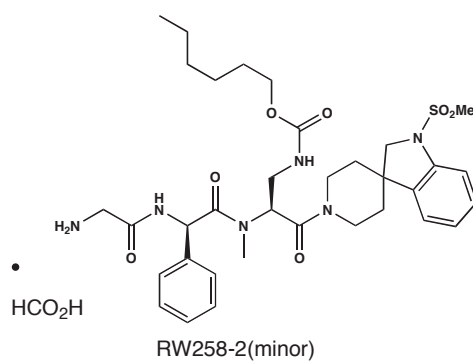
RW197



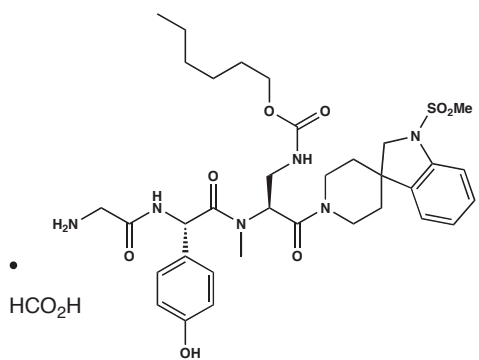
RW220



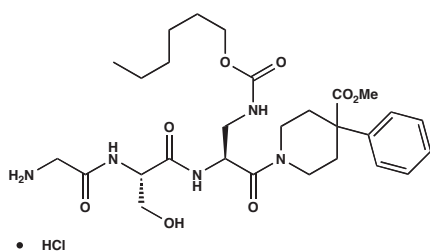
RW258-1



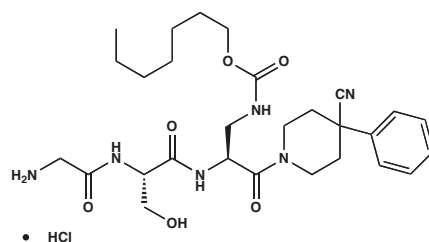
RW258-2



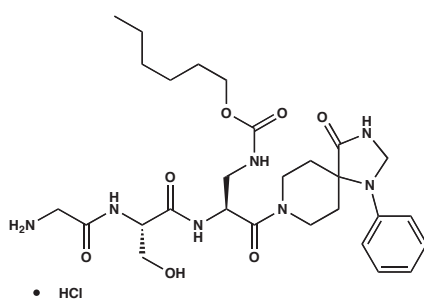
RW260



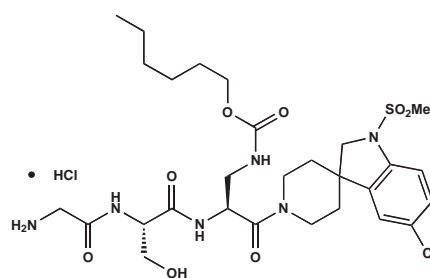
RAH-1-46



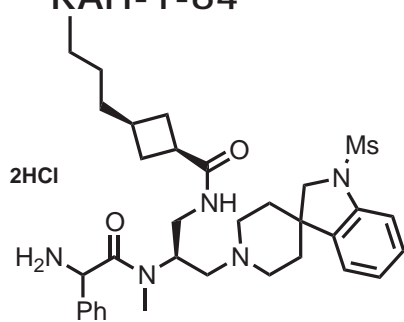
RAH-1-50



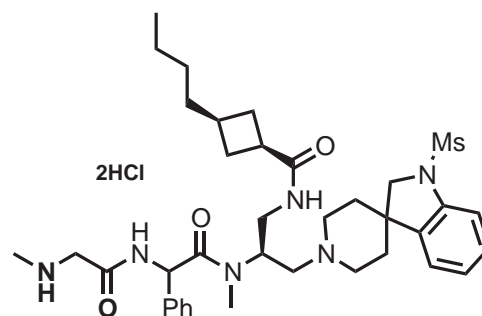
RAH-1-64



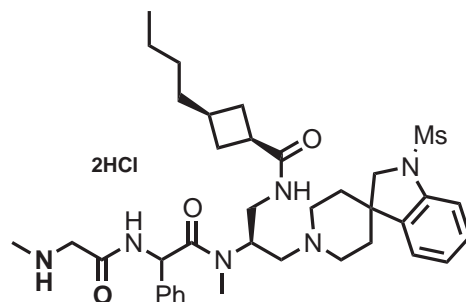
RAH-1-89



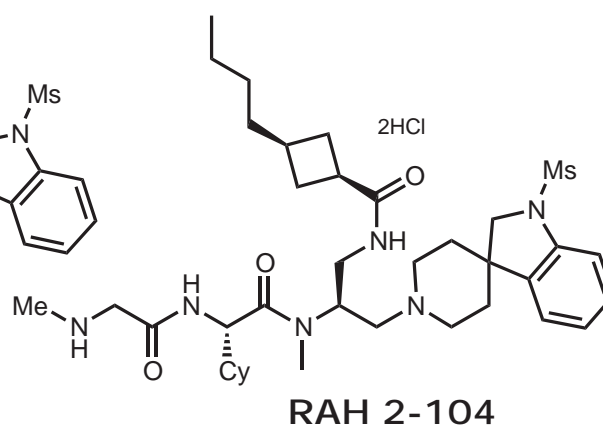
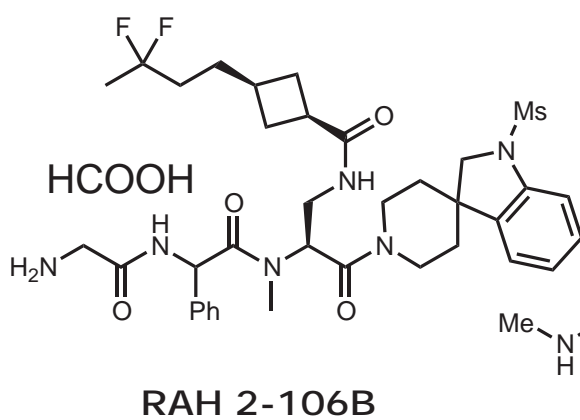
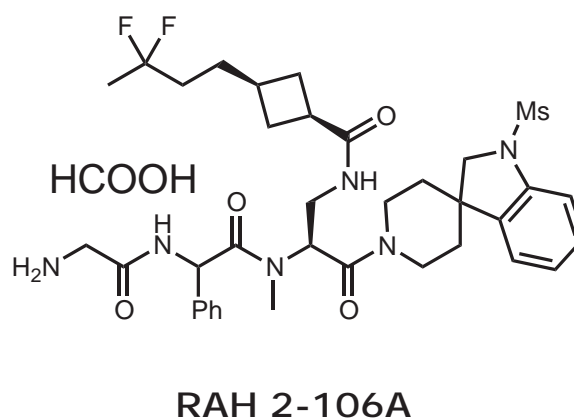
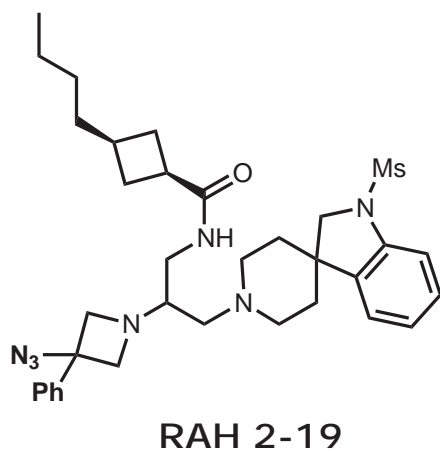
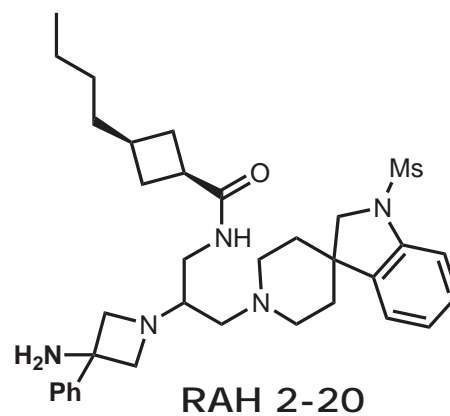
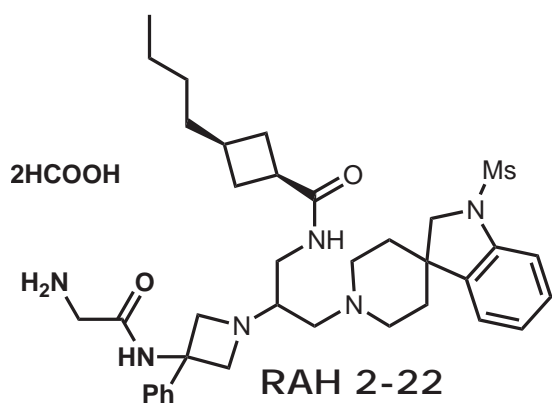
RAH 2-57

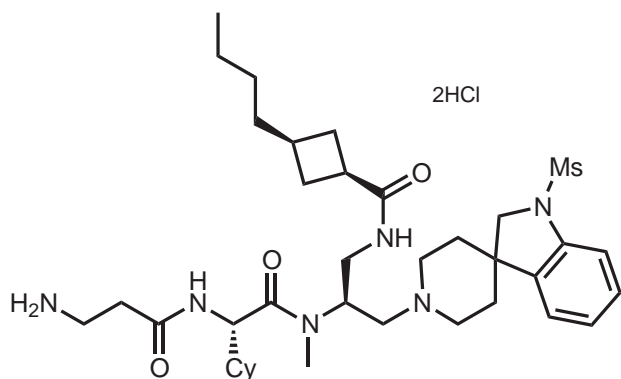


RAH 2-58B

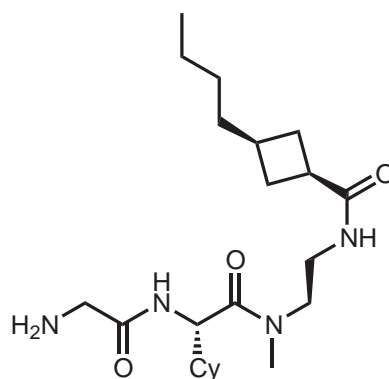


RAH 2-58T

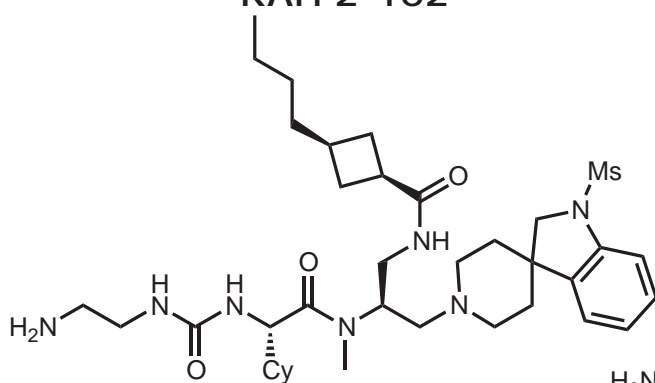




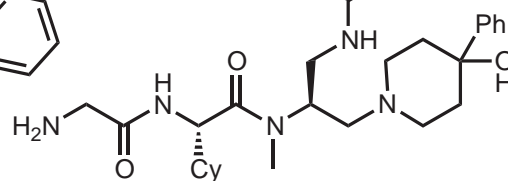
RAH 2-102



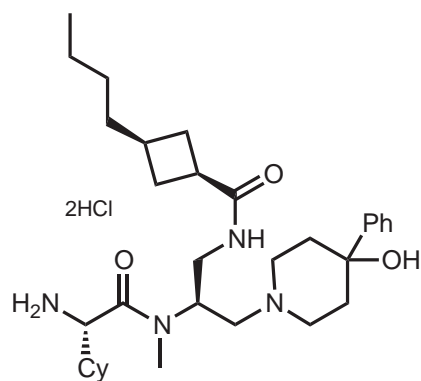
RAH 2-101



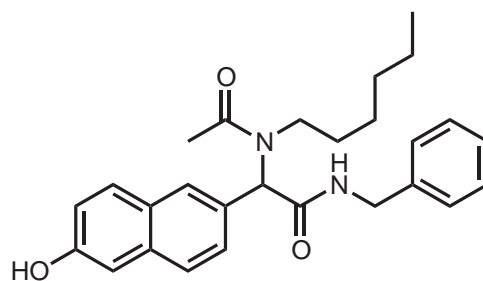
RAH 2-100



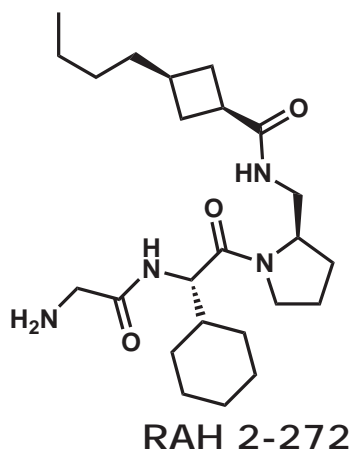
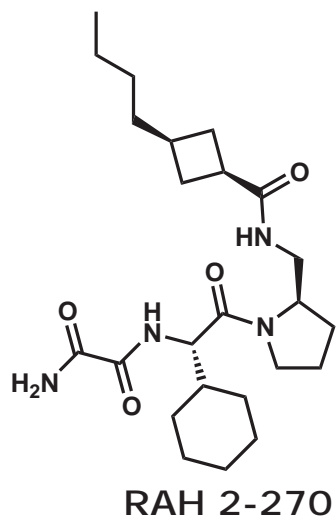
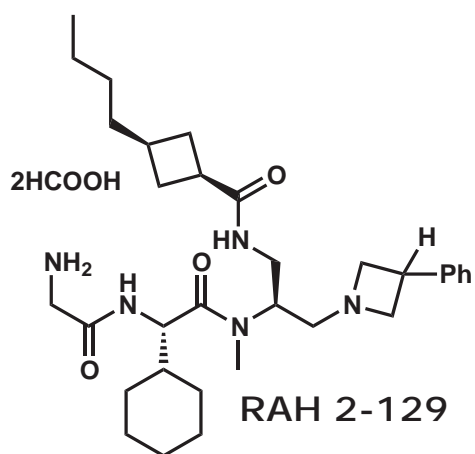
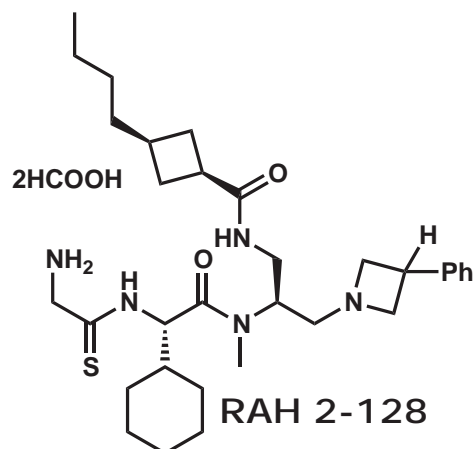
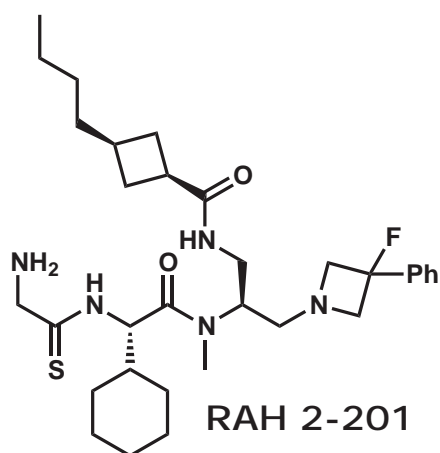
RAH 2-81

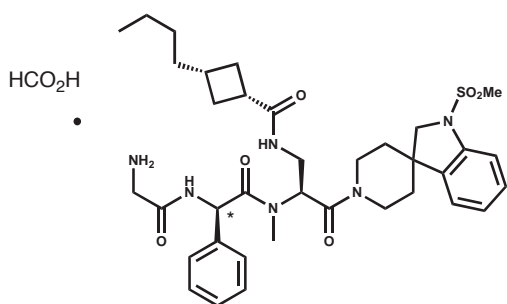


RAH 2-77

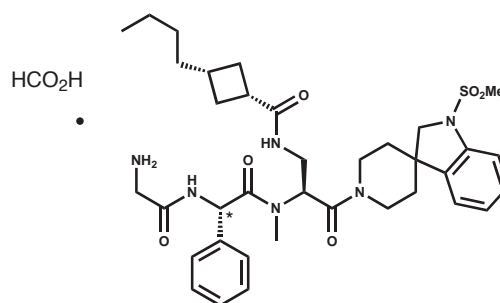


RAH 2-109

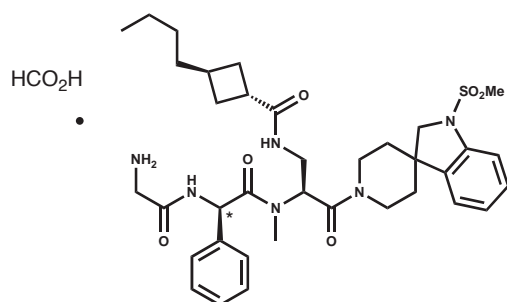




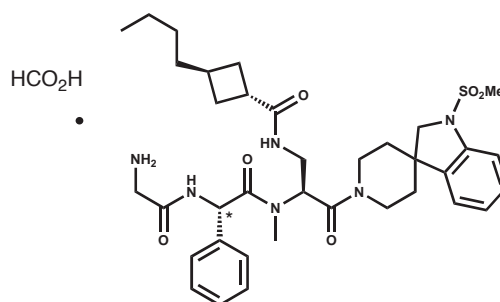
LHX_3_90A



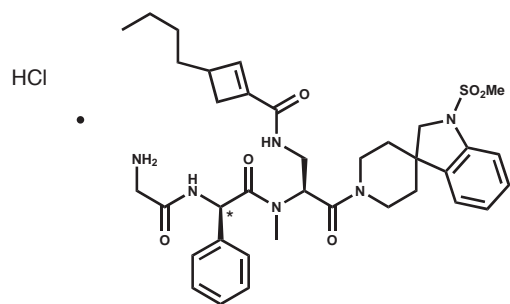
LHX_3_90B



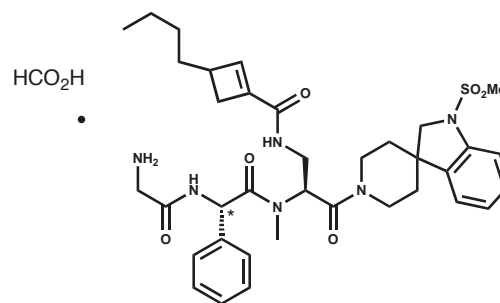
LHX_3_96A



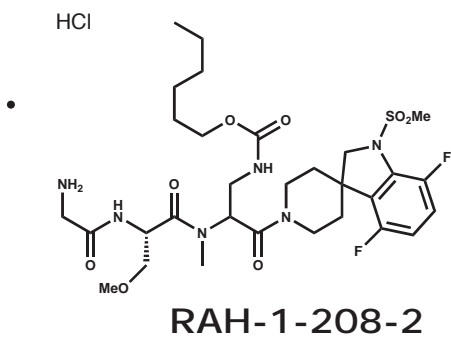
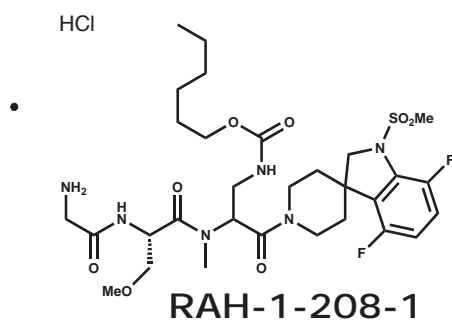
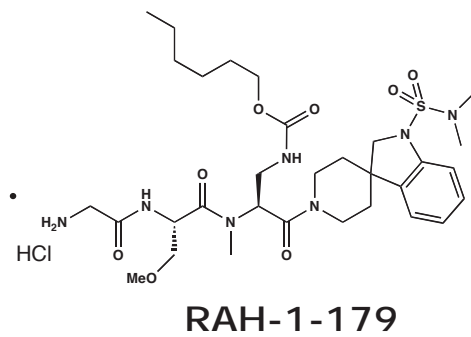
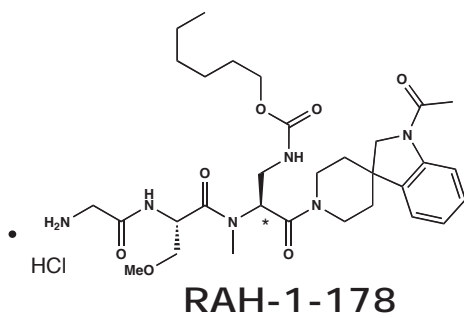
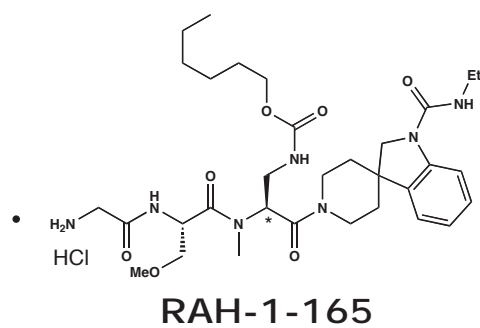
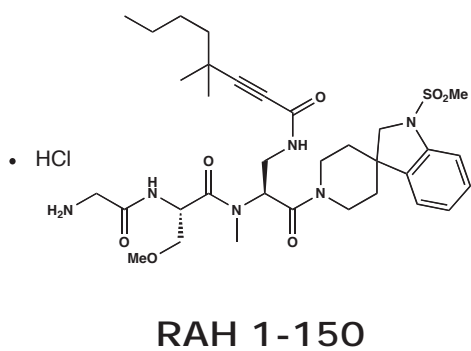
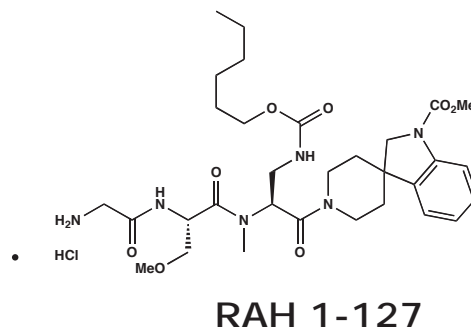
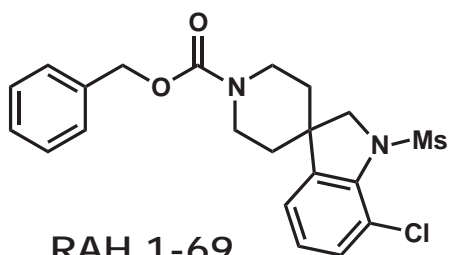
LHX_3_96B

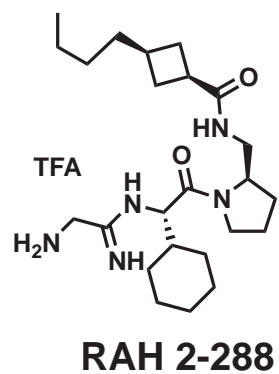
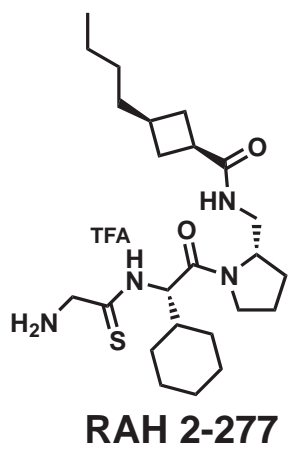
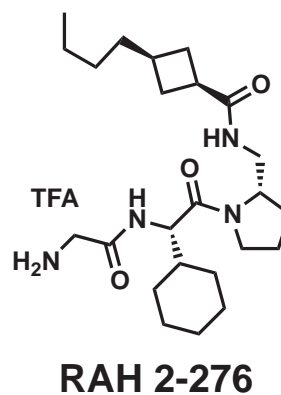
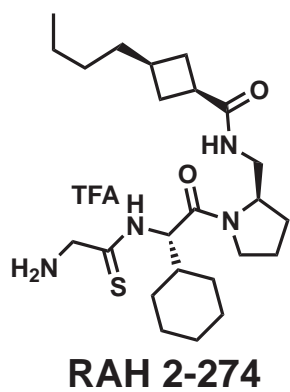
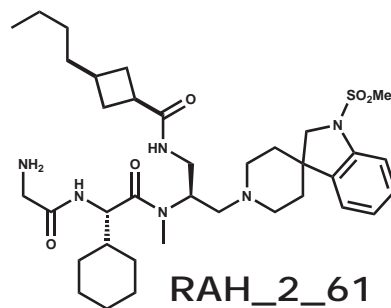
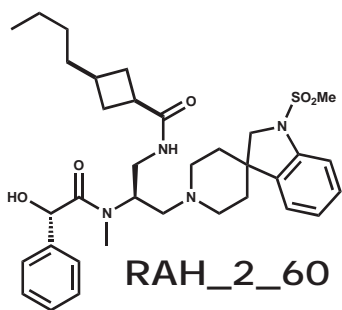
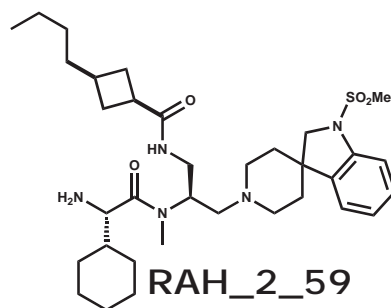
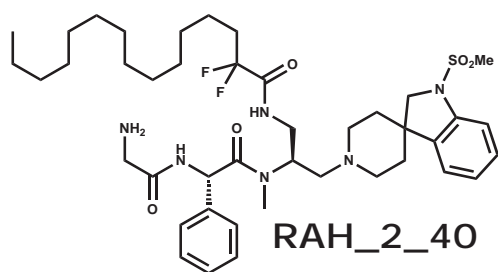


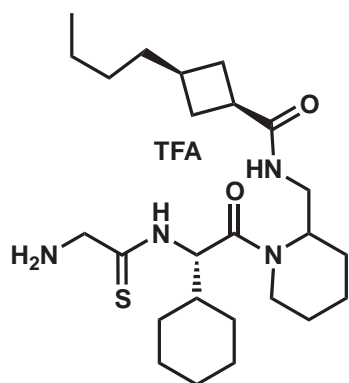
LHX_3_97A



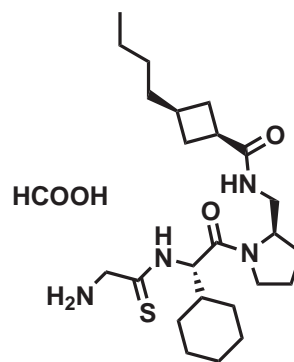
LHX_3_97B



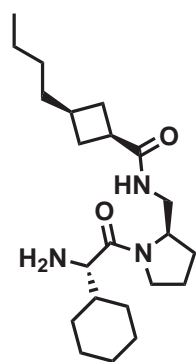




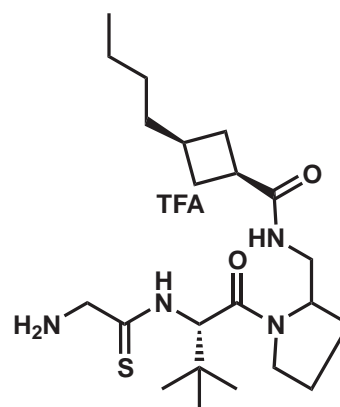
RVQ 1-72



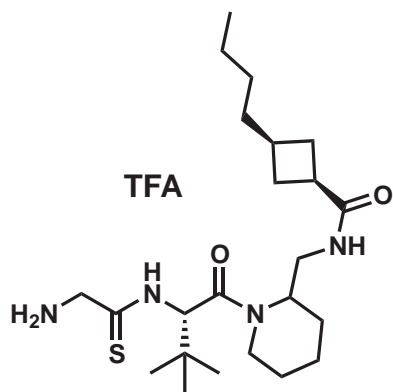
RVQ 1-33



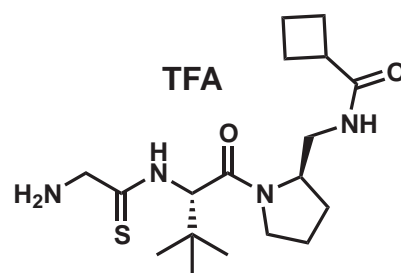
RVQ 1-47



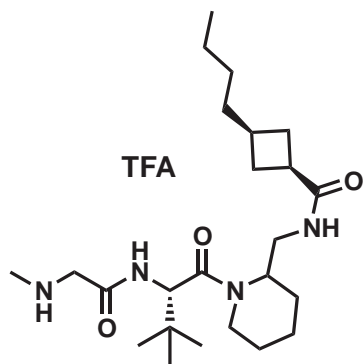
RVQ 1-75



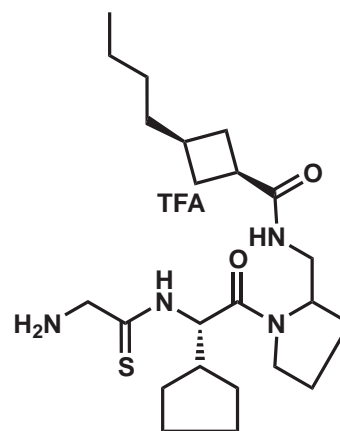
RVQ 1-95



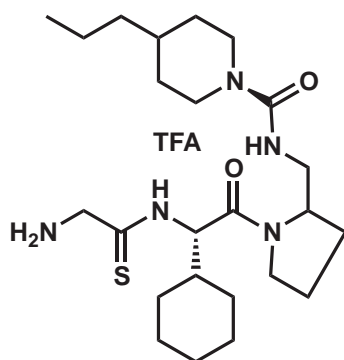
RVQ 1-99



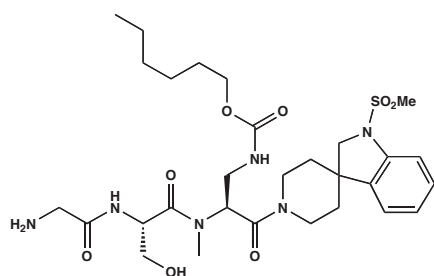
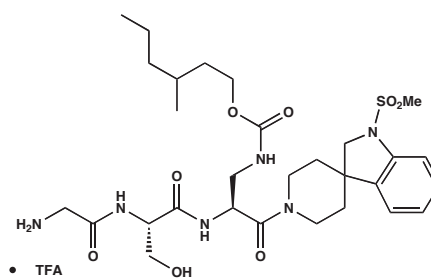
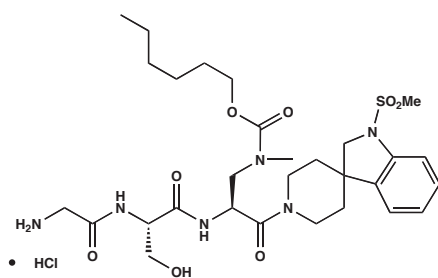
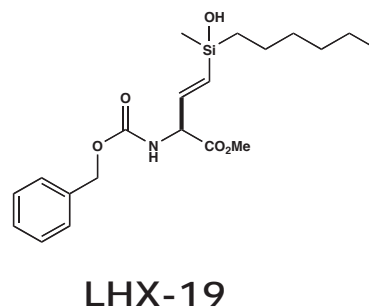
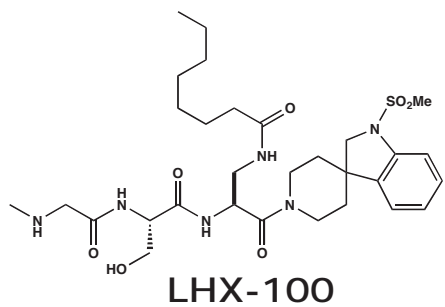
RVQ 1-96



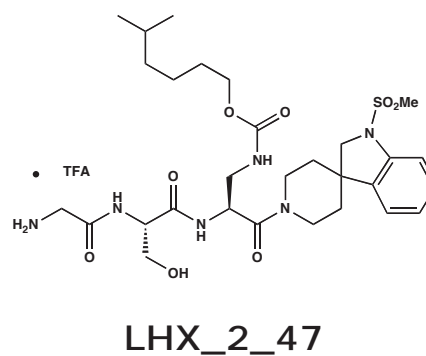
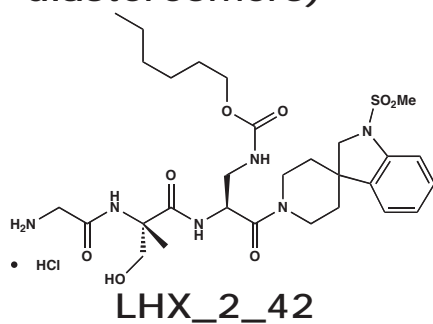
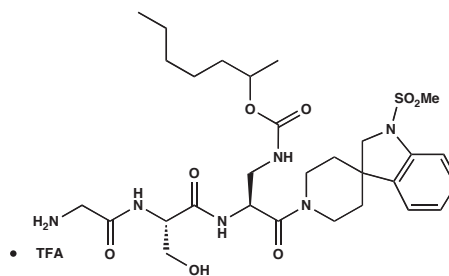
NE 1-124

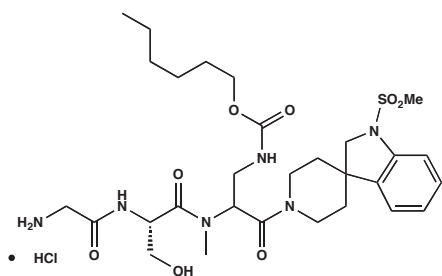


NE 1-116

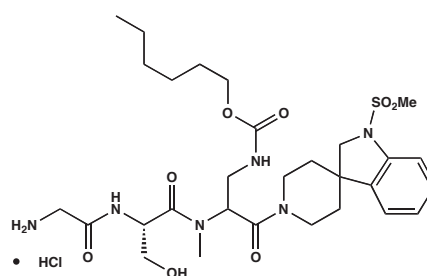


(mixture of two diastereomers)

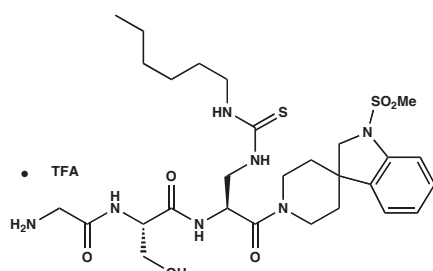




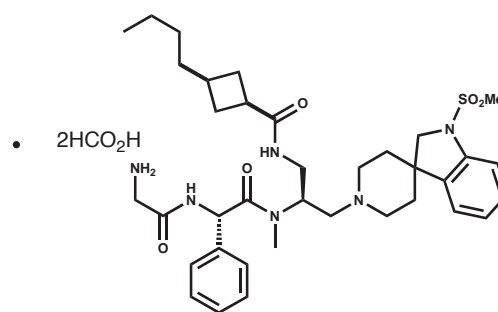
LHX_2_43A
diastereomer A



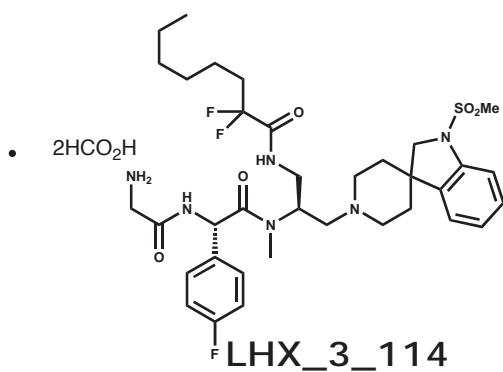
LHX_2_43B
diastereomer B



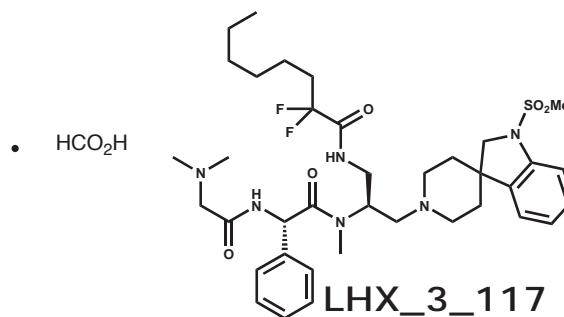
LHX_2_51



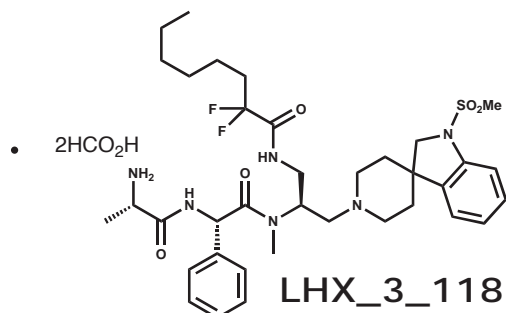
LHX_3_105



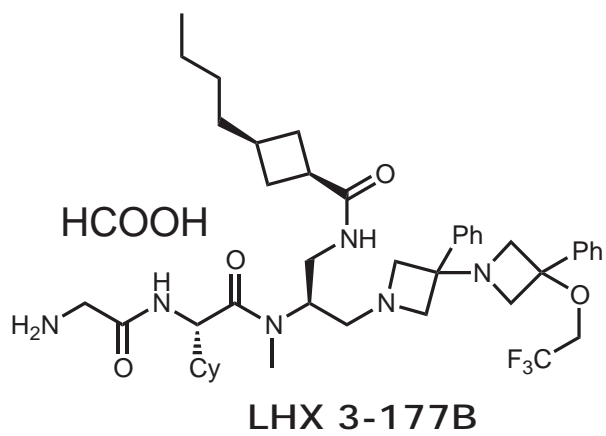
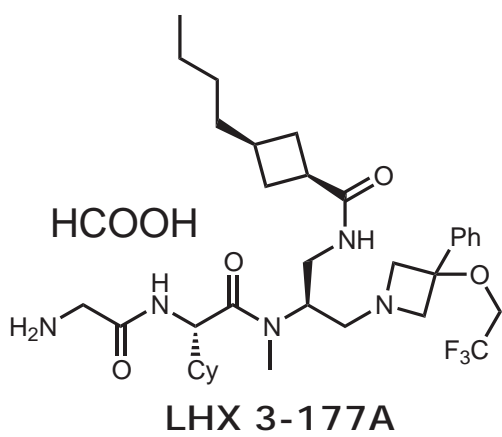
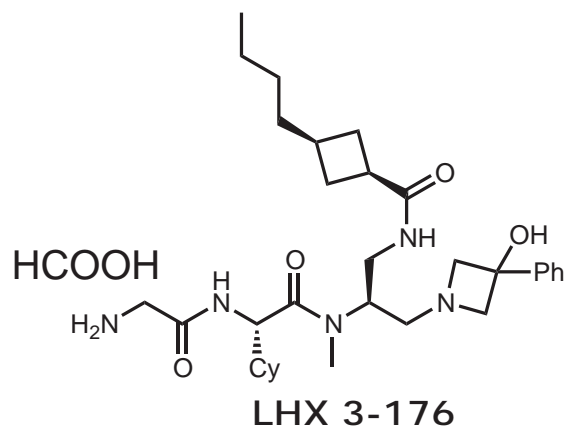
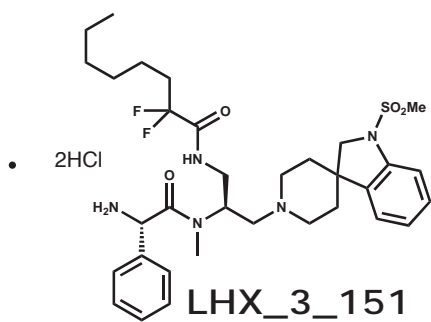
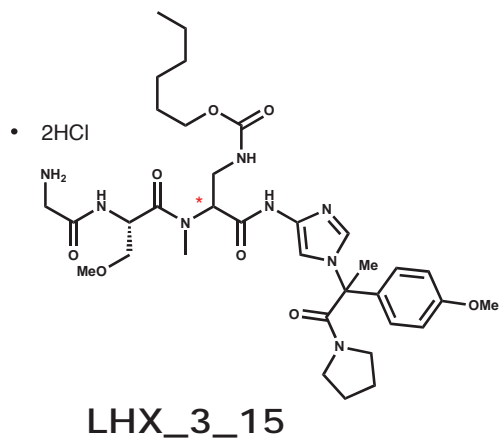
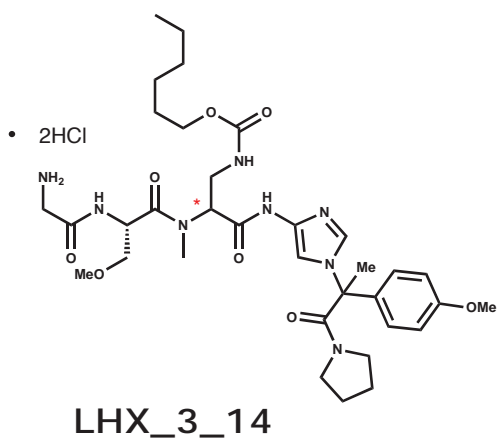
LHX_3_114

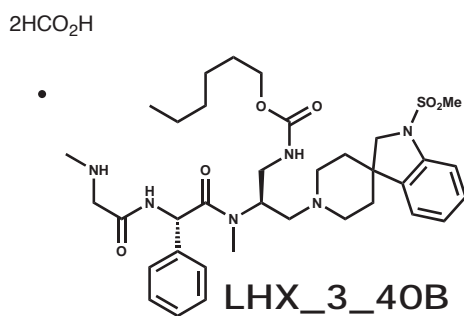
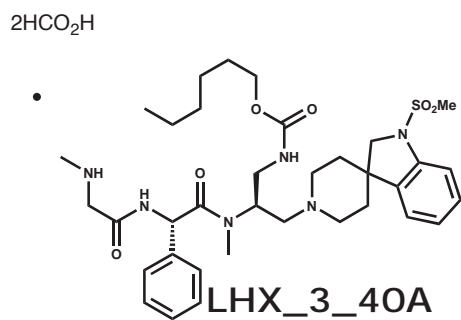
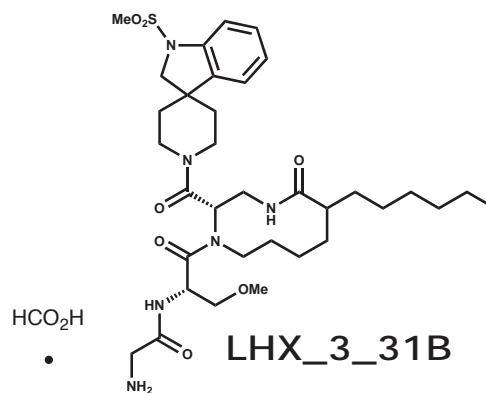
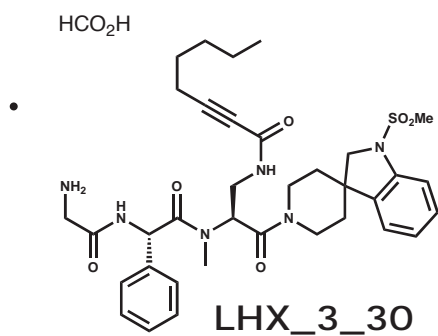
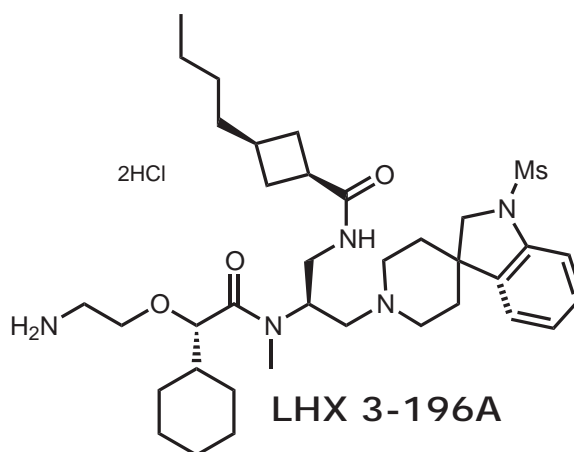
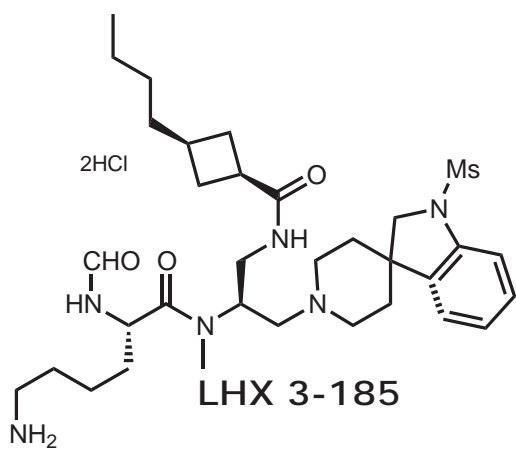


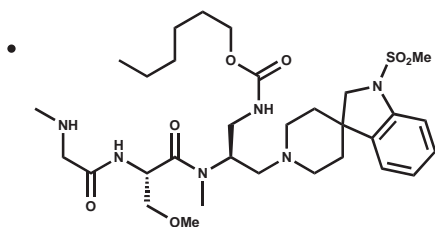
LHX_3_117



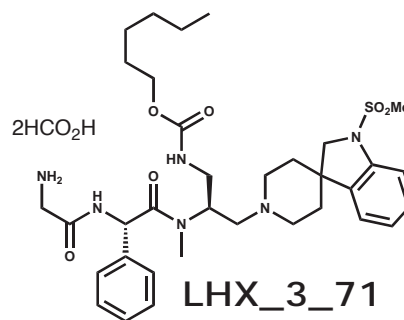
LHX_3_118



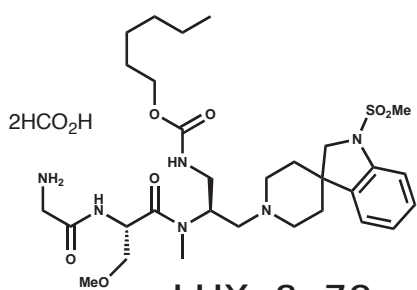


2HCO₂H

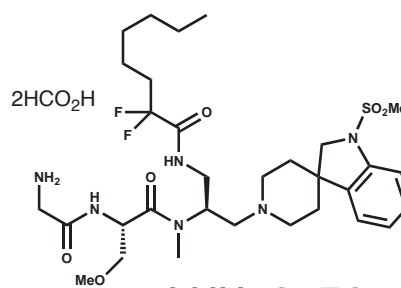
LHX_3_42



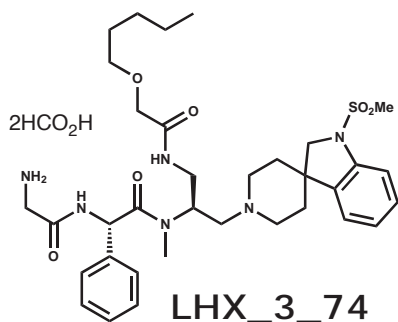
LHX_3_71



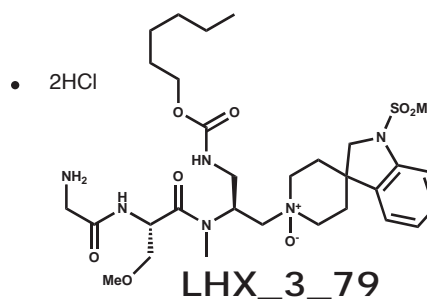
LHX_3_72



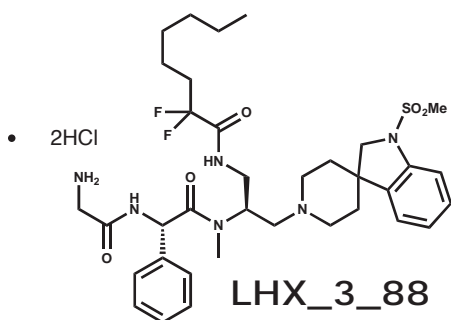
LHX_3_73



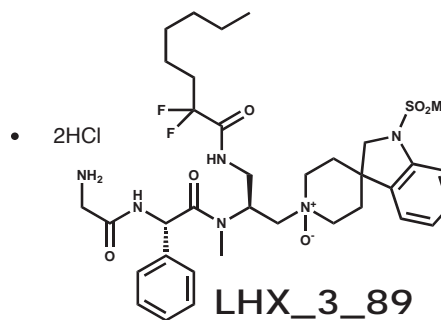
LHX_3_74



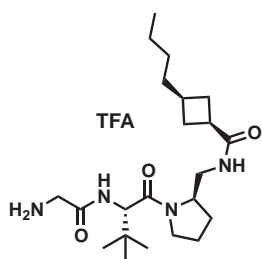
LHX_3_79



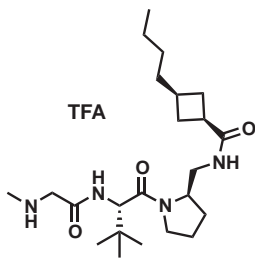
LHX_3_88



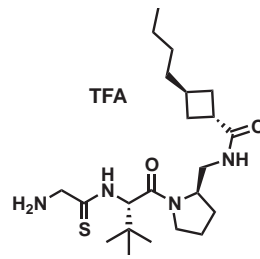
LHX_3_89



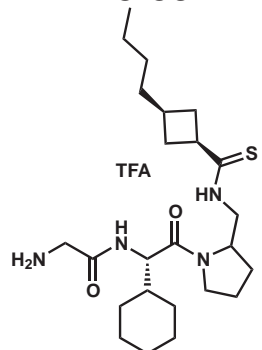
RAH 3-59



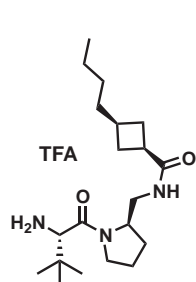
RAH 3-60



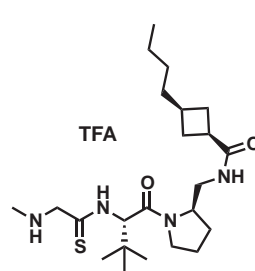
RAH 3-64



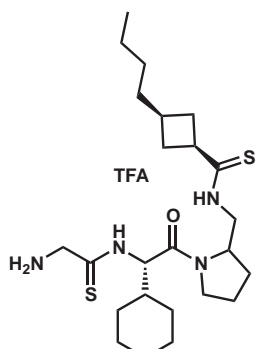
RAH 3-30



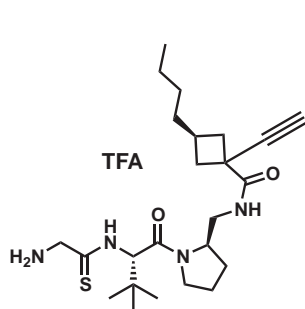
RAH 3-65



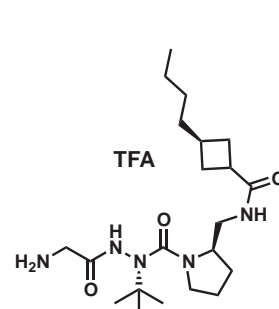
RAH 3-63



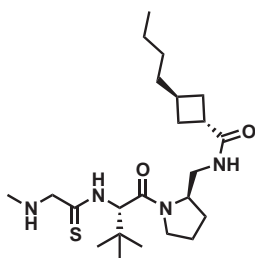
RAH 3-28



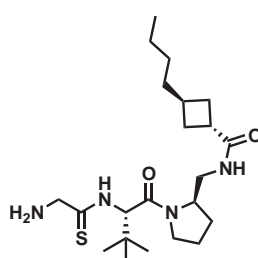
RAH 3-79



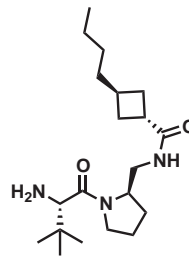
RAH 3-88



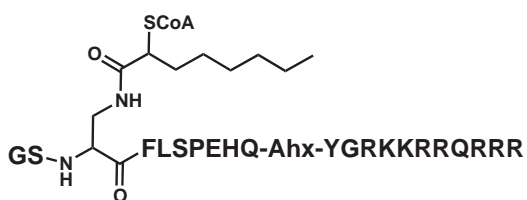
RAH 3-163



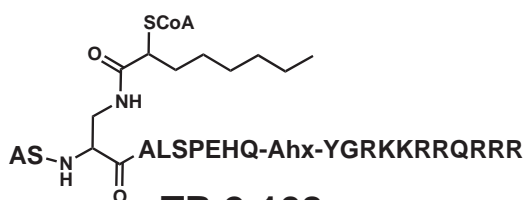
RAH 3-164



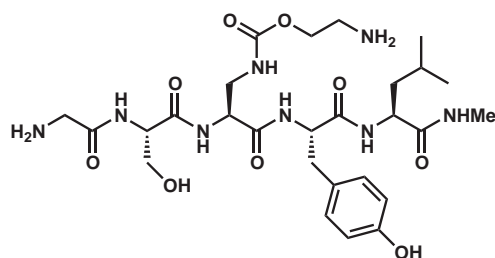
RAH 3-167



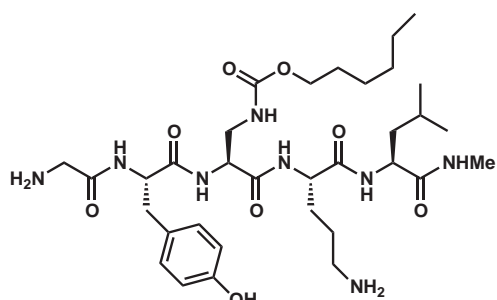
TR 2-98A
GO-CoA-Tat



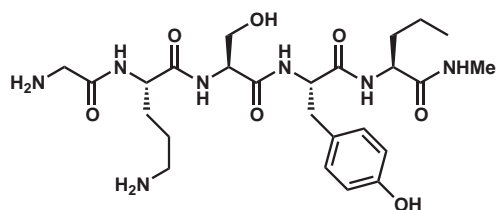
TR 2-108
GO-CoA-Tat
G1A, F4A mutant



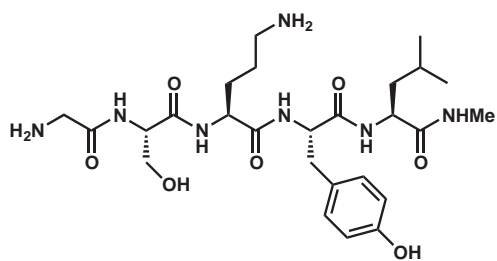
TR 1-296A



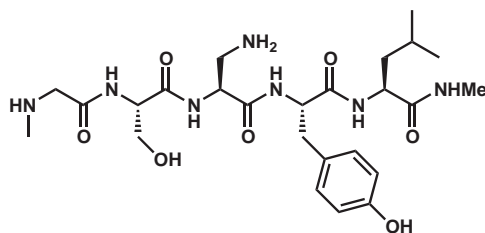
TR 1-296E



TR 1-296C

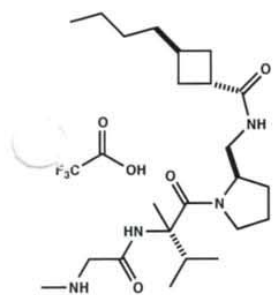


TR 1-296B

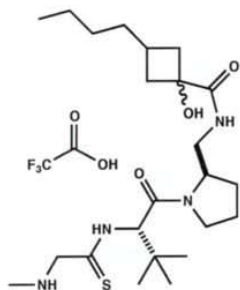


TR 1-296D

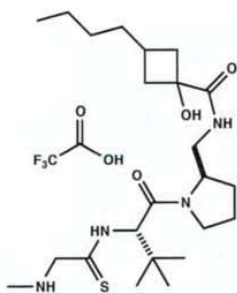
36



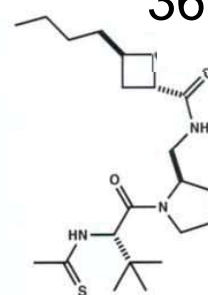
HD 5-240



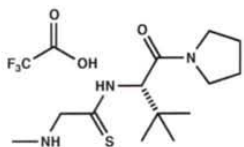
HD 5-259-2A



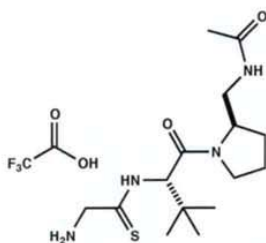
HD 5-259-2B



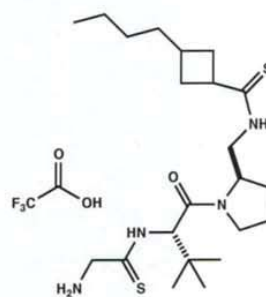
RAH 3-220



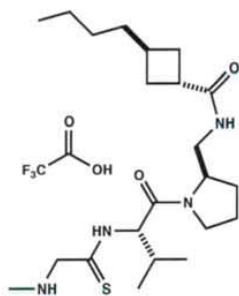
RAH 3-209



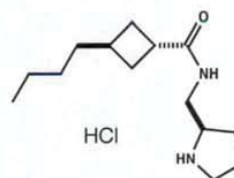
RaH 3-228



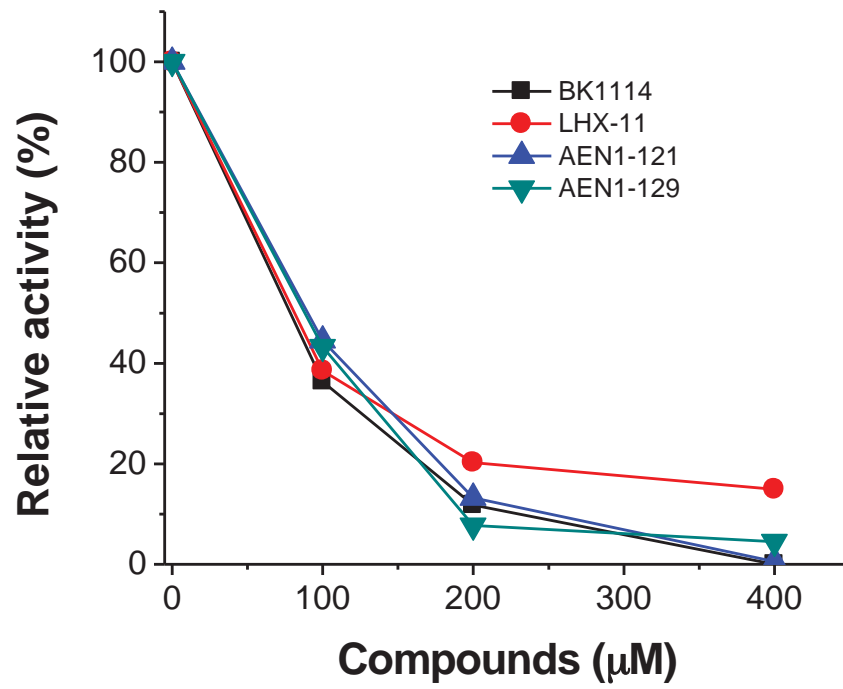
RAH 3-203

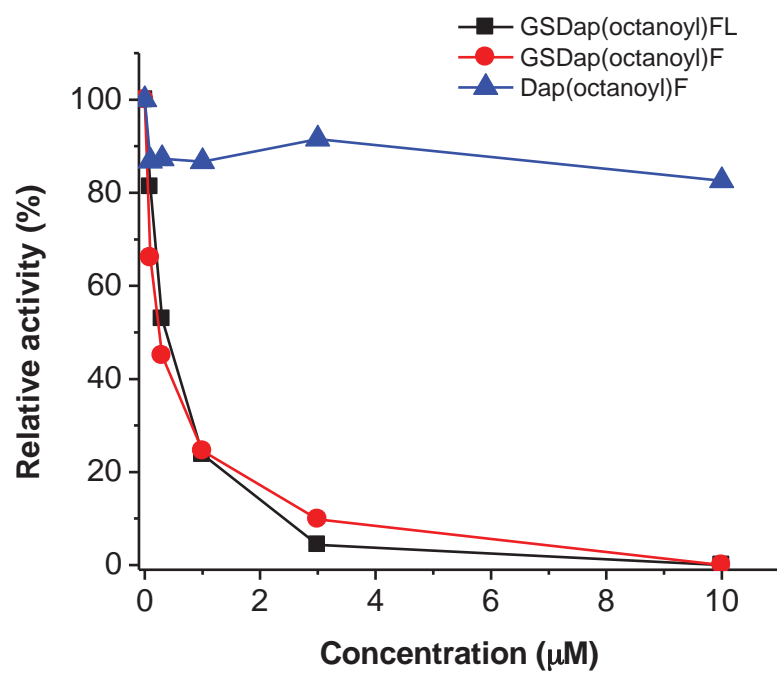


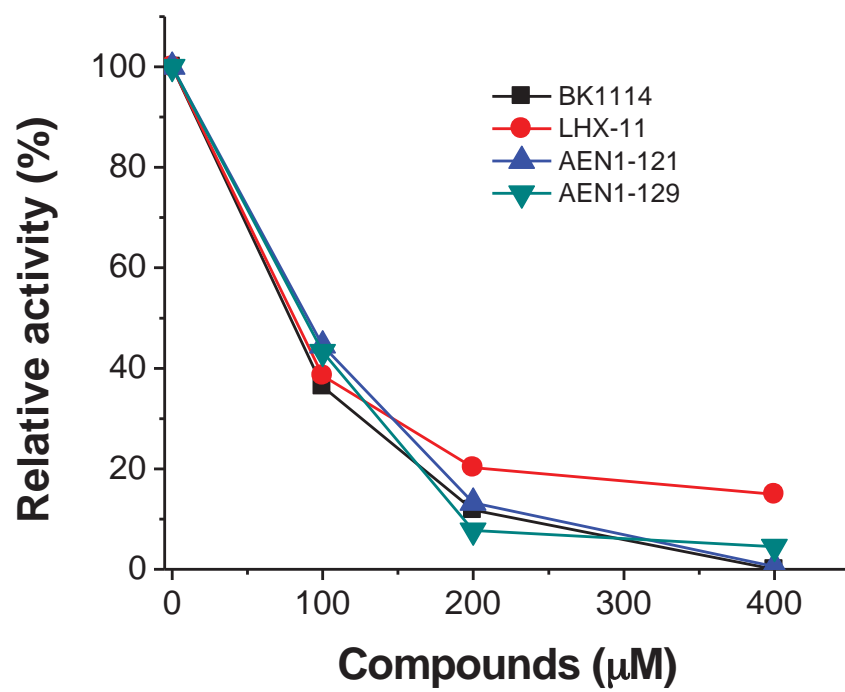
RAH 3-224

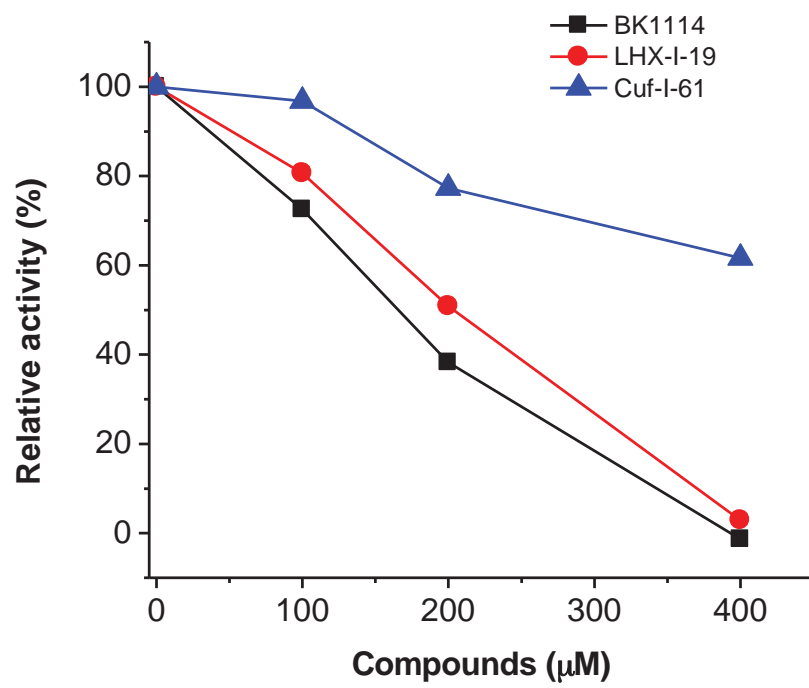


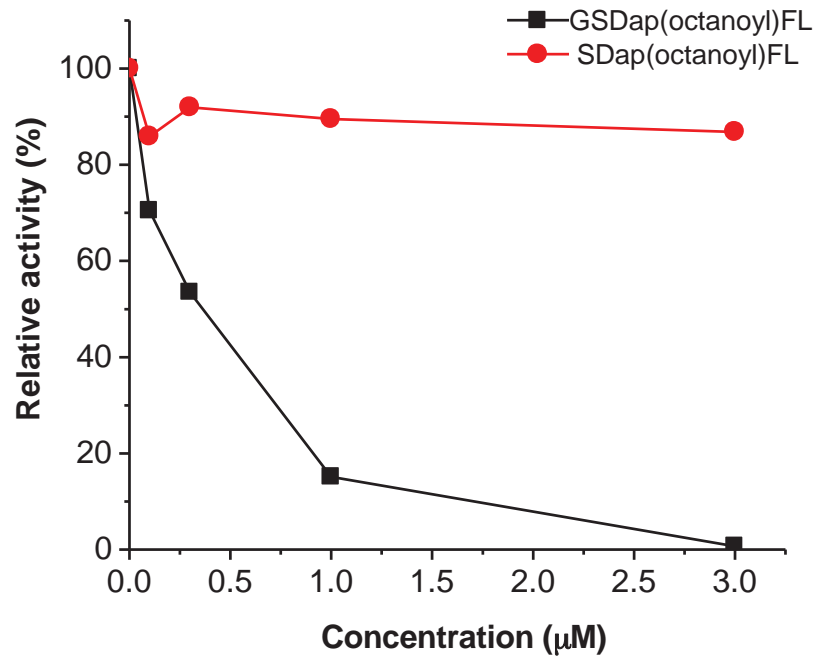
RAH 3-134

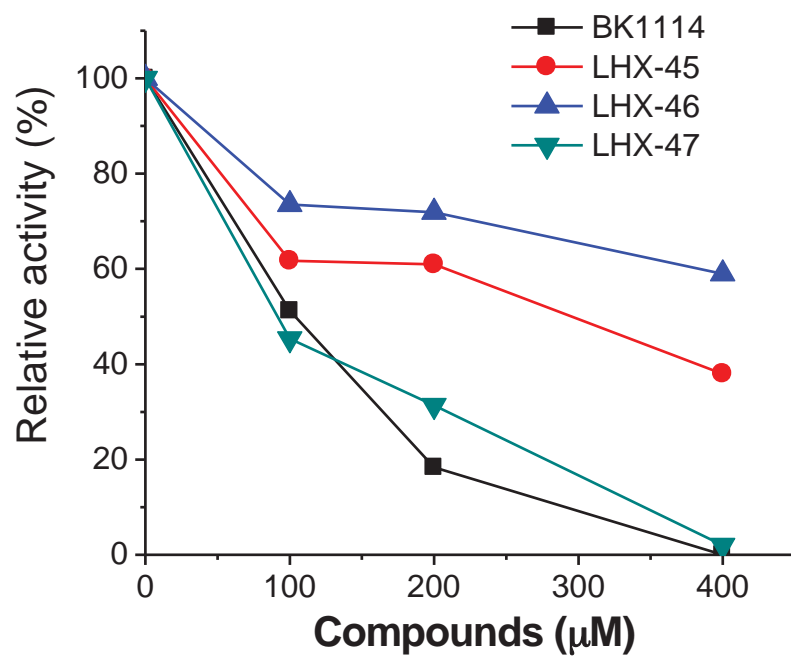


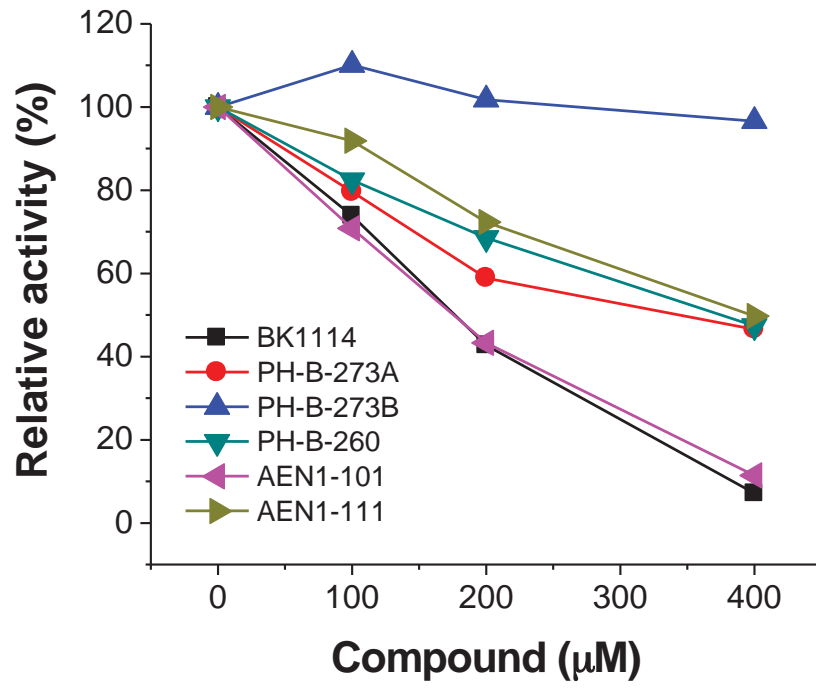


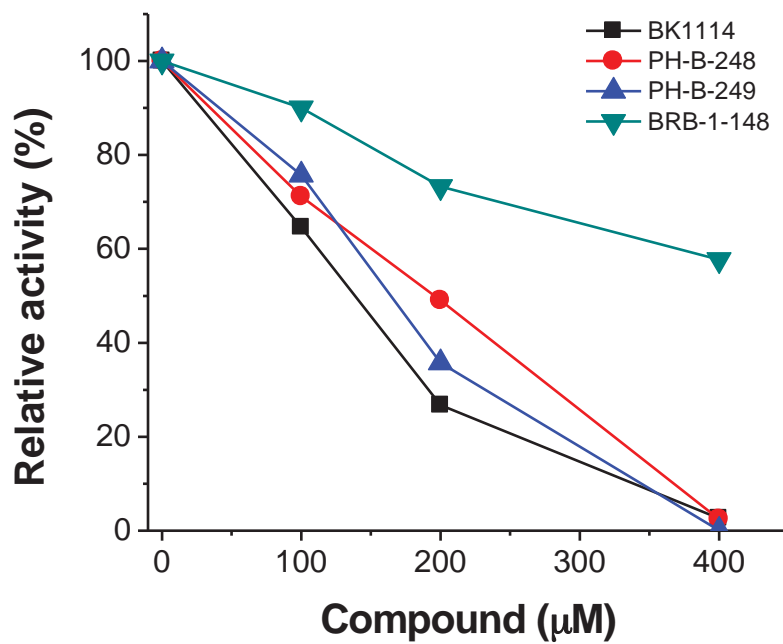
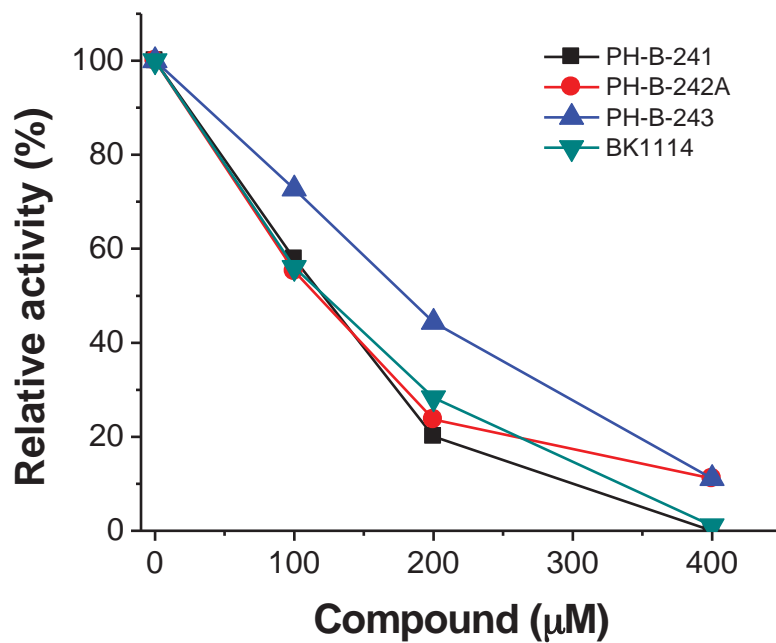


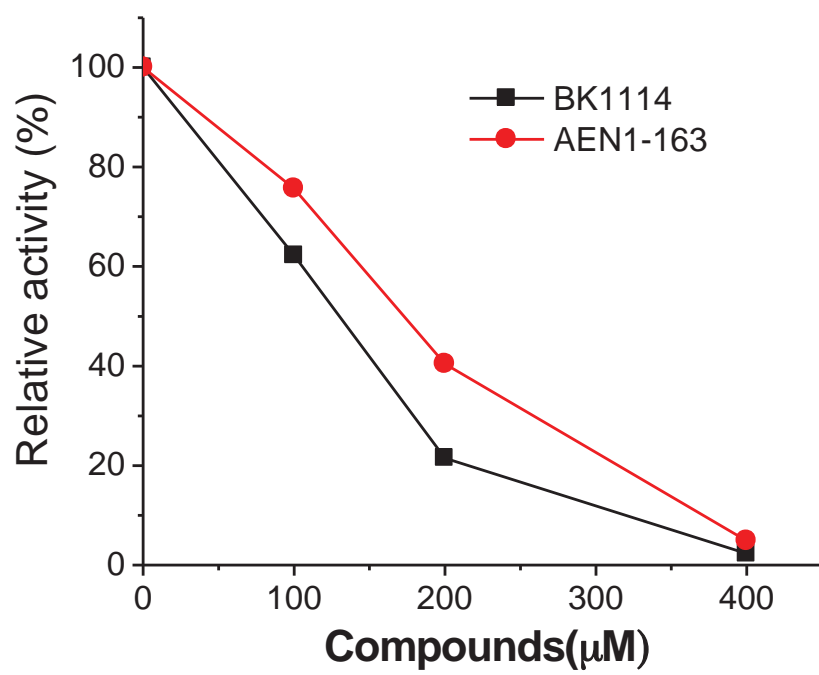


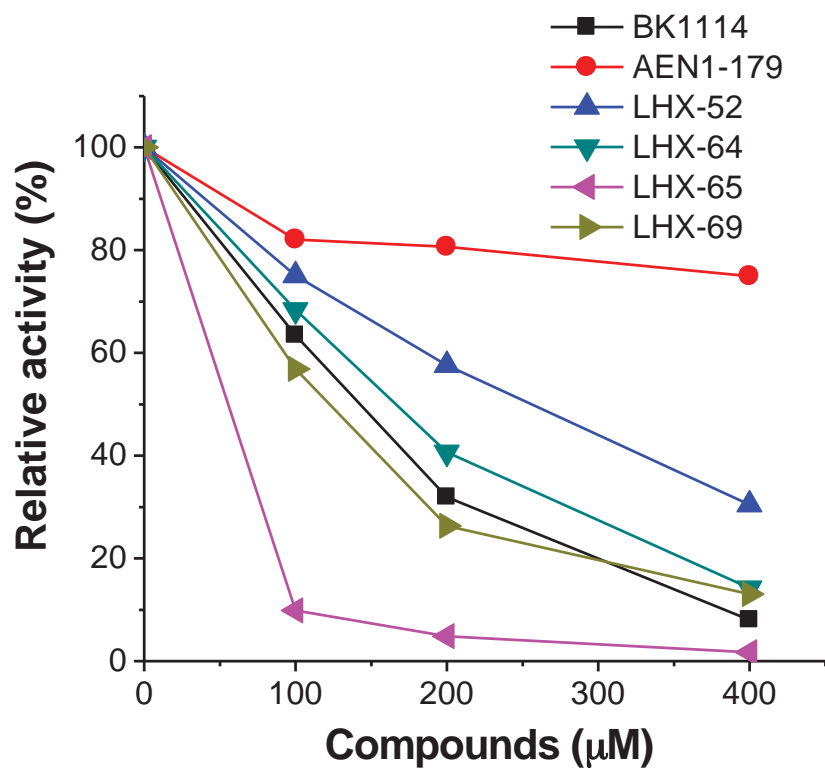


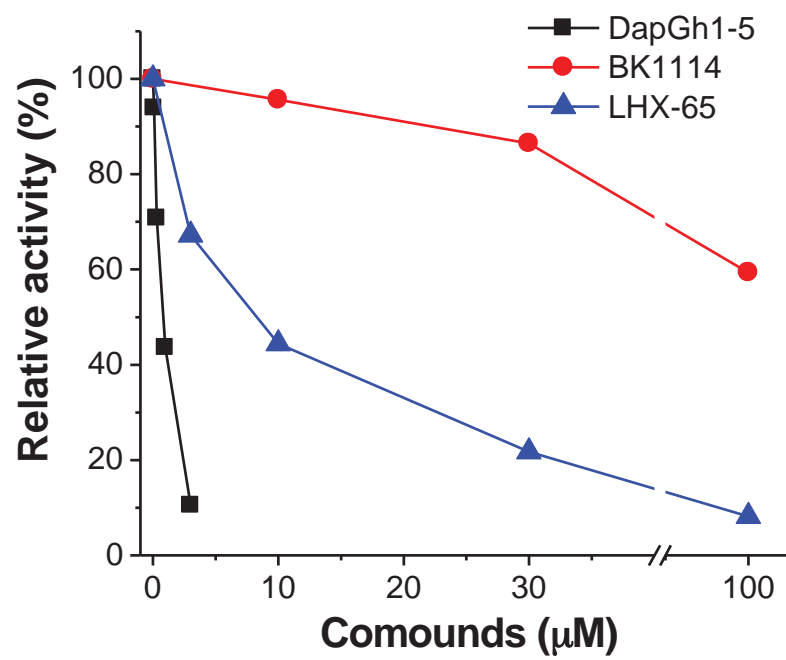


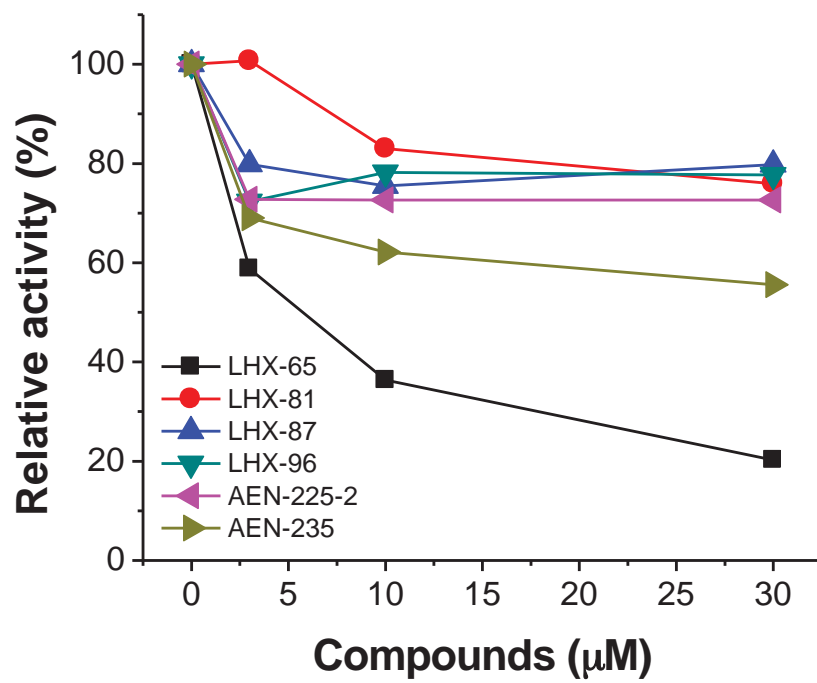


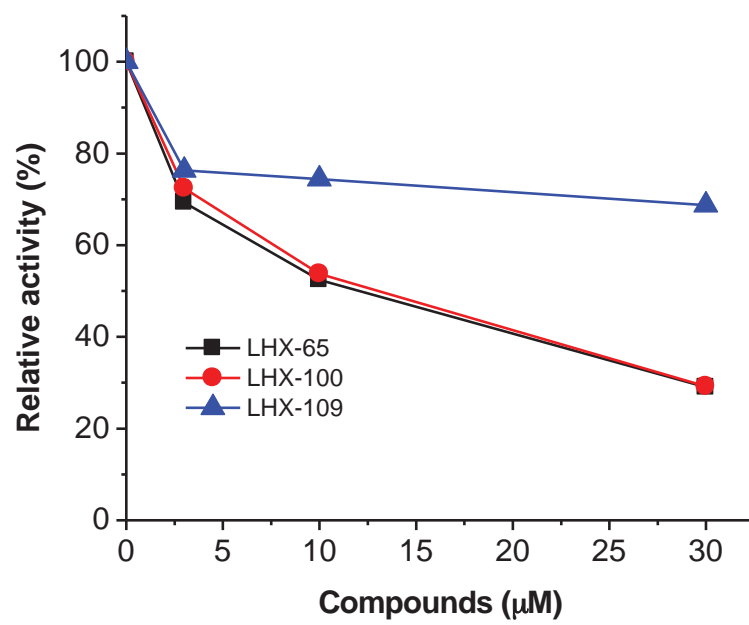


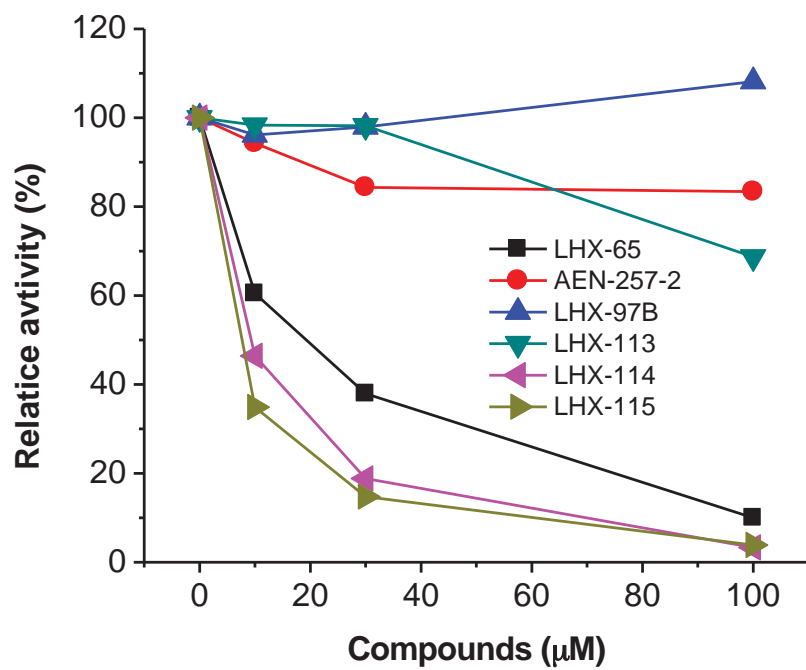


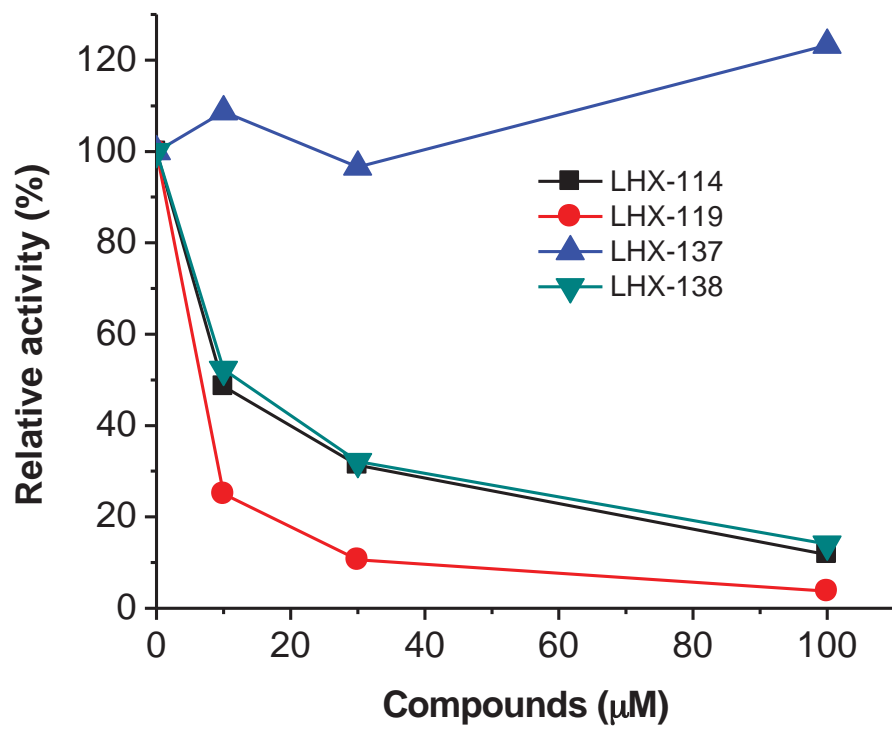


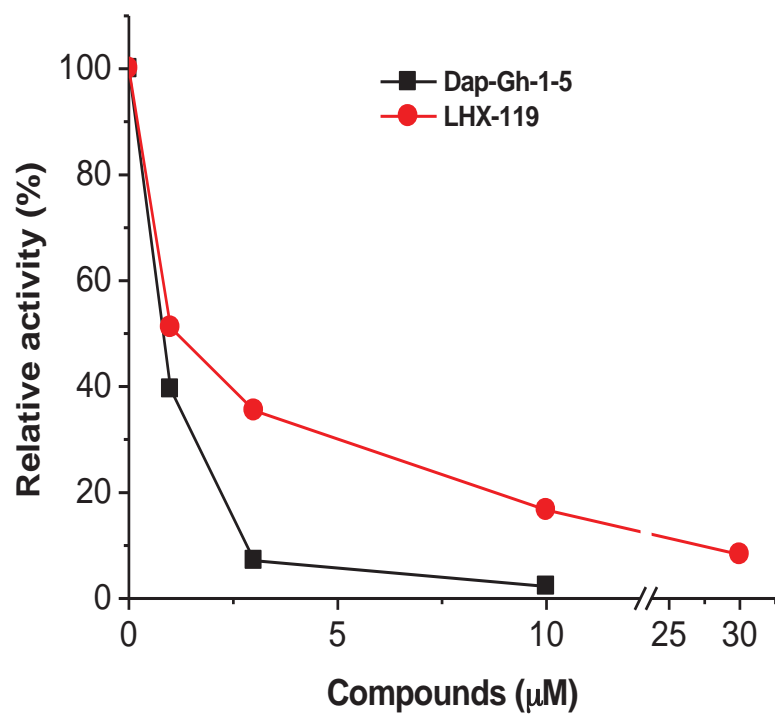


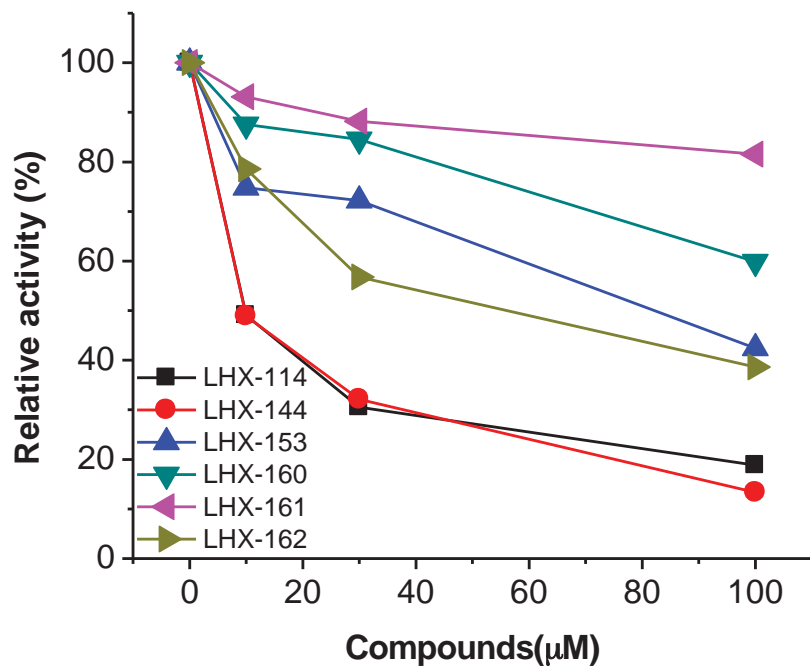


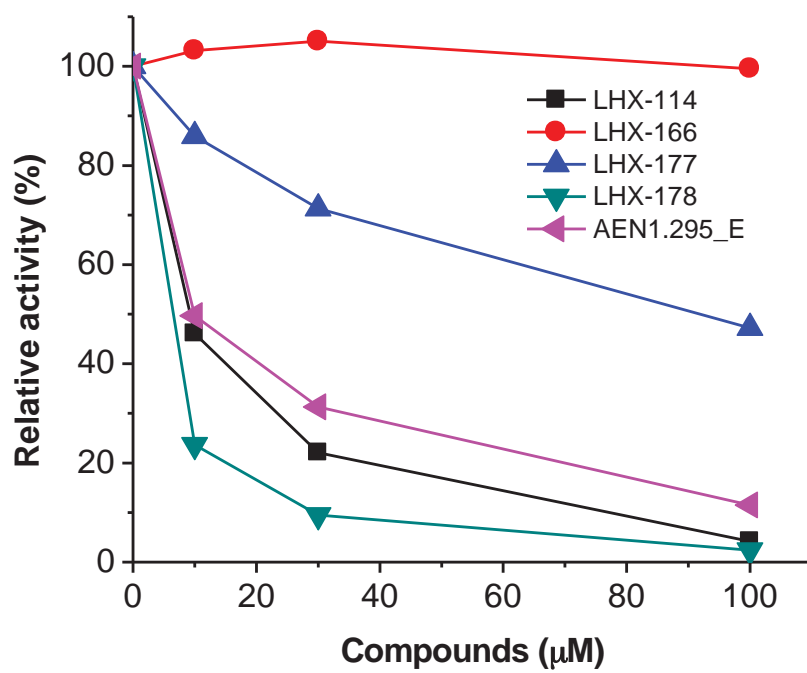


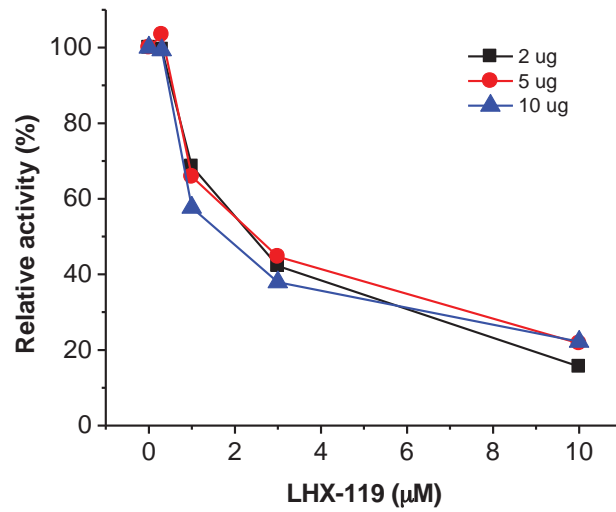
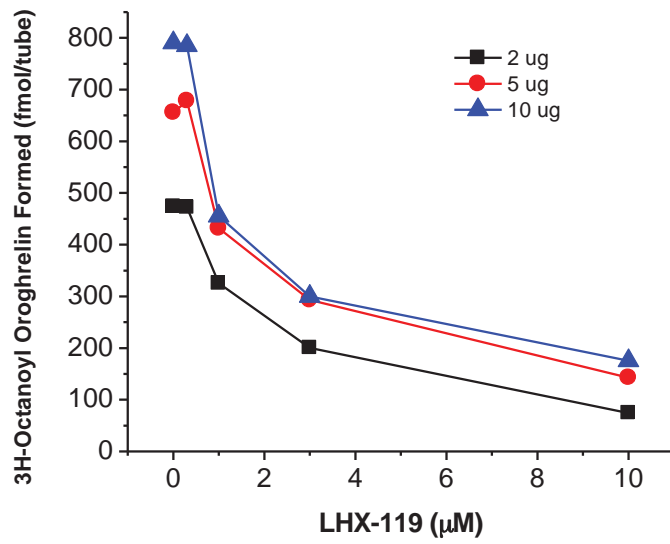


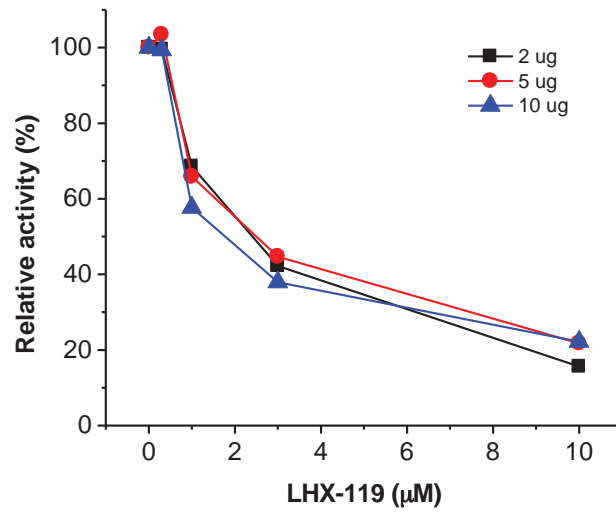
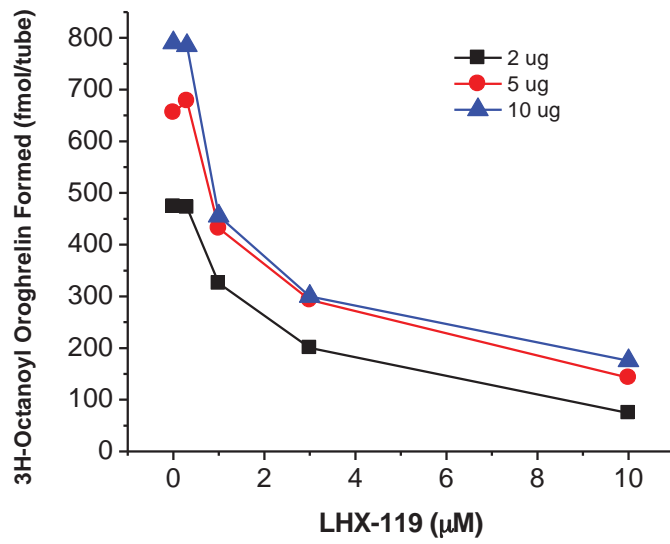


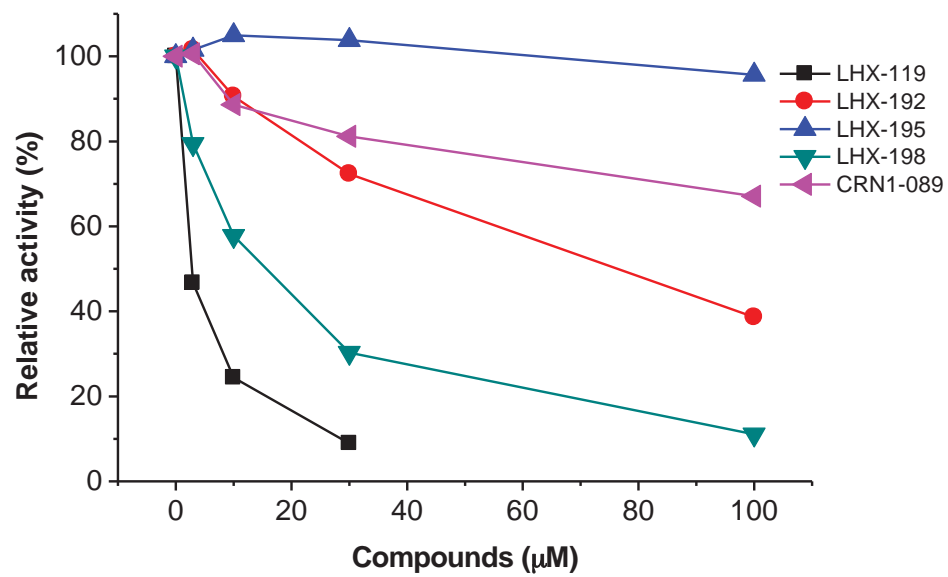


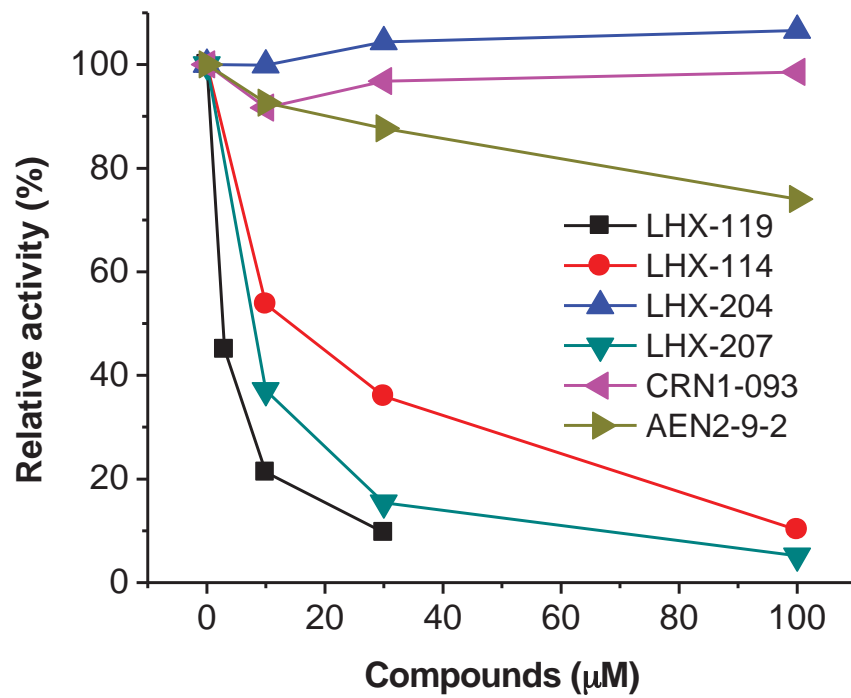


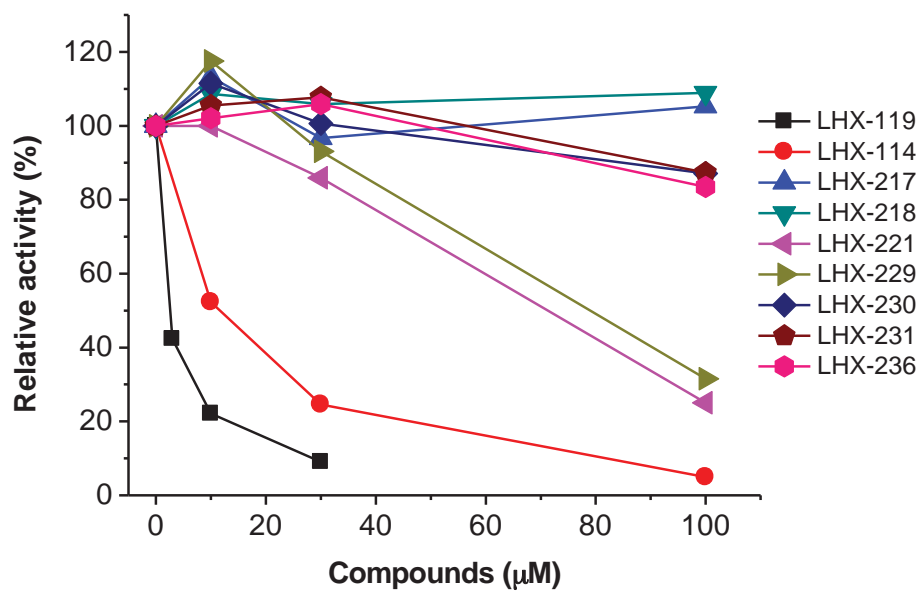


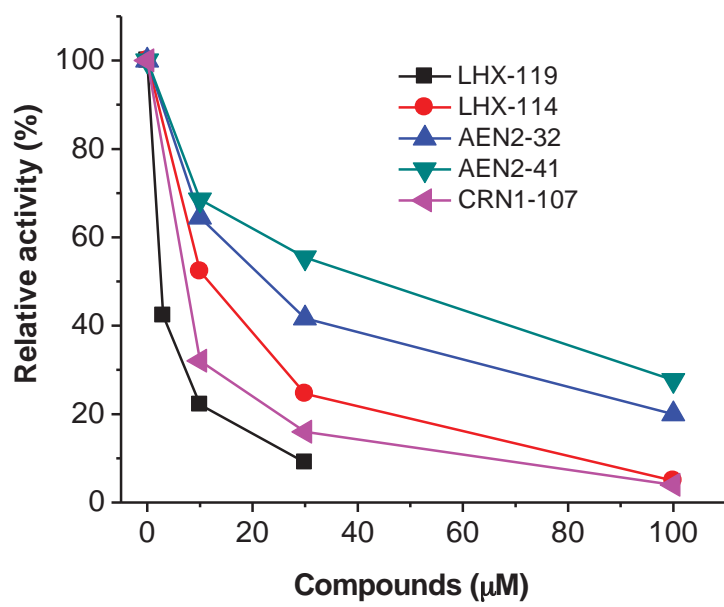


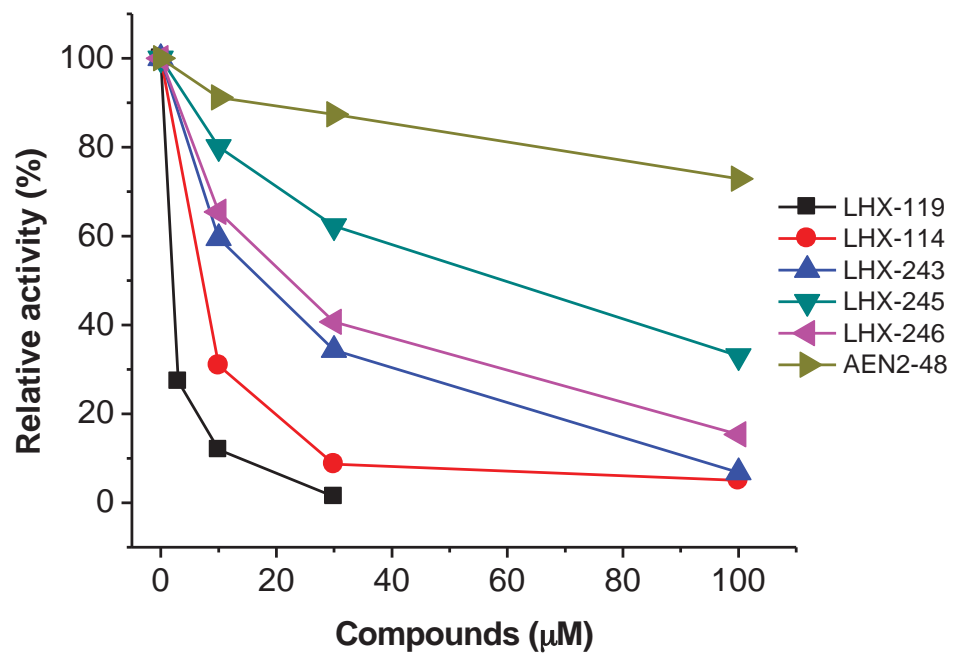


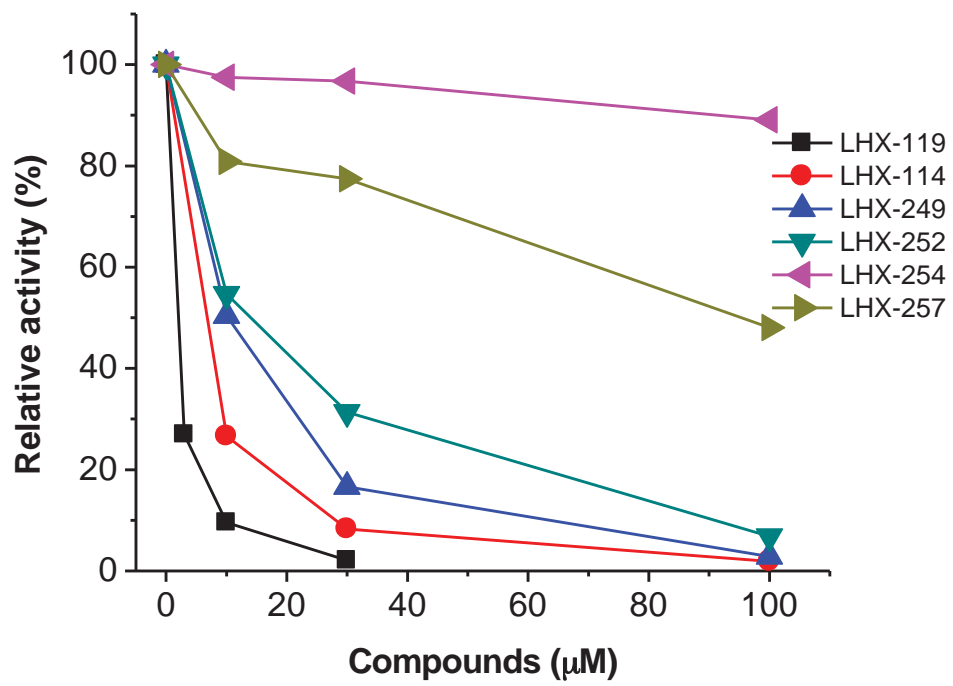


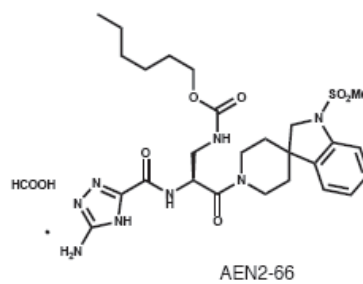
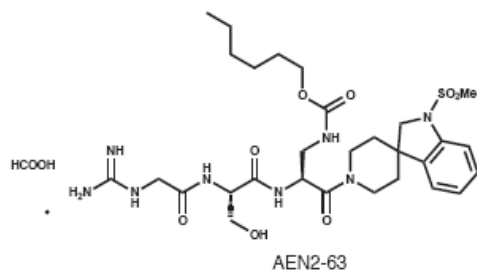
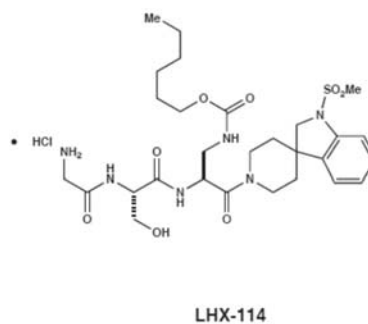
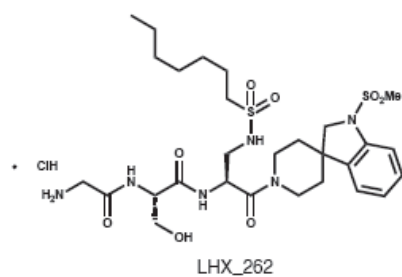
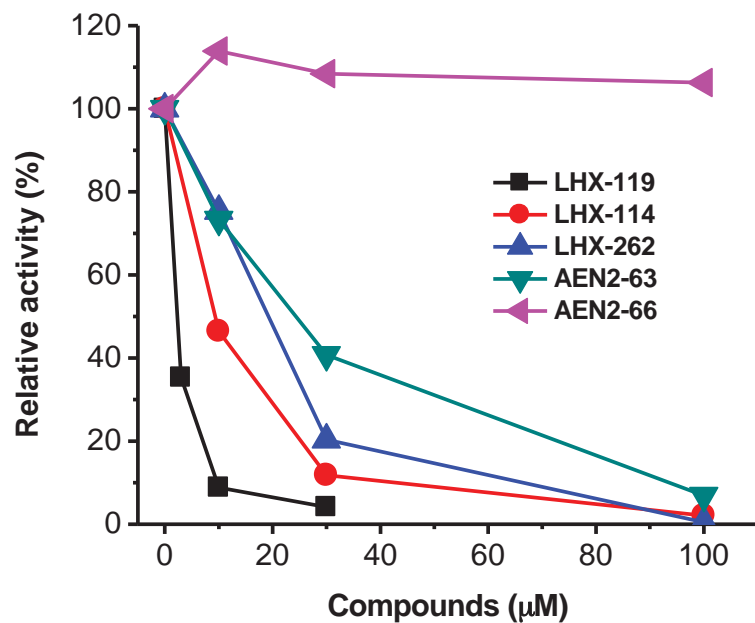


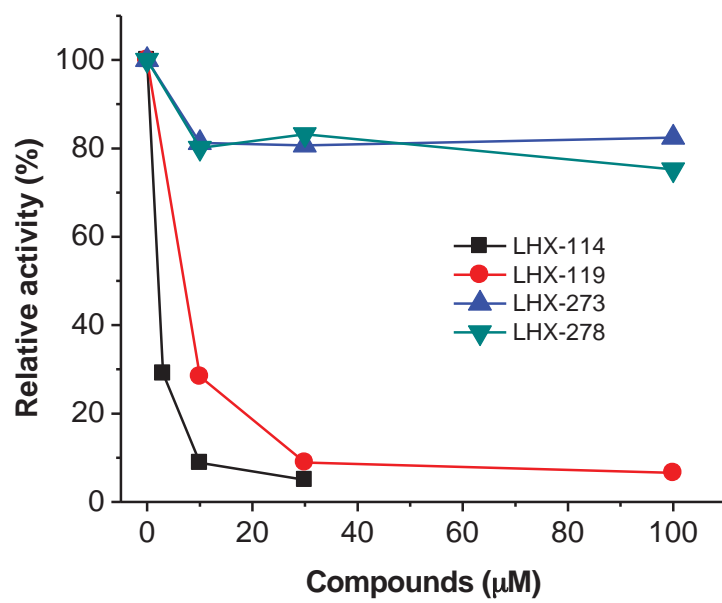


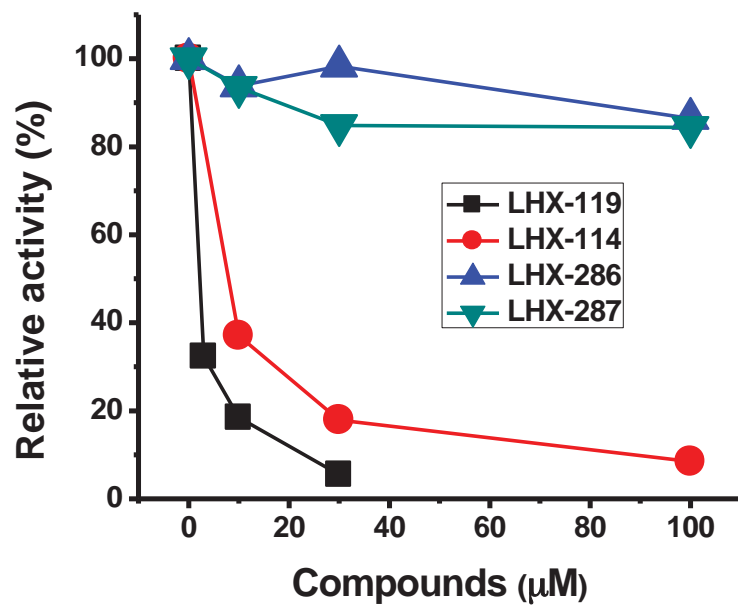


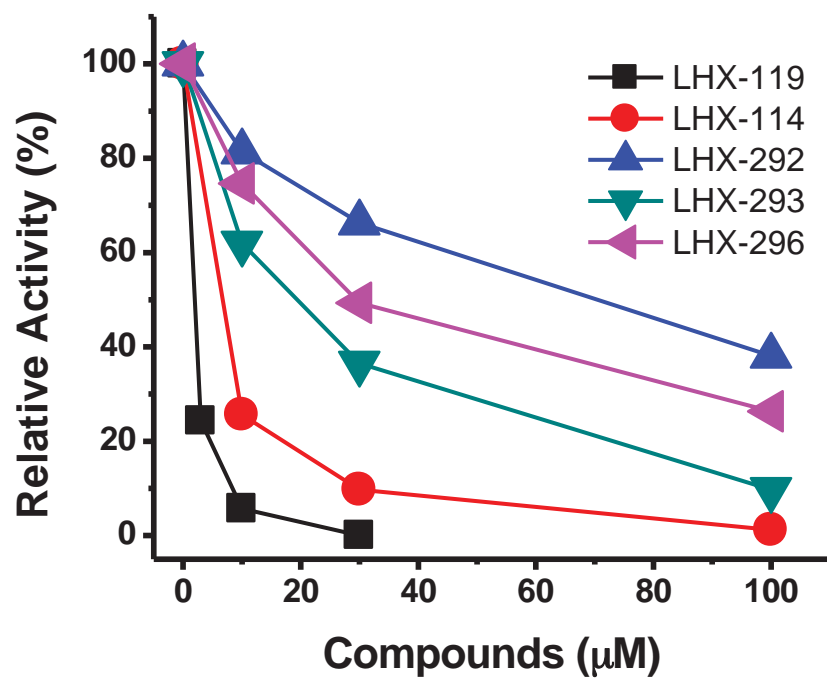


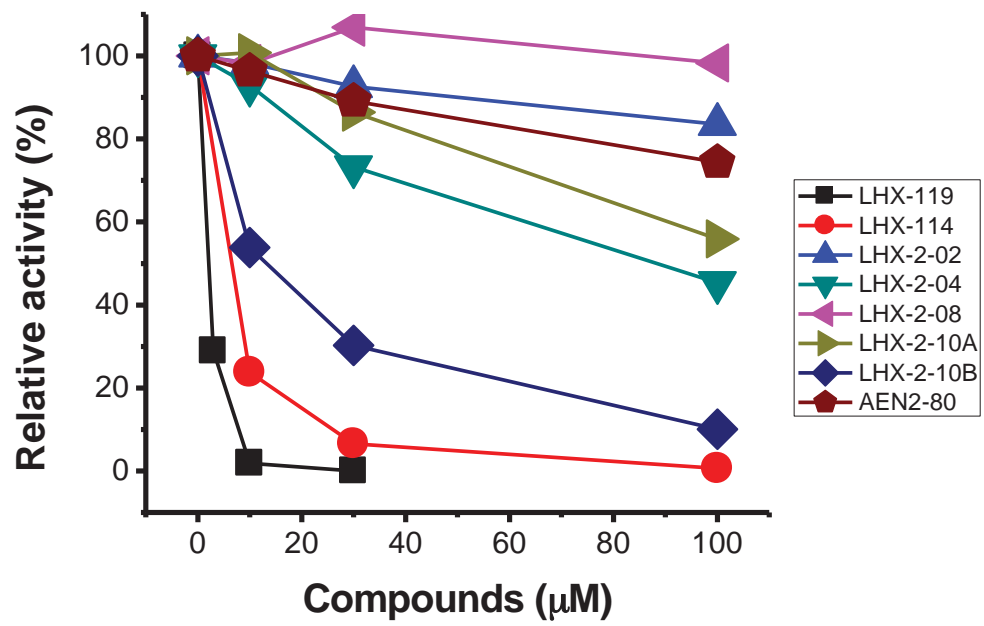


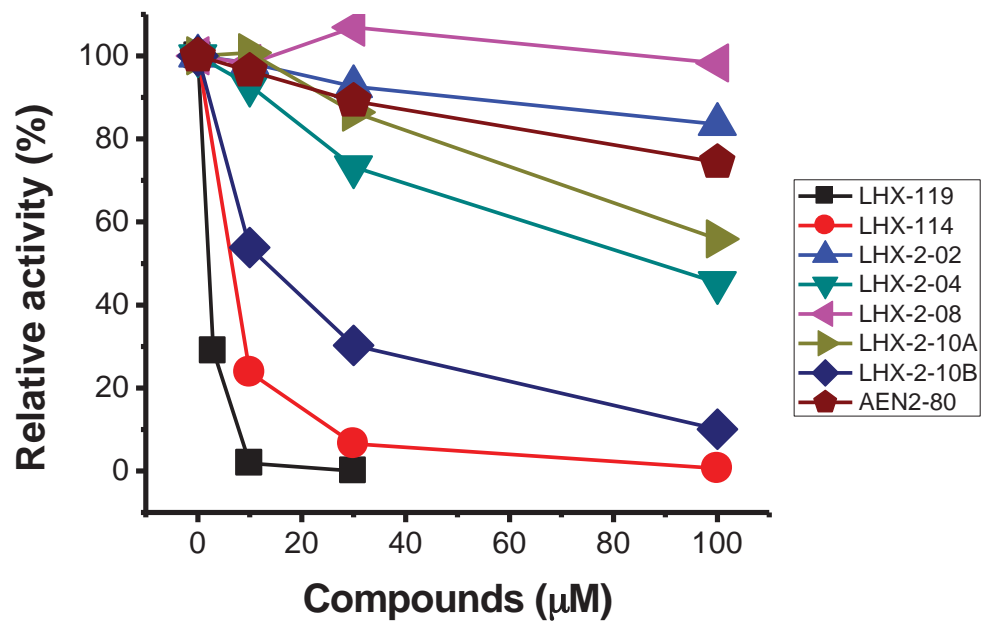


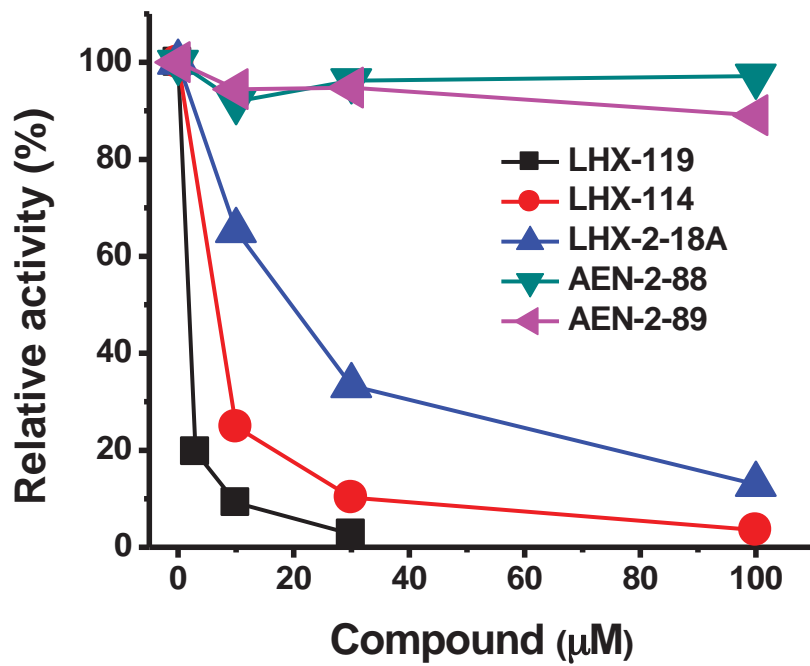


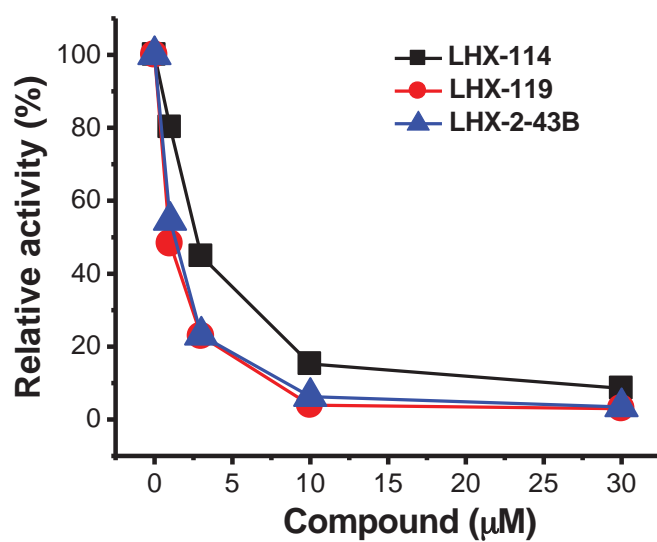
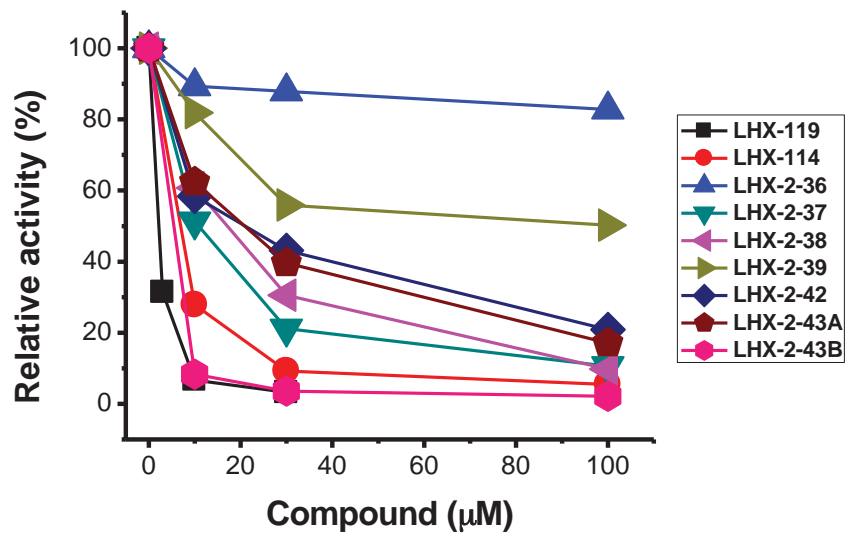


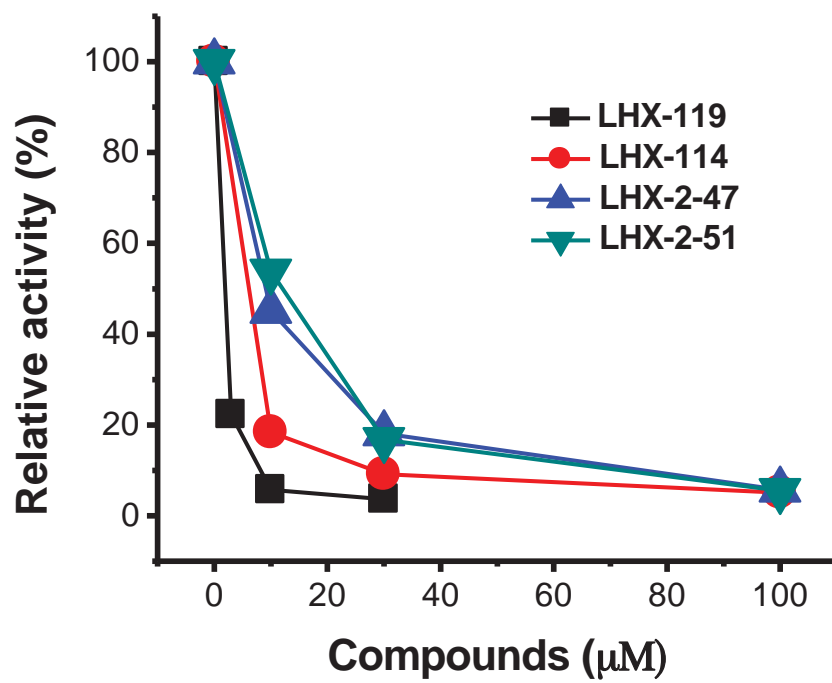


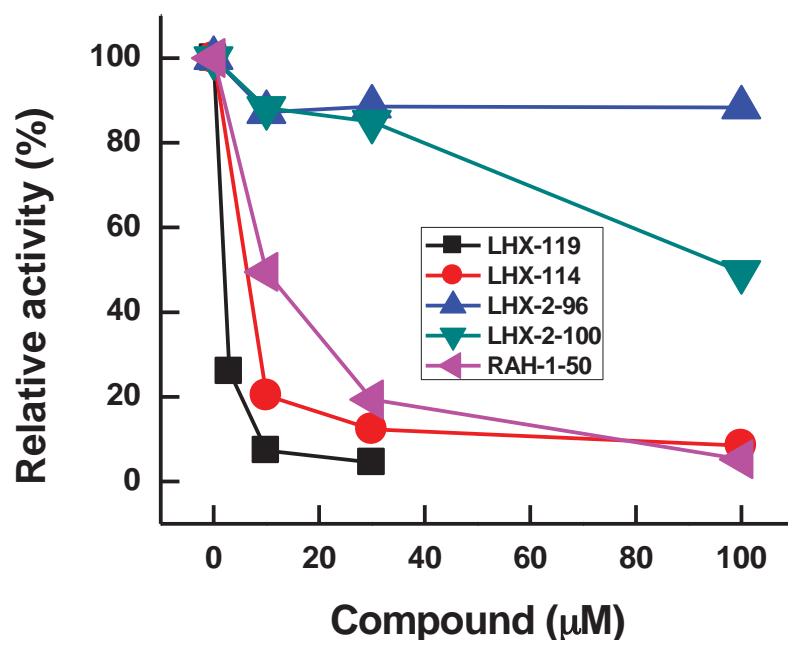


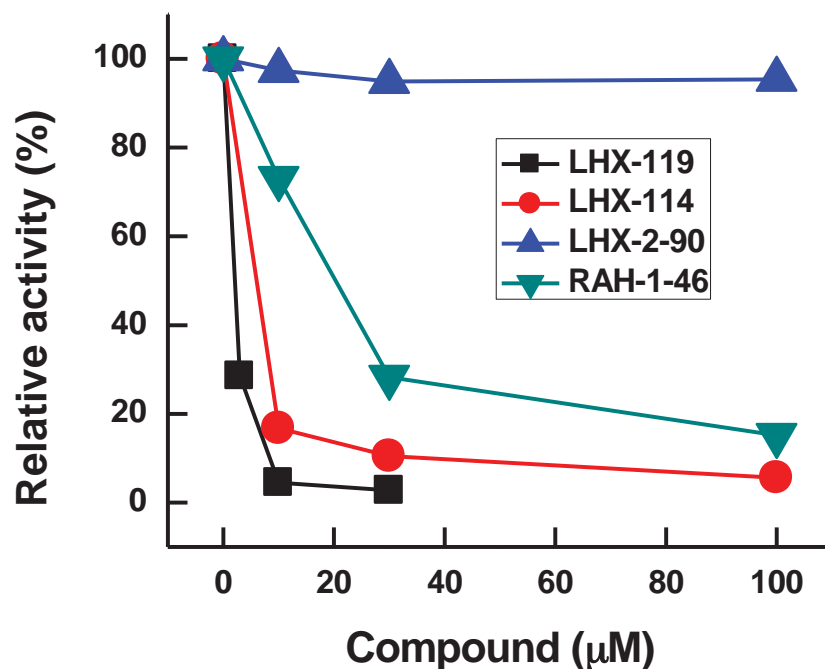


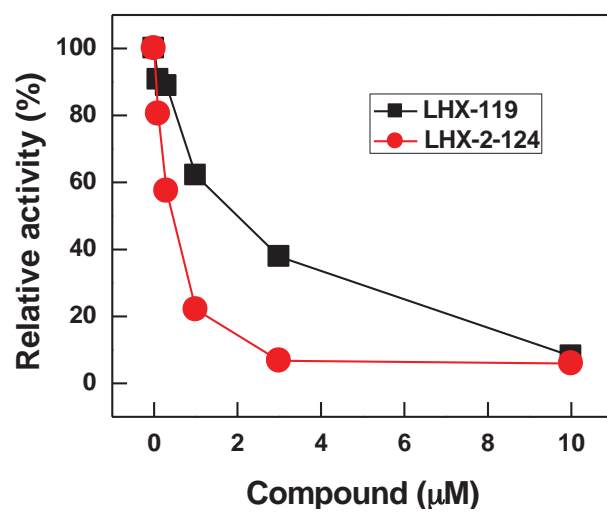
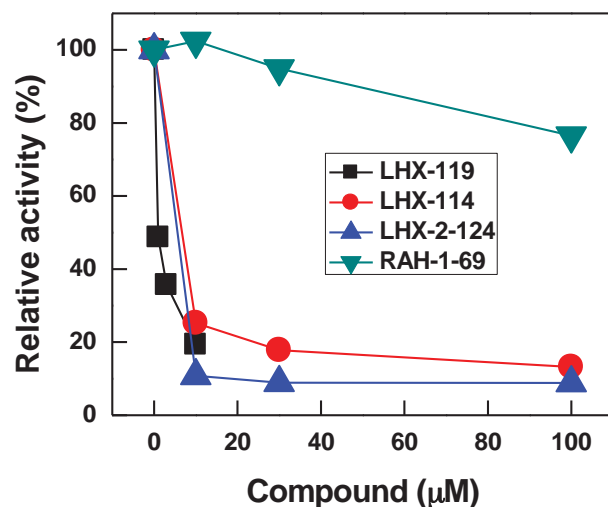


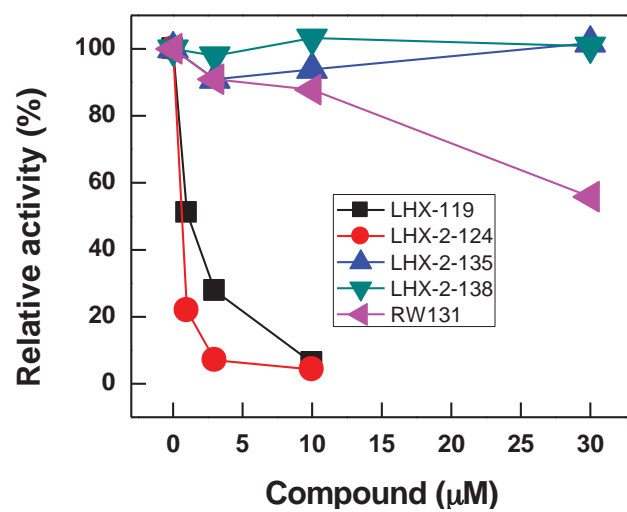


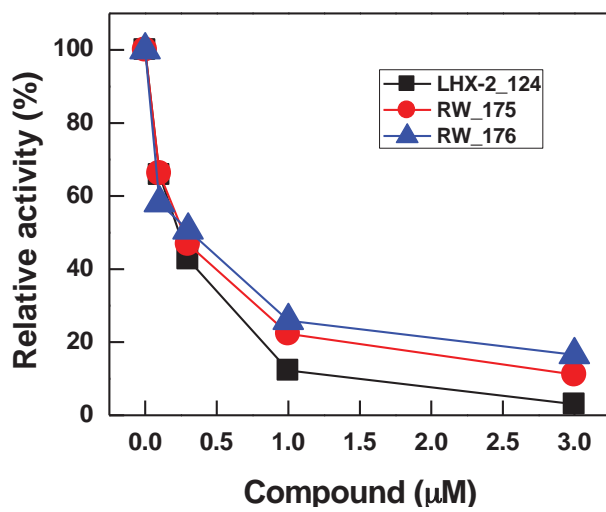
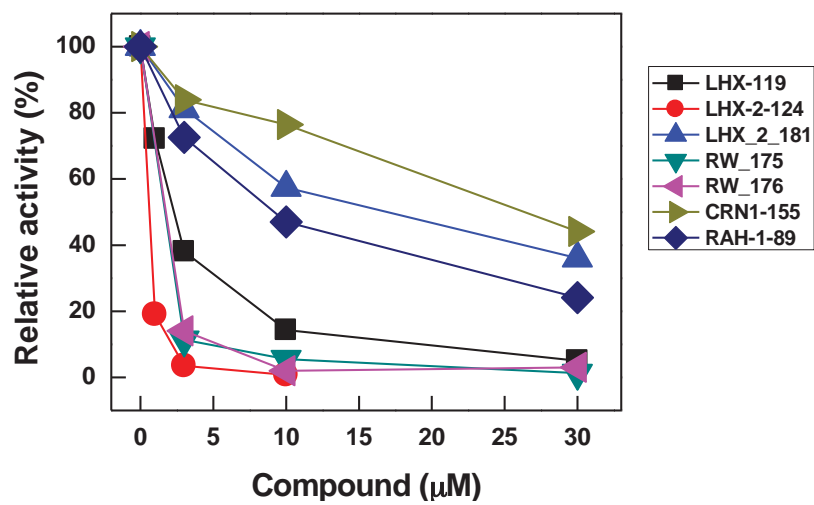


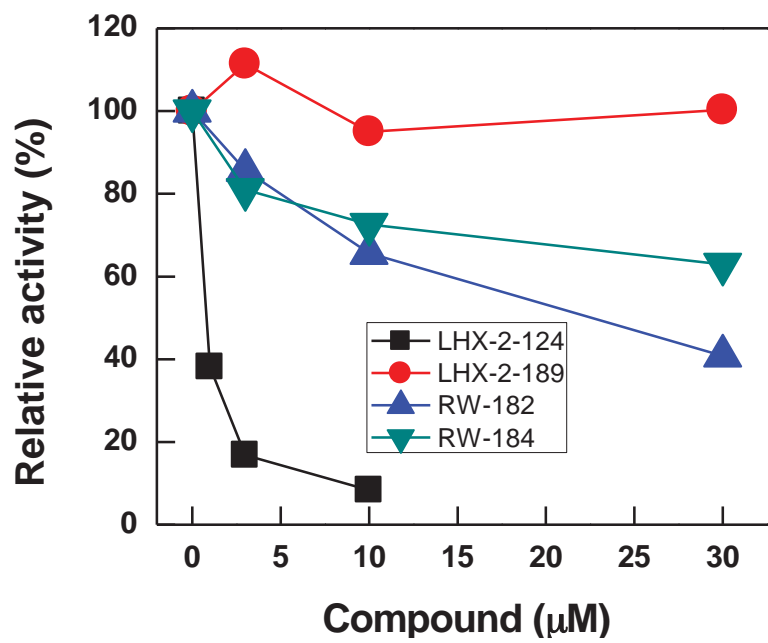


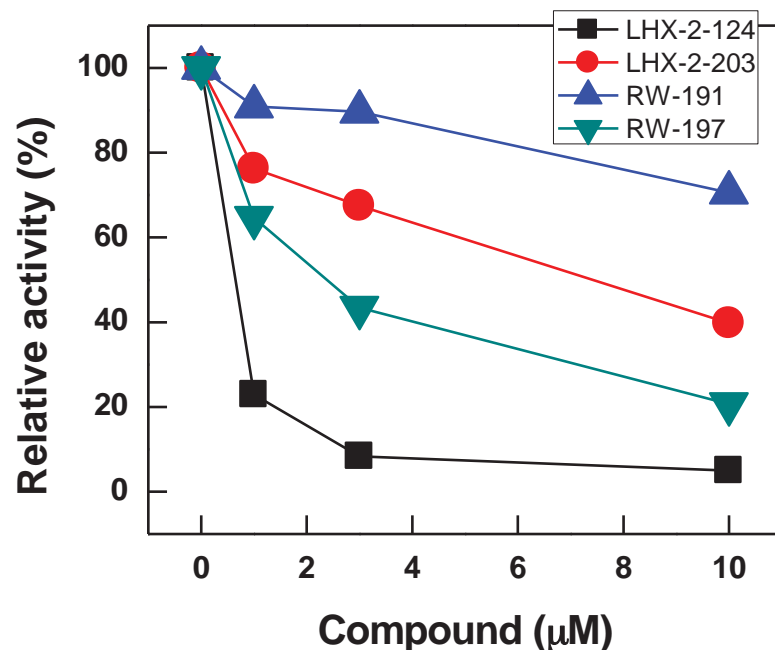


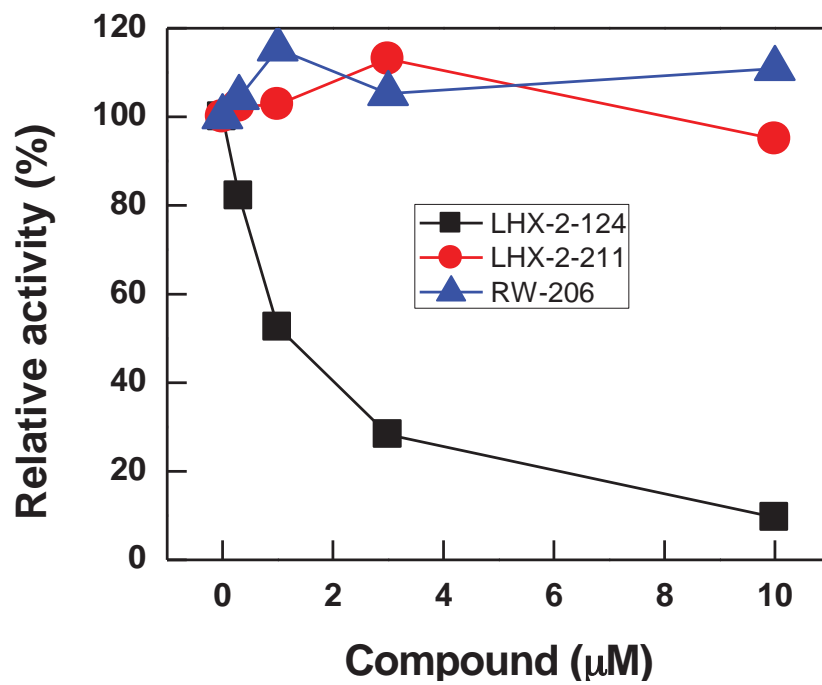


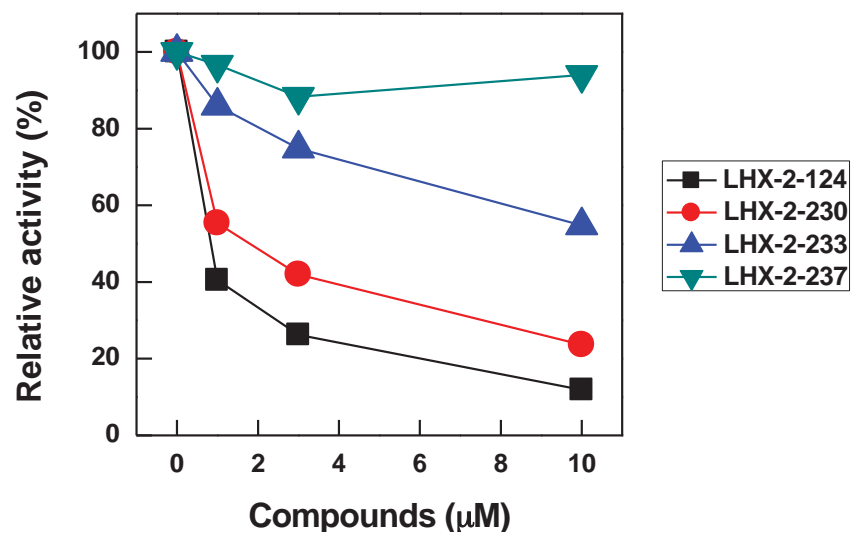


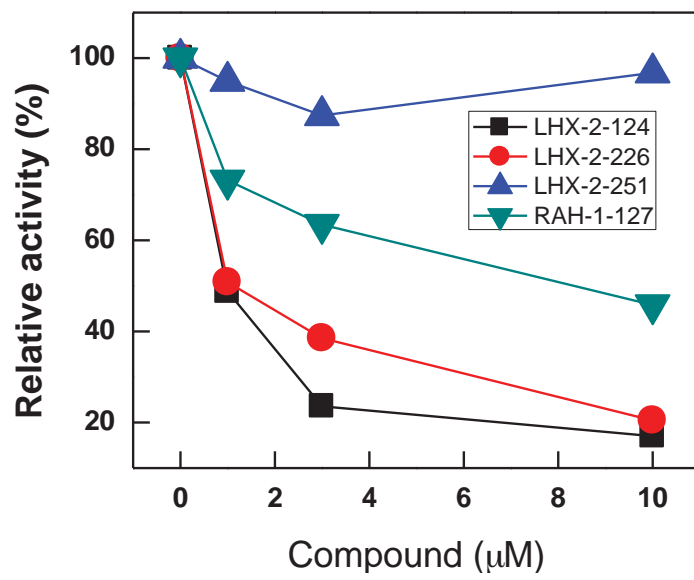


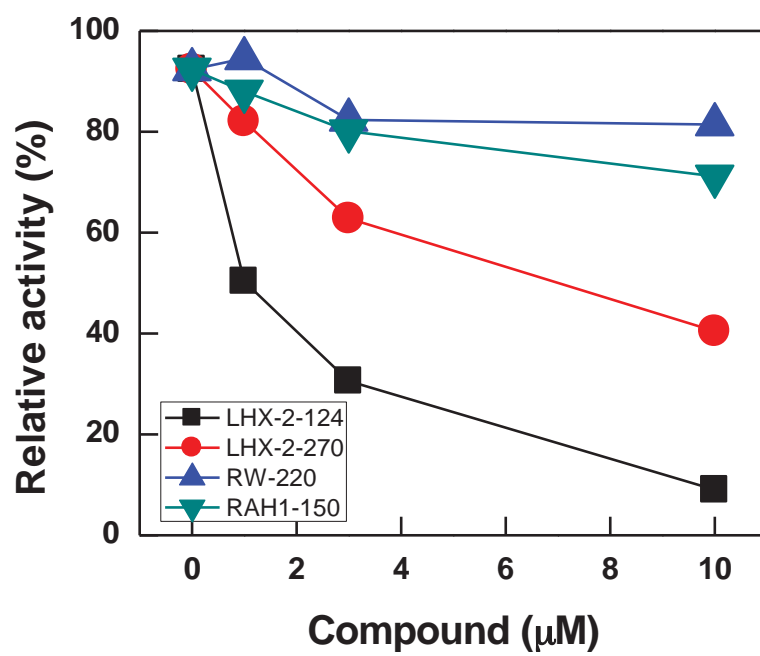


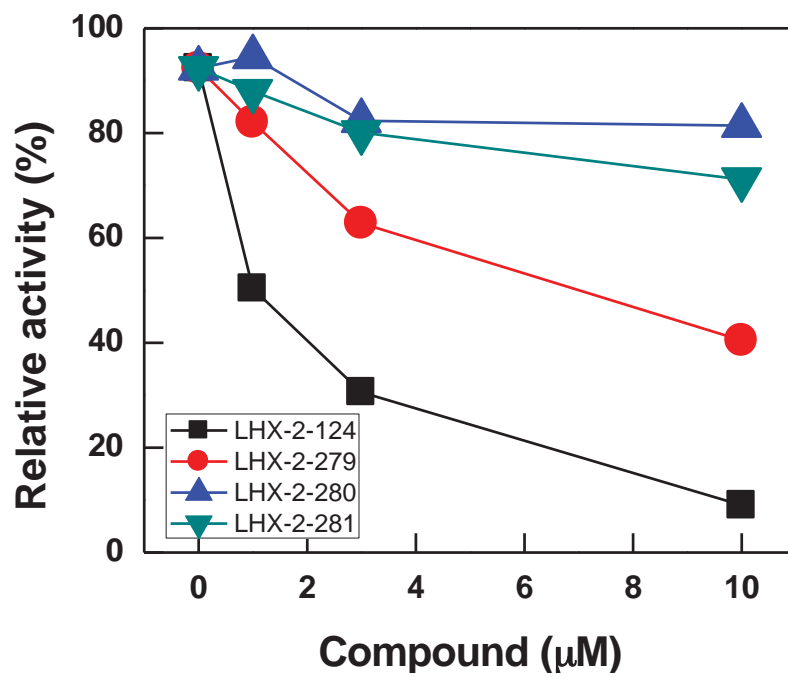


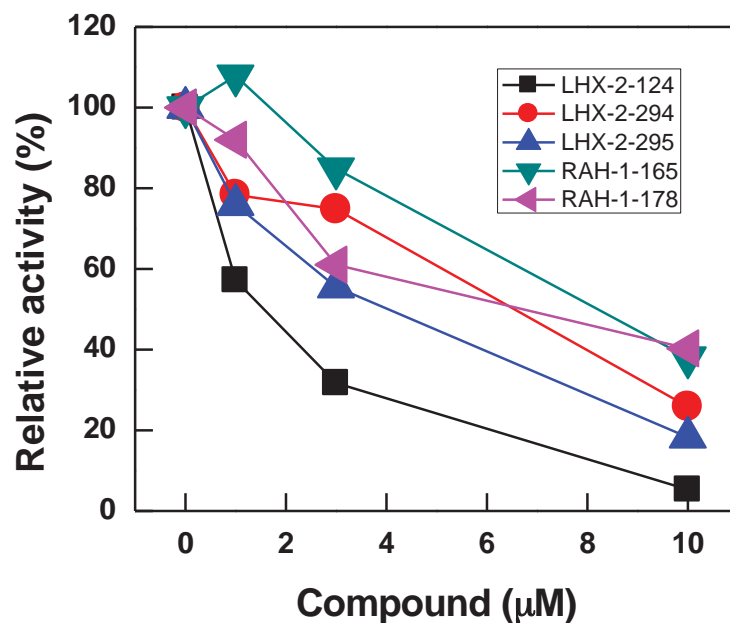


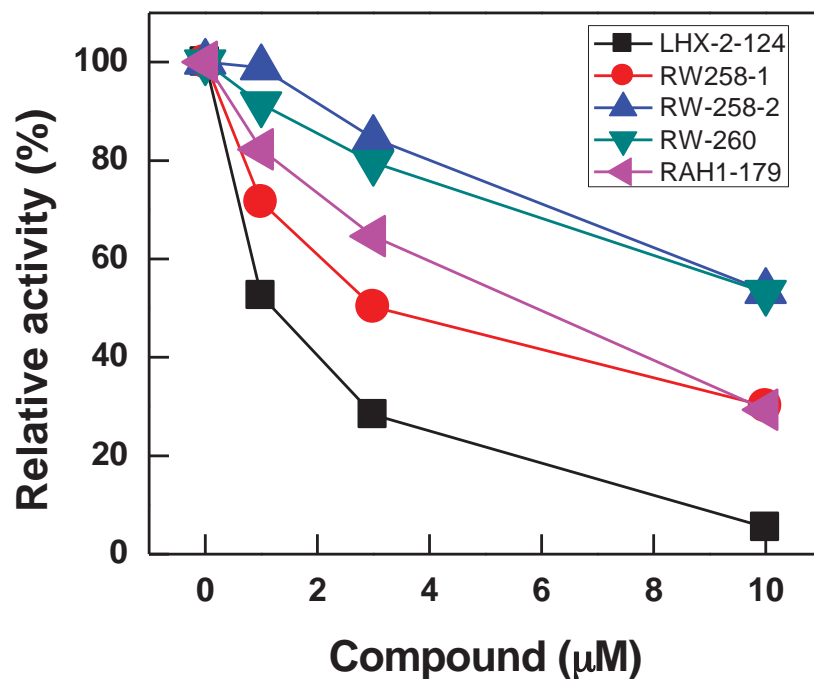


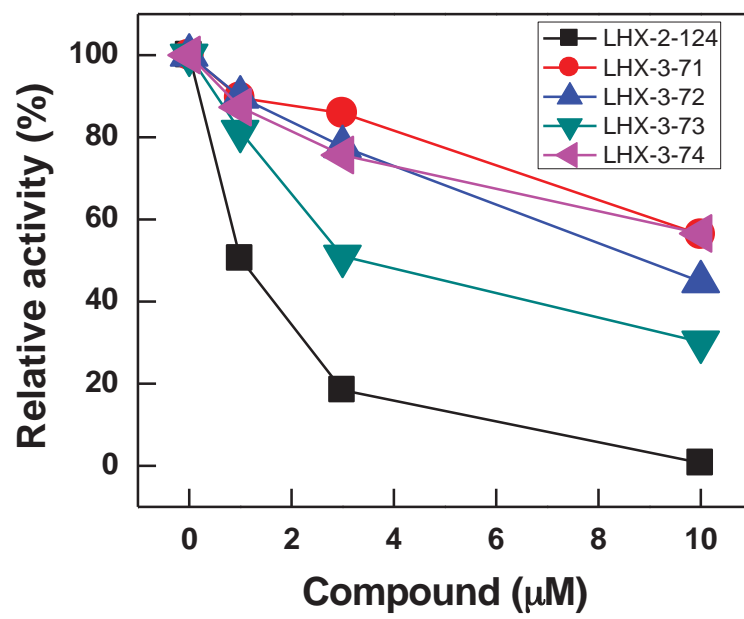


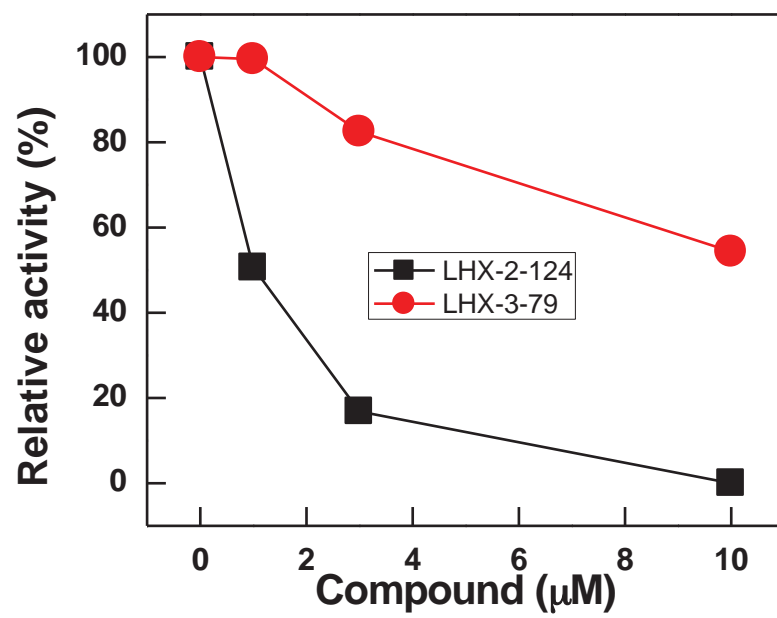


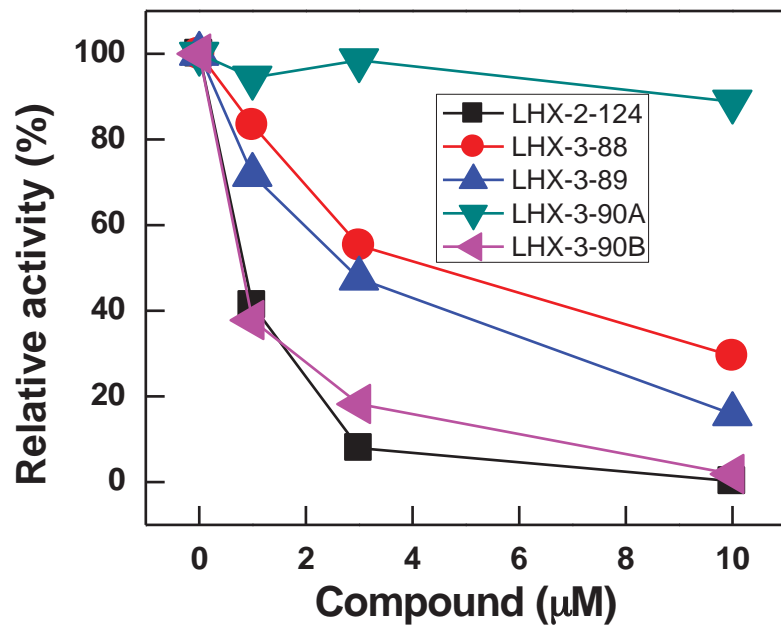


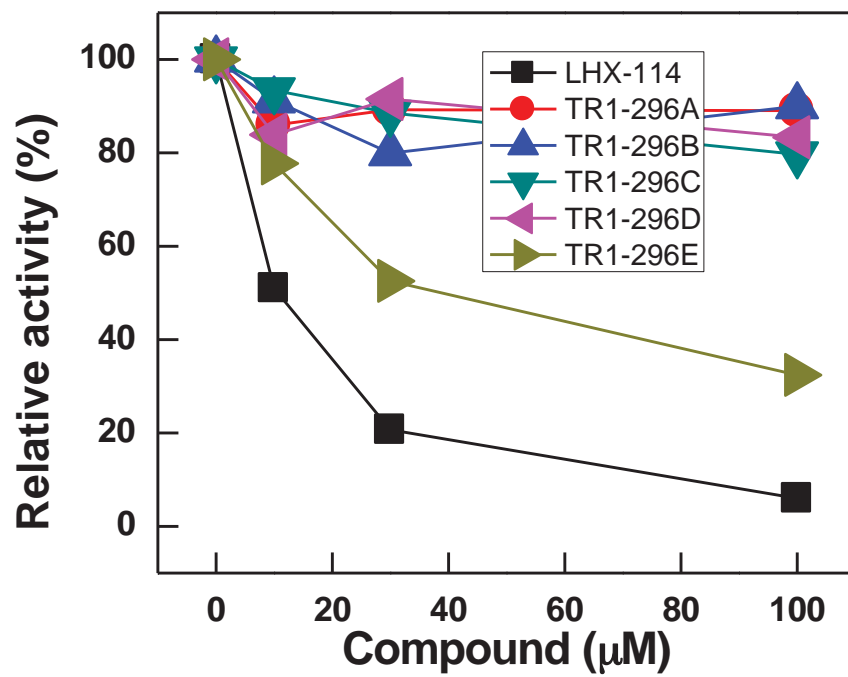


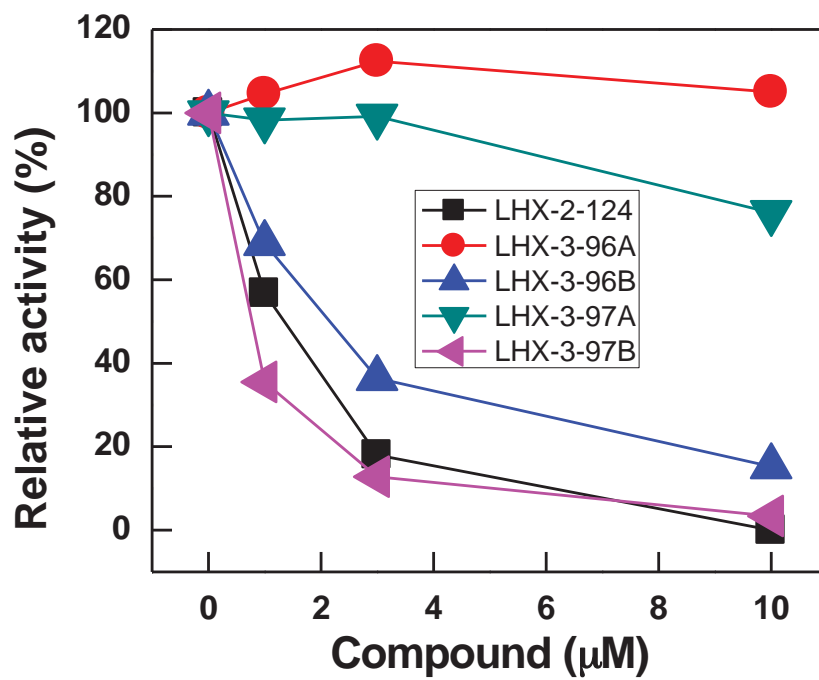


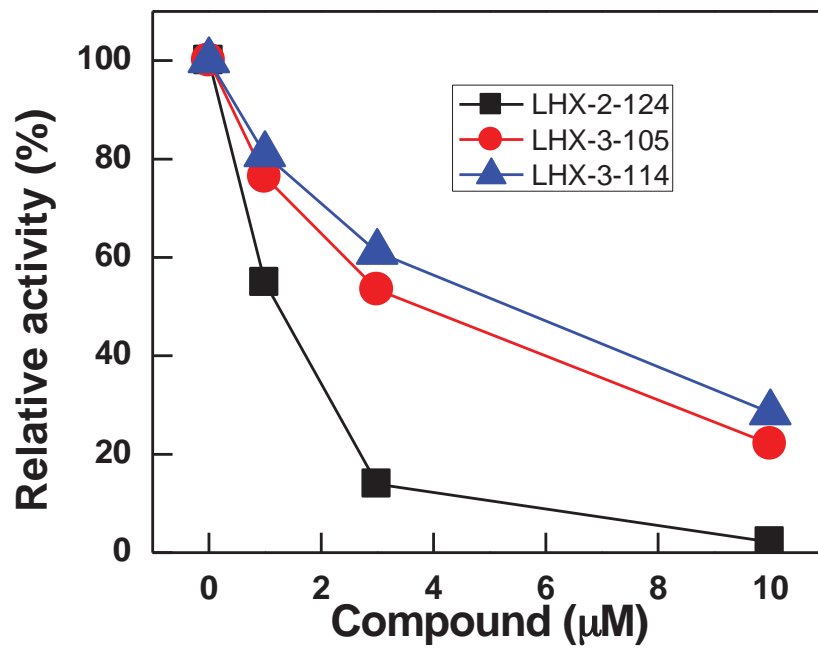


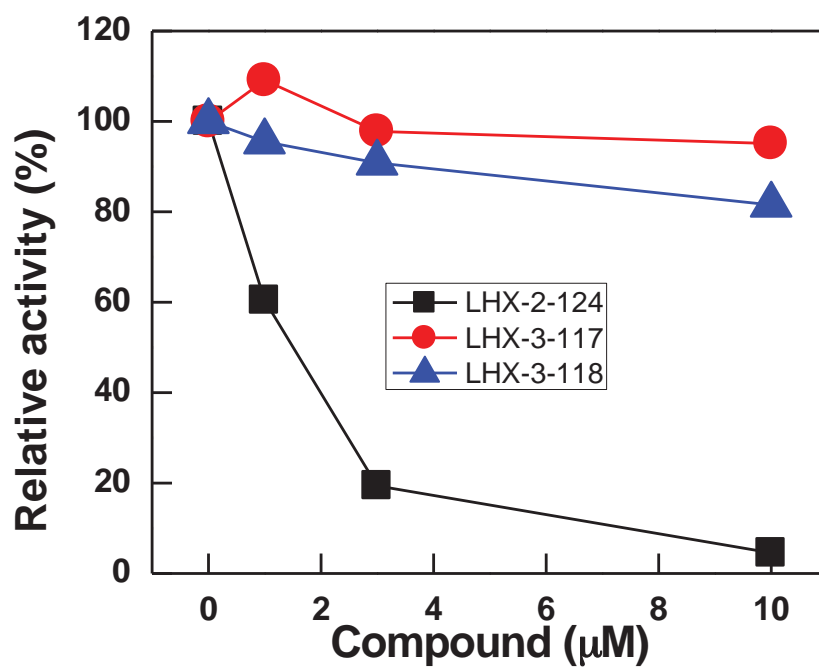


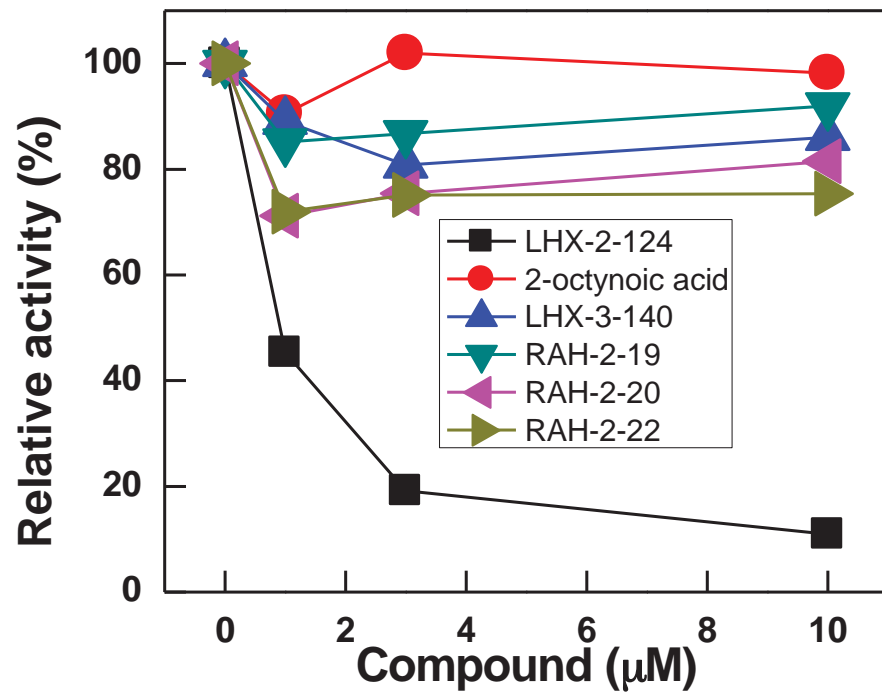


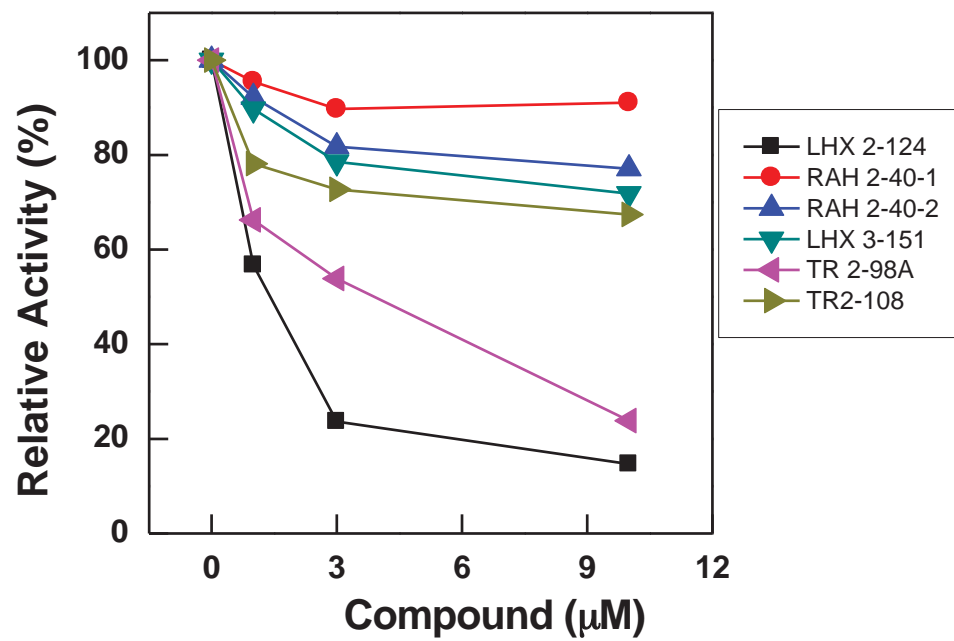


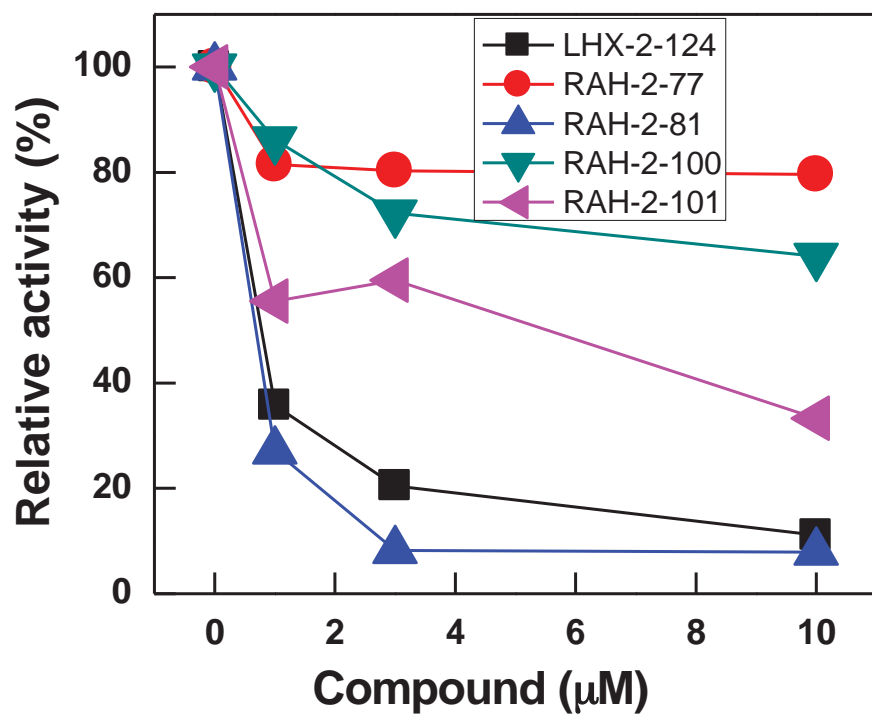


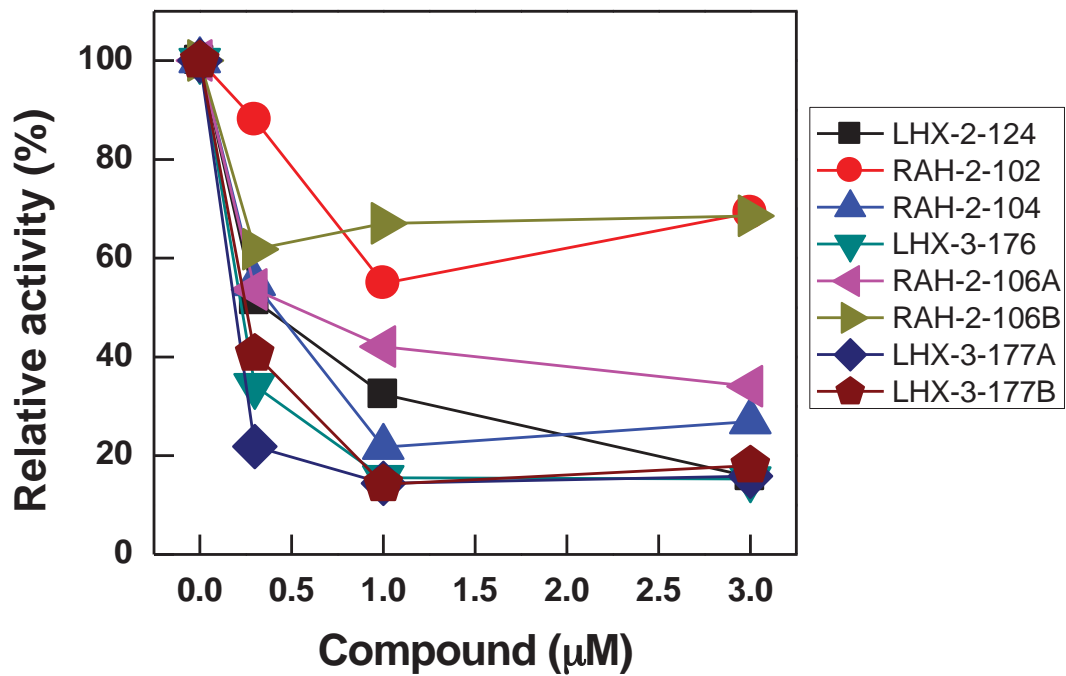


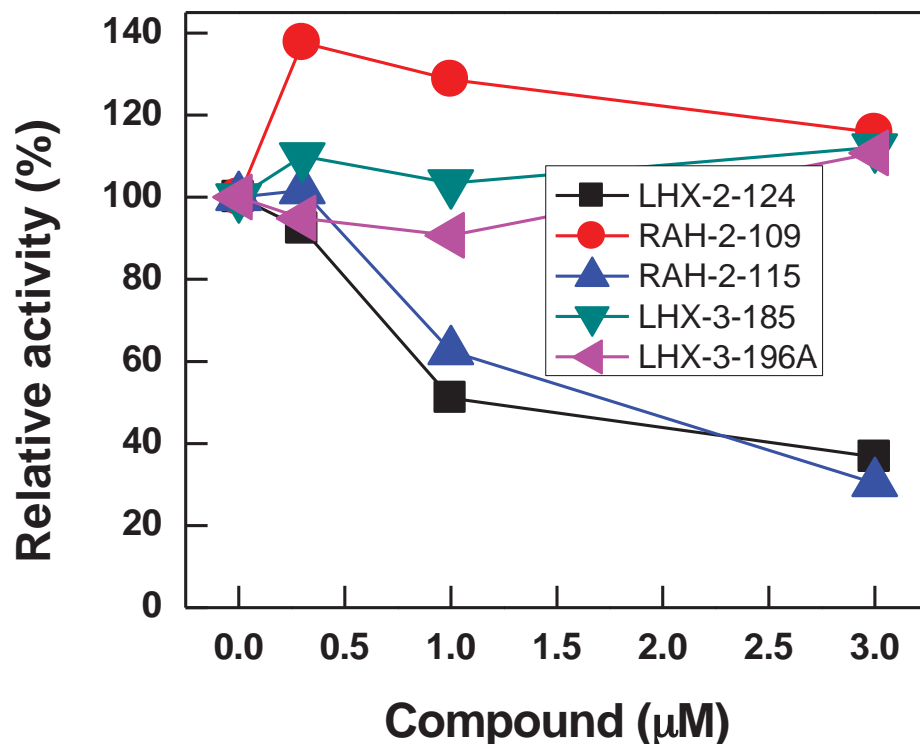


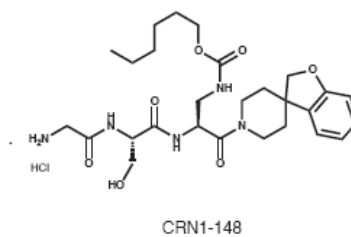
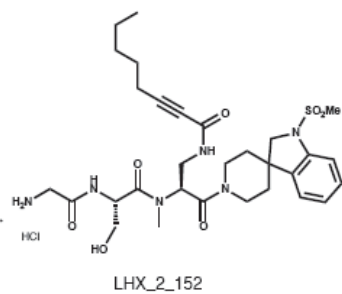
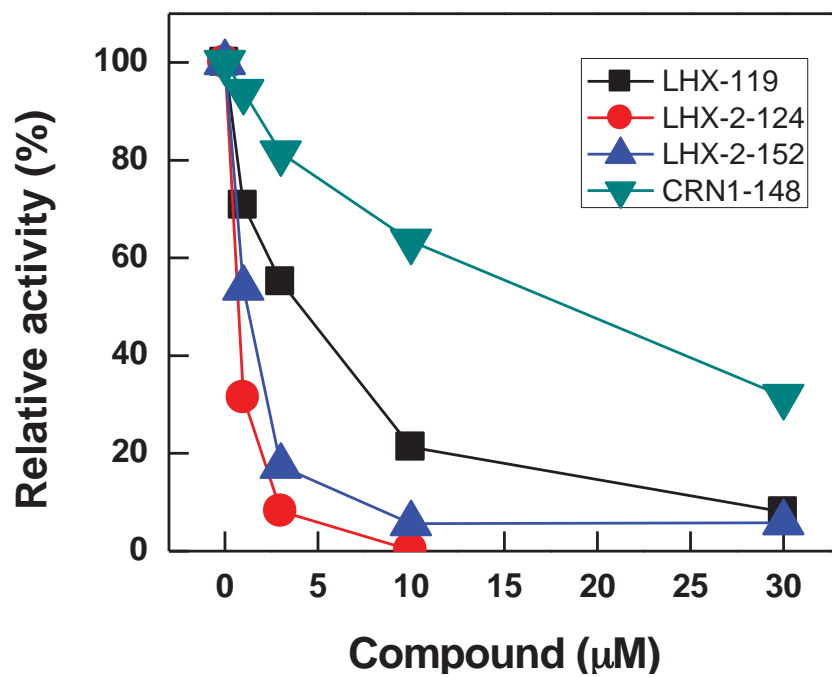


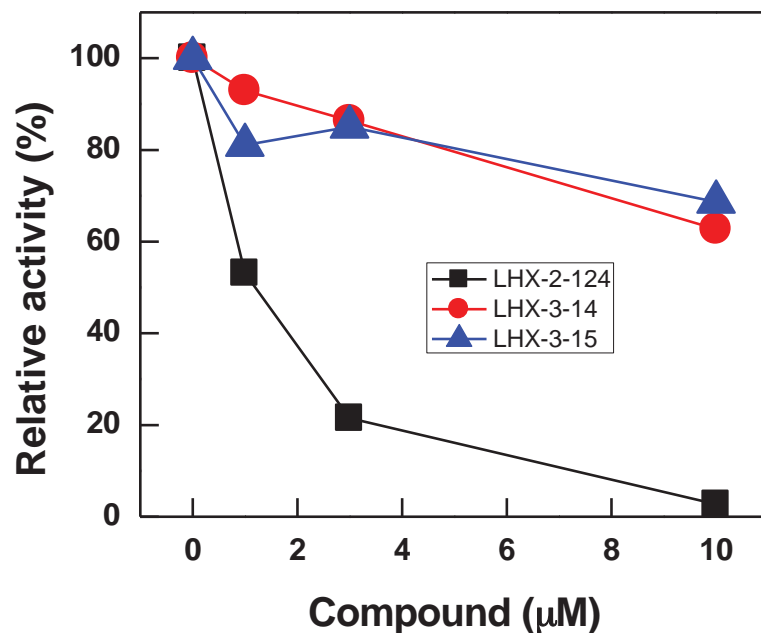


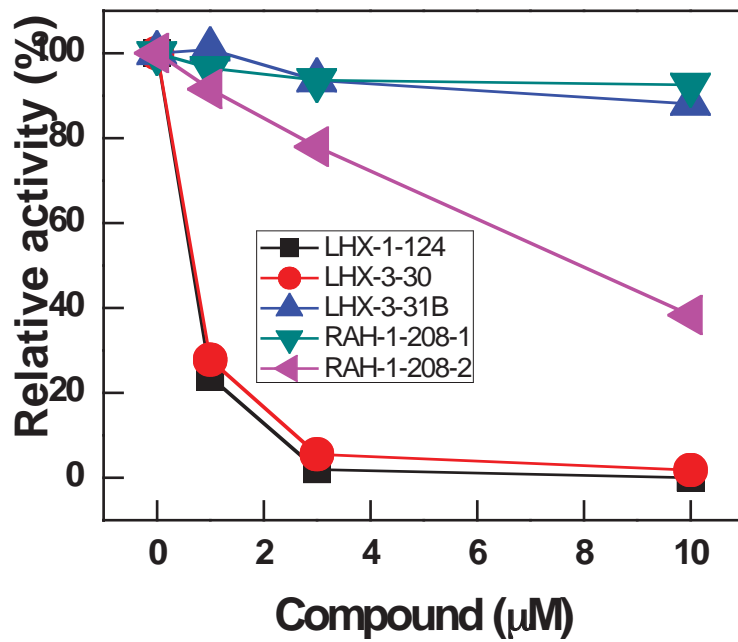


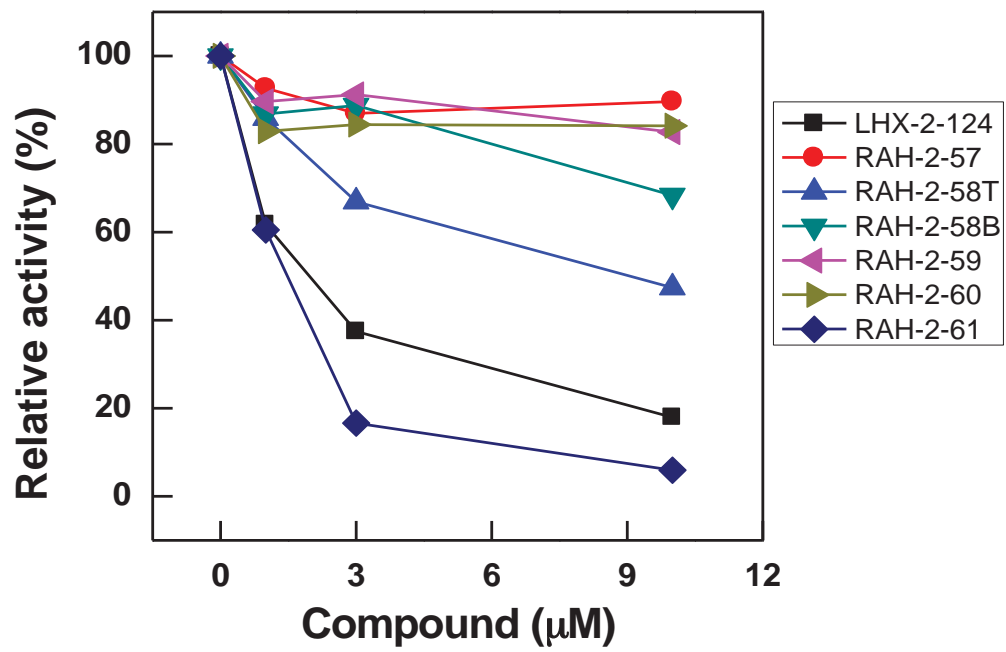


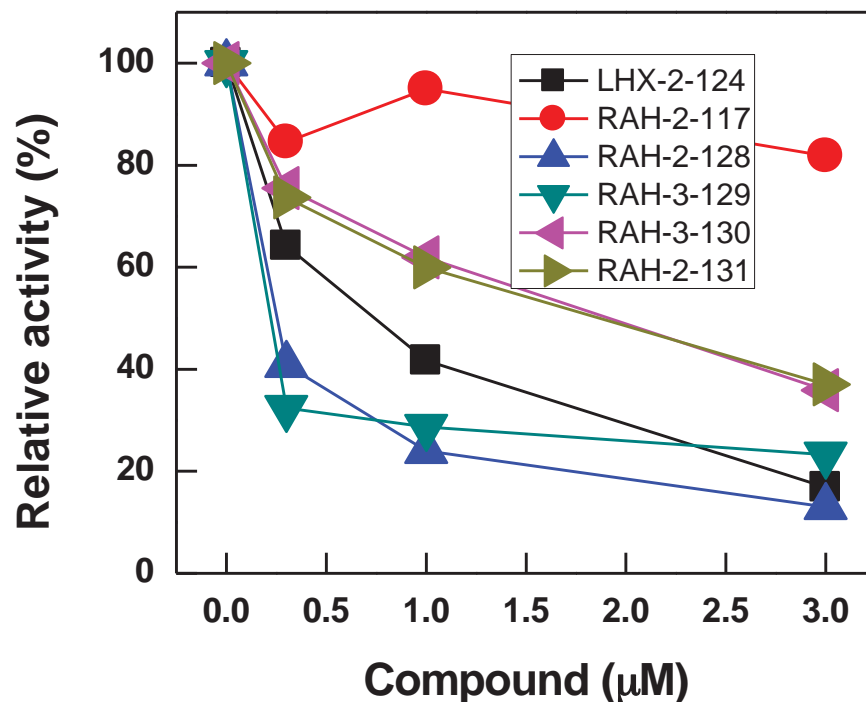


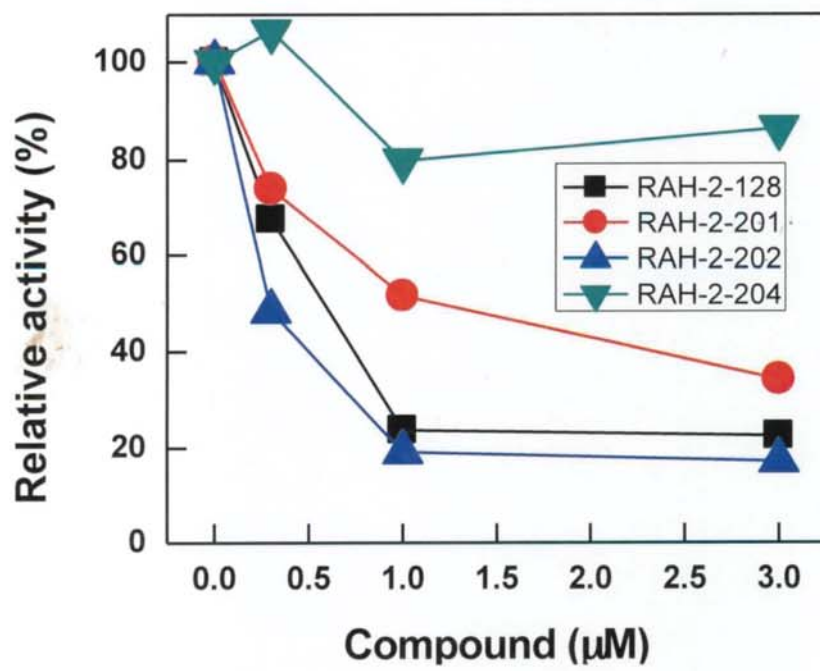


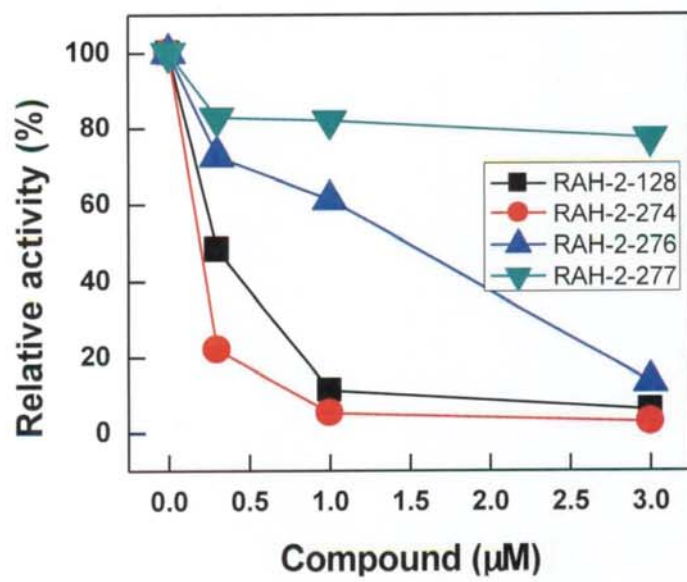


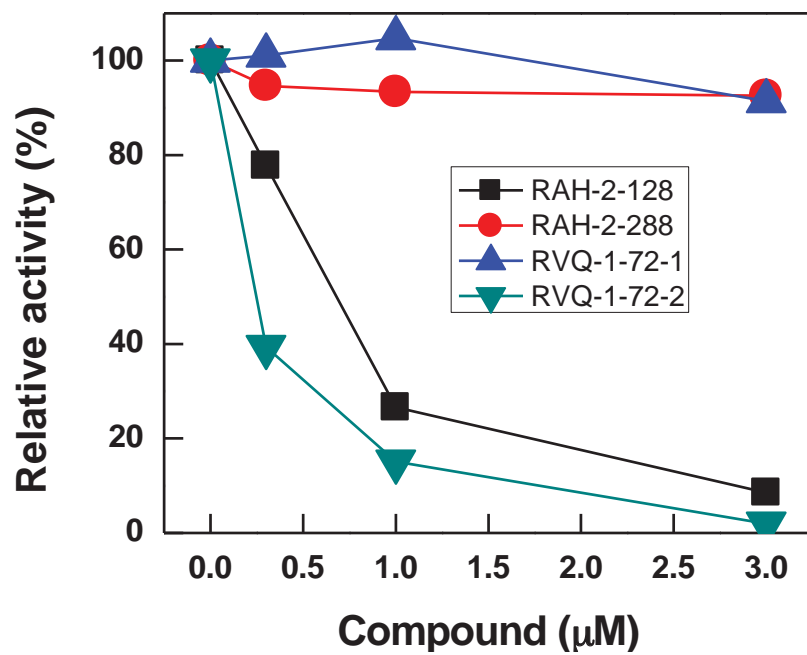


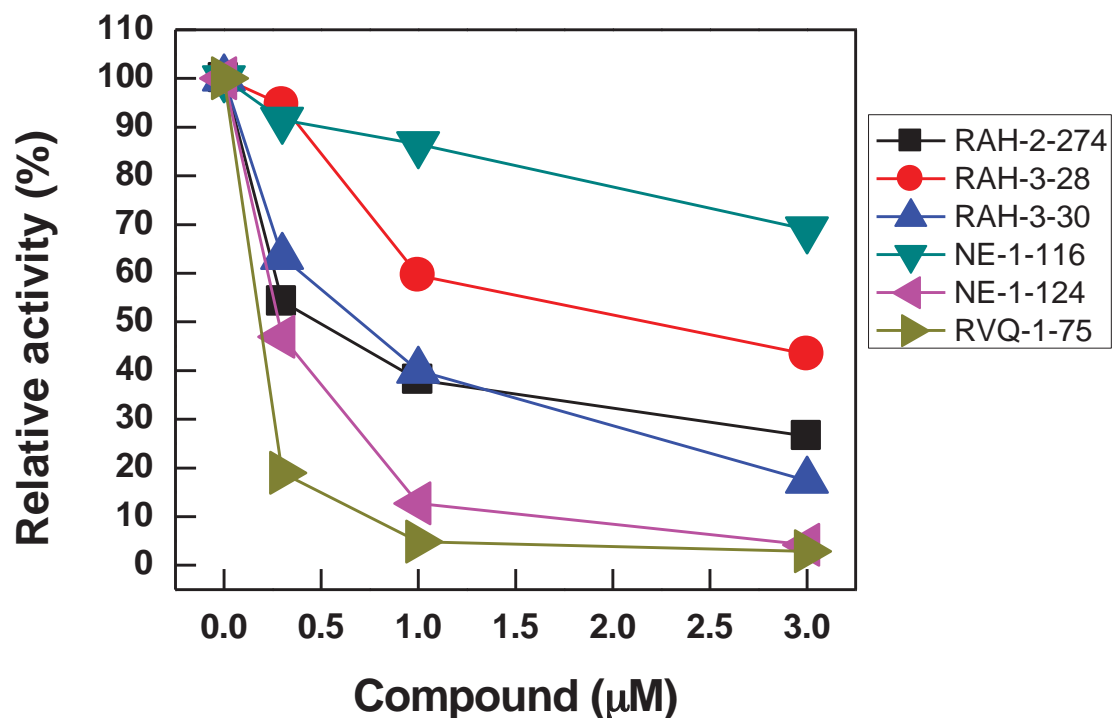


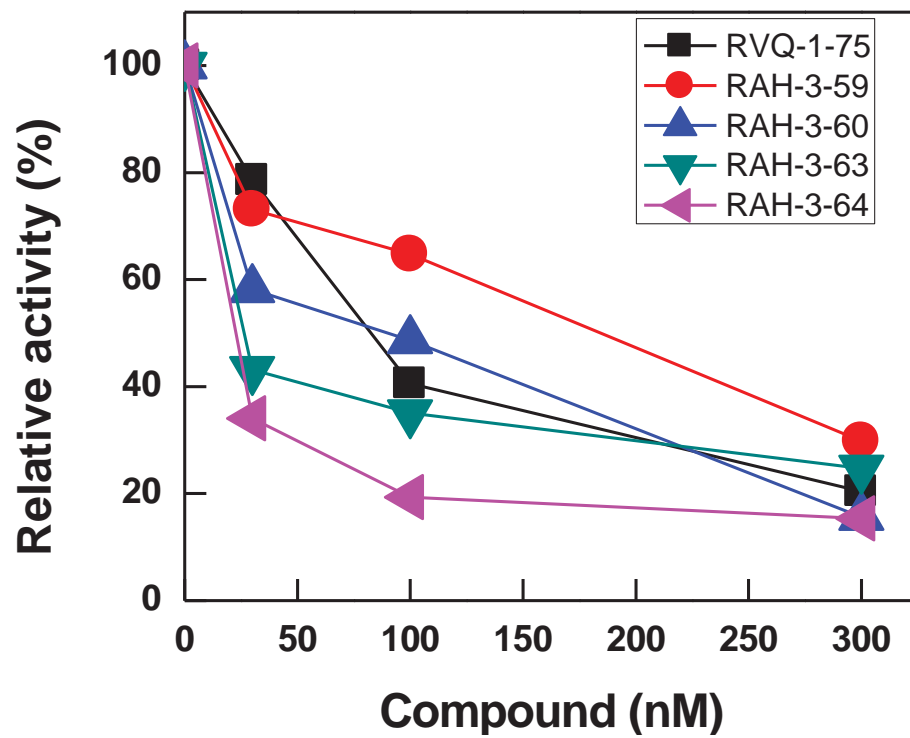


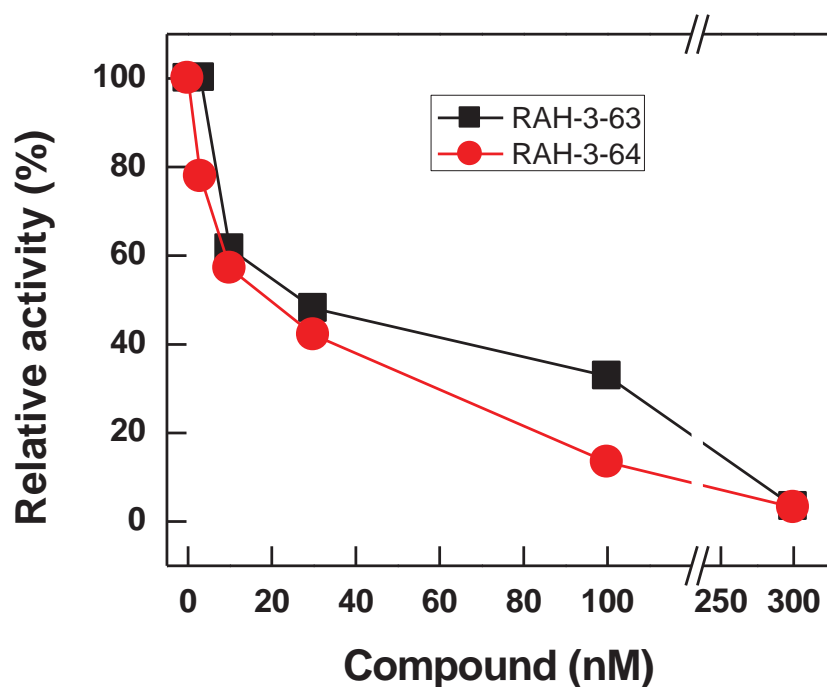


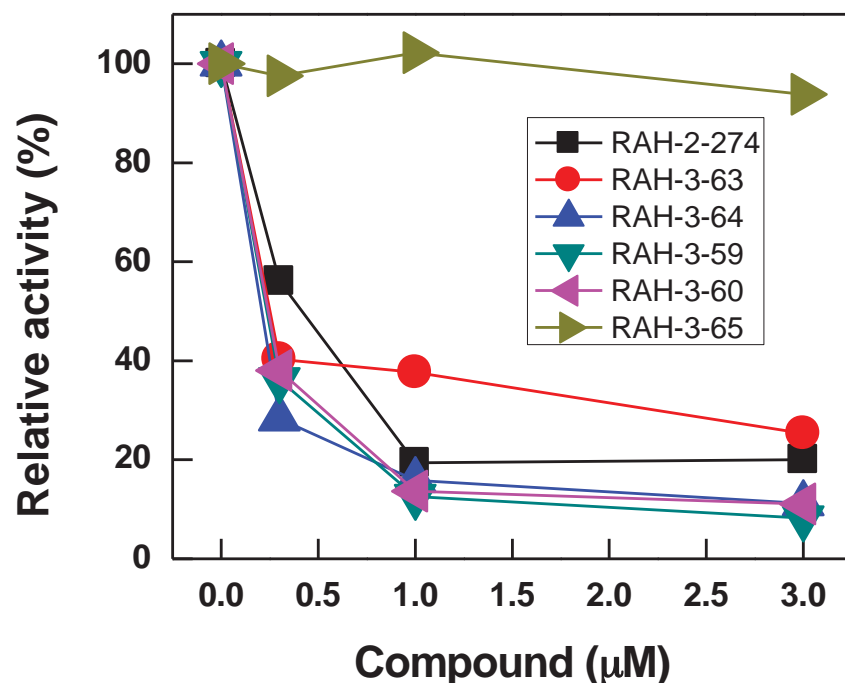


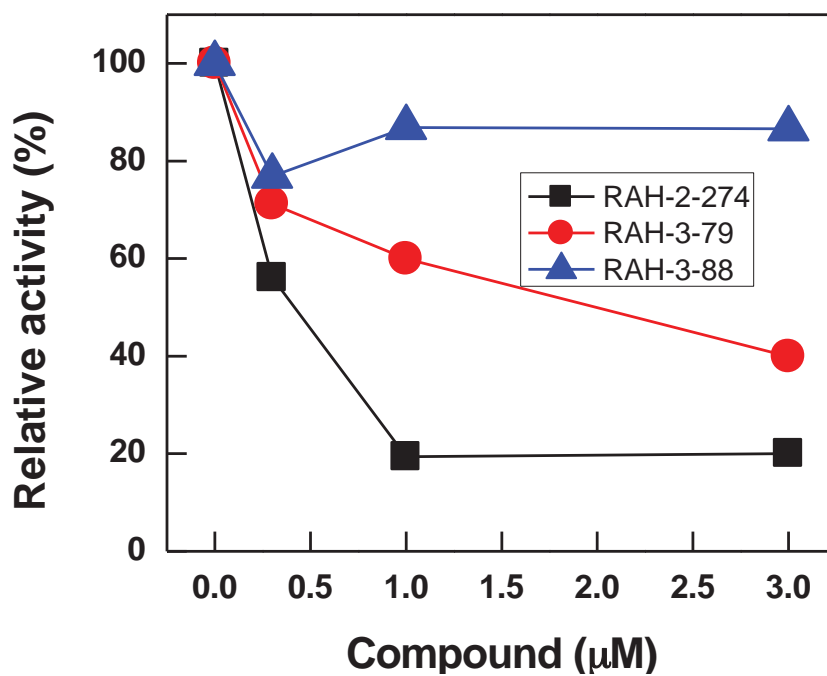
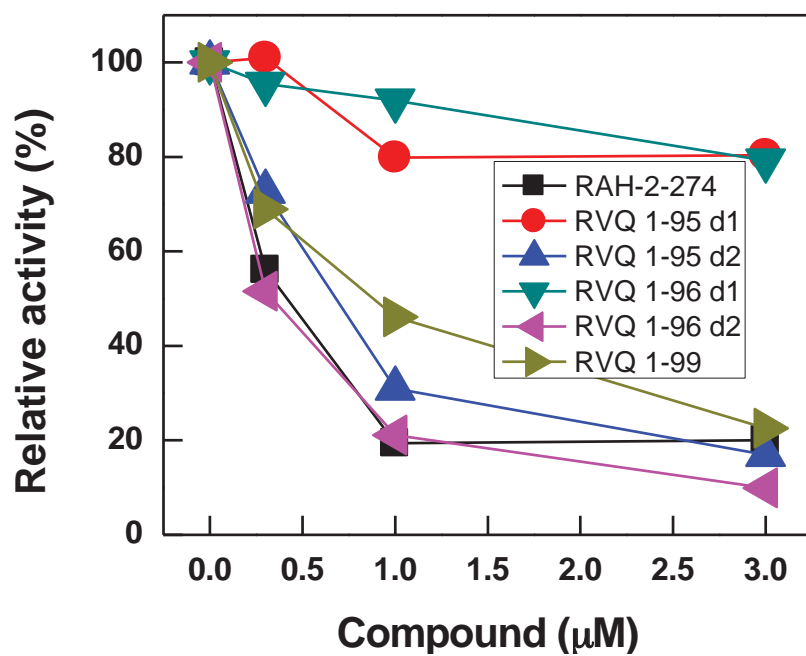


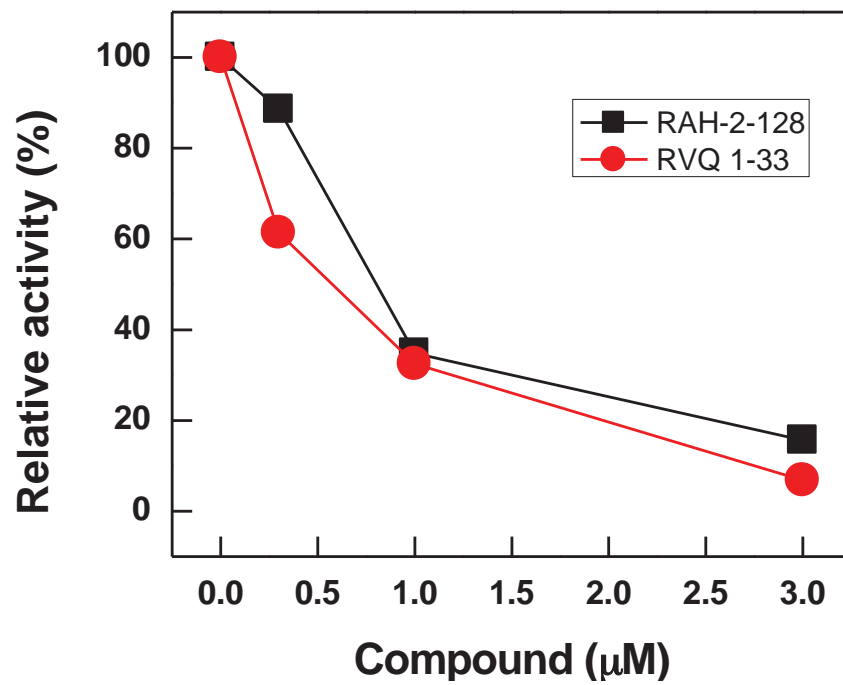


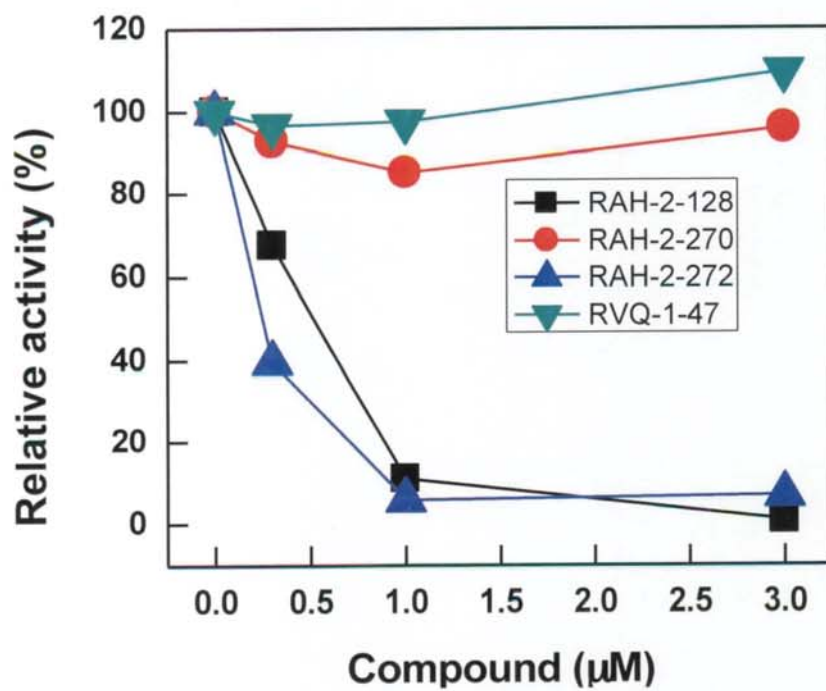


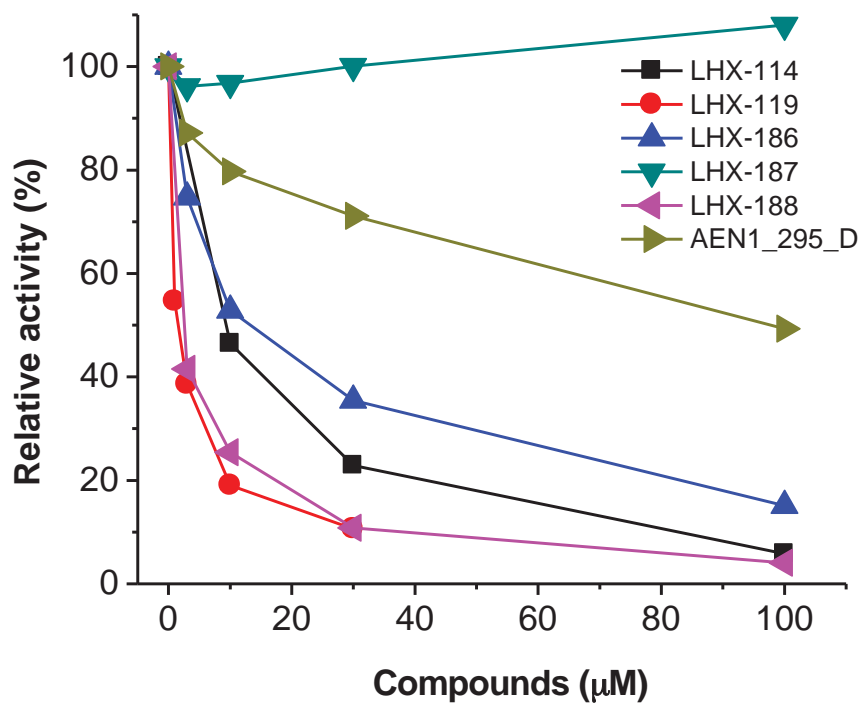








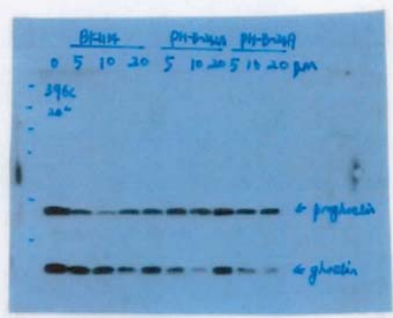
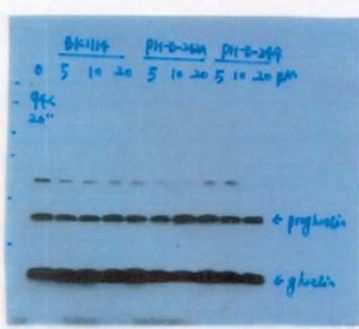
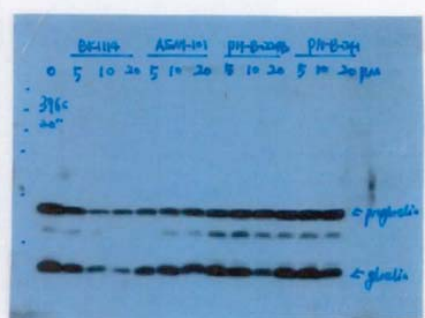
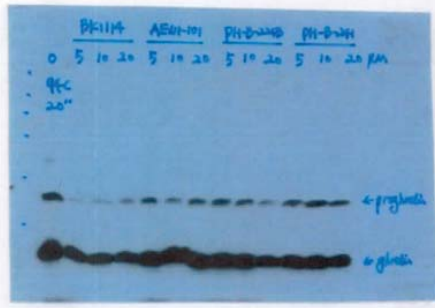




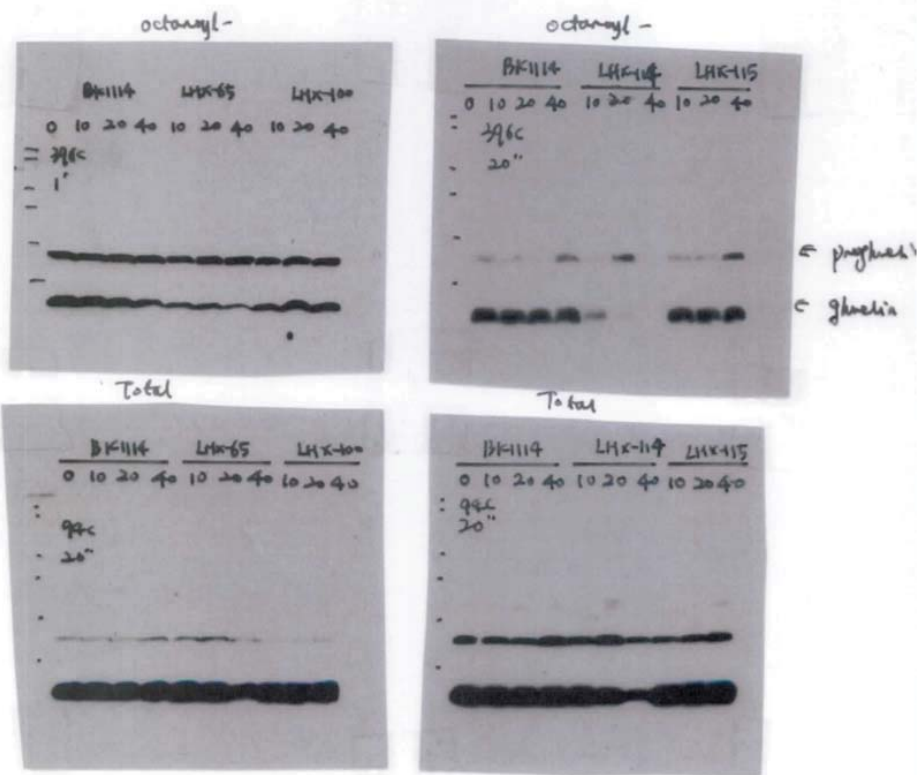
Day 0: set up 3930-112 (GDF-T7, propr-galactin) at $1.5 \times 10^6 / 10$ cm dish.
Day 4: treat the cells with 50 μ M Cs-FA, and 0, 5, 10 or 20 μ M
BK114, AEW1-101, PH-B-224B, PH-B-241, PH-B-242A and PH-B-249.
Day 5: Harvest the cells.

Glnelin (Total)

Glnelin (occluding)



Day 0: Set up 3930-112 at 1.5×10^6 /dish.
 Day 3: Change Medium.
 Day 4: Treat cells with 0, 10, 20, 40 μ M of BK1114, LHX-6^{and}
 LHX-100, LHX-114 and LHX-115
 Day 5: Harvest cells.



10/7-10/11

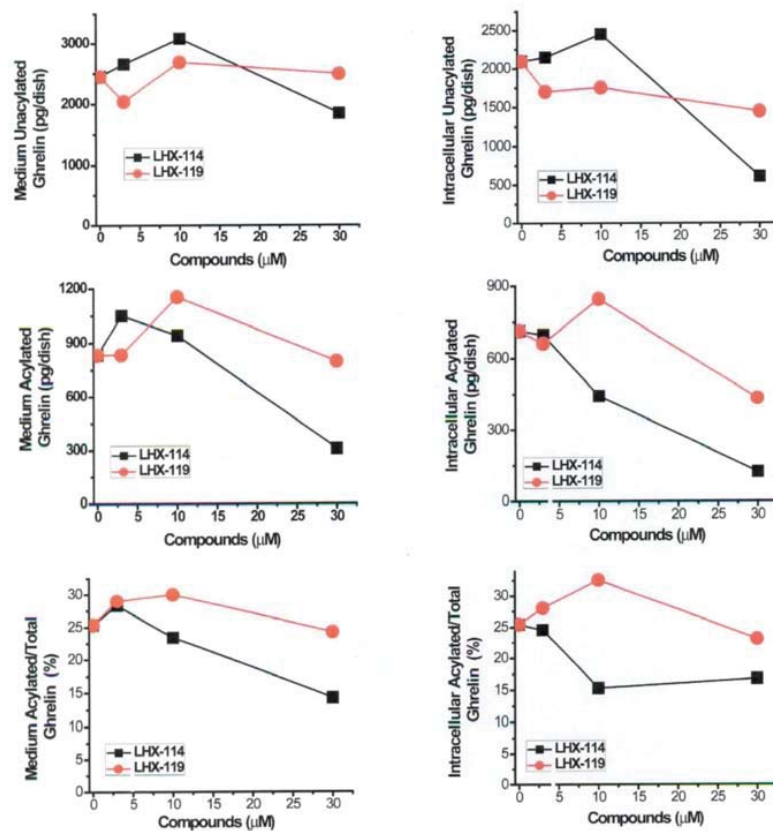
TJ-150 test LHX-11 and LHX-119 in the stomach tumor cells

Day 0, set up 1672s at 600K/12 ml in DHG (10% FCS, 1% ITS)

Day 2, combine the cells, spin down .

Resuspend the cells in 22 ml DMEM (no serum, no glucose, no sodium pyruvate), 1% ITS, add 49 ul 45% glucose stock. Add 110 ul C8-FA.

Aliquot 16 ml of the cells into 16 wells, treat the cells with different concentrations of LHX-114 or LHX-119.

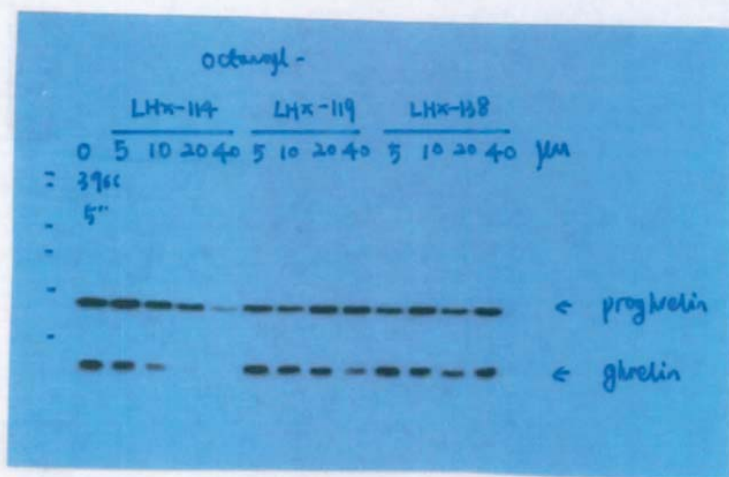


Day 0: Set up 3930-1-12 (progesterin, GAT-T1) at 1.5×10^5 /dish.

Day 3: Change medium

Day 4: Treat cells with 0, 5, 10, 20 and 40 μ M LHX-114, 119 and 138.

Day 5: Harvest cells.

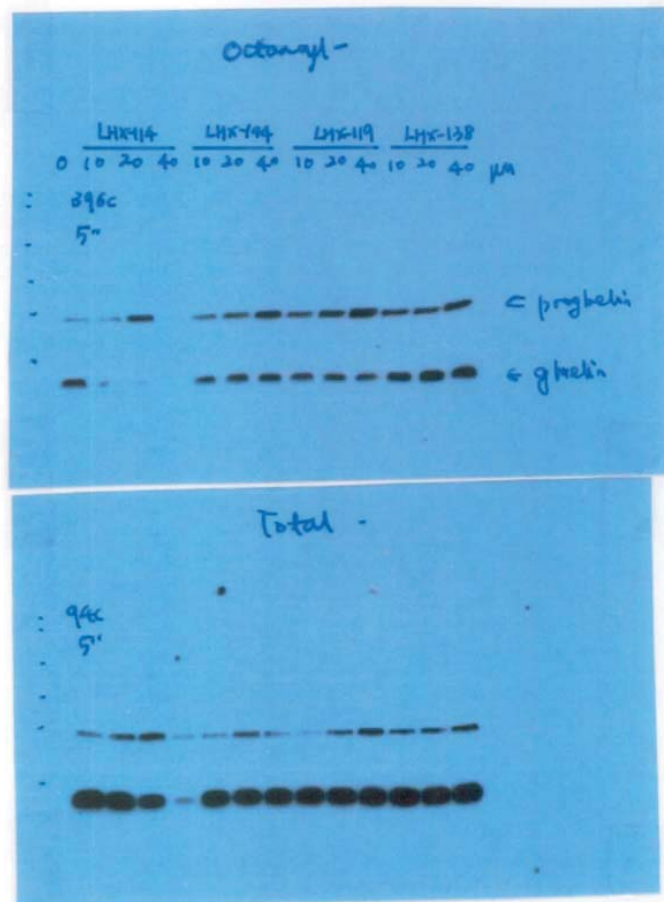


Day 0: Set up 3930-1-12 (G6AT-T7, preproghelin) at 1.5×10^6 /dish

Day 3: Change medium

Day 4: Treat cells with LHX-114 at 10, 20 and 40 μ M.
LHX-114
LHX-119
and LHX-138.

Day 5: Harvest cells.



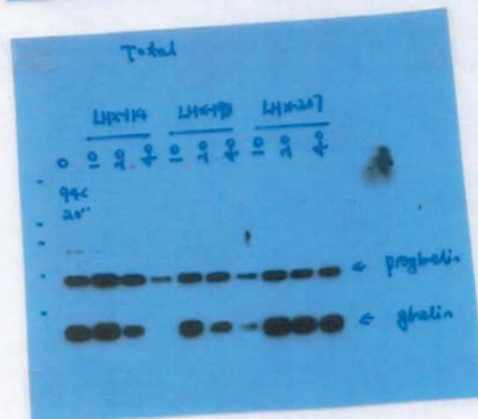
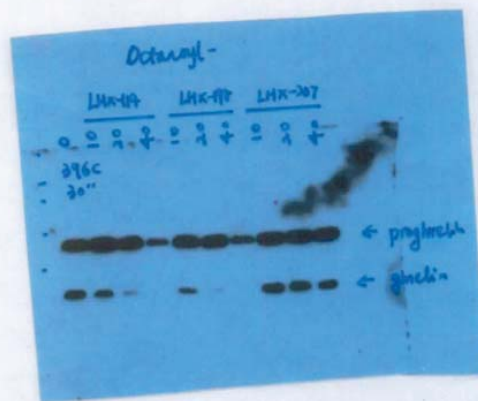
TJ-121

Day 0: Set up 3T3⁺-1-12 (propranolol and G₁T-17) at 1.5×10^6 /dish.

Day 3: Refeed cells.

Day 4: Treat cells with 0, 10, 20, 40 μ M LHX-198 or LHX-207. With LHX-114 as control

Day 5: Harvest cells 16 h after treatment.



5/12/10 - 5/17/10

Day 0, set up TR303-12 (96wells, 600T) at $1.5 \times 10^6 / 10$ cm dishes.

Day 3. Change medium.

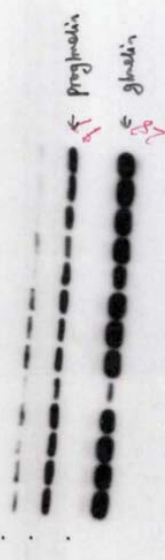
Day 4. treat cells with 0, 5, 10, 20 μ M LHx-114, puw-175, and puw-176.

Day 5. Harvest cells.

Ic50: LHx-114: 10 μ M
 puw-175: 0.2 μ M
 puw-176: 0.2 μ M

Protein glnelin

LHX-114	puw-175	puw-176
0 5 10 20 40	0 5 10 20 40	0 5 10 20 40



Glnelin

LHX-114	puw-175	puw-176
0 5 10 20 40	0 5 10 20 40	0 5 10 20 40



BSU/110

- Day 0. T23910-1-12 were set up in 1% FCS at 1.5×10^6 cells/dish.
Day 1. Refresh the cells.
Treat cells with 0, 5, 10, 20 and 40 μ M compounds.
Day 4 Harvest cells.

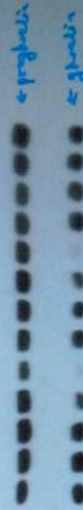
Octanoyl - ghrelin

LM-114 LM-2103 LM-2104
0 5 10 20 40 5 10 20 40 5 10 20 40 μ M
: 30%
100



Total Ghrelin

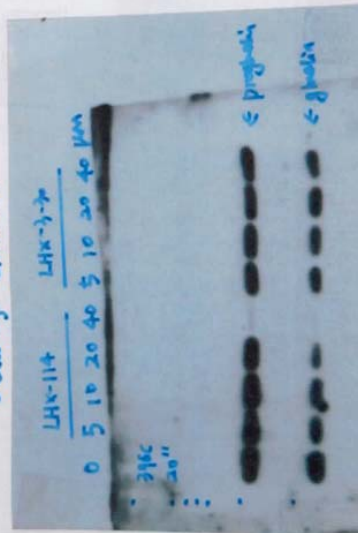
LM-114 LM-2103 LM-2104
0 5 10 20 40 5 10 20 40 5 10 20 40 μ M
: 30%
100



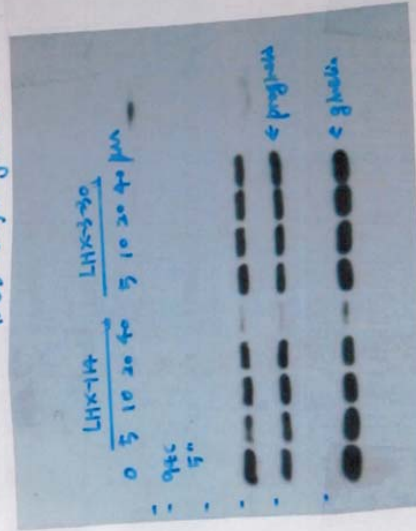
10/18/10-19/14/10

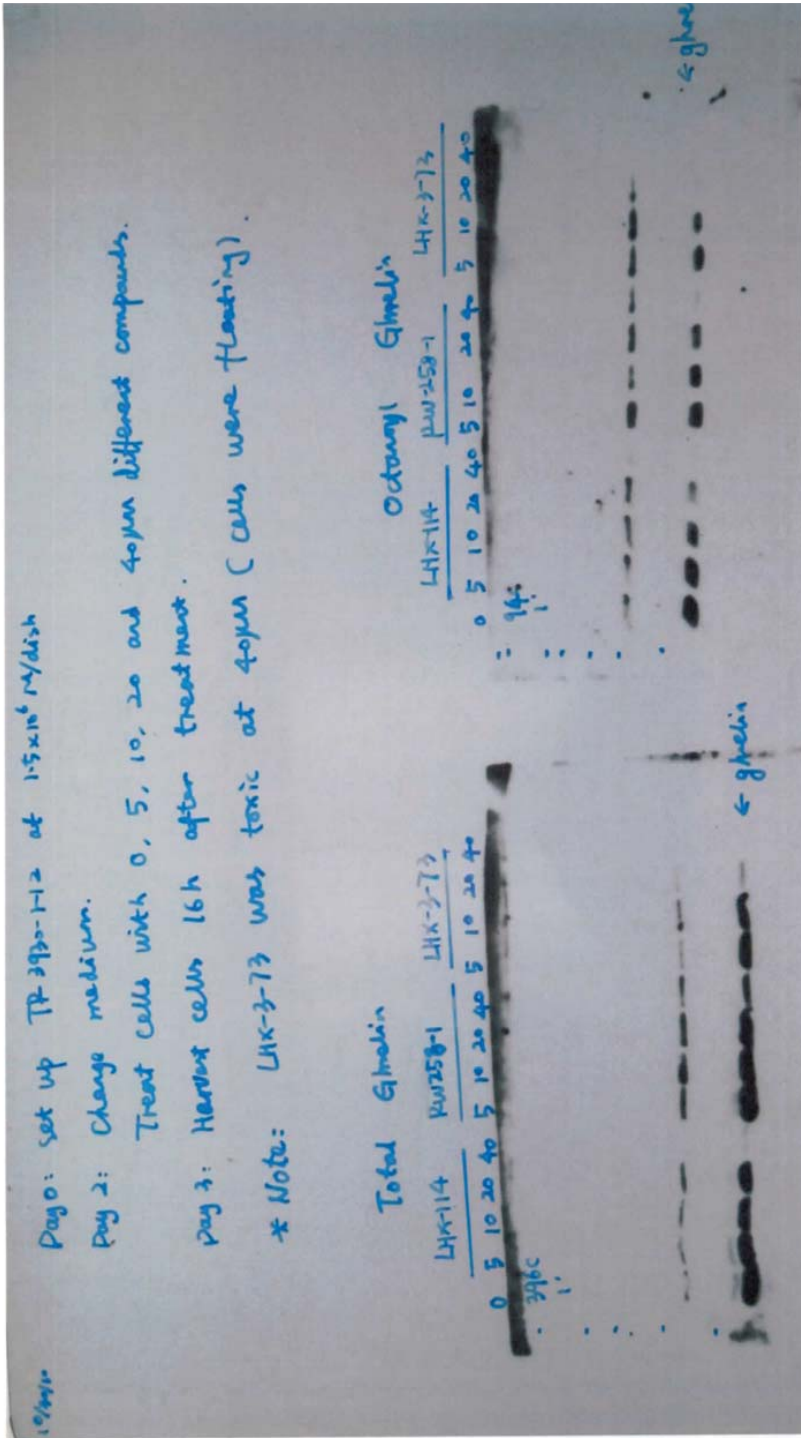
Day 0, Set up T4-3930 CGANT, progesterone in RPM2164 with 10% FCS, 1.5×10^6 cells.
Day 3, change medium.
Treat cells with 0, 5, 10, 20 and 40 μ M LHX-114 or LHX-330.
Day 4, Harvest cells. Peptide extraction.

Octanoyl Ghrelin



Des-acyl ghrelin





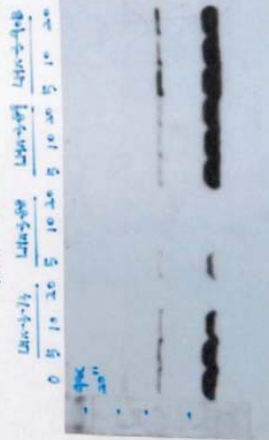
Day 0, set up TH-330-1-2 in Apmite with 12 Fcs. 1.5x10⁶/well.

Day 1, change medium.

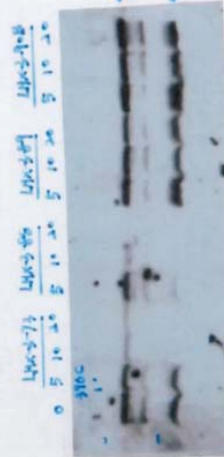
Treat cells with 0, 5, 10 and 20 μM LHX-3-73, LHX-3-80
LHX-3-89 and LHX-3-90b for 16h.

Day 3, Harvest cells.

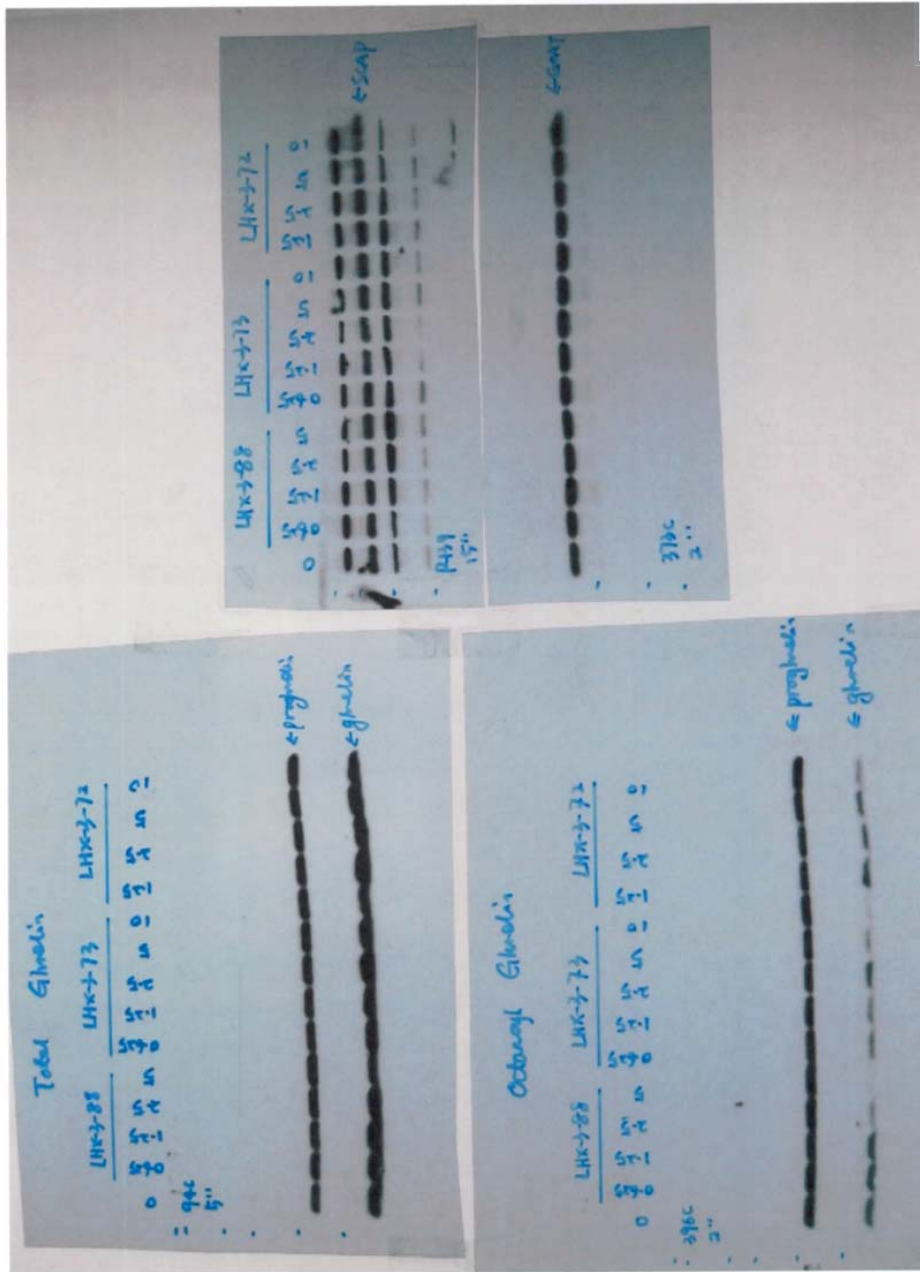
Total Glucan

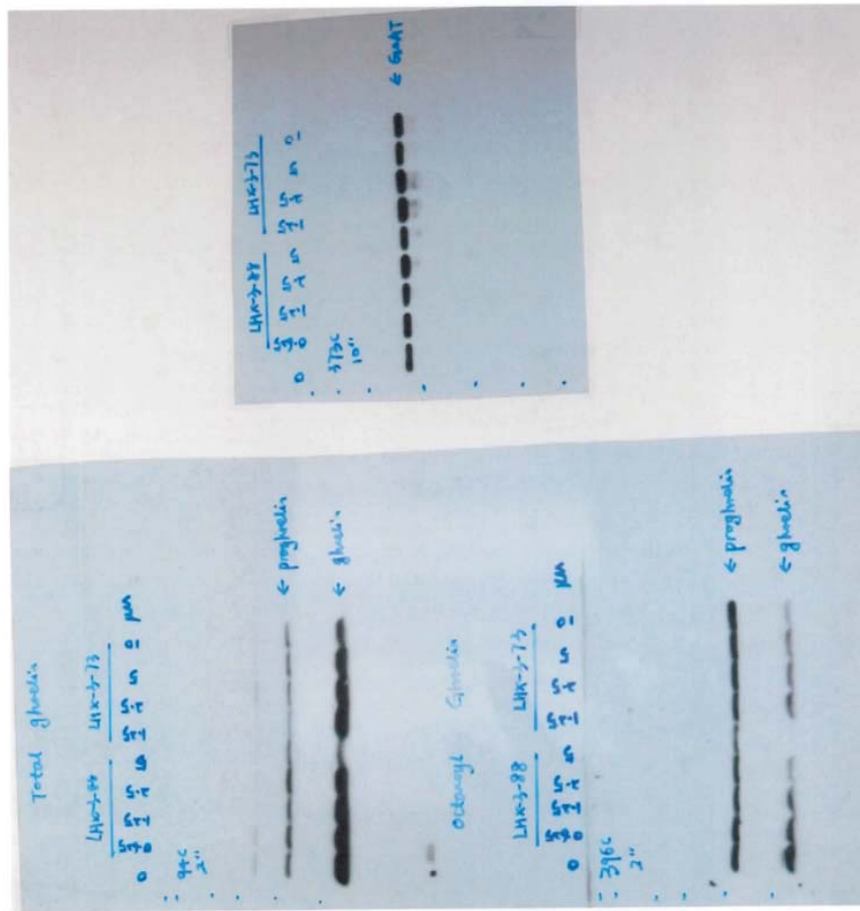


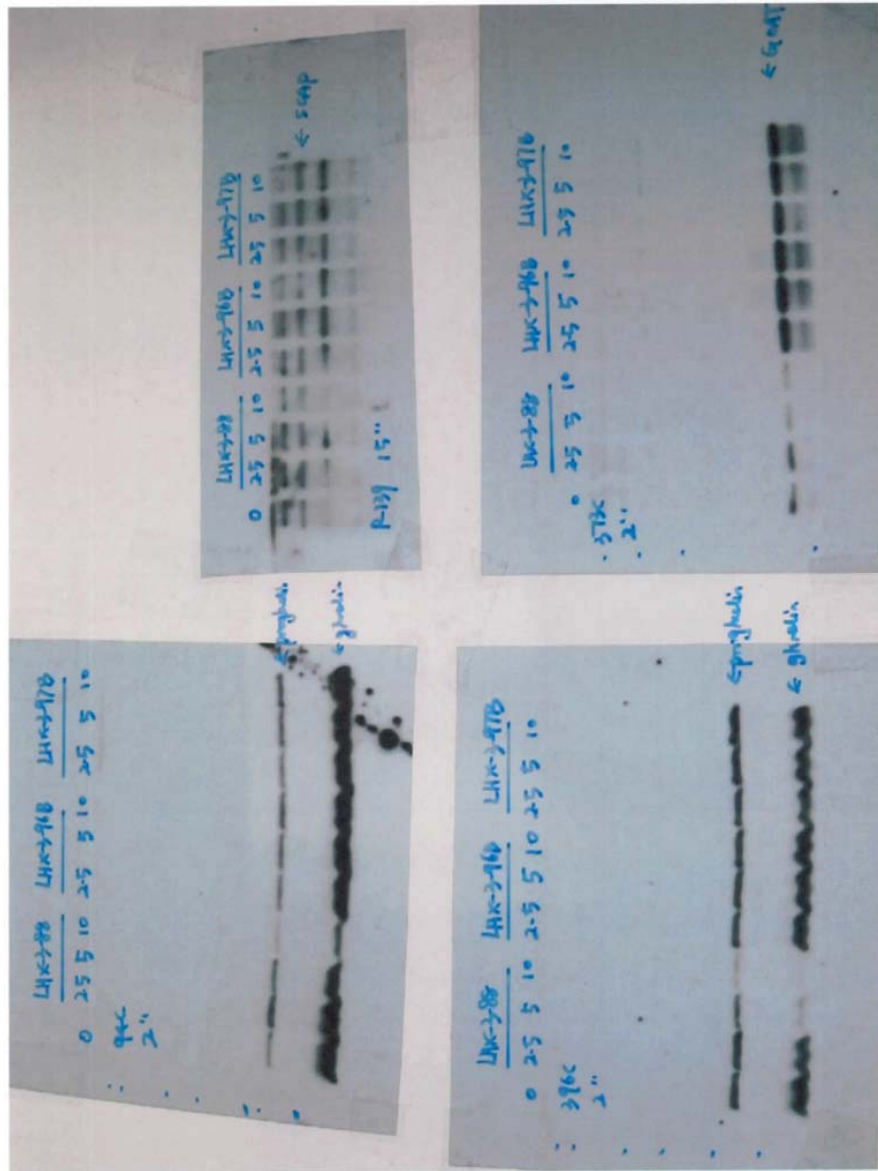
Orthomyl Glucan



* Note: Cells were floccing at 20 μM LHX-3-80.

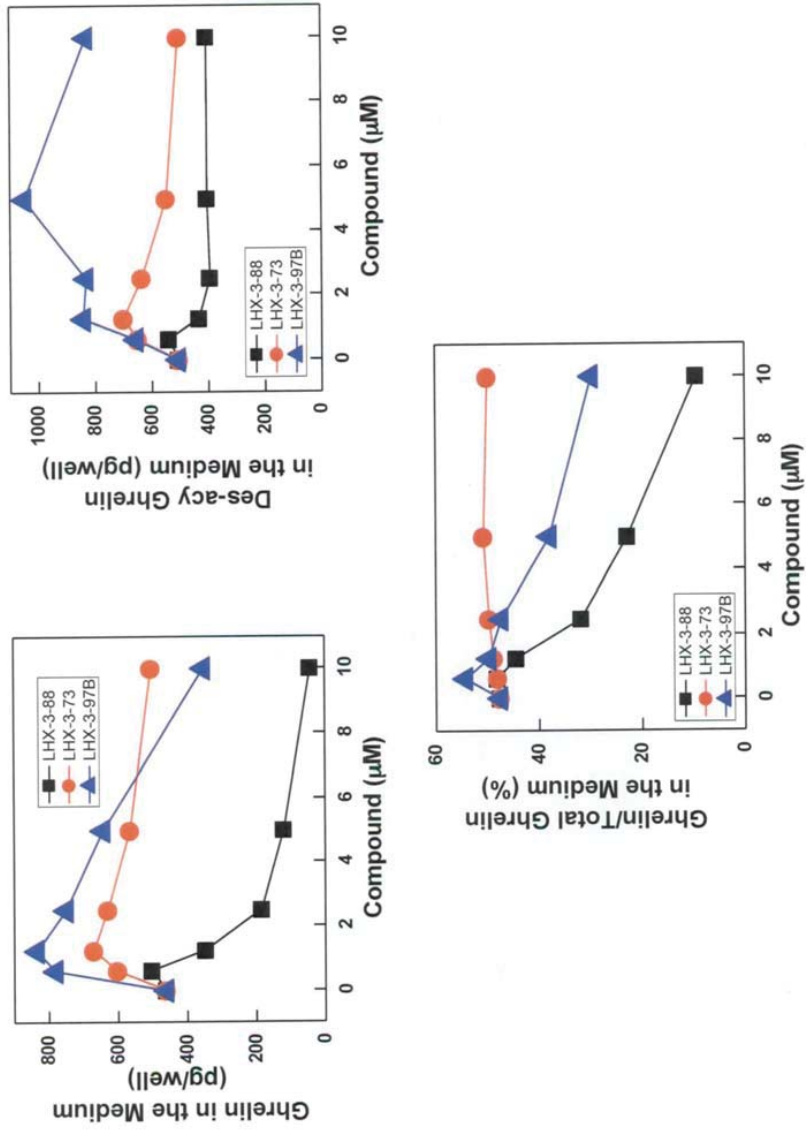






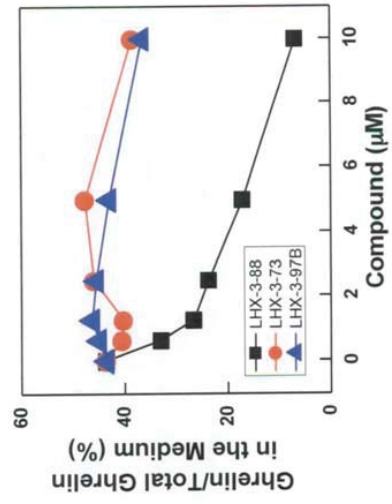
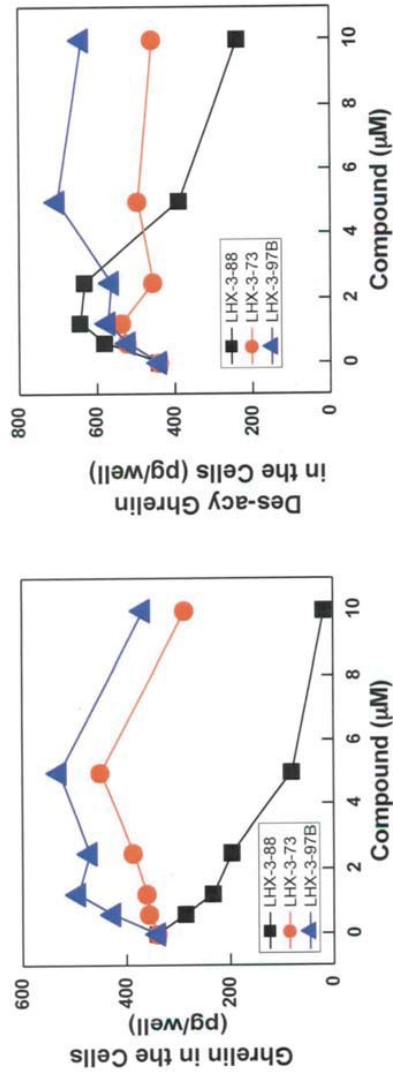
TJ-313

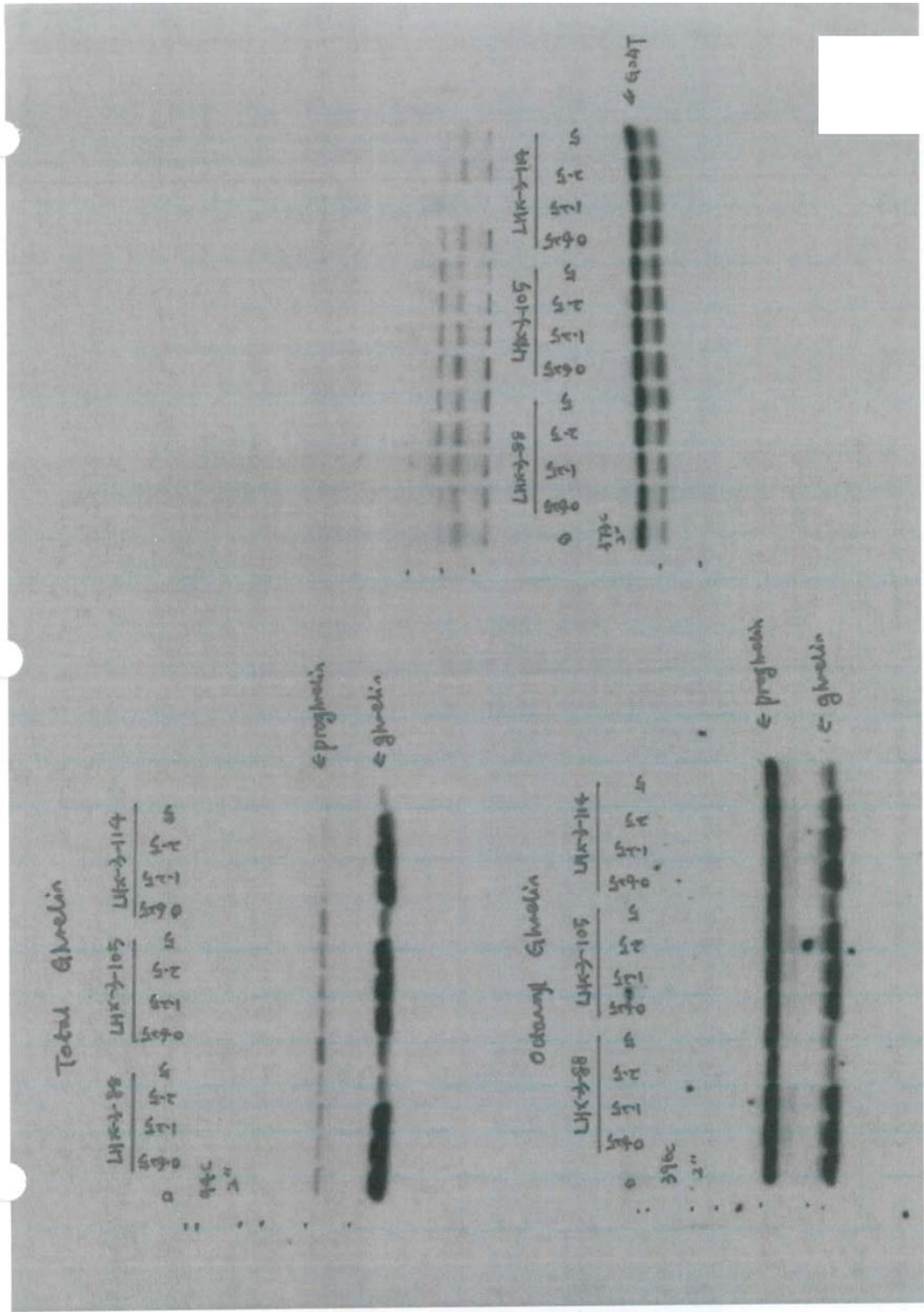
Ghrelin levels in the Medium



TJ-313

Ghrelin levels in the Cells

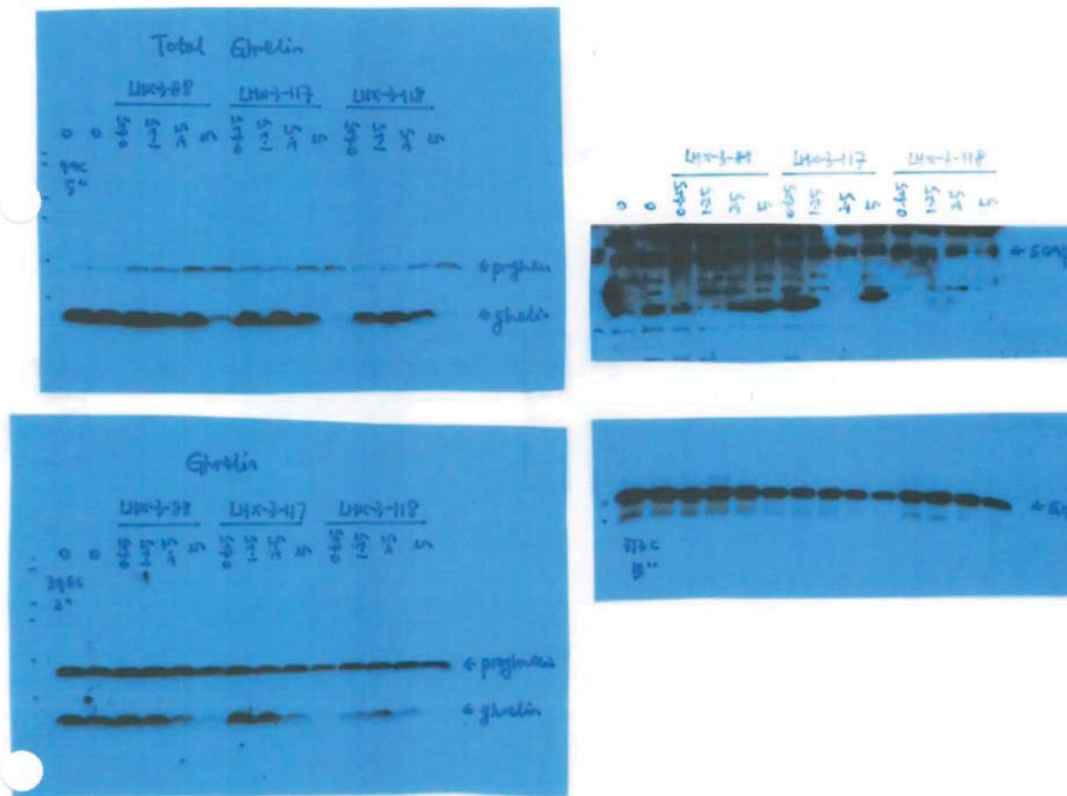




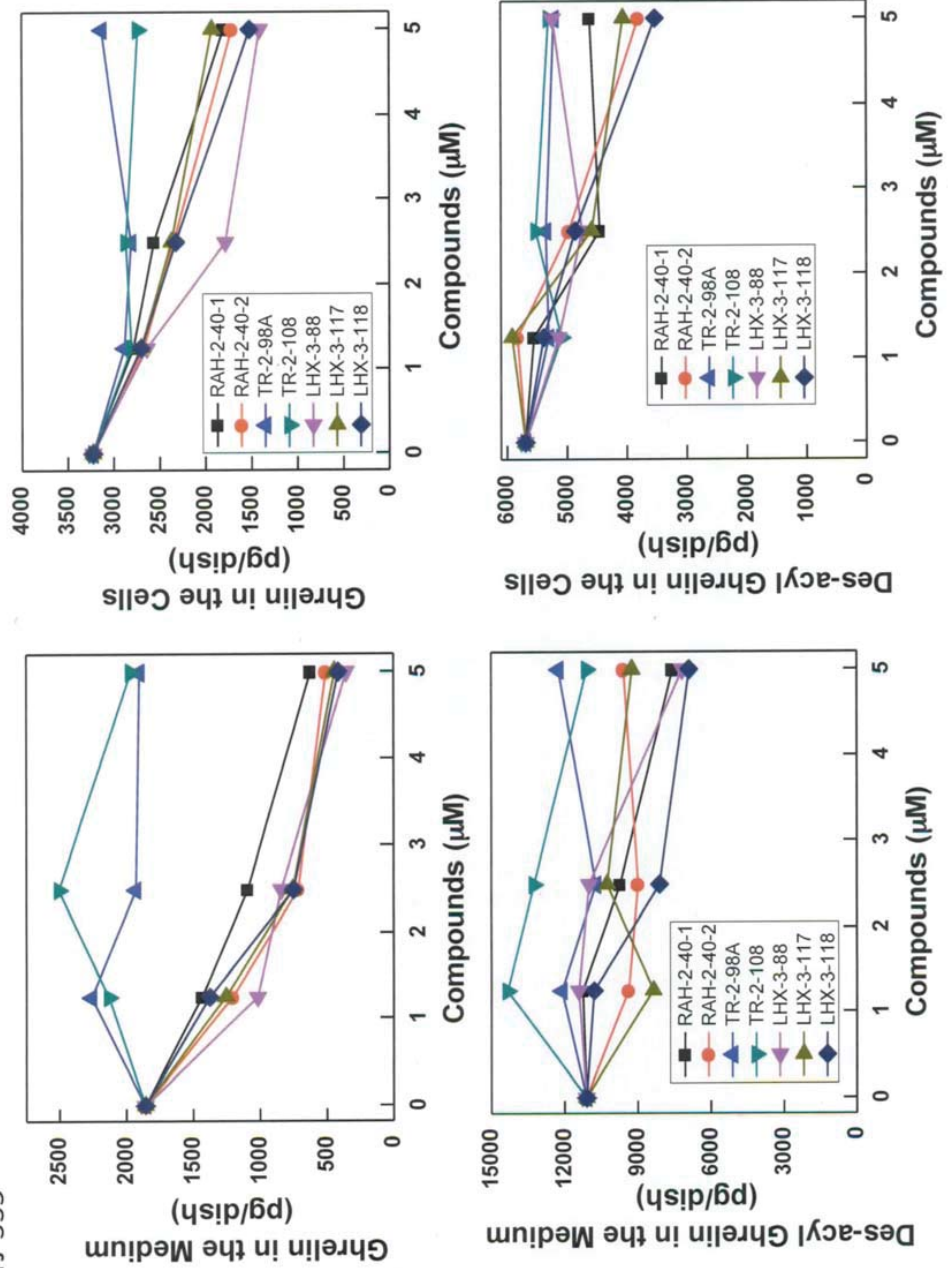
Day 0, Set up TR3930-1-12 cells at 1.5×10^6 cells/dish.

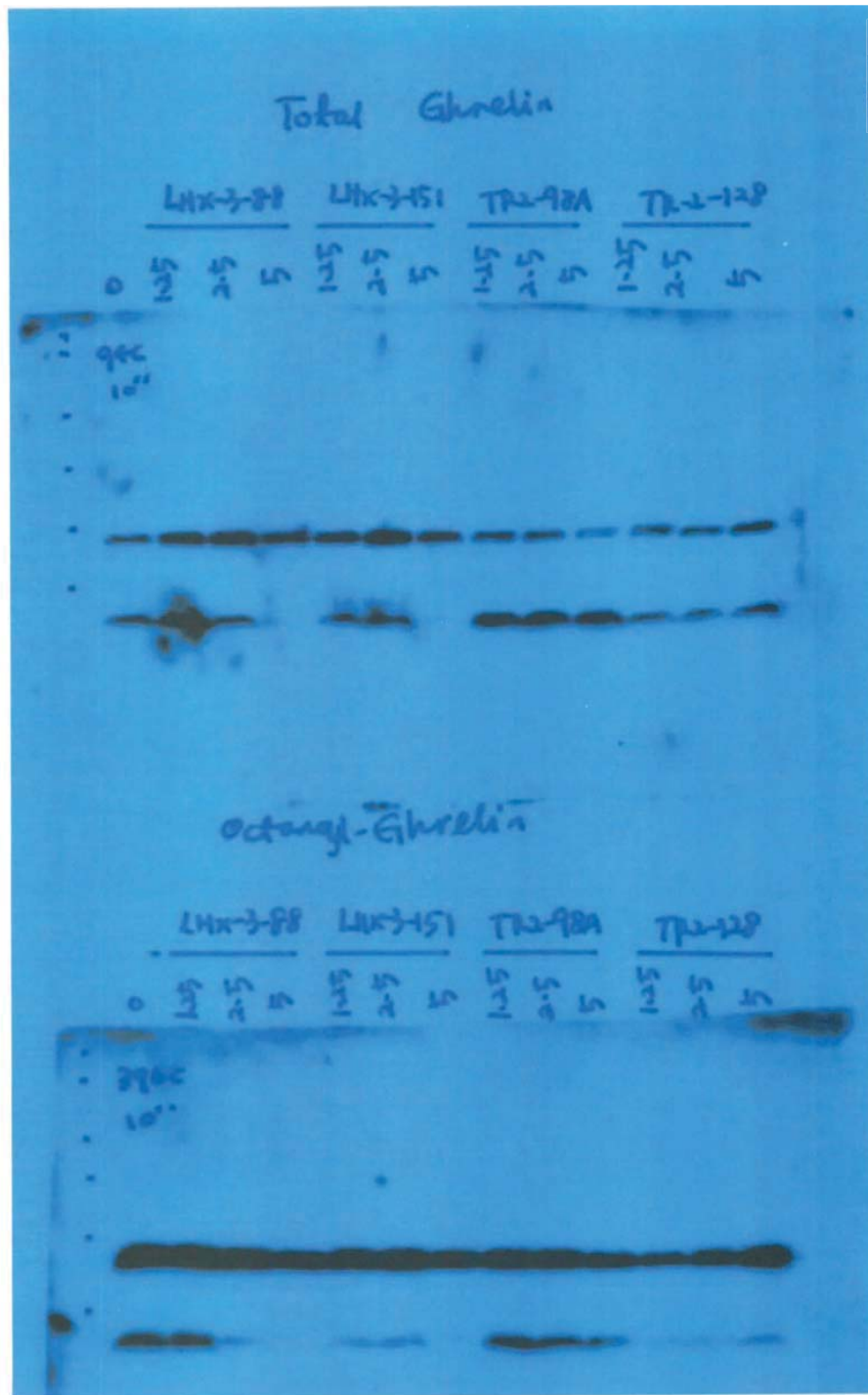
Day 2, change medium. Treat cells with 0, 0.625, 1.25, 2.5, and 5 μ M of
LXR-3-88, 3-117 or 3-118.

Day 3, Harvest cells 16h after treatment.



TJ-335





2/11 - 4/28/11

54 Test RAH-2-20 and RAH-2-22 in IWS-1 cells

Day 0, Set up TR2930-1-12 (GAT-T7, proglucalin) cells at 1.5×10^6 cells/dish.

Day 2, Change medium.

Treat cells with 0, 1.25, 2.5 and 5 μ M of LHX-3-151, or RAH-2-20, or RAH-2-22 or 5, 10 and 20 μ M of TR-2-908.

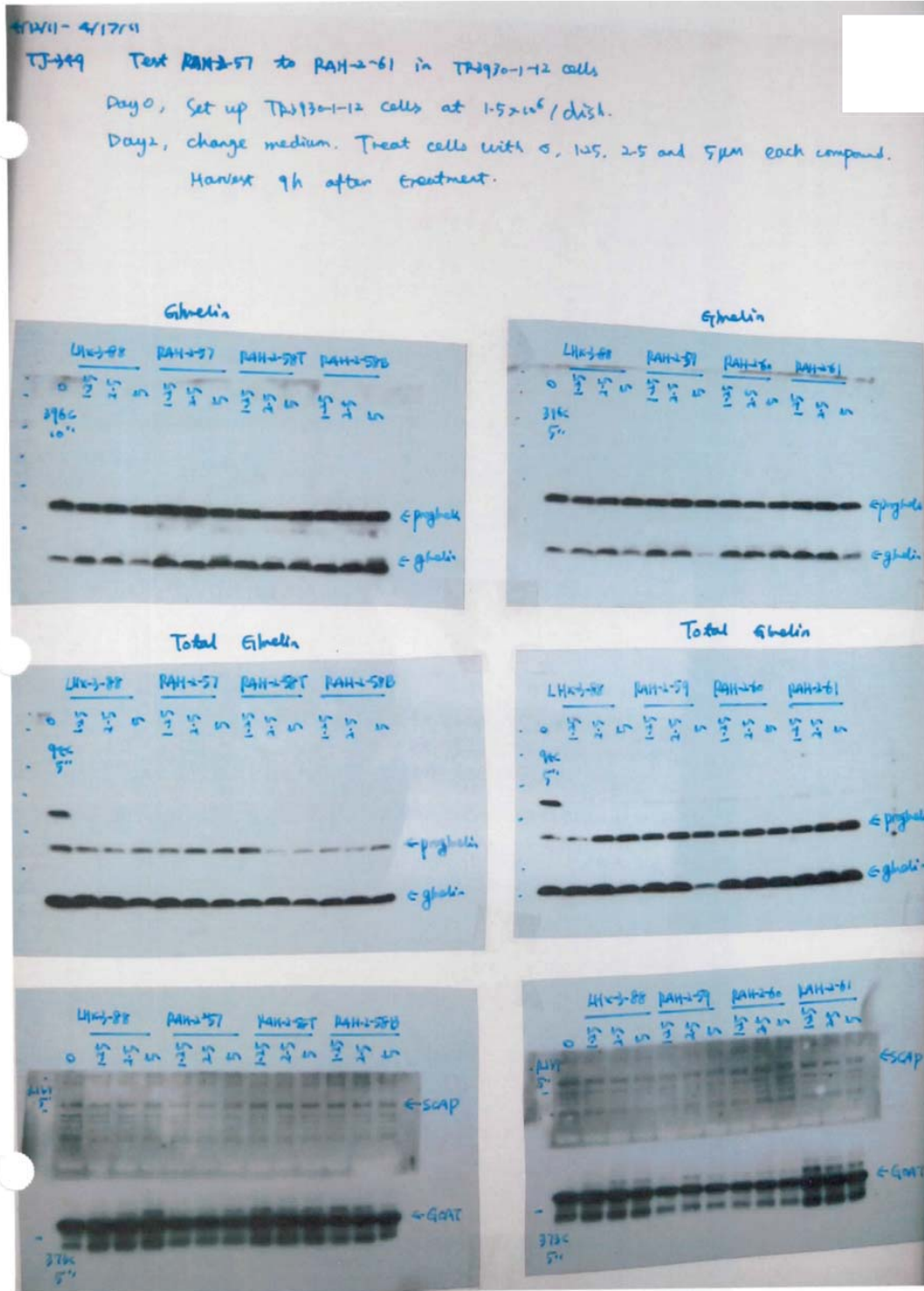
Harvest cells 9h after treatment.

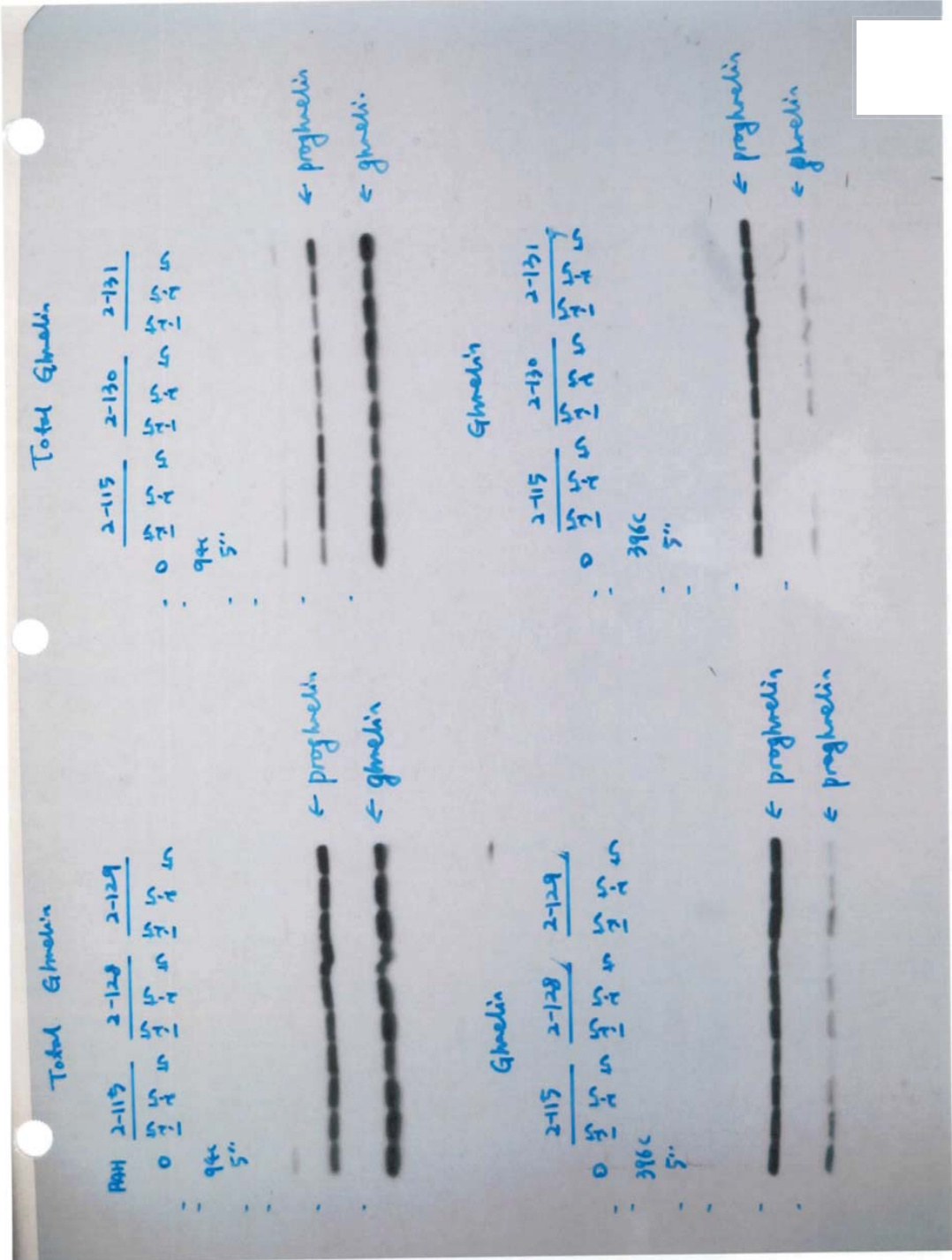
LHX-3-151		RAH-2-20		RAH-2-22		TR-2-908	
0	5	0	5	0	5	0	5
396c							

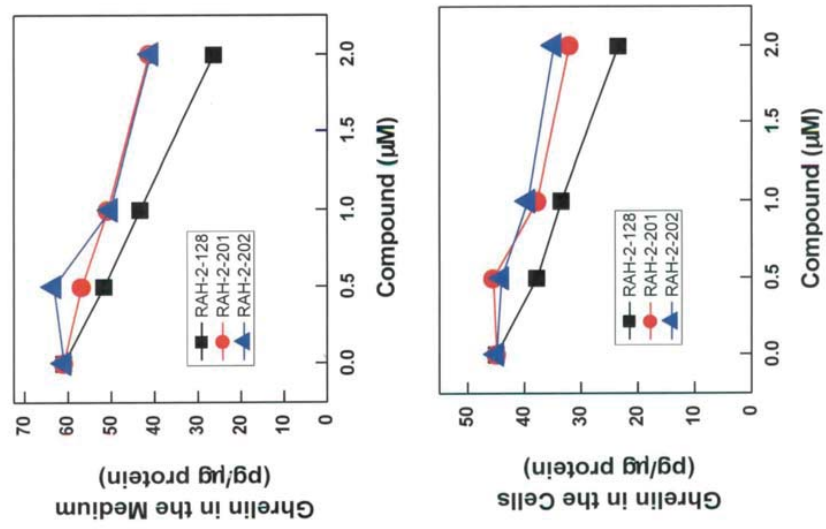
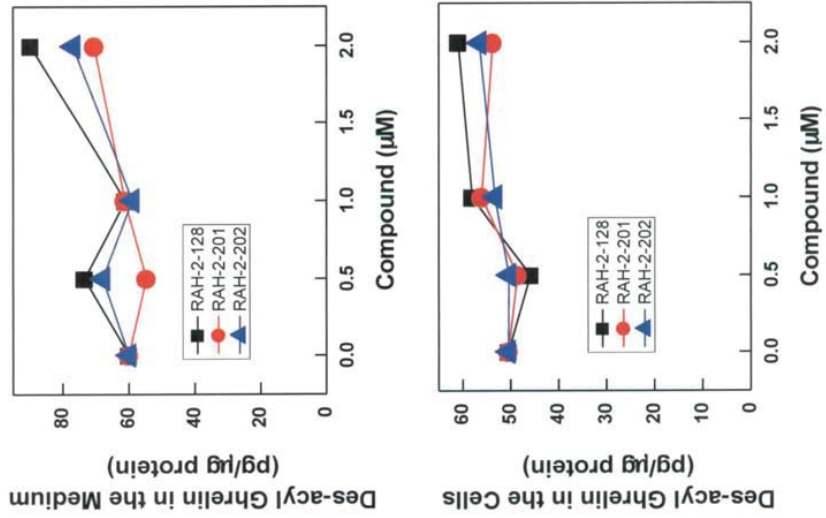
Total Glucalin

LHX-3-151		RAH-2-20		RAH-2-22		TR-2-908	
0	5	0	5	0	5	0	5
98c							

LHX-3-151		RAH-2-20		RAH-2-22		TR-2-908	
0	5	0	5	0	5	0	5
370c							

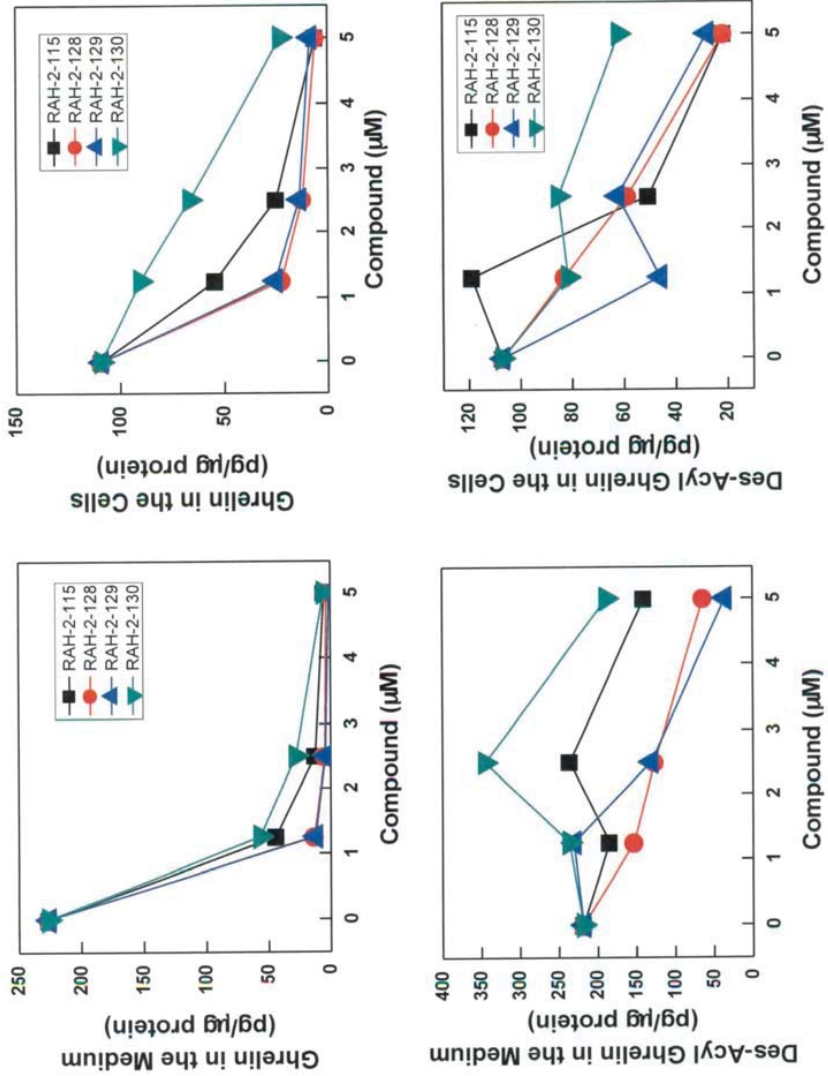




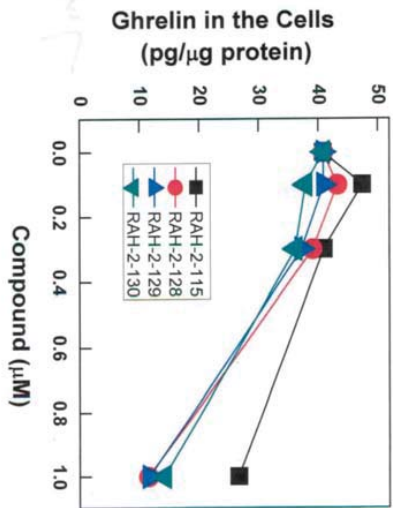
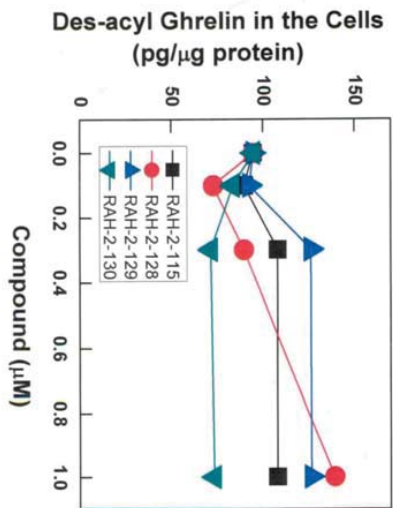
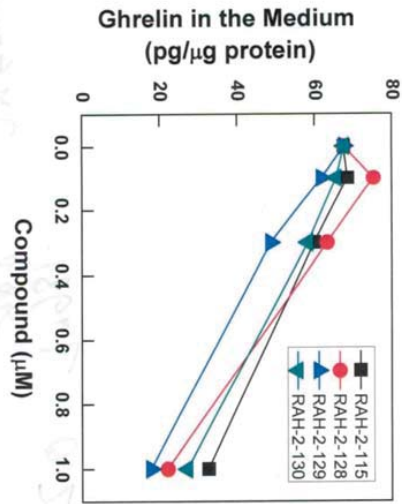
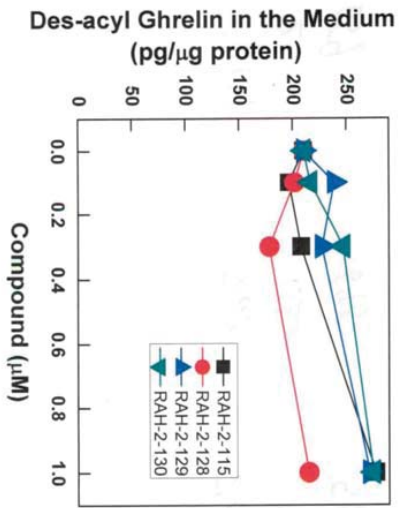


TJ-411

TJ-395



Compounds are toxic to the cells.



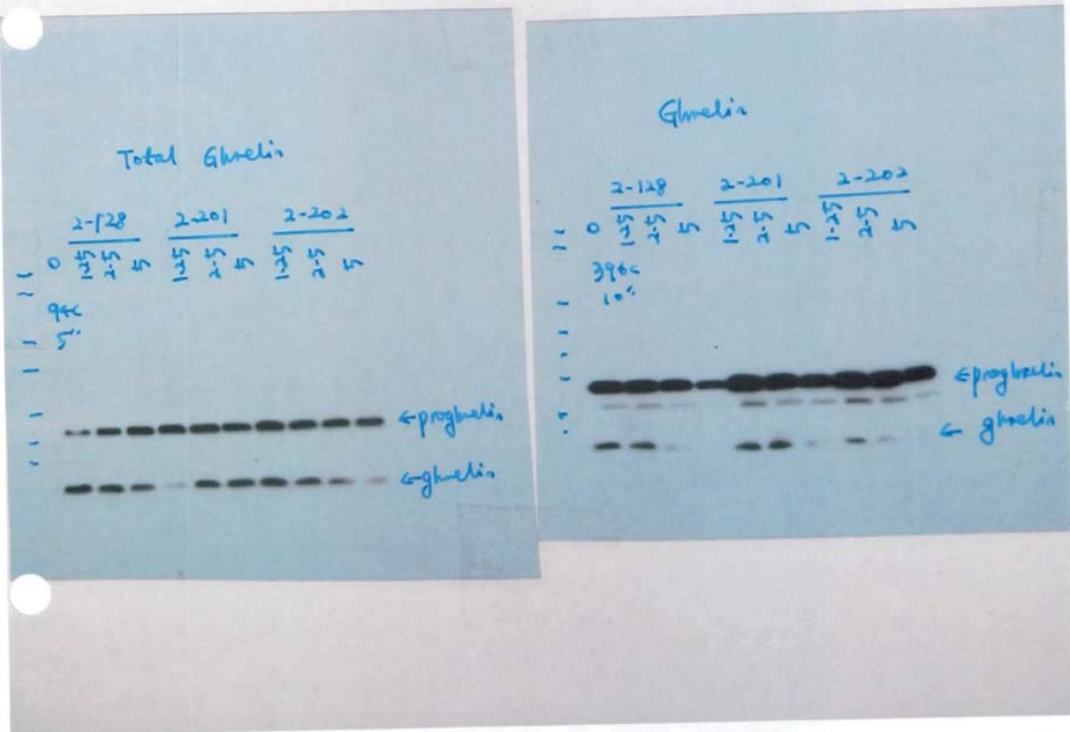
1/12/11
 F-406 Test AAH-2-201, 2-202 in IWS-1 cells

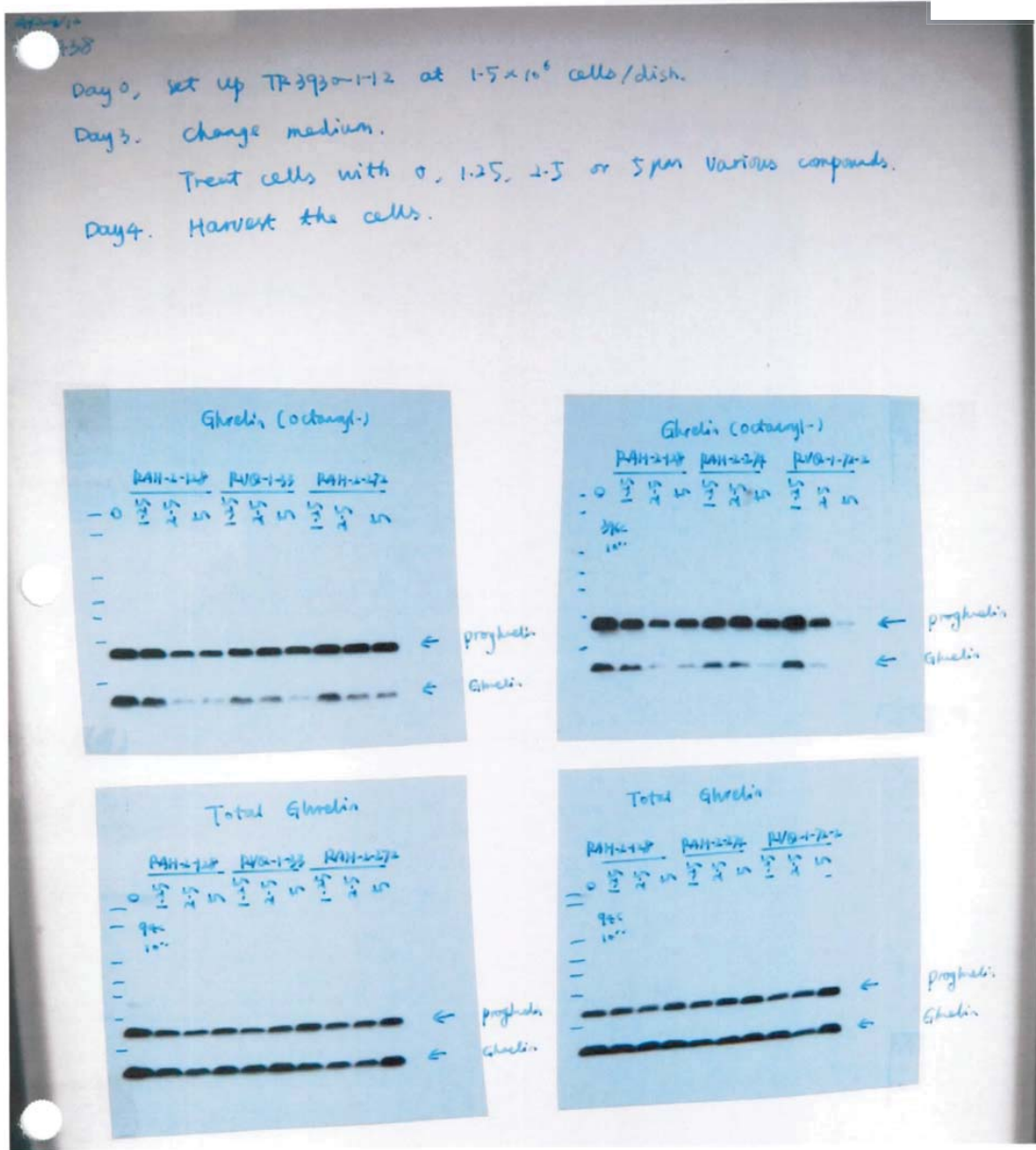
Day 0, set up TA3930-1-12 cells

Day 2, change medium

Treat cells with 0, 1.25, 2.5 and 5 μ M of the indicated compounds

Day 3, Harvest cells.





5/1/12 - 5/7/12

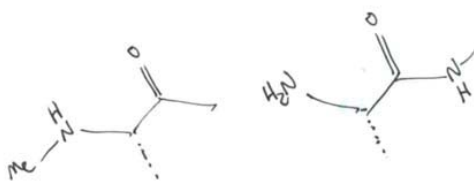
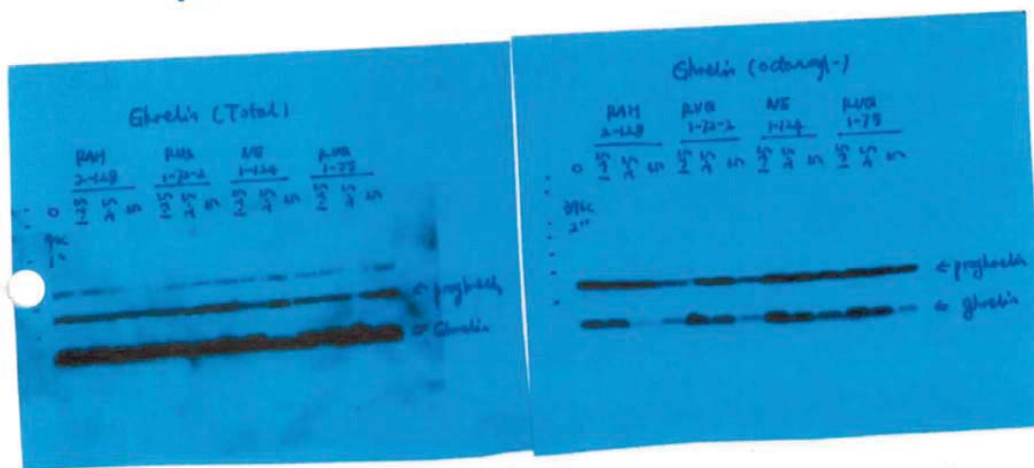
Test NE-1-124 and AVO-1-75 in the IWS-1 cells

Day 0, set up TR-3930-1-12 cells, 1.5×10^6 cells/dish.

Day 3, change medium

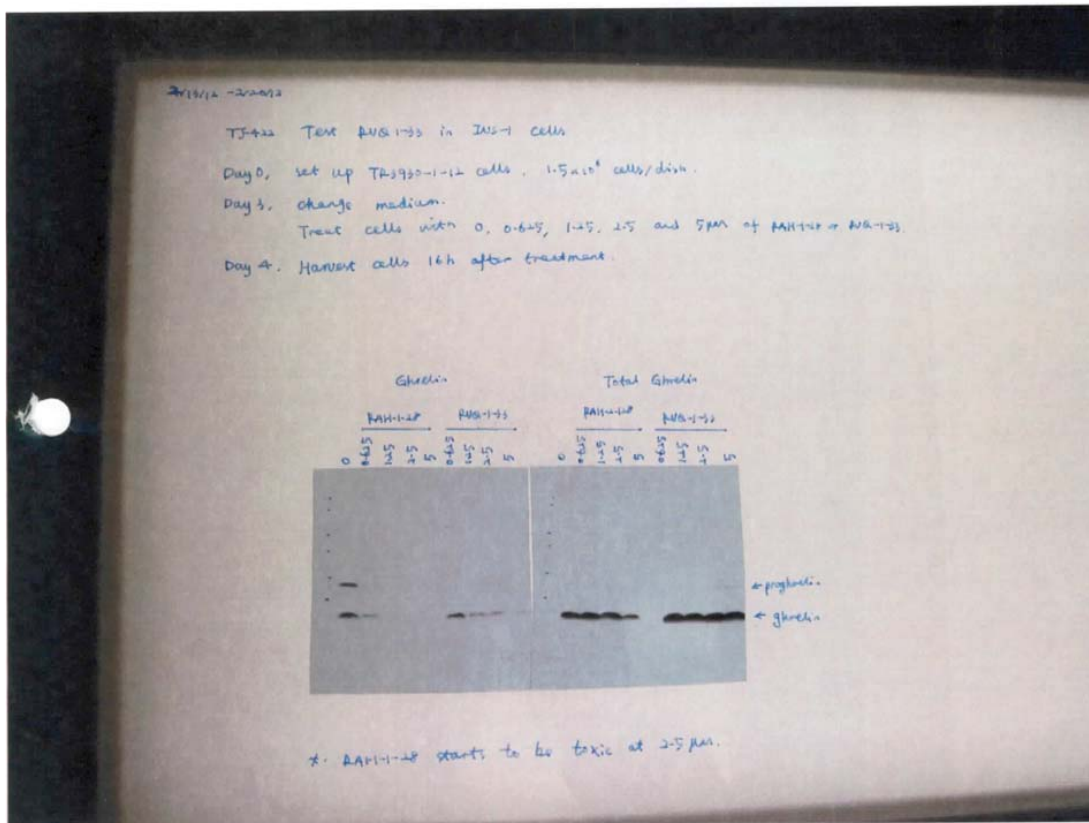
Treat cells with 0, 1.25, 2.5 and 5 μ M of the indicated compounds for 16h.

Day 4, Harvest the cells.



- 5 \downarrow trans \downarrow trans amide
- 5 \downarrow cis \downarrow NMe
- 5 \downarrow cis \downarrow NMe
- 6 tBu NMe
- 6 tBu NMe
- ~~6 tBu NMe~~
- + Ryan

7

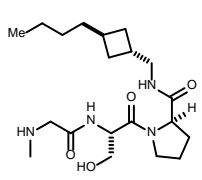


Dr. David Strugatsky Results

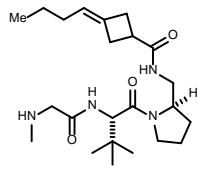
Compound	Structure Page	In Vitro Data Page
Ghrelin 1-28 octanamide		14
BS 1-27	1	1
BS 1-78	1	2
BS 1-120	1	13
BS 1-123	1	13
BS 1-138	1	13
BS 1-149	1	8
BS 1-150	1	8
BS 1-151	1	8
BS 1-152	1	8
Go-CoA-TAT TR2-98A		10
LHX 1'-65	1	21
LHX 1-114	1	21
LHX 3'-88	1	11
RAH 2-109	1	10
RAH 2-274	1	4
RAH 2-277	1	13
RAH 3-64	1	5, 14, 15, 16, 20
RAH 3-131	1	11
RAH 3-163	1	4, 16, 17, 18, 25, 27
RAH 3-181	1	7, 9, 10
RAH 3-209	1	11
RAH 3-285	1	12
RAH 4-40	2	2, 13
RAH 4-84'	2	7
RAH 4-89	2	11
RAH 4-143	2	2
RAH 4-144	2	1
RAH 4-147	2	12
RAH 4-199	2	3

RAH 4-247	2	11
RAH 4-252	2	10, 14
RAH 4-253	2	10
RAH 4-272A	2	15
RAH 4-272B	2	15
RAH 4-277	2	15
RAH 4-278A	2	15
RAH 4-278B	2	15
RAH 4-295-1	2	16
RAH 4-295-2	2	16
RAH 5'-82R	3	17, 18, 19
RAH 5'-85	3	17
RAH 5-98iPR	3	19
RAH 5-98Et	3	19
RAH 5'-99	3	19
RAH 5-101A	3	20
RAH 5-101B	3	20
RAH 5-116	3	21
RAH 5-118A	3	22
RAH 5-118B	3	22
RAH 5-118C	3	22
RAH 5-118D	3	23
RAH 5-118E	3	23
RAH 5-125A	4	25
RAH 5-125B	4	25
RAH 5-131	4	25
RAH 5-142A	4	26
RAH 5-142B	4	26
RAH 5-142C	4	26
RAH 5-142D	4	26
RAH 5-142E2	4	27
RAH 5-142E3	4	27
RAH 5-145	4	27
TKA 1-79	4	3

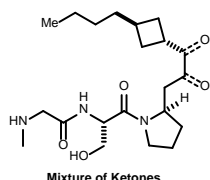
TKA 1-92	4	5
TKA 1-217	4	3, 6
TKA 1-218	4	5, 6
TKA 1-244A	4	6
TKA 1-244B	4	4, 6
TKA 3-195	5	23
TKA 3-196	5	24
TKA 3-197	5	24
TKA 3-198	5	24



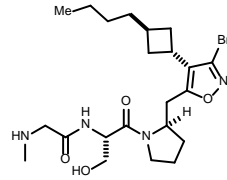
BS 1-27



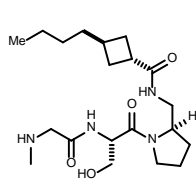
BS 1-78



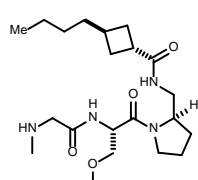
Mixture of Ketones
BS 1-120



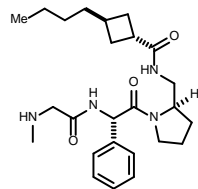
With Regioisomeric isoxazole
BS 1-38



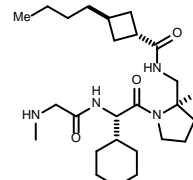
BS 1-150



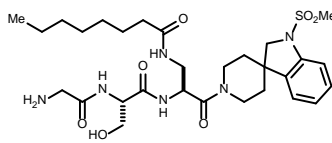
BS 1-151



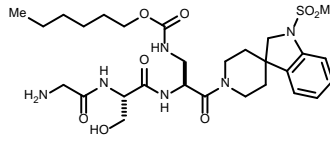
BS 1-149



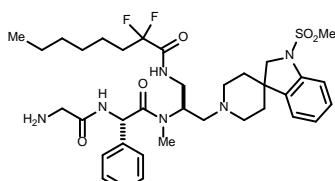
BS 1-152



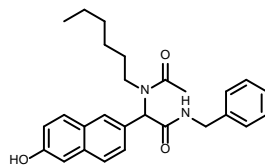
Ihx 1-65



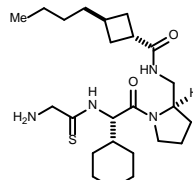
Ihx 1-114



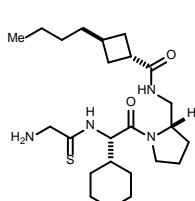
Ihx 3-88



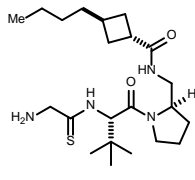
RAH 2-109



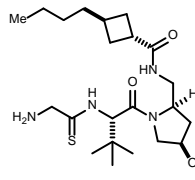
RAH
274



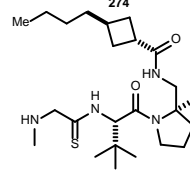
RAH
277



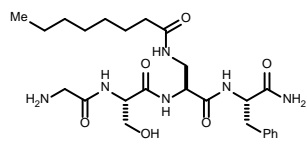
3-64



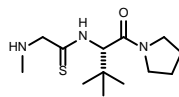
3-131



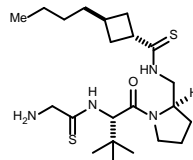
3-163



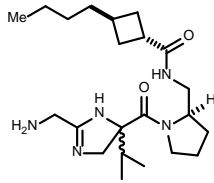
181



3-209

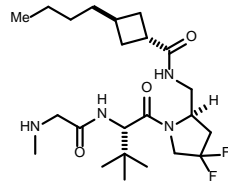


3-285

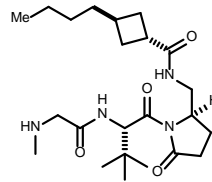


1:1 diastereomers
Unstable

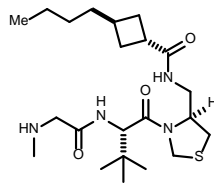
4-40



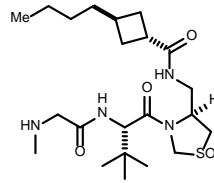
4-84



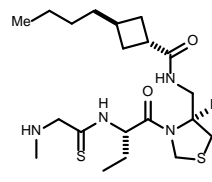
4-89



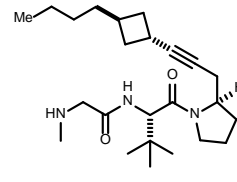
4-143



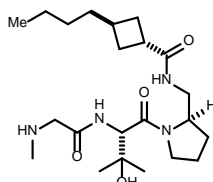
4-144



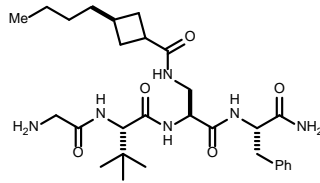
4-147



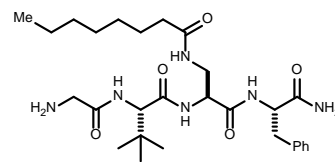
4-199



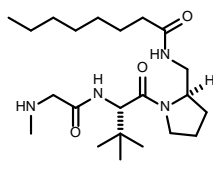
247



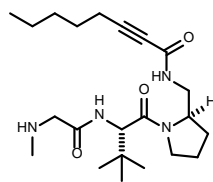
252



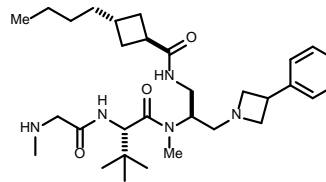
253



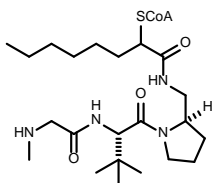
4-272a



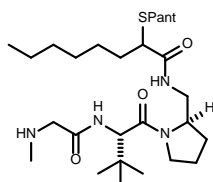
4-272b



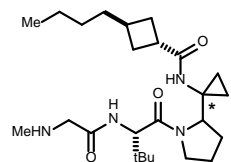
4-277



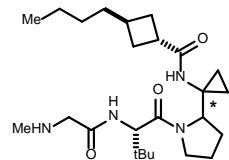
278A



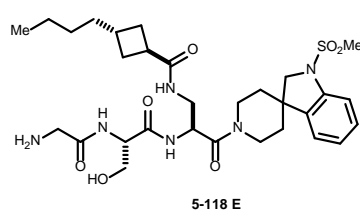
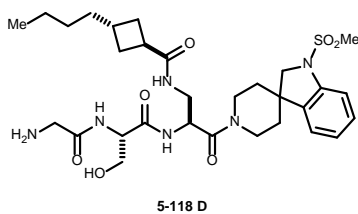
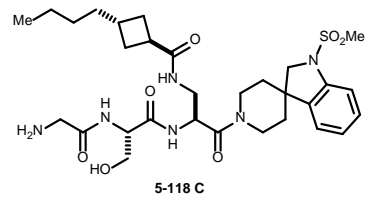
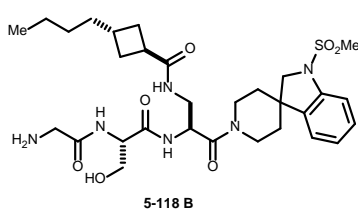
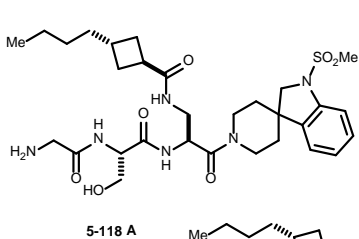
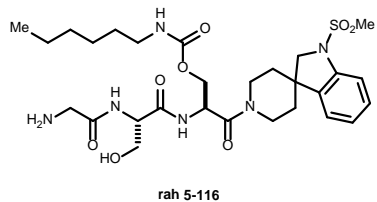
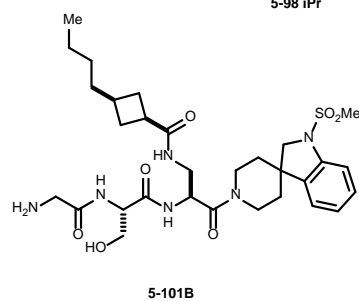
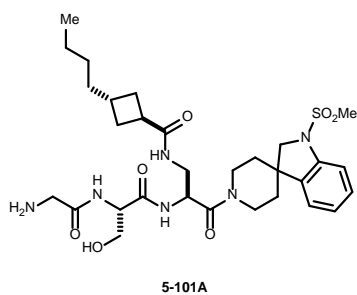
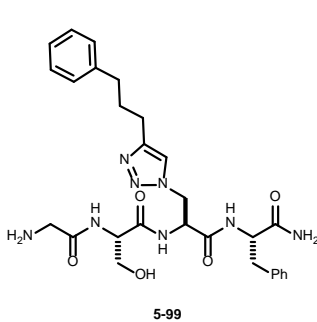
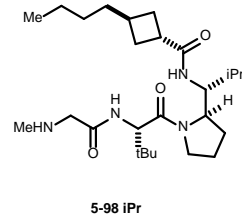
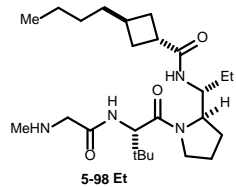
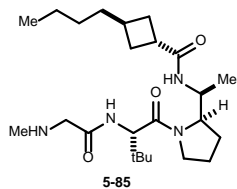
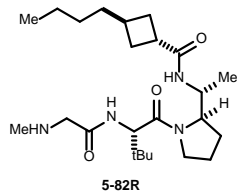
278B

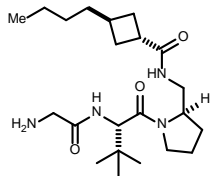


4-295-1

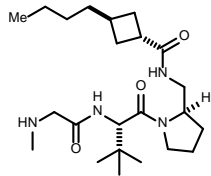


4-295-2

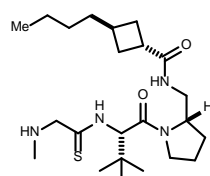




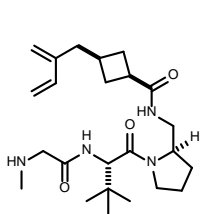
5-125A



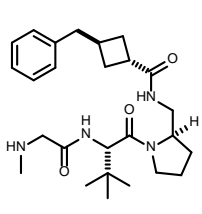
5-125B



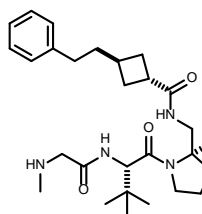
5-131



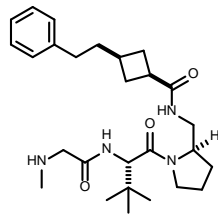
5-142A



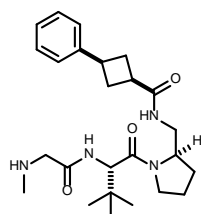
5-142B



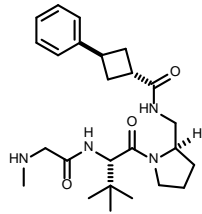
5-142C



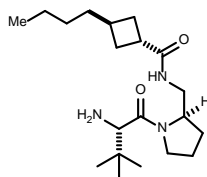
5-142D



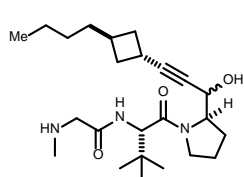
5-142E2



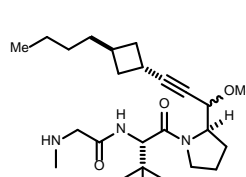
5-142E3



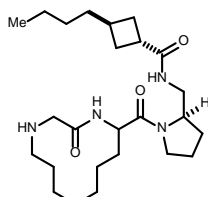
5-145



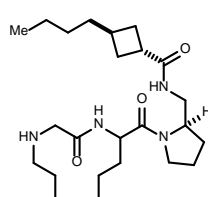
TKA 1-79



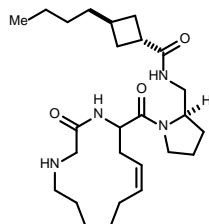
TKA 1-92



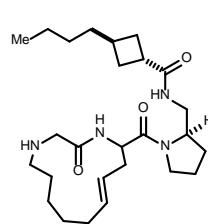
TKA 1-217



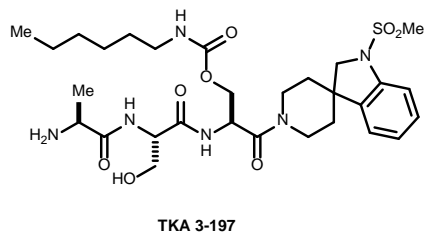
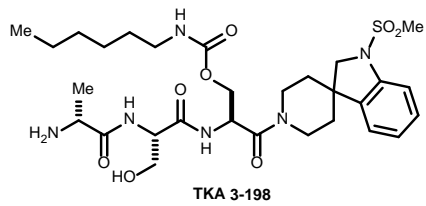
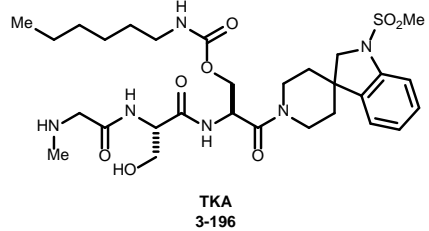
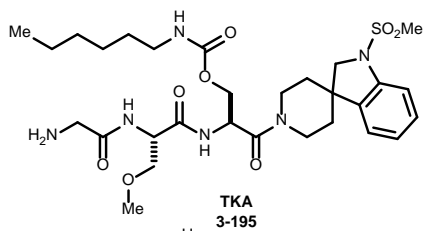
TKA 1-218



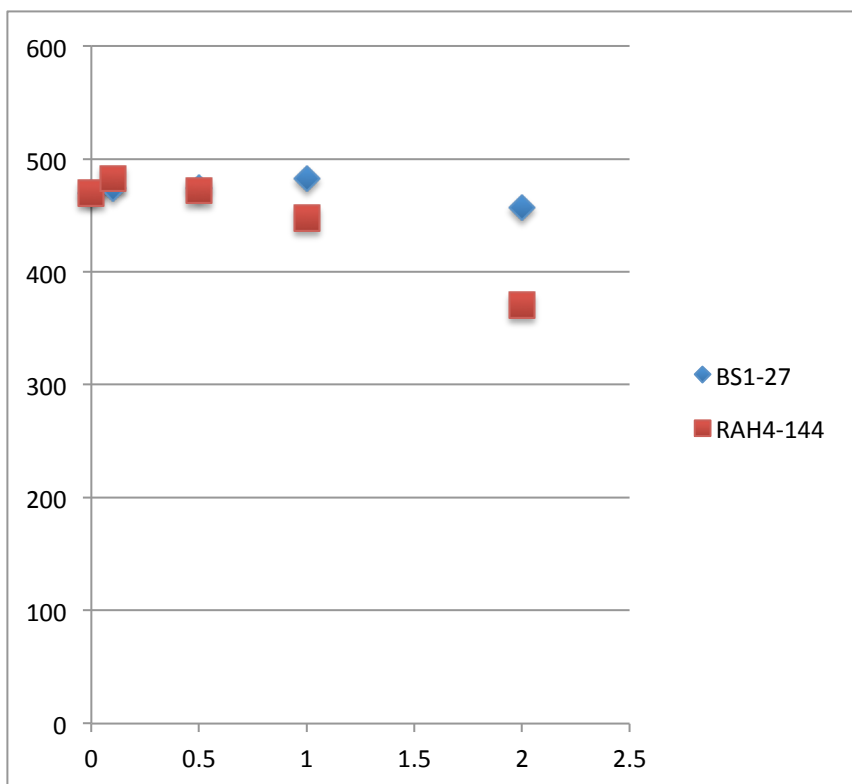
TKA 1-244A/B



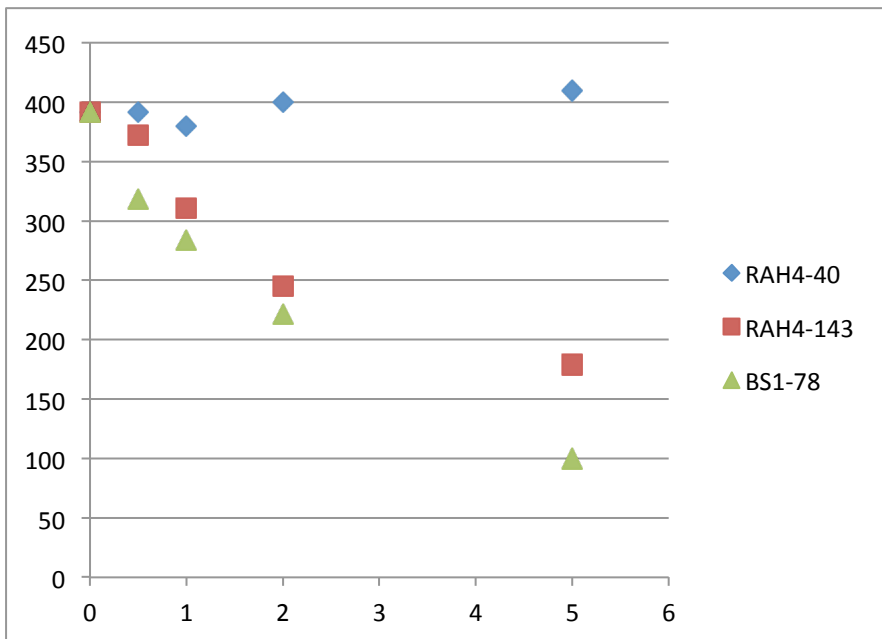
TKA 1-244A/B



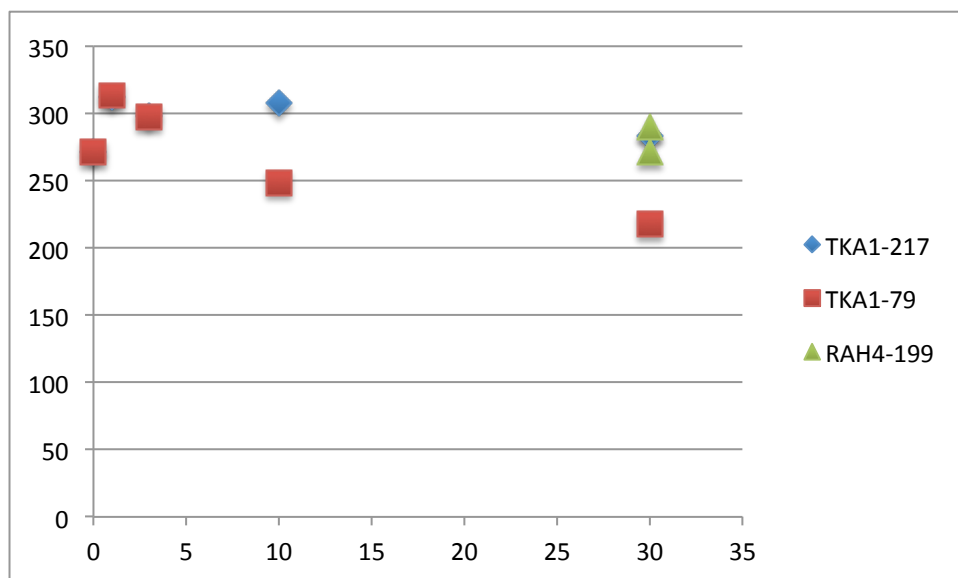
	dpm	fmol	% activity	
control	0	3109	470	100.0
		3255		
BS1-27	0.1	3159	474	100.9
		3263		
BS1-27	0.5	3312	474	100.9
		3108		
BS1-27	1	3146	483	102.7
		3383		
BS1-27	2	3150	457	97.2
		3043		
BS1-27	0.1	3371	483	102.8
		3164		
RAH4-144	0.5	3317	472	100.4
		3074		
RAH4-144	1	2947	448	95.2
		3122		
RAH4-144	2	2796	370	78.8
		2254		



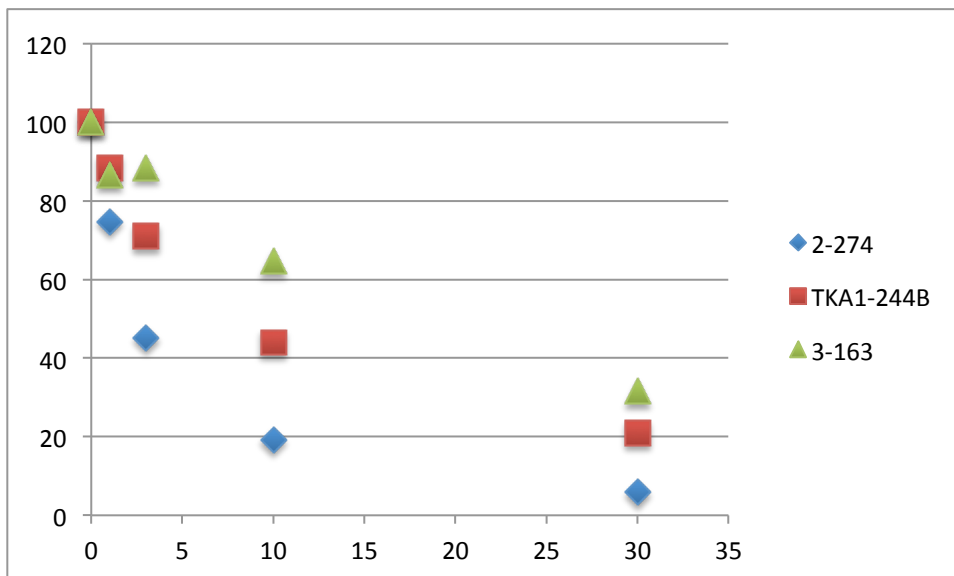
	dpm	avr. Dpm	fmol	fmol	% activity	
RAH4-40	0	2652	2602.5	387	391	100
		2553		372		
	0.5	2672	2606	390	392	100
		2540		370		
	1	2477	2527.5	360	380	97
		2578		376		
	2	2686	2660.5	392	400	102
		2635		384		
	5	2623	2723.5	382	410	105
		2824		413		
RAH4-143	0.5	2451	2472	357	372	95
		2493		363		
	1	2150	2065	311	311	79
		1980		286		
	2	1639	1631	234	245	63
		1623		232		
	5	1264	1189.5	178	179	46
		1115		156		
	0.5	2149	2120.5	311	319	82
		2092		303		
BS1-78	1	1959	1886	283	284	73
		1813		261		
	2	1451	1473.5	206	222	57
		1496		213		
	5	700	665	93	100	26
		630		83		



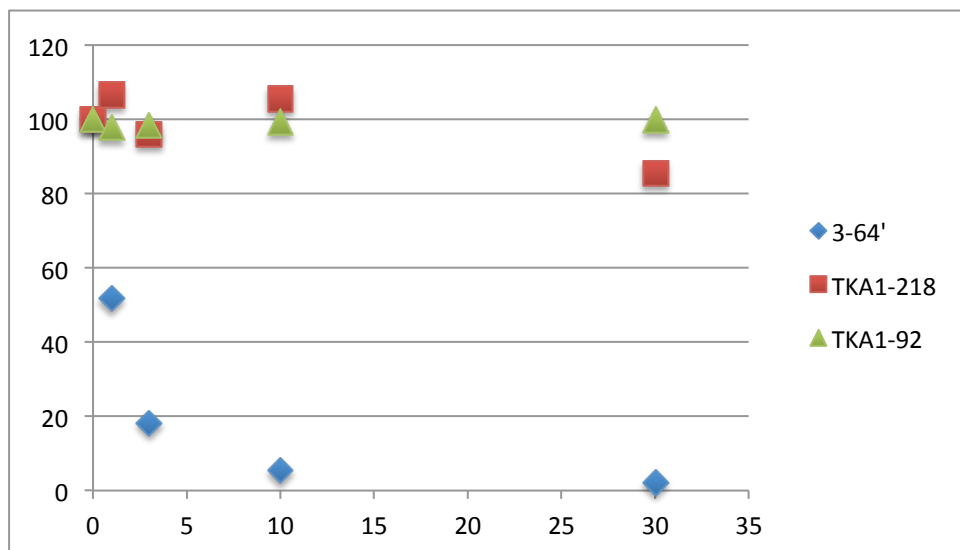
	dpm	fmol	% activity	
control	0	1857	271	100
		1885		
	1	2049	313	115
TKA1-217	3	2021	298	110
		2072		
	10	2253	308	114
		1970		
	30	1817	283	105
	2084			
TKA1-79	1	1996	313	116
		2301		
	3	2049	298	110
		2038		
	10	1860	249	92
	1582			
RAH4-199	30	1474	218	80
		1562		
	1	1974	290	107
		2017		
	3	1770	277	102
	2044			
RAH4-199	10	1839	259	96
		1740		
	30	1821	272	100
		1924		



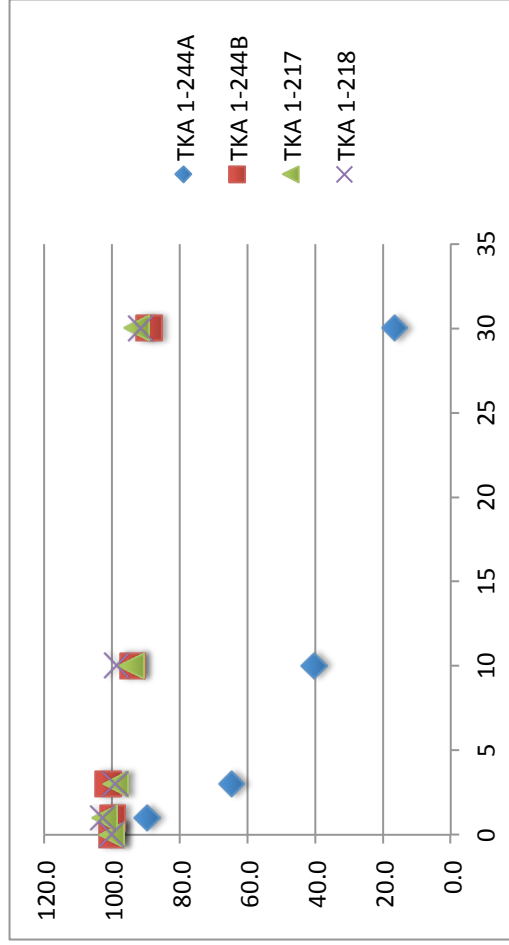
	dpm	fmol	percent activity	
control	0	1465	207	100
		1388		
	1	1042	155	75
2-274		1130		
	3	678	93	45
		694		
	10	324	40	19
		351		
TKA1-244B	30	172	12	6
		147		
	1	1376	183	88
		1163		
	3	1025	147	71
		1044		
	10	579	91	44
	766			
3-163	30	367	44	21
		360		
	1	1345	179	87
		1148		
	3	1249	183	88
	1289			
3-163	10	942	134	65
		956		
	30	460	66	32
	552			



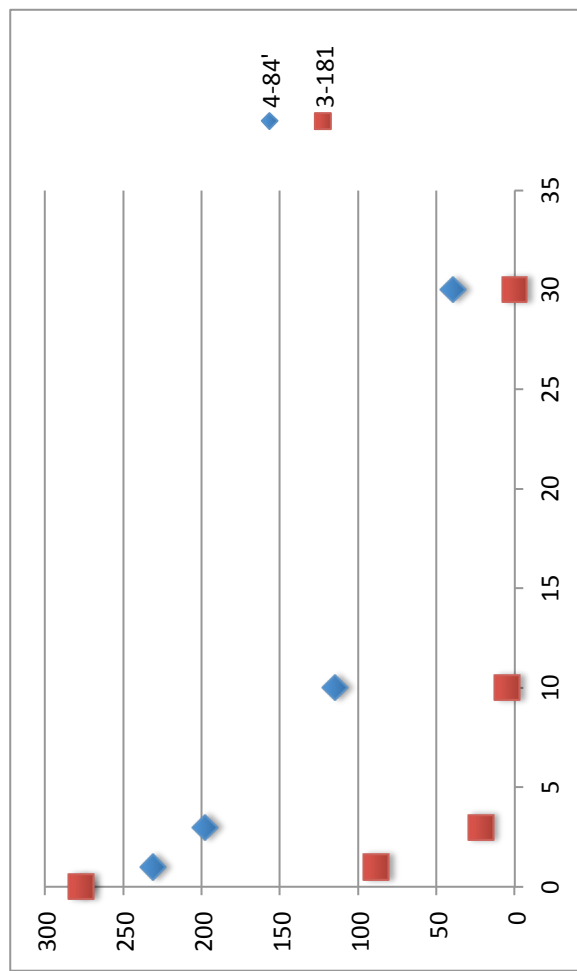
	dpm	fmol	percent activity	
control	0	1299	173	100
		1145		
	1	663	96	52
3-64'		759		
	3	307	34	18
		297		
	10	148	10	5
		142		
TKA1-218	30	99	4	2
		112		
	1	1288	197	107
		1473		
	3	1264	178	96
		1242		
TKA1-92	10	1352	195	106
		1387		
	30	1246	158	86
		1002		
TKA1-92	1	1277	181	98
		1270		
	3	1272	182	98
		1292		
	10	1299	184	99
	1285			
TKA1-92	30	1150	185	100
		1448		



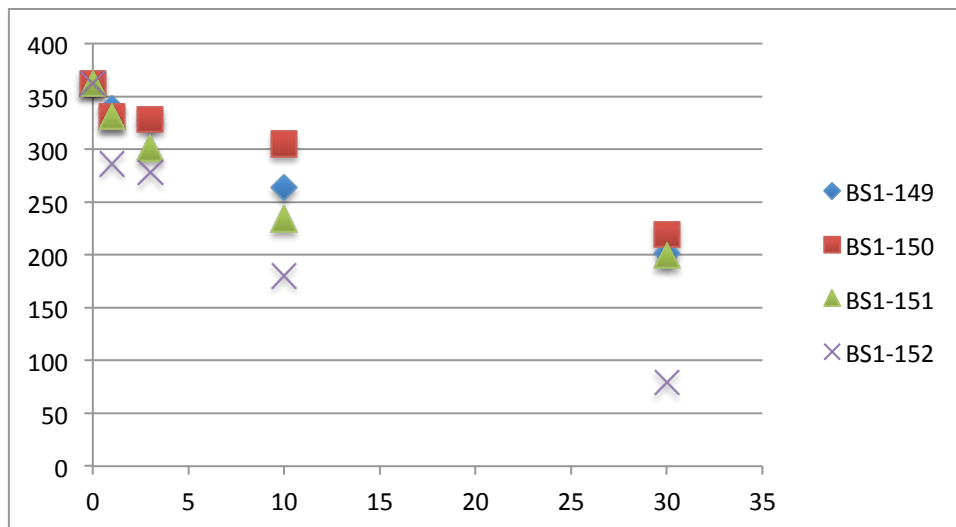
control	dpm	fmol	percent activity
	0	2387	100.0
		2575	
	1	2421	89.6
		2028	
TKA 1-244A	3	1644	64.6
		1564	
	10	984	40.4
		1020	
	30	370	16.6
		452	
	1	2327	99.8
		2624	
	3	2435	101.2
		2586	
TKA 1-244B	10	2245	94.1
		2423	
	30	2090	89.1
		2330	
	1	2400	102.1
		2666	
	3	2501	98.9
		2408	
TKA 1-217	10	2209	94.4
		2475	
	30	2300	92.6
		2295	
	1	2499	102.8
		2605	
	3	2403	99.0
		2509	
TKA 1-218	10	2460	98.6
		2436	
	30	2252	91.4
		2285	



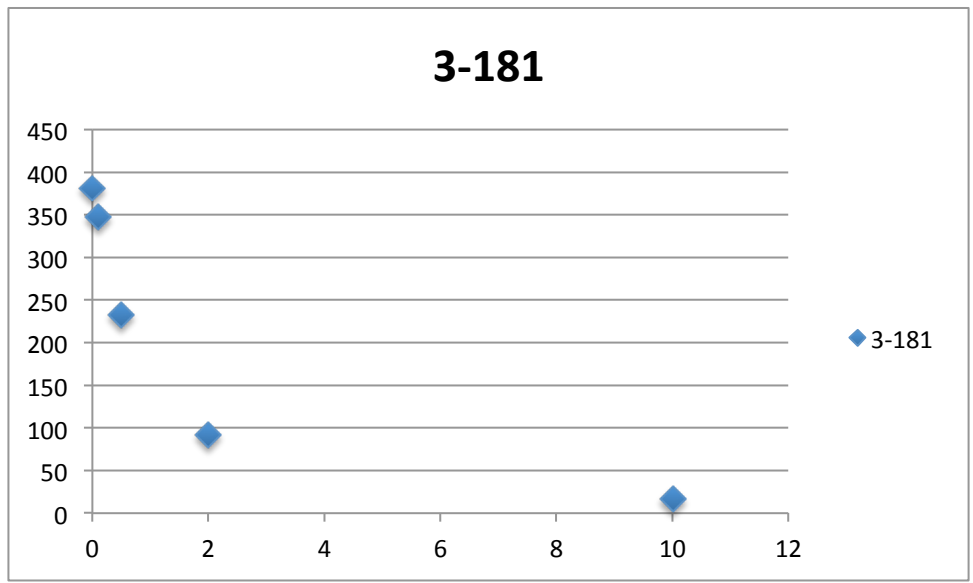
control	dpm	fmol	% activity
	0	1876	100
	1	1935	
	3	1596	83
	10	1616	
4-84'	3	1388	71
	10	1378	
	30	856	41
	1	818	
	3	341	14
	10	339	
	30	635	32
	1	693	
	3	220	8
	10	227	
	30	90	2
baseline	30	137	0
		89	0
		73	0
		83	0
sf9 mGOAT		287	
sf9 control		12	



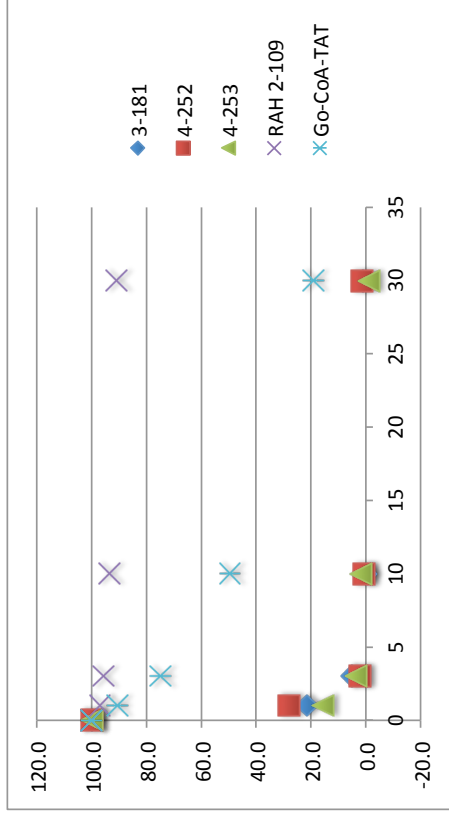
	dpm	fmol	avr fmol	% activity	
control	0	2531	371	363	100
		2418	354		
	1	2440	358	339	93
BS1-149	3	2194	320		
		2301	337	327	90
	10	2181	318		
		1864	270	264	73
	30	1776	257		
		1438	206	201	55
BS1-150	1	1380	197		
		2222	325	331	91
	3	2307	337		
		2180	318	329	91
	10	2320	339		
		2111	308	305	84
BS1-151	30	2072	302		
		1622	234	220	60
	1	1436	205		
		2324	340	331	91
	3	2207	322		
		1811	262	301	83
BS1-151	10	2325	340		
		1674	242	234	64
	30	1573	226		
		1441	206	200	55
	1	1357	193		
		2175	317	286	79
BS1-152	3	1765	255		
		1888	274	278	77
	10	1943	282		
		1180	167	180	50
	30	1355	193		
		622	82	79	22
		581	76		



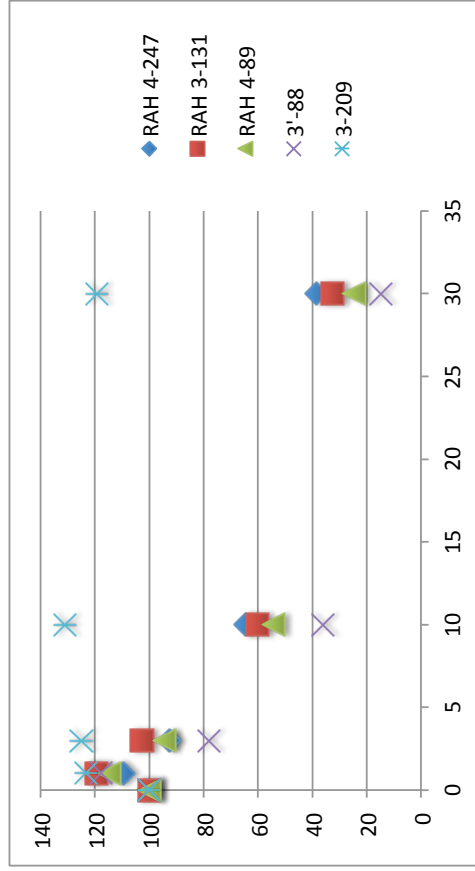
	dpm1	dpm2	famol	
3-181	0	2423	2610	381
	0.1	2328	2254	347
	0.5	1558	1512	233
	2	624	590	92
	10	114	106	17



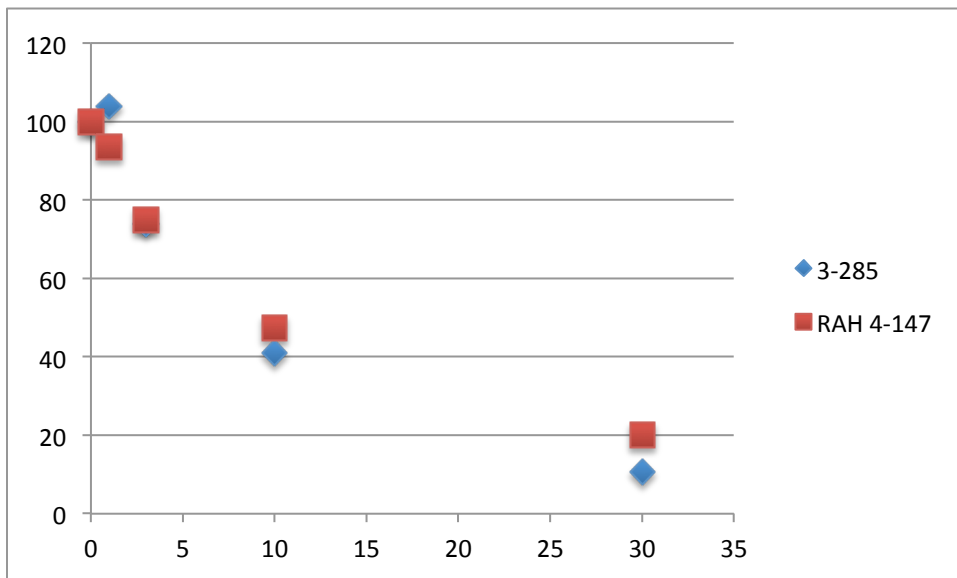
	dpm	avr	% activity	IC50
	0	1523 1555	100.0	
	1	377 407	21.4	
	3	156 147	4.9	
3-181	10	81 71	-0.3	0.24
	30	72 122	1.2	
	1	512 471	28.2	
	3	90 134	2.2	
4-252	10	95 86	0.7	0.32
	30	87 113	1.4	
	1	302 317	15.7	
	3	140 123	3.5	
35	10	93 120	1.8	0.17
4-253	30	64 67	-1.0	
	1	1485 1504	96.9	
	3	1477 1480	95.9	
RAH 2-109	10	1465 1426	93.6	
	30	1536 1276	90.9	
	1	1441 1364	90.6	
	3	1236 1106	74.8	
Go-CoA-TAT	10	847 763	49.7	8.9
	30	401 315	19.1	



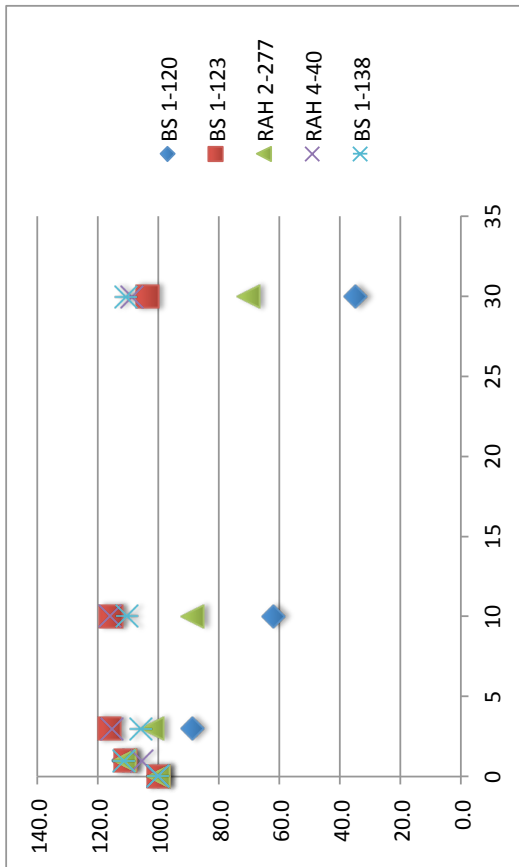
control	dpm	avr	% of activity IC50
	0	2023	100
	1	1748	109
	3	1633	92
	10	2015	65
	30	1912.5	39
RAH 4-247	1	1677	119
	3	1715	103
	10	1616	60
	30	1129.5	32
	1	1148	115
	3	755	94
	10	2300	54
	30	2037	25
RAH 3-131	1	1860	118
	3	1794	78
	10	1888	36
	30	1080	15
	1	1179	124
	3	769	125
	10	527	131
	30	2066	119
RAH 4-89	1	2098	119
	3	1711	119
	10	1750	119
	30	995	119
	1	1057	119
	3	482	119
	10	540	119
	30	2051	119
3'-88	1	2235	119
	3	1507	119
	10	1383	119
	30	730	119
	1	695	119
	3	316	119
	10	357	119
	30	2233	119
3-209	1	2247	119
	3	2206	119
	10	2323	119
	30	2425	119
	1	2316	119
	3	2213	119
	10	2084.5	119
	30	2116	119



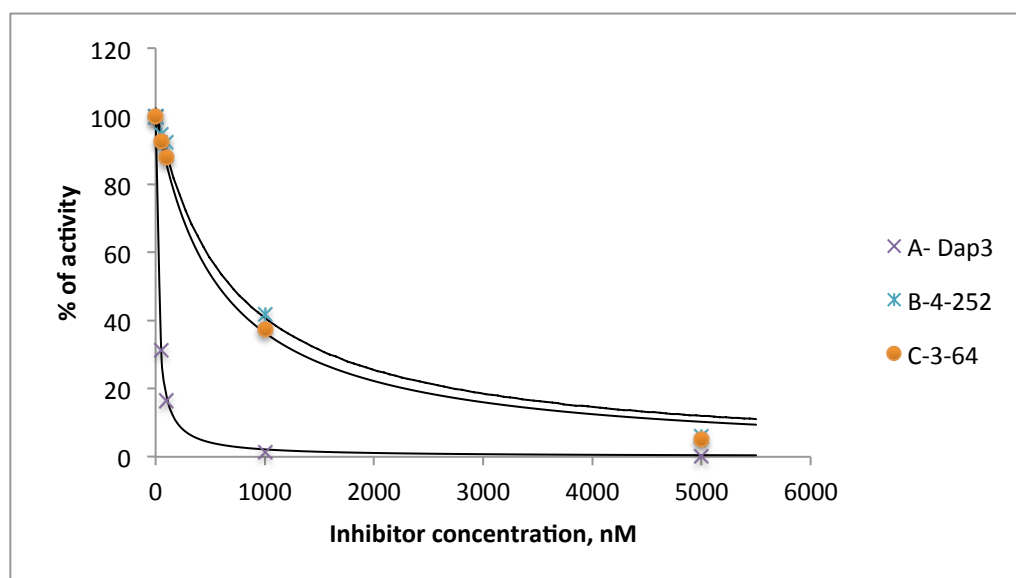
	dpm	avr	% activity	IC50
control	0	2031	1992.5	100
		2114		
3-285	1	2169	2068	104
		2127		
3-285	3	1545	1475.5	74
		1566		
3-285	10	875	818.5	41
		922		
3-285	30	361	213.5	11
		226		
RAH 4-147	1	1891	1861	93
		1991		
RAH 4-147	3	2661	1491	75
		1491		
RAH 4-147	10	1041	945.5	47
		1010		
RAH 4-147	30	492	400.5	20
		469		



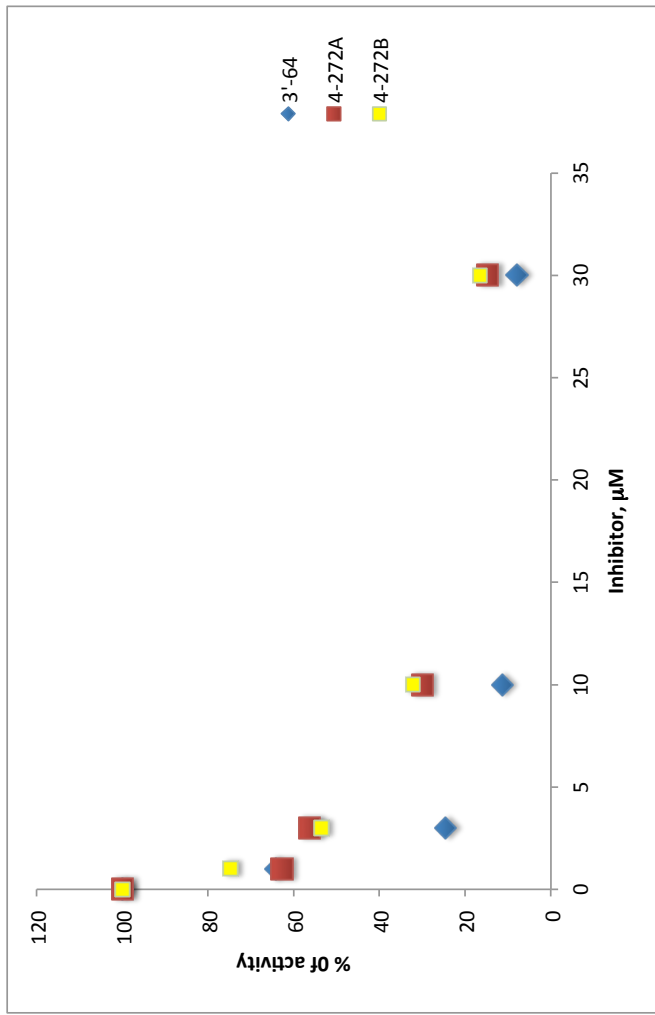
	dpm	avr	% activity	IC50
control	0	1963	1791.5	100.0
	1	1780	1996	111.4
	3	1762	1591.5	88.9
	10	1581	1107	61.9
BS 1-120	30	1271	622.5	34.8
	1	691	1987.5	111.0
	3	1950	2083	116.3
	10	2181	2071	115.6
BS 1-123	30	2078	1857.5	103.7
	1	1923	1994.5	111.4
	3	1937	1824.5	101.9
	10	1668	1585.5	88.5
RAH 2-277	30	1663	1258.5	70.3
	1	1248	1891	105.6
	3	1984	2069.5	115.5
	10	2339	2073.5	115.8
RAH 4-40	30	1968	1947.5	108.7
	1	2076	1992.5	111.3
	3	2128	1895.5	105.8
	10	2015	1977.5	110.4
BS 1-138	30	2052	1982.5	110.7
	1	1970		
	3			
	10			



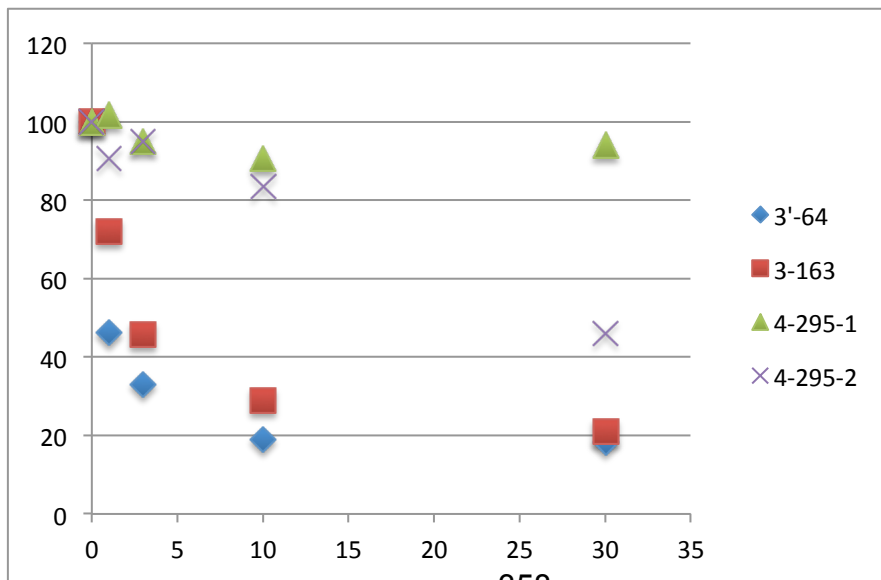
	dpm	avr.	% of activity	
control	0	2142	2109	100.0
		2235		
A- Dap3	50	838	660	31.3
		641		
	100	428	348	16.5
		427		
	1000	132	29	1.4
B-4-252	5000	85	4	0.2
		84	4	
		84		
	50	1870	1995	94.6
		2280		
C-3-64	100	2097	1951	92.5
		1964		
	1000	925	882	41.8
		998		
	5000	181	129	6.1
	236			
B-4-252	50	1884	1954	92.6
		2183		
	100	2024	1852	87.8
		1840		
	1000	901	792	37.5
	842			
C-3-64	5000	192	108	5.1
		184		



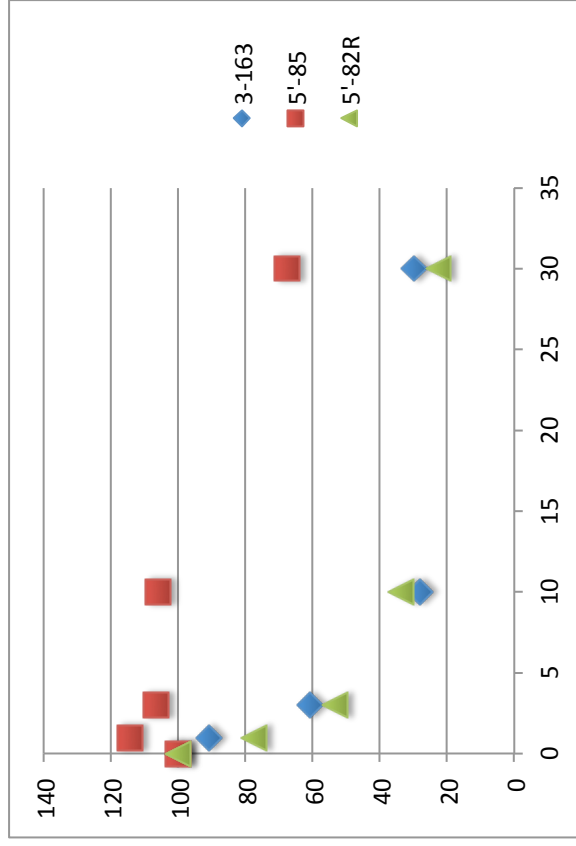
	cpm	avr cpm	% of activity
control	0	1575	100
3'-64	1	1815	64
	3	773	25
	10	1404	11
4-272A	30	442	8
	1	389	63
	3	207	56
4-272B	10	146	30
	30	125	15
	1	260	75
4-277	3	243	54
	10	1199	32
	30	1338	17
4-278A	10	837	68
	30	982	63
	10	536	45
4-278B	30	554	30
	1	291	61
	3	270	56
3'-64	10	1146	53
	30	1170	66
	1	1020	61
4-272A	3	1101	61
	10	1021	61
	30	1035	61
4-272B	10	975	56
	30	917	53
	1	847	66
4-277	30	954	61
	1	1173	54
	3	1069	38
4-278A	10	1019	54
	30	1056	68
	1	912	54
4-278B	30	920	54
	1	664	45
	3	631	45



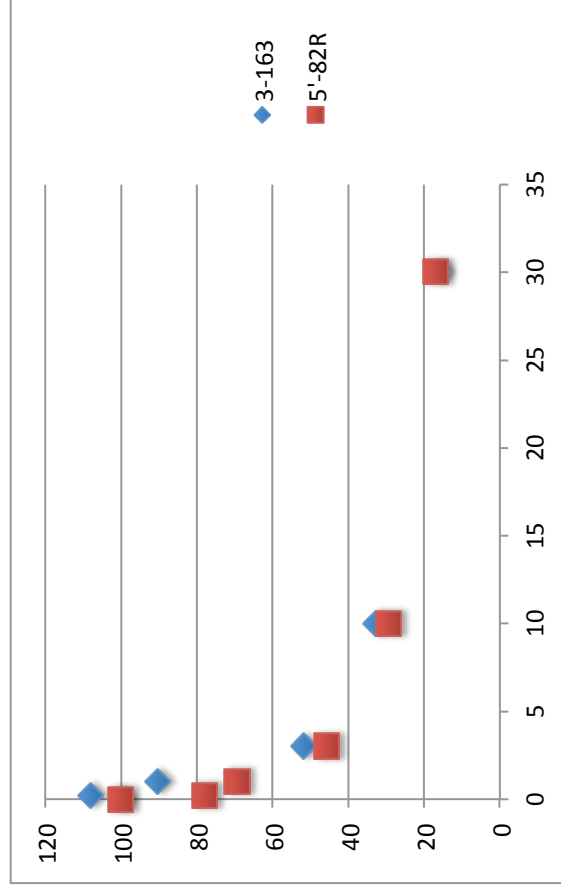
	cpm	avr cpm	% of activity	dpm	avr dpm	% of activity	
control	0	618	657	100	1378	1416	100
		695			1454		
	1	290	304	46	741	733	49
3'-64		318			724		
	3	242	218	33	592	561	36
		193			530		
	10	128	125	19	267	313	17
		122			359		
3-163	30	92	121	18	249	295	16
		150			340		
	1	447	473	72	1135	1243	87
		499			1351		
	3	347	301	46	881	784	53
		254			687		
	10	211	190	29	627	575	37
4-295-1		169			522		
	30	152	138	21	401	381	23
		124			361		
	1	675	669	102	1546	1513	107
		662			1480		
	3	626	625	95	1551	1497	106
		624			1442		
4-295-2	10	565	596	91	1473	1597	114
		626			1720		
	30	629	618	94	1493	1540	109
		607			1586		
	1	587	596	91	1533	1502	106
4-295-2		604			1470		
	3	675	623	95	1757	1504	107
		571			1250		
	10	561	549	83	1440	1322	93
		536			1204		
	30	334	303	46	760	728	48
		271			695		



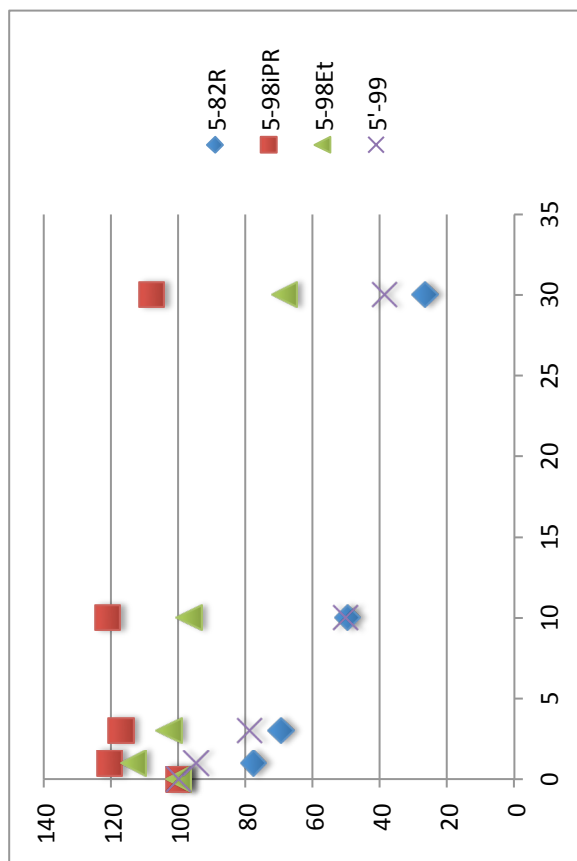
	dpm	corr dpm	avr dpm	fmol	% activity	
1	0	1302	1740	1685	306	100
2		1629				
3	1	1353	1526	277	91	
4		1699				
5	3	510	1111	1023	186	61
6		934				
7	10	471	471	471	86	28
8		6755				
9	30	532	501	91	30	
10		470				
11	1	1197	2238	1924	350	114
12		1610				
13	3	1912	1792	326	106	
14		1671				
15	10	1772	1772	324	106	
16		1797				
17	30	1079	1138	207	68	
18		1197				
19	1	1308	1302	237	77	
20		1296				
21	3	965	898	163	53	
22		478				
23	10	559	566	103	34	
24		573				
25	30	350	379	69	22	
26		407				
1*		438				
5*		601				
11*		1041				
22*		353				



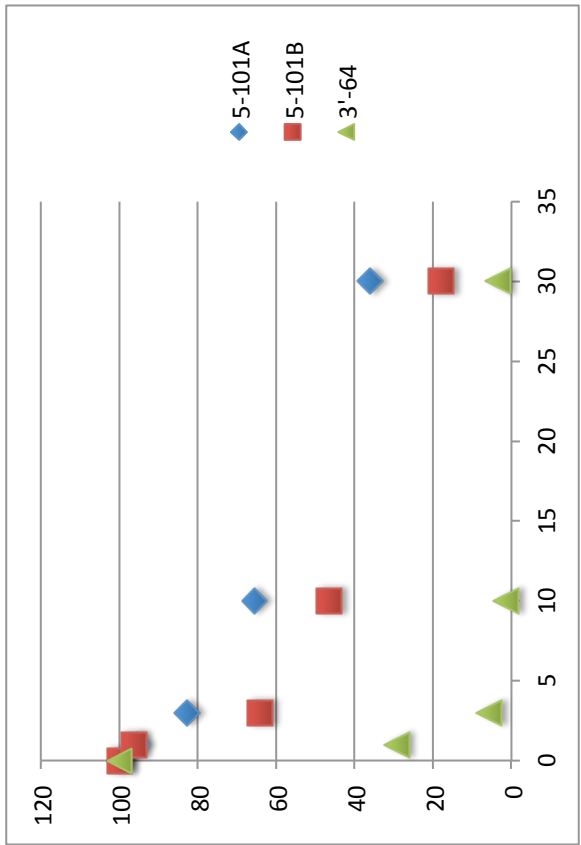
control	dpm	avr dpm	fmol	% activity
	0	4072	716	100
	0.2	3807		
	0.2	4361	773	108
	0.2	4147		
	1	3474	647	90
	1	3638		
3-163	3	1709	371	52
	3	2370		
	10	1210	235	33
	10	1380		
	30	722	117	16
	30	567		
	0.2	3085	558	78
	0.2	3052		
	1	2481	497	69
	1	2984		
5'-82R	3	1490	327	46
	3	2102		
	10	1232	210	29
	10	1082		
	30	585	122	17
	30	752		



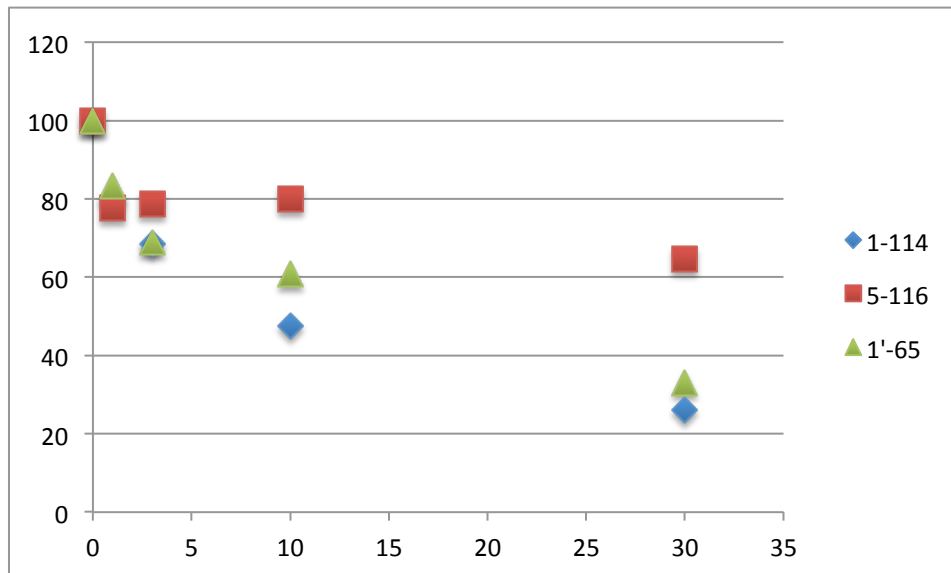
	dpm	avr dpm	fmol	% activity
5-82R	0	1699	281	100
		1387		
	1	1226	218	78
		1174		
	3	1080	195	69
		1066		
	10	853	139	50
		681		
	30	389	74	26
		430		
5-98iPR	1	1830	338	120
		1893		
	3	1927	329	117
		1692		
	10	1866	340	121
		1872		
	30	1578	303	108
		1758		
	1	1800	318	113
		1702		
5-98Et	3	1709	288	103
		1463		
	10	1543	272	97
		1448		
	30	1005	193	69
		1113		
	1	1606	266	95
		1324		
	3	1200	221	79
		1236		
5'-99	10	716	141	50
		836		
	30	544	109	39
		652		



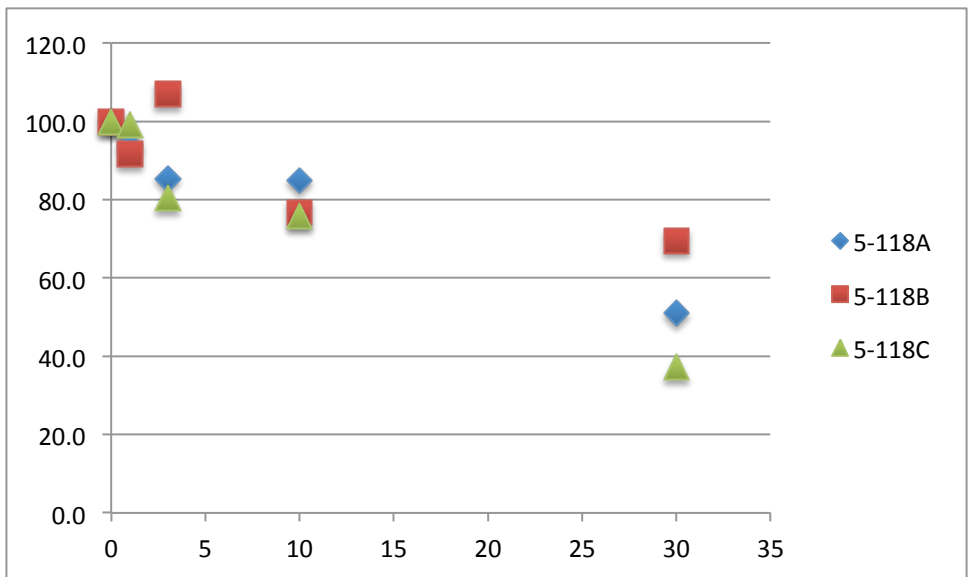
	dpm	avr dpm	avr dpm - bkgr	% of activity
	2051	2141	1782	100
0.0001	2231			
1	1940	2059	1700	95
	2178			
3	1865	1832	1473	83
	1798			
10	1330	1527	1168	66
	1723			
30	1037	1000	641	36
	962			
1	2141	2076	1717	96
	2011			
3	1529	1500	1141	64
	1470			
10	1288	1186	827	46
	1083			
30	572	680	321	18
	787			
1	908	880	521	29
	852			
3	466	459	100	6
	451			
10	430	383	24	1
	336			
30	519	421	62	3
	322			
background	305	359	0	
	413			



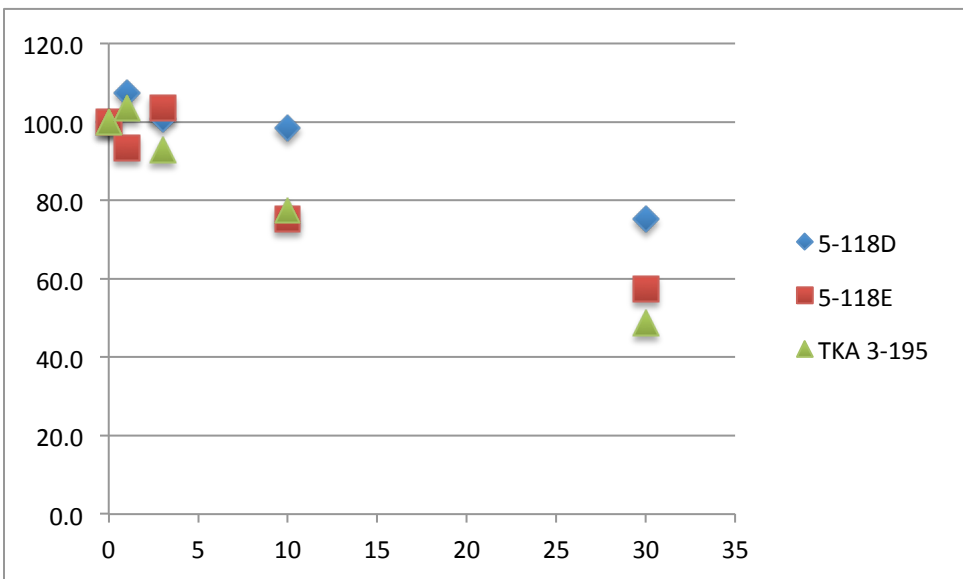
	dpm	avr dpm	norm to Dap3	
1-114	0	2339	2412	100
		2485		
	1	1986	1953.5	79
		1921		
	3	1697	1712.5	68
		1728		
5-116	10	1406	1249	47
		1092		
	30	827	774.5	26
		722		
	1	1852	1920	78
		1988		
1'-65	3	1774	1942	79
		2110		
	10	1821	1970.5	80
		2120		
	30	1574	1629.5	65
		1685		
Dap3-'A'	1	2063	2042.5	83
		2022		
	3	1774	1722.5	69
quenched		1671		
	10	1663	1546	61
		1429		
	30	823	932.5	33
		1042		
	239	200.5		
	162			
	360	339		
	318			



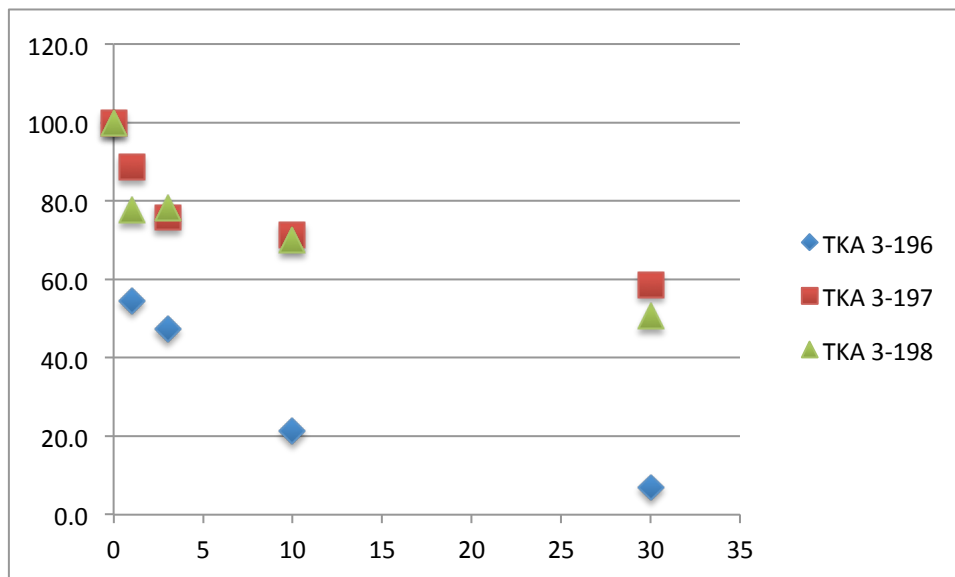
	dpm	avr dpm	norm to bkgr
5-118A	0	2128 2395	2262 100.0
	1	2254 2018	2136 93.7
	3	2105 1830	1968 85.3
	10	1922 1995	1959 84.9
	30	1094 1464	1279 51.0
	1	2228 1961	2095 91.7
5-118B	3	2183 2623	2403 107.0
	10	1612 1977	1795 76.7
	30	1466 1833	1650 69.5
	1	2101 2388	2245 99.1
5-118C	3	1893 1840	1867 80.3
	10	1700 1853	1777 75.8
	30	1034 969	1002 37.2
	Dap3(1-28) bkgr	291 219	255



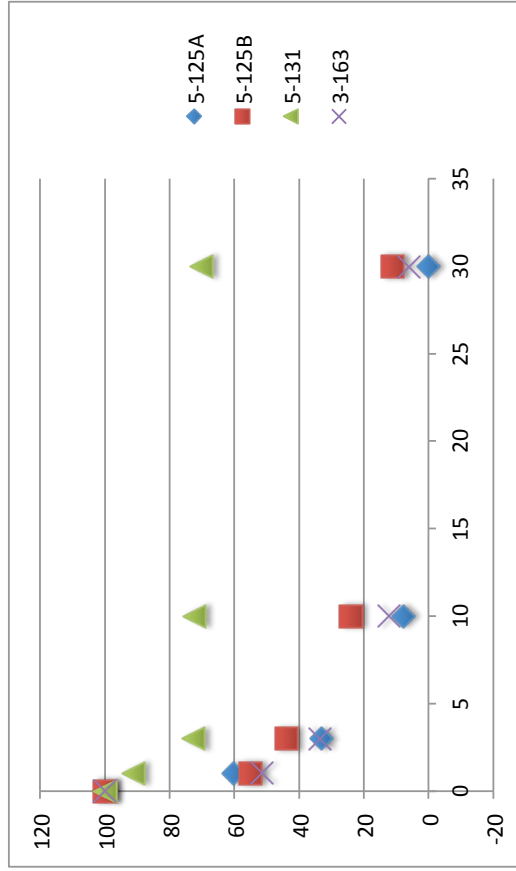
	dpm	avr dpm	norm to Dap3
5-118D	0	2379 2340	2360 100.0
	1	2520 2498	2509 107.5
	3	2472 2281	2377 100.8
	10	2356 2306	2331 98.6
	30	1979 1751	1865 75.3
	1	2300 2155	2228 93.4
	3	2499 2360	2430 103.5
5-118E	10	1748 1983	1866 75.3
	30	1547 1467	1507 57.4
	1	2202 2659	2431 103.5
	3	2211 2218	2215 92.7
TKA 3-195	10	1747 2071	1909 77.5
	30	1411 1257	1334 48.7
	Dap3(1-28) bkgr	371 348	360



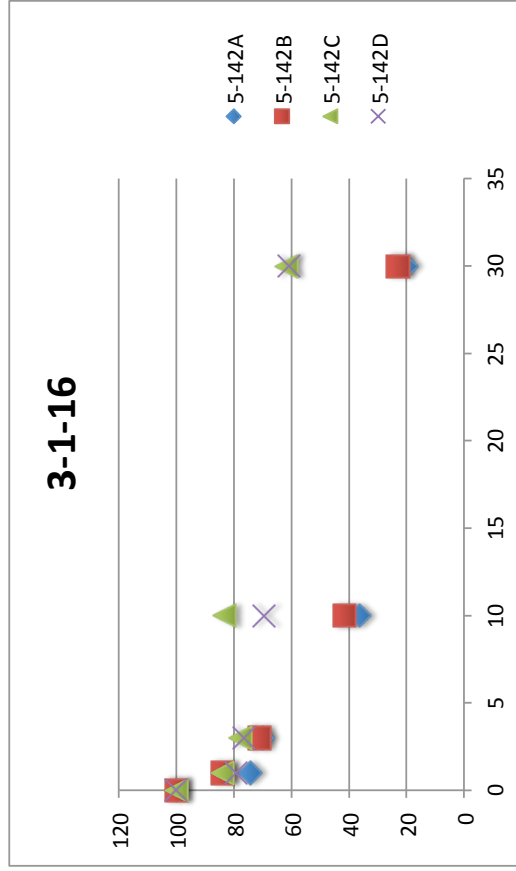
	dpm	avr dpm	norm to Dap3	
TKA 3-196	0	2704 2577	2641 100.0	
	1	1600 1586	1593 54.7	
	3	1360 1492	1426 47.4	
	10	871 770	821 21.2	
	30	446 537	492 7.0	
	TKA 3-197	1	2307 2452	2380 88.7
		3	2036 2127	2082 75.8
		10	1872 2086	1979 71.4
		30	1696 1672	1684 58.6
		TKA 3-198	1	2291 1964
3			2271 2002	2137 78.2
10	1883 2015		1949 70.1	
30	1523 1476		1500 50.6	
Dap3(1-28) bkgr		365 295	330	



	dpm	avr dpm	norm to Dap3
control	0	2010	100
		2210	
	1	1348	60
		1516	
5-125A	3	986	33
		947	
	10	475	8
		595	
	30	392	0
		412	
	1	1198	55
		1483	
5-125B	3	1138	44
		1165	
	10	760	24
		866	
	30	599	11
		588	
	1	1877	91
		2038	
5-131	3	1592	73
		1691	
	10	1500	72
		1771	
	30	1619	70
		1576	
	1	1221	51
		1342	
	3	994	33
		953	
	10	499	12
		723	
	30	377	6
		632	
Dap3(1-28)		509	
bkgr		299	



control	dpm	avr dpm	nor to Dap3
	0	2282	100
	1	2352	
	1	1867	74
	1	1801	
A	3	1766	70
	10	1740	
	10	1182	36
	10	1065	
	30	831	20
	30	804	
	1	1968	84
	1	2068	
B	3	1814	71
	3	1741	
	10	1172	41
	10	1270	
	30	796	23
	30	948	
	1	2040	84
	1	1997	
C	3	1870	78
	3	1934	
	10	2158	83
	10	1843	
	30	1594	62
	30	1604	
	1	1772	79
	1	2088	
D	3	1923	76
	3	1831	
	10	1669	69
	10	1819	
	30	1682	61
	30	1488	
		441	
		445	
		449	
			bkg



	dpm	avr dpm	nor to Dap3
	0	2130	100
		2035	
	1	1677	77
		1730	
	3	1536	72
		1711	
	10	1203	54
		1437	
	30	853	28
		919	
	1	1970	92
		1936	
	3	2101	89
		1694	
	10	1833	79
		1622	
	30	1400	58
		1359	
	1	1935	96
		2112	
	3	2032	103
		2230	
	10	1661	80
		1830	
	30	1792	81
		1744	
	1	1396	66
		1640	
	3	1384	41
		831	
	10	864	23
		740	
	30	326	-7
		296	
		317	
		420	
			bkgr
			523

